DISSERTATION

# ELUCIDATION OF THE BIOGENESIS OF THE PARAHERQUAMIDES, MALBRANCHEAMIDES, CITRINALINS, AND BREVIANAMIDES

Submitted by

Kimberly R. Klas

Department of Chemistry

In partial fulfillment of the requirements

For the Degree of Doctor of Philosophy

Colorado State University

Fort Collins, Colorado

Summer 2019

Doctoral Committee:

Advisor: Robert M. Williams

Yian Shi
Eugene Chen
Dean Crick

ABSTRACT

ELUCIDATION OF THE BIOGENESIS OF THE PARAHERQUAMIDES, MALBRANCHEAMIDES, CITRINALINS, AND BREVIANAMIDES

Various fungi of the genera *Aspergillus, Penicillium* and *Malbranchea* produce prenylated indole alkaloids that possess a bicyclo[2.2.2]diazaoctane ring system and a variety of biological activities such as insecticidal, cytotoxic, anthelmintic, and antibacterial properties. After the discovery of distinct enantiomers of the natural alkaloids Stephacidin A, Notoamide B and their corresponding diastereomers, from *Aspergillus protuberus* MF297-2, *Aspergillus amoenus* NRRL 35660 and *Aspergillus taichungensis*, the structurally diverse metabolites became of particular biosynthetic interest. The bicyclo[2.2.2]diazaoctane core of the divergent natural metabolites may be enzymatically derived via a putative intramolecular hetero-Diels-Alder cycloaddition. We completed the total synthesis of ZwtP and MeZwtP, unveiling the role of a newly discovered Diels-Alderase. We are also undergoing further synthetic efforts to access other novel natural products, as well as further understand additional unprecedented transformations in nature.

ACKNOWLEDGEMENTS

"Only those who dare to fail greatly can ever achieve greatly" – Robert F. Kennedy

The path to success comes with great risks, failure, persistence, and motivation. It is rarely attained without moments of self-doubt and obstacles you once thought you didn't have the ability to overcome. Thankfully, I have been incredibly blessed with a network of supportive family, friends, and colleagues. Below is a partial list of the people who have been by my side throughout my journey. Thank you for helping me achieve my goals.

Professor Robert M. Williams—For giving me the opportunity to succeed, demonstrating patience and encouragement, and believing in me when I had a hard time believing in myself. I am forever grateful for your influence, mentorship and the opportunity to be trained under you.

Past and present committee members: Professor Tomislav Rovis, Professor Andrew McNally, Professor Tony Rappe, Professor Yian Shi, Professor Eugene Chen, and Professor Dean Crick—For your professional support and pushing me to overcome my weaknesses.

Dr. Justin Wyatt—For taking a chance on me, giving me the opportunity to develop a love for research, and showing me the joys of synthetic chemistry. I am forever grateful for your influence and mentorship.

Christine Dunne, Nathan Bair, Jonathan Thielman, and Heather Rubin—For being great friends and supportive colleagues. I am forever grateful to have made lifelong friends from this experience.

My siblings Ashleigh Langheim, Lauren Hunt, and Andrew Klas and their families—For your love and encouragement throughout this process.

My parents, Don and Jeannie Klas—For your love, understanding and support in fulfilling my dreams.

My husband, Jordan Koehn—A very special thanks for being my number one support system. You have helped me grow as a person and a scientist. I am forever grateful to have you by my side.

TABLE OF CONTENTS

# Chapter 1: Prenylated Indole Alkaloids[1]

## I. Introduction

The isolation of natural products from marine and terrestrial-derived fungal species of the *Aspergillus* genus has allowed for a widely studied diverse class of secondary metabolites. The focus is on prenylated indole alkaloids, specifically the paraherquamides, brevianamides, aspergamides, versicolamides, notoamides, stephacidins, and recently the taichunamides. The presence of a bicyclo[2.2.2]-diazaoctane ring system and indole-derived unit are reasons for the structural attraction of these naturally occurring metabolites, but does not alone account for their popularity. Many of these alkaloids have been found to maintain a variety of biological activity such as insecticidal, cytotoxic, anthelmintic, and antibacterial properties.[2-3] We have greatly studied the notoamides, paraherquamides, malbrancheamides, and brevianamides as well as contributed to developments in the biosynthesis of these compounds and the discovery of unexpected enantiomeric and diasteromeric relationships.[2-8] Herein this introductory chapter, we will focus on the biogenesis of these metabolites and their congeners (Figures 1.1 and 1.2), and provide our current understanding of the structural and stereochemical homologies and disparities that are of particular biosynthetic intrigue.

[1]This chapter is published in part or in full in *Natural Product Reports*[1]

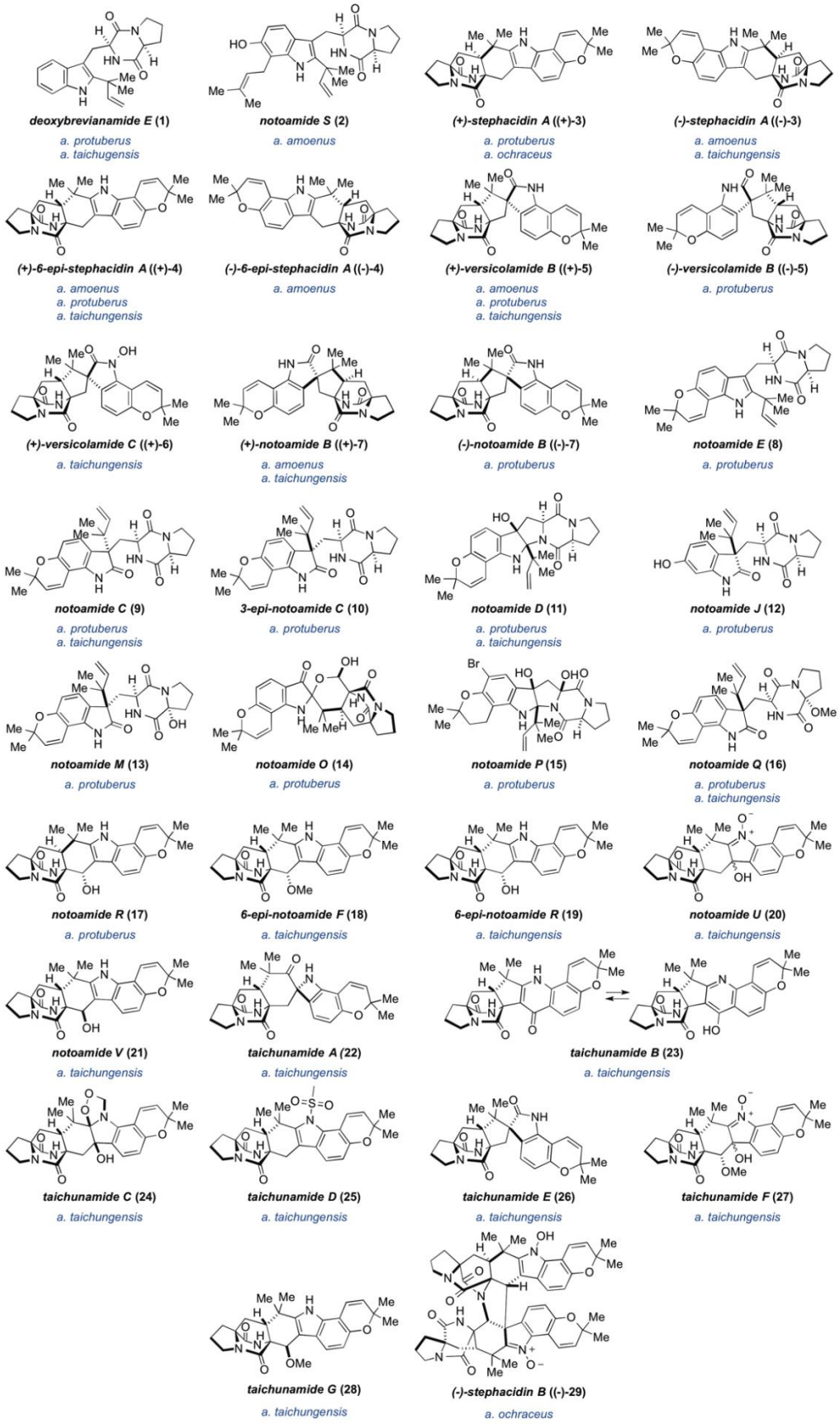


*Figure 1.1*. Select prenylated indole alkaloids isolated from the *Aspergillus* genus.

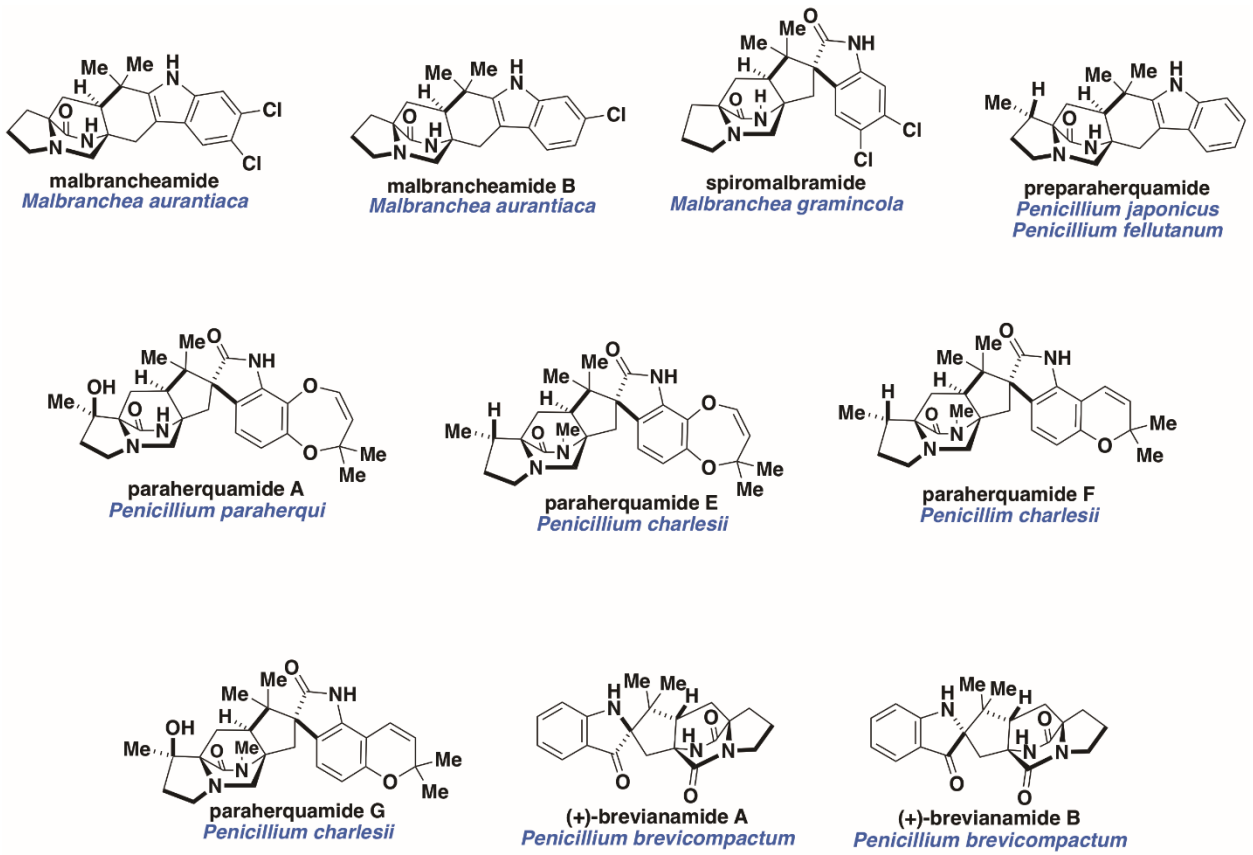


*Figure 1.2.* Select prenylated indole alkaloids isolated from the *Penicillium* and *Malbranchea* genera.[9-10]

## II. Fungal Metabolites and Biosynthetic Studies of Prenylated Indole Alkaloids in the *Aspergillus* genus

Elucidation of the biogenesis of these compounds became of particular interest upon the isolation of antipodal metabolites from different species of the *Aspergillus* genus. Initial studies from our laboratory,[11] with great influence from Sammes[12] and Birch,[13] have shown that these natural metabolites arise from L-tryptophan, one or two isoprene units, and L-proline, β-methylproline, or pipecolic acid.[6] This led to speculations of the early biogenesis of these antipodal metabolites. Although, advancements in identifying these stages were not made until identification of the notoamide gene cluster *(vide infra)* as well as feeding studies of anticipated intermediates.

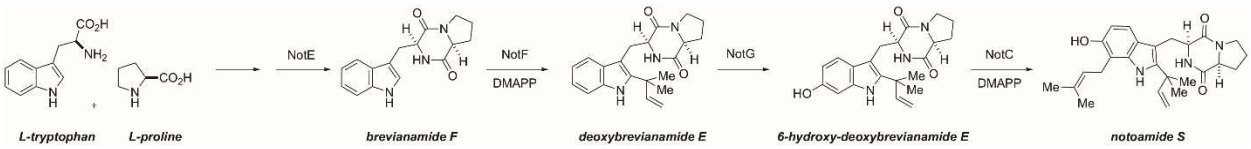


*Figure 1.1*. Early stages in the biogenesis of the *Aspergillus* genus.[8, 14]

Bioinformatics analysis and biochemical characterization of purified and bio-expressed enzymes helped to identify a normal prenyltransferase, NotF, and a reverse prenyltransferase, NotC.[14] Enzymatic conversion of brevianamide F into deoxybrevianamide E by the NotF enzyme was confirmed by gene expression of *notF* in the *Aspergillus* genus.[14] Confirmation of NotC enzyme activity in the transformation of 6-hydroxy-deoxybrevianamide E into notoamide S was performed in a similar procedure. The two prenyltransferases demonstrated high substrate selectivity in labeling studies and have provided evidence for the early stages of the biosynthesis (Figure 1.1).[14]

An understanding of the enantio- and diastereo-divergence of the biosynthetic pathways led Williams and coworkers to propose the presence of a putative Diels-Alderase, an enzyme scant in nature. Theoretical[15-16] and experimental[17-21] studies from our labs have provided sufficient evidence for the existence of the controversial enzyme in the biosynthesis of the orthologs (Figure 1.2).[5, 22]

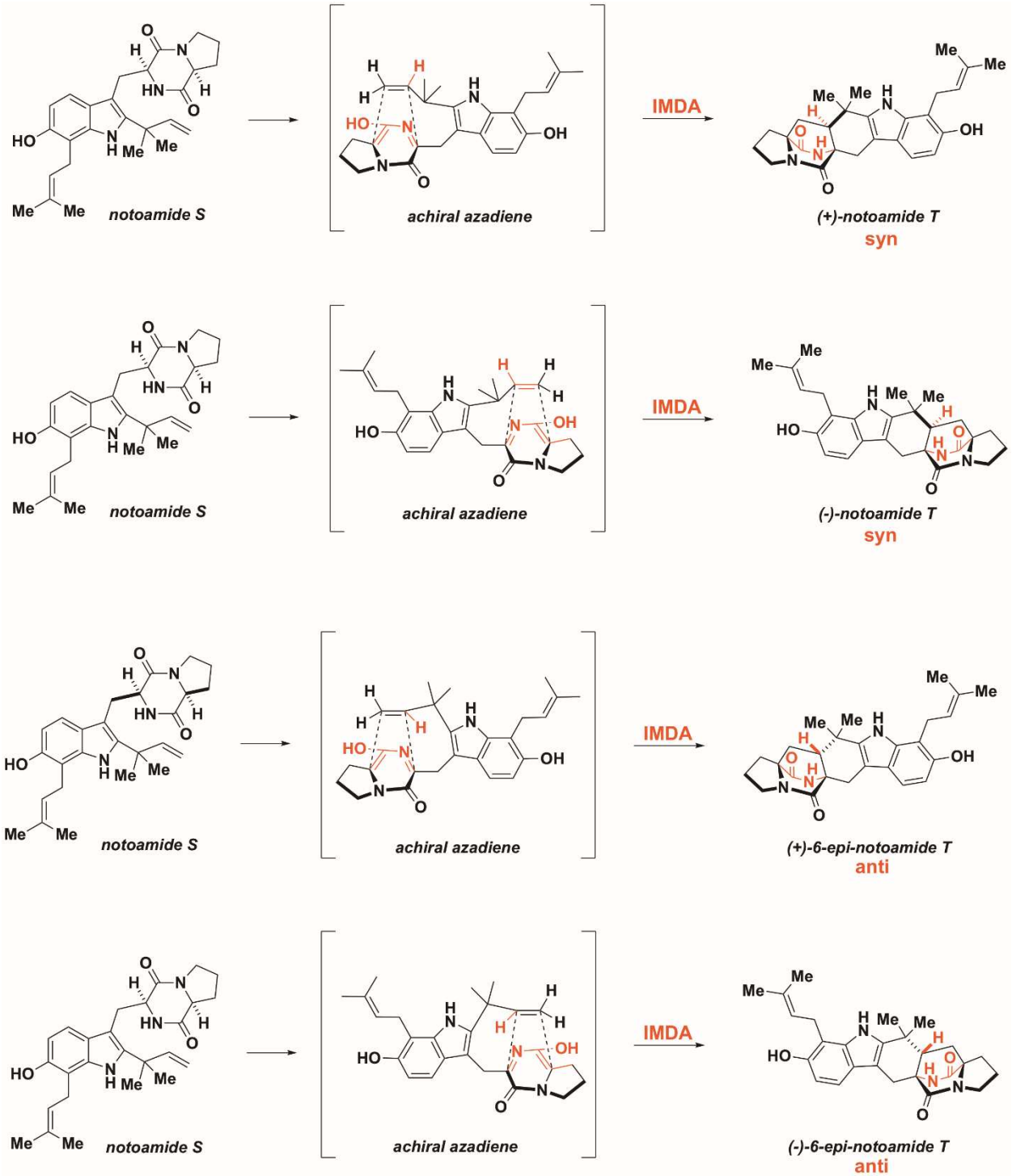


*Figure 1.2.* Putative IMDA in the enzymatic transformation of notoamide S to notoamide T and 6-epi-notoamide T.

This transformation is presented as an Intramolecular Diels-Alder (IMDA) reaction with NotH *(A. amoenus)* or NotH' *(A. protuberus)* as the enzyme (Figures 1.3 and 1.14). The stereospecific

enzyme-mediated IMDA reaction is thought to proceed via an achiral azadiene intermediate in an endo or exo configuration.[5] While it has been determined that these two fungal strains produce antipodal metabolites, the 71% overall nucleotide identity between *A. protuberus* and *A. amoenus* for genes *notA-notJ* and *notA'-notJ'* can be rationalized by the presence of the claimed Diels-Alderase.[23-24] This enzyme should be distinctive for each transition in order to achieve enantio- and diastereo-divergence, resulting in differences between the sequences of the active sites. Sherman and colleagues are currently investigating this hypothesis to elucidate the biological origins of this elusive enzyme and the mechanistic pathway that such an enzyme would utilize to carry out this transformation.[23, 25]

### *i. Aspergillus protuberus*

Notoamide T and its C6 epimer, 6-epi-notoamide T have not been isolated from the *Aspergillus* genus, but there is evidence for their presence among the metabolites. Incorporation of $^{13}C$ isotope labeled (±)-notoamide T resulted in enantiomerically distinct metabolites of stephacidin A and notoamide B in both *A. protuberus* and *A. amoenus*.[26] Contrarily, the bioconversion of racemic 6-epi-notoamide T into versicolamide B resulted in both of its enantiomers, after incubation with the fungal cells of *A. protuberus*.[27] While (-)-versicolamide B has been isolated from the fungal species, it is proposed to arise from notoamide E, possibly through isolated intermediate notoamide M, as shown in Figure 1.3.[28-29] This raises the question of whether or not the fungus produces (-)-versicolamide B by two different biosynthetic pathways, while also maintaining the opposite enantiomer of 6-epi-stephacidin A. It should also be noted that incorporation studies of both notoamide T and its diastereomer 6-epi-notoamide T resulted in the identification of new possible metabolites, which have not been isolated.[27]

Figure 3 shows the anticipated biogenesis of 6-epi-notoamide T3 and T4. Oxidation and consequential pinacol rearrangement would form the spirooxindole. Successive oxidation and incorporation of glycine would eventually result in the oxazolidine in 6-epi-notoamide T3. Oxygenation at this unit would produce the oxazolidinone in 6-epi-notoamide T4.[27]

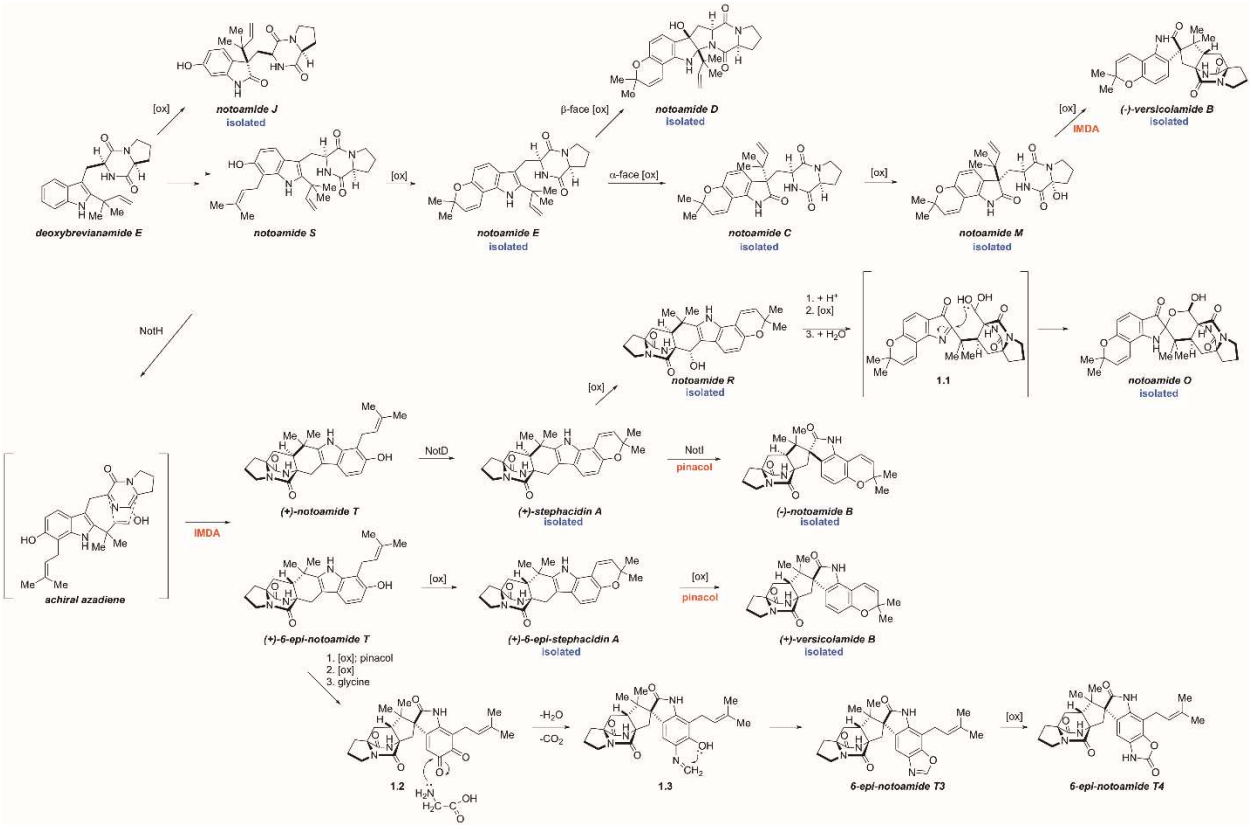


*Figure 1.3.* Biosynthesis of Aspergillus protuberus.

In 2010, Tsukamoto and coworkers isolated notoamide O, which contains an unprecedented, among this family of indole alkaloids, hemiacetal/hemiaminal ether functionality.[30] With this isolation, notoamides P-R were also found in the marine-derived fungus. The probable biosynthetic pathway for notoamides O and R is represented in Figure 1.3. Notoamide R is expected to arise directly from stephacidin A.[30] The dehydration of notoamide R, facilitated by the aromatic indole, provides natural metabolite aspergamide B.[30] Further oxidation, followed by hydrolysis, leads to intermediate **1.1,** which subsequently undergoes nucleophilic addition

onto the imine to afford notoamide O.[30] There currently are no feeding studies to support this transformation, nor biosynthetic implications for notoamides P and Q.

### *ii. Aspergillus amoenus*

The isolation of notoamide S, from *A. amoenus,* provided further support for the claimed enzyme-catalyzed enantiomeric and diastereomeric IMDA reaction.[8, 24] As precursor studies indicate,[31] this transformation would give rise to expected intermediates, (-)-notoamide T and (-)-6-epi-notoamide T, prior to oxidation to form the isolated metabolites, (-)-stephacidin A, and its C-6 epimer, 6-epi-stephacidin A in an enantio-rich mixture (Figure 1.4).[25-26] The fungal species contains some enantio-selective oxidase that accepts the (+)-enantiomer of 6-epi-stephacidin A, and transforms it into (+)-versicolamide B.[24] This enzyme is not identified as the same oxidase that converts (-)-stephacidin A into (+)-notoamide B, a transformation that has been validated by $^{13}$C-labeled feeding studies in both *A. amoenus* and *A. protuberus*.[32] Even though (-)-6-epi-stephacidin A is the enriched diastereomer, it may very well be a shunt metabolite in the biogenesis of *A. amoenus*. While the formation of an enantio-enriched metabolite has not yet been represented in any of the other species, it leaves the question of why this occurs in *A. amoenus*.

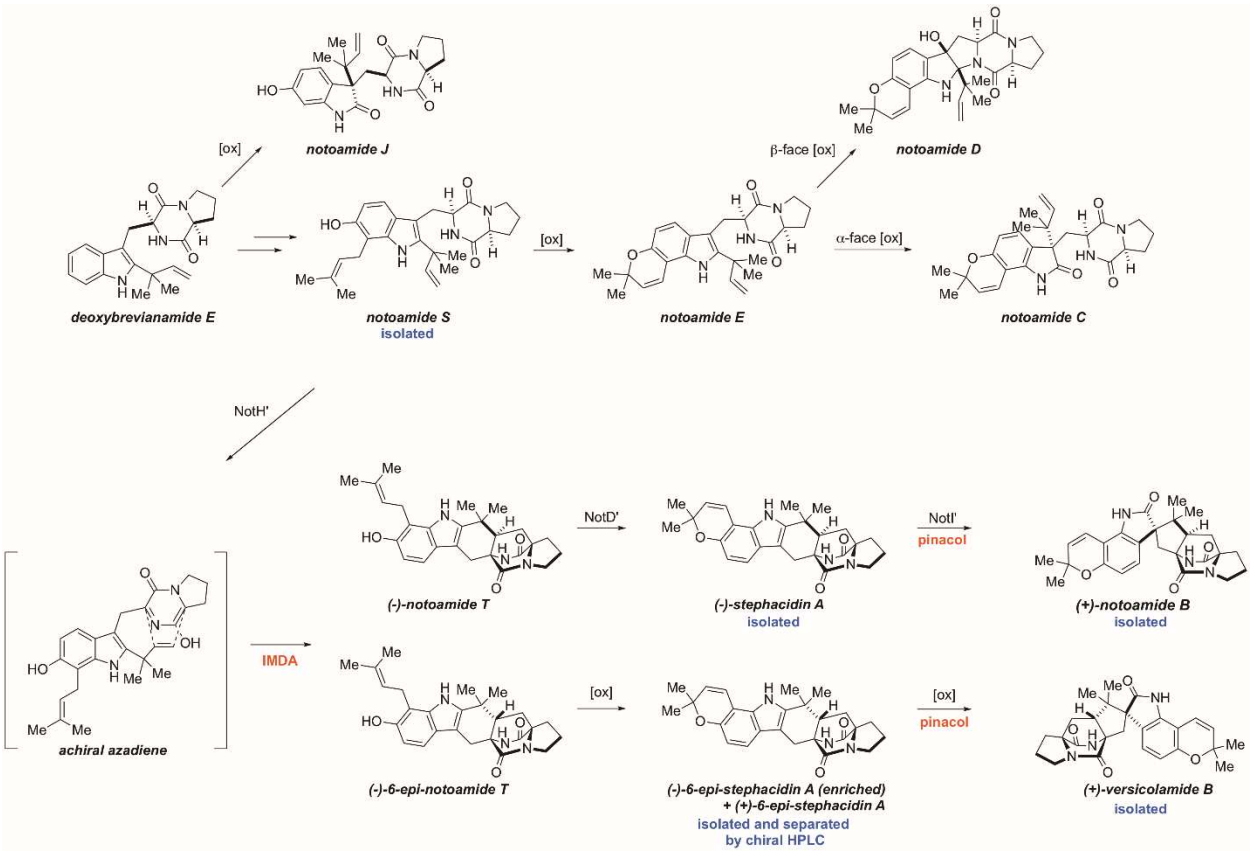


*Figure 1.4*. Biosynthesis of Aspergillus amoenus.

The total synthesis of notoamide E aided in the identification of the precursor within the metabolites,[33] which also allowed for $^{13}$C-labeled experiments to recognize if the intermediate was involved in the biogenesis.[34] It was originally understood that notoamide E may be part of the same biogenesis as stephacidin A.[35] Incubation of the $^{13}$C-labeled notoamide E surprisingly resulted in the detection of notoamides C and D in cultures of *A. amoenus* and *A. protuberus* with no observed stephacidin A.[36] Meanwhile, bioconversion of notoamide S into notoamides C and D, as well as (-)-stephacidin A, (+)-notoamide B, and (+)-versicolamide B is shown in the terrestrial derived species.[31] This provides evidence for the formation of notoamide E, from notoamide S, by some oxidase other than that is involved in the formation of stephacidin A. It can also be concluded that notoamides C and D are involved in the same biogenesis as notoamide E.

Meanwhile, it is suggested from a biogenetic standpoint that they are formed independently of one another.

Notoamide J has only been isolated from *A. protuberus*, but feeding studies with $^{13}C$-labeled 6-hydroxydeoxybrevianamide E in *A. amoenus* show incorporation into the indole alkaloid.[37] This implies that the fungus must preserve an indole oxidase capable of undergoing the Pinacol rearrangement that affords notoamide J. It should also be noted that it is likely a dead-end metabolite due to the lack of $^{13}C$ incorporation into more advanced intermediates.[37]

### *iii. Aspergillus taichungensis*

Versicolamide B and 6-epi-stephacidin A, recently isolated by Cai *et.al*., were the first prenylated indole alkaloids to be isolated from *A. taichugensis*.[38] This led to an array of metabolites, known and new to this family, to be isolated from the fungal species by Tsukamoto and coworkers.[23] Biochemical implications are presented herein (Figure 1.5) for new metabolites taichunamides A, B, and E as well as (+)-versicolamide C.[23] β-face oxidation (anti- to the bridged amide) of 6-epi-stephacidin A allows for the formation of a non-isolatable epoxide intermediate which subsequently undergoes a Pinacol rearrangement within the active site to form the spirooxindole in (+)-versicolamide B or the azetidine in taichunamide A.[23] Further oxidation of (+)-versicolamide B allows for the formation of the hydroxypiperidinone in (+)-versicolamide C. Oxidation at the α-face and Pinacol rearrangement would allow for formation of taichunamide E, from 6-epi-stephacidin A. Also, formation of peroxide **1.4** via oxidation of (+)-6-epi-stephacidin A would ultimately lead to the ring system found in taichunamide B, theoretically through compound **1.5**.[23] The isolation of these compounds from *A. taichunamide* has greatly broadened the library of these secondary metabolites. Future biochemical studies and genome mining will

aid in the identification of genes or gene clusters responsible for the convergent evolution of these unprecedented metabolites.

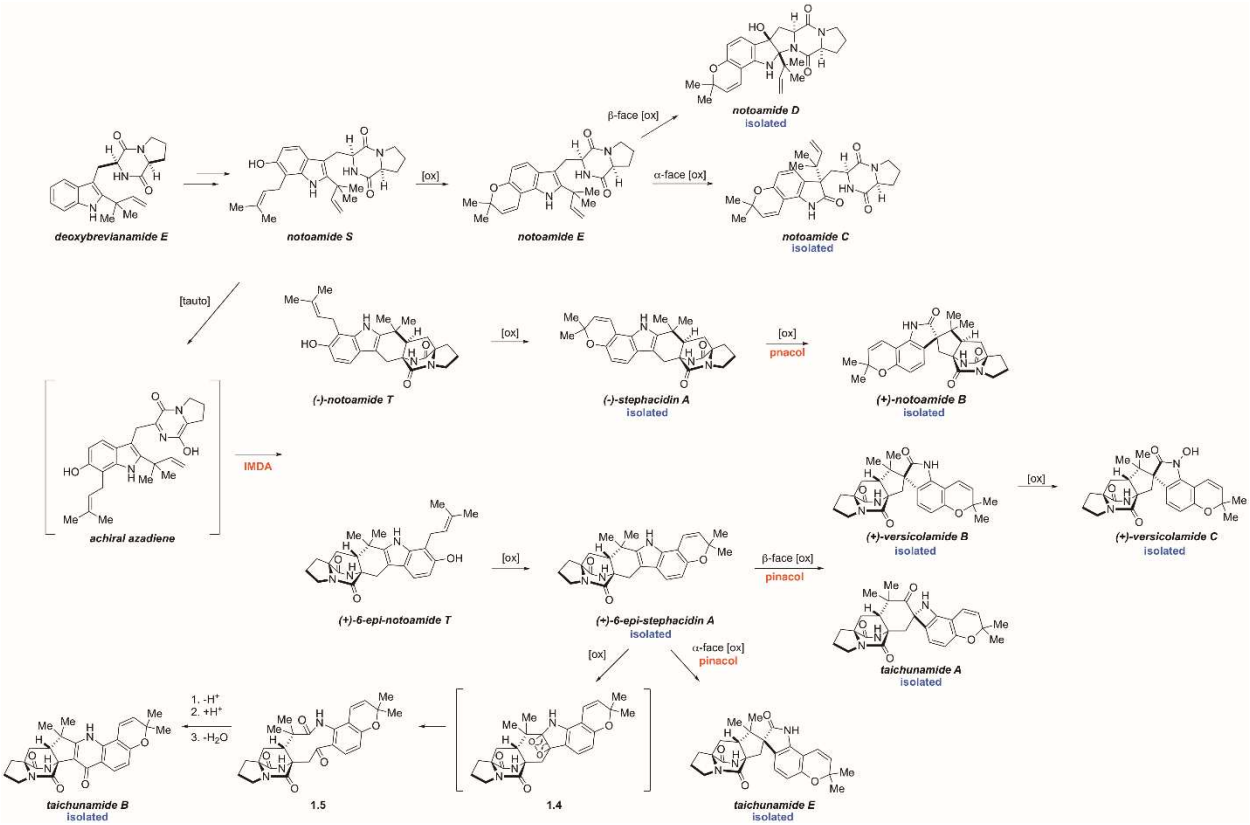


*Figure 1.5*. Biosynthesis of Aspergillus taichungensis.

### *iv. Aspergillus ochraceus*

The mitosporic fungal species, *A. ochraceus*, has been found to produce natural metabolites, among others, (+)-stephacidin A and (-)-stephacidin B.[39] The isolation of these compounds by Bristol-Meyers Squibb led to the discovery of the cytotoxic levels of the prenylated indole alkaloids, particularly against carcinoma and prostate cancer.[39-40] The complex structure of stephacidin B may reason for the increased toxicity levels of this natural product, compared to stephacidin A.[39] This motivated the outstanding synthetic developments of these compounds by Williams[41], Myers, and Baran.[42]

## III. Biomimetic Total Syntheses of Prenylated Indole Alkaloids in the *Aspergillus* genus

Biomimetic syntheses of the secondary metabolites are important, primarily to confirm the proposed biosyntheses. It is reported herein the total syntheses of several of the previously discussed prenylated indole alkaloids achieved by Williams and coworkers. Most notably, the IMDA reaction claimed to proceed via a Diels-Alderase has been successfully carried out synthetically in our labs.[17-21] Model studies for this reaction show optimized conditions for these alkaloids to be mild, since the dienes are activated (Figure 1.6).[20]

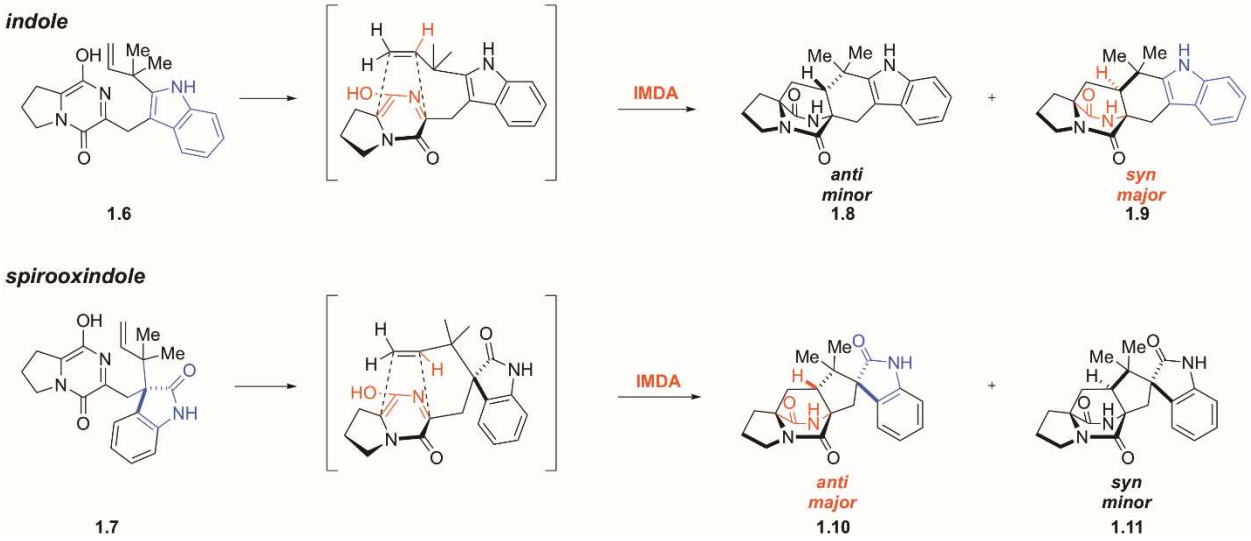


*Figure 1.6.* Initial IMDA studies.

Theoretical and experimental studies yield the expected diastereochemical outcome based on the nature of the substituents.[15-17] Studies show that the alkaloids containing a spirooxindole system favor anti- formation (**1.10**) whereas the indole system favors syn- stereochemistry (**1.9**).[17] Syn- formation is achieved for the indole system due to the sterically preferred spatial arrangement of the isoprene unit to the diene. The stereochemistry provided by the spirooxindole forces anti- conformation in the product. This development within our group has not only presented a basis for synthesizing these natural products, but also provided validity to

the proposed biosynthetic formation of the bicyclo[2.2.2]diazaoctane core via an innovative Diels-Alderase.

The most recent total synthesis of stephacidin A and its C-6-epimer (6-epi-stephacidin A) reported by Williams and coworkers, mimics the enzymatic formation of the natural products from notoamide T and 6-epi-notoamide T, respectively, as shown in Figure 1.7.[26, 43] Indole **1.13** is prepared by protection of alcohol **1.12** followed by the Leimgruber-Batcho indole synthesis and re-protection of the phenol group. Indole **1.13** is chlorinated, which then undergoes reverse prenylation with **1.14** to provide **1.15**. The reverse prenylated indole was subsequentially treated with dimethylamine and formaldehyde to afford the gramine that was coupled with glycine derived benzophenone imine **1.16** and treated with acid to offer reverse prenyl tryptophan **1.17** by a Somei-Kametani coupling method. Amine protected hydroxyproline **1.18** was coupled with tryptophan product **1.17** employing peptide coupling reagent, HATU. This provided the dipeptide, which was then deprotected, allowing cyclization to dioxopiperazine **1.19**. Upon deprotection of Boc protected **1.19**, the free phenol underwent prenylation with carbonate **1.20** via a Tsuj-Trost type reaction. Mesylation of the free alcohol in **1.21** allows for elimination, followed by tautomerization upon treatment with base and thereafter, the IMDA to provide a diastereomeric mixture of notoamide T and 6-epi-notoamide T. The basic conditions used for the Diels-Alder reaction also facilitate a Claisen rearrangement of the reverse-prenyl phenol in **1.21**. Upon separation of the diastereomers, cyclodehydrogenation was used to convert the notoamides into racemic mixtures of stephacidin A and 6-epi-stephacidin A, respectively.

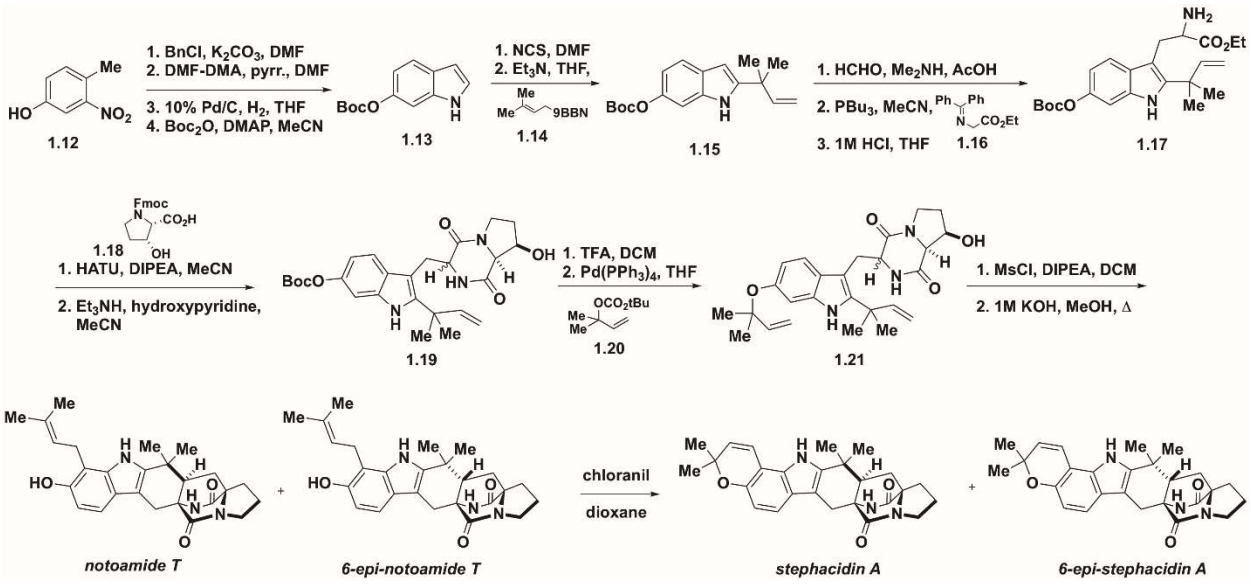


*Figure 1.7.* Biomimetic total synthesis of stephacidin A and 6-epi-stephacidin A.

The total synthesis of notoamide J was recently achieved by Williams and coworkers, from previously synthesized tryptophan **1.22** (see Figures 1.7 and 1.8).[43] Protection of the free amine and ester hydrolysis allows for HATU coupling providing dipeptide **1.24**. Upon deprotection of the free amine, cyclization affords dioxopiperazine **1.25**, as seen in the synthesis of stephacidin A (Figure 1.7). Oxidation at the aromatic indole with Davis' Oxaziridine (D.O.) allows for the formation of an unstable epoxide intermediate which subsequently undergoes a Pinacol type rearrangement, mimicking the proposed biochemical transformation from deoxybrevianamide E (Figure 1.4), to afford notoamide J as a racemate.

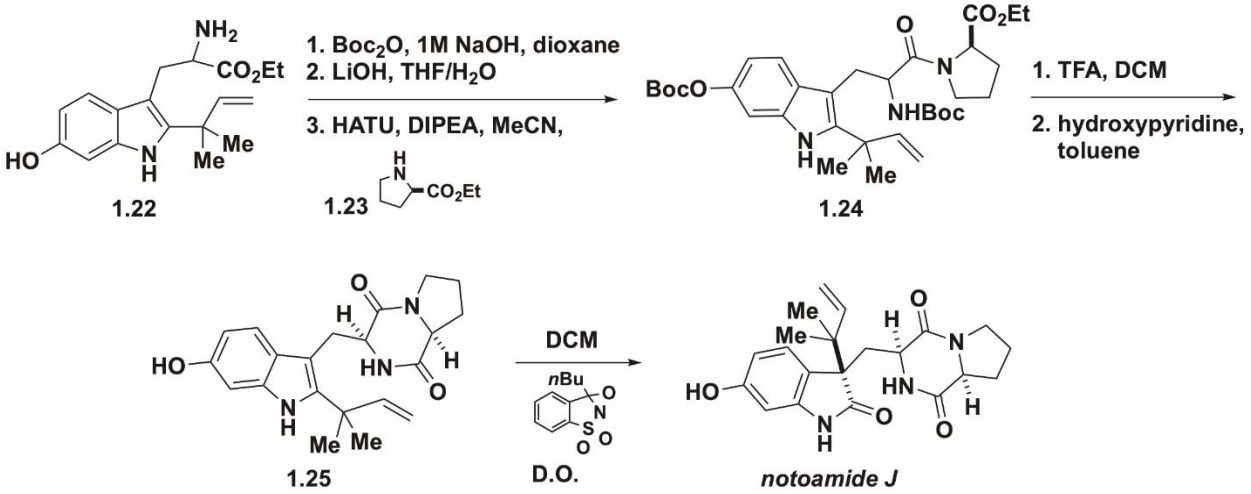


*Figure 1.8.* Biomimetic total synthesis of notoamide J.

Reverse prenylated indole **1.26**, developed from alcohol **1.12** as shown in the synthesis of stephacidin A (Figure 1.7), also led to the formation of notoamide B and its' diastereomer, versicolamide B.[40, 43-46] This synthesis is biomimetic as they both arise from a Pinacol rearrangement via aromatic indole oxidation. The total synthesis of these metabolites is represented in Figure 1.9.

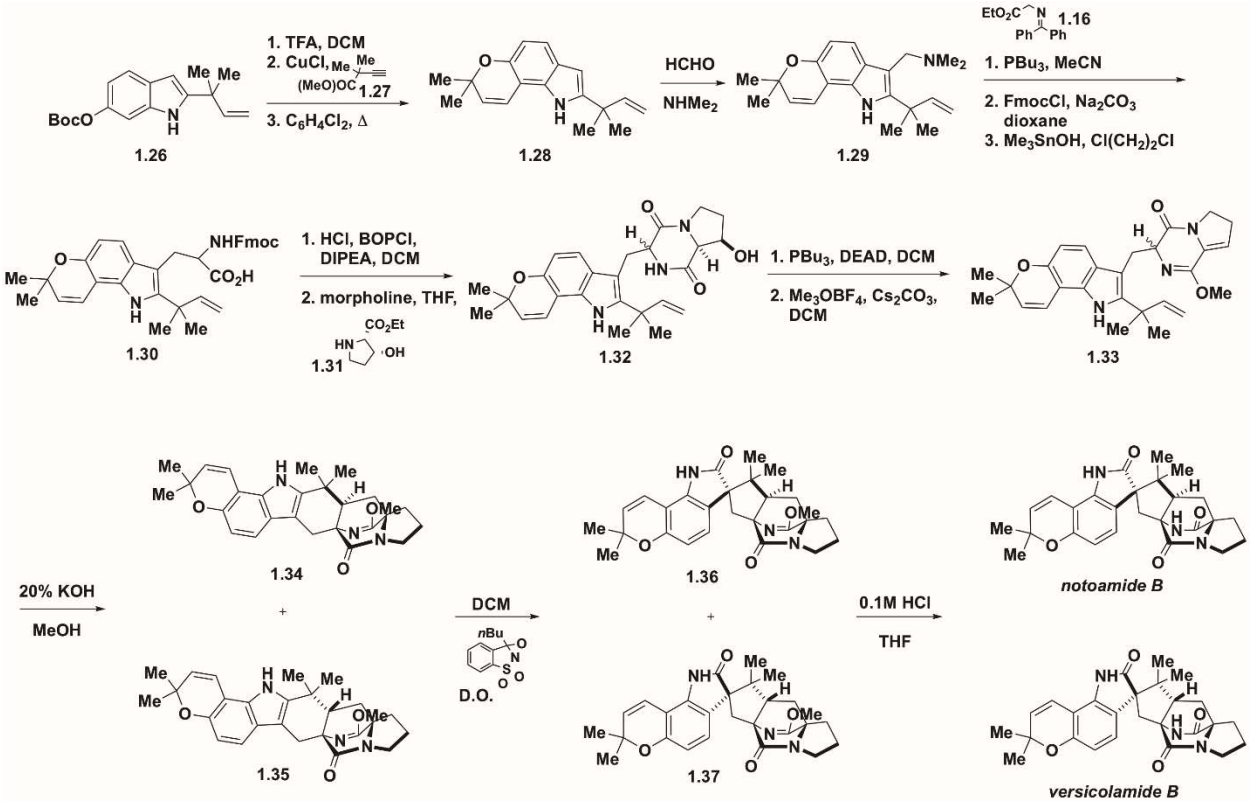


*Figure 1.9.* Biomimetic Total Synthesis of notoamide B and versicolamide B.

Deprotection of indole **1.26** allows for prenylation of the free phenol and thereafter, cyclization to provide pyran **1.28**. Formation of gramine **1.29** allows for coupling with glycine derivative **1.16** to eventually afford tryptophan **1.30**. Deprotection, cyclization, elimination, and formation of the aza enol ether in intermediate **1.33** allows for the IMDA to afford precursors **1.34** and **1.35**. Upon treatment of the isolated diastereomers with D.O., the Pinacol rearrangement takes place to eventually afford metabolites notoamide B and versicolamide B as racemic mixtures.

While the current total synthesis that has been developed in our laboratories for notoamide E does not mimic its biosynthesis, it has been found useful in feeding studies, as well as a gateway to the biomimetic syntheses of other metabolites *(vide infra).* The synthesis of notoamide E, and its epimer, epi-notoamide E, results in 13 steps from commercially available material, as shown

in Figure 1.10.[25, 47] Diazotization and reduction of benzyl amine **1.38** led to the formation of hydrazine **1.39**, which was subsequently submitted to Dean-Stark conditions with substrate **1.40** and Fischer indolization to achieve the prenylated indole (**1.41**). Prenylation at the deprotected phenol sets up for a thermal Claisen rearrangement of dipeptide **1.47** after Somei-Kametani coupling of gramine **1.44** and peptide coupling of tryptophan **1.45** to accomplish a diastereomeric mixture of the natural product.

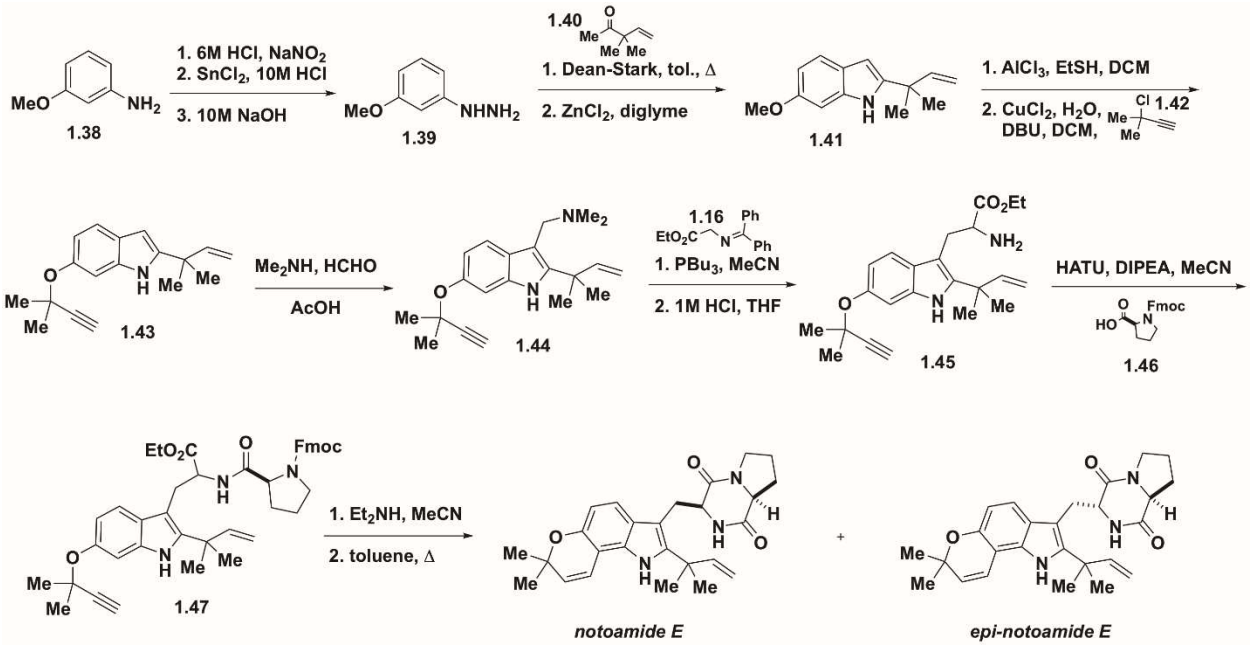


*Figure 1.10.* Total Synthesis of notoamide E.

Notoamide S is also accomplished synthetically from dipeptide **1.48**, along the notoamide E pathway (Figure 1.11).[25] In place of pyran formation, the terminal alkyne undergoes reduction to afford an alkene. Cleavage of the Fmoc group allows for cyclization to the diketopiperazine and the prenylated phenol consequentially undergoes a Claisen rearrangement to attain notoamide S and its epimer (epi-notoamide S).

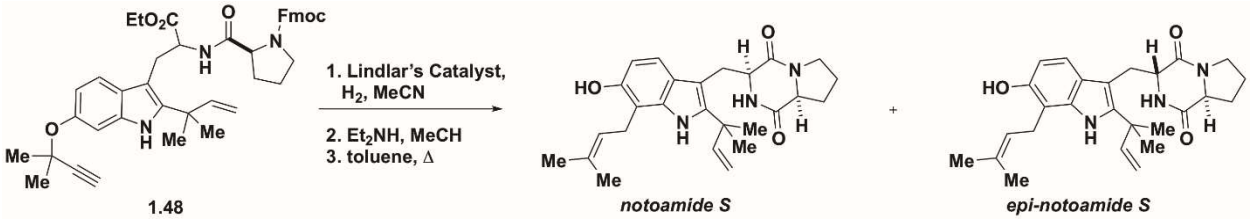


*Figure 1.11.* Total Synthesis of notoamide S.

Notoamides C and D can be achieved directly from notoamide E by oxidation (Figure 1.12),[25, 45, 47] as predicted in the biosynthesis (refer to Figures 1.3 and 1.4). Treatment of notoamide E and its diastereomer with D.O. produces a mixture of three products. Notoamide C and its C3 epimer, which may be an artifact of isolation,[31] are produced by a Pinacol type rearrangement of the non-isolatable epoxide intermediate. Notoamide D is a result of the epoxide opening to form the more stable hydroxyindoline species. This transformation is symbolic, among many others like the IMDA *(vide supra),* of the stereochemical diversity found among these compounds. The notoamide C pathway is suspected to arise via α-face oxidation and notoamide D by β-face oxidation. The role of the electronics within the indole ring system impacts the formation of the metabolites and is likely a result of which face of the molecule the oxidation takes place.[45]

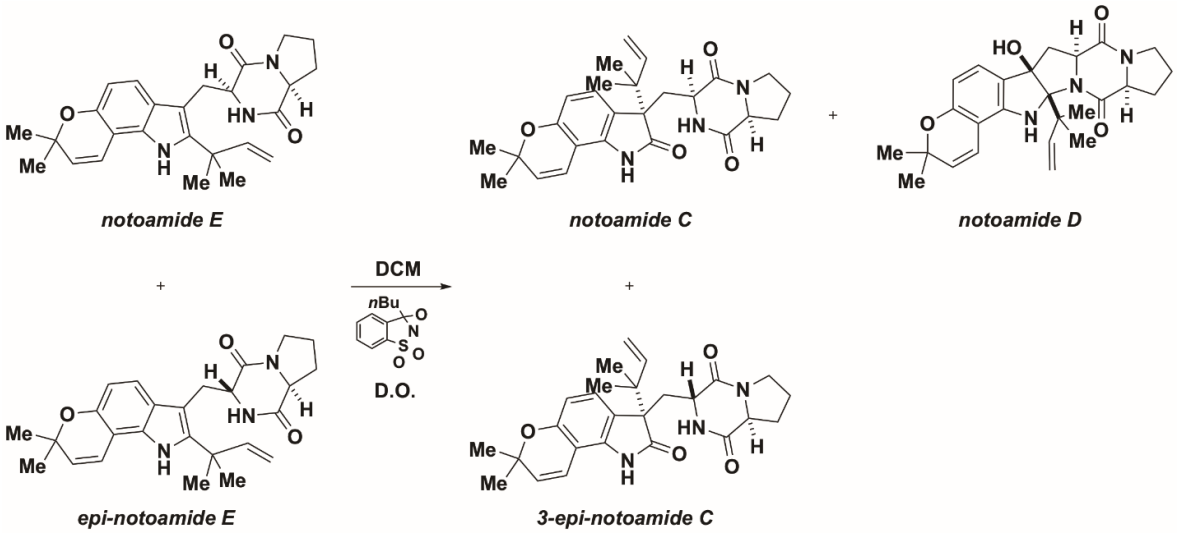


*Figure 1.12.* Biomimetic Total Synthesis of notoamide C and notoamide D.

Asymmetric total syntheses are found attractive within the field of synthetic chemistry and more importantly, are considered extremely beneficial to feeding studies. The metabolic profile of fungal species can more easily be understood with the use of enantiopure materials, rather than those in racemic form. With this, our laboratories aim at achieving asymmetric syntheses alongside their racemates. Within this family, the total syntheses of (+)-versicolamide B, (-)-versicoloamide B, (-)-stephacidin A, (+)-notoamide B, (-)-avrainvillamide, and (+)-stephacidin B have been achieved by Williams and coworkers.

Coupling of Fmoc protected tryptophan **1.30** with the salt form of proline derivative **1.31** provides dipeptide **1.32** as a single diastereomer, upon separation of the diastereomers. Oxidation and Pinacol rearrangement offers both diastereomers which are separated and converted into each enantiomer of versicolamide B (Figure 1.13) upon treatment with Mitsunobu conditions and successively base to afford the spirooxindole and bridged amide, respectively.[28, 46]

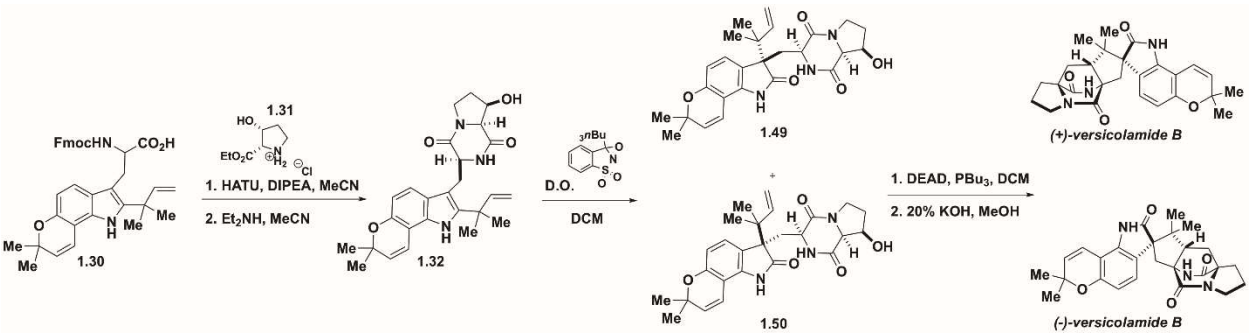


*Figure 1.13.* Asymmetric Total Synthesis of versicolamide B.

The asymmetric total synthesis of (-)-stephacidin A, (+)-notoamide B, and (+)-stephacidin B is achieved from hydroxy indole **1.51**.[41] Protection of the indole and phenol deprotection allows for prenylation of the phenol and thereafter, thermal cyclization to afford the pyran. Treatment with dimethyl amine and formaldehyde in acidic conditions allows for formation of the gramine and

consequent deprotection of the boc group to achieve **1.52**. Somei-Kametani coupling, protection of the free amine, and ester hydrolysis allows for tryptophan **1.53** to undergo peptide coupling, deprotection, and cyclization to present dioxopiperazine **1.55** in enantiopure form. Aza enol ether **1.56** is treated with Grubbs' catalyst (**1.58**) to achieve an aldehyde, which then gets reduced and mesylated to achieve **1.59**. Construction of the bicyclo core is succeeded under basic conditions, as seen before. Carbon-carbon coupling and deprotection of IMDA product **1.60** completes the synthesis of enantiomeric (-)-stephacidin A (Figure 1.14). Further treatment with D.O. presents the spirooxindole established in (+)-notoamide B. Reduction of (-)-stephacidin A to the dihydroindole allows for catalytic oxidation to natural product (-)-avrainvillamide and thereafter, coupling with itself in the presence of non-nucleophilic base to provide (+)-stephacidin B (Figure 1.15).

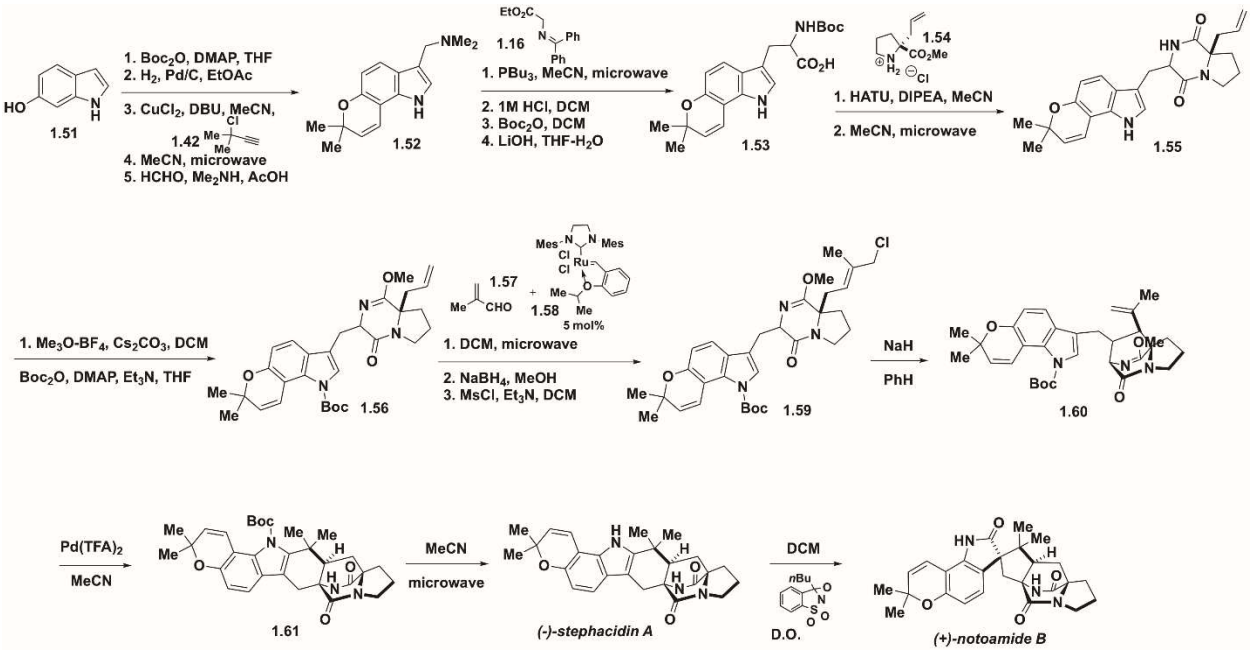


*Figure 1.14.* Asymmetric Total Synthesis of (-)-stephacidin A and (+)-notoamide B.

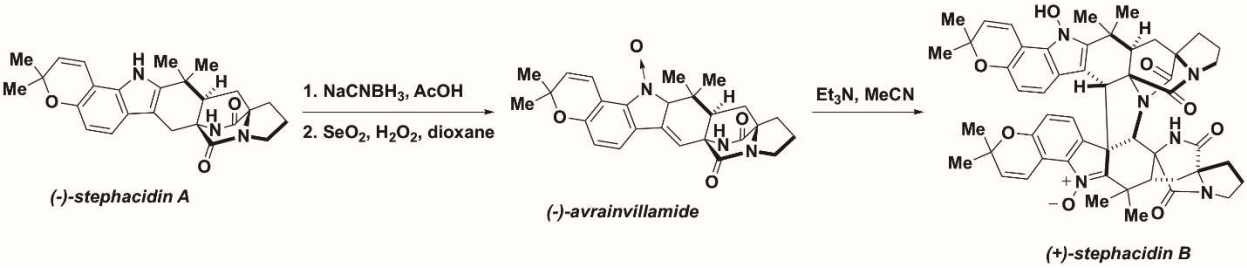


*Figure 1.15.* Assymmetric Total Synthesis of (+)-stephacidin B.

## IV. Fungal Metabolites and Biosynthetic Studies of Prenylated Indole Alkaloids in the *Malbranchea* and *Penicillium* genera.

Efforts to elucidate the biogenesis of the malbracheamides, paraherquamides, and brevianamides have been under way since the initial discovery of the paraherquamides and brevianamides, and the later discovery of the malbrancheamides. These metabolites possess the bicyclo[2.2.2]diazaoctane core and are believed to arise from an IMDA, like that of the notoamides, stephacidins, and taichunamides *(vide supra).* However, the paraherquamides and malbrancheamides differ at their core as they arise from monodiketopiperazines, rather than the diketopiperazine that is observed among the notoamides, stephacidins, taichunamides, and brevianamides. This leaves the question as to whether the monoketo- substrates arise in nature via reduction of the diketo- compounds or via an alternate reaction pathway. However, the lack of observance of the diketo- metabolites among the same fungal strains of the monoketo- metabolites suggests they arise through a different reactive species. With this being said, our initial proposals suggest their biochemical pathways to be nearly analogous.

### *i. Malbrancheamides.*

Malbrancheamide was isolated in 2006 from *Malbranchea aurantiaca* and was the first of the malbrancheamides to be discovered.[48] Shortly after, malbrancheamide B, which is the presumed

precursor to malbrancheamide, was isolated from the same fungal strain in 2008.[49] These metabolites have been evidenced to arise from premalbrancheamide by halogenase, Mal A (Figure 1.16).[50] Precursor incorporation studies with premalbrancheamide in *Malbranchea aurantiaca* show that premalbrancheamide can be incorporated into malbrancheamide B with 5.5% incorporation.[51] However, malbrancheamide was not detected from incorporation studies, suggesting a very slow second chlorination. Even though premalbrancheamide has not been isolated from the fungus, these results verify its existence as a natural metabolite.[50-51] Based on what we know about the biosynthesis of the notoamide and stephacidins *(vida supra)*, we can speculate that premalbrancheamide arises directly from the IMDA reaction with reactive achiral azadiene **1.64**.[10] Spiromalbramide was more recently isolated from *Malbranchea graminicola* in 2011 by Crews *et. al.* and is believed to arise from the oxidation and pinacol rearrangement of premalbrancheamide (Figure 1.16).[52] From here, MalA would also need to halogenate the species as shown in the biosynthesis of malbrancheamide. An alternate route would suggest spiromalbramide to arise from the oxidation and pinacol rearrangement of malbrancheamide. As of now, we can only speculate its biochemical destiny based on a biogenetic standpoint.

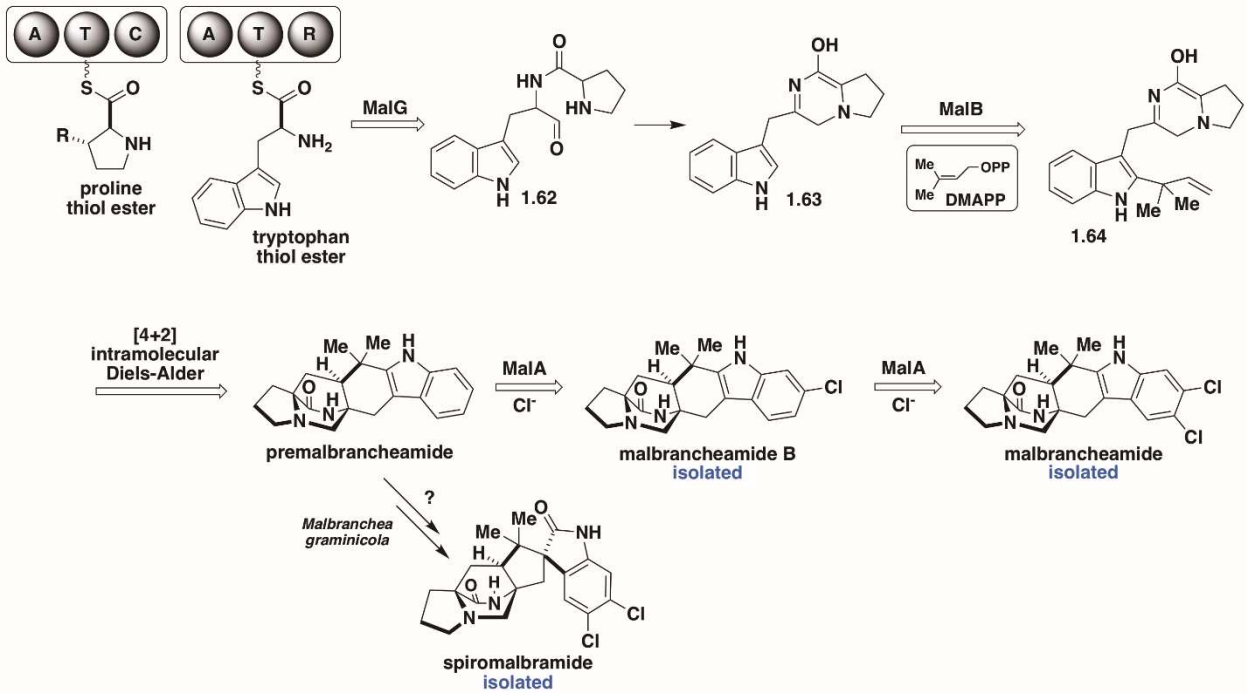


*Figure 1.16.* Earlier proposed biosynthesis of the Malbrancheamides.

### *ii. Paraherquamides.*

The paraherquamides were first discovered in 1989 upon the isolation of paraherquamide A from *Penicillium paraherqui.*[53] Preparaherquamide was isolated from *Penicillium japonicas* and *fellutanum* in 2008,[54] a few years after it was shown to biosynthetically incorporate into paraherquamide A. Feeding studies with preparaherquamide in *Penicillium fellutanum* exhibit 0.72% incorporation into paraherquamide A, whereas preparaherquamide's diketo- and diastereomeric counterparts show 0% incorporation.[9] This not only suggested preparaherquamide's existence as a natural metabolite before its' isolation, but also provides further evidence that the monoketo- substrates do not arise from the diketo- substrates.

Preparaherquamide is thought to arise in parallel to the biosynthesis of premalbrancheamide, through achiral azadiene **1.67**.[55] The only structural difference between premalbrancheamide and preparaherquamide is the methyl group that is present at the $\beta$

position of the proline unit of preparaherquamide. β-methyl proline is a presumed NRPS substrate and is believed to be fashioned from natural amino acid L-isoleucine.[56]

Paraherquamides E-G have also been isolated, but from *Penicillium charlesii.*[57] While these metabolites are found in a different species, we can speculate they are part of the same biosynthesis of paraherquamide A.[10] Based on a biogenetic standpoint, we can speculate paraherquamide F to arise from the oxidation and pinacol rearrangement of preparaherquamide, followed by oxidation, prenylation, and cycloaddition. Paraherquamides G and E can both arise from paraherquamide F through two different oxidations, yielding a hydroxyl group in paraherquamide G and a dioxene in paraherquamide E. From here, paraherquamide A can be achieved, exhibiting both newly biosynthesized functional groups.[56, 58-61]

The total synthesis of paraherquamide A has been achieved,[62-67] as well as efforts towards the total synthesis of paraherquamides E and F.[47, 68] Paraherquamide A is not only structurally attractive, but is also on the market to treat parasites in sheep.[69] This biological activity, alongside that of many other metabolites, helped this family of natural products receive further attention from scientists.

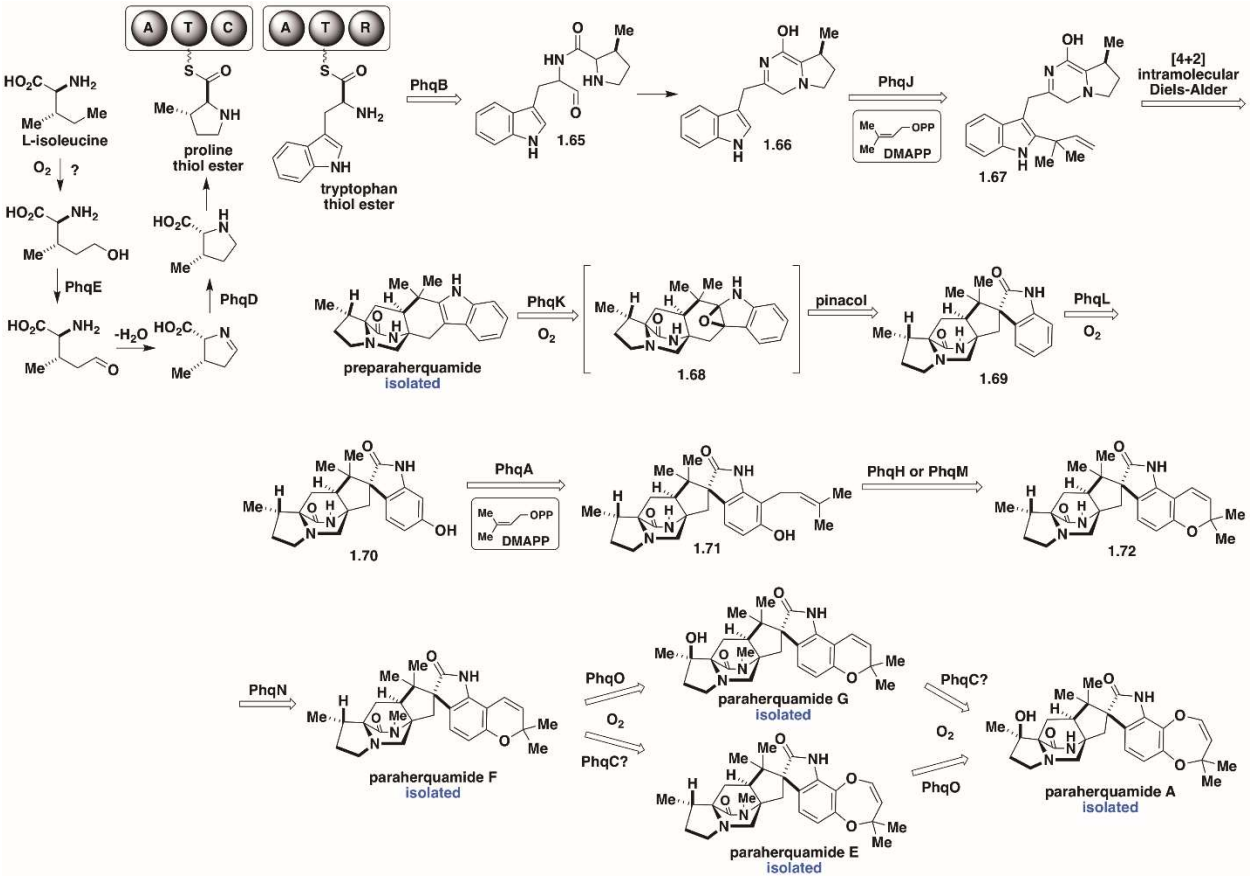


*Figure 1.17*. Earlier proposed biosynthesis of the Paraherquamides.

### *iii. Brevianamides.*

Being a member of the dioxopiperazine family and found in *Penicillium brevicompactum,* the brevianamides are an interesting family of natural products among this class of prenylated indole alkaloids. Some of these metabolites possess a unique spiroindoxyl moiety and the brevianamides are the only metabolites among this class of prenylated indole alkaloids that have this functionality. Brevianamide A was first discovered in 1969 by Birch and Wright[70] and brevianamides B and F were discovered shortly after.[71-72] It was after this discovery, alongside the isolation of antipodal metabolites from *Aspergillus,* that Birch and Wright first theorized the intramolecular Diels-Alder reaction through an achiral azadiene intermediate for the formation of the characteristic bicyclo core found among these metabolites.[71-74]

Incorporation studies show brevianamide A to arise from brevianamide F,[75] likely through that of the presumed IMDA.[74] Brevianamides A and B possess the aforementioned indoxyl unit, which is speculated to arise from the oxidation of presumed IMDA products **1.73** and the pinacol rearrangement of hydroxyindolines **1.74** and **1.75**.[76] At this point in time, biosynthetic studies of the brevianamides remain in need of further investigation.

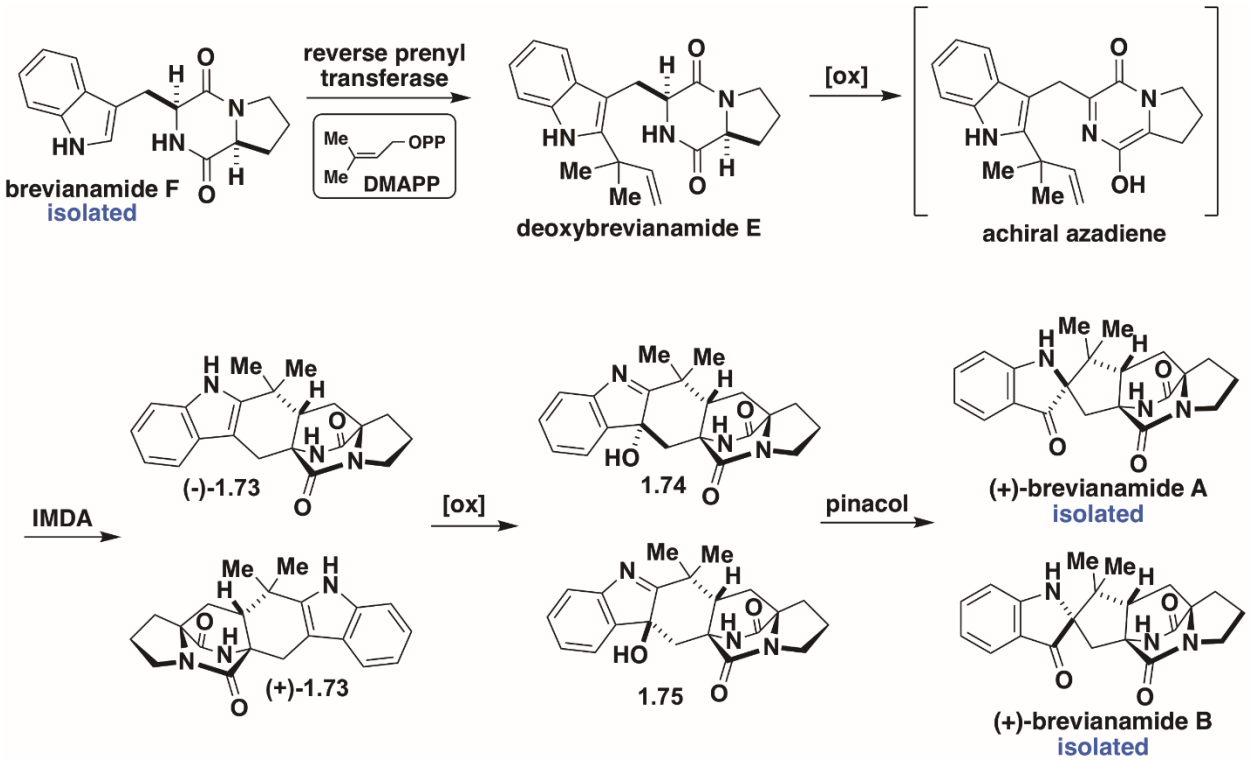


*Figure 1.18.* Earlier proposed biosynthesis of the brevianamides.

## V. Biomimetic Total Syntheses of Prenylated Indole Alkaloids in the *Malbranchea* and *Penicillium* genera

### *i. Malbrancheamides.*

The first-generation total synthesis of premalbrancheamide was reported by Williams *et. al.* in 2008 for $^{13}C$ labelling studies.[51] $^{13}C$-labelled premalbrancheamide was accessed from HATU coupling of Boc-protected tryptophan **1.76** and ethyl ester proline **1.77**, followed by deprotection

and cyclization to produce diketopiperazine **1.79**. Treatment with base allows for tautomerization to form the reactive achiral azadiene that subsequentially undergoes 1,4-cycloaddition to form a 2:1 ratio of syn:anti- diastereomers. Final conversion to premalbrancheamide requires selective amide reduction of the syn- diastereomer (Figure 1.19).

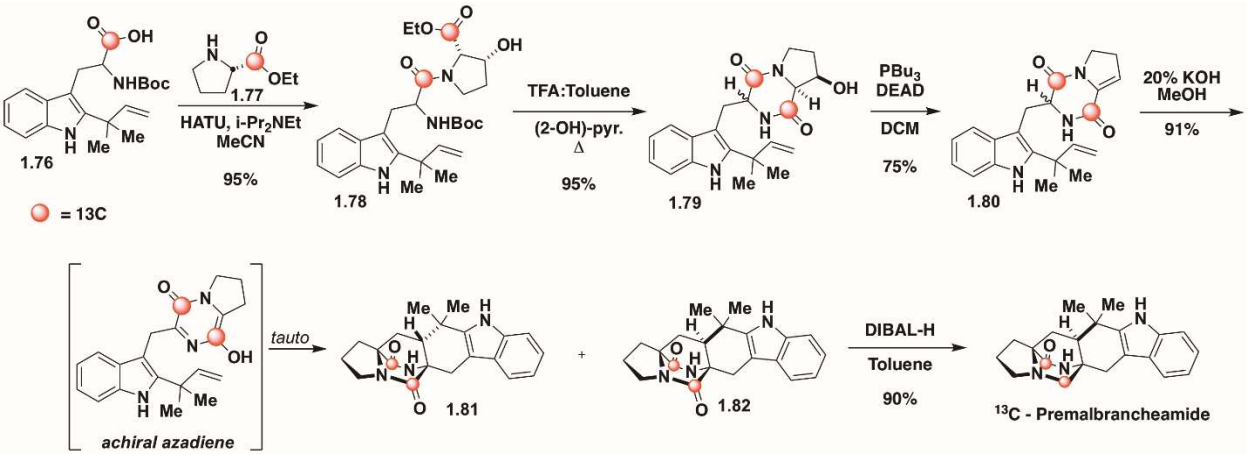


*Figure 1.19.* First generation total synthesis of premalbrancheamide for $^{13}$C-labeling studies.

The total synthesis of malbrancheamide and malbrancheamide B converge on mono- or di-chloro substituted indole **1.83** and proceed forward in parallel.[77] Chlorination and reverse prenylation of indole **1.83** yields prenylated indole **1.84**. Tryptophan **1.85** is formed through the gramine intermediate, followed by Somei-Kametani type coupling and hydrolysis. Reduction of the ester, followed by peptide coupling with HATU yields dipeptide **1.86**. Deprotection of the Boc group allows for cyclization, then Mitsunobu conditions forms enamine diketopiperazine **1.87**. Tautomerization of the diketopiperazine moiety under basic conditions allows for the spontaneous IMDA reaction from the reactive achiral azadiene intermediate. Selective reduction of the tertiary amide in **1.90** yields natural metabolites malbrancheamide and malbrancheamide B (Figure 2.10).

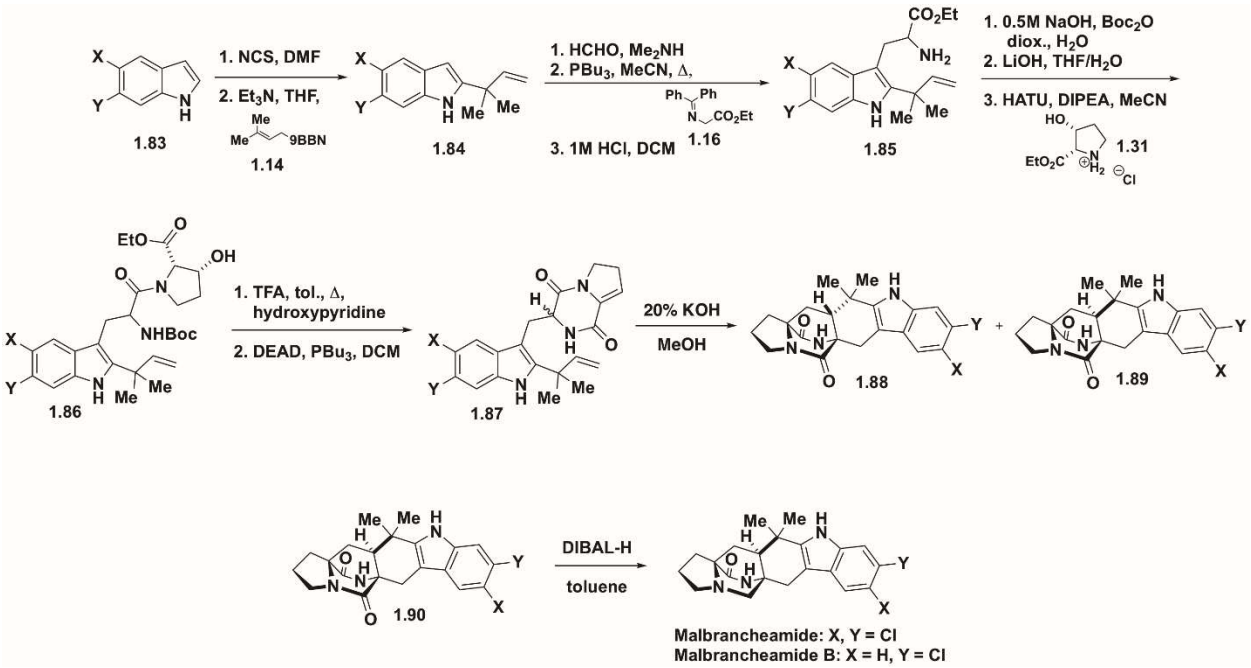


*Figure 1.20.* Total synthesis of the Malbrancheamides.

### *ii. Brevianamides.*

Since the enzymatic intramolecular diels-alder reaction was theorized by Birch and Wright around 1970, many biomimetic studies of these metabolites have been carried out.[78-80] With this, we have been able to complete the synthesis of brevianamide B.[81] Formation of the lactim ether in **1.91** from deoxybrevianamide E allows for the IMDA reaction to form the bicyclo core in **1.92** and **1.93**. Treatment with oxidant, *m*CPBA, forms the hydroxyindoline intermediate that is hypothesized in the biosynthesis *(vide supra)*. The pinacol rearrangement to form the indoxyl unit is initiated with base, then the lactim ether is cleaved upon treatment with acid to yield brevianamide B and its diastereomer (Figure1.21).

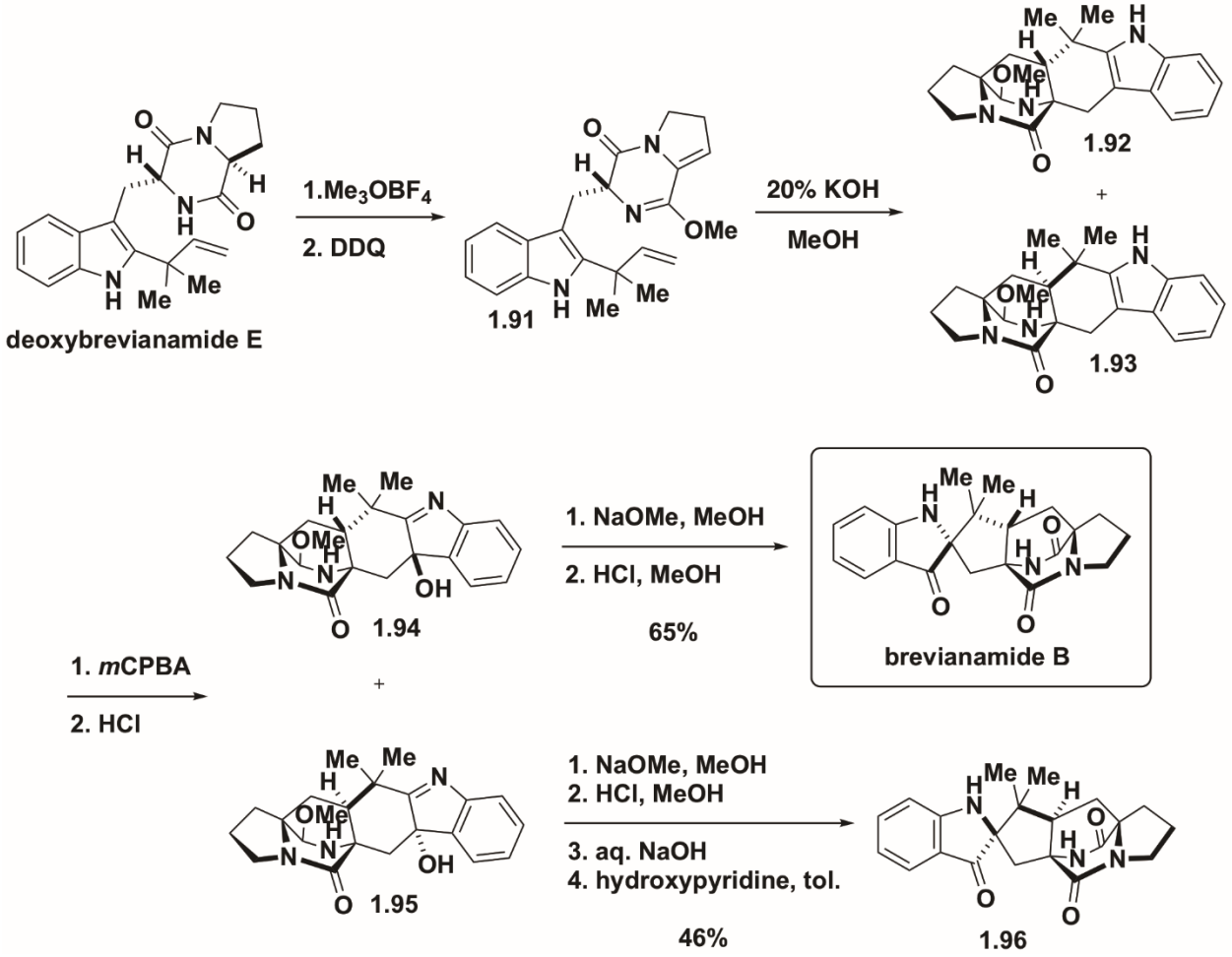


*Figure 1.21.* Total synthesis of brevianamide B.

## VI. Conclusion and Perspective

The biogenesis of the notoamides, paraherquamides, malbrancheamides, brevianamides and their congeners from the prenylated indole alkaloid family of metabolites that have been isolated from the *Aspergillus* and *Penicillium* genera has been demonstrated. The total syntheses of these metabolites are important in guiding our understanding of their biochemical destinies. These total syntheses have greatly adapted throughout the generations, exemplifying the complexity of these molecules and the continued growth of knowledge this project facilitates. Genome-based experiments, feeding studies, and the total synthesis of these natural products are currently ongoing in order to gain a deeper understanding of the role each enzyme plays in the

formation of these captivating natural metabolites. Complete knowledge of the structural and stereochemical homologies and disparities among these compounds continues to motivate the progression in this area of prenylated indole alkaloids.

This overview outlines what we knew about the biogenesis of these metabolites before I began my graduate career. My dissertation work has contributed to the complete elucidation of the malbrancheamide pathway, the development of a deeper understanding of the stereochemistry that arises from the pinacol reaction, and the unprecedented opening of the Diels-Alder core that is represented in a new class of metabolites *(vide infra)*, and most notably understanding the intramolecular Diels-alder construction of the bicyclo core of the syn-metabolites. The work we do facilitates the discovery of new enzymes and the characterization of their mechanistic roles. This aids in the development of new tools for drug discovery which is incredibly important to the pharmaceutical industry and ultimately, the well-being of others.

# Chapter 2: Diels-Alderases in Nature[2]

## I. Introduction

Eight examples of biosynthetic pathways wherein a natural enzyme has been identified and claimed to function as a catalyst for the [4+2] cycloaddition reaction, namely, Diels-Alderase, are briefly reviewed. These are discussed in the context of the mechanistic challenges associated with the technical difficulty of proving that the net formal [4+2] cycloaddition under study, indeed proceeds through a synchronous mechanism and that the natural protein catalyst deploys the pericyclic transition state required for a Diels-Alder cycloaddition reaction.

Among the family of concerted pericyclic reactions governed and understood by the theoretical underpinnings of the conservation of orbital symmetry rules advanced by Woodward and Hoffmann, the [4 + 2] cycloaddition reaction, namely the Diels-Alder reaction, is among one of the most useful and widely studied reactions in synthetic organic chemistry. A vast array of publications concerning the synthetic utility, mechanism, catalysis and theoretical bases of the Diels-Alder reaction are evident in the literature. An area of particular controversy concerns the fundamental question regarding the existence of natural enzymes that have evolved to catalyze this tremendously important synthetic construction. Our laboratory published a review of biosynthetic Diels-Alder constructions in 2003 covering primarily secondary metabolites that had been suggested by researchers to arise by potential biosynthetic Diels-Alder constructions, both enzyme-catalyzed and non-enzyme-catalyzed.[5, 83] Herein, we survey and provide a contextual perspective of the publications claiming to have identified biosynthetic genes coding for the

[2]This chapter is published in part or in full in the *Journal of Organic Chemistry.*[82]

expression of natural enzymes that catalyze the Diels-Alder reaction in the formation of primary or secondary metabolites.

## II. Diels Alder Reaction Mechanism

The mechanistic argument about whether the Diels-Alder reaction proceeds *via* a concerted or stepwise mechanism dates back to studies carried out by Woodward *et. al.* suggesting a synchronous concerted transition state.[84] Early theoretical calculations of kinetic isotope effects and reaction rates were found to not be conclusive,[85] and the mechanism of the [4+2] cycloaddition reaction has been extensively studied experimentally and theoretically by numerous researchers. Figure 1 represents the four transition state (TS) structures through which the net redox-neutral [4+2] cycloaddition may be envisioned to proceed.

Based on earlier calculations conducted with lower levels of theory by Dewar *et. al*.,[85-87] the Diels-Alder reaction has been rationalized to proceed through a biradical intermediate suggesting that multi-bond reactions cannot proceed *via* a synchronous transition state.[88] This theory quickly became discredited as Houk *et. al*. showed that geometries are more sensitive to electron correlation than to the basis set as it exceeds 3-21G.[89] Further investigations by Houk *et. al.* based on Becke3LYP/6-31G* calculations suggested the concerted transition state is lower in energy than the biradical transition state in the retro-Diels-Alder reaction of norbornene[90] while highly substituted dienes were found to favor a stepwise mechanism.[91]

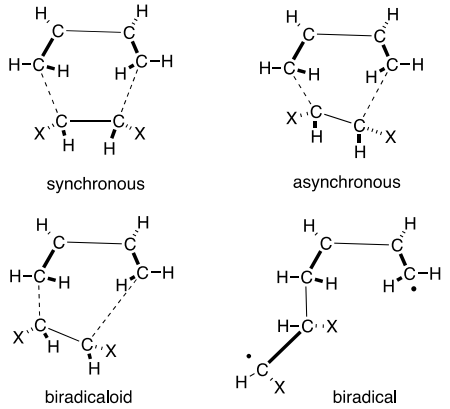


*Figure 1.* Possible Transition Structures in the Diels-Alder reaction

### *i. The [4+2] Cycloaddition Reaction with Symmetrical Addends*

The simplest or "parent" Diels-Alder reaction, is the reaction of 1,3-butadiene with ethylene to form cyclohexene (Figure 2). Early high-level *ab initio* and RH calculations by Burke *et. al.* and Townshend *et. al.* predicted a symmetrical transition state, with perfect synchronicity of formation of the two new C-C bonds.[92-93] Using the highest level of theory (STO-3G and 4-31G basis sets at CAS1 and CAS2 level) at the time, *ab initio* calculations by Bernardi *et. al.* suggest a synchronous transition state for the parent DA reaction.[94] While the basis sets for the MC-SCF study was limited, Becke3LP and CASSCF calculations at the higher 6-31G* level of theory and CASSCF calculations at the STO-3G level of theory predict a synchronous transition structure for the reaction of ethylene with butadiene (Figure 2).[89, 94] The calculated transition structure for the reaction of ethylene with butadiene was favored over a stepwise mechanism by 5 kcal/mol in calculations by Houk *et. al.*[89] Secondary kinetic isotope effects interrogated by Gajewski *et. al.*, suggest the reaction of nearly symmetrical dienes and dienophiles is nearly synchronous.[95] These 'nearly synchronous' addends refer to alkyl substituents, none of which have significant electronic activating or deactivating effects.

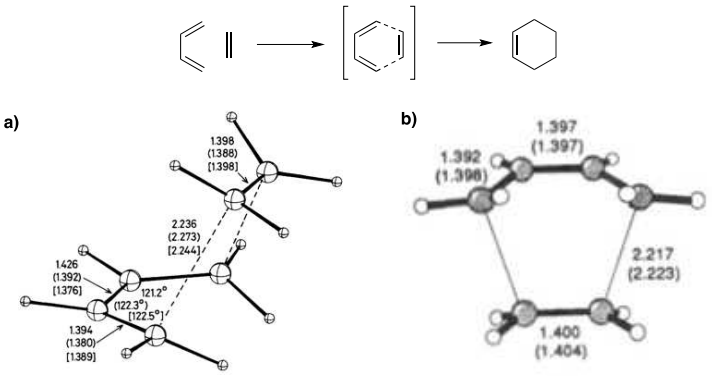


*Figure 2.* Parent Diels-Alder Reaction. Bond lengths in Angstroms. a) CASSCF/STO-3G calculated transition structures from Bernardi *et. al.* 1985. CAS2 and CAS1 are in parentheses and lower-level 4-31G basis set calculations are in brackets. b) CASSCF/STO-3G calculated transition structures by Houk et. al. 1993.

### *ii. Diels-Alder Reaction with Unsymmetrical Addends*

The first *ab initio* calculations and semiemperical studies on a reaction of 1,3-butadiene with an unsymmetrical dienophile were performed by Houk *et. al.* on the reaction of acrolein and 1,3-butadiene.[96] *Ab initio* quantum mechanical calculations at the 3-21G basis set suggests an asynchronous TS (Figure 3).[96]

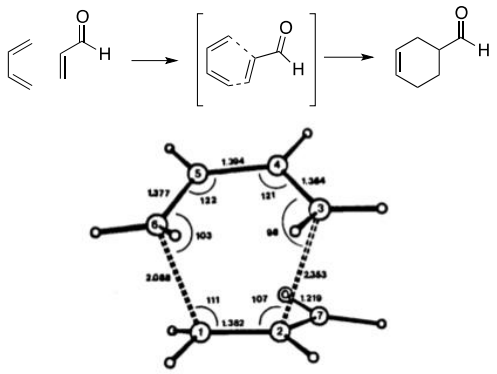


*Figure 3.* Orbital calculations for the asymmetric endo transition structure in the reaction of acrolein with butadiene.

These calculations suggest that substituents, particularly ones that create an asymmetric diene, create asynchronicity within the transition state. RHF calculations predict one substituent to give a 0.3 Å difference in the bond lengths of the forming new sigma bonds within the

transition state.[96] Orbital calculations are given for the *endo* transition structure as they were found most favorable. While the theoretical underpinnings for *endo* preferences are not clear, secondary orbital overlap interactions (now largely assumed moot based on theoretical work) as well as dipolar, electrostatic and van der Waals forces have been attributed to govern *endo*-selectivity.[96]

Further investigations by Bernardi et al. with MC-SCF studies at the minimal STO-3G level predict that reaction of vinylcylcobutane and 1,3-butadiene undergo a two-step asynchronous (diradicaloid nature) mechanism, suggesting steric effects can significantly increase the amount of asynchronicity.[97] Based on symmetry, McIver has suggested it is highly unlikely that a symmetric transition structure would be relevant.[98-99]

### *iii. Diels-Alder Reactions with Activating Symmetrical Addends*

While recent studies reveal that Diels-Alder reactions with unsymmetrical addends undergo cycloaddition through asynchronous transition states, it was accepted that reactions with symmetrical addends would undergo cycloaddition through synchronous or nearly synchronous transition states.[85, 100] Singleton *et. al.,* was interested if this would apply to doubly activated dienophiles,[100] due to the observation of attenuated activation by a second activating group.[85, 101] Reaction of 1,3-butadiene with bis(boryl)-acetylene is predicted by density functional theory to undergo cycloaddition through a highly unsymmetrical transition state.[100] Becke3LYP calculations with a 6-31G* basis set predict the symmetrical structure, forced $C_s$ symmetry, to be 6.5 kcal/mol higher in energy than the unsymmetrical transition structure.[100] Due to the size of the boron groups and the favorable HOMO-LUMO overlap of the first boryl group with the $\pi$-system of 1,3-butadiene, further investigation with other activating groups was found necessary

and the results somewhat surprising.[100] Becke3LYP/6-31G* theoretical calculations predicted unsymmetrical and nearly symmetrical transition states for the reaction of acetylenedicarboxylate with isoprene (Figure 4)[100] and an unsymmetrical transition state with cyclopentadiene.[102]

Experimental kinetic isotope effects support asynchronous character as well as theoretical kinetic isotope effects for the reaction of acetylene dicarboxylate with isoprene.[100, 103] The asynchronous character of the symmetrical reaction can be explained by the difference in activation by the two activating groups. Stronger activation by the first group over that of the second group accounts for the asynchronous nature of the transition state.

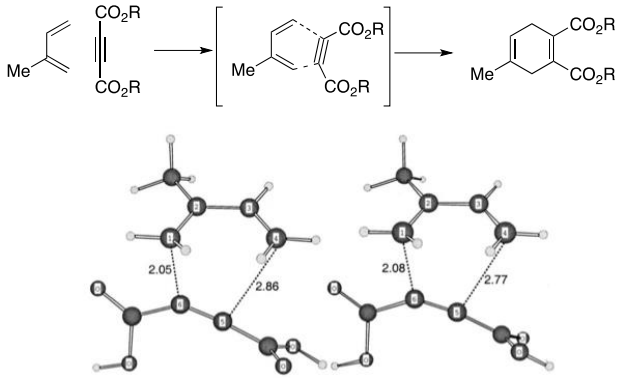


*Figure 4.* Becke3LYP/6-31G* calculations for the asynchronous endo and exo transition structures for the reaction of acetylene dicarboxylic acid with isoprene by Singleton *et. al.* 2001.

Becke3LYP/6-31G* calculations for the reaction with the highly reactive parent triazolinedione (TAD) represents a highly unsymmetrical transition state being favored by 1.1 kcal/mol by Singleton *et. al.* (Figure 5)[100] and 1.0 kcal/mol by Houk *et. al.*[91] over the second-order saddle point.

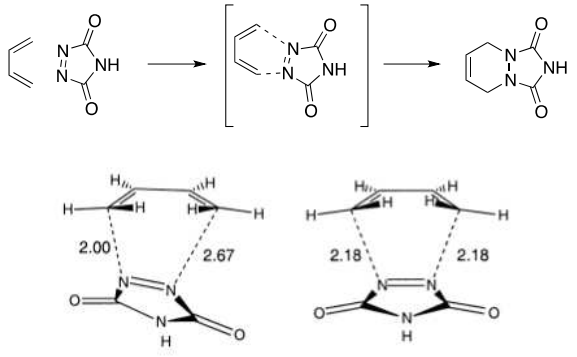


*Figure 5.* Becke3LYP/6-31G* calculated asynchronous and forced Cs symmetry saddle point synchronous transition structures for the reaction of TAD with 1,3-butadiene by Singleton et. al. 2001. Asynchronous TS 1.1 kcal/mol lower in energy than synchronous TS.

While Houk *et. al.* found an alternative stepwise diradicaloid mechanism for the reaction of TAD with *tert*-butyl butadiene 3 kcal/mol lower in energy[91] than the concerted transition state, Singleton et al. suggests the reaction can undergo a stepwise or concerted asynchronous transition structure.[100] Calculated kinetic isotope effects of phenyltriazolinedione (PTAD) suggest very little asynchronicity due to the closeness in experimental proton KIE. Theoretical calculations suggest a different interpretation. Beck3LYP/6-31G* calculations suggest a highly asynchronous TS (Figure 6) while predicted KIEs follow suit. The concern remains if a symmetrical transition structure can account for the observed kinetic isotope effects. Fortunately, calculated isotope effects of the synchronous transition structure are symmetrical and do not agree with the experimental values. Therefore, due to agreement of theoretical isotope effects with the highly unsymmetrical Becke3LYP/6-31G* calculation transition state, reaction of PTAD with butadiene supports highly asynchronous mechanisms and asymmetrical transition states.[100]

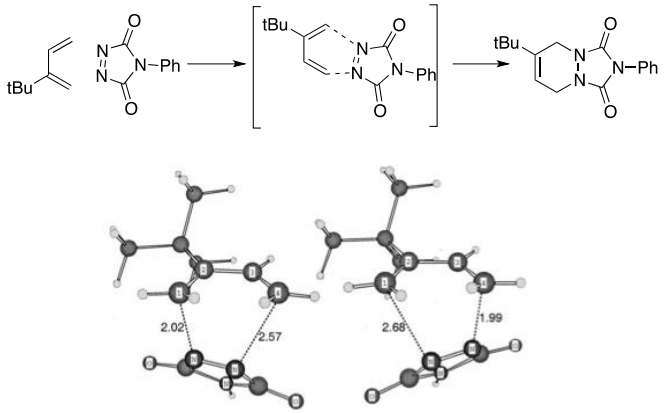


*Figure 6.* Becke3LYP/6-31G* calculated asynchronous *endo*- and *exo*- transition structures for the reaction of PTAD with *tert*-butyl-butadiene.

It can be concluded that while there has been a lot of attention towards establishing a specific reaction mechanism for the Diels-Alder reaction, many questions still remain. Theoretical evidence suggests that symmetrical substrates undergo cycloaddition *via* a concerted transition state. Determination of the synchronicity *versus* asynchronicity of the transition state seems to be highly substituent dependent. The presence of activating groups, which is most common in the putative natural substrates to be discussed below, creates intrinsic asymmetry and attendant asynchronicity within the transition structure. It should also be appreciated that the concertedness of a putative Diels-Alder reaction, whether it be a synthetic laboratory system or a putatively enzyme-catalyzed or enzyme-mediated system, lie on a continuum with symmetrical and concerted on one end to highly asynchronous and non-concerted on the other.

## III. Diels-Alderases

The possible involvement of Diels-Alder reactions in biosynthesis has been an area of intense interest and attempts at identifying enzymes that might function as catalysts for the Diels-Alder reaction has been an active area of research since the late 1970's.[104] While numerous examples of non-enzyme-catalyzed biosynthetic Diels-Alder constructions are evident in the literature,[5] the

question of evolutionary selection pressure leading to the creation of enzymes that have specifically evolved to catalyze the [4+2] cycloaddition reaction *via* a true pericyclic transition state have attracted the attention of numerous research groups, particularly in the past twenty years. These will be briefly surveyed herein.

### *i. Solanapyrone Synthase*

Ichihara and coworkers performed feeding studies in *Alternaria solani*, that provided evidence of oxidation of prosolanapyrone **1** to prosolanapyrone **2** (Figure 7), followed by a subsequent [4+2] cycloaddition in the biosynthesis of Solanapyrones A (**4**) and B (**3**),[105] Ichihara *et. al.* isolated a partially purified protein that was named Solanapyrone synthase and were the first to claim the identification of a natural Diels-Alderase.[104]

The enzymatic and non-enzymatic reaction of prosolanapyrone **2** was monitored by HPLC analysis utilizing UV and CD detectors. The reaction did occur without presence of crude enzyme but produced a 3:97 ratio of *exo:endo* adducts; whereas in the presence of the partially purified enzyme, the reaction proceeded, from **1** and **2**, in about a 6:1 *exo*-selective ratio. A control experiment with denatured enzyme was carried out to establish the reactivity of the enzyme. While the reaction does occur non-enzymatically, the enzyme-catalyzed reaction proceeded 4.1 times faster with an increase in enzyme concentration.[104] The question remained on whether the two-step reaction was carried out by one or two enzymes. Further investigations by Oikawa et al. suggest that Solanapyrone synthase is an oxidase that catalyzes the oxidation of **1** to aldehyde **2**, followed by Diels-Alder cylclization in a two-step manner.[106-107] In this instance, conformational restriction of the in situ-generated aldehyde **2**, seems a plausible mechanistic explanation for the differences in *endo:exo*-selectivity between the laboratory and protein-mediated reactions.

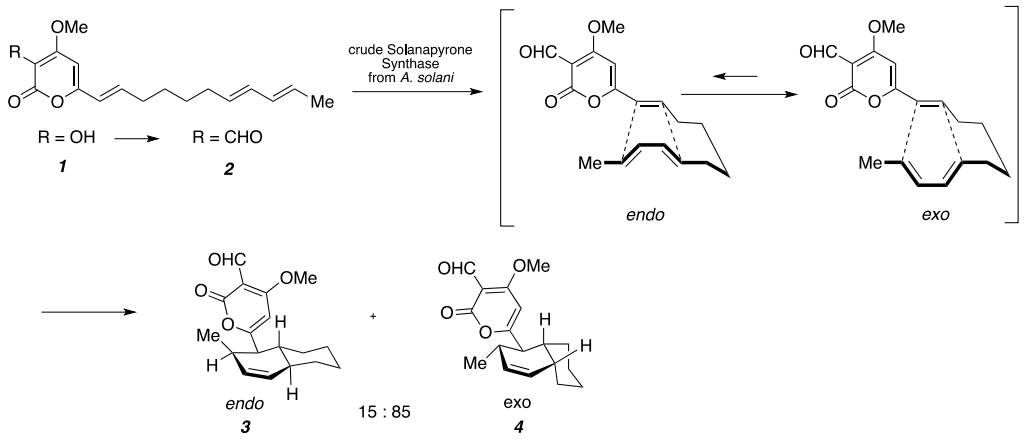


*Figure 7.* Biosynthesis of solanapyrone A (4) and B (3) with solanapyrone synthase as putative cyclase.

More recently, Oikawa and co-workers have succeeded in cloning and functionally expressing solanapyrone synthase in the heterologous host *Aspergillus oryzae*. Using purified enzyme, they were able to confirm that this single enzyme effects the net two-electron oxidation of prosolanapyrone **1** to the *achiral* substrate aldehyde **2**, and mediates the formal [4+2] cycloaddition forming optically pure Solanapyrone.[108] These workers concluded that: *"Expression and purification of SPS confirmed that this single protein catalyzes both the oxidation and the [4+2] cycloaddition, probably acting as a Diels–Alderase."*

The Solanapyrone system therefore also introduces the concept that the "Diels-Alderase" function of Solanapyrone synthase may be an accidental or spontaneous manifestation of producing the reactive aldehyde substrate (**2**) in the conformationally restricted and chiral environment of the active site of this oxidase. In other words, solanapyrone synthase is functionally constituted as an oxidase and the "Diels-Alderase" activity is a subsequent fortuitous side-show to the primary biochemical purpose of the enzyme's major function: which is the oxidation of a primary alcohol to an aldehyde. It is significant that the in situ-generated aldehyde substrate **2** is *achiral*, and the enzymatic product is optically pure clearly revealing that the

enzyme pre-organizes the transition state conformation to proceed in an enantioselective and diastereoselective manner. The high stereoselectivity of the enzyme-mediated process does not provide experimental support for a Diels-Alder transition state and mechanism but seems highly likely based on the corresponding laboratory reaction. The implications of this conceptual framework will be discussed in more detail below.

### *ii. Lovastatin Nonaketide Synthase*

Vederas, Hutchinson and co-workers have studied the fascinating formation of the decalin system (**7**) in the biosynthesis of the HMG CoA-reductase inhibitor Lovastatin (**10**).[109] The lovastatin nonaketide synthase (LNKS) was shown to participate in the synthesis of polyketides,[110] particularly pyrones **5** and **6**[111] and the formation of dihydromonacolin L (**9)** in Figure 8, with the *lovC* protein, in the synthesis of Lovastatin.[109]

To interrogate the involvement of this enzyme in the formation of hexaketide **9**, purified, recombinant enzyme was submitted to reaction with dihydromonacolin L (**9**).[109] UV spectroscopy shows formation of pyrones **5** and **6** in the presence of malonyl CoA, FAD, S-adenosylmethionine and NADPH in buffer.[109] Further investigation with NMR studies revealed formation of **12** and **13** from **11**, non-enzymatically and formation of **12**, **13**, and **14** enzymatically in the presence of LNKS in a 15:15:1 ratio, respectively (Figure 9).[109] The stereochemistry of *endo*-product **13**, corresponds to the natural stereochemistry in the biosynthesis of lovastatin. The authors conclude that the *endo* transition state is a manifestation of van der Waals interactions occurring in the hydrophobic active site of the enzyme.[109]

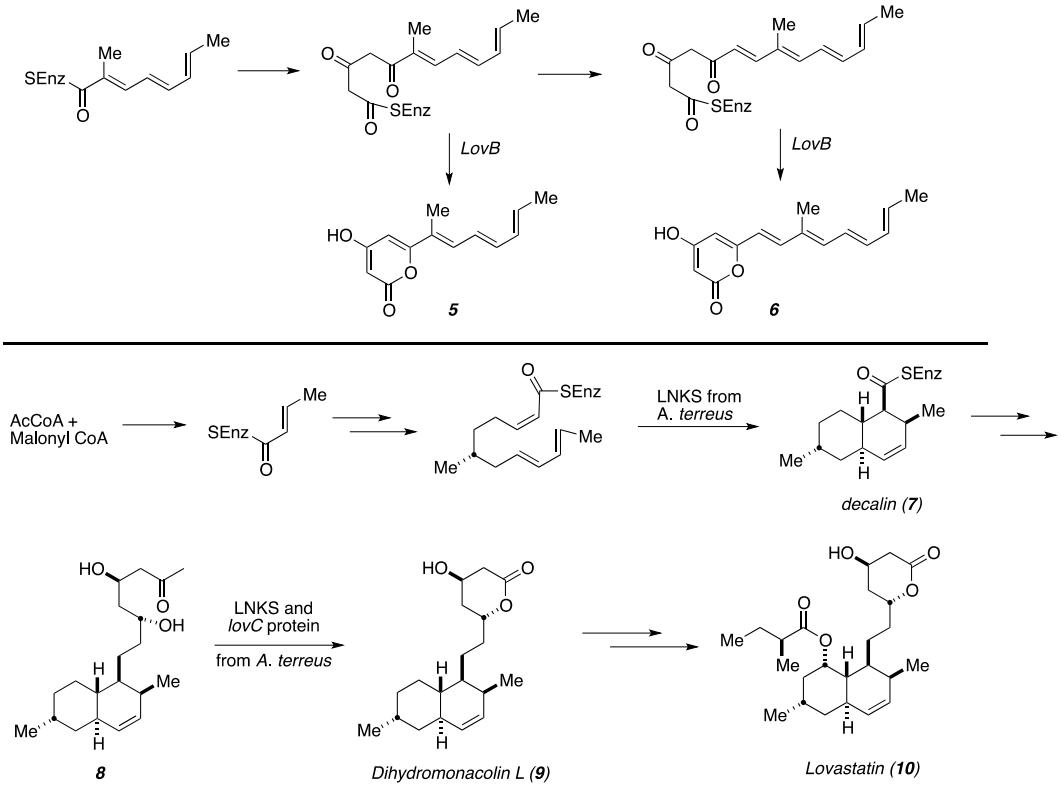


*Figure 8.* Biosynthesis of lovatastatin (**10**) with LNKS as cyclase.

As in virtually all of the systems studied prior to and subsequent to this seminal work, rigorous biophysical evidence corroborating a concerted, pericyclic transition state mechanism for the construction of the decalin ring system in lovastatin biosynthesis has not been secured and alternative step-wise and/or highly asynchronous mechanisms might indeed be operative and await further, deeper experimental interrogation.

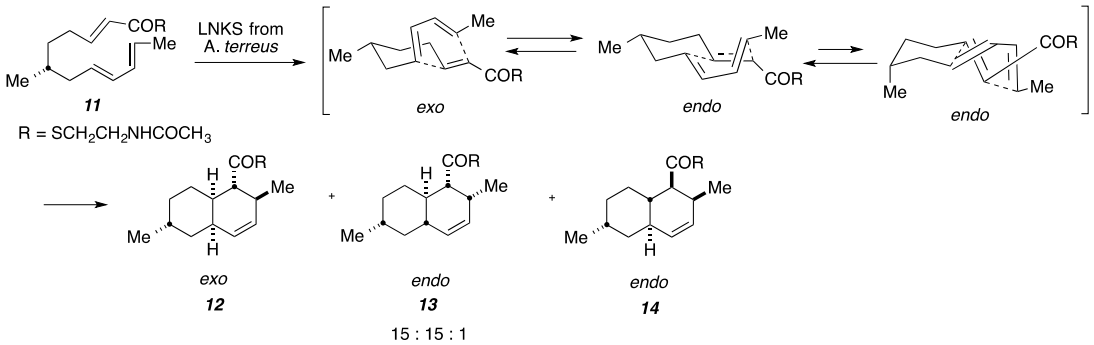


*Figure 9.* Model reaction with LNKS as cyclase in the enzymatic reaction of **11**.

### *iii. Macrophomate Synthase*

The biosynthesis of macrophomate has been the subject of particular controversy and was first proposed by Oikawa, *et. al.,* to proceed *via* an enzyme-catalyzed intermolecular Diels-Alder reaction. The putative Diels-Alderase, macrophomate synthase (MPS) was demonstrated by Oikawa, *et. al.,* to catalyze a multi-step reaction from 2-pyrone (**17**) and oxaloacetate **15** to ultimately furnish macrophomate. These workers postulated that the key transformation proceeded *via* the intermolecular Diels-Alder reaction of enol pyruvate **16** and pyrone **17** to furnish the unstable bicyclo[2.2.2] Diels-Alder adduct **18**.[112] Dehydration of **18** to **20** and decarboxylation with concomitant aromatization through the proposed enzyme-catalyzed Diels-Alder reaction mechanism is illustrated in Figure 10.[112]

The authors speculated that, upon coordination with $Mg^{2+}$, decarboxylation of **15** occurs to form enolpyruvate **16**. Intermolecular Diels-Alder cycloaddition was proposed to furnish the bicyclo[2.2.2] species **18** which, followed by dehydration and decarboxylation furnishes macrophomate. In order to determine the stereochemical outcome of the $Mg^{2+}$-dependent enzymatic cycloadditon proposed, deuterium-labeled oxaloacetate and NMR spectroscopy revealed retention of the deuterium in the final macrophomate product.[112] This revealed the high stereospecificity of the transformation that was ascribed as evidence for a concerted process. While the experimental evidence based on NMR studies is only circumstantial, the authors concluded that the enzymatic reaction proceeded *via* the Diels-Alder route due to the high stereospecificity observed.[112] It should be noted that these studies only revealed that the net process was highly stereospecific and does not conclusively corroborate a concerted or pericyclic mechanism catalyzed by MPS.

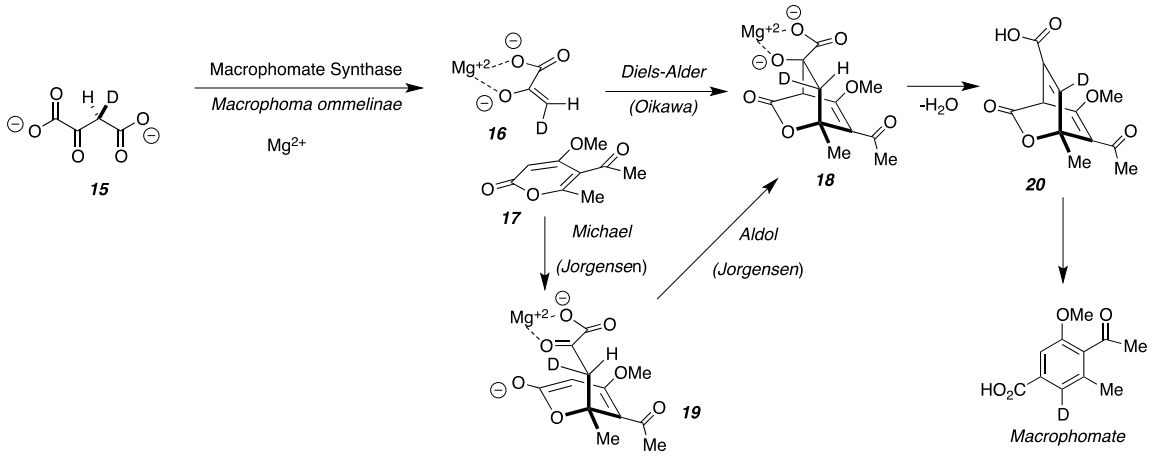


*Figure 10.* Proposed biosynthesis of macrophomate where macrophomate synthase functions as cyclase.

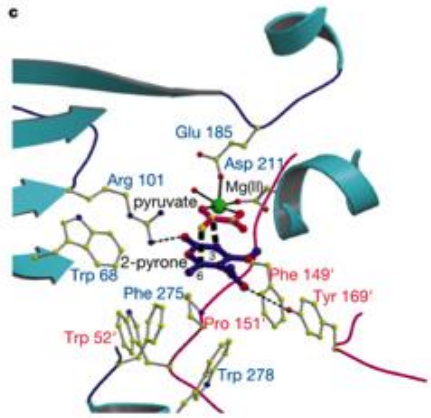


*Figure 11.* Model active site of MPS with binding of 15 and 17 utilizing crystal structure information and proposed transition structure.

Protein X-ray crystallography studies by Oikawa and coworkers provided further insight into the active site of MPS.[113] A binding model was built by Oikawa *et. al.* based on the transition structure of the presumed Diels-Alder cyclization and structural insights from the crystal structure (Figure 11). The carbonyl oxygen of 2-pyrone can hydrogen bond to residue $Arg^{101}$ and the acyl oxygen can hydrogen bond to Tyr 169 which undergoes π-stacking with the $Phe^{149}$ residue, placing residue $Tyr^{169}$ in the correct orientation.[113] Experimental evidence with two

mutants represents the importance of hydrogen-bonding in the active site, supporting evidence for the binding site represented in Figure 11.[113]

Jorgensen and coworkers investigated this reaction from a theoretical perspective and conducted mixed quantum and molecular mechanics (QM/MM) combined with Monte Carlo simulations and free-energy perturbation (FEP) calculations and found a lower energy step-wise reaction pathway involving intermolecular Michael addition through intermediate **19**, followed by intramolecular aldol condensation to provide the same bicyclo[2.2.2]intermediate **18** proposed by the Oikawa group.[114] The Jorgensen investigations revealed that the Diels-Alder TS model is 17.7 and 12.1 kcal/mol less stable than the Michael and aldol TSs in the stepwise route, respectively. Jorgensen states in their paper: *"Therefore, this work indicates that the Michael-aldol mechanism is the route used by MPS to catalyze the second step of the overall transformation, and that the enzyme is not a natural Diels-Alderase, as claimed by Ose and co-workers (Nature 2003, 422, 185-189; Acta Crystallogr. 2004, D60, 1187-1197)."*

Significantly, Hilvert and coworkers subsequently demonstrated that MPS was a very competent aldolase, corroborating the second arm of the Jorgensen Michael-aldol mechanism.[115] Hilvert *et. al.,* demonstrated that MPS is highly homologous to a known aldolase DDG (2-dehydro-3-deoxygalactarate) and concluded that this lends plausibility to the two-step Michael-aldol alternative originally proposed by Jorgensen.[115] This work, taken in context with the penetrating theoretical insights of Jorgensen, reveals that extreme care must be taken when presuming that a putative Diels-Alder transformation, wherein the substrates appear to be structurally viable Diels-Alder substrates, form a product, that ostensibly appears to be the result of a concerted [4+2] cycloaddition, can arise by distinct, step-wise, non-concerted mechanisms

that are not bona fide Diels-Alder constructions mechanistically. However, it is my understanding that the Michael-Aldol reaction pathway was later disproven.[116]

### *iv. Riboflavin Synthase*

Riboflavin synthase of *Escherichia coli* is an enzyme that has been extensively studied that appears to be responsible for multiple functions in the biosynthesis of the essential enzymatic co-factor riboflavin.[117-118] This enzyme catalyzes the fascinating transfer of a four-carbon unit derived from one of the two equivalents of the common substrate, 6,7-dimethyl-8-ribityllumazine (**22**), culminating in the formation of riboflavin and 5-amino-6-ribitylamino-2,4(1H,3H)-pyrimidinedione (**26**). The mechanism proposed by Bacher, *et. al.* is illustrated in Figure 12 and features the key intermolecular Diels-Alder condensation between **22** and the oxidized diene species **23** derived from **22** to form **24** – a substance that these workers have isolated and structurally characterized.

Bacher proposes that the enzyme specifically functions as a Diels-Alderase, but there has been no experimental data published supporting this provocative mechanistic hypothesis. The authors discuss that the electronics of the proposed Diels-Alder substrates favor an inverse-electron-demand [4+2] reaction wherein overlap of the HOMO of the dienophile (**22**) and the LUMO of the diene (**23**). No corresponding laboratory reaction was reported that would have provided additional mechanistic insight.

Access to the purified enzyme provides ample opportunity to study the detailed mechanism of the very interesting heterodimerization of **22** where kinetic isotope effects and double isotope fractionation would be particularly revealing. It is also appreciated that tedious, expensive and

time-consuming experiments are required to conduct such a rigorous mechanistic inquiry; a problem encountered by all workers in this field

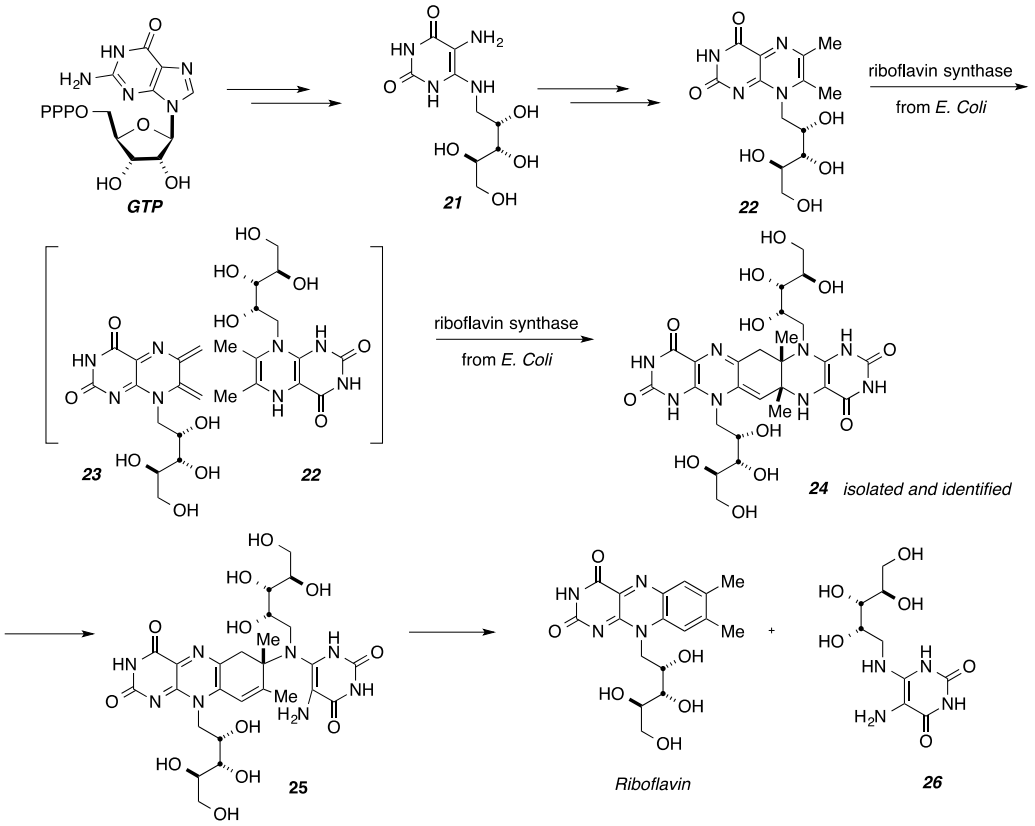


*Figure 12.* Proposed biosynthesis of riboflavin *via* a key [4+2] cycloaddition to provide the isolated and structurally characterized intermediate **24**.

### *v. Spinosyn A Biosynthesis*

The fascinating biosynthesis of Spinosyn A, was recently investigated by Liu et al., and these workers identified the polyketide synthase expressed from the *spnF* gene of *Saccharopolyspora spinosa* and suggested that SpnF was a natural Diels-Alderase that catalyzes a [4+2] cycloaddition in the formation of the cyclohexene ring core of Spinosyn A.[119] The authors suggest that this represents the first example of an enzyme whose sole purpose is to catalyze a Diels-Alder reaction, although the basis for such a claim appears curious in light of earlier claims of Diels-Alderases, such as the lovastatin biosynthesis discussed above. The biosynthetic gene cluster of

*S. spinosyn* for spinosyn A also includes *spnJ, spnL, spnM* which were also initially proposed to code for an enzyme that converts product **27** to **29** (Figure 13).[119]

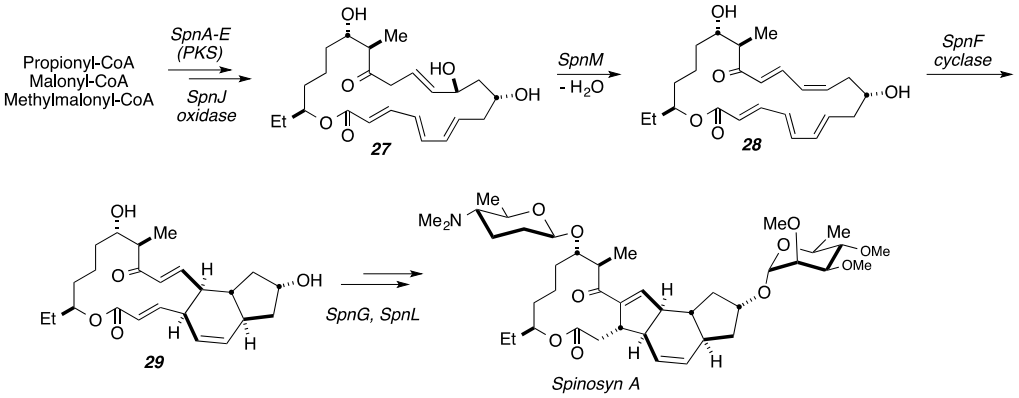


*Figure 13.* Biosynthesis of spinosyn A (24) where PKS has been proposed as the putative cyclase.

To elucidate if the SpnF cyclase was a true Diels-Alderase, conversion of **27** to cyclized product **29** was observed after a two hour incubation period with the *spnM* gene product and monitored by HPLC.[119] Analysis by NMR, mass spectrometry and further investigation by HPLC of the reaction time-course led to the discovery of intermediate **28**, identified by spectral analysis.[119] The presence of the monocyclic macrolactone intermediate represents a possible 2-step process that includes a dehydration step followed by the cycloaddition as shown in Figure 13.[119] To determine if the enzyme expressed by the *spnM* gene catalyzes both the dehydration and cycloaddition steps, dependence of the rate of each step on the concentration of the *spnM*-coded enzyme was determined by HPLC (consumption vs. time).[119] Rate enhancement of the dehydration step was observed with an increase in *SpnM* gene product concentration and the cyclization step was unaffected.[119] While data from Michaelis-Menten kinetics and first order kinetics suggest the cyclization can take place non-enzymatically, the remaining genes from the gene cluster were in turn interrogated. Incubation of SpnF with **22** produced the desired bicyclic species **23** in twenty minutes, which was compared to the two hour non-enzymatic reaction

time.[119] In order to measure the effect of the SpnF enzyme on the rate of cyclization, HPLC was used with a fixed concentration of SpnM with time as a function of SpnF. Michaelis-Menten kinetics established that SpnF coded a polyketide synthase as a potential Diels-Alderase in the catalytic conversion of **22** to **23** with an apparent $k_{cat}$ of 14 +/- 1.6 $min^{-1}$ for an approximated rate enhancement of 500-fold.[119]

Recent X-ray crystal structure elucidation of the enzyme by Liu *et. al.* was used to support the putative mechanism of the *spnF*-coded PKS-catalyzed cyclization.[120] While the enzyme of interest resembles S-adenosylmethionine (SAM)-dependent methyltransferases (SAM MTs), the activity of SAM MTs could give insight to the activity of the stand-alone enzyme. The activity of SAM MTs in these particular cyclization reactions is currently unknown.[120] The authors conclude however, that: *"The mechanisms by which SpnF and SpnL catalyse their respective cyclization reactions are a point of interest. The SpnF-catalysed endo mode syn-addition of an alkenyl to a dienyl functionality seems consistent with a Diels–Alder reaction; however, confirmation of this hypothesis will require demonstrating that the reaction progresses through a single pericyclic transition state such as [**6**]. Therefore, a stepwise [4+2] cycloaddition mechanism, for example, one involving a dipolar intermediate such as [**7**], cannot at present be ruled out."* This comment again gets to the heart of the purely academic argument pervasive in this field regarding the high-resolution details of the synchronicity of the C-C bond-forming step and the exact nature of the transition state.

### *vi. Biosynthesis of Pyrroindomycins*

Biosynthetic studies of the naturally occurring pyrroindomycins, the first naturally occurring spirotetramates, isolated by Ding *et. al.,* suggests that the pentacyclic core is constructed *via* two

distinct, sequential [4+2] cycloadditions.[121-123] Bioinformatic analysis of the previously established biosynthetic gene cluster provided two candidates, *pyrE3* and *pyrI4*.[123] Known functions of enzymes homologous to PyrE3 and PyrI4 suggested that PyrI4 to be responsible for the formation of *spiro*-indole **32**, via dialkydecalin (**31**) construction by PyrE3 (Figure 14).[123]

Deactivation of PyrE3 resulted in the isolation of intermediate **30** while inactive enzyme, PyrE3 and PyrI4, did not lead to the formation of pyrroindomycin A and pyrroindomycin B.[123] Structure elucidation of **30** was confirmed by NMR and mass spectrometry analysis and is consistent with the previously proposed biosynthesis.[123] Further investigation required addition of both purified enzymes, PyrE3 and PyrI4, to intermediate **30** with no additional cofactors.[123] The enzymes collectively converted **30** into **32**, validated by characterization.

Independent function of each enzyme was investigated. Incubation of **30** with PyrE3 resulted in essentially complete conversion into **31**, but no reaction occurred in the presence of PyrI4 alone. ESI-MS analysis and site-directed mutagenic studies were successful in identifying and subsequently determining the dependence of co-factor FAD for PyrE3 activity. It was assumed that FAD influences the geometry of the active site during the PyrE3-mediated cycloaddition which was further supported by ECD spectra analysis of related proteins in the presence and absence of FAD cofactor. Intermediate **31** did not suffer transformation into **32** upon incubation in aqueous media without the presence of PyrI4.[123] While this suggests a non-spontaneous, and specifically enzyme-mediated [4+2] reaction, initial studies revealed a dependence of PyrI4 activity on the dialkyldecalin system represented as intermediate **31**. Steady-state kinetics indicate a moderate efficiency for the enzymatic conversion of **30** into **31** and **31** into **32**. To further confirm the existence of PyrI4 and PyrE3 their crystal structures were recently reported

by Zheng *et. al.*[124-125] The homolog of PyrI4, AbyU, has also recently been isolated and identified as Diels-Alderase that is proposed to occur mechanistically identical to that of PyrI4.[126]

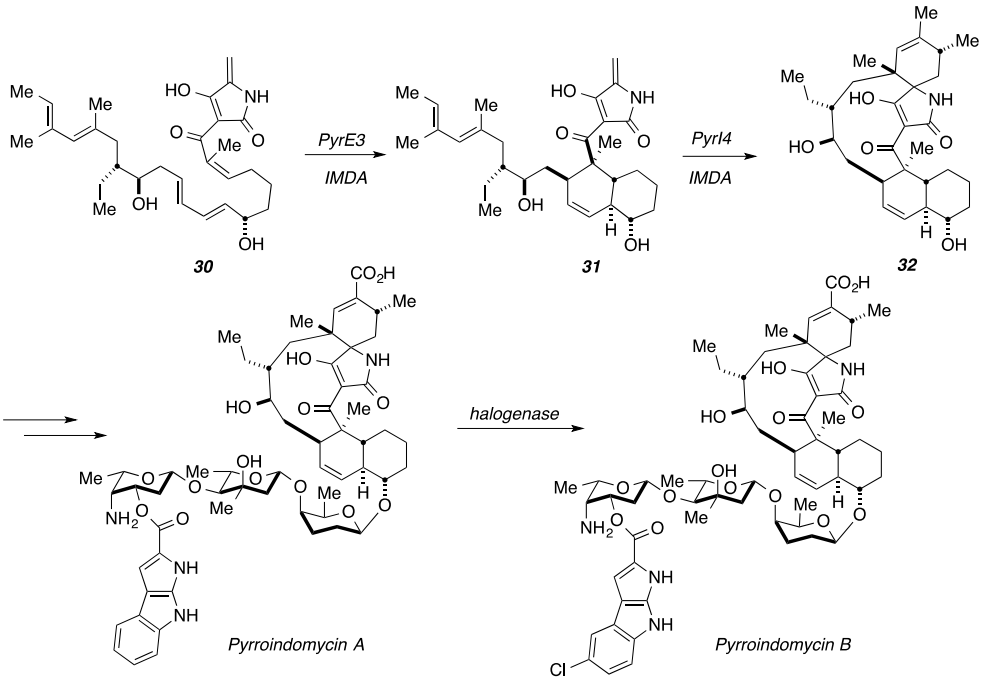


*Figure 14.* Proposed biosynthesis of pyrroindomycins with PyrE3 and PyrI4 as cyclases.

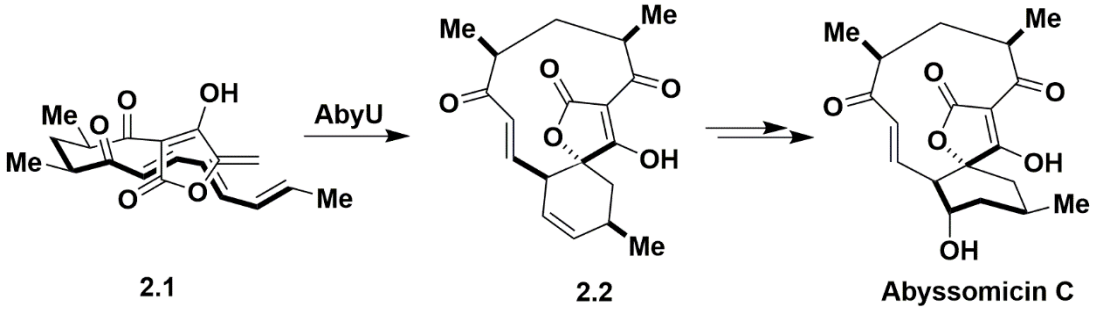


*Figure 15.* Proposed biosynthesis of abyssomicin C with AbyU as cyclase.

### *vii. Biosynthesis of Leporin C*

In the biosynthesis of leporin C, LepI has been identified as the enzyme to catalyze a hetero-Diels-Alder reaction to build the pyran moiety from the alpha, beta unsaturated ring in **2.3** (Figure 16).[127] Recent experimental reports by Tang *et. al.* classifies LepI as a SAM-dependent enzyme that first functions as a stereoselective dehydratase to form the reactive hetero diene that

subsequentially undergoes a spontaneous 4+2 cyclization to produce the natural metabolite. This represents a common theme among these Diels-Alderases where they were designed to perform some other particular function, then by chance undergo spontaneous cyclization within the active site.

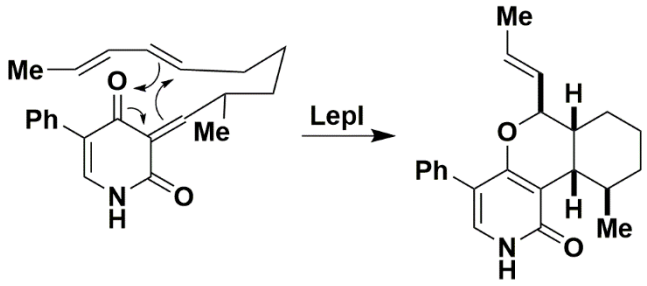


**2.3** **Leporin C**

*Figure 16.* Proposed biosynthesis of leporin C with LepI as cyclase.

***viii.****Thiazolyl Peptide Biosynthesis*

Recent investigations of the incredibly complex thiazolyl peptide biosynthesis by Bowers and co-workers, suggests that a single enzyme, TclM catalyzes the final macrocyclization step that was previously suggested to proceed *via* a [4+2] cycloaddition between dehydroalanine residues (Dha).[128] These workers synthesized Thiocillin **33** to undergo enzymatic reaction with TclM in hopes of forming cycloaddition product **26** (Figure 17).[128]

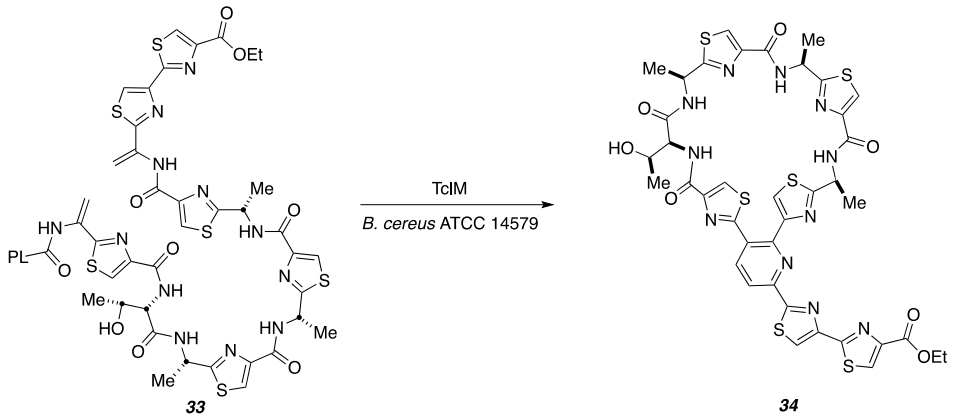


*Figure 17.* Biosynthesis of thiocillin **34** *via* TclM as cyclase.

Substrate **33** was incubated with purified TclM gene for 20 hours and monitored by high-resolution QTOF LC/MS and UV-vis. Overtime, a new absorption peak was observed as well as full consumption of the peak indicative of substrate **33**. The new peak was potentially **34** as the wavelength observed is consistent with that of thiazolyl peptides with the same trisubstituted pyridine core. Further investigation by NMR spectroscopy shows evidence of aromatic protons from the pyridine ring and observation by LC/MS shows an m/z that matches the desired product as well as appropriate fragmentation patterns.[128]

While it is evident that TclM catalyzes the formation of the tri-substituted core present in product **34**, the nature of the mechanism remains unclear. Figure 18 represents the proposed [4+2] cycloaddition mechanism for the net transformation of **33** to **34**.[128] The authors were careful to designate this assembly as a "formal [4+2] cycloaddition" and did not over-state the case for Tc1M necessarily being a true Diels-Alderase. The aromatization to the final pyridine ring is also apparently conducted by Tc1M as putative intermediates corresponding to the intermediate species **36** and **37** were not detectable. Here again, access to the recombinant enzyme provides for the opportunity to study the mechanism of this fascinating macrocyclic assembly at high resolution that might involve the intermediacy of a biosynthetic Diels-Alder construction.

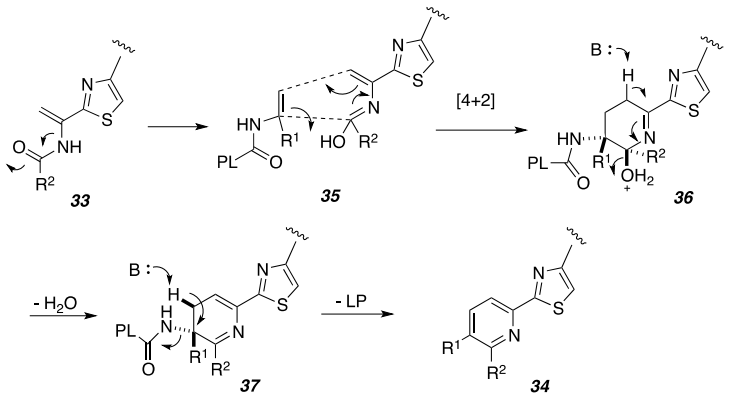


*Figure 18.* Proposed mechanism for the transformation of **25** to **26** in presence of TclM.

### *ix. Stephacidin-Notoamide and Paraherquamide Biosynthesis*

Our laboratories have been studying the biosynthesis of a large family of fungal alkaloids including the dioxopiperazine-containing stephacidins, notoamides, brevianamides, and the related monooxopiperazine alkaloids including the paraherquamides, marcfortines, malbrancheamides and asperparalines for some time.[129-133] All of these alkaloids contain a bicyclo[2.2.2]diazaoctane core that is the result of the net oxidative cyclization of a reverse-isoprene moiety to the two $\alpha$-carbons of the amino acid units, typically derived from tryptophan and proline or a proline analog. Biomimetic laboratory intramolecular Diels-Alder reactions, which occur at ambient temperature and below in aqueous media, provide indirect support for the putative biosynthetic constructions.

What is even more interesting in the stephacidin-notoamide biosynthesis, is the observation that two distinct pairs of terrestrial and marine-derived orthologous *Aspergillus* sp. produce opposite enantiomers of stephacidin A and notoamide B (100% er). We have postulated that the key enantiodivergent step is also the formal [4+2] cycloaddition step that all experimental evidence indicates arises through a common *achiral* azadiene (**38**) as shown in Figure 19.

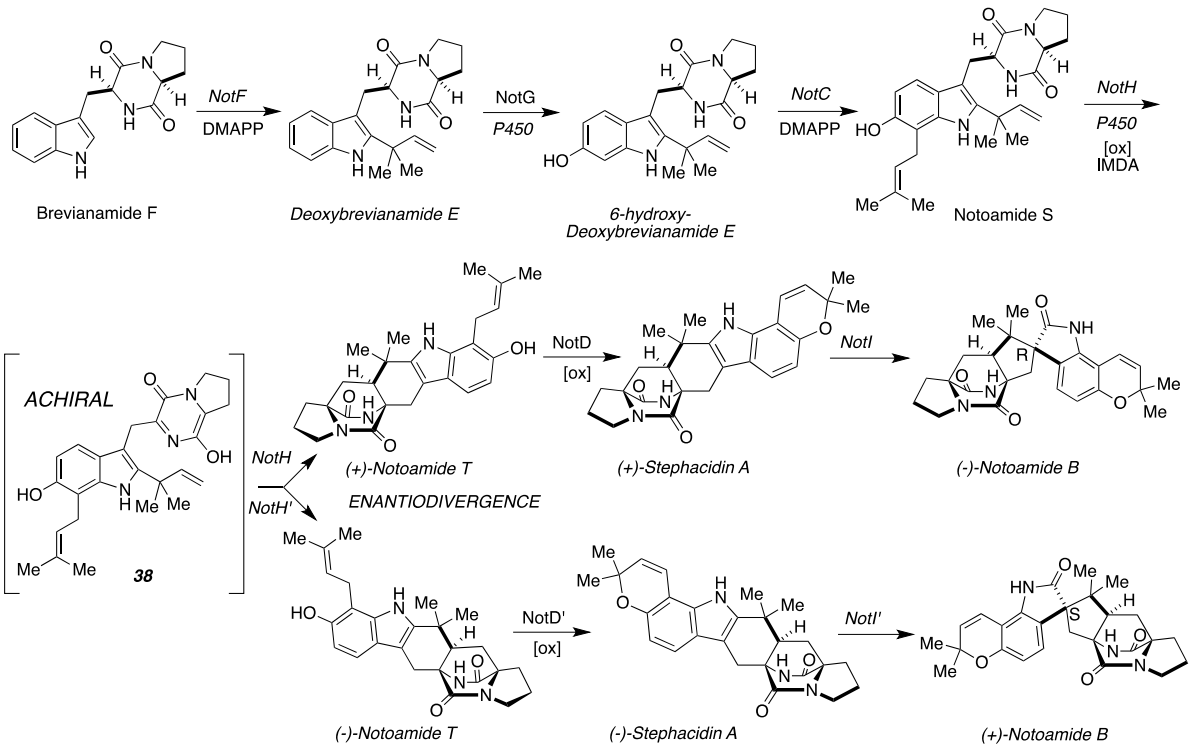


*Figure 19.* Proposed enantio-divergent biogenesis of the stephacidins and notoamides through a formal [4+2] cycloaddition.

Whole genome sequencing and bioinformatics analyses of the identified gene clusters has revealed that the conversion of notoamide S into notoamide T, appears to be conducted by a cytochrome P450 NotH.[42] That the putative intermediate IMDA substrate **38** is *achiral*, and that the final natural products are optically pure, strongly implicates pre-organization of the isoprene moiety relative to the azadiene in the active site of the enzyme. It is also noteworthy that the identical laboratory Diels-Alder reaction has been successfully conducted producing racemic notoamide T in a 2.4:1 *syn:anti*-diasteromeric ratio.

We have recently determined that the biosynthesis of the monooxopiperazine alkaloids (such as paraherquamide and malbrancheamide) and the dioxopiperazine alkaloids (such as stephacidin and notoamide B) arise by distinct pathways, but appear to converge on the formation of an azadiene intermediate (**41**) that suffers a net formal [4+2] cycloaddition to form

the bicyclo[2.2.2]diazaoctane ring system, albeit in two distinct oxidation states (Figure 20, Z = O or $H_2$). In both instances, we have acknowledged that the primary function of the enzyme responsible for fashioning the bicyclo[2.2.2]diazaoctane ring systems, are oxidation (for the diooxopiperazines) and possibly prenyl transfer or reduction for the monooxopiperazines, and are not specifically cyclases. Attempts to functionally express *NotH* in a heterologous host have not been successful to date and constitute a major focus of our current efforts. In both families of alkaloids, a reactive intermediate is formed in the chiral and conformationally restricted environment of the enzyme active site which presumably pre-organizes the conformation of the azadiene relative to the isoprene moiety resulting in highly enantioselective and diastereoselective cycloadditions. Here as in other systems discussed in this article, the cycloaddition reaction appears to be a fortuitous “side-reaction” leading to new molecular complexity.

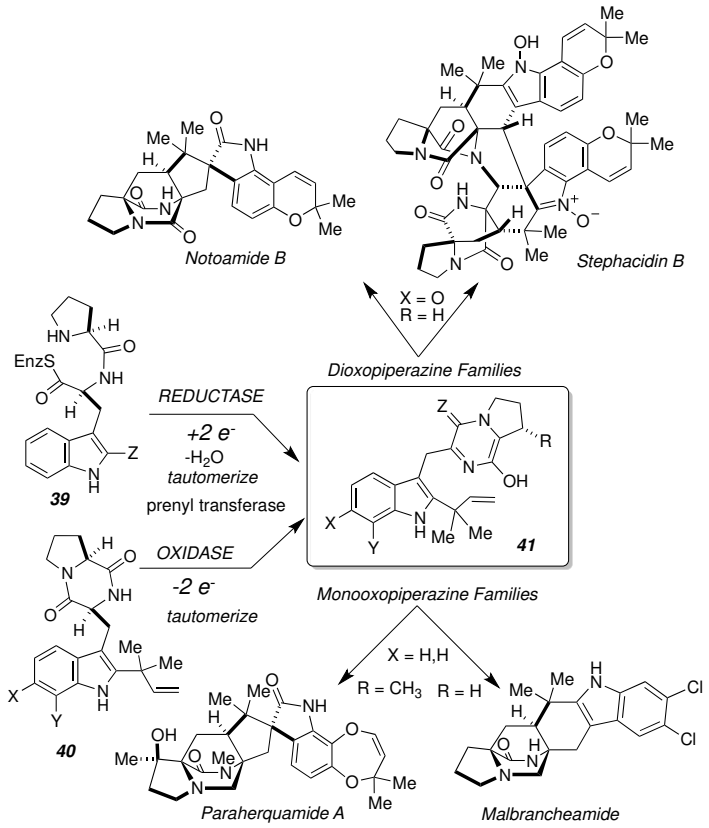


*Figure 20.* Unified biosynthesis of the monooxopiperazine and dioxopiperazine families of alkaloids containing a bicyclo[2.2.2]diazaoctane ring system.

## IV. Conclusion

There are at least eight biosynthetic systems to date that have been identified to contain natural enzymes claimed to function as the key cyclase in biosynthetic transformations that appear to constitute biosynthetic formal [4+2] cycloadditions or Diels-Alder-type constructions. Despite the increasing sophistication of mechanistic tools – both theoretical and experimental- to study the concertedness of putative enzyme-mediated and/or specifically enzyme-catalyzed biosynthetic Diels-Alder constructions, much remains to be investigated and rigorous, corroborating biophysical evidence remains elusive.

The fundamental mechanistic conundrum for Diels-Alderases, is the issue of turnover. Virtually all known enzymatic reactions lower the activation energy to affect rate acceleration by

stabilizing the structure, charge and geometry of the developing transition state, which does not typically structurally resemble the product. For the Diels-Alder reaction however, the transition state and the product are highly structurally homologous which would manifest as product inhibition begging the question of how turnover is achieved. This very problem of turnover was evident in the work of Schultz and Hilvert who designed and generated catalytic antibodies for the Diels-Alder reaction using transition state mimics as haptens.[134-140]

In the case of systems where the putative Diels-Alderase is an enzyme that evolved to perform a distinct biochemical transformation, such as oxidation, generating the reactive substrate in the chiral environment of the active site, turnover is presumably not affected by product inhibition. In such systems, such as the Solanapyrone and Stephacidin biosyntheses discussed above, conformational restriction of the reactive substrate as it generated in the active site, is pre-disposed to undergo the subsequent "side-reaction" of cycloaddition. The entropic benefit of conformational restriction, certainly must contribute to increase the rate of the cycloaddition step relative to the laboratory reaction and would also plausibly impact stereoselectivity relative to the laboratory reaction. In fact, the relative changes in stereoselectivity between the cycloadition reaction in the presence and absence of enzyme has been used, perhaps incorrectly, as "experimental evidence" to support the pericyclic mechanism of these enzyme-mediated transformations. Extreme care should be exercised in this regard when comparing the laboratory reaction (where feasible) to the protein-mediated transformation. Differences in stereoselectivity only reveals that the protein-mediated reaction has a distinct stereoselectivity and does not penetrate the subtle mechanistic details of the protein-mediated reaction.

These authors remain circumspect as to whether a true Diels-Alderase exists that evolved to specifically catalyze the Diels-Alder reaction through the concerted, synchronous pericyclic transition state required. Yet this becomes essentially a philosophical argument as the experimental rigor required to prove that a pericyclic transition state is operative to the exclusion of alternative stepwise, non-synchronous or highly asynchronous mechanisms will inevitably loom. In particular, non-enzymatic, laboratory Diels-Alder reactions where the spectrum of substrates, which can undergo cycloaddition through a strictly concerted, synchronous mechanism controlled by orbital symmetry considerations, typically require symmetrical substrates, rarely found in natural products studied to date in this context. The polyketide synthases identified in the Lovastatin and Spinosyn biosyntheses, appear to constitute enzymes identified to catalyze a formal [4+2] cycloaddition reaction as their sole function.[47] Chemists have been irresistibly drawn to the biosynthetic Diels-Alder construction for the allure of penetrating how Nature has been able to exploit so many chemical reactions familiar in synthetic chemistry to assemble molecular complexity and molecular diversity in primary metabolites and especially secondary metabolites. That Nature might have "accidentally" stumbled upon the Diels-Alder reaction or, more precisely based on the current body of experimental evidence, formal [4+2] cycloaddition reactions, in the course of secondary metabolic enzyme tailoring is certainly evident and numerous examples of non-enzyme-catalyzed biosynthetic Diels-Alder constructions are known.[2] The biological activity of such natural substances, if providing an adaptive benefit to the producing organism, furnishes the evolutionary driving force to preserve, propagate and modify such enzymes. This field remains an area worthy of additional experimentation, theoretical analysis and pedagogical vetting. As one of the most significant reactions in laboratory

synthetic organic chemistry, it is very exciting to contemplate the extent to which Nature has interrogated formal [4+2] cycloaddition constructions.

# Chapter 3: Elucidation of the Malbrancheamide Pathway and the Discovery of a Novel Diels-Alderase

## I. Introduction

Among the prenylated indole alkaloids isolated from various strains of fungi from the *Aspergillus*, *Penicillium,* and *Malbranchea* genera, two distinct families have evolved: the dioxopiperazines and the monooxopiperazines. It has long been hypothesized these families of metabolites originate from similar stereochemically divergent biochemical mechanisms in the IMDA construction of the bicyclo[2.2.2]diazaoctane core (Figure 3.1).[1, 22, 141-142] The bicyclo core of the antipodal metabolites is enzymatically derived via a stereocontrolled intramolecular hetero-Diels-Alder cycloaddition. With only five crystal structures reported to date, this enzyme remains incredibly rare in nature.

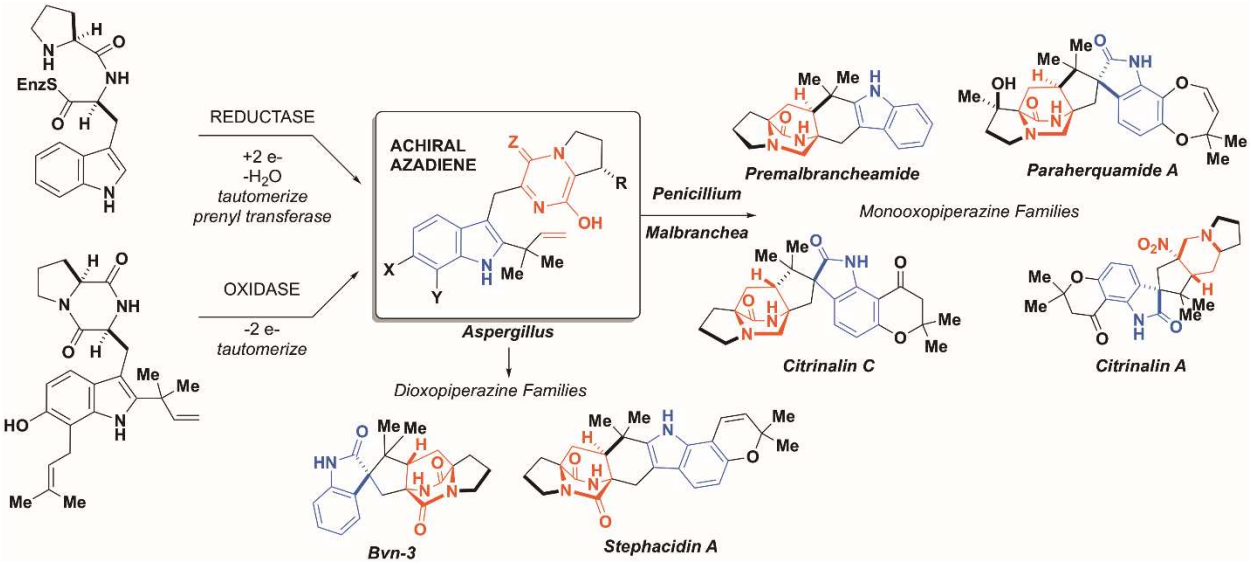


*Figure 3.1.* Unified biosynthesis of the monooxopiperazines and dioxopiperazines.

Many of the biosynthetic pathways in the *Aspergillus* genus have long been studied and many hypotheses, supported by theoretical and experimental studies, have been made to date.

However, up to this point, very few conclusions have been made about the biological destiny of the metabolites in the *Malbranchea* and *Penicillium* genera. We recently isolated two Diels-Alderases, MalC and PhqE, from *Malbranchea* and *Penicillium sp.* and successfully obtained high-resolution X-ray crystal structures of PhqE bound to the IMDA substrate, ZwtP, and the product, premalbrancheamide (Figure 3.2).[143-144] As shown in Figure 3.2, the indole units of premalbrancheamide and ZwtP are bound in the same pocket, while the pyrazinone of ZwtP is in close proximity to the cofactor, which was determined to be NADPH (*vide infra)*. As discussed herein, this was determined to be due to the role of NADPH as a reducing agent for ZwtP in the active site. Molecular dynamics simulations also revealed this enzyme-cofactor complex to play a crucial role in the stereocontrol of the IMDA by aiding in the spatially confined pre-organization of the substrate within the complex.[144] This is a very exciting discovery as we have been searching for this stereoselective Diels-Alderase for at least 30 years. In order to study the role of the enzyme and perform *in vitro* reconstitution studies, the total synthesis of natural products ZwtP, MeZwtP, premalbrancheamide, and other biochemical intermediates was required.[143-144] Herein is reported the total synthesis of two new natural products, the complete elucidation of the malbrancheamide pathway, and the discovery of a novel Diels-Alderase.

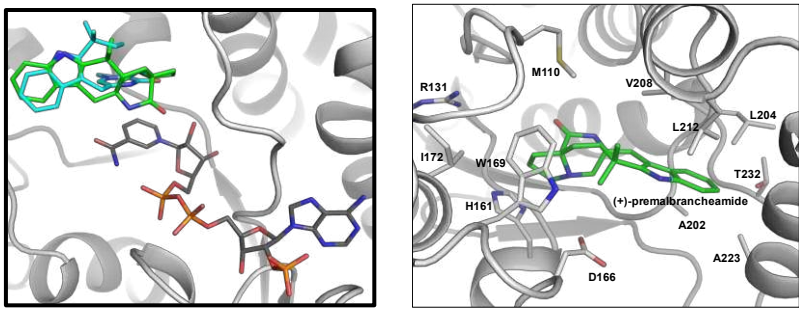


*Figure 3.2.* On left: Premalbrancheamide (IMDA substrate) inside active site of PhqE. On right: ZwtP (IMDA product) inside active site of PhqE.

## II. Total Synthesis of Premalbrancheamide and ZwtP

Numerous anti- metabolites have been observed in the stephacidins, notoamides, brevianamides, and citrinadins; however, only syn- metabolites have been detected among the malbrancheamides and paraherquamides. This suggests the possibility of a different biosynthetic pathway in the IMDA construction of the aza bicyclo core of premalbrancheamide and preparaherquamide. The first-generation synthesis of premalbrancheamide by Williams *et. al.* in 2008 was carried out for feeding studies (Figure 1.19).[51] The most important take away from the first generation synthesis is at this point, we only knew how to access these substrates from the reduction of the dioxopiperazine compound. We don't observe any dioxo compounds in these fungal strains, so we don't believe this is how nature implements the production of the mono substrates. With this in mind, we investigated a new biomimetic synthetic route to access premalbrancheamide.

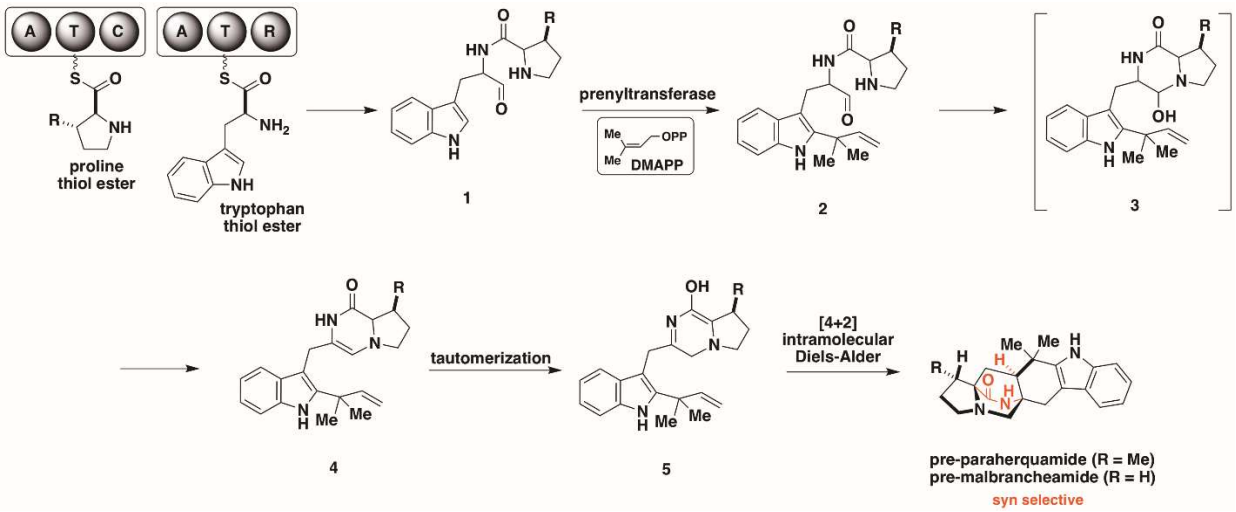


*Figure 3.1.* Original hypothesized biosynthesis of premalbrancheamide and preparaherquamide

We initially assumed the construction of the IMDA arises from dienamine **3.5**, which is fashioned from the cyclization and elimination of L-Pro-L-Trp dipeptide **1** (MalG NRPS domain product) as shown in Figure 3.1. In order to test this hypothesis, the biomimetic total synthesis

of premalbrancheamide was explored (Figures 3.2 and 3.3). Chlorination, followed by reverse prenylation of the commercially available indole led to prenylated indole **3.3**. Somei-Kamatani coupling of gramine **3.4** with glycine derivative **3.5** yielded tryptophan **3.7**, which was then reduced to provide peptide coupling substrate **3.8**. Peptide coupling of proline **3.9** with reduced tryptophan **3.8** afforded alcohol **3.10**, which was subsequently oxidized under Parikh-Doering conditions to yield dipeptide aldehyde **3.11**. Deprotection of Fmoc on dipeptide **3.11** followed by treatment with 1% TFA, all under anaerobic conditions, generates premalbrancheamide in low yield. We long explored this transformation directly from the aldehyde because we initially believed this is how nature implemented the IMDA. At this point, we were still convinced dienamine **3.5** was the substrate for the IMDA *in vitro.* However, enzymatic reconstitution revealed a native substrate for the Intramolecular Diels-Alder reaction, ZwtP. ZwtP can be accessed from aldehyde **3.11** upon deprotection and oxidative aromatization in good yields.[143-144]

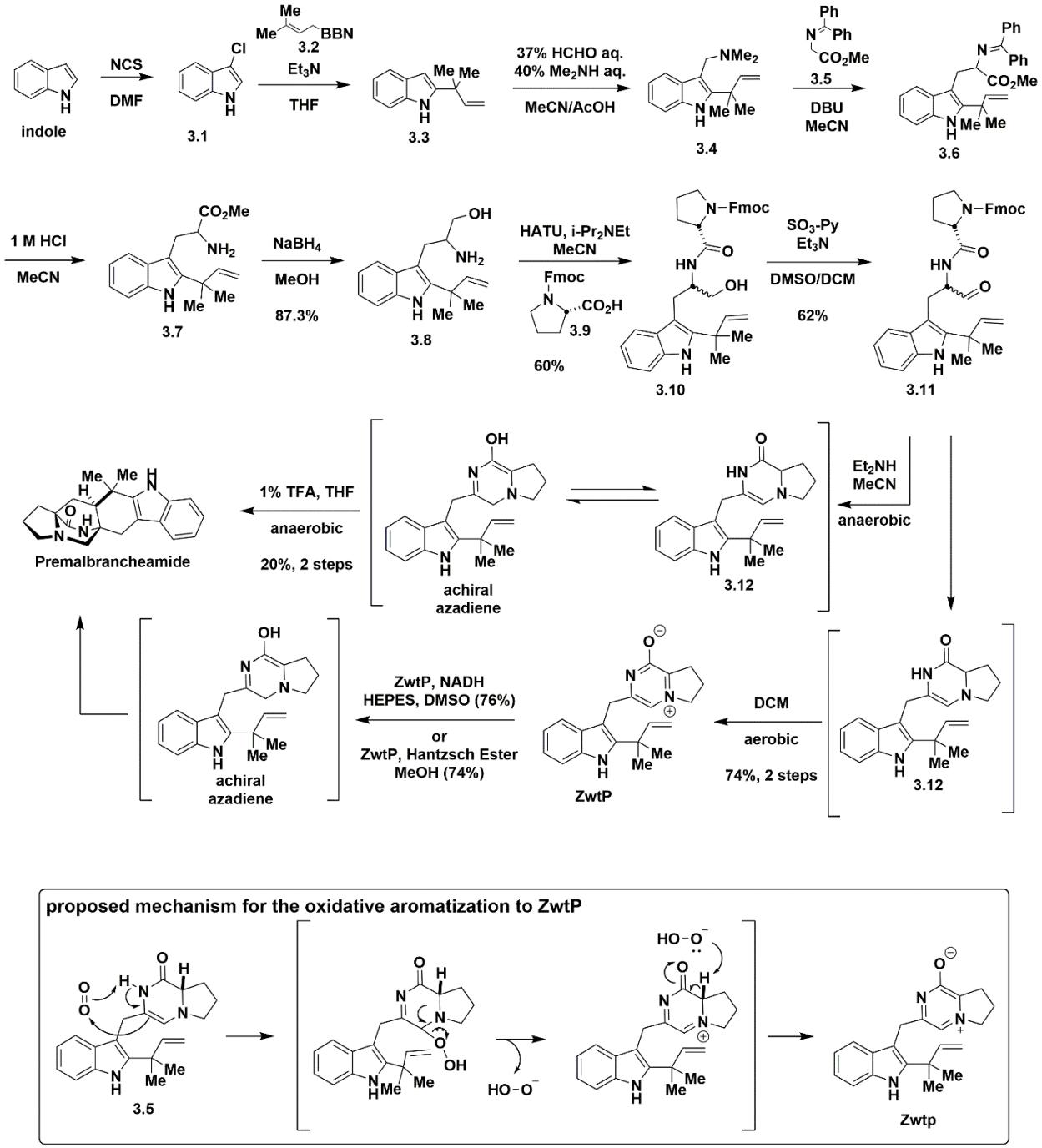


*Figure 3.2.* Total synthesis of ZwtP and second-generation synthesis of premalbrancheamide.

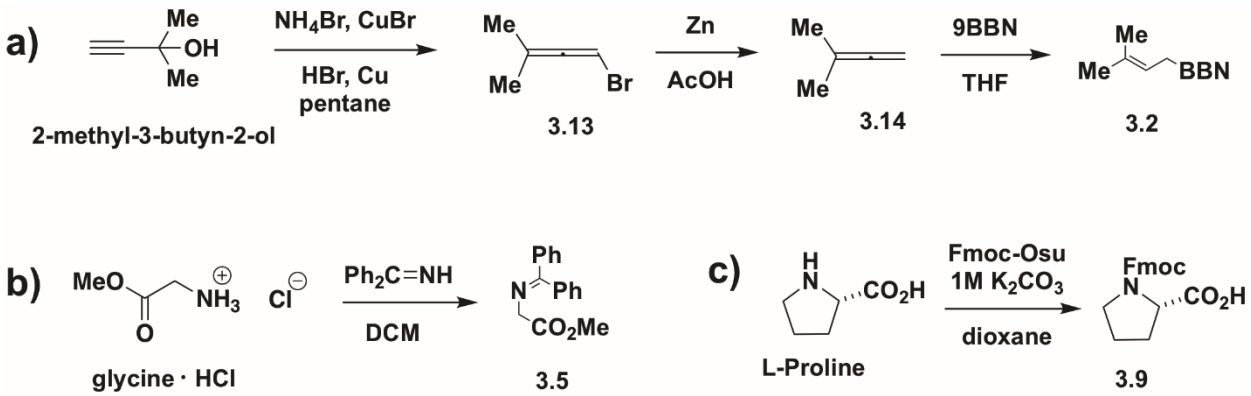


*Figure 3.3.* Synthesis of reagents for the total synthesis of ZwtP and premalbrancheamide. a) Synthesis of 9BBN allene **3.2**. b) Synthesis of glycine derivative **3.5**. c) Synthesis of Fmoc protected proline **3.9**.

## III. *In Vitro* Reconstitution of the Malbrancheamide Pathway

Initial efforts to reconstitute the first step of the malbrancheamide pathway, which is hypothesized to involve coupling of L-proline and L-tryptophan by MalG (dimodular nonribosomal peptide synthetase containing 6 domains) to afford L-Pro-L-Tryp dipeptide **3.15**, included incubation of substrates L-proline and L-tryptophan with the MalG NRPS domain and the presumed NADPH cofactor. Analysis by LC/MS identified aromatic zwitterion species **3.17** as the main product instead of the presumed dipeptide intermediate **3.16**. While formation of the zwitterion was suppressed under anaerobic conditions, it was determined that the zwitterion is formed from spontaneous oxidation of dienamine **3.16**.[143-144]

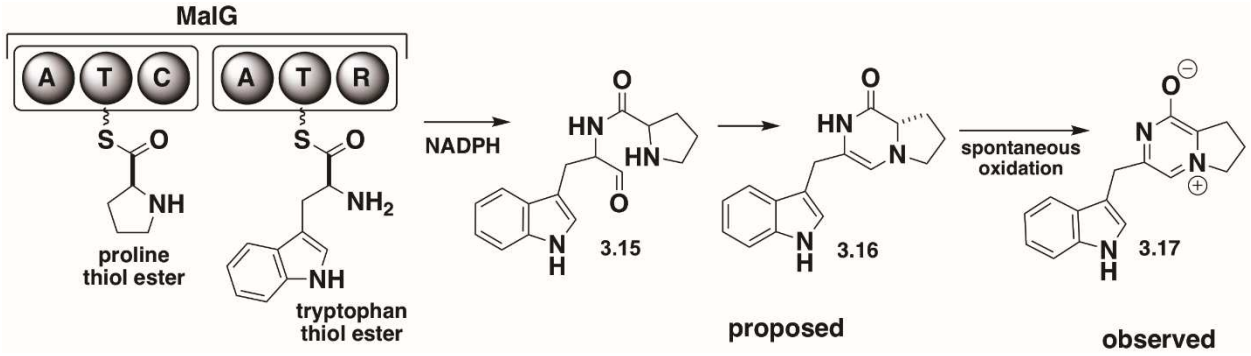


*Figure 3.4. In vitro* assay to determine the NRPS product resulting from the MalG domain in the biosynthesis of malbrancheamide.

The formation of zwitterion **3.17** was confirmed by chemical synthesis (Figure 3.5). Reduction of L-Tryptophan methyl ester **3.18** with $NaBH_4$, followed by peptide coupling with Fmoc protected L-Proline **3.19** yields alcohol **3.20**. Oxidation of the alcohol under Parikh-Doering conditions allowed for cyclization and spontaneous oxidation upon deprotection and controlled exposure to air. Initial exploration of the oxidative aromatization of aldehyde **3.21** was found challenging due to the temperamental nature of the zwitterion. However, these challenges were overcome in all syntheses of the zwitterions, providing us with no less than a 47% yield, over two steps. At this stage, we believed the zwitterion species were shunt metabolites in the biogenesis of malbrancheamide.[143-144]

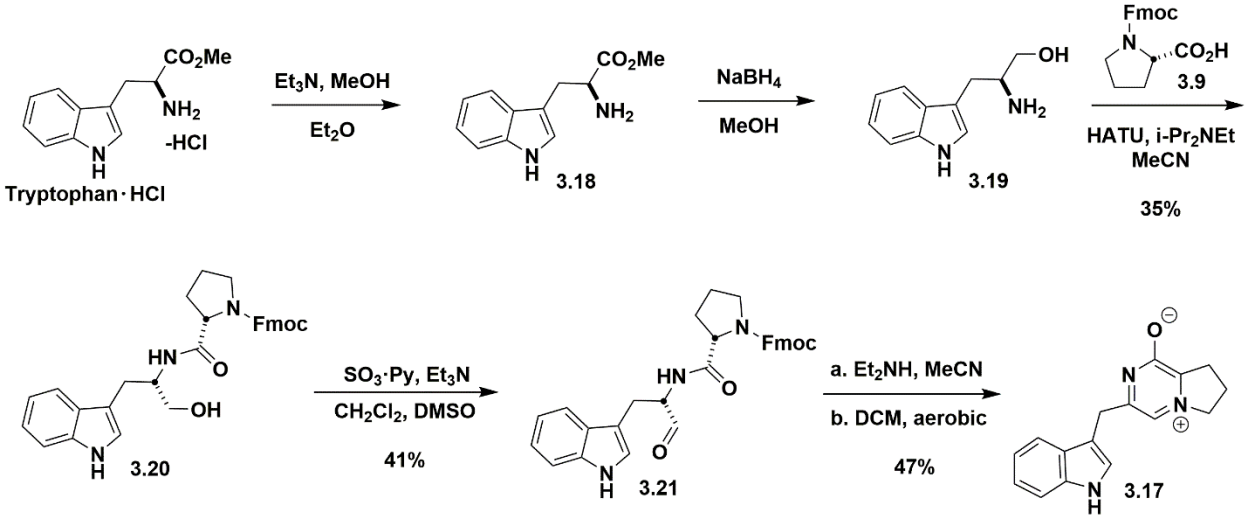


*Figure 3.5.* Synthesis of Zwt for *in vitro* assays.

In exploring the prenylation step, we expected to observe dienamine 4 (Figure 3.1) as the product, which is the anticipated substrate for the IMDA. However, incubation of the substrate loaded MalG (NRPS) domain with presumed cofactor and the enzyme conditions for the reverse prenylation step formed the prenylated zwitterion, ZwtP (Figure 3.6). Since the nonprenylated dienamine spontaneously oxidizes to its subsequent zwitterion as shown in Figure 3.4, this wasn't

really that surprising. Even though everything is carried out in a glovebox under anaerobic conditions, the product must be removed from the anaerobic environment to undergo analysis by LCMS. Therefore, dienamine 4 is likely the pathway intermediate and immediate oxidation is occurring when removed from the glovebox. Because of this stability issue, we can't really know for sure which of these two substrates is the product from reverse prenyl transferase, MalE *in vitro*. However, we can figure this out by providing synthetic material to be used for the *in vitro* assays. We already know how to synthesize Zwt **3.17** (Figure 3.5), but we face a challenge in synthesizing the very aerobically unstable dienamine (**3.16**). We proposed synthesizing the aldehyde with a protecting group that is easily removable within the glovebox under anaerobic conditions. We, in turn, decided to use *ortho*-nitrobenzyl because it is known to undergo photolysis relatively easily at a wavelength of 355 nm.

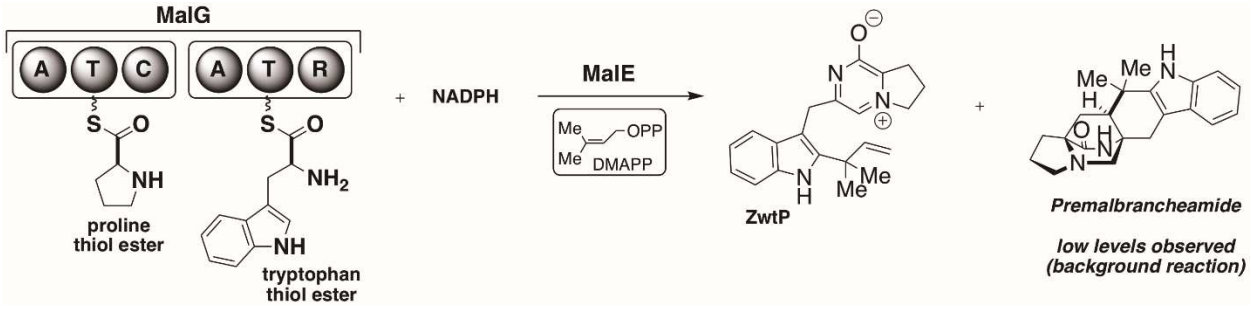


*Figure 3.6. In vitro* assay to determine the prenylation product resulting from reverse prenyl transferase MalE in the biosynthesis of malbrancheamide.

*Ortho*-nitrobenzyl protected proline can be accessed from chloroformate **3.22** utilizing Schotten-Baumann conditions. This technique proved to be challenging as the rate and order of addition is extremely critical. Peptide coupling of ONB proline with reduced tryptophan, followed by oxidation provided aldehyde **3.25** for *in vitro* studies (Figure 3.7). Upon completion of the synthesis, I shipped the ONB protected aldehyde **3.25** to our collaborators in Michigan to be used in accessing the dienamine (**3.16**) *in situ.* They incubated the material in the glovebox with the

enzyme conditions and exposed it to an ultraviolet tanning light, which worked out great exhibiting rapid and full conversion to ZwtP (Figure 3.8). However, incubation of zwitterion **3.17** with the enzyme conditions was not as efficient with only low levels being observed and at a much slower rate.[143-144]

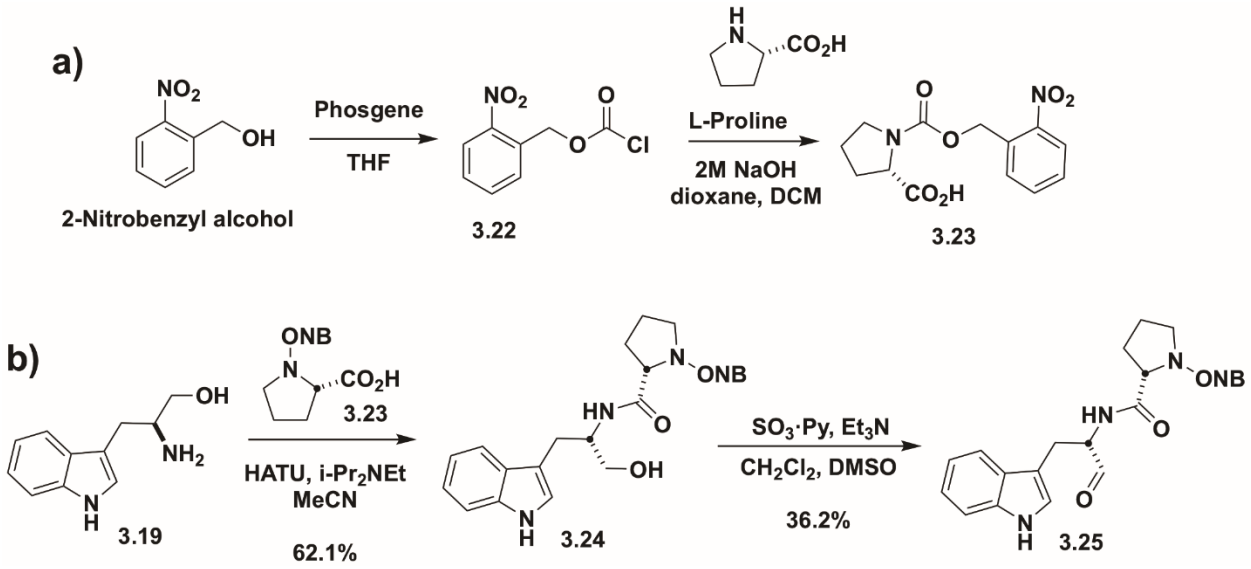


*Figure 3.7.* Synthesis of nonprenylated ONB proline for *in vitro* studies.

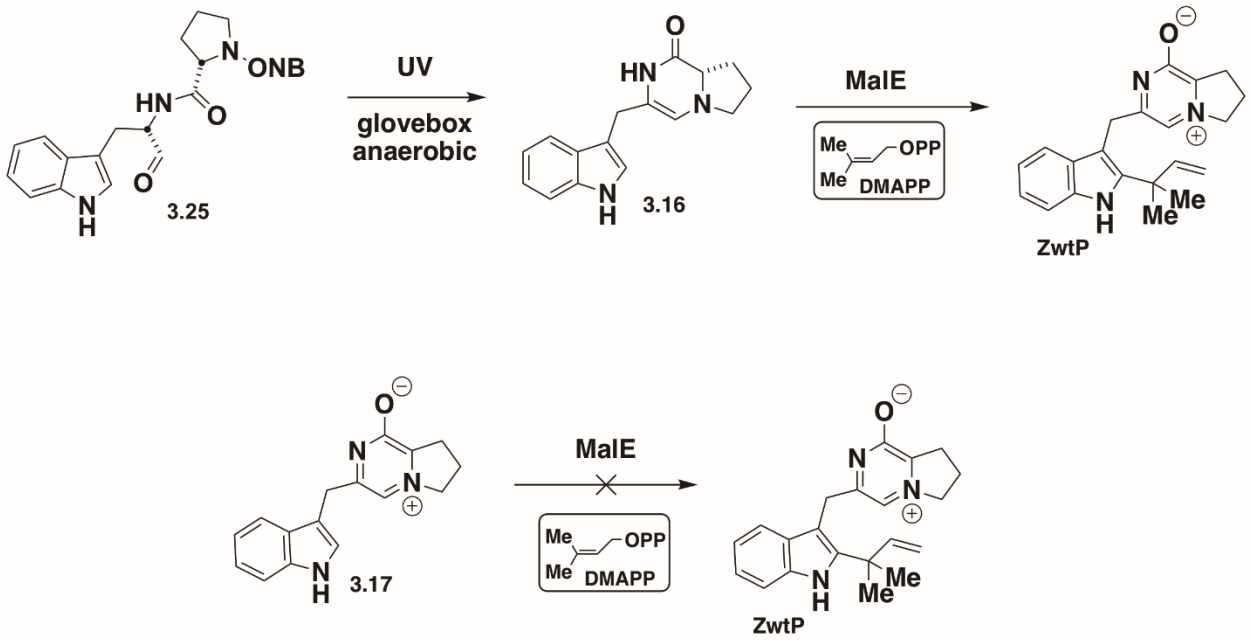


*Figure 3.8. In vitro* assays to determine the prenylation substrate for reverse prenyl transferase MalE in the biosynthesis of malbrancheamide.

Even though all our hypotheses have been correct up to this point, the most important question lies in defining the substrate for the intramolecular Diels-Alder reaction. We continued *in vitro* studies to determine if dienamine **3.28** is in fact our IMDA substrate. We first confirmed that the isolated enzyme, MalC, does in fact function as a Diels-Alderase in the formation of enantiopure premalbrancheamide via incubation of the substrate loaded MalG domain with presumed cofactors, the reverse prenyl transferase MalE, and the presumed Diels-Alderase MalC (Figure 3.9). As previously mentioned, the zwitterion species were initially presumed to be shunt metabolites; however, the observance of premalbrancheamide from earlier *in vitro* studies (Figure 3.6) raised questions about the role of ZwtP. With the consideration that ZwtP may actually play an important role in the formation of premalbrancheamide, we tested the ability of MalC to react with ZwtP. We expected to observe no reaction since we believe it to be just a shunt metabolite; however, we observed full and rapid conversion to enantiopure premalbrancheamide (Figure 3.9). At this stage, we were still convinced that the dienamine is the active substrate within the cell, so we considered ZwtP must be behaving as an alternate intermediate in the biogenesis of premalbrancheamide. With this in mind, I synthesized substrates ZwtP (Figure 3.2) and ONB protected aldehyde **3.27** (Figure 3.10) to be used for *in vitro* studies in testing our hypothesis.

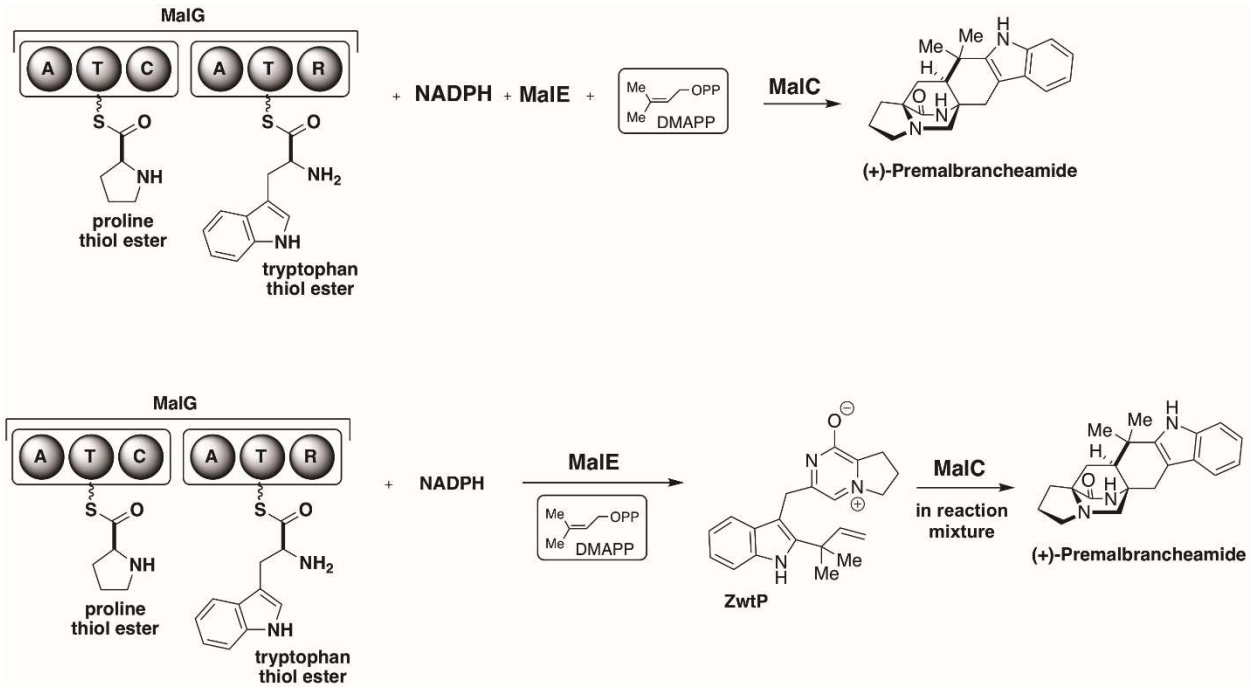


*Figure 3.9. In vitro* assays to determine the role of intramolecular Diels-Alderase MalC in the biosynthesis of malbrancheamide.

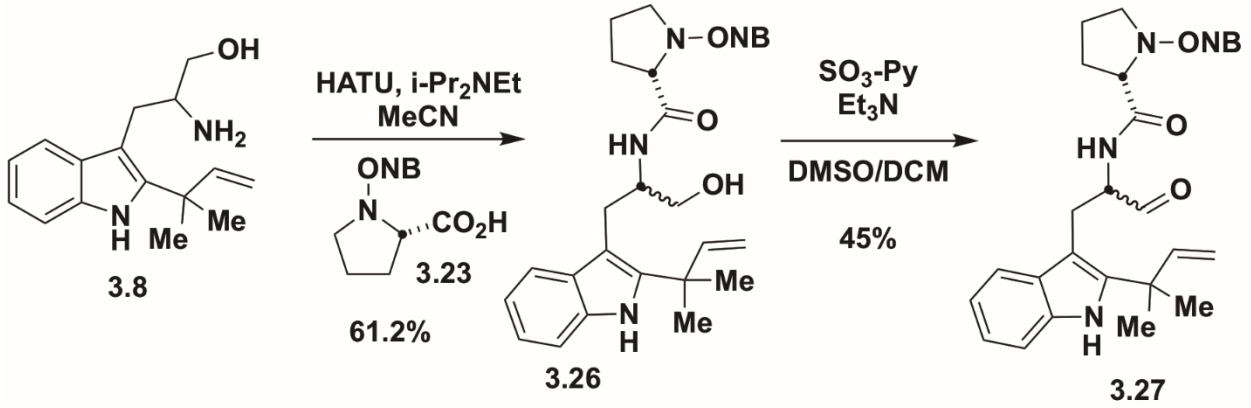


*Figure 3.10.* Synthesis of *ortho*-nitrobenzyl protected proline **3.27** for *in vitro* studies.

Peptide coupling of reduced tryptophan **3.8** with *ortho*-nitro benzyl protected proline **3.23**, followed by Parikh-Doering oxidation provides ONB protected aldehyde **3.27** (Figure 3.10). Removal of the ONB group within the glovebox will allow for *in situ* formation of the aerobically unstable dienamine **3.28** (Figure 3.11). Removal of the Fmoc group from aldehyde **3.11** permits cyclization and spontaneous oxidation to yield ZwtP (Figure 3.2). While we already know that

incubation of the zwitterion with enzyme conditions rapidly forms premalbrancheamide, we were surprised to see that the dienamine did not (Figure 3.11). We know that the dienamine is in fact forming because when NADPH was used under anaerobic conditions, it formed over-reduced product **3.29**. When $NADP^+$ is used, premalbrancheamide does form but only 50% is converted over 18 hours (Figure 3.11). So, we can conclude from these results that our original hypothesis that the dienamine is the IMDA substrate and MalC serves as a rate-enhancing enzyme wasn't completely accurate. However, more interestingly, we have discovered an authentic pathway intermediate![143-144]

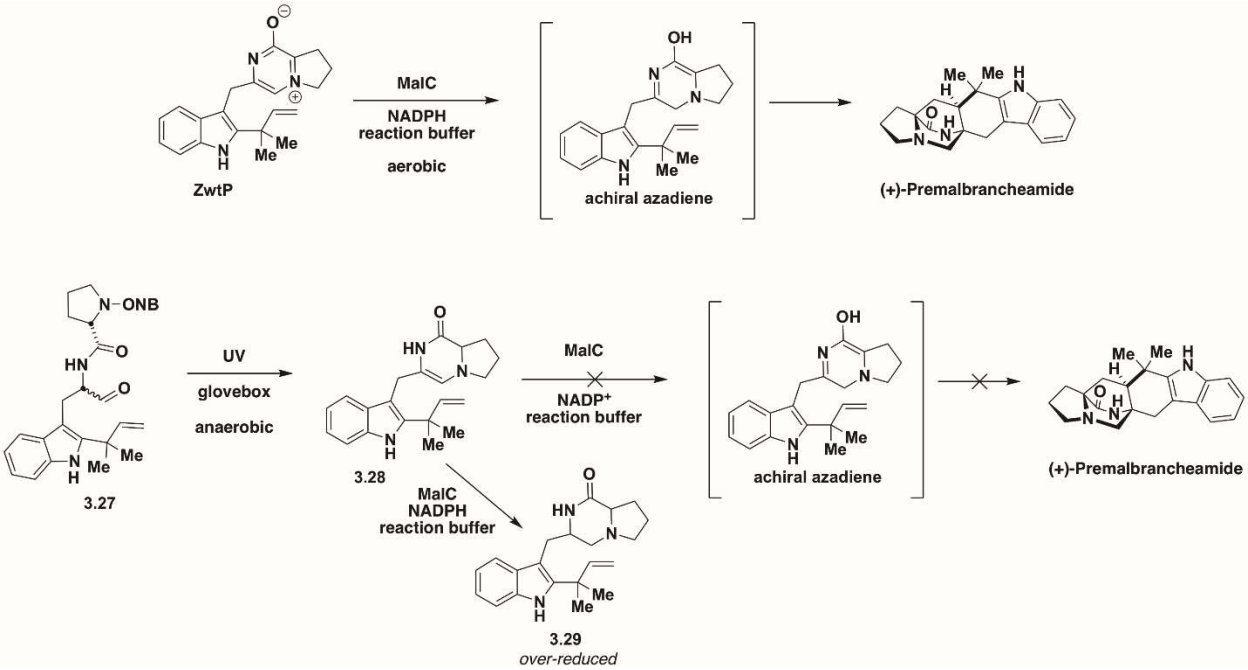


*Figure 3.11. In vitro* assays to determine the IMDA substrate for Diels-Alderase MalC in the biosynthesis of malbrancheamide.

While these results were initially much to our dismay, we speculate that the issue with the dienamine qualifying as the substrate for the intramolecular diels-alder enzymatic transformation is due to the tautomerization step to form the azadiene. Not only is there likely

not a carboxylate amino acid residue in close enough proximity to help facilitate the mechanism, but it would also likely require an antiaromatic intermediate (Figure 3.12).

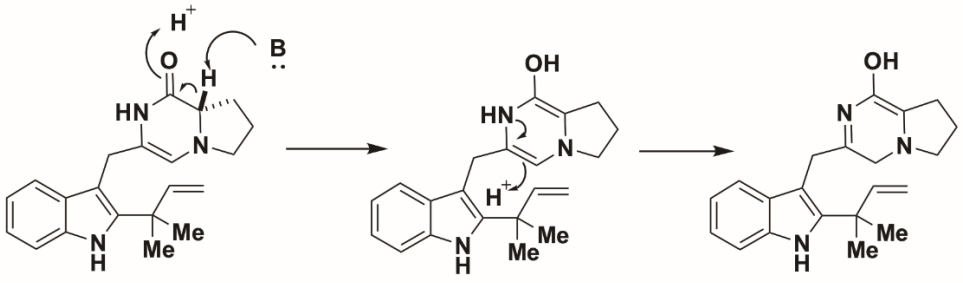


*Figure 3.12.* Tautomerization of dienamine 3.29 to yield achiral azadiene for the IMDA to product premalbrancheamide requires a disfavored anti-aromatic intermediate.

To further confirm what we have observed from our data, I chemically synthesized premalbrancheamide from ZwtP (Figure 3.2). This reaction proceeds forward beautifully in the presence of a reducing agent (Hantzsch ester or NADH) as well as a proton source (MeOH or HEPES buffer). Together with results from the *in vitro* assays that studied the efficacy of the zwitterion compared to that of the dienamine, the proposed disfavored intermediate the dienamine would require to form the azadiene, chemical syntheses, and the isolation of MeZwtP from *phqE* strains *(vida infra),* we can confidently conclude that ZwtP is the native substrate for the IMDA reaction.[143-144] This is an incredibly intriguing finding as we have never observed a metabolite characteristically like that of ZwtP among any of the genera. This unique IMDA substrate also highlights the difficulties surrounding the ability to find the enzyme in the first place.

With the ability to access premalbrancheamide from that of the IMDA substrate, ZwtP, in good yields, we began to question the role of MalC. It is important to note that premalbrancheamide is formed as an enantiomerically pure metabolite *in vitro*, so we continued

studies to further articulate the role of MalC (Figure 3.13). Treatment of chemically synthesized ZwtP with presumed cofactor NADPH, but in the absence of the enzyme produces premalbrancheamide as a racemate in 80-90% conversion by LCMS. When MalC is used in the presence of NADH, we observe full conversion to premalbrancheamide enriched in its (+)-enantiomer (63%). However, when we use MalC in the presence of NADPH, we observe full conversion to enantiopure (+)-premalbrancheamide. With these results, we can conclude that NADPH rescues the over-oxidized ZwtP to form the reactive dienamine which in turn, by chance, undergoes a spontaneous 4+2 cycloaddition in the MalC active site, catalyzed by the spatial restriction and proximity of the diene to the prenyl group.[143-144] The utility of NADPH over NADH within the active site is also further evidenced by Michaelis-Menten kinetic constants for both cofactors with MalC and ZwtP revealing NADPH to have a 10-fold greater catalytic efficiency ($k_{cat}/K_M$) than NADH and a 6-fold greater biding affinity ($K_M$).[143-144]

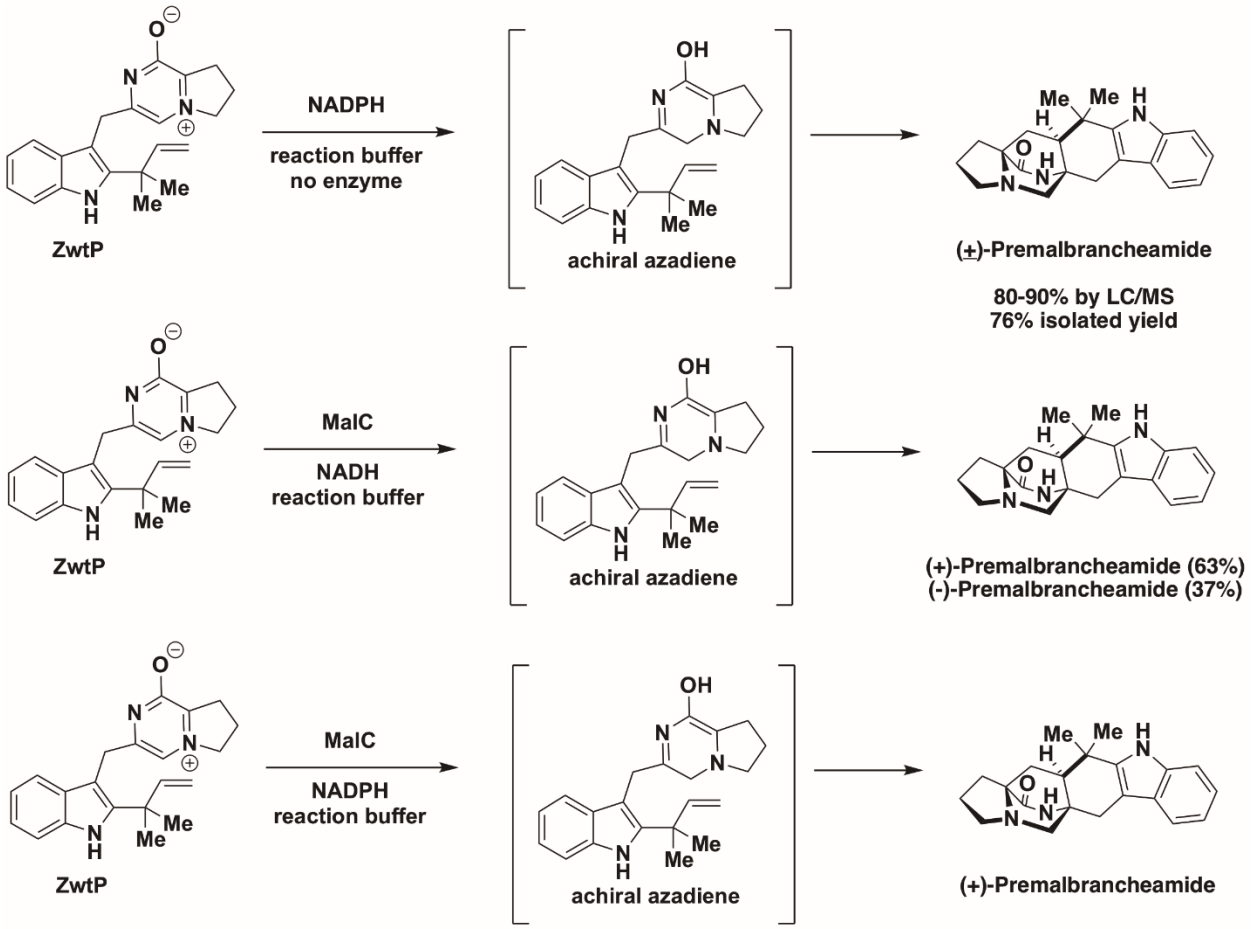


*Figure 3.13. In vitro* assays to determine the stereospecificity of MalC for the IMDA formation of premalbrancheamide in the biosynthesis of malbrancheamide.

Together with these data, we have been able to put together the puzzle pieces for the biosynthesis of malbrancheamide (Figure 3.14). Dienamine **3.16** is the NRPS product, which is subsequently and rapidly picked up by the prenyl transferase to form dienamine **3.28**, which then undergoes spontaneous oxidation to form natural product ZwtP. ZwtP is the native substrate for the IMDA and forms enantiomerically pure premalbrancheamide in the presence of MalC and cofactor NADPH.[143-144] Other studies have shown that malbrancheamide is formed from premalbrancheamide by double chlorination by MalA.[50]

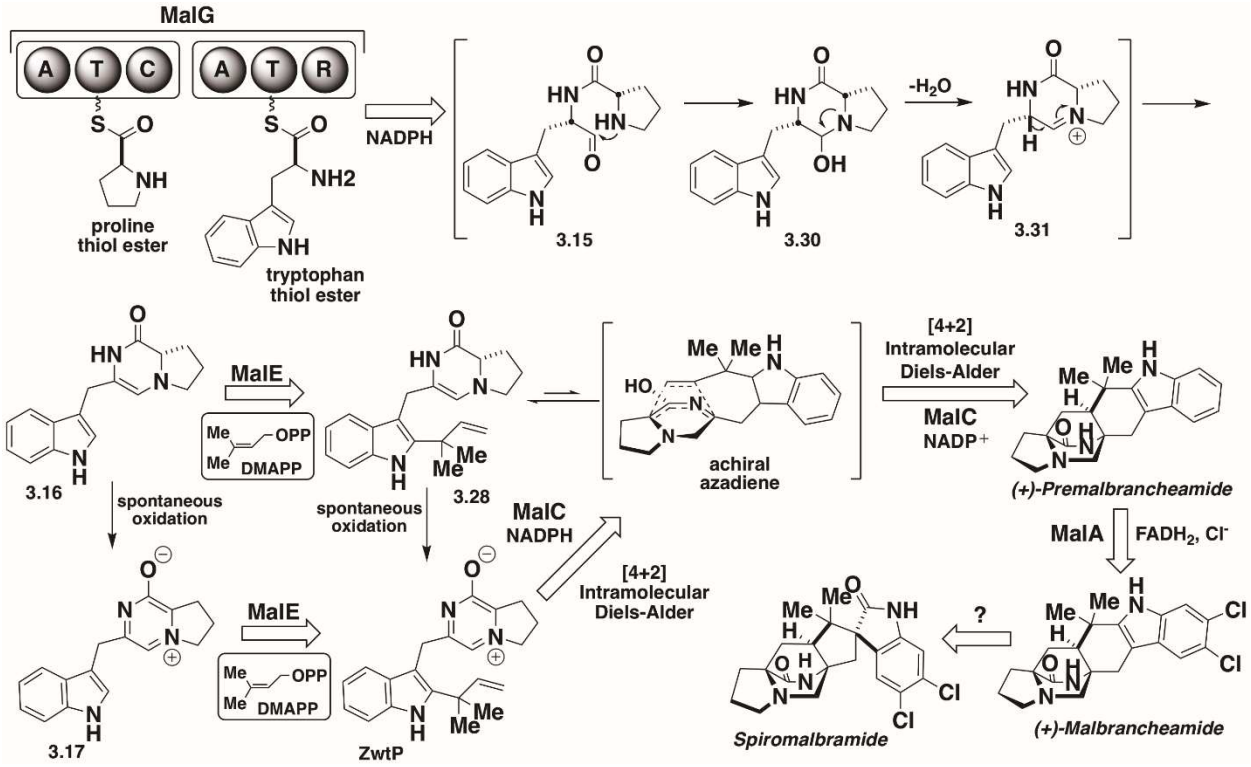


*Figure 3.14.* The biosynthesis of malbrancheamide.

## IV. Total Synthesis of MeZwtP and Elucidation of the Paraherquamide Pathway

Upon the identification of PhqE as the Diels-Alderase among the paraherquamides, the isolation of MeZwtP from PhqE strains, and our recent findings of the IMDA among the malbrancheamides, we can propose a new biosynthetic route to preparaherquamide. The newly isolated natural product, MeZwtP, can be synthesized in a similar manner to that of ZwtP (Figure 3.15). β-methyl proline **3.34** is synthesized from isoleucine via the already established Hoffman-Loeflller-Freytag synthesis. Fmoc protected proline **3.35** is accessed by the reduction, deprotection, and reprotection of Boc protected proline **3.34**. Peptide coupling with reduced tryptophan **3.8**, oxidation, deprotection, cyclization, and oxidative aromatization proceeded forward to provide MeZwtP in good yields. From here, MeZwtp was used for *in vitro* studies with the isolated Diels-Alderase, PhqE, to confirm its proposed transformation into enantiopure (+)-

preparaherquamide (Figure 3.16). With this, we can envision the paraherquamides biosynthesized in a similar way to the malbrancheamides, where MeZwtP is the substrate for the IMDA (Figure 3.17).

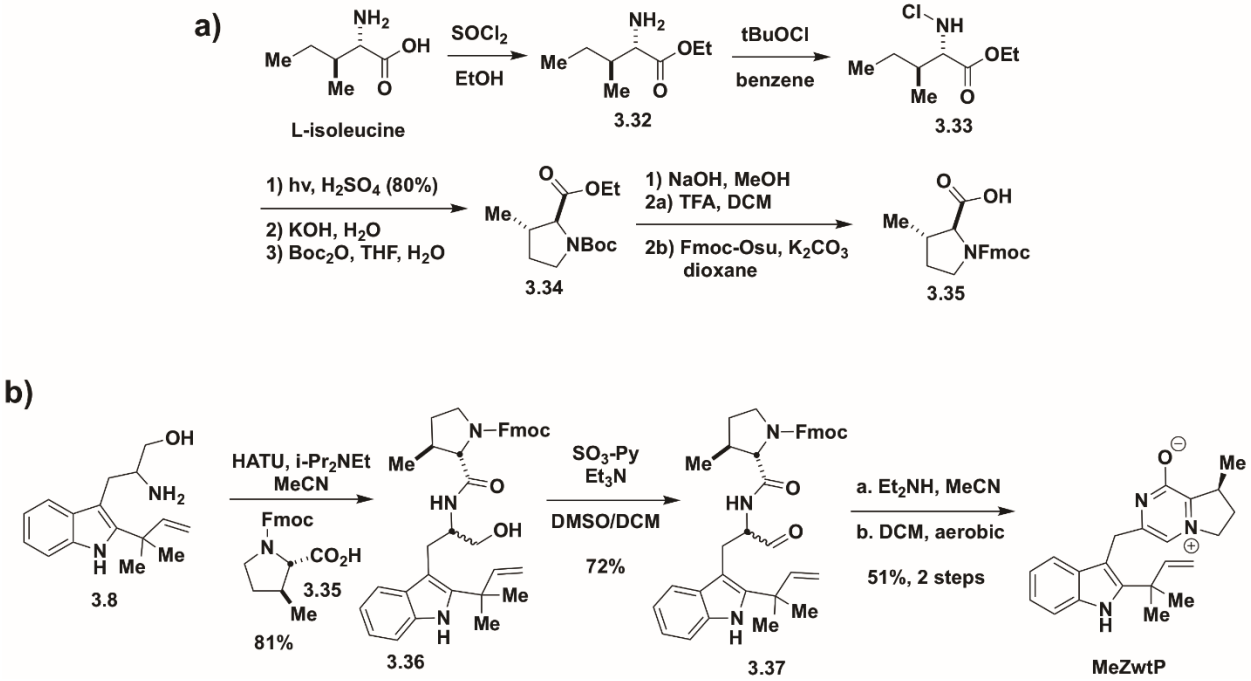


*Figure 3.15.* Total Synthesis of MeZwtP.

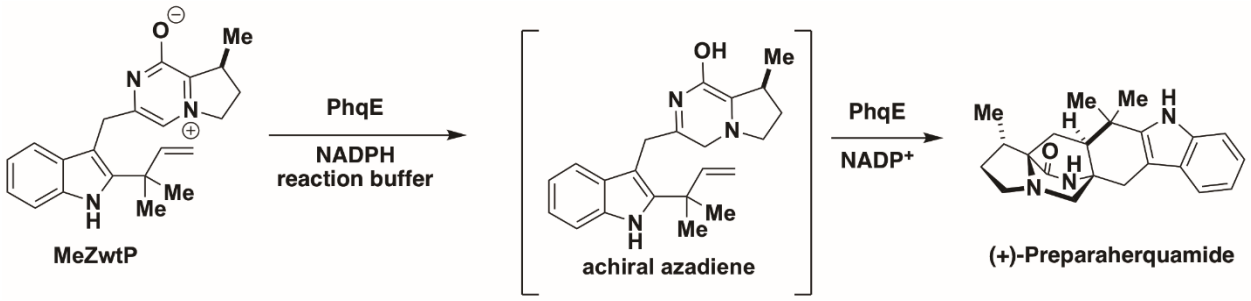


*Figure 3.16. In vitro* assays to determine the IMDA substrate for Diels-Alderase PhqE in the biosynthesis of paraherquamide.

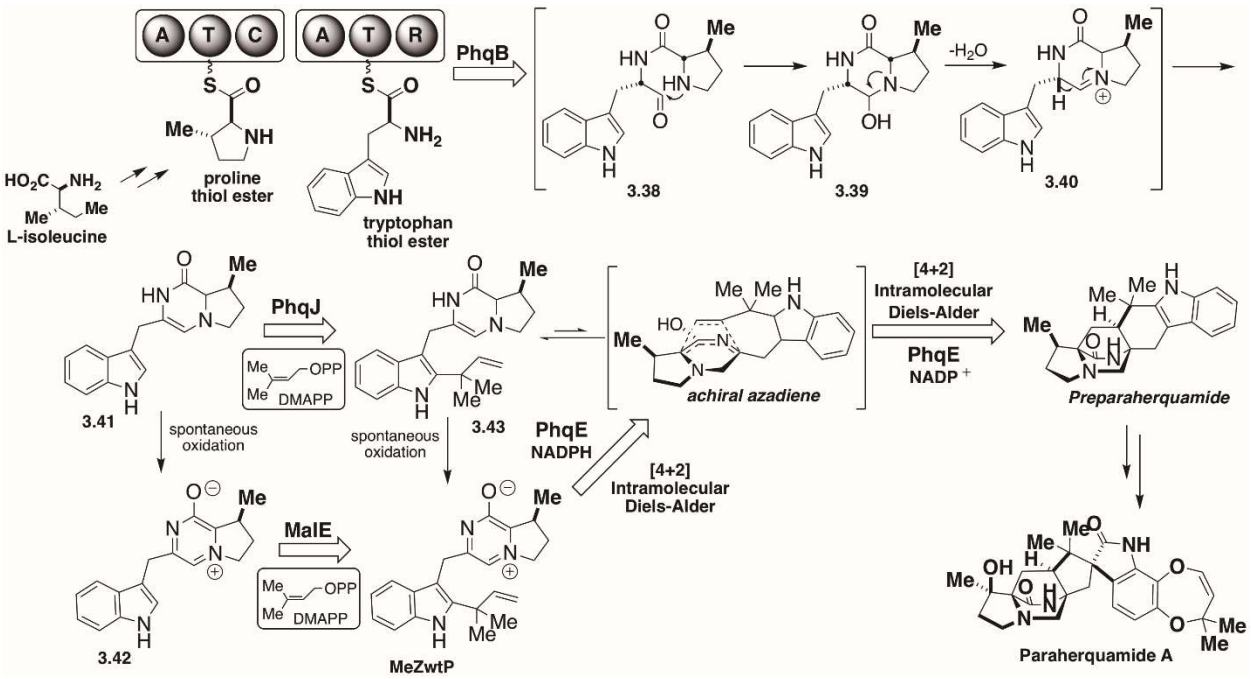


*Figure 3.17.* The proposed biosynthesis of paraherquamide A.

## V. Conclusions and Future Directions

In conclusion, I have successfully completed the total synthesis of newly discovered natural products ZwtP and MeZwtP and accomplished a new and improved biomimetic route to premalbrancheamide. With the improved biomimetic route to premalbrancheamide, we have established a more direct and efficient route to the monoketo- syn- metabolites. I have also completed syntheses to at least three other biological intermediates required for *in vitro* enzymatic reconstitution studies, which helped uncover the role of the elusive Diels-Alderases. My synthetic efforts have allowed us to understand the minimal changes within the active site that are required for the divergence of antipodal natural products, complete the elucidation of the malbrancheamide biosynthetic pathway, and further understand the biochemical destiny of the *Penicillium* and *Malbranchea* metabolites. Our exciting discoveries will aid in unveiling the

enantioselective and diastereoselective mechanisms of other [4+2] cycloadditions in nature and develop new molecular diversity using biological enzymes.

Future directions for this project include investigating the anti- vs syn- formation of the Diels-Alder core. We now fully understand the formation of the syn-premalbrancheamide metabolites among the malbrancheamide pathway; however, the anti- metabolites have not been observed among the malbrancheamide and paraherquamide pathways as they have among the stephacidin and notoamide pathways. Interestingly, DFT calculations performed by Paton and Williams *et. al.* reveal a substantial IMDA transition state (TS) difference among the syn-/anti-diastereomers of the monooxo- compounds (syn- favored over anti- by 2.6 kcal/mol) compared to that of the much more modest TS difference among the dioxo- compounds (syn- favored over anti- by only 0.3 kcal/mol).[143-144] This leaves the perplexing question of whether the anti-metabolites arise from a different pathway intermediate. We plan on figuring this out!

# Chapter 4: Towards the Total Synthesis of Citrinalins A and B

## I. Biosynthetic Insights

Citrinalins A and B are part of a new family of metabolites, the citrinadins, that lack the bicyclo core (Figure 4.1).[145] These new metabolites were isolated from *Penicillium citrinum* by Berlinck and coworkers in 2010.[146] Biosynthetic studies are in the early stages and Berlinck *et. al.* have primarily identified glucose, anthranilic acid and ornithine as precursors through results of $^{13}C$-labeling experiments.[147] They also believe these metabolites to possibly be just an artifact of isolation. However, Williams *et. al.* suggests an alternative mode of action for this new family of metabolites within the cell. More interestingly, we believe citrinalins A and B are likely biosynthesized from the biologically unprecedented loss of CO at the proline unit and decarbonylative deconstruction of the azabicyclo core from a precursor like citrinalin C, a metabolite also isolated from *Penicillium citrinum* (Figure 4.1). For this reason, biomimetic syntheses of Citrinalins A and B are desirable for incorporation studies by Sherman and coworkers. This will aid in determining if these natural metabolites are indeed formed from the opening of the diels-alder core.

Theoretical calculations performed by Tantillo and coworkers suggest citrinalin B to be the thermodynamically favored product over citrinalin A.[148] This suggests that citrinalin A should be present in very low quantities, within the genome, since citrinalin B is likely formed from epimerization of citrinalin A through a Nitro-Mannich type mechanism.[148] While Berlinck and coworkers isolated citrinalin A in a significantly high abundance, isotope-labeled incorporation

studies would also be of use to determine if citrinalin B is in fact a natural product in *P. citrinium* or just an artifact of isolation.

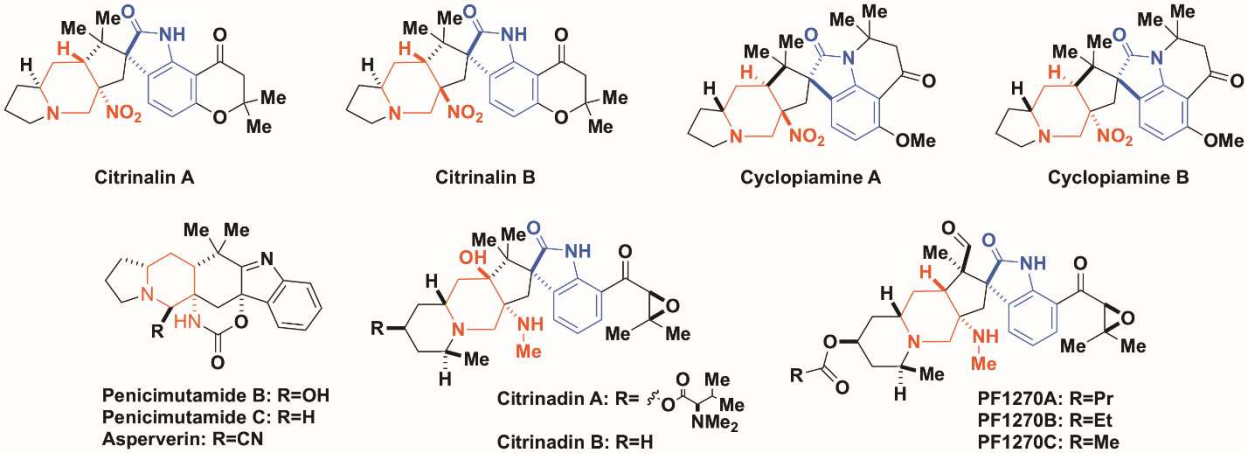


*Figure 4.1.* New family of isolated metabolites from *Penicillium*.

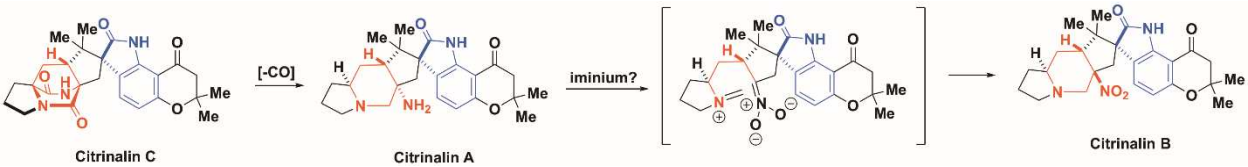


*Figure 4.1.* Williams proposed biosynthesis of citrinalins A and B.

## II. Total Synthesis of *ent*-Citrinalin B by Sarpong *et. al.*

The total synthesis of *ent*-citrinalin B, the unnatural enantiomer of citrinalin B, has recently been reported by Sarpong and coworkers (Figure 4.2).[147] This synthesis was designed to access a different known natural product, cyclopiamine B, found in *Penicillium cyclopium*.[147] Even though Sarpong *et. al.* established many important synthetic steps in accessing the citrinalins, it is important to note our interest lies in synthetically mimicking the proposed biotransformation, which requires accessing these compounds from the opening of the azabicyclo ring. This is a transformation we found to be incredibly challenging.

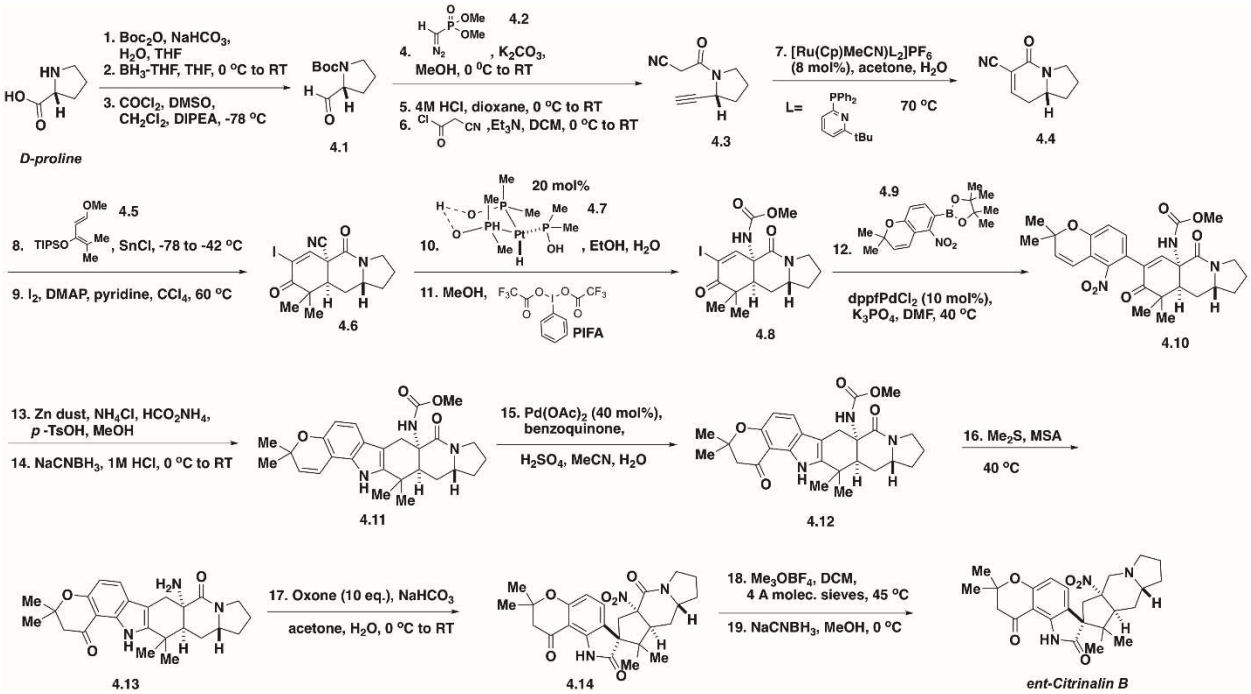


*Figure 4.2.* Sarpong's synthesis of *ent*-citrinalin B.

In the total synthesis of *ent*-citrinalin B, Sarpong builds the proline-derived, pyran substituted indole backbone of these metabolites utilizing Suzuki coupling to circumvent the azabicyclo ring that arises from the Williams' established intramolecular Diels-Alder reaction. From coupled and dehydrated product **4.11**, *ent*-citrinalin B is synthesized via Wacker oxidation of the pyran ring, followed by hydrolysis, oxidation of the free amine, and selective reduction of the tertiary amide.[147] We will be able to implement the use of the Wacker oxidation and the oxidation of the free amine with DMDO in our future synthesis of citrinalins A and B *(vide infra).*

## III. Retrosynthetic Analysis

As previously mentioned, we plan to synthesize these metabolites by opening the azabicyclo core via a decarbonylative deconstruction. In planning the biomimetic synthesis of these metabolites, we can envision synthesizing these compounds from known metabolite versicolamide B (Figure 4.3). Versicolamide B is a natural product found in *Aspergillus* that we

already know how to make chemically *(vide infra).*[44] However, it is important to note that synthesizing this compound is a long feat, requiring 17 linear steps. With this in mind, we decided to utilize a model study to establish the unprecedented chemistry before applying it to the natural product.

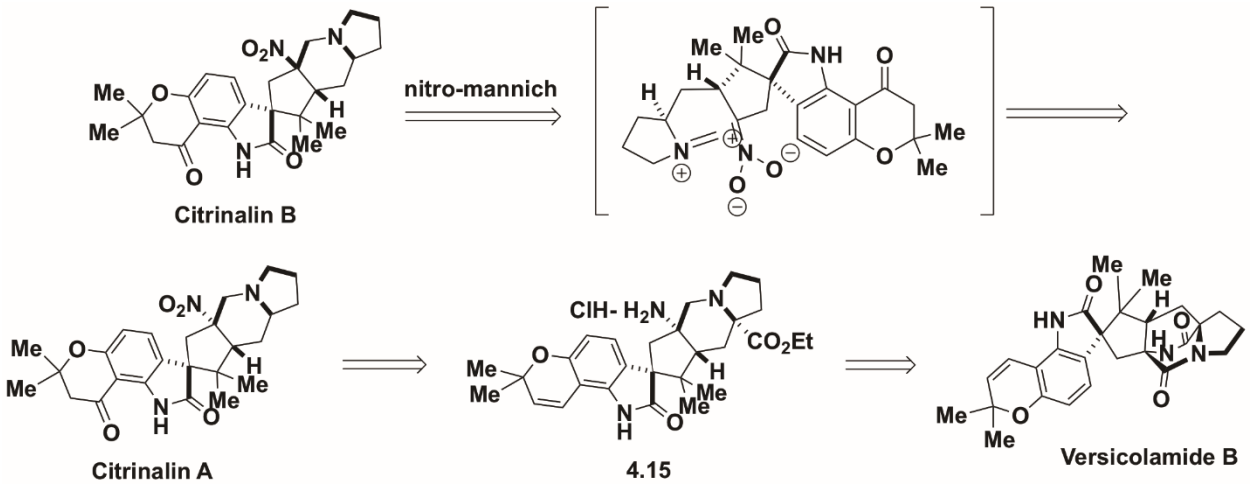


*Figure 4.3.* Retrosynthetic analysis of Citrinalins A and B.

## IV. Model Study for the Biomimetic Synthesis of Citrinalins A and B

The model compound (**4.30**) to be used for the study lacks the pyran ring and therefore can be accessed in 10 linear steps (Figure 4.4).[149] Chlorination of commercially available indole **4.16**, followed by prenylation with freshly made 9-BBN substituted methylene yields prenylated indole **4.19**. Treatment with formaldehyde and dimethyl amine produces gramine **4.20**, which is sub sequentially coupled with glycine derivative **4.21** through Somei-Kametani type coupling conditions. Hydrolysis of **4.22** yields tryptophan **4.23** for peptide coupling with Fmoc protected β-hydroxy proline **4.24**. Deprotection of the Fmoc group on dipeptide **4.25** allows for cyclization onto the ester to form diketopiperazine **4.26** in good yields. Mesylation and elimination of the hydroxyl group from the proline unit produces the enamine that is, in turn, tautomerized under basic conditions to access the reactive achiral azadiene substrate for the intramolecular diels-

alder reaction. It is important to note that the Diels-Alder reaction that takes place from the indole substituted diketopiperazine (**4.28**) forms a diastereomeric ratio (anti- vs syn-) with the anti- product being the less favorable diastereomer. This is a very important stereochemical difference that arises from the intramolecular diels-alder reaction at the tertiary carbon of the bicyclo core.

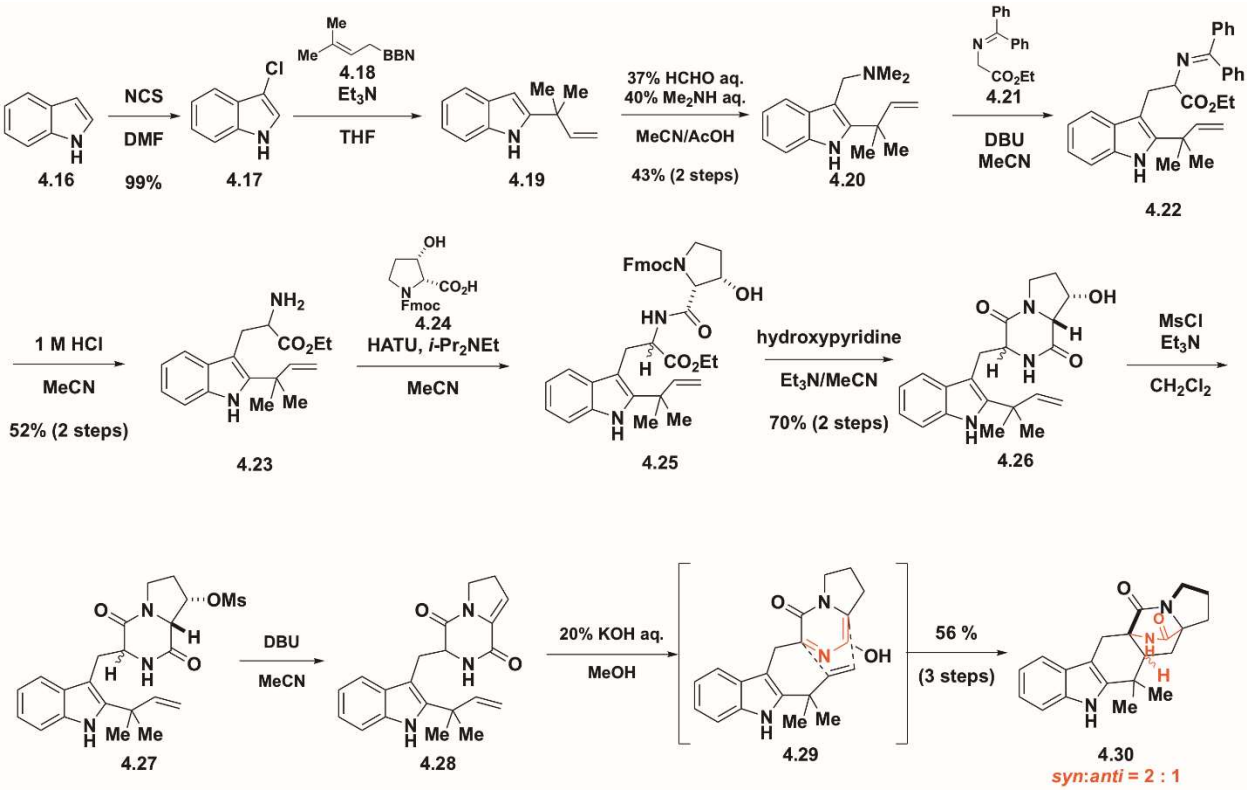


*Figure 4.4.* Synthesis of the Model Diels-Alder Product **4.30**.

The citrinalins possess stereochemistry that is adapted from the anti- Diels-Alder products. Even though the only reported synthesis of the model Diels-Alder products produces the compounds in a syn- dominant ratio, former theoretical and experimental studies from our research group prove that we can chemically make the anti- products as the major or sole product (Figure 4.5).[64, 73, 150]

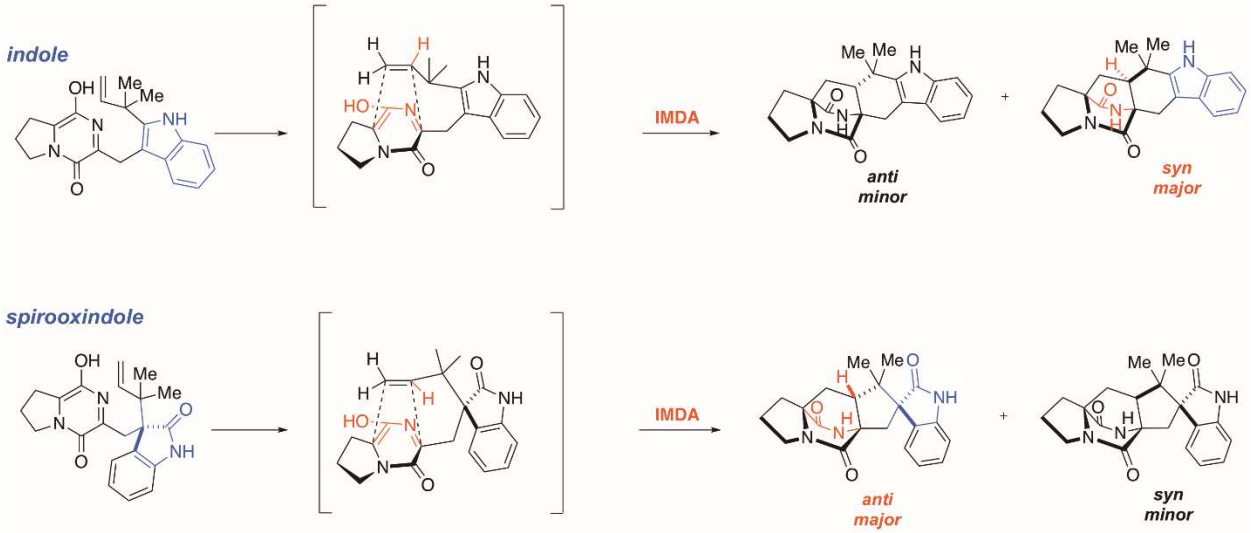


*Figure 4.5* Theoretical and experimental studies for the diastereoselective evalution of the intramolecular diels-alder reaction.

The spirooxindole substituted diketopiperazine compounds produce the anti- Diels-Alder diastereomer as the major product upon tautomerization and spontaneous 4+2 cyclization. This is also represented in the synthesis of versicolamide B (Figure 4.6).[44] Even though the anti-dominant formation of the Diels-Alder product from the model compounds has yet to be established, we already know how to make spirooxindole compound **4.34** directly from the anti-model Diels-Alder product (Figure 4.6). The difference between these two routes is in the synthesis of versicolamide B, the Pinacol reaction to form the oxindole takes place before the IMDA, whereas in the synthesis of the model compounds, the Pinacol reaction is implemented after the IMDA.

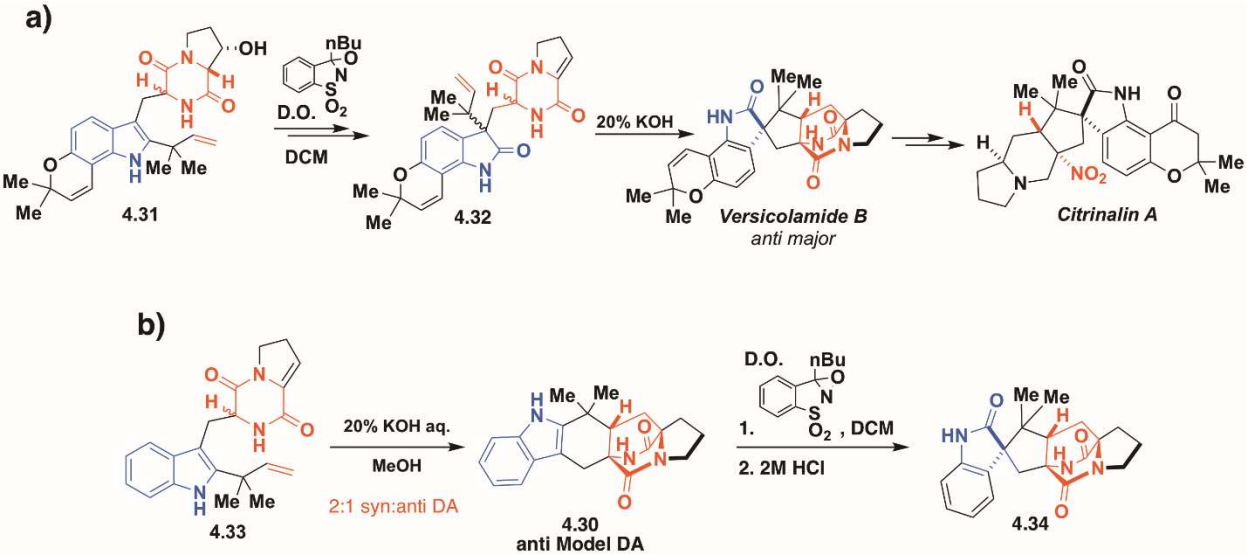


*Figure 4.6.* Syn vs anti- formation for the synthetic intramolecular diels-alder reaction.

In an attempt to more accurately model the synthesis of citrinalins A and B, it is important to consider the synthetic requirements for producing the anti- and syn- metabolites in the desired dominant ratio. With this in mind, I attempted to synthesize the model Diels-Alder product from that of the spirooxindole to yield the anti- dominant product (Figure 4.7). Treatment of indole **4.26** with Davis' Oxaziridine was not successful. I ultimately reasoned that the presence of the electronic system from the pyran ring in the versicolamide B synthesis did not only help aid in forming the desired spirooxindole product at a higher abundance over the undesired side hydroxyl cyclized product (Figure 4.7),[44] but the electronic system is also absolutely necessary in driving the reaction forward at all under Davis' Oxaziridine conditions. I later found out that this was due to the initial formation of the epoxide intermediate. Even though this felt defeating and was a dead end at the moment, the knowledge gained from these results aided in the progression of future work, which will be discussed in the brevianamide chapter (Chapter 5).

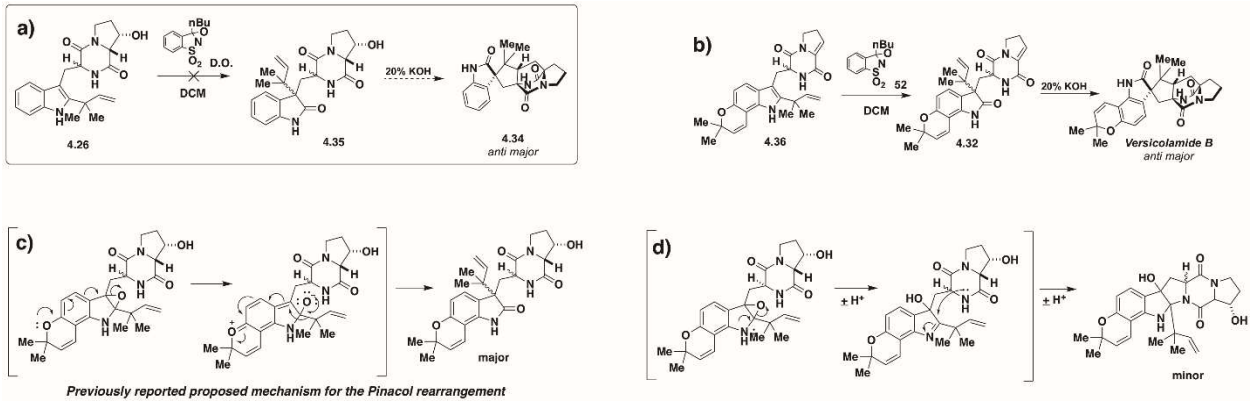


*Figure 4.7.* Initial model study attempts. a) Failed pinacol rearrangement on model substrate 4.26. b) Previously established pinacol rearrangement on diketopiperazine **4.36** in the total synthesis of versicolamide b. c) proposed mechanism for the pinacol rearrangement in formation of the spirooxindole product. d) proposed mechanism for the formation of the undesired cyclized hydroxyl side product.

With the use of the non-substituted indole model compounds for the pinacol reaction initially being unsuccessful, I decided to utilize the already synthesized 3-Oboc substituted compounds in hopes that it would aid in driving the reaction forward (Figure 4.8). Protection of nitro phenol, followed by Leimgruber-Batcho indole synthesis yields hydroxyindole **4.40**. Despite the indole formation reaction being previously reported with the use of $H_2$ as the hydrogen source,[151] when I started on this project we found that the original conditions and yields were not very reproducible and it was causing a lot of problems because we weren't able to make sufficient quantities of material. This was due to polymerization of the hydroxyindole. Fortunately, after reviewing the literature I was able to develop a set of conditions that solved this problem giving us excellent yields on large scales.[152] From here, Boc protection of **4.40** proceeded forward smoothly to yield indole **4.41**. With this in hand, chlorination, prenylation, and formation of gramine **4.44** allows for Somei-Kamatani coupling and hydrolysis to yield tryptophan **4.46**. HATU coupling for the formation of dipeptide **4.47**, followed by deprotection of the Fmoc group and cyclization gives the intended pinacol precursor **4.48**.

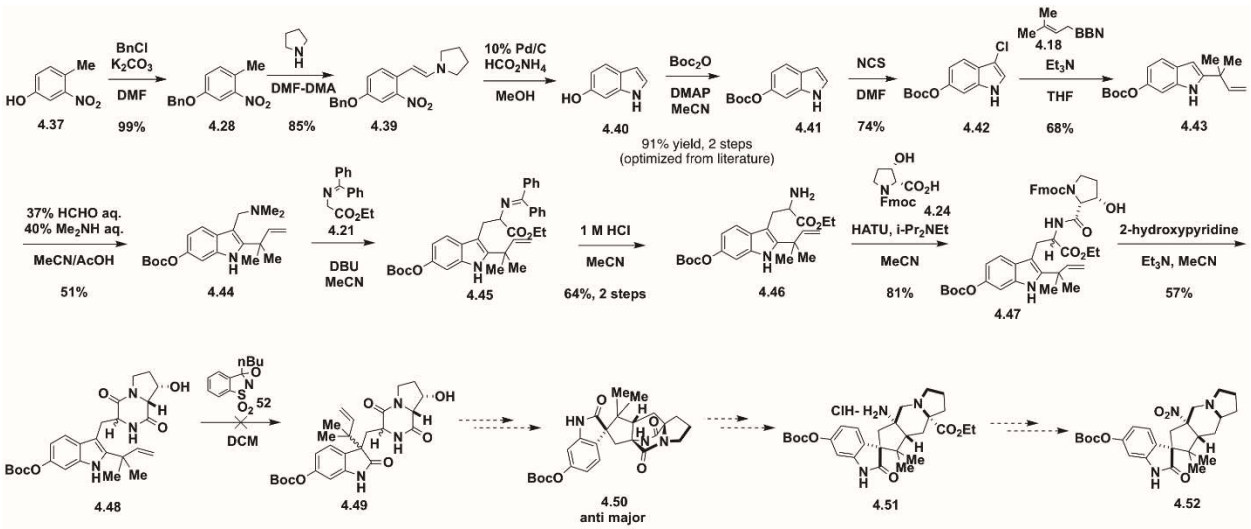


*Figure 4.8.* Model study attempt 2. Synthesis of 3-OBoc indole substituted substrates.

Unfortunately, the pinacol rearrangement did not work. While the reaction did proceed forward as predicted, the hydroxyl cyclized product was the major product (Figure 4.9). I reasoned this was likely due to the electrons being nearly fully tied up in resonance with the Boc group. While I could have proceeded forward with other protecting groups, like methoxymethyl ether, that would likely produce better results, it did not seem reasonable to devote much time to it since this transformation wouldn't be of concern when applying it to the natural product.

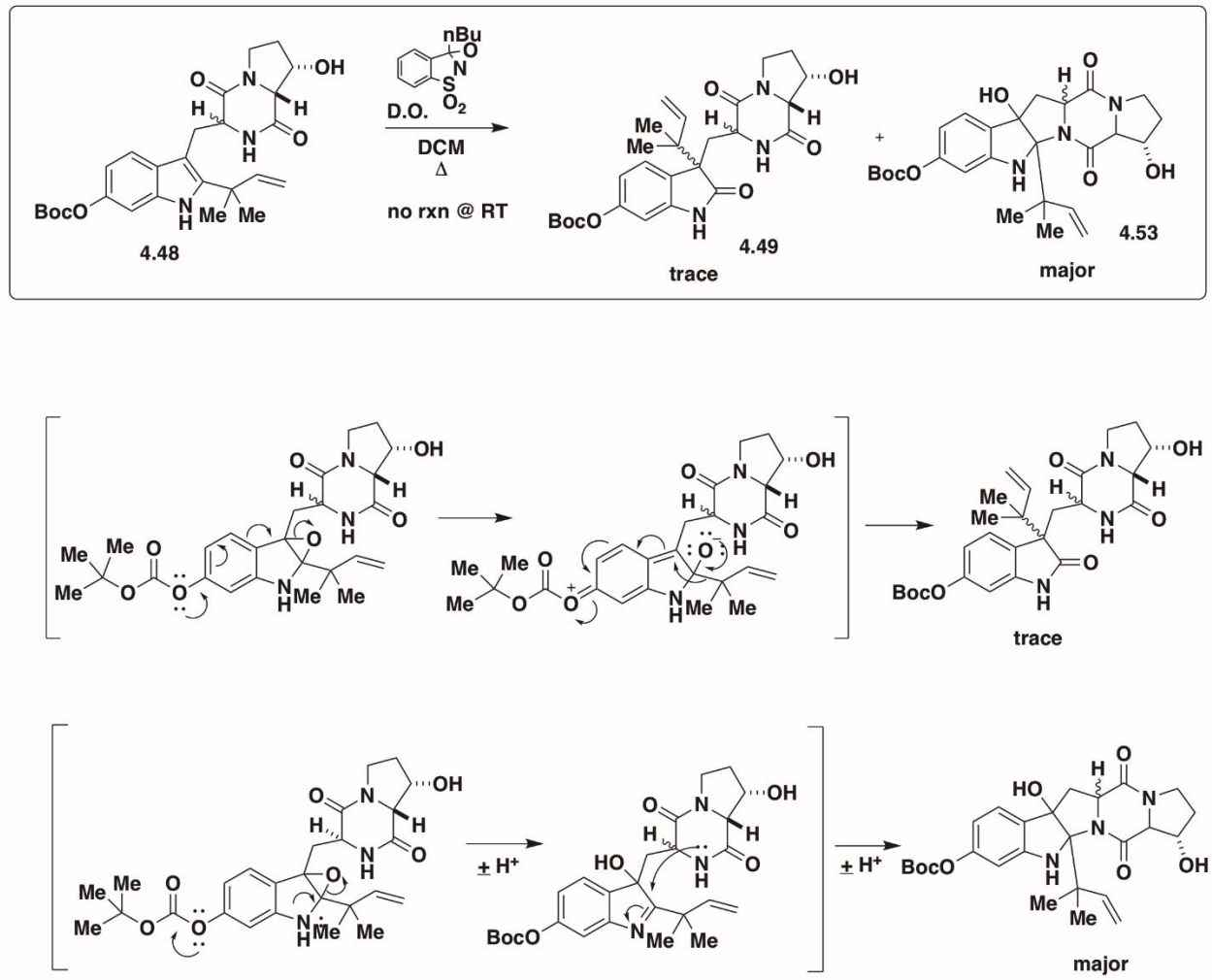


*Figure 4.9.* Oxidation of 3-OBoc diketopiperazine 4.48 with Davis' Oxiziridine and mechanistic rationale for the observed results.

With these results in hand, I found it most reasonable to proceed forward with the model study utilizing the already synthesized model DA compound (Figure 4.4). We found that conversion of the bridged amide in **4.30** to the lactim ether allowed us to open up the bicyclo ring when treated with acid, as long as we could trap the resulting amine as a salt and immediately oxidize or protect it. This transformation created a lot of issues because the ring continuously wanted to collapse back onto itself. However, we were able to find success with this transformation on both the indole and spirooxindole scaffolds. We came across many challenges with the oxidation step as well, because all other conditions that were tried also caused the ring

to collapse back onto itself, or the material to degrade. This is why we used DMDO, which Sarpong also used in his synthesis.[145] This likely worked because the reaction with DMDO does not form any harsh side products. Once we found success with opening the bicyclo ring and were able to effectively protect the amide, we could hydrolyze the ester to the carboxylic acid. Decarboxylation through Curtius type conditions was also found successful by Dr. Ikeuchi. Most importantly from these results, we can conclude that we successfully figured out how to open the azabicylo ring in a similar way that we believe nature intended.

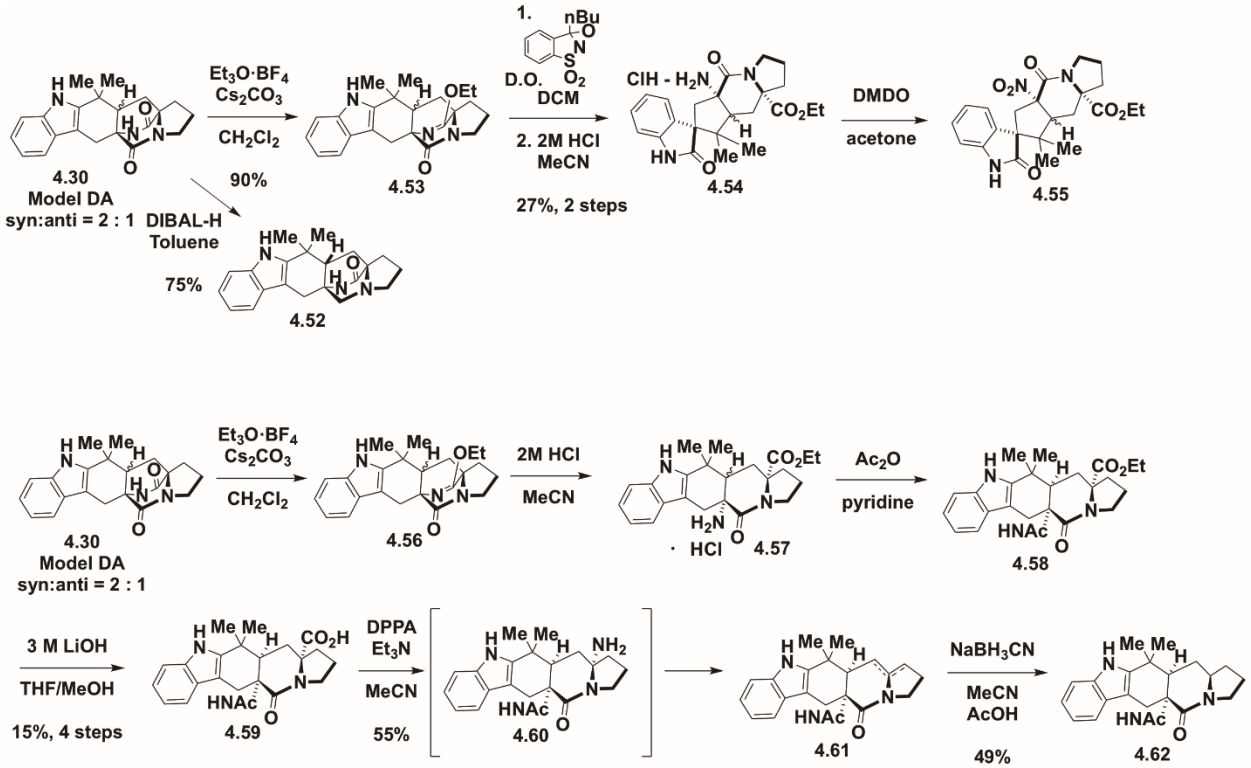


*Figure 4.10.* Completed model study work by Klas and Ikeuchi.

## V. Conclusions and Future Directions

Based on what we have learned from initial efforts on the model study, we can foresee implementing the model chemistry in a linear manner before applying it to the natural products (Figure 4.11). Selective reduction of the tertiary amide proceeds forward in good yields (see

Figure 4.10). From reduced substrate **4.52**, the spirooxindole should be able to form in the presence of Davis' Oxaziridine. If this does not work, then the spiro- compound can be formed before the selective reduction is implemented. Formation of the lactim ether in **4.64** will allow for opening of the azabicyclo ring, followed by immediate protection, reduction, and decarboxylation to form compound **4.69**. deprotection of the amine and oxidation to form the characteristic nitro group should provide us with citrinalin A model substrate **4.71**. From here, we will be able to explore the nitro mannich reaction to form citrinalin B model substrate **4.72**.

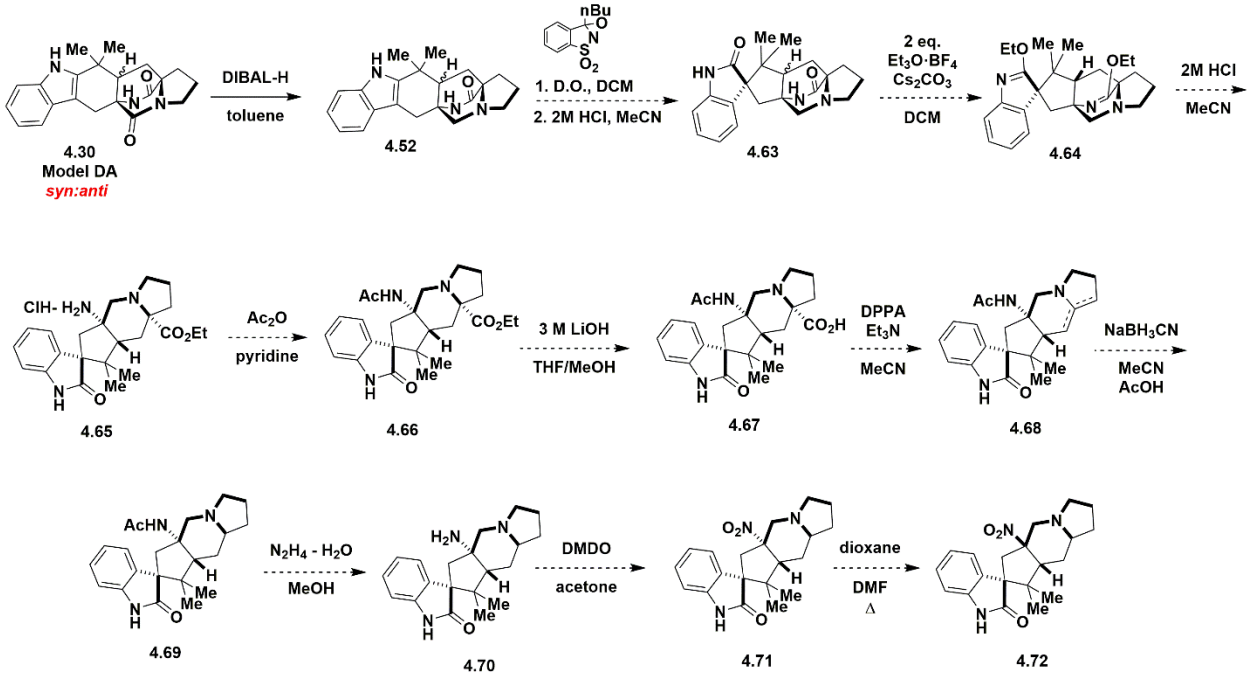


*Figure 4.11.* Future directions for the model study.

From our work on the citrinalins, we have learned more about the reactivity of the Pinacol reaction among the substituted and non-substituted substrates. Even though initial work on the model study led to a dead-end, these results created a foundation of knowledge that allowed us to find a lot of rapid initial success in the brevianamide project (Chapter 5).

While model studies can sometimes be very useful in understanding new chemical transformations quickly, very small changes in the electronics can hugely impact results among the different scaffolds. We found this to be the case with our model study. However, we were able to work through many challenges and successfully open the azabicyclo core. This is truly impactful for this project and will aid in synthesizing the natural products. Utilizing what we learned from the model study and what we know from Sarpong's synthesis of *ent*-citrinalin B, we can carefully plan an educated synthetic route to the citrinalins from versicolamide B (Figure 4.12).

Deprotection of the previously synthesized Boc protected 3-OH prenylated indole, followed by Pd-catalyzed allylic alkylation and Claisen rearrangement yields compound **4.76**. Cyclodehydrogenation allows for formation of the pyran ring on indole **4.77**. Pinacol rearrangement of diketopiperazine **4.82** with Davis' Oxaziridine successfully yields the spirooxidindole that ultimately undergoes the intramolecular Diels-Alder reaction to form versicolamide B as the major product. We then should be able to implement the chemistry we established in the model study to synthesize citrinalin A. From here, we can look at the efficacy of the Nitro-Mannich reaction for the formation of citrinalin B.

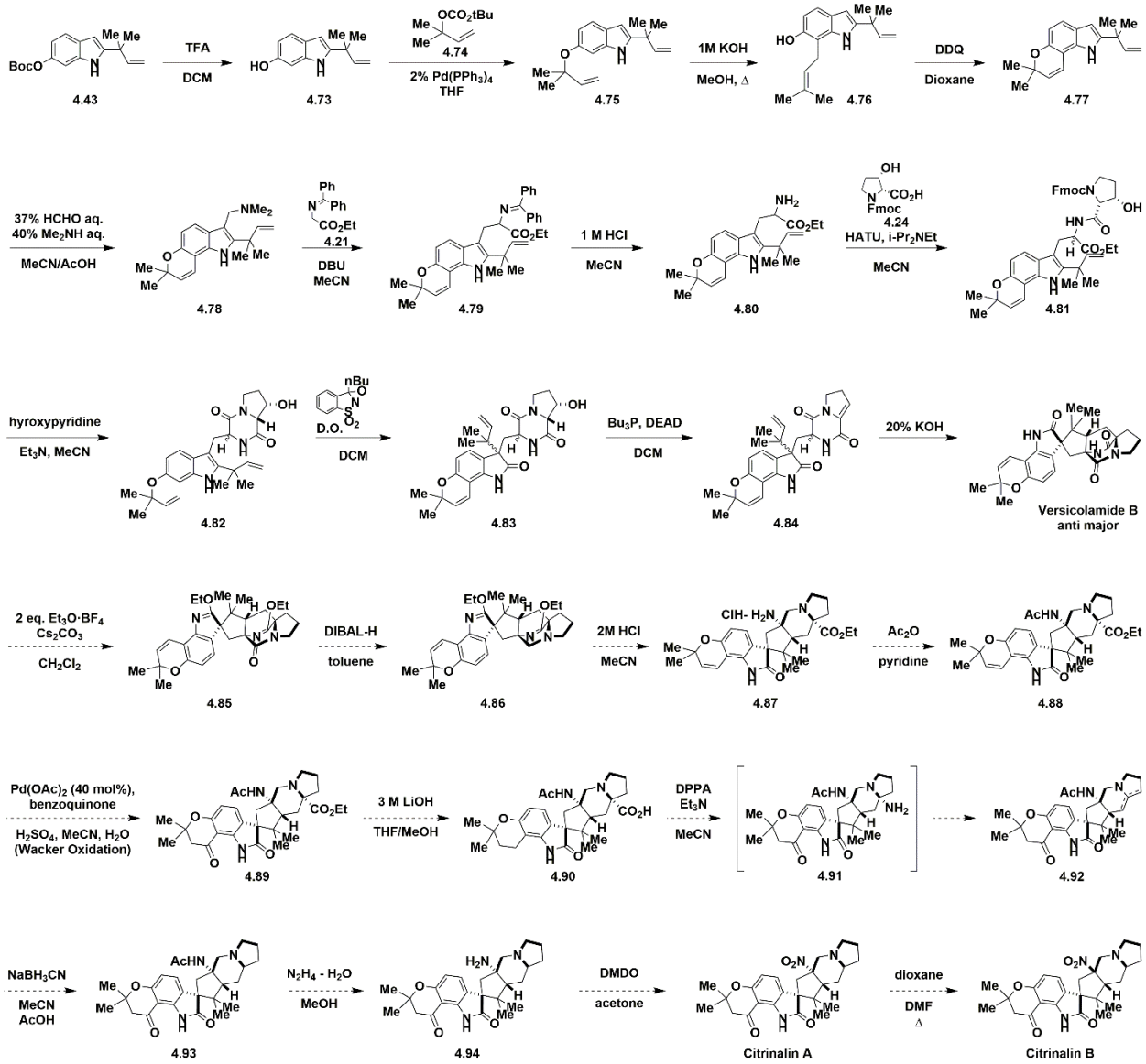


*Figure 4.12.* The planned total synthesis of Citrinalins A and B.

# Chapter 5: Toward the Total Synthesis of Bvn3/Brevianamide Y and Brevianamide A

## I. Introduction

The brevianamides were first discovered in 1969 by Birch and Wright when brevianamide A was isolated from *Penicillium brevicompactum* (Figure 5.1).[70] Brevianamide B was isolated shortly after,[71-72] which was followed by a total synthesis (Figure 5.2) reported by our group in 1998.[78-79] These metabolites present an indole-derived moiety (spiroindoxyl) that arise from the oxidation and Pinacol rearrangement of indole and is unique among all the genera. Bvn3, also known as brevianamide Y, was recently isolated by our group in 2018. The observance of this metabolite created more structural diversity (exhibiting a spirooxindole, which has been observed in other species and is too derived from the oxidation and Pinacol rearrangement of the indole) among this family of metabolites and more stereochemical diversity within the entire class of prenylated indole alkaloids.

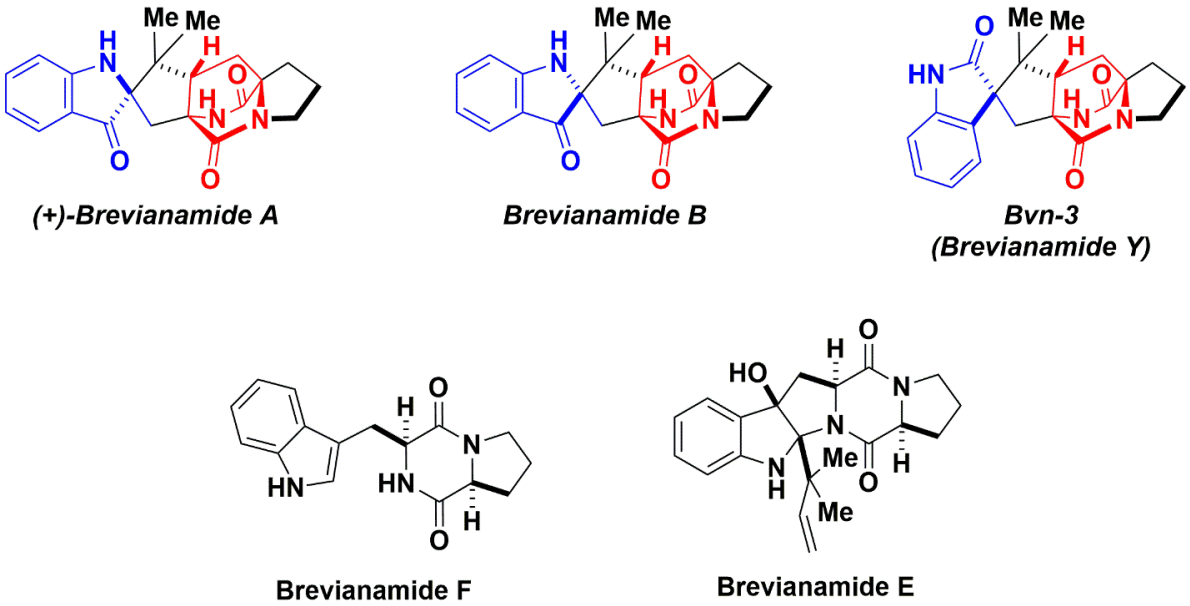


*Figure 5.1.* Isolated metabolites from *Penicillium brevicompactum.*

These metabolites present an interesting stereochemical challenge. The structural hindrance is determined by the stereochemistry at the indole unit in relation to the bicyclo core stereochemistry (Figure 5.2). For this reason, brevianamide A has yet to be synthesized since its 1969 isolation and is why we have been able to successfully synthesize all of the less hindered diastereomers, but not their more hindered counterparts. However, it was upon the very recent isolation of Bvn3 and the observance of the more hindered *para*-methoxy benzyl (pMB) protected analog of **5.5** from synthetic studies reported by our group in 1989[62] *(vide infra)* that provided us with an idea on how to make all of these compounds.

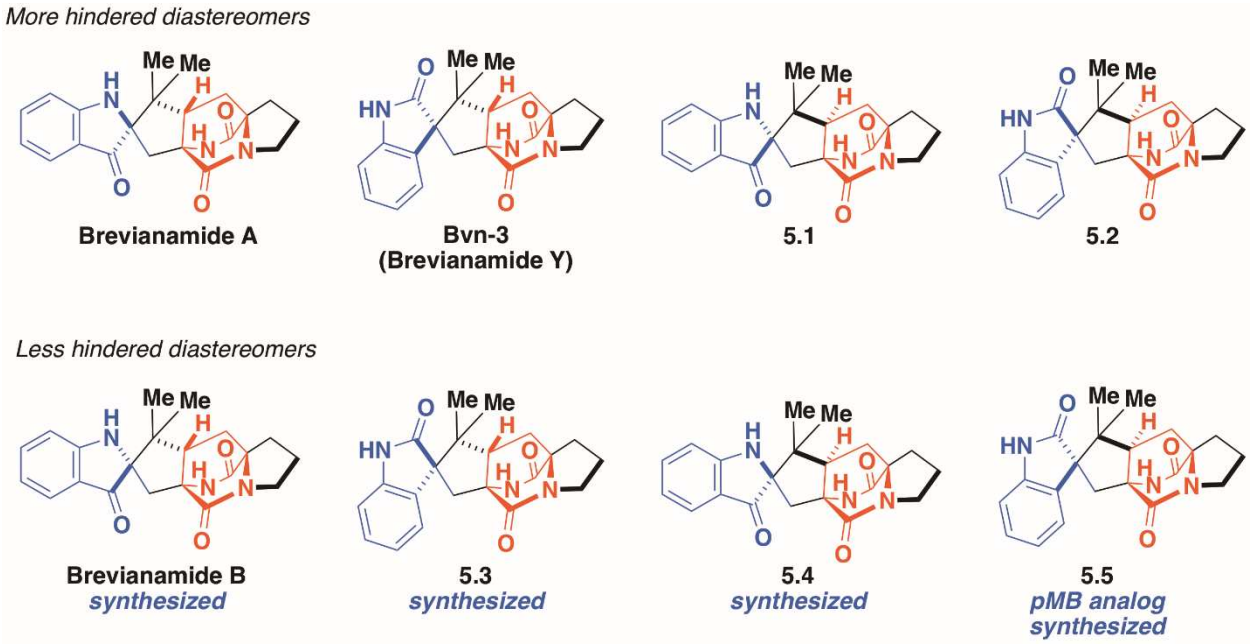


*Figure 5.2.* Stereochemistry of the brevianamides.

## II. Previous Work and Syntheses of the Brevianamides

The synthesis of oxindoles **5.11** and **5.12** was reported by Williams *et*. *al.* in 1989 (Figure 5.1).[62] In an attempt to synthesize target compound **5.11** from pMB protected **5.8** with *tert*-butyl hypochlorite, low levels of the more hindered compound were observed. This is likely due to the presence of the pMB group on the backside (less hindered side) of the molecule, ultimately

reducing facial selectivity of the oxidation. However, the presence of this product (hindered syn-product) later motivated us to explore the total synthesis of newly isolated metabolite Bvn3/brevianamide Y (hindered anti- product).

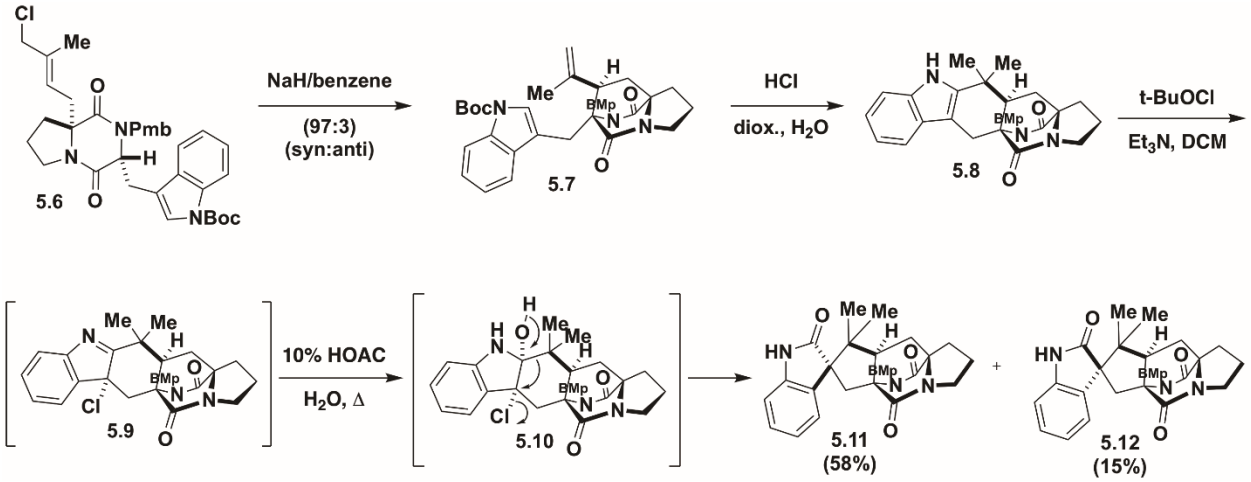


*Figure 5.1.* Synthesis of both diastereomers of the pMB spirooxindole analogs.

The total synthesis of brevianamide B was reported in 1998 by Williams *et. al.* Facial selective oxidation at the indole unit of lactim ether **5.16** yields hydroxyindoline **5.18** via a non-isolatable epoxide intermediate. Treatment of the hydroxyindoline with base yields the spiroindoxyl in brevianamide B. It is important to note that brevianamide B was synthesized as the sole diastereomer, exhibiting anti- stereochemistry at the azabicyclo unit and less hinderance at the indoxyl unit. The less hindered oxindole can be made as the sole product from the same hydroxyindoline intermediate under acidic conditions. It can be concluded from all of the syntheses that have been reported to date, the only observance of the more hindered spiro compounds was in the 1989 synthesis of the pMB oxindole analogs. At this point, we had only explored accessing these metabolites from the Diels-Alder product, with the azabicyclo core stereochemistry already established. It can be reasoned that if the stereochemistry at the azabicyclo core is already set, then we will less likely be able to access the more hindered spiro

compounds. This is because the oxidation preceding the Pinacol rearrangement must occur solely on the less hindered face of the molecule.

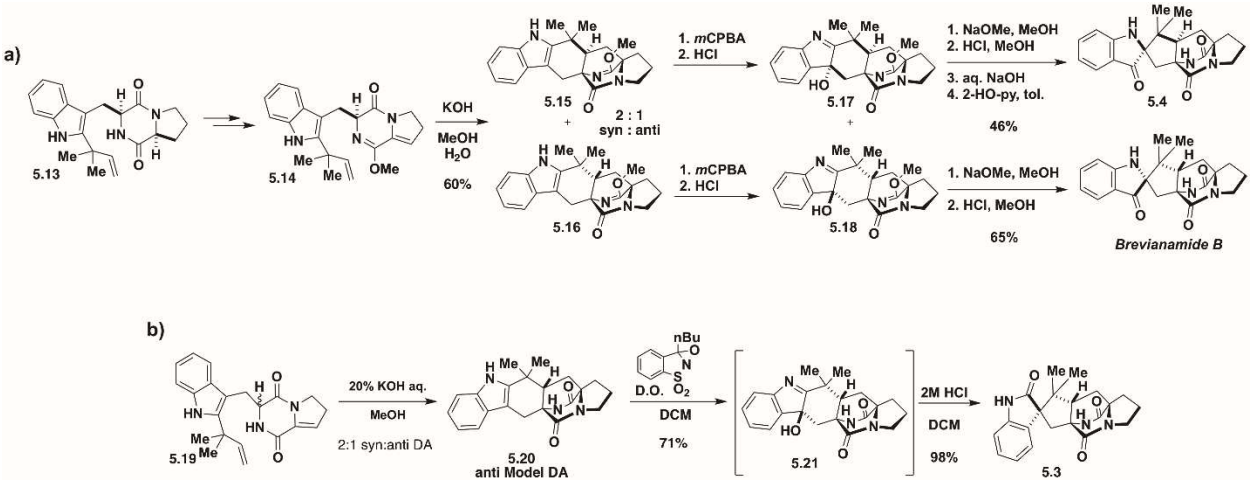


*Figure 5.2.* Synthesis of brevianamide B, less hindered indoxyl **5.5**, and less hindered oxindole **5.3**.

## III. Synthetic Efforts Toward Brevianamide A and Brevianamide Y (Bvn3)

In developing our route to access the more hindered metabolites, Bvn3 and brevianamide A, we aim to establish the stereochemistry at the indole unit with the Pinacol reaction before setting the stereochemistry at the azabicyclo core with the IMDA reaction. I briefly had explored this transformation utilizing Davis' Oxaziridine as the oxidant (Figure 5.3a). This transformation did not work due to the inability to form the epoxide on the inactivated indole. However, we used this scaffold to further troubleshoot this transformation, utilizing conditions that would proceed through a different intermediate. We decided to use the *t*-butyl hypochlorite conditions that were used in the 1989 synthesis since we had already established a precedent for its transformation on a similar analog and because it proceeds through a chloroindoline intermediate, rather than the epoxide.

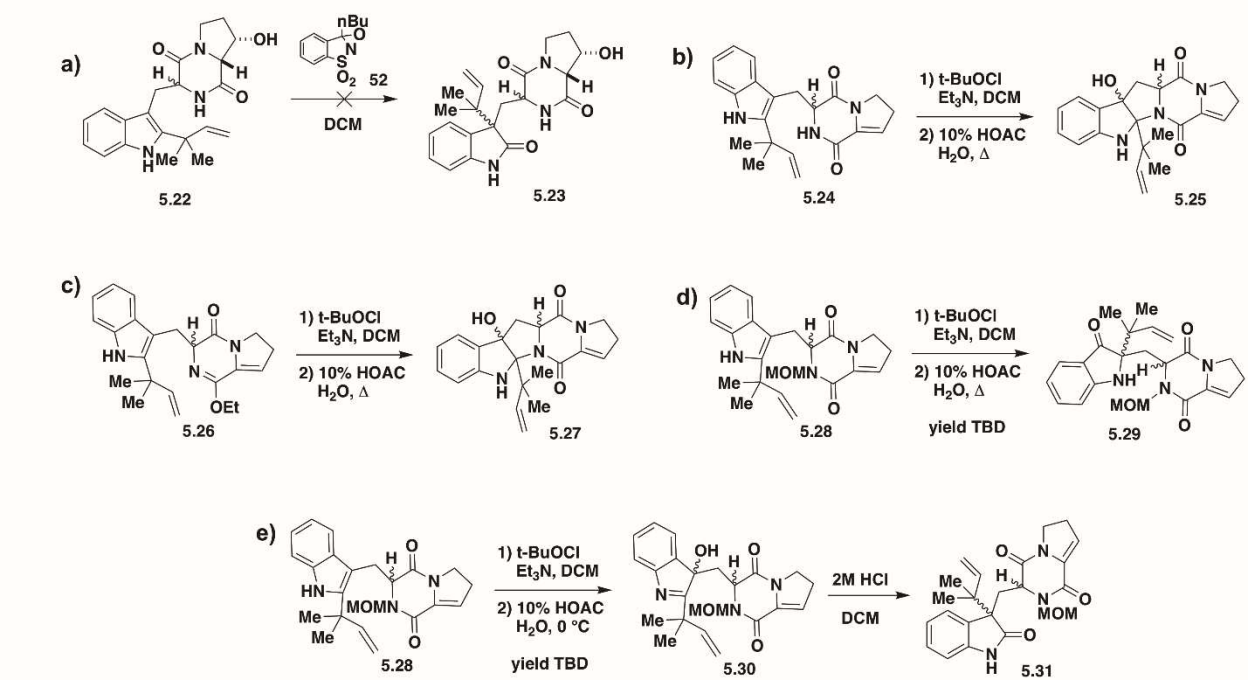


*Figure 5.3.* Synthetic studies to overcome the stereochemical conundrum among the brevianamides by Kimberly Klas (a) and Morgan McCauley (b-e).

Initial attempts with the *t*-butyl hypochlorite conditions proved to successfully oxidize the indole; however, it confirmed that protection of the amide is necessary to avoid cyclization onto the indole unit via the chloroindoline intermediate, forming the undesired hydroxyl product (Figure 5.3b). In choosing a protecting group, we need to consider easy removal without the group being too labile under acidic conditions. Even though we know pMB works as a protecting group and may also help aid in the formation of the more hindered product, we don't want to use it because earlier synthetic studies proved it near impossible to remove. We first explored the use of the lactim ether as the protecting group, but we found that it was too labile and could not hold up to the oxidation conditions (Figure 5.3c). However, the use of MOM has proven to be very promising. The use of the tbutyl hypochlorite conditions on MOM protected diketopiperazine **5.28** formed a mixture of diastereomers of the indoxyl product in the presence of heat (Figure 5.3d). However, when the reaction was run at 0°C, the hydroxyindoline

intermediate was observed as a mixture of diastereomers of similar abundance. From here, the use of acid drives the reaction forward to the oxindole (Figure 5.3e). This data proves that we have begun to overcome this stereochemical conundrum.

## IV. Future Directions for the Total Synthesis of Brevianamide A and Brevianamide Y (Bvn3)

Future directions for this project are underway and include exploring deprotection conditions to remove the MOM group while avoiding the undesired beta-hydride elimination side reaction. Once this is achieved, the IMDA reaction will be explored, ultimately revealing natural metabolites Bvn3 and brevianamide A (Figure 5.4). Since the stereochemically unfavored products are being sought out, harsher conditions for the IMDA reaction may be required to achieve these natural metabolites. This is an incredibly exciting discovery that helps us further understand the stereochemical diversity among these metabolites. It also opens up many more opportunities for synthesizing a number other metabolites.

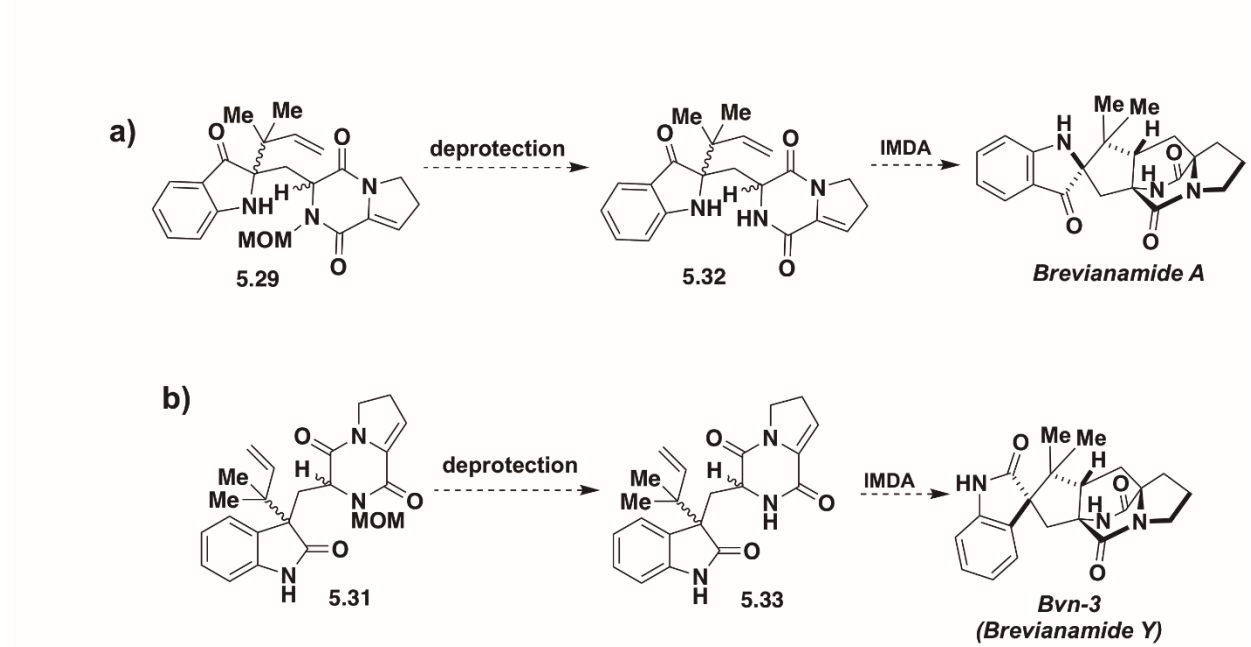


*Figure 5.4.* Future directions for synthesizing the brevianamides.

## V. New Biosynthetic Insights

Upon the isolation of Bvn3 and with the new synthetic data, we can begin to better understand the construction of these stereochemically hindered metabolites. With these findings, we can better speculate how these metabolites are formed in nature. Brevianamides A, B, and Y likely converge on the same hydroxyindoline intermediate. From here, we can envision the Pinacol rearrangement to proceed through two different mechanisms to yield indoxyl **5.35** and oxindole **5.36**. These spiro compounds can then undergo an IMDA reaction through their corresponding achiral azadiene intermediate to produce the anti- metabolites. Providing access to synthetic **5.35** and **5.36**, as well as their enamine counter parts, would be of use and should strongly be considered for feeding studies. Once we achieve this, as well as the biomimetic total syntheses of brevianamide A and Bvn3, we will be able to provide corroborative evidence for the proposed unique construction of the brevianamides and have uncovered an authentic pathway for the biosynthesis of this family of prenylated indole alkaloids.

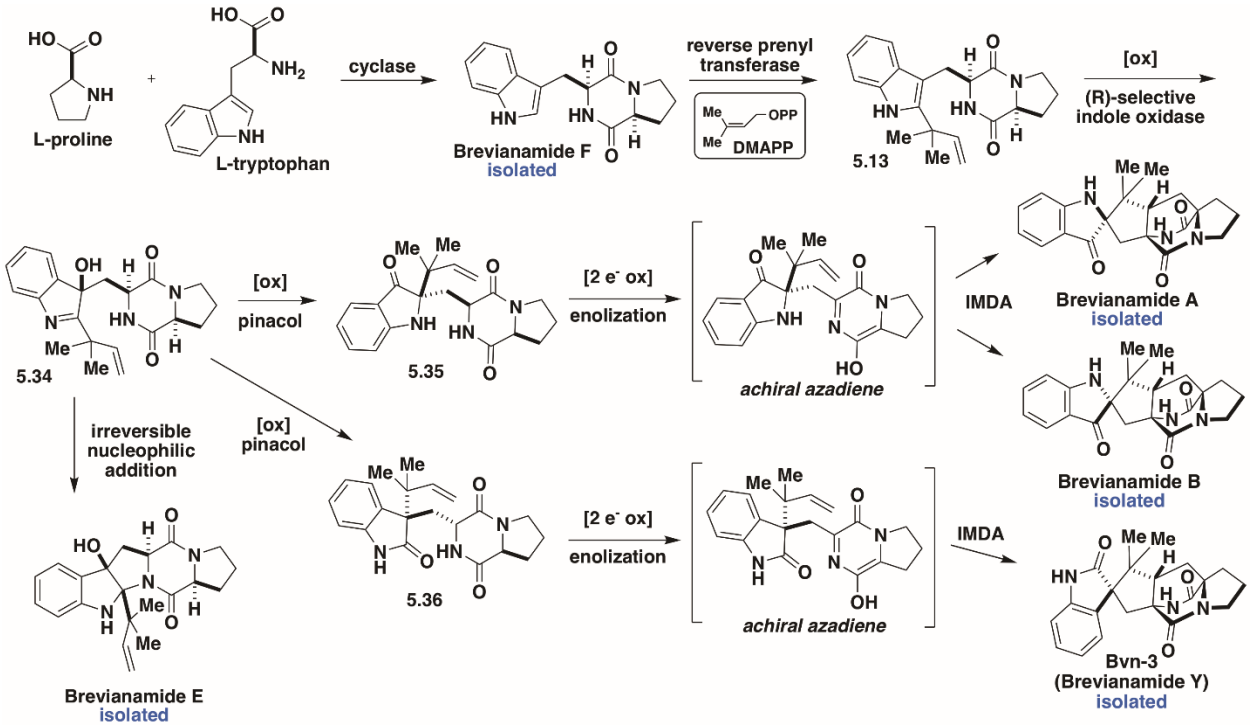


*Figure 5.5.* New proposed biosynthesis of the brevianamides.

# References


1. Klas, K. R.; Kato, H.; Frisvad, J. C.; Yu, F.; Newmister, S. A.; Fraley, A. E.; Sherman, D. H.; Tsukamoto, S.; Williams, R., Structural and stereochemical diversity in prenylated indole alkaloids containing the bicyclo[2.2.2]diazaoctane ring system from marine and terrestrial fungi. *Nat. Prod. Rep.* **2018,** *35*, 532-558.
2. Finefield, J. M.; Frisvad, J. C.; Sherman, D. H.; Williams, R. M., Fungal Origins of the Bicyclo[2.2.2]diazaoctane Ring System of Prenylated Indole Alkaloids. *J. Nat. Prod.* **2012,** *75*, 812-833.
3. Finefield, J. M.; Sherman, D. H.; Kreitman, M.; Williams, R. M., Enantiomeric Natural Products: Occurrence and Biogenesis. *Angew. Chem. Int. Ed.* **2012,** *51*, 4802-4836.
4. Williams, R. M., Paraherquamide Review. *Chem. Pharm. Bull.* **2002,** *50*, 711-740.
5. Stocking, E. M.; Williams, R. M., chemistry and biology of biosynthetic diels-alder reactions. *Angew. Chem. Int. Ed.* **2003,** *42*, 3078-3115.
6. Williams, R. M.; Cox, R. J., paraherquamides, brevianamides, and asperparalines: laborator synthesis and biosynthesis. an interim report. *Acc. Chem. Res.* **2003,** *36*, 127-139.
7. Miller, K. A.; Williams, R. M., synthetic approaches to the bicyclo [2.2.2] ring system *Chem. Soc. Rev.* **2009,** *38*, 3160-3174.
8. Sunderhaus, J. D.; Sherman, D. H.; Williams, R. M., Studies of the Biosynthesis of the Stephacidin and Notoamide Natural Products: A Stereochemical and Genetic Conundrum. *Isr. J. Chem.* **2011,** *51*, 442-452.
9. Williams, R. M.; Cox, R. J., Paraherquamides, Brevianamides, and Asperparalines: Laboratory Synthesis and Biosynthesis. An Interim Report. *Acc. Chem. Res.* **2003,** *36* (2), 127-139.
10. Li, S.; Srinivasan, K.; Tran, H.; Yu, F.; Finefield, J. M.; Sunderhaus, J. D.; McAfoos, T. J.; Tsukamoto, S.; Williams, R. M.; Sherman, D. H., Comparative analysis of the biosynthetic systems for fungal bicyclo[2.2.2]diazaoctane indole alkaloids: the (+)/(-)-notoamide, paraherquamide and malbrancheamide pathways. *Med. Chem. Comm.* **2012,** *3* (8), 987-996.
11. Williams, R. M.; Stocking, E. M.; Sanz-Cervera, J. F., *Top. Curr. Chem.* **2000,** *209*, 97-173.
12. Porter, A. E. A.; Sammes, P. G., *Chem. Commun.* **1970**, 1103.
13. Baldas, J.; Birch, A. J.; Russell, R. A., *J. Chem. Soc. Perkin Trans.* **1974,** *1*, 50.
14. Ding, Y.; Wet, J. R. d.; Cavalcoli, J.; Li, S.; Greshock, T. J.; Miller, K. A.; Finefield, J. M.; Sunderhaus, J. D.; McAfoos, T. J.; Tsukamoto, S.; Williams, R. M.; Sherman, D. H., Genome-Based Characterization of Two Prenylation Steps in the Assembly of the Stephacidin and Notoamide Anticancer Agents in a Marine-Derievd Aspergillus sp. *J. Am. Chem. Soc.* **2010,** *132*, 12733-12740.
15. Domingo, L. R.; Zaragozá, R. J.; Williams, R. M., thereotical studies on IMDA. *J. Org. Chem.* **2003,** *68*, 2895-2902.
16. Domingo, L. R.; Sanz-Cervera, J. F.; Williams, R. M.; Picher, M. T.; Marco, J. A., ab initio study on IMDA. *J. Org. Chem.* **1997,** *62*, 1662-1667.
17. Adams, L. A.; Gray, C. R.; Williams, R. M., *Tetrahedron Lett.* **2004,** *45*, 4489-4493.
18. Sanz-Cervera, J. F.; Williams, R. M., *J. Am. Chem. Soc.* **2002,** *124*, 2556-2559.

19. Stocking, E. M.; Sanz-Cervera, J. F.; Williams, R. M., *J. Am. Chem. Soc.* **2000,** *122*, 1675-1683.
20. Sanz-Cervera, J. F.; Williams, R. M.; Marco, J. A.; López-Sánchez, J. M.; González, F.; Martínez, M. E.; Sancenón, F., *Tetrahedron Lett.* **2000,** *56*, 6345-6358.
21. Williams, R. M.; Sanz-Cervera, J. F.; Sancenón, F.; Marco, J. A.; Halligan, K. M., *Bioorg. Med. Chem.* **1998,** *6*, 1233-1241.
22. Klas, K.; Tsukamoto, S.; Sherman, D. H.; Williams, R. M., Natural Diels-Alderases: Elusive and Irresistable. *J. Org. Chem.* **2015,** *80*, 11672-11685.
23. Kagiyama, I.; Kato, H.; Nehira, T.; Frisvad, J. C.; Sherman, D. H.; Williams, R. M.; Tsukamoto, S., Taichunamides biosynth. *Angew. Chem. Int. Ed.* **2016,** *55*, 1128-1132.
24. Kato, H.; Nakahara, T.; Sugimoto, K.; Matsuo, K.; Kagiyama, I.; Frisvad, J. C.; Sherman, D. H.; Williams, R. M.; Tsukamoto, S., isolation of Not Sand 6-epi-steph A from a .amoenus. *Org. Lett.* **2015,** *17*, 700-703.
25. McAfoos, T. J.; Li, S.; Tsukamoto, S.; Sherman, D. H.; Williams, R. M., Biosynth studies of Stephs and Nots, Total synth Not S. *Heterocycles* **2010,** *82*, 461-472.
26. Sunderhaus, J. D.; McAfoos, T. J.; Finefield, J. M.; Kato, H.; Li, S.; Tsukamoto, S.; Sherman, D. H.; Williams, R. M., Synth of Not T and Steph A and Biocoversion of Not T into STeph A and Not B. *Org. Lett.* **2013,** *15*, 22-25.
27. Kato, H.; Nakahara, T.; Yamaguchi, M.; Kagiyama, I.; Finefield, J. M.; Sunderhaus, J. D.; Sherman, D. H.; Williams, R. M.; Tsukamoto, S., bioconversion of C6 Not T in a. protuberus. *Tetrahedron Lett.* **2015,** *56*, 247-251.
28. Miller, K. A.; Tsukamoto, S.; Williams, R. M., assym. total synth of versi B. *Nature Chem.* **2009,** *1*, 63-68.
29. Tsukamoto, S.; Kawabata, T.; Kato, H.; Greshock, T. J.; Hirota, H.; Ohta, T.; Williams, R. M., isolation of (-)-Versi B and Nots L-N from Marine Derived Asp. sp. *Org. Lett.* **2009,** *11*, 1297-1300.
30. Tsukamoto, S.; Umaoka, H.; Yoshikawa, K.; Ikeda, T.; Hirota, H., Not O, P-R isolation from a. protuberus. *J. Nat. Prod.* **2010,** *73*, 1438-1440.
31. Li, S.; Finefield, J. M.; Sunderhaus, J. D.; McAfoos, T. J.; Williams, R. M.; Sherman, D. H., NotB biochemical characterization. *J. Am. Chem. Soc.* **2012,** *134*, 788-791.
32. Finefield, J. M.; Kato, H.; Greshock, T. J.; Sherman, D. H.; Tsukamoto, S.; Williams, R. M., Biosyth studies Nots. isotope synth of Steph A. incorp into Not B. *Org. Lett.* **2011,** *13*, 3802-3805.
33. Tsukamoto, S.; Kato, H.; Greshock, T. J.; Hirota, H.; Ohta, T.; Williams, R. M., NotE isolation. *J. Am. Chem. Soc.* **2009,** *131*, 3834-3835.
34. Kato, H.; Nakamura, Y.; FInefield, J. M.; Umaoka, H.; Nakahara, T.; Williams, R. M.; Tsukamoto, S., biosynth of nots: pinacol-type rearr. of isoprenyl unit in deoxyvrev E and 6-hydroxybrev E. *Tetrahedron Lett.* **2011,** *52*, 6923-6926.
35. Kato, H.; Yoshida, T.; Tokue, T.; Nojiri, Y.; Hirota, H.; Ohta, T.; Williams, R. M.; Tsukamoto, S., Nots A-D isolation. *Angew. Chem. Int. Ed.* **2007,** *46*, 2254-2256.
36. Finefield, J. M.; Greshock, T. J.; Sherman, D. H.; Tsukamoto, S.; Williams, R. M., Not E: biosynth incorp into Nots C and D in a. amoenus. *Tetrahedron Lett.* **2011,** *52*, 1987-1989.
37. Finefield, J. M.; Sherman, D. H.; Tsukamoto, S.; Williams, R. M., Biosynth incorp into Not J. *J. Org. Chem.* **2011,** *76*, 5954-5958.
38. Cai, S.; Luan, Y.; Kong, X.; Zhu, T.; Gu, Q.; Li, D., *Org. Lett.* **2013,** *15*, 2168-2171.

39. Qian-Cutrone, J.; Huang, S.; Shu, Y.-Z.; Vyas, D.; Fairchild, C.; Menendez, A.; Krampitz, K.; Dalterio, R.; Klohr, S. E.; Gao, Q., Stephs A and B in Asp. Och. *J. Am. Chem. Soc.* **2002,** *124*, 14556-14557.
40. Grubbs, A. W.; ArtmanIII, G. D.; Williams, R. M., Synthesis of stephs aspergamides and norgeamides. *Tetrahedron Lett.* **2005,** *46*, 9013-9016.
41. ArtmanIII, G. D.; Grubbs, A. W.; Williams, R. M., assym. stephs A, B Not B. *J. Am. Chem. Soc.* **2007,** *129*, 6336-6342.
42. Baran, P. S.; Hafensteiner, B. D.; Ambhaikar, N. B.; Guerrero, C. A.; Gallagher, J. D., assym. synth. of avrainvillamide and stephacidins (Baran). *J. Am. Chem. Soc.* **2006,** *128*, 8678-8693.
43. Finefield, J. M.; Williams, R. M., Synthesis of Not J. *J. Org. Chem.* **2010,** *75*, 2785-2789.
44. Greshock, T. J.; Grubbs, A. W.; Jiao, P.; Wicklow, D. T.; Gloer, J. B.; Williams, R. M., Isolation, Structure Elucidation, and Biomimetic Total Synthesis of Versi B, and the Isolation of antipodal (-)-Stephacidin A and (+)-Notoamide B from a. amoenus. *Angew. Chem. Int. Ed.* **2008,** *47*, 3573-3577.
45. Greshock, T. J.; Grubbs, A. W.; Tsukamoto, S.; Williams, R. M., A Concise, Biomimetic Total Synthesis of Stephacidin A and Notoamide B. *Angew. Chem. Int. Ed.* **2007,** *46* (13), 2262-2265.
46. Greshock, T. J.; Grubbs, A. W.; Tsukamoto, S.; Williams, R. M., Biomimetic total synth of Steph A and Not B. *Angew. Chem. Int. Ed.* **2007,** *46*, 2262-2265.
47. Cox, R. J.; Williams, R. M., synthetic studies towards paraherquamide F *Tetrahedron Lett.* **2002,** *43*, 2149-2152.
48. Martínez-Luis, S.; Rodríguez, R.; Acevedo, L.; González, M. C.; Lira-Rocha, A.; Mata, R., Malbrancheamide, a new calmodulin inhibitor from the fungus Malbranchea aurantiaca. *Tetrahedron* **2006,** *62* (8), 1817-1822.
49. Figueroa, M.; Gonzalez Mdel, C.; Mata, R., Malbrancheamide B, a novel compound from the fungus Malbranchea aurantiaca. *Natural product research* **2008,** *22* (8), 709-714.
50. Fraley, A. E.; Garcia-Borràs, M.; Tripathi, A.; Khare, D.; Mercado-Marin, E. V.; Tran, H.; Dan, Q.; Webb, G. P.; Watts, K. R.; Crews, P.; Sarpong, R.; Williams, R. M.; Smith, J. L.; Houk, K. N.; Sherman, D. H., Function and Structure of MalA/MalA', Iterative Halogenases for Late-Stage C–H Functionalization of Indole Alkaloids. *J. Am. Chem. Soc.* **2017,** *139* (34), 12060-12068.
51. Ding, Y.; Greshock, T. J.; Miller, K. A.; Sherman, D. H.; Williams, R. M., Premalbrancheamide: Synthesis, Isotopic Labeling, Biosynthetic Incorporation, and Detection in Cultures of Malbranchea aurantiaca. *Org. Lett.* **2008,** *10* (21), 4863-4866.
52. Watts, K. R.; Loveridge, S. T.; Tenney, K.; Media, J.; Valeriote, F. A.; Crews, P., Utilizing DART Mass Spectrometry to Pinpoint Halogenated Metabolites from a Marine Invertebrate-Derived Fungus. *J. Org. Chem.* **2011,** *76* (15), 6201-6208.
53. Yamazaki, M.; Okuyama, E.; Kobayashi, M.; Inoue, H., The structure of paraherquamide, a toxic metabolite from penicillium paraherquei. *Tetrahedron Lett.* **1981,** *22* (2), 135-136.
54. Ding, Y.; Gruschow, S.; Greshock, T. J.; Finefield, J. M.; Sherman, D. H.; Williams, R. M., Detection of VM55599 and Preparaherquamide from Aspergillus japonicus and Penicillium fellutanum: Biosynthetic Implications. *J. Nat. Prod.* **2008,** *71* (9), 1574-1578.
55. Williams, R. M., Total Synthesis and Biosynthesis of the Paraherquamides: An Intriguing Story of the Biological Diels-Alder Construction. *Chem. Pharm. Bull.* **2002,** *50* (6), 711-740.

56. Stocking, E. M.; Sanz-Cervera, J. F.; Unkefer, C. J.; Williams, R. M., Studies on the biosynthesis of paraherquamide. Construction of the amino acid framework. *Tetrahedron* **2001,** *57* (25), 5303-5320.
57. Liesch, J. M.; Wichmann, C. F., Novel antinematodal and antiparasitic agents from Penicillium charlesii. II. Structure determination of paraherquamides B, C, D, E, F, and G. *J. Antibiot.* **1990,** *43* (11), 1380-1386.
58. Stocking, E. M.; Sanz-Cervera, J. F.; Williams, R. M., Studies on the Biosynthesis of Paraherquamide: Synthesis and Incorporation of a Hexacyclic Indole Derivative as an Advanced Metabolite. *Angew. Chem. Int. Ed.* **2001,** *40* (7), 1296-1298.
59. Sommer, K.; Williams, R. M., Studies on paraherquamide biosynthesis: synthesis of deuterium-labeled 7-hydroxy-pre-paraherquamide, a putative precursor of paraherquamides A, E, and F. *Tetrahedron* **2009,** *65* (16), 3246-3260.
60. Stocking, E. M.; Sanz-Cervera, J. F.; Williams, R. M.; Unkefer, C. J., Studies on the Biosynthesis of Paraherquamide A. Origin of the β-Methylproline Ring. *J. Am. Chem. Soc.* **1996,** *118* (29), 7008-7009. Addition/Correction: J. Am. Chem. Soc., 1997, 119, 9588.
61. Stocking, E. M.; Martinez, R. A.; Silks, L. A.; Sanz-Cervera, J. F.; Williams, R. M., Studies on the Biosynthesis of Paraherquamide: Concerning the Mechanism of the Oxidative Cyclization of l-Isoleucine to β-Methylproline. *J. Am. Chem. Soc.* **2001,** *123* (14), 3391-3392.
62. Williams, R. M.; Glinka, T.; Kwast, E., Synthetic studies on paraherquamide: Regioselectivity of indole oxidation. *Tetrahedron Letters* **1989,** *30* (41), 5575-5578.
63. Williams, R. M.; Cushing, T. D., Synthetic studies on paraherquamide: synthesis of the 2H-1,5. Benzodioxepin ring system. *Tetrahedron Lett.* **1990,** *31* (44), 6325-6328.
64. Adams, L. A.; Gray, C. R.; Williams, R. M., Concise synthesis of the core bicyclo[2.2.2]diazaoctane ring common to asperparaline, paraherquamide, and stephacidin alkaloids. *Tetrahedron Lett.* **2004,** *45* (23), 4489-4493.
65. Williams, R. M.; Cao, J., Studies on the total synthesis of paraherquamide A. Stereocontrolled, asymmetric synthesis of α-alkyl-β-hydroxyproline derivatives. *Tetrahedron Lett.* **1996,** *37* (31), 5441-5444.
66. Lee, B. H.; Clothier, M. F., Conversion of Marcfortine A to Paraherquamide A via Paraherquamide B. The First Formal Synthesis of Paraherquamide A. *J. Org. Chem.* **1997,** *62* (6), 1795-1798.
67. Williams, R. M.; Cao, J.; Tsujishima, H., Asymmetric, Stereocontrolled Total Synthesis of Paraherquamide A. *Angew. Chem. Int. Ed.* **2000,** *39* (14), 2540-2544.
68. Sommer, K.; Williams, R. M., Studies Towards Paraherquamides E & F and Related C-labeled Putative Biosynthetic Intermediates: Stereocontrolled Synthesis of the alpha-Alkyl-beta-Methylproline Ring System. *Tetrahedron* **2008,** *64* (30), 7106-7111.
69. Shoop, W. L.; Egerton, J. R.; Eary, C. H.; Suhayda, D., Anthelmintic Activity of Paraherquamide in Sheep. *J. Parasitol.* **1990,** *76* (3), 349-351.
70. Birch, A. J.; Wright, J. J., The Brevianamides: A New Class of Fungal Alkaloid. *J. Chem. Soc., Chem. Commun.* **1969,** (12), 644b-645.
71. Birch, A. J.; Wright, J. J., Studies in relation to biosynthesis—XLII: The structural elucidation and some aspects of the biosynthesis of the brevianamides-A and -E. *Tetrahedron* **1970,** *26* (10), 2329-2344.

72. Birch, A. J.; Russell, R. A., Studies in relation to biosynthesis—XLIV: Structural elucidations of brevianamides-B, -C, -D and -F. *Tetrahedron* **1972,** *28* (11), 2999-3008.
73. Domingo, L. R.; Sanz-Cervera, J. F.; Williams, R. M.; Picher, M. T.; Marco, J. A., Biosynthesis of the Brevianamides. An ab Initio Study of the Biosynthetic Intramolecular Diels−Alder Cycloaddition. *J. Org. Chem.* **1997,** *62* (6), 1662-1667.
74. Sanz-Cervera, J. F.; Glinka, T.; Williams, R. M., Biosynthesis of brevianamides A and B: in search of the biosynthetic diels-alder construction. *Tetrahedron* **1993,** *49* (38), 8471-8482.
75. Baldas, J.; Birch, A. J.; Russell, R. A., Studies in relation to biosynthesis. Part XLVI. Incorporation of cyclo-L-tryptophyl-L-proline into brevianamide A. *J. Chem. Soc., Perkin Trans. 1* **1974,** (0), 50-52.
76. Kato, H.; Nakamura, Y.; Finefield, J. M.; Umaoka, H.; Nakahara, T.; Williams, R. M.; Tsukamoto, S., Study on the biosynthesis of the notoamides: pinacol-type rearrangement of the isoprenyl unit in deoxybrevianamide E and 6-hydroxydeoxybrevianamide E. *Tetrahedron Lett.* **2011,** *52* (51), 6923-6926.
77. Miller, K. A.; Welch, T. R.; Greshock, T. J.; Ding, Y.; Sherman, D. H.; Williams, R. M., Biomimetic Total Synthesis of Malbrancheamide and Malbrancheamide B. *J. Org. Chem.* **2008,** *73* (8), 3116-3119.
78. Williams, R. M.; Sanz-Cervera, J. F.; Sancenón, F.; Marco, J. A.; Halligan, K., Biomimetic Diels−Alder Cyclizations for the Construction of the Brevianamide, Paraherquamide Sclerotamide, and VM55599 Ring Systems. *J. Am. Chem. Soc.* **1998,** *120* (5), 1090-1091.
79. Williams, R. M.; Sanz-Cervera, J. F.; Sancenón, F.; Marco, J. A.; Halligan, K. M., Biomimetic diels–alder cyclizations for the construction of the brevianamide, paraherquamide, sclerotamide, asperparaline and VM55599 ring systems. *Bioorg. Med. Chem.* **1998,** *6* (8), 1233-1241.
80. Sanz-Cervera, J. F.; Williams, R. M.; Alberto Marco, J.; Marı; x; a López-Sánchez, J.; González, F.; Eugenia, M.; x; nez, M.; x; Sancenón, F., A Synthetic Model for the [4+2] Cycloaddition in the Biosynthesis of the Brevianamides, Paraherquamides, and Related Compounds. *Tetrahedron* **2000,** *56* (34), 6345-6358.
81. Adams, L. A.; Valente, M. W. N.; Williams, R. M., A concise synthesis of d,l-brevianamide B via a biomimetically-inspired IMDA construction. *Tetrahedron* **2006,** *62* (22), 5195-5200.
82. Klas, K.; Tsukamoto, S.; Sherman, D. H.; Williams, R. M., Natural Diels–Alderases: Elusive and Irresistable. *J. Org. Chem.* **2015,** *80* (23), 11672-11685.
83. Laschat, S., Pericyclic Reactions in Biological Systems--Does Nature Know About the Diels-Alder Reaction? *Angew. Chem. Int. Ed.* **1996,** *35*, 289-291.
84. Woodward, R. B.; Katz, T., The Mechanism of the Diels Alder Reaction. *Tetrahedron* **1959,** *5*, 70.
85. Dewar, M. J. S.; Olivella, S.; Rzepa, H. S., Ground States of Molecules. 40. MINDO/3 Study of the Retro-Diels-Alder Reaction of Cyclohexene. *J. Am. Chem. Soc.* **1978,** *100*, 5650-5660.
86. Dewar, M. J. S.; Griffin, A. C.; Kirschner, S., MINDO/3 Study of Some Diels-Alder Reactions. *J. Am. Chem. Soc.* **1974,** *96*, 6225-6226.
87. Dewar, M. J. S.; Olivella, S.; Stewart, J. J. P., Mechanism of the Diels Alder Reaction: Reactions of Butadiene with Ethylne and Cyanoethylenes. *J. Am. Chem. Soc.* **1986,** *108*, 5771-5779.
88. Dewar, M. J. S., Multibond Reactions Cannot Normally Be Synchronous. *J. Am. Chem. Soc.* **1984,** *106*, 209-219.

89. Li, Y.; Houk, K. N., Diels-Alder Dimerization of 1, 3-Butadiene: An an Initio CASSCF Study of the Concerted and Stepwise Mechanisms and Butadiene-Ethylene Revisited. *J. Am. Chem. Soc.* **1993,** *115*, 7478-7485.
90. Beno, B. R.; Wilsey, S.; Houk, K. N., The C7H10 Potential Energy Landscape: Concerted Transition States and Diradical Intermediates for the Retro-Diels-Alder Reaction and [1, 3] Sigmatropic Shifts of Norbornene. *J. Am. Chem. Soc.* **1999,** *121*, 4816-4826.
91. Chen, J. S.; Houk, K. N.; Foote, C. S., Theoretical Study of the Concerted and Stepwise Mechanisms of Triazolinedione Diels-Alder Reactions. *J. Am. Chem. Soc.* **1998,** *120*, 12303-12309.
92. Townshend, R. E.; Ramunni, G.; Segal, G.; Hehre, W. J.; Salen, L., Organic Transition States. V. The Diels-Alder Reaction. *J. Am. Chem. Soc.* **1976,** *98*, 2190-2098.
93. Burke, L. A.; Leroy, G.; Sana, M., *Theor. Chim. Acta* **1975,** *40*, 313.
94. Bernardi, F.; Bottini, A.; Robb, M. A.; Field, M. J.; Hillier, I. H.; Guest, M. F., Towards an Accurate ab initio Calculation of the Transition State Structures of the Diels-Alder Reaction. *J. Chem. Soc., Chem. Commun.* **1985**, 1051-1052.
95. Gajewski, J. J.; Peterson, K. B.; Kagel, J. R.; Huang, Y. C. J., Transition-State Structure Variation in the Diels-Alder Reaction from Secondary Deuterium Kinetic Isotope Effects: The Reaction of Nearly Symmetrical Dienes and Dienophiles Is Nearly Synchronous. *J. Am. Chem. Soc.* **1989,** *111*, 9078-9081.
96. Loncharich, R. J.; Brown, F. K.; Houk, K. N., Transition Structures of the Diels-Alder Reaction of Butadiene with Acrolein. *J. Org. Chem.* **1989,** *54*, 1129-1135.
97. Bernardi, F.; Bottoni, A.; Field, M. J.; Guest, M. F.; Hillier, I. H.; Robb, M. A.; Venturini, A., MC-SCF Study of the Diels-Alder Reaction between Ethylene and Butadiene. *J. Am. Chem. Soc.* **1988,** *110*, 3050-3055.
98. McIver, J. W., *J. Am. Chem. Soc.* **1975,** *97*, 3632.
99. McIver, J. W., *Acc. Chem. Res.* **1974,** *7*, 72.
100. Singleton, D. A., Isotope effects and the distinction between synchronous, asynchronous, and stepwise Diels-Alder reactions. *Tetrahedron* **2001,** *57*, 5149-5160.
101. Hancock, R. A.; Wood, B. F., Evidence for Non-biradicaloid Transition States in Diels-Alder Reactions. *J. Chem. Soc., Chem. Commun.* **1988**, 351-353.
102. Froese, R. D. J.; Coxon, J. M.; West, S. C.; Morokuma, K., Theoretical Studies of DIels-ALder REactions of Acetylenic COmpounds. *j. org. chem.* **1997,** *62*, 6991-6996.
103. Singleton, D. A.; Thomas, A. A., High-Precision Simultaneous Determination of Multiple Small Kinetic Isotope Effects at Natural Abundane. *J. Am. Chem. Soc.* **1995,** *117*, 9357-9358.
104. Oikawa, H.; Katayama, K.; Suzuki, Y.; Ichihara, A., Enzymatic Activity Catalysing Exo-selective Diels-Alder Reaction in Solanapyrone Biosynthesis. *J. Chem. Soc., Chem. Commun.* **1995**, 1321-1322.
105. Oikawa, H.; Suzuke, Y.; Naya, A.; Katayama, K.; Ichihara, A., First Direct Evidence in Biological Diels-Alder Reaction of Incorporation of Diene-Dienophile Precursors in the Biosynthesis of Solanapyrones. *J. Am. Chem. Soc.* **1994,** *116*, 3605-3606.
106. Katayama, K.; Kobayashi, T.; Oikawa, H.; Honma, M.; Ichihara, A., partial purification and properties of solanapyrone synthase. *Biochim. Biophys. Acta* **1998,** *1384*, 387-395.
107. Oikawa, H.; Kobayashi, T.; Katayama, K.; Suzuki, Y.; Ichihara, A., Total Synthesis of (-)-Solanapyrone A via Enzymatic Diels-ALder Reaction of Prosolanapyrone. *J. Org. Chem.* **1998,** *63*, 8748-8756.

108. Kashara, K.; Miyamoto, T.; Fujimoto, T.; Oguri, H.; TOkiwano, T.; Oikawa, H.; Ebizuka, Y.; Fujii, I., Solanapyrone Synthase, a Possible Diels-Alderase and Iterative Tupe I Polyketide Synthase Encoded in a BIosynthetic Gene Cluster from Alternaria solani. *ChemBioChem* **2010,** *11*, 1245-1252.
109. Auclair, K.; Sutherland, A.; Kennedy, J.; Witter, D. J.; Heever, J. P. V. d.; Hutchinson, C. R.; Vederas, J. C., Lovastatin Nonaketide Synthase Catalyzes an Intramolecular Diels-Alder Reaction of a Substrate Analogue. *J. Am. Chem. Soc.* **2000,** *122*, 11519-11520.
110. Ma, S. M.; Li, J. W.; Choi, J. W.; Zhou, H.; Lee, K. K.; Moorthie, V. A.; Xie, X.; Kealey, J. T.; DaSilva, N. A.; Vederas, J. C.; Tang, Y., Complete Reconstitution of a Highly Reductin Iterative Polyketide Synthase. *Science* **2009,** *326*, 589-593.
111. Kennedy, J.; Auclair, K.; Kendrew, S. G.; Park, C.; Vederas, J. C.; Hutchinson, C. R., LNKS for pyrone formation. *Science* **1999,** *284*, 1368-1372.
112. Watanabe, K.; Mie, T.; Ichihara, A.; Oikawa, H.; Honma, M., Detailed Reaction Mechanism of Macrophomate Synthase. *The Journal of Biological Chemistry* **2000,** *275* (49), 38393-38401.
113. Ose, T.; Watanabe, H.; Yao, M.; Tanaka, I.; Watanabe, K.; Mie, T.; Honma, M.; Oikawa, H., Insight into a Diels-Alder reaction from the structure of macrophomate synthase. *Nature* **2003,** *422*, 185-189.
114. Guimaraes, C. R. W.; Udier-Blagovic, M.; Jorgensen, W. L., Macrophomate Synthase: QM/MM Simulations Address the Diels-Alder versus Michael-Aldol Reaction Mechanism. *J. Am. Chem. Soc.* **2005,** *127*, 3577-3588.
115. Serafimov, J. M.; Gillingham, D.; Kuster, S.; Hilvert, D., The Putative Diels-Alderase Macrophomate Synthase is an Efficient Aldolase. *J. Am. Chem. Soc.* **2008,** *130*, 7798-7799.
116. Minami, A.; Oikawa, H., Recent advances of Diels–Alderases involved in natural product biosynthesis. *J. Antibiot.* **2016,** *69*, 500.
117. Eberhardt, S. Z., N.; Kemter, K.; Richter, G.; Cushman, M.; Bacher, A., Domain Structure of Riboflavin Synthase. *Eur. J. Biochem.* **2001,** *268*, 4315-4323.
118. Kim, R.; Illarionov, B.; Joshi, M.; Cushman, M.; Lee, C. Y.; Eisenreich, W.; Fischer, M.; Bacher, A., Mechanistic Insights on Riboflavin Synthase Inspired by Selective Binding of the 6,7-Dimethyl-8-fibityllumazine Exomethylene Anion. *J. Am. Chem. Soc.* **2010,** *132*, 2983-2990.
119. Kim, H. J.; Ruszczycky, M. W.; Choi, S.-h.; Liu, Y.-n.; Liu, H.-w., Enzyme-catalysed [4 + 2] cycloaddition is a key step in the biosynthesis of spinosyn A. *Nature* **2011,** *473*, 109-112.
120. Fage, C. D.; Isiorho, E. A.; Liu, Y.; Wagner, D. T.; Liu, H., The Structure of SpnF, a standalone enzyme that catalyzes [4+2] cycloaddition. *Nature* **2015,** *11*, 256-260.
121. Ding, W.; Williams, D. R.; Northcote, P.; Siegel, M. M.; Tsao, R.; Ashcroft, J.; Morton, G. O.; Alluri, M.; Abbanat, D.; Maiese, W. M.; Ellestad, G. A., Pyrroindomycins, novel antibiotics produced by Streptomyces rugosporus sp. LL-42D005. I. Isolation and structure determination *J. Antibiot.* **1994,** *47*, 1250-1257.
122. Singh, M. P.; Petersen, P. J.; Jacobus, N. V.; Mroczenski-Wildey, M. J.; Maiese, W. M.; Greenstein, M.; Steinberg, D. A., *J. Antibiot.* **1994,** *47*, 1258-1265.
123. Tian, Z.; Sun, P.; Yan, Y.; Wu, Z.; Zheng, Q.; Zhou, S.; Zhang, H.; Yu, F.; Jia, X.; Chen, D.; Mandi, A.; Kurtan, T.; Liu, W., An enzymatic [4+2] cyclization cascade creates the pentacyclic core of pyrroindomycins. *Nature* **2015,** *11*, 259-268.
124. Zheng, Q.; Guo, Y.; Yang, L.; Zhao, Z.; Wu, Z.; Zhang, H.; Liu, J.; Cheng, X.; Wu, J.; Yang, H.; Jiang, H.; Pan, L.; Liu, W., Enzyme-Dependent [4 + 2] Cycloaddition Depends on Lid-like Interaction

of the N-Terminal Sequence with the Catalytic Core in PyrI4. *Cell. Chem. Biol.* **2016,** *23* (3), 352-60.
125. Zheng, Q.; Gong, Y.; Guo, Y.; Zhao, Z.; Wu, Z.; Zhou, Z.; Chen, D.; Pan, L.; Liu, W., Structural Insights into a Flavin-Dependent [4 + 2] Cyclase that Catalyzes trans-Decalin Formation in Pyrroindomycin Biosynthesis. *Cell. Chem. Biol.* **2018,** *25* (6), 718-727.e3.
126. Byrne, M. J.; Lees, N. R.; Han, L.-C.; van der Kamp, M. W.; Mulholland, A. J.; Stach, J. E. M.; Willis, C. L.; Race, P. R., The Catalytic Mechanism of a Natural Diels–Alderase Revealed in Molecular Detail. *J. Am. Chem. Soc.* **2016,** *138* (19), 6095-6098.
127. Ohashi, M.; Liu, F.; Hai, Y.; Chen, M.; Tang, M.-c.; Yang, Z.; Sato, M.; Watanabe, K.; Houk, K. N.; Tang, Y., SAM-dependent enzyme-catalysed pericyclic reactions in natural product biosynthesis. *Nature* **2017,** *549*, 502.
128. Wever, W. J.; Bogart, J. W.; Baccile, J. A.; Chan, A. N.; Schroeder, F. C.; Bowers, A. A., Chemoenzymatic Synthesis of Thiazolyl Peptide Natural Products Featuring an Enzyme-Catalyzed Formal [4+2] Cycloaddition. *J. Am. Chem. Soc.* **2015**.
129. Li, S.; Srinivasan, K.; Tran, H.; Yu, F.; Finefield, J. M.; Sunderhaus, J. D.; McAfoos, T. J.; Tsukamoto, S.; Williams, R. M.; Sherman, D. H., Comparative Analysis of the Biosynthetic Systems for Fungal Bicyclo[2.2.2]diazaoctane Indole Alkaloids: The (+)/(-)-Notoamide, Paraherquamide and Malbrancheamide Pathways. *Med. Chem. Commun.* **2012,** *3*, 987-996.
130. Finefield, J. M.; Frisvad, J.; Williams, R. M., Fungal Origins of the Bicyclo[2.2.2]diazaoctane Ring System of Prenylated Indole Alkaloids. *J. Nat. Prod.* **2012,** *75*, 812-833.
131. Sunderhaus, J. D.; Williams, R. M., Studies on the Biosynthesis of the Stephacidin and Notoamide Natural Products: A Stereochemical and Genetic Conundrum. *Israel J. Chem.* **2011,** *51*, 442-452.
132. Ding, Y.; Wet, J. R. d.; Cavalcoli, J.; Li, S.; Greshock, T. J.; Miller, K. A.; Finefield, J. M.; Sunderhaus, J. D.; McAfoos, T.; Tsukamoto, S.; Williams, R. M.; Sherman, D. H., Genome-based Characterization of Two Prenylation Steps in the Assembly of the Stephacidin and Notoamide Anticancer Agents in a Marine Aspergillus sp. . *J. Am. Chem. Soc.* **2010,** *132*, 12733-12740.
133. Townsend, C. A., A "Diels-Alderase" At Last. *ChemBioChem* **2011,** *12*, 2267-2269.
134. Romesberg, F. E.; Spiller, B.; Schultz, P. G.; Stevens, R. C., Immunological Origins of Binding and Catalysis in a DIels-Alderase Antibody. *Science* **1998,** *279*, 1929-1934.
135. Xu, J.; Deng, Q.; Chen, J.; Houk, K. N.; Bartek, J.; Hilvert, D.; Wilson, I. A., Evolution of Shape Complementarity and Catalytic Efficiency from a Primordial Antibody Template. *Science* **1999,** *286*, 2345-2349.
136. Piatesi, A.; Hilvert, D., Immunological Optimization of a Generic Hydrophobic Pocket for High Affinity Hapten Binding and Diels-Alder Activity. *ChemBioChem* **2004,** *5*, 460-466.
137. Braisted, A. C.; Schultz, P. G., An Antibody-Catalyzed Bimolecular DIels-Alder Reaction. *J. Am. Chem. Soc.* **1990,** *112*, 7430-7431.
138. Hilvert, D.; Hill, K. W.; Nared, K. D.; Auditor, M.-T. M., Antibody Catalysis of a Diels-Alder Reaction. *J. Am. Chem. Soc.* **1989,** *111*, 9261-9262.
139. Piatesti, A.; Aldag, C.; Hilvert, D., Switching Antibody Specificity through Minimal Mutation. *J. Mol. Biol.* **2008,** *377*, 993-1001.
140. Verdino, P.; Aldag, C.; Hilvert, D.; Wilson, I. A., Closely related antibody receptors exploit fundamentally different strategies for steroid recognition. *PNAS* **2008,** *105*, 11725-11730.

141. Finefield, J. M.; Sherman, D. H.; Kreitman, M.; Williams, R. M., Enantiomeric Natural Products: Occurrence and Biogenesis. *Angew. Chem. Int. Ed.* **2012,** *51* (20), 4802-4836.
142. Stocking, E. M.; Williams, R. M., Chemistry and Biology of Biosynthetic Diels–Alder Reactions. *Angew. Chem. Int. Ed.* **2003,** *42* (27), 3078-3115.
143. Dan, Q.; Newmister, S. A.; Klas, K. R.; Fraley, A. E.; McAfoos, T. J.; Somoza, A. D.; Sunderhaus, J. D.; Ye, Y.; Shende, V. V.; Yu, F.; Sanders, J. N.; Brown, W. C.; Zhao, L.; Paton, R. S.; Houk, K. N.; Smith, J. L.; Sherman, D. H.; Williams, R. M., Fungal Indole Alakloid Biogenesis Through Evolution of a BIfunctional Reductase/Diels-Alderase. **2018**, http://doi.org/10.26434/chemrxiv.7505486.v1 (published on-line December 26, 2018).
144. Dan, Q.; Newmiter, S. A.; Klas, K. R.; Fraley, A. E.; McAfoos, T. J.; Somoza, A. D.; Sunderhaus, J. D.; Ye, Y.; Shende, V. V.; Yu, F.; Sanders, J. N.; Brown, W. C.; Zhao, L.; Paton, R. S.; Houk, K. N.; Smith, J. L.; Sherman, D. H.; Williams, R. M., Fungal Indole Alkaloid Biogenesis Through Evolution of a BIfunctional Reductase/Diels-Alderase. *Nat. Chem.* **2019**, (under revision).
145. Mercado-Marin, E. V.; Garcia-Reynaga, P.; Romminger, S.; Pimenta, E. F.; Romney, D. K.; Lodewyk, M. W.; Williams, D. E.; Andersen, R. J.; Miller, S. J.; Tantillo, D. J.; Berlinck, R. G. S.; Sarpong, R., Total synthesis and isolation of citrinalin and cyclopiamine congeners. *Nature* **2014,** *509*, 318-324.
146. Pimenta, E. F.; Vita-Marques, A. M.; Tininis, A.; Seleghim, M. H. R.; Sette, L. D.; Veloso, K.; Ferreira, A. G.; Williams, D. E.; Patrick, B. O.; Dalisay, D. S.; Andersen, R. J.; Berlinck, R. G. S., Use of Experimental Design for the Optimization of the Production of New Secondary Metaboliters by Two Penicillium Species. *J. Nat. Prod.* **2010,** *73*, 1821-1832.
147. Mercardo-Marin, E. V.; Garcia-Reynaga, P.; Romminger, S.; :imenta, E. F.; Romney, D. K.; Lodewyk, M. W.; Williams, D. E.; Anderson, R. J.; Miller, S. J.; Tantillo, D. J.; Berlinck, R. G. S.; Sarpong, R., Total synthesis and isolation of citrinalin and cyclopiamine congeners. *Nature* **2014,** *509*, 318-324.
148. Wood, J. L., Collaborative synthesis. *Nature* **2014,** *509*, 293-294.
149. Greshock, T. J.; Williams, R. M., improved biomimetic total synth of D, L-Steph A. *Org. Lett.* **2007,** *9*, 4255-4258.
150. Domingo, L. R.; Zaragozá, R. J.; Williams, R. M., Studies on the Biosynthesis of Paraherquamide A and VM99955. A Theoretical Study of Intramolecular Diels−Alder Cycloaddition. *J. Org. Chem.* **2003,** *68* (7), 2895-2902.
151. Finefield, J. M.; Williams, R. M., Synthesis of Notoamide J: A Potentially Pivotal Intermediate in the Biosynthesis of Several Prenylated Indole Alkaloids. *J. Org. Chem.* **2010,** *75* (9), 2785-2789.
152. Lerman, L.; Weinstock-Rosin, M.; Nudelman, A., An Improved Synthesis of Hydroxyindoles. *Synthesis* **2004,** (18), 3043-3046.
153. Sommer, K.; Williams, R. M., Synthetic studies toward paraherquamides E and F and related 13C-labeled putative biosynthetic intermediates: stereocontrolled synthesis of the α-alkyl-β-methylproline ring system. *Tetrahedron* **2008,** *64* (30), 7106-7111.
154. Hu, L.-C.; Yonamine, Y.; Lee, S.-H.; van der Veer, W. E.; Shea, K. J., Light-Triggered Charge Reversal of Organic–Silica Hybrid Nanoparticles. *J. Am. Chem. Soc.* **2012,** *134* (27), 11072-11075.
155. Haridasan, V. K.; Pillai, V. N. R., Peptide Synthesis Using Photolytically Cleavable 2-Nitrobenzyloxycarbonyl Protecting Group. *Proc. Indian Natn. Sci. Acad.* **1987,** *53* (6), 717-728.

156. Chong, H.-S.; Song, H. A.; Dadwal, M.; Sun, X.; Sin, I.; Chen, Y., Efficient Synthesis of Functionalized Aziridinium Salts. *J. Org. Chem.* **2010,** *75* (1), 219-221.
157. Davis, F. A.; Towson, J. C.; Vashi, D. B.; ThimmaReddy, R.; McCauley, J. P.; Harakal, M. E.; Gosciniak, D. J., Chemistry of oxaziridines. 13. Synthesis, reactions, and properties of 3-substituted 1,2-benzisothiazole 1,1-dioxide oxides. *J. Org. Chem.* **1990,** *55* (4), 1254-1261.
158. Taber, D. F.; DeMatteo, P. W.; Hassan, R. A., Simplified Preparation of Dimethyldioxirane. *Organic syntheses; an annual publication of satisfactory methods for the preparation of organic chemicals* **2013,** *90*, 350-357
159. Vane, J.; Botting, R., Inflammation and the mechanism of action of anti-inflammatory drugs. *FASEB J.* **1987,** *1* (2), 89-96.
160. Mitchell, J. A.; Warner, T. D., COX isoforms in the cardiovascular system: Understanding the activities of nonsteroidal anti-inflammatory drugs. *Nat. Rev. Drug Discov.* **2006,** *5*, 75-85.
161. Tabas, I.; Glass, C. K., Anti-Inflammatory Therapy in Chronic Disease: Challenges and Opportunities. *Science* **2013,** *339* (6116), 166-172.
162. Li, C.-Y.; Meng, Y.-H.; Ying, Z.-M.; Xu, N.; Hao, D.; Gao, M.-Z.; Zhang, W.-J.; Xu, L.; Gao, Y.-C.; Ying, X.-X., Three Novel Alkaloids from Portulaca oleracea L. and Their Anti-inflammatory Effects. *J. Agric. Food Chem.* **2016,** *64* (29), 5837-5844.
163. Li, C.-Y.; Meng, Y.-H.; Ying, Z.-M.; Xu, N.; Hao, D.; Gao, M.-Z.; Zhang, W.-J.; Xu, L.; Gao, Y.-C.; Stien, D.; Ying, X.-X., Correction to Three Novel Alkaloids from Portulaca oleracea L. and Their Anti-inflammatory Effects. *J. Agric. Food Chem.* **2017,** *65* (4), 993-994.
164. Meng, Y.; Ying, Z.; Xiang, Z.; Hao, D.; Zhang, W.; Zheng, Y.; Gao, Y.; Ying, X., The anti-inflammation and pharmacokinetics of a novel alkaloid from Portulaca oleracea L. *J. Pharm. Pharmacol.* **2016,** *68*, 397-405.
165. Rao, P. P. N.; Kabir, S. N.; Mohamed, T., Nonsteroidal Anti-Inflammatory Drugs (NSAIDs): Progress in Small Molecule Drug Development. *Pharmaceuticals* **2010,** *3* (5), 1530-1549.

# Appendix I: Contributions to Work

## I. Chapter 3

Former postdoc, Jim Sunderhaus, initially worked on the second-generation synthesis of premalbrancheamide (Figure 3.2; route via dieneamine **3.12**). Former postdoc, Tim McAfoos, also worked on the second-generation synthesis of premalbrancheamide. Tim's focus was on the intramolecular diels-alder reaction from the aldehyde, through the dienamine.

Sean Newmister and Dan Qingyun of David Sherman's group in Michigan performed all of the biological data for this project. They also contributed to the experimental design, alongside Robert M. Williams, David H. Sherman, and Janet Smith.

## II. Chapter 4

Former postdoc, Kazutada Ikeuchi performed initial work on the model study with Model DA **4.30** (Figures 4.4 and 4.10; route from **4.30** to **4.62**). His author contribution is also recognized within the chapter.

## III. Chapter 5

Graduate student, Morgan McCauley, performed the chemistry on this project (Figure 5.3b-3e). Kimberly Klas, Morgan McCauley, and Robert M. Williams all contributed to experimental and rational design. Morgan's synthetic contributions are also recognized in the Figure headings within the chapter.

# Appendix II: Supporting Information

## I. Experimentals

### General Chemical Procedures

$^{1}H$ and $^{13}C$ spectra were obtained using 300 MHz, 400 MHz or 500 MHz spectrometers. The chemical shifts are given in parts per million (ppm) relative to residual $CDCl_3$ δ 7.26 ppm, $CD_3OD$ δ 3.31 ppm, $(CD_3)_2CO$ δ 2.05 ppm or $(CD_3)_2SO$ δ 2.50 ppm for proton spectra and relative to $CDCl_3$ at δ 77.23 ppm, $CD_3OD$ δ 49.00 ppm, $(CD_3)_2CO$ δ 29.84 ppm or $(CD_3)_2SO$ δ 39.52 ppm for carbon spectra. IR spectra were recorded on an FT-IR spectrometer as thin films. Mass spectra were obtained using a high/low resolution magnetic sector mass spectrometer. Flash column chromatography was performed with silica gel grade 60 (230-400 mesh). Preparative TLC was performed with silica gel 60 $F_{254}$ 20 x 20 cm plates. Unless otherwise noted materials were obtained from commercially available sources and used without further purification. Dichloromethane ($CH_2Cl_2$), tetrahydrofuran (THF), N, N-dimethylformamide (DMF), acetonitrile ($CH_3CN$), triethylamine ($Et_3N$), and methanol (MeOH) were all degassed with argon and passed through a solvent purification system containing alumina or molecular sieves in most cases.

We attempted to coalesce rotomeric peaks by heating to 100°C. In some cases it was successful, and others it was not. Reports show data of rotomeric compounds taken at 100°C in DMSO.

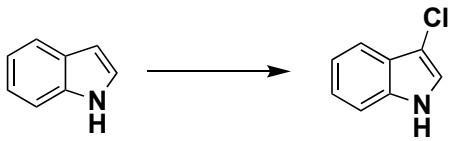


**Chlorinated Indole 3.1.** NCS (18 g, 135 mmol) was added to a solution of indole **3.1** in DMF (375 mL) and the reaction was stirred at room temperature for 3 h. The solution was added saturated aqueous NaCl (200 mL) and washed with EtOAc (3 x 200 mL). The combined organic phase was washed with $H_2O$ (375 mL), saturated aqueous NaCl (375 mL), then dried ($Na_2SO_4$), filtered and concentrated under reduced

pressure. The crude reside was purified by flash chromatography, eluting with 10% - 50% EtOAc/Hex to yield chlorinated indole **3.1** as a yellow solid. $^{1}$H NMR (400 MHz, $CDCl_3$, 25 °C) $\delta$ 8.02 (bs, 1H), 7.67 (d, *J* = 7.84 Hz, 1 H), 7.36 (d, *J* = 7.92 Hz, 1 H), 7.09 (m, 2 H), 7.17 (d, *J* = 2.52 Hz, 1H).; $^{13}$C NMR (400 MHz, $CDCl_3$, 25 °C) $\delta$ 135.07, 125.51, 123.27, 120.94, 120.60, 118.40, 111.60, 106.69.

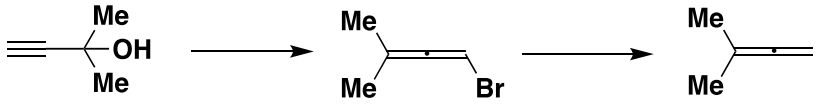


**Allene.** A mixture of 2-methyl-3-butyn-2-ol (90 mL) in pentane (225 mL) were added dropwise to a solution of $NH_4Br$ (37.35 g), CuBr (46.65 g), and Cu (2.37 g) in HBr (180 mL) at room temperature, then stirred at 30 °C for 3 h. The crude mixture was filtered over glass wool, washed with HBR (2 x equal parts), $H_2O$ (3 x equal parts), dried @ 0 °C ($MgSO_4$), filtered through an $SiO_2$ plug, and concentrated @ 0 °C under reduced pressure to yield bromoallene.

Bromoallene (74.2 g, 505 mmol) was added dropwise to a solution of Zn dust (42.8 g, 656 mmol) in AcOH (400 mL) at 50 °C. The temperature was gradually increased to 75 °C and the product was collected via short path distillation apparatus to yield allene as a clear liquid. All spectra matched that of previously reported.

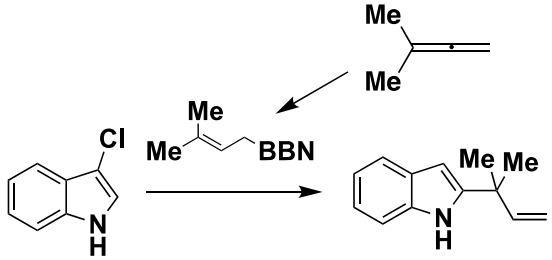


**Prenylated Indole 3.3.** Allene (70.12 mmol, 6.95 mL) was added to 9BBN (0.5M in THF, 58.43 mmol, 117 mL) at 0 °C. The solution was allowed to warm to room temperature and ran for 18 h. Chlorinated indole **3.1** (19.86 mmol, 3 g) was added to the solution at room temperature and stirred for 15 min. $Et_3N$ (59.00 mmol, 8.23 mL) was added and the reaction ran for 8 h at the same temperature. The resulting solution was washed with 1 M HCl (140 mL), then $NaHCO_3$ (140 mL). The organics were cooled to 0 °C then added 2 M NaOH (125 mL) and $H_2O_2$ (125 mL), subsequently, while maintaining an internal temperature of 0-5 °

C. The resulting solution was allowed to warm to room temperature and stir for 1.5 h. The resulting mixture was partitioned then the aqueous layer was washed with $Et_2O$ (2 x 280 mL). The combined organics were washed with saturated aqueous NaCl (2 x 140 mL), dried ($MgSO_4$), filtered, and concentrated under reduce pressure. Purification by flash chromatography eluting with 3 % - 5 % EtOAc/Hexanes yielded 2 g (60%) prenylated indole **3.3** as a yellow solid. $^1$H NMR (400 MHz, $CDCl_3$, 25 °C) $\delta$ 7.89 (bs, 1 H), 7.57 (d, *J* = 7.76 Hz, 1 H), 7.31 (d, *J* = 7.52 Hz, 1 H), 7.15 (t, *J* = 7.12 Hz, 1 H), 7.09 (t, *J* = 7.80 Hz, 1 H), 6.34 (s, 1 H), 6.07 (dd, *J* = 10.28, 17.64 Hz, 2 H), 5.16 (d, *J* = 5.36 Hz, 1 H), 5.12 (s, 1 H), 1.50 (s, 6 H). $^{13}$C NMR (400 MHz, $CDCl_3$, 25 °C) $\delta$ 146.22, 145.88, 136.01, 128.66, 121.42, 120.24, 119.74, 112.35, 110.57, 98.09, 38.32, 27.55.

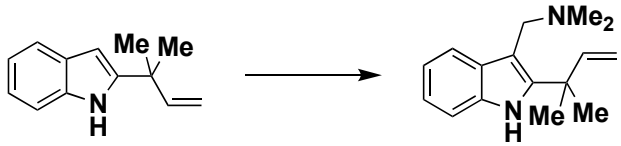


**Gramine 3.4.** $Me_2NH$ (40% in $H_2O$, 10.52 mmol, 1.33 mL) and $H_2CO$ (37% in $H_2O$, 10.04 mmol, 0.75 mL) were added to a solution of prenylated indole **3.3** (9.56 mmol, 1.77 g) in glacial acetic acid (9.2 mL) and MeCN (1 mL) at 0 °C. The solution ran for 5 min., was allowed to warm to room temperature and stirred for an addition 1.5 h. The crude mixture was partitioned between 1 M HCl (50 mL) and $Et_2O$ (100 mL) and the organics were washed with 1 M HCl (2 x 50 mL). The aqueous layer was basified with 2 M NaOH (~175 mL) then washed with $Et_2O$ (1 x 200 mL, 2 x 100 mL). The resulting organics were washed with $NaHCO_3$ (2 x 50 mL), then saturated aqueous NaCl (2 x 100 mL), dried ($MgSO_4$), filtered and concentrated under reduced pressure. Purification by flash chromatography eluting with 10 % - 80 % EtOAc/Hexanes to yield 1.16 g (50%) gramine **3.4**.

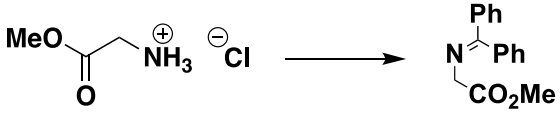


**Glycine Derivative 3.5.** A solution of glycine HCl (11 mmol, 1.37 g) was added to benzophenone (11 mmol, 2 g) at room temperature. The flask was equipped with a $CaCl_2$ drying tube and ran at the same

temperature for 24 h. The salts were filtered off and the solution was concentrated to an oil. The residue was taken up in $Et_2O$ (40 mL), washed with $H_2O$ (2 x 20 mL), dried ($MgSO_4$), filtered and concentrated to yield 2.7 g (97%) glycine derivative **3.5** as a white solid. $^1$H NMR (400 MHz, $CDCl_3$, 25 °C) $\delta$ 7.66 (m, 2H), 7.38-7.48 (comp, 4H), 7.35 (m, 2H), 7.18 (m, 2H), 4.22 (s, 2H), 3.75 (s, 3H); $^{13}$C NMR (400 MHz, $CDCl_3$, 25 °C) $\delta$ 172.06, 171.23, 139.34, 136.05, 132.53, 130.62, 130.18, 128.98, 128.90, 128.83, 128.40, 128.20, 127.77.

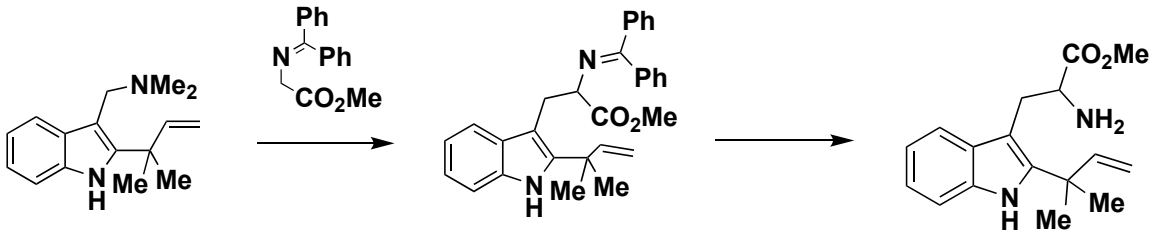


**Tryptophan 3.7.** Freshly distilled DBU (1.97 mmol, 0.294 mL) was added to a solution of gramine **3.4** (1.54 mmol, 373 mg) and glycine derivative **3.5 (**1.54 mmol, 390 mg) in MeCN (9 mL) at 0 °C. The solution was allowed to warm to room temperature, then was heated to reflux and ran overnight. The resulting solution was allowed to cool to room temperature and was add $NH_4Cl$ (10 mL). The crude mixture was washed with $Et_2O$ (10 mL), saturated aqueous NaCl (2 x 10 mL), dried ($Na_2SO_4$), filtered, and concentrated under reduced pressure to yield intermediate **3.6** as a crude orange oil that was carried forward immediately for hydrolysis.

1M HCl (4.5 mmol, 4.5 mL) was added to a solution of **3.6** in MeCN (9 mL) at 0 °C. The solution was allowed to warm to room temperature, then stirred for 3 h. The crude mixture was basified with 1M NaOH (~10 mL) at 0 °C. The resulting solution was allowed to warm to room temperature, then was extracted with $Et_2O$ (50 mL). The organics were washed with saturated aqueous NaCl (2 x 25 mL), dried ($MgSO_4$), filtered and concentrated. Purification by $SiO_2$ plug, eluting with DCM (85 mL), then 3% MeOH/DCM (100 mL). The fractions from the 3% MeOH/DCM eluent were collected and concentrated under reduced pressure to yield 254 mg (57.6%) tryptophan **3.7** as an orange/yellow oil.

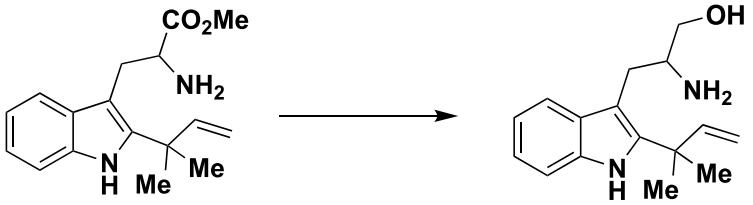


**Reduced Tryptophan 3.8.** $NaBH_4$ (84 mg, 2.22 mmol) was added to a solution of tryptophan **3.7** in MeOH (1.16 mL) and the reaction was stirred at room temperature for 1 h. The reaction was quenched with saturated $NH_4Cl$ (6.5 mL) and washed with EtOAc (13 mL). The layers were separated, and the organic phase was washed with saturated aqueous NaCl (6.5 mL), then dried ($MgSO_4$), filtered and concentrated under reduced pressure to yield 139.2 mg (87.3 %) of alcohol **3.8** as a white solid. $^1$H NMR (400 MHz, $CDCl_3$, 25 °C) $\delta$ 7.98 (bs, 1 H), 7.55 (d, *J* = 7.8 Hz, 1 H), 7.29 (d, *J* = 7.88 Hz, 1 H), 7.14 (t, *J* = 6.94 Hz, 1 H), 7.07 (t, *J* = 7.44 Hz, 1 H), 6.13 (dd, *J* = 10.56, 17.36 Hz, 1 H), 5.18 (d, *J* = 6.08 Hz, 1 H), 5.14 (s, 1 H), 3.67 (dd, *J* = 2.96, 11.12 Hz, 1 H), 3.46 (t, *J* = 7.14 Hz, 1 H), 3.30 (bs, 1 H), 2.95 (dd, *J* = 5.6, 14.5 Hz, 1H), 2.86 (dd, *J* = 8.68, 14.52 Hz, 1H), 2.27 (s, 3 H), 1.54 (s, 6 H), 1.26; $^{13}$C NMR (400 MHz, $CDCl_3$, 25 °C) $\delta$ 146.27, 140.25, 134.31, 130.05, 121.62, 119.48, 118.73, 112.09, 110.55, 107.83, 66.46, 54.26, 39.25, 29.59, 28.01, 27.94; Maxis Q-TOF (ESI) *m/z* 259.1806 [$C_{16}H_{22}N_2O$ (M+H) requires 259.1810].

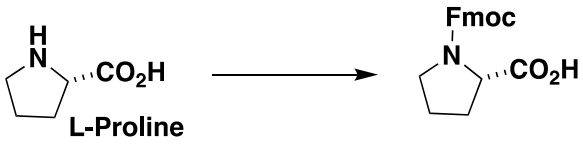


**Fmoc Proline 3.9.** Aqueous $K_2CO_3$ (1M, 87 mL, 87 mmol) then FmocOSu (6.65 g, 19.7 mmol) were added to a solution of L-proline (2.0 g, 17.4 mmol) in dioxane (87 mL) and the reaction was stirred at room temperature for 18 h. The solution was diluted with $H_2O$ (116 mL) and extracted with $Et_2O$ (290 mL x 2). The layers were separated, and the aqueous phase was acidified with 2M HCl (100 mL), then extracted with EtOAc (290 mL x 1, 145 mL x 2). The organic phase was washed with saturated aqueous NaCl (290 mL x 2), then dried ($MgSO_4$), filtered and concentrated under reduced pressure to yield amine protected proline **3.9** as a yellow solid. $^1$H NMR (400 MHz,

DMSO, 25 °C) δ 12.68 (bs, 1H), 7.89 (t, *J* = 5.86 Hz, 2H), 7.64-7.68 (comp, 2H), 7.42 (t, *J* = 7.45 Hz, 2H), 7.30-7.36 (comp, 2H), 4.28 (s, 1H), 4.14-4.21 (comp, 2H), 3.34-3.44 (comp, 3H), 2.01-2.12 (comp, 1H), 1.82-2.01 (comp, 3H);□$^{13}$C NMR (400 MHz, DMSO, 25 °C) δ 174.00, 173.62, 153.92, 153.77, 143.84, 143.78, 143.76, 143.70, 140.75, 140.69, 140.66, 140.64, 127.72, 127.69, 127.18, 127.16, 125.29, 125.25, 125.17, 125.13, 120.16, 120.14, 120.10, 66.96, 66.58, 58.84, 58.41, 46.76, 46.71, 46.63, 46.09, 30.53, 29.39, 23.92, 22.93.

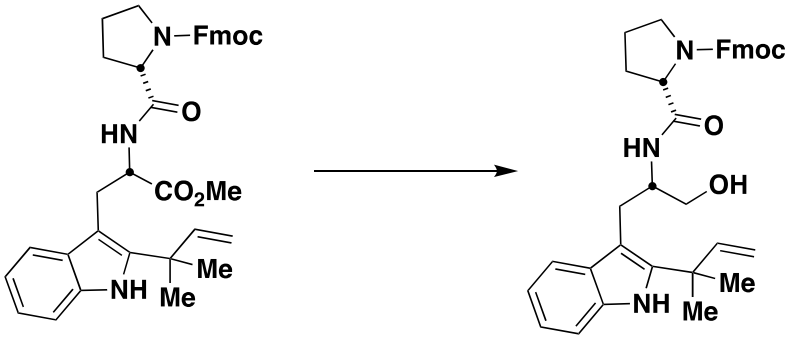


**Alcohol 3.10.** $NaBH_4$ (56 mg, 1.48 mmol) was added to a suspension of methyl ester dipeptide (286 mg, 0.47 mmol) and LiCl (72 mg, 1.70 mmol) in THF (2.19 mL) and the reaction stirred for 5 min at room temperature. MeOH (2.19 mL) was then added and the reaction stirred for 7 h. The reaction was quenched with saturated $NH_4Cl$ (8 mL) and extracted with EtOAc (16 mL). The layers were separated, and the organic phase was washed with saturated aqueous NaCl (8 mL), then dried ($MgSO_4$), filtered and concentrated under reduced pressure. The residue was purified by flash chromatography eluting with 60-70% EtOAc/hexane to give 135.5 mg (50 %) of alcohol **3.10** as a white foamy solid. $^1$H NMR (300 MHz, DMSO, 100 °C) δ 10.02 (s, 1 H), 7.82 (d, *J* = 7.5 Hz, 2 H), 7.57-7.64 (comp, 3 H), 7.37 (t, *J* = 7.3 Hz, 2 H), 7.29 (t, *J* = 7.3 Hz, 2 H), 7.24 (d, *J* = 7.9 Hz, 1 H), 7.09 (d, *J* = 6.9 Hz, 1 H), 6.94 (t, *J* = 7.5 Hz, 1 H), 6.85 (t, *J* = 7.5 Hz, 1 H), 6.13 (dd, *J* = 17.4, 10.6 Hz, 1 H), 4.98 (d, *J* = 17.4 Hz, 1 H), 4.96 (d, *J* = 10.6 Hz, 1 H), 4.60 (dd, *J* = 15.3, 7.6 Hz, 1 H), 4.10-4.12-4.30 (comp, 5 H), 3.22-3.36 (comp, 4 H), 3.00 (dd, *J* = 14.5, 8.2 Hz, 1 H), 2.86 (dd, *J* = 14.5, 6.4 Hz,

1 H), 1.96-2.08 (m, 1 H), 1.55-1.77 (comp, 3 H), 1.48 (s, 3 H), 1.47 (s, 3 H); $^{13}$C NMR (75 MHz, DMSO, 100 °C) $\delta$ 170.9, 153.9, 146.0, 143.5, 140.3, 140.0, 134.4, 129.2, 127.0, 126.5, 124.5, 119.7, 119.4, 117.8, 117.5, 110.4, 110.1, 106.3, 66.3, 62.1, 59.9, 52.2, 46.6, 46.3, 38.4, 29.8, 27.4, 27.3, 26.2, 22.7; IR (thin film) 3308, 1685, 1655, 1520, 1415, 1352, 1119, 910, 738 cm$^{-1}$; HRMS (ESI-APCI) *m/z* 578.3023 [$C_{36}H_{40}N_3O_4$ (M+H) requires 578.3019].

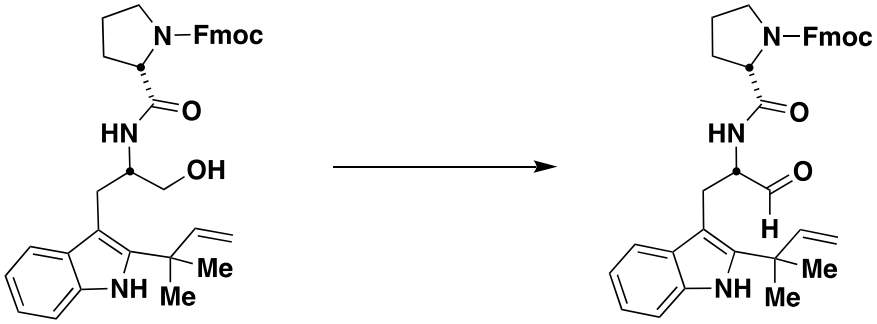


**Aldehyde 3.11.** $SO_3$·Py (180 mg, 1.13 mmol) was added to a solution of alcohol **3.10** (160 mg, 0.28 mmol), $Et_3N$ (0.2 mL, 145 mg, 1.43 mmol) and DMSO (1.5 mL) in $CH_2Cl_2$ (3 mL) and the reaction stirred for 2 h at room temperature. The reaction was partitioned between water (10 mL) and EtOAc (10 mL). The layers were separated, and the organic phase was washed with 1 M HCl (10 mL) and saturated aqueous NaCl (10 mL), and then dried ($MgSO_4$), filtered and concentrated under reduced pressure. The residue was purified by flash chromatography eluting with 45% EtOAc/hexane to give 115 mg (72%) of aldehyde **3.11** as dark yellow solid. $^1$H NMR (500 MHz, DMSO, 100 °C) $\delta$ 10.22 (bs, 1 H), 9.42 (s, 1 H), 7.90 (bs, 1 H), 7.85 (d, *J* = 7.55 Hz, 2 H), 7.61-7.65 (comp, 2 H), 7.46 (m, 1 H), 7.40 (t, *J* = 7.65 Hz, 2 H), 7.32 (m, 3 H), 7.00 (m, 1 H), 6.91 (m, 1 H), 6.18 (m, 1 H), 5.04 (m, 2 H), 4.44 (m, 1 H), 4.22-4.31 (comp, 4 H), 3.29-3.38 (comp, 3 H), 3.08 (m, 1 H), 2.00-2.10 (comp, 1 H), 1.70-1.80 (comp, 3 H), 1.51 (d, *J* = 3.45 Hz, 3 H) 1.50 (d, *J* = 2.05 Hz, 3H); $^{13}$C NMR (75 MHz, DMSO, 100 °C) $\delta$ 199.67, 199.54, 171.72, 171.67, 153.80, 153.73, 145.85, 145.79, 143.50, 143.48, 143.41, 140.40, 140.37, 140.29, 134.45, 128.84, 127.05, 126.51,

124.56, 124.49, 119.98, 119.95, 119.41, 117.84, 117.82, 117.41, 117.28, 110.71, 110.69, 110.39, 110.36, 104.42, 104.36, 78.59, 66.27, 66.24, 59.47, 59.03, 58.95, 46.54, 46.51, 46.28, 38.36, 27.41, 27.40, 27.27, 27.26, 24.16, 24.07; IR (thin film) 3281, 1684, 1508, 1416, 1341, 1119, 912, 739 $cm^{-1}$; HRMS (ESI-APCI) *m/z* 576.2884 [$C_{36}H_{38}N_3O_4$ (M+H) requires 576.2862].

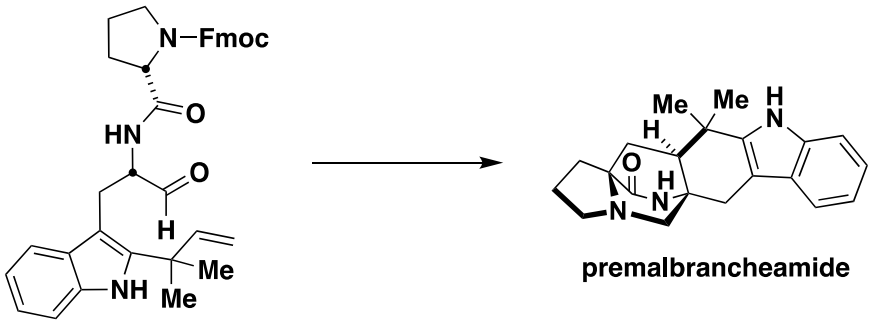


**Premalbrancheamide.** $Et_2NH$ (0.7 mL) was added to $CH_3CN$ (3.52 mL) and the resulting solution was sparged with argon for 15 min. The 5:1 $CH_3CN$:$Et_2NH$ solution (4.22 mL) thus prepared was added to aldehyde **3.11** (121.3 mg, 0.211 mmol) and the reaction was stirred for 2 h at room temperature and the reaction was concentrated under reduced pressure. The residue was dissolved in the THF (4.22 mL) and TFA (0.045 mL, 67.36 mg, 0.6 mmol) was added. The reaction stirred for 24 h at 50 °C. The reaction was quenched with saturated aqueous $NaHCO_3$ (20 mL) and the resulting mixture was extracted with $CH_2Cl_2$ (3 x 20 mL). The combined organic phases were dried ($MgSO_4$), filtered and concentrated under reduced pressure. The residue was purified by flash chromatography eluting with 2% MeOH/$CH_2Cl_2$. Further purification by flash chromatography eluting with 50% EtOAc/hexane gave 12.7 mg (18%) of **premalbrancheamide** as a white solid. $^1$H NMR (400 MHz, $CDCl_3$, 25 °C) $\delta$ 7.83 (bs, 1 H), 7.44 (d, *J* = 7.76 Hz, 1 H), 7.33 (d, *J* = 8 Hz, 1 H), 7.17 (t, *J* = 8.12 Hz, 1 H), 7.11 (t, *J* = 7.84 Hz, 1 H), 6.08 (bs, 1 H), 3.04-3.09 (comp, 1 H), 2.88 (diastereotopic, *J* = 15.2 Hz, 2 H), 2.59-2.66 (comp, 1 H), 2.05-2.36 (comp, 6 H), 1.89-1.93 (comp, 3 H), 1.25 (s, 6 H).

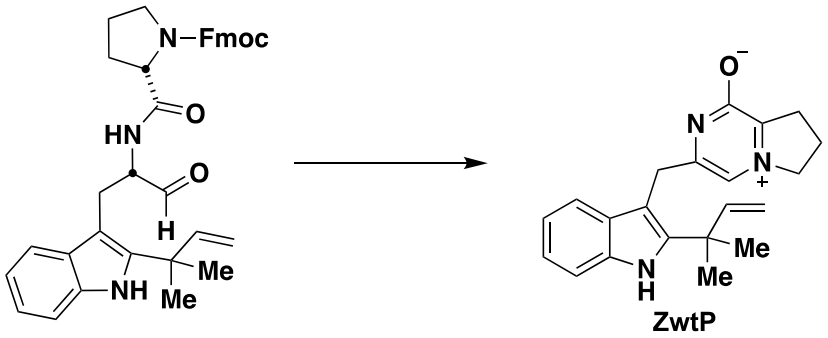


**ZwtP.** $Et_2NH$ (0.09 mL) was added to a solution of aldehyde **3.11** (16 mg, 0.028 mmol) in MeCN (0.47 mL) and the reaction stirred at room temperature for 2 h. The reaction was concentrated under reduced pressure, the residue was taken up in $CH_2Cl_2$ (1.40 mL) and allowed to stand for 2 days. The resulting solution was concentrated under reduced pressure. The residue was purified by preparative thin layer chromatography eluting with 5% MeOH/$CH_2Cl_2$ to give 6.90 mg (74.4 %) of **ZwtP** as a yellow solid. $^1$H NMR (500 MHz, DMSO, 25 °C) $\delta$ 10.61 (s, 1 H), 7.33 (d, *J* = 7.95 Hz, 1 H), 7.28 (d, *J* = 7.75 Hz, 1 H), 7.01 (dd, *J* = 7.30, 7.75 Hz, 1 H), 6.89 (dd, *J* = 7.25, 7.65 Hz, 1 H), 6.66 (s, 1 H), 6.18 (dd, *J* = 10.50, 17.45 Hz, 1 H), 5.06 (d, *J* = 17.45 Hz, 1 H), 5.01 (d, *J* = 10.45 Hz, 1 H), 4.39 (t, *J* = 7.8 Hz, 2 H), 4.00 (s, 2 H), 2.95 (t, *J* = 7.45 Hz, 2 H), 2.11 (m, *J* = 7.5 Hz, 2 H), 1.48 (s, 6 H). $^{13}$C NMR (500 MHz, DMSO, 25 °C) $\delta$ 173.63, 146.03, 141.64, 140.89, 136.49, 134.76, 129.05, 126.45, 120.50, 118.44, 117.79, 110.91, 105.25, 101.93, 64.08, 58.25, 34.64, 31.25, 29.61, 27.73; (ESI-M-TOFMS) *m/z* 334.1939 [$C_{21}H_{23}N_3O$ (M+H) requires 334.1919].

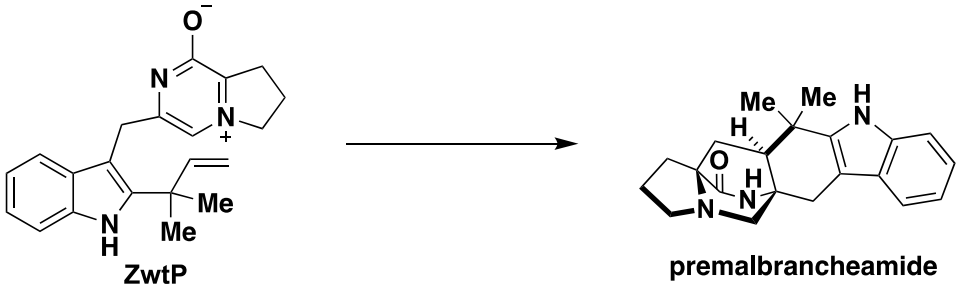


**Premalbrancheamide.** A solution of **ZwtP** (3.9 mg, 0.0117 mmol) in DMSO (0.65 mL) was added to a solution of NADH (89.36 mg, 0.117 mmol) in HEPES buffer (50 mM, 23.4 mL) and the resulting

solution was sparged with argon for 15 min, then stirred for 18 h at room temperature. The resulting mixture was extracted with EtOAc (3 x 20 mL). The combined organic phases were washed with saturated aqueous NaCl, dried ($Na_2SO4$), filtered and concentrated under reduced pressure. The residue was purified by preparative thin layer chromatography eluting with 80% EtOAc/Hex to give 3 mg (76.5%) of **premalbrancheamide** as a white solid. All spectral data matched those reported above.

**Premalbrancheamide.** Hantzsch Ester (12.54 mg, 0.05 mmol) was added to a solution of **ZwtP** (3.3 mg, 0.01 mmol) in MeOH (0.2 mL) and the resulting solution was sparged with argon for 15 min, then stirred for 18 h at room temperature. The resulting mixture was concentrated under reduced pressure. The residue was purified by preparative thin layer chromatography eluting with 80% EtOAc/Hex to yield 2.5 mg (74.6%) of **premalbrancheamide** as a white solid. All spectral data matched those reported above.

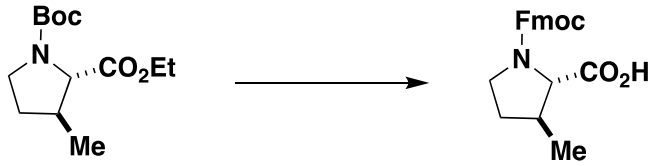


***N*-Fmoc-$\beta$-methyl-L-proline (3.35).** NaOH (4.05 g, 15.75 mmol) was added to a solution of **3.34**[153] **i**n MeOH (315 mL) and the reaction was heated to reflux for 18 h. The resulting solution was acidified (pH = 2) with 0.1M HCl (900 mL) and washed with EtOAc (3 x 500 mL). The combined organic phases were dried ($Na_2SO_4$), filtered and concentrated under reduced pressure. The residue was recrystallized from EtOAc and Hexanes to yield 2.29 g (63.4%) of proline as a white solid. TFA (9.92 mL) was added to the solution of $\beta$-MeProline (1 g, 4.36 mmol) in DCM (9.92 mL) and the reaction stirred at 0 °C for 1 h. The reaction was concentrated under reduced pressure, the residue was taken up in dioxane (21.8 mL) and Fmoc-Osu (1.67 g, 4.95 mmol) and $K_2CO_3$ (21.8

mL ,21.8 mmol) were added. The reaction was allowed to stir at room temperature for 18 h. The resulting solution was diluted with deionized $H_2O$ (30 mL) and extracted with EtOAc (2 x 50 mL). The aqueous phase was acidified with 2M HCl (25 mL) and washed with EtOAc (1 x 50 mL, 2 x 25 mL). The combined organic phases were washed with NaCl (2 x 75 mL), dried ($Na_2SO_4$), filtered and concentrated under reduced pressure. The residue was purified by flash chromatography eluting with 20-50% EtOAc/Hexanes to yield 1.39 g (91.1%) of proline **3.35** as a foamy white solid. $^1$H NMR (400 MHz, DMSO, 25 °C) $\delta$ 12.65 (bs, 1 H), 7.89 (t, *J* = 6.60 Hz, 2 H), 7.65 (m, 2 H), 7.42 (t, *J* = 7.42 Hz, 2 H), 7.33 (m, 2 H), 3.51 (m, 1 H), 3.37 (m, 1 H), 2.29 (m, 1 H), 1.99 (m, 1 H), 1.53 (m, 1 H), 1.11 (dd, *J* = 6.78, 17.10 Hz, 3H); $^{13}$C NMR (400 MHz, DMSO, 25 °C) $\delta$ 173.66, 173.19, 153.90, 153.85, 143.83, 143.76, 143.68, 140.75, 140.66, 140.63, 127.69, 127.15, 127.14, 125.28, 125.21, 125.18, 125.10, 120.12, 66.94, 66.52, 65.74, 65.30, 46.74, 46.66, 45.92, 45.40, 37.88, 31.92, 30.87, 18.63, 18.28; Maxis Q-TOF (ESI) *m/z* 352.1547 [$C_{21}H_{21}NO_4$ (M+H) requires 352.1549]. Maxis Q-TOF (ESI) *m/z* 352.1547 [$C_{21}H_{21}NO_4$ (M+H) requires 352.1549].

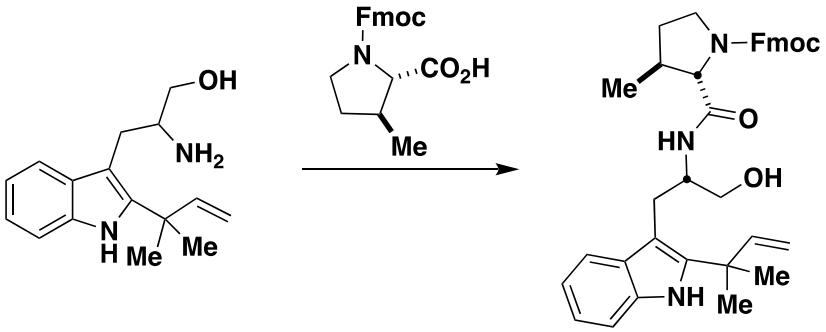


**Methyl Alcohol 3.36.** HATU (1.96 g, 5.16 mmol) and *i*-$Pr_2$NEt (3 mL, 2.22 g, 17.2 mmol) were added to a solution of *N*-Fmoc-$\beta$-methyl-L-proline **3.35** (1.59 g, 4.73 mmol) and reduced tryptophan **3.8** (1.11 g, 4.3 mmol) in $CH_3CN$ (43 mL) and the reaction was stirred at room temperature for 4 h. The reaction was concentrated under reduced pressure, the residue was dissolved in EtOAc and partitioned between $Et_2O$ (118 mL) and 1 M HCl (84 mL). The layers were

separated, and the organic phase was washed with saturated aqueous NaCl (84 mL), then dried ($MgSO_4$), filtered and concentrated under reduced pressure. The residue was purified by flash chromatography eluting with 60-80% EtOAc/hexane to give 2 g (81%) of alcohol **3.36** as a white foamy solid. $^1$H NMR (500 MHz, DMSO, 100 °C) $\delta$ 10.05 (s, 1 H), 7.85 (d, *J* = 7.45 Hz, 2 H), 7.59-7.66 (comp, 3 H), 7.40 (t, *J* = 7.4 Hz, 2 H), 7.27-7.35 (comp, 3H), 6.95-6.99 (comp, 1 H), 6.87-6.93 (comp, 1 H), 6.14-6.26 (comp, 1 H), 4.97-5.09 (comp, 2 H), 4.22-4.33 (comp, 3 H), 4.16 (bs, 2 H), 3.73 (bs, 1 H), 3.34-3.44 (comp, 4 H), 3.02-3.07 (comp, 3 H), 2.86-2.96 (comp, 2 H), 2.06 (m, 1 H), 1.53 (s, 3 H), 1.51 (d, *J* = 3.95 Hz, 3 H), 0.99 (dd, *J* = 6.8, 22.3 Hz, 3 H) $^{13}$C NMR (500 MHz, DMSO, 100 °C) $\delta$ 173.08, 146.24, 146.17, 142.35, 139.99, 139.97, 139.06, 137.09, 134.44, 129.28, 129.18, 128.31, 126.65, 120.67, 119.68, 119.66, 119.31, 117.96, 117.80, 117.46, 117.45, 110.34, 110.12, 110.06, 108.38, 106.37, 106.50, 78.58, 67.37, 67.28, 62.66, 62.30, 51.53, 51.30, 44.90, 44.59, 38.40, 38.17, 38.02, 33.98, 33.82, 27.51, 27.48, 27.37, 27.30, 26.32, 26.04, 18.88, 18.77; (ESI-M-TOFMS) *m/z* 592.3156 [$C_{37}H_{41}N_3O_4$ (M+H) requires 592.3175].

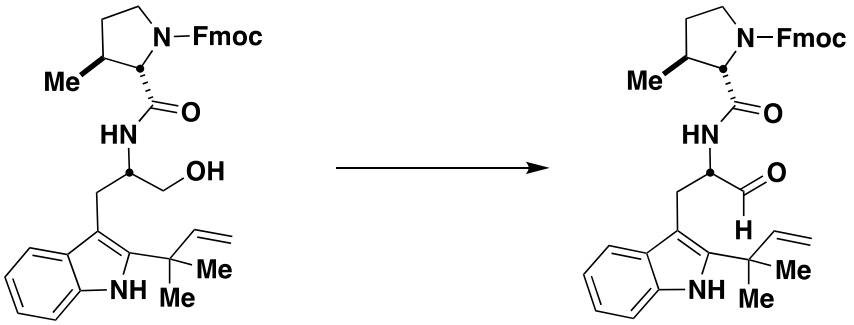


**Methyl Aldehyde 3.37.** $SO_3$·Py (180 mg, 1.13 mmol) was added to a solution of alcohol **3.36** (160 mg, 0.28 mmol), $Et_3N$ (0.2 mL, 145 mg, 1.43 mmol) and DMSO (1.5 mL) in $CH_2Cl_2$ (3 mL) at 0°C and the reaction stirred for 2 h at the same temperature. The reaction was partitioned between water (10 mL) and EtOAc (10 mL). The layers were separated, and the organic phase was washed with 1 M HCl (10 mL) and saturated aqueous NaCl (10 mL), and then dried ($MgSO_4$), filtered and

concentrated under reduced pressure. The residue was purified by flash chromatography eluting with 45% EtOAc/hexane to give 115 mg (72%) of aldehyde **3.37** as dark yellow solid. $^{1}$H NMR (500 MHz, DMSO, 100 °C) $\delta$ 10.21 (s, 1 H), 9.37 (s, 1 H), 7.85 (d, *J* = 7.55 Hz, 2 H), 7.61-7.64 (comp, 2 H), 7.38-7.48 (comp, 3 H), 7.29-7.33 (comp, 3 H), 6.97-7.01 (comp, 1 H), 6.88-6.93 (comp, 1 H), 6.17 (m, 1 H), 5.00-5.07 (comp, 2 H), 4.46 (bs, 1 H), 4.22-4.32 (comp, 4 H), 3.77 (d, *J* = 5 Hz, 1 H), 3.44 (bs, 1 H), 3.25-3.37 (comp, 2 H), 3.07 (m, 1 H), 2.05-2.14 (comp, 1 H), 1.51 (d, *J* = 4.05 Hz, 3 H), 1.49 (s, 3 H), 1.26 (d, *J* = 17.65 Hz, 3 H), 1.00 (d, *J* = 6.75 Hz, 2 H); $^{13}$C NMR (500 MHz, DMSO, 100 °C) $\delta$ 199.68, 199.55, 171.32, 171.24, 153.80, 153.75, 145.82, 145.80, 145.78, 143.46, 143.41, 140.39, 140.36, 140.29, 134.45, 134.43, 128.84, 128.80, 127.03, 126.49, 126.47, 124.52, 124.47, 119.95, 119.39, 119.38, 117.80, 117.38, 117.28, 110.69, 110.66, 110.35, 104.41, 104.28, 78.58, 66.56, 66.19, 59.01, 58.80, 46.56, 46.53, 38.35, 27.39, 27.24, 24.15, 18.02, 17.86; (ESI-M-TOFMS) *m/z* 590.3029 [$C_{37}H_{39}N_3O_4$ (M+H) requires 590.3019].

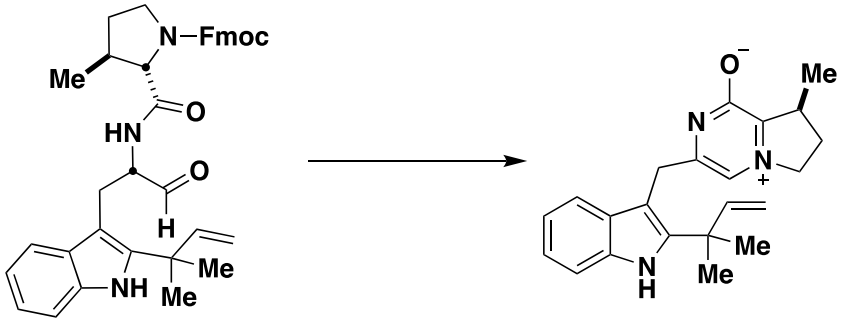


**MeZwtP.** $Et_2NH$ (0.102 mL) was added to a solution of aldehyde **36** in MeCN (0.51 mL) and the reaction stirred at room temperature for 2 h. The reaction was concentrated under reduced pressure, the residue was taken up in $CH_2Cl_2$ (1.55 mL) and allowed to stand for 2 days. The resulting solution was concentrated under reduced pressure. The residue was purified by preparative thin layer chromatography eluting with 5% MeOH/$CH_2Cl_2$ to give 4.65 mg (45%) of **38** as a yellow solid. $^{1}$H NMR (400 MHz, DMSO, 25 °C) $\delta$ 10.61 (s, 1 H), 7.33 (d, *J* = 8.00 Hz, 1 H),

7.30 (d, *J* = 7.92 Hz, 1 H), 7.01 (td, *J* = 1.10, 7.56 Hz, 1 H), 6.89 (td, *J* = 0.96, 7.92 Hz, 1 H), 6.65 (s, 1 H), 6.18 (dd, *J* = 10.52, 17.40 Hz, 1 H), 5.06 (dd, *J* = 1.16, 17.44 Hz, 1 H), 5.02 (dd, *J* = 1.20, 10.52 Hz, 1 H), 4.45 (m, 1 H), 4.30 (m, 1 H), 4.00 (s, 2 H), 3.37 (m, 1 H), 2.29-2.39 (comp, 1 H), 1.68-1.76 (comp, 1 H), 1.49 (d, *J* = 2.0 Hz, 6 H), 1.28 (d, *J* = 7.08 Hz, 3 H); $^{13}$C NMR (400 MHz, DMSO, 25 °C) δ 164.31, 160.02, 146.17, 141.52, 141.00, 134.75, 129.06, 120.51, 118.45, 117.82, 110.98, 110.90, 108.59, 105.24, 57.14, 38.74, 37.31, 31.25, 27.74, 27.46, 16.40; HRMS (BTOF) *m/z* 364.20162 [$C_{22}H_{25}N_3O$ (M+NH4) requires 364.22576].

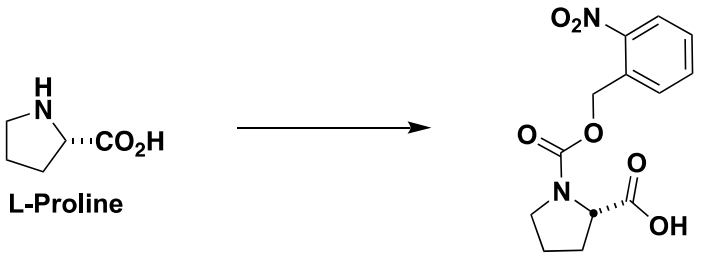


**ONB-L-proline 3.23.** A solution of previously prepared chloroformate[154] in DCM (8.6 mL) and dioxane (2.15 mL) at 0°C was added in turn, alongside 2.37 mL NaOH (2M), to a solution of L-proline in 2M NaOH (2.15 mL) at 0°C. The solution ran at the same temperature for 1 h, then was allowed to warm to room temperature and run for another 18 h. The resulting organic phase was removed, and the aqueous phase was acidified (pH = 3-4) with 5M HCl and washed with equal parts EtOAc. The combined organic phases were dried ($MgSO_4$), filtered and concentrated under reduced pressure. The crude reside was taken up in DCM and washed with equal parts 0.1M HCl, dried over $MgSO_4$, filtered and concentrated. The residue was purified by flash chromatography eluting with 20% - 80% EtOAc/Hexanes to give 386 mg (30.6%) of proline **3.23**[155] as a yellow oil. $^1$H NMR (400 MHz, DMSO, 25 °C) δ 12.69 (bs, 1 H), 8.06-8.15 (comp, 1 H), 7.50-7.84 (comp, 3 H), 5.34-5.55 (comp, 2 H), 4.34 (m, 1 H), 4.34-3.53 (comp, 2 H), 2.14-2.36 (comp, 1 H), 1.76-2.03 (comp, 3 H); $^{13}$C NMR (400 MHz, DMSO, 25 °C) δ 173.92, 173.47, 171.98, 171.62, 153.52, 153.41,

153.19, 152.98, 147.44, 147.36, 147.27, 146.96, 146.82, 134.27, 134.08, 134.02, 134.00, 132.84, 132.33, 132.25, 132.15, 131.03, 130.79, 130.66, 129.66, 129.51, 129.49, 129.44, 129.07, 129.02, 128.95, 128.78, 128.74, 128.56, 128.20, 124.96, 124.89, 124.85, 124.74, 63.15, 63.06, 62.89, 62.84, 59.01, 58.98, 58.45, 58.37, 46.89, 46.85, 46.20, 46.11, 30.46, 30.30, 29.37, 29.34, 23.95, 23.86, 23.03, 22.97.

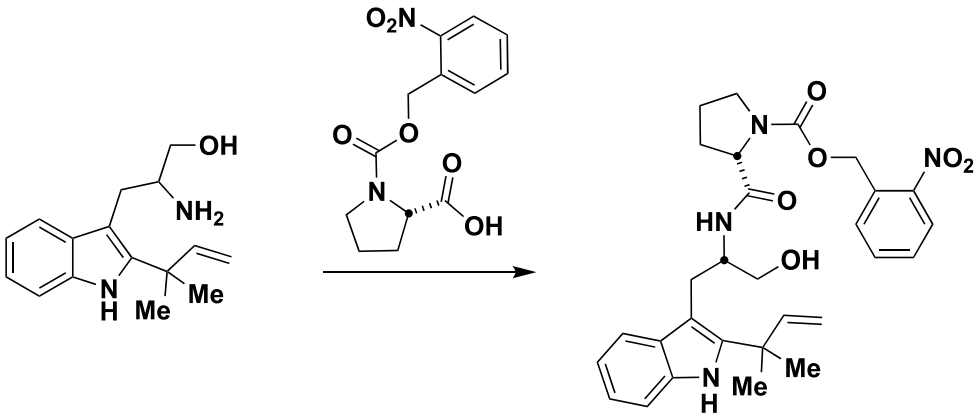


**ONB Alcohol 3.26.** HATU (182.15 mg, 0.65 mmol) and *i*-$Pr_2NEt$ (0.45 mL, 336.02 mg, 2.6 mmol) were added to a solution of **3.23** (229.4 mg, 0.78 mmol) and **3.8** (168 mg, 0.65 mmol) in $CH_3CN$ (6.5 mL) and the reaction was stirred at room temperature for 2 h. The reaction was concentrated under reduced pressure, the residue was dissolved in 20 mL EtOAc and washed with 1 M HCl (20 mL), saturated aqueous NaCl (20 mL), dried ($MgSO_4$), filtered and concentrated under reduced pressure. The residue was purified by flash chromatography eluting with 80% EtOAc/hexane to give 212.4 mg (61.2%) of alcohol **3.26** as a yellow solid. $^1$H NMR (500 MHz, DMSO, 100 °C) $\delta$ 10.04 (s, 1 H), 8.05 (d, *J* = 8.05 Hz, 1 H), 7.62-7.74 (comp, 3 H), 7.56 (q, *J* = 7.8 Hz, 1 H), 7.28 (t, *J* = 8 Hz, 1 H), 7.17, (bs, 1 H), 6.95-6.99 (comp, 1 H), 6.88-6.93 (comp, 1 H), 6.20 (dq, *J* = 10.55, 6.8 Hz, 1 H), 5.36 (s, 2 H), 5.00-5.07 (comp, 2 H), 4.19-4.24 (comp, 2 H), 4.13 (bs, 1 H), 3.37-3.44 (comp, 4 H), 2.99-3.06 (m, *J* = 8.4 Hz, 2 H), 2.86 (m, *J* = 7.05 Hz, 1 H), 1.71-1.81 (comp, 2 H), 1.62-1.68 (comp, 1H), 1.54 (d, *J* = 1.5 Hz, 3 H), 1.51 (d, *J* = 2.75 Hz, 3 H); $^{13}$C NMR (500

MHz, DMSO, 100 °C) δ 170.86, 170.79, 153.24, 153.12, 146.16, 146.14, 146.07, 139.94, 139.90, 134.40, 133.20, 133.17, 129.24, 129.21, 128.41, 128.36, 128.21, 128.17, 123.79, 123.78, 119.68, 119.65, 117.96, 117.81, 117.51, 117.46, 110.37, 110.34, 110.11, 110.08, 106.45, 106.36, 78.58, 62.20, 62.12, 59.82, 59.69, 52.23, 46.38, 38.40, 38.37, 37.70, 27.47, 27.46, 27.31, 26.19, 26.14; Maxis Q-TOF (ESI) *m/z* 535.2560 [$C_{29}H_{34}N_4O_6$ (M+H) requires 535.2557].

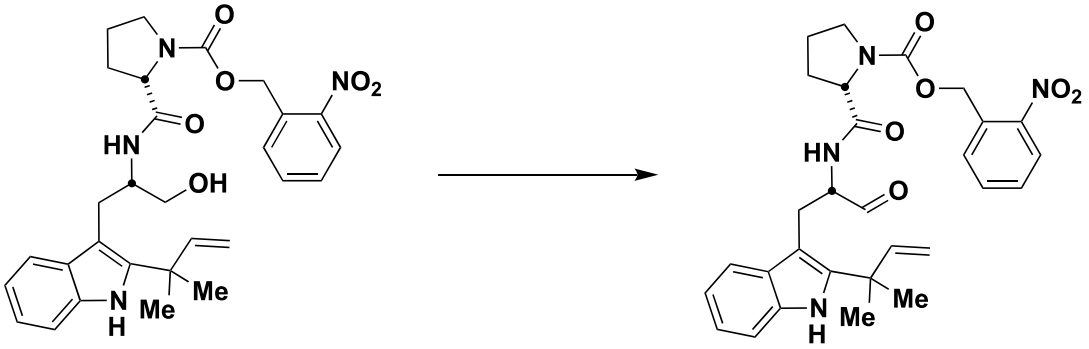


**ONB Aldehyde 3.27.** $SO_3$·Py (204.25 mg, 1.28 mmol) was added to a solution of alcohol **3.26** (171.4 mg, 0.321 mmol), $Et_3N$ (0.23 mL, 165.7 mg, 1.64 mmol) and DMSO (1.72 mL) in $CH_2Cl_2$ (3.6 mL) and the reaction stirred for 3 h at room temperature. The reaction was partitioned between water (20 mL) and EtOAc (20 mL). The layers were separated, and the organic phase was washed with 1 M HCl (20 mL) and saturated aqueous NaCl (20 mL), and then dried ($MgSO_4$), filtered and concentrated under reduced pressure. The residue was purified by flash chromatography eluting with 50% - 60% EtOAc/hexanes to give 75.6 mg (45%) of aldehyde **3.27** as yellow solid. $^1$H NMR (500 MHz, DMSO, 100 °C) δ 10.22 (s, 1 H), 9.39 (s, 1 H), 8.05 (d, *J* = 8.15 Hz, 1 H), 7.94, (bs, 1 H), 7.68-7.71 (comp, 1 H), 7.62-7.65 (comp, 1 H), 7.57 (t, *J* = 7.6 Hz, 1 H), 6.44 (d, *J* = 7.95 Hz, 1 H), 7.30 (d, *J* = 7.9 Hz, 1 H), 7.00 (t, *J* = 7.55 Hz, 1 H), 6.92 (t, *J* = 7.35 Hz, 1 H), 6.17 (dd, *J* = 10.6, 17.45 Hz, 1 H), 5.31-5.39 (comp, 2 H), 5.02-5.09 (comp, 2 H), 4.3 (m, 1 H), 4.27-4.30 (comp, 1 H), 3.35-3.44 (comp, 2 H), 3.31 (q, *J* = 7.40 Hz, 1 H), 3.07 (m, 1 H), 2.10 (bs, 1 H), 1.68-1.81 (comp, 3 H), 1.50 (d, *J* = 1.80 Hz, 6 H); $^{13}$C NMR (500 MHz, DMSO, 100 °C) δ 199.60, 171.62, 153.15, 145.81,

145.79, 140.36, 134.43, 133.15, 131.77, 128.83, 128.42, 128.27, 123.82, 119.94, 117.79, 117.28, 110.70, 110.36, 104.39, 62.19, 59.43, 58.98, 46.37, 38.35, 27.38, 27.26, 24.01, 22.70; Maxis Q-TOF (ESI) *m/z* 533.2398 [$C_{29}H_{32}N_4O_6$ (M+H) requires 533.2400].

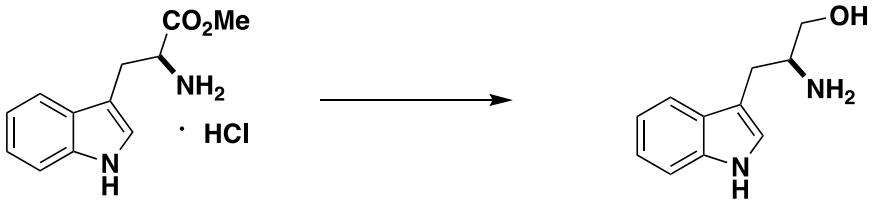


**Reduced Tryptophan 3.19.**[156] $Et_3N$ (1.26 mL, 9.04 mmol) was added to a solution of tryptophan methyl ester HCl salt (1 g, 4.00 mmol) in MeOH (0.75 mL) and $Et_2O$ (25 mL) at -10 °C and stirred for 1 h at the same temperature. The salts were filtered off and the solution was concentrated under reduce pressure to yield 328.1 mg (43.15%) of reduced tryptophan **3.19** as a yellow foam. $^1$H NMR (400 MHz, DMSO, 25 °C) $\delta$ 10.89 (s, 1 H), 8.34 (s, 2 H), 7.55 (d, *J* = 7.84 Hz, 2 H), 7.35 (d, *J* = 8.04 Hz, 1 H), 7.16 (s, 1 H), 7.07 (t, *J* = 7.24 Hz, 1 H), 6.97 (t, *J* = 7.4 Hz, 1 H), 3.40 (dd, *J* = 4.32, 10.36 Hz, 2 H), 3.27 (t, *J* = 7.9 Hz, 1 H), 3.04 (bs, 1 H), 2.83 (dd, *J* = 6.16, 14.12 Hz, 1 H), 2.64 (dd, *J* = 6.92, 14,04 Hz, 1 H); $^{13}$C NMR (400 MHz, DMSO, 20 °C) $\delta$ 136.29, 127.58, 123.42, 120.84, 118.47, 118.20, 111.38, 79.26, 65.38, 53.58, 29.12.

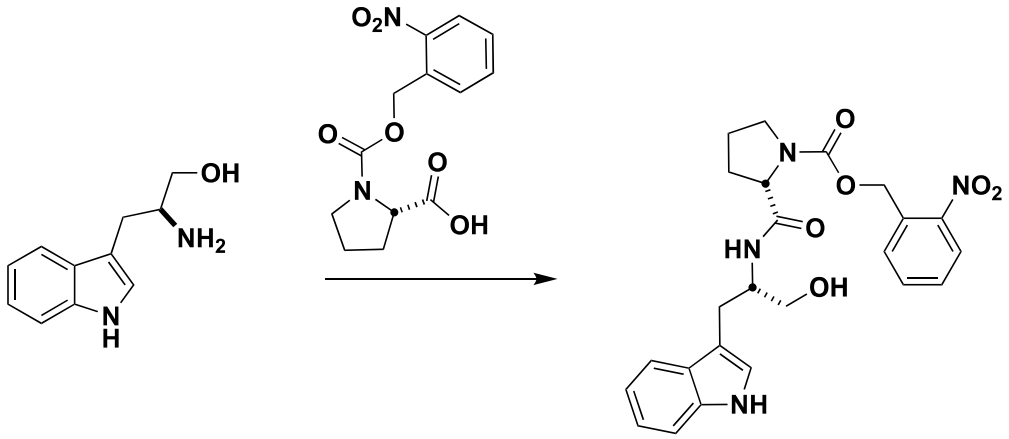


**ONB Alcohol 3.24.** HATU (144 mg, 0.513 mmol) and *i*-$Pr_2NEt$ (0.3 mL, 222 mg, 1.72 mmol) were added to a solution of ONB-L-proline **3.23** (151 mg, 0.513 mmol) and previously prepared

reduced tryptophan **3.19** .[156] 81.34 g, 0.43 mmol) in $CH_3CN$ (4.3 mL) and the reaction was stirred at room temperature for 2 h. The reaction was concentrated under reduced pressure, the residue was dissolved in EtOAc (10 mL) and washed with 1 M HCl (10 mL), saturated aqueous NaCl (10 mL), dried ($MgSO_4$), filtered and concentrated under reduced pressure. The residue was purified by flash chromatography eluting with 20-80% EtOAc/hexane to give 124.4 mg (62.1%) of alcohol **3.24** as a yellow solid. $^1$H NMR (500 MHz, DMSO, 100 °C) $\delta$ 10.44 (bs, 1 H), 8.03 (d, *J* = 8.1 Hz, 1 H), 7.64 (bs, 2 H), 7.57, (d, *J* = 7.9 Hz, 1 H), 7.52-7.55 (comp, 1 H), 7.48 (m, 1 H), 7.29 (d, *J* = 8.05 Hz, 1 H), 7.07 (bs, 1 H), 7.02 (t, *J* = 7.5 Hz, 1 H), 6.94 (t, *J* = 7.43 Hz, 1 H), 5.31-5.39 (comp, 2 H), 4.26 (dd, *J* = 3.2, 8.45 Hz, 1 H), 4.04 (m, 1 H), 3.42 (m, 4 H), 2.91 (m, 1 H), 2.82 (m, 1 H), 2.07-2.15 (comp, 1 H), 1.83-1.88 (comp, 1 H), 1.78 (m, 2 H); $^{13}$C NMR (500 MHz, DMSO, 100 °C) $\delta$ 150.33, 135.87, 133.13, 128.36, 128.17, 128.07, 127.25, 123.76, 122.57, 120.17, 119.94, 117.81, 117.58, 110.89, 110.64, 75.21, 62.17, 62.13, 59.69, 56.13, 51.48, 46.39, 37.69, 25.91. HRMS (BTOF) *m/z* 467.19234 [$C_{24}H_{26}N_4O_6$ (M+H) requires 467.19251].

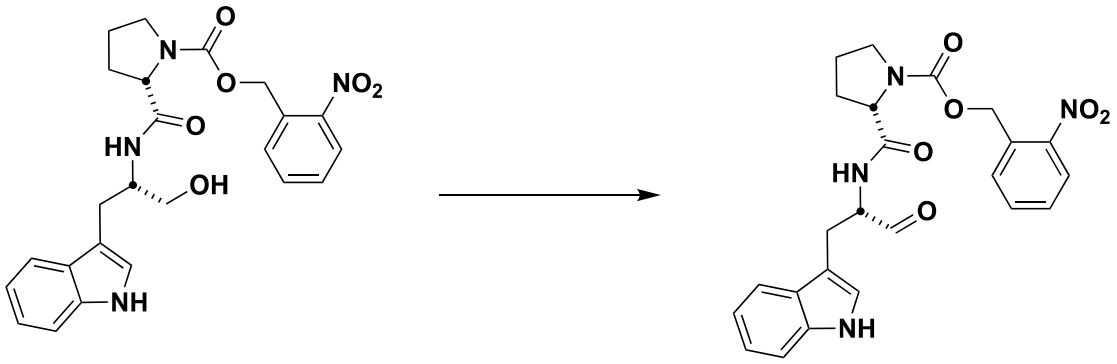


**ONB Aldehyde 3.25.** $SO_3$·Py (8.33 mg, 0.052 mmol) was added to a solution of alcohol **3.24** (6.1 mg, 0.0131 mmol), $Et_3N$ (0.01 mL, 6.75 mg, 0.07 mmol) and DMSO (0.07 mL) in $CH_2Cl_2$ (0.15 mL) and the reaction stirred for 3 h at 0°C. The reaction was partitioned between water (2 mL) and EtOAc (2 mL). The layers were separated, and the organic phase was washed with 1 M HCl (2 mL)

and saturated aqueous NaCl (2 mL), and then dried ($MgSO_4$), filtered and concentrated under reduced pressure. The residue was purified by preparative thin layer chromatography eluting with 3% MeOH/$CH_2Cl_2$ to give 2.2 mg (36.2%) of aldehyde **3.25** as dark yellow solid. $^1$H NMR (500 MHz, DMSO, 100 °C) $\delta$ 10.56 (bs, 1 H), 9.51 (s, 1 H), 8.04 (d, *J* = 8.2 Hz, 1 H), 8.01 (bs, 1 H), 7.60-7.73 (comp, 2 H), 7.56 (m, 1 H), 7.50 (dd, *J* = 3.02, 7.77 Hz, 1 H), 7.32 (t, *J* = 7.00 Hz, 1 H), 7.10-7.12 (comp, 1 H), 7.03-7.07 (comp, 1 H), 6.95-6.99 (comp, 1 H), 5.36 (s, 2 H), 4.42 (q, *J* = 7.05 Hz, 1 H), 4.30-4.33 (comp, 1 H), 3.42-3.44 (comp, 2 H), 3.22 (m, 1 H), 3.04 (m, 2 H), 1.75-1.83 (comp, 3 H); $^{13}$C NMR (500 MHz, DMSO, 100 °C) $\delta$ 199.72, 199.69, 171.73, 153.11, 135.89, 133.16, 133.13, 128.28, 128.26, 126.84, 123.81, 123.05, 120.41, 117.84, 117.54, 117.52, 110.81, 109.08, 62.21, 59.33, 58.39, 45.97, 40.42, 28.35, 23.63, 23.57, 8.16; HRMS (BTOF) *m/z* 465.17617 [$C_{24}H_{24}N_4O_6$ (M+H) requires 465.1774].

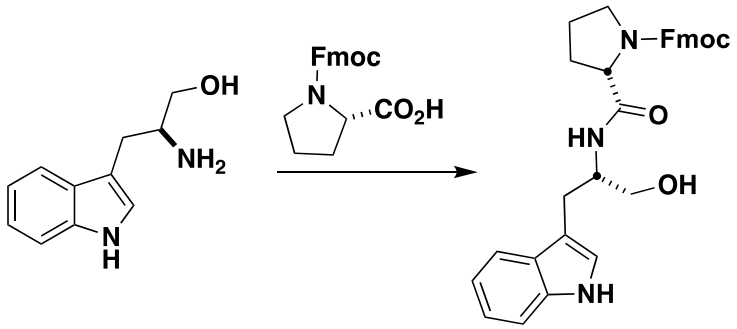


**Alcohol 3.20.** HATU (496 mg, 1.3 mmol) and *i*-$Pr_2$NEt (0.4 mL, 300 mg, 2.32 mmol) were added to a solution of tryptophan **3.19** (212 mg, 1.115 mmol) and **L-Proline 3.9** (451 mg, 1.34 mmol) in DMF (11.15 mL) and the reaction was stirred at room temperature for 2 h. The reaction was concentrated under reduced pressure, taken up in EtOAc, and added $Et_2O$ (20 mL). The organics were washed with 1 M HCl (20 mL), saturated aqueous NaCl (20 mL), dried ($MgSO_4$), filtered and concentrated under reduced pressure. The residue was purified by flash chromatography eluting

with 40 - 60% EtOAc/hexane to yield 128.2 mg (22.6%) of alcohol **3.20** as a white solid. The material as not analyzed by NMR due to the presence of rotomers.

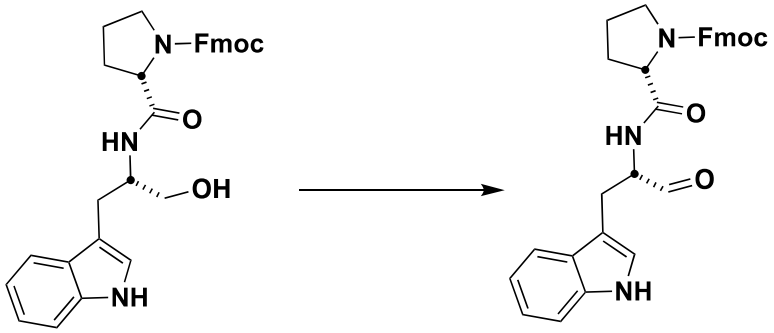


**Aldehyde 3.21.** $SO_3$·Py (159.16 mg, 1 mmol) was added to a solution of alcohol **3.20** (128.2 mg, 0.251 mmol), $Et_3N$ (0.18 mL, 129.5 mg, 1.28 mmol) and DMSO (1.34 mL) in $CH_2Cl_2$ (2.8 mL) and the reaction stirred for 3 h at room temperature. The reaction was partitioned between water (7 mL) and EtOAc (7 mL). The layers were separated, and the organic phase was washed with 1 M HCl (7 mL) and saturated aqueous NaCl (7 mL), and then dried ($MgSO_4$), filtered and concentrated under reduced pressure. The residue was purified by preparative thin layer chromatography eluting with 45% EtOAc/hexanes to yield aldehyde **3.21** as a yellow solid. The material was not analyzed by NMR due to the presence of rotomers.

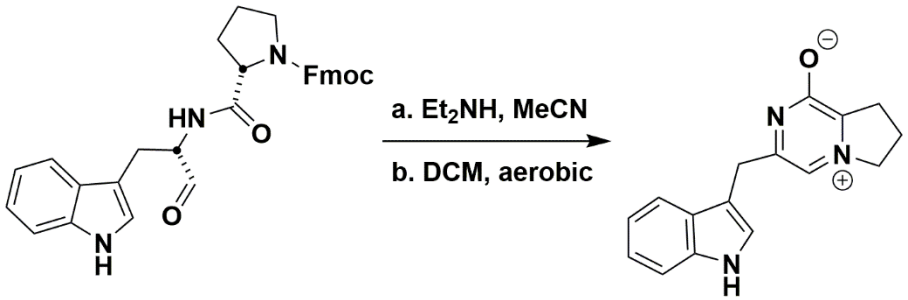


**Zwt 3.17.** $Et_2NH$ (0.08 mL) was added to a solution of aldehyde **3.21** (12.1 mg, 0.024 mmol) in MeCN (0.40 mL) and the reaction stirred at room temperature for 2 h. The reaction was concentrated under reduced pressure, the residue was taken up in $CH_2Cl_2$ (1.20 mL) and allowed to stand for 2 days. The resulting solution was concentrated under reduced pressure. The residue was purified by preparative thin layer

chromatography eluting with 5% MeOH/$CH_2Cl_2$ to give 3.0 mg (47.2%) of **Zwt 3.17** as a yellow solid. $^1$H NMR (400 MHz, DMSO, 25 °C) $\delta$ 10.90 (s, 1 H), 7.53 (d, *J* = 7.84 Hz, 1 H), 7.33 (d, *J* = 8.08 Hz, 1 H), 7.21 (d, *J* = 2.24 Hz, 1 H), 7.14 (s, 1 H), 7.05 (t, *J* = 7.04 Hz, 1 H), 6.95 (t, *J* = 7.04 Hz, 1 H), 4.46 (t, *J* = 7.75 Hz, 2 H), 3.89 (s, 2 H), 2.95 (t, *J* = 7.58 Hz, 2 H), 2.13 (m, *J* = 7.6 Hz, 2 H). $^{13}$C NMR (400 MHz, DMSO, 25 °C) $\delta$ 164.82, 159.04, 140.13, 136.24, 127.06, 123.75, 120.99, 118.67, 118.39, 111.38, 111.17, 109.30, 59.02, 31.69, 29.61, 19.09.

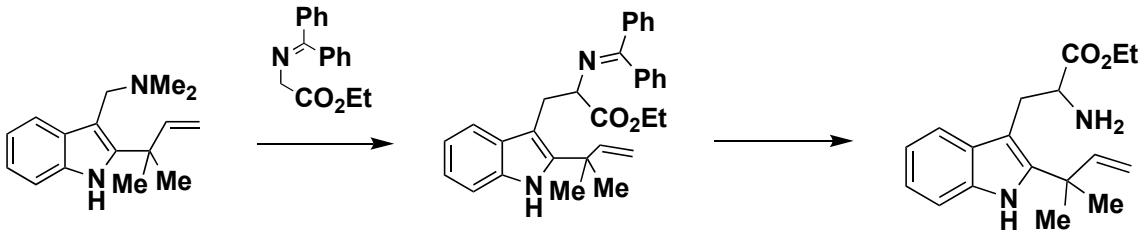


**Tryptophan 4.23.** Freshly distilled DBU (6.70 mmol, 1.0 mL) was added to a solution of gramine **4.20** (5.24 mmol, 1.27 g) and glycine derivative **4.21 (**5.24 mmol, 1.4 g) in MeCN (24 mL) at 0 °C. The solution was allowed to warm to room temperature, then was heated to reflux and ran overnight. The resulting solution was allowed to cool to room temperature and was added aqueous $NH_4Cl$ (20 mL). The crude mixture was washed with $Et_2O$ (20 mL x 2), saturated aqueous NaCl (2 x 20 mL), dried ($MgSO_4$), filtered, and concentrated under reduced pressure to yield intermediate **4.22** as a crude orange oil that was carried forward immediately for hydrolysis.

1M HCl (50.8 mmol, 51 mL) was added to a solution of **4.22** in MeCN (24 mL) at 0 °C. The solution was allowed to warm to room temperature, then stirred for 3 h. The crude mixture was basified with 1M NaOH (~20 mL) at 0 °C. The resulting solution was allowed to warm to room temperature, then was extracted with DCM (50 mL x 2). The organics were washed with saturated aqueous NaCl (2 x 50 mL), dried ($Na_2SO_4$), filtered and concentrated. Purification by $SiO_2$ plug, eluting with DCM, then 3% MeOH/DCM. The fractions from the 3% MeOH/DCM eluent were

collected and concentrated under reduced pressure to yield 560 mg (47%) tryptophan **4.23** as an orange/yellow oil.

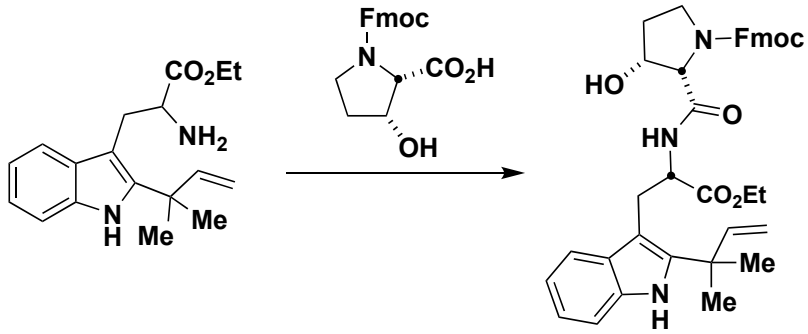


**Dipeptide 4.25.** HATU (967 mg, 2.54 mmol) and *i*-$Pr_2NEt$ (0.742 mL, 551 mg, 4.26 mmol) were added to a solution of *N*-Fmoc-β-hydroxy-L-proline **4.24** (946 mg, 2.50 mmol) and tryptophan **4.23** (560 mg, 1.87 mmol) in $CH_3CN$ (13 mL) at 0 °C. The solution was allowed to warm to room temperature and stirred for 18 h. The reaction was concentrated under reduced pressure, and the residue was taken up in DCM (40 mL). The solution was washed with 1 M HCl (40 mL). The layers were separated, and the aqueous phase was washed with DCM (15 mL x 2). The organic phase was washed with saturated aqueous NaCl (21 mL), then dried ($Na_2SO_4$), filtered and concentrated under reduced pressure. The residue was purified by flash chromatography eluting with 10% - 80% EtOAc/hexane to yield dipeptide **4.25** as an off-white foamy solid. All spectral data matched that of previously reported.

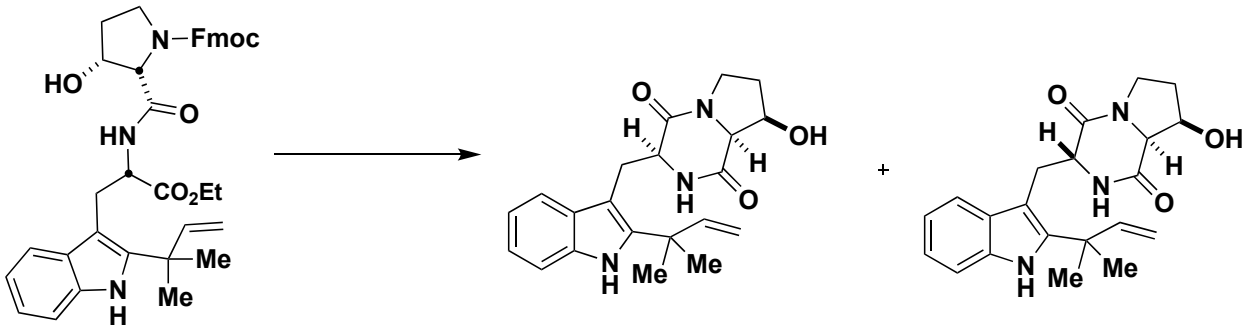


**Hydroxy Diketopiperazine 4.26.** $Et_3N$ (2.6 mL, 19.0 mmol), then hydroxypyridine (40 ml, 309 mg, 0.42 mmol) were added to a solution of dipeptide **4.25** (1.2 g, 1.90 mmol) in $CH_3CN$ (30 mL). The

reaction was heated to reflux and stirred for 23 h. The resulting solution was allowed to cool to room temperature and was partitioned between DCM (76 mL) and 1 M HCl (38 mL). The layers were separated, and the aqueous phase was washed with DCM (20 mL x 2). The combined organic layers were washed thoroughly with saturated aqueous NaCl (80 mL), then dried ($MgSO_4$), filtered and concentrated under reduced pressure. The residue was purified by flash chromatography eluting with 3% - 5% MeOH/DCM to yield 360 mg (51.6%) of a diastereomeric mixture of diketopiperazines **4.26** as an off-white foamy solid. ROESY and NOESY data were obtained for the separated diastereomers; however, the data did not reveal the identity of the diastereomers. Diastereomer 1: $^{1}$H NMR (400 MHz, $CDCl_3$, 25 °C) $\delta$ 8.06 (bs, 1 H), 7.49 (d, *J* = 7.84 Hz 1 H), 7.33 (d, *J* = 8.00 Hz, 1 H), 7.18 (t, *J* = 7.5 Hz, 1 H), 7.12 (t, *J* = 7.96 Hz, 1 H), 6.13 (dd, *J* = 10.2, 16.92, 1 H), 5.85 (bs, 1 H), 5.21 (s, 1 H), 5.17 (d, *J* = 6.2 Hz, 1 H), 4.69 (bs, 1 H), 4.43 (d, *J* = 9.36 Hz, 1 H), 4.12 (bs, 1 H), 3.89 (m, 1 H), 3.77 (dd, *J* = 4, 15.32 Hz, 1 H), 3.71 (t, *J* = 10.04 Hz, 1 H), 3.20 (dd, *J* = 11.72, 15.28 Hz, 1 H), 2.98 (t, *J* = 1.88 Hz, 1 H), 2.17 (s, 2 H), 1.56 (s, 6 H).; $^{13}$C NMR (400 MHz, $CDCl_3$, 25 °C) $\delta$ 167.73, 165.90, 145.65, 141.73, 134.48, 129.15, 122.39, 120.35, 117.98, 113.10, 111.06, 104.61, 71.01, 64.66, 55.01, 44.19, 39.15, 30.33, 28.09, 26.30.

Diastereomer 2: $^{1}$H NMR (400 MHz, $CDCl_3$, 25 °C) $\delta$ 7.99 (bs, 1 H), 7.52 (d, *J* = 7.28 Hz, 1 H), 7.24 (bs, 1 H), 7.10 (m, 2 H), 6.12 (dd, *J* = 10.56, 17.44 Hz, 1 H), 5.92 (bs, 1 H), 5.18 (m, 2 H), 4.59 (bs, 1 H), 4.29 (m, 1 H), 3.85 (m, 1 H), 3.70 (d, *J* = 3.08 Hz, 1 H), 3.19-3.31 (comp, 2 H), 2.89 (bs, 1 H), 2.05 (m, 1 H), 1.54 (s, 3 H), 1.53 (s, 3 H); $^{13}$C NMR (400 MHz, $CDCl_3$, 25 °C) $\delta$ 167.16, 166.06, 145.94, 141.43, 134.20, 128.91, 121.98, 119.87, 118.48, 112.09, 110.57, 104.98, 70.98, 63.82, 58.50, 47.49, 44.20, 39.09, 29.95, 29.58, 27.97, 27.78, 8.70.

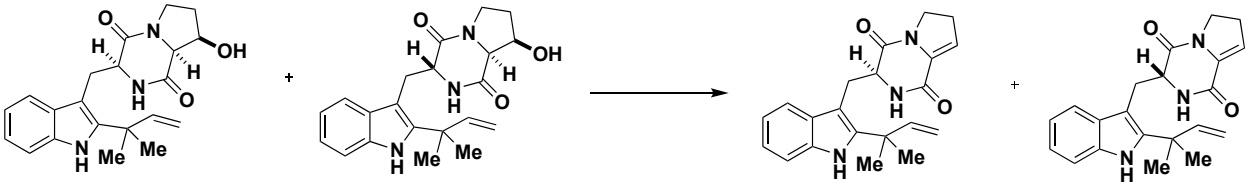

**Enamine Diketopiperazine 4.28.** $Et_3N$ (44.0 mg, 0.061 mL, 0.435 mmol), then MsCl (24.21 mg, 0.016 mL, 0.211 mmol) were added to a solution of diketopiperazine **4.26** (38.8 mg, 0.106 mmol) in DCM (2 mL) at 0 °C. The reaction ran at the same temperature for 1 h, then was poured into saturated aqueous $NaHCO_3$ (5 mL). The resulting solution was extracted with DCM (5 mL), dried ($Na_2SO_4$), filtered and concentrated under reduced pressure to yield 47.19 mg of crude diastereomeric mesylated diketopiperazine **4.27**.

DBU (0.048 mL, 48.4 mg, 0.318 mmol) was added to a solution of the mesylated diketopiperazines **4.27** (47.19 mg, 0.106 mmol) in MeCN (3 mL) at 0 °C. The reaction was allowed to warm to room temperature and stirred for 12 h. The resulting solution was poured into saturated aqueous $NH_4Cl$ (5 mL) at 0 °C, then was extracted with EtOAc (5 mL). The layers were separated, and the organic phase was washed with saturated aqueous NaCl (5 mL), dried ($Na_2SO_4$), filtered and concentrated under reduced pressure to afford enamine diketopiperazine **4.28** as a crude diastereomeric mixture.

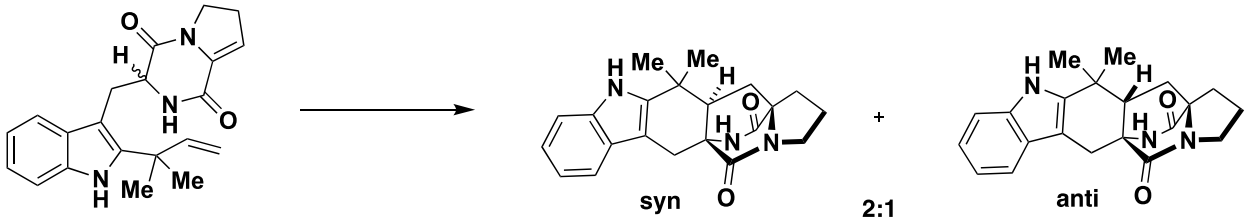


**Model DA 4.30.** Aqueous 20% KOH (0.49 mL, 1.04 g, 3.71 mmol) was added to a solution of enamine diketopiperzines **4.28** (37 mg, 0.106 mmol) in MeOH (3 mL). The reaction was heated to 60 °C and stirred for 12 h, then was poured into 1 M HCl (5 mL) at 0 °C. The resulting solution was extracted with EtOAc (5 mL), and the organic phase was washed with saturated aqueous

NaCl (5 mL), dried ($Na_2SO_4$), filtered and concentrated under reduced pressure. The residue was purified by flash column chromatography, eluting with 25% - 100% EtOAc/hexanes to yield a 2:1 syn:anti ratio of Model DA **4.30** as a white solid. $^1$H NMR (400 MHz, 5:2 $CDCl_3$:MeOD, 25 °C) δ 7.27-7.32 (comp, 1 H), 7.10-7.15 (comp, 1 H), 6.83-6.95 (comp, 2 H), 3.59 (m, 1 H), 3.18-3.37 (comp, 2 H), 2.53-2.81 (comp, 2 H), 2.11-2.42 (comp, 1 H), 1.95-2.04 (comp, 1 H), 1.78-1.98 (comp, 3 H), 1.68-1.75 (comp, 1 H), 1.02 (m, 6 H); $^{13}$C NMR (400 MHz, 5:2 $CDCl_3$:MeOD, 25 °C) δ 174.12, 173.65, 169.96, 139.97, 139.81, 136.61, 126.87, 126.52, 121.12, 121.03, 118.63, 118.50, 117.67, 117.59, 110.60, 110.51, 103.32, 102.35, 67.02, 66.61, 61.44, 60.33, 49.39, 45.76, 43.95, 43.88, 34.59, 34.44, 32.35, 30.65, 28.99, 28.75, 28.13, 27.85, 24.24, 24.17, 24.08, 22.96, 21.62.

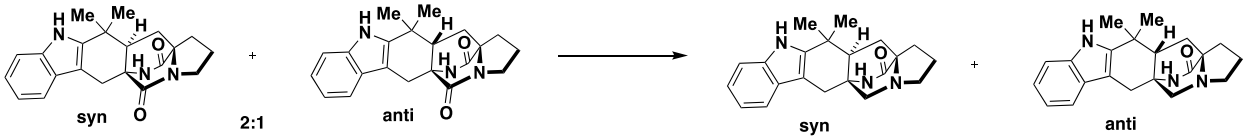


**Monoketopiperazine 4.52.** DIBAL-H (1M in toluene, 1.14 mL, 1.14 mmol) was added to a solution of **model DA 4.30** (20 mg, 0.057 mmol) in toluene (11.46 mL) at 0 °C. The solution was allowed to warm to room temperature and stirred for 25 h. The reaction was brought back down to 0 °C and $Na_2SO_4$ decahydrate was added slowly until bubbling subsided. The resulting to solution was allowed to warm to room temperature and stirred for 30 min. The salts were filtered off and the mixture evaporated. The crude material was purified by PTLC, eluting with 2% MeOH/DCM to yield a diastereomeric ratio of monoketopiperazine **4.52**.

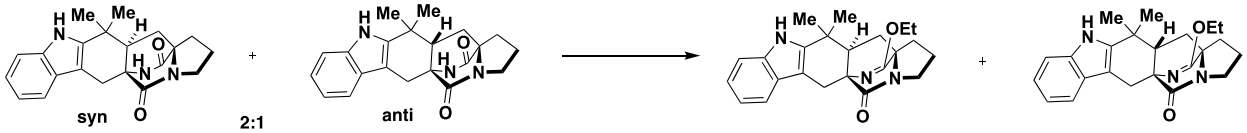


**Lactim Ether 4.53.** $Et_3OBF_4$ (326.7mg, 1.72 mmol) and $Cs_2CO_3$ (839.5 g, 2.58 mmol) were added to a solution of **Model DA 4.30** (300 mg, 0.86 mmol) in DCM (60 mL) at 0 °C. The solution was allowed to warm to room temperature, then was heated to reflux and stirred for 18 h. The

resulting solution was allowed to cool to room temperature, the salts were filtered off over celite, and rinsed with DCM. The resulting organics were washed with saturated aqueous $NH_4Cl$ (50 mL) and saturated aqueous NaCl (50 mL), dried ($Na_2SO_4$), filtered, and concentrated under reduced pressure to yield lactim ether **4.53** as a crude product. $^1H$ NMR (400 MHz, $CDCl_3$, 25 °C) $\delta$ 8.88 (bs, 1 H), 7.47 (d, *J* = 7.20 Hz, 1 H), 7.20 (d, *J* = 7.72 Hz, 1 H), 7.01 (t, *J* = 7.04 Hz, 1 H), 6.96 (t, *J* = 7.76 H, 1 H), 4.02 (m, 1 H), 3.92 (m, 1 H), 3.77 (d, *J* = 17.04 Hz, 1 H), 3.39 (s, 3 H). 3.36 (bs, 1 H), 3.18 (d, *J* = 17.04 Hz, 1 H), 2.60 (m, 1 H), 2.24 (dd, *J* = 4.08, 9.76 Hz, 1 H), 1.91 (m, 5 H). 1.76 (dd, *J* = 4.12, 13.08 Hz, 1 H), 1.15 (s, 6 H).

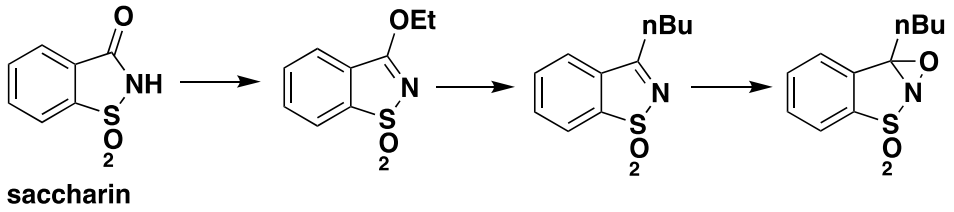

saccharin

**Davis Oxaziridine (D.O.).**[157] $PCl_5$ (8 g, 0.039 mol) was carefully added to saccharin (5.49 g, 0.03 mol) under argon. An air condenser was attached and the solids were slowly heated to 175 °C as they reacted and formed a liquid. The reaction was allowed to stir at the same temperature for 1.5 h. The resulting mixture was allowed to cool to room temperature, and the $POCl_3$ side product was concentrated under reduce pressure. The resulting crude material was dissolved in EtOH (400 mL) and the mixture heated to reflux for 1 h. The solution was allowed to cool to room temperature, the stored in the fridge overnight while crystallization occurred. The resulting crystals were collected by vacuum filtration to yield ethyl ether saccharin.

nBuLi was added to a solution of ethyl ether saccharin (1 g, 4.7 mmol) in THF (95 mL) at -78 °C. The reaction stirred for 4 h at the same temperature, then was quenched with saturated aqueous $NH_4Cl$ (9.5 mL). The resulting mixture was allowed to warm to room temperature, then was

extracted with $Et_2O$ (143 mL). The organics were washed with saturated aqueous NaCl (95 mL x 2), dried ($MgSO_4$), filtered and concentrated to yield 860 mg (82% yield) of butyl saccharin as a white solid.

A solution of 95% mCPBA (1.05 g, 5.8 mmol) in DCM (38.5 mL) was added dropwise over the course of 30 minutes to a solution of butyl saccharin (860 mg, 3.85 mmol) in saturated aqueous $K_2CO_3$ (58 mL) and DCM (58 mL) at room temperature. The solution stirred at the same temperature for 2 h. The layers were separated and the organic phase was washed with saturated aqueous $Na_2SO_3$ (60 mL), saturated aqueous $NaHCO_3$ (60 mL), and saturated aqueous NaCl (60 mL), dried ($MgSO_4$), filtered, and concentrated under reduced pressure to yield a yellow oil. The crude material was recrystallized from EtOH to yield davis' oxaziridine as a white crystal. All spectral data matched that of previously reported.

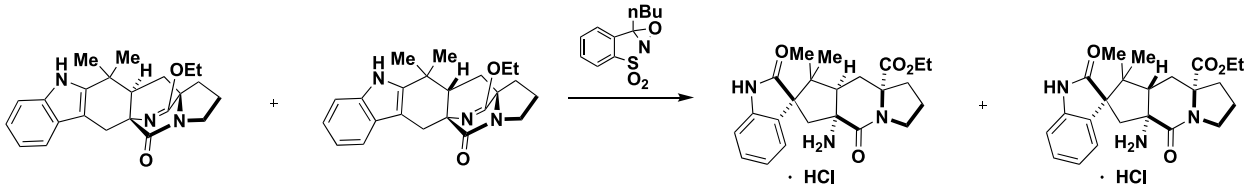


**Amine 4.54.** Davis' oxaziridine (636 mg, 2.6 mmol) was added to a solution of lactim ether **4.53** (324 mg, 0.86 mmol) in DCM (100 mL) at 0 °C. The reaction was allowed to warm to room temperature, then was heated to reflux and ran for 18 h. The resulting mixture was concentrated under reduced pressure and purified by flash chromatography elution with 100% EtOAc to yield the hydroxyindoline intermediate, which was sub sequentially dissolved in MeCN (10 mL) and added 1M HCl (1.426 mL, 1.426 mmol) at 0 *C. The reaction was allowed to warm to room temperature and stirred for 18 h. The solution was concentrated under reduced pressure to yield amine **4.54** as a crude salt. $^1$H NMR (400 MHz, $CDCl_3$, 25 °C) $\delta$ 7.57 (bs, 1 H), 7.49 (d, *J* = 7.47 Hz, 1 H), 7.18 (t, *J* = 7.38 Hz, 1 H), 7.01 (t, *J* = 7.68 Hz, 1 H), 6.83 (d, *J* = 7.44, 1 H), 4.16 (m, 2 H), 3.33-

3.61 (comp, 4 H), 2.99 (m, 1 H), 2.68 (m, 1 H), 2.55 (d, *J* = 13.5 Hz, 1 H), 1.31 (t, *J* = 7.08 Hz, 6 H), 1.25 (s, 3 H), 0.85 (s, 3 H), 0.83 (s, 3 H); HRMS (ESI-APCI) *m/z* 412.23 [$C_{23}H_{29}N_3O_4$ (M+H) requires 411.22].

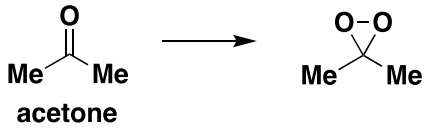

acetone

**Dimethyl Dioxirane (DMDO).**[158] $NaHCO_3$ (5 g) was added to a mixture of $H_2O$ (20 mL) and anhydrous acetone (15 mL) at 0 °C and stirred for 20 minutes at the same temperature. Oxone (10 g) was added to the solution in portions, then stirred for 15 minutes at the same temperature. DMDO was collected by vacuum distillation and titrated (see procedure below) with thioanisole to determine the concentration of 0.06M DMDO in acetone.

Titration: DMDO/acetone (0.5 mL) was added to a solution of thioanisole (0.03 mL, 0.25 mmol) in anhydrous acetone (1.3 mL) and stirred at room temperature for 10 minutes. The resulting solution was concentrated under reduced pressure, and an NMR was taken to reveal an integration ratio of 1:8.6.

Calculations: (1/8.6) x 0.25 mmol = 0.03 mmol DMDO in 0/5 mL DMDO/acetone. (0.03 mmol/0.5 mL) = 0.06 M DMDO in acetone.

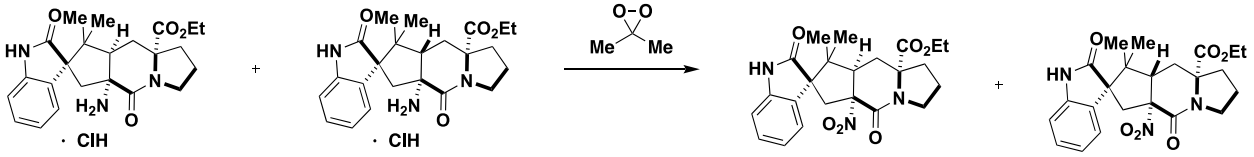


**Nitro 4.55.** A freshly prepared solution of 0.05M DMDO in acetone (0.18 mL, 0.0214 mmol, 0.12 M) was added to a solution of amine **4.54** in anhydrous acetone at -78 °C. The reaction ran at the same temperature for 3 h, then was concentrated to yield nitro **4.55** as a crude product. The product needs to be separated from the starting material for full analysis.

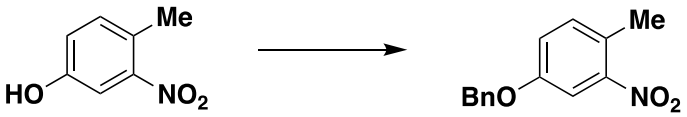


**Nitro Benzene 4.38.** $K_2CO_3$ (45.13 g, 326.5 mmol) and BnCl (43.4 mL, 48 g, 378.7 mmol) were added to a solution of 2-nitro-3-methylphenol **4.37** (50 g, 326.5 mmol) in DMF (350 mL). The solution was heated to reflux and stirred for 18 h. The reaction was allowed to cool to room temperature, then was partitioned between EtOAc (500 mL) and $H_2O$ (500 mL). The layers were separated and the aqueous phase was washed with EtOAc (250 mL x 2). The combined organics were washed with 1M NaOH (500 mL x 2) and saturated aqueous NaCl (500 mL x 2), dried ($MgSO_4$), filtered and concentrated under reduced pressure to yield 78.6 g (99%) nitro benzene **4.38** as a yellow solid. $^1$H NMR (400 MHz, $CDCl_3$, 25 °C) $\delta$ 7.60 (d, *J* = 2.72 Hz, 1H), 7.35-7.45 (comp, 5 H), 7.23 (d, *J* = 8.48 Hz, 1H), 7.13 (dd, *J* = 2.68, 8.48 Hz, 1H), 5.10 (s, 2H), 2.53, s, 3H); $^{13}$C NMR (400 MHz, $CDCl_3$, 25 °C) $\delta$ 157.29, 149.51, 136.07, 133.64, 128.86, 128.46, 127.67, 125.98, 120.80, 110.37, 70.68, 19.89.

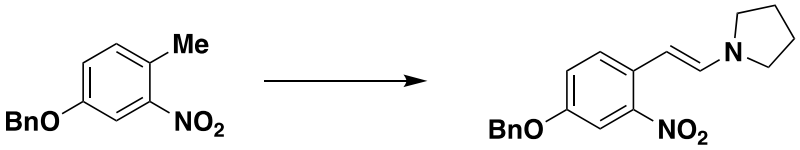


**Enamine 4.39.** DMF-DMA (135.7 mL, 121.74 g, 1.022 mol) was added to a solution of nitro benzene **4.38** in pyrrolidine (83.3 mL, 70.9 g, 0.98 mol). The reaction was heated to reflux and stirred for 18 h. The resulting solution was allowed to cool completely to room temperature and added EtOH until crystals formed. The resulting purple crystals were filtered off and washed with EtOH to yield 90.33 g (85.3%) of enamine **4.39** as a purple crystal. $^1$H NMR (400 MHz, $CDCl_3$, 25 °C) $\delta$ 7.50 (d, *J* = 2.8 Hz, 1H), 7.34-7.44 (comp, 6H), 7.11 (d, *J* = 13.52 Hz, 1H), 7.05 (dd, 2.8, 8.96 Hz, 1H), 5.86 (d, *J* = 13.56 Hz, 1H), 5.04 (s, 2H), 3.29 (t, *J* = 6.68 Hz, 4H), 1.93 (t, *J* = 6.70, 4H); $^{13}$C

NMR (400 MHz, $CDCl_3$, 25 °C) δ 154.11, 144.41, 139.64, 136.43, 130.12, 128.74, 128.27, 127.70, 125.80, 122.28, 109.58, 91.57, 70.57, 49.22, 25.36.

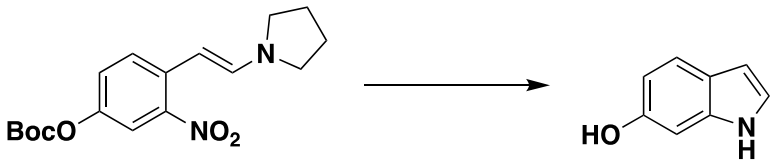


**Hydroxyindole 4.40.** 10% Pd/C (2.62 g, 24.64 mmol) was added to a solution of enamine **4.39** (20 g, 61.6 mmol) and $HCO_2NH_4$ (19.4 g, 308 mmol) in MeOH (200 mL). The solution was purged with argon for 10 minutes, the ran at room temperature for 3 h. The Pd/C was filtered off over celite and the solution was concentrated under reduce pressure. The resulting material was taken up in acetone and the ammonium formate salts were filtered off over celite, and the solution concentrated under reduced pressure. The crude product was dissolved in a little bit of acetone and a $SiO_2$ plug was ran eluting with 100% $Et_2O$. The resulting solution was concentrated under reduced pressure to yield hydroxyindole **4.40** as a yellow solid. The product was carried forward immediately. $^1$H NMR (400 MHz, $CDCl_3$, 25 °C) δ 10.64 (s, 1 H), 8.84 (s, 1 H), 7.28 (d, *J* = 8.44 Hz, 1 H), 7.08 (t, *J* = 2.72 Hz, 1 H), 6.74 (s, 1 H), 6.52 (dd, *J* = 2.12, 8.44 Hz, 1 H), 6.25 (bs, 1 H); $^{13}$C NMR (400 MHz, $CDCl_3$, 25 °C) δ 152.85, 136.97, 123.10, 120.97, 120.25, 109.44, 100.82, 96.42.

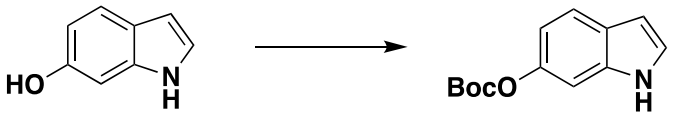


**Boc Indole 4.41.** $Boc_2O$ (15.6 mL, 14.8 g, 67.7 mmol) and DMAP (75.3 mg, 0.616 mmol) were added to a solution of hydroxyindole **4.40** (8.2 g, 61.6 mmol) in MeCN (120 mL) at 0 °C. The ice bath was removed and the reaction was allowed to run for 10 minutes. The solution was partitioned between $Et_2O$ (500 mL) and 1M HCl (250 mL). The organic phased was washed with 1M NaOH (500 mL) and saturated aqueous NaCl (500 mL x 2), dried ($MgSO_4$), filtered, and

concentrated under reduced pressure. Purification by flash chromatography eluting with 20% - 50% EtOAc/hexanes yielded 13.25 g (92%) of boc indole **4.41** as a white solid. $^{1}$H NMR (400 MHz, $CDCl_3$, 25 °C) $\delta$ 8.20 (bs, 1H), 7.58 (d, *J* = 8.52 Hz, 1H), 7.20 (d, *J* = 1.92 Hz, 1H), 7.14 (t, *J* = 2.8 Hz, 1H), 6.94 (dd, *J* = 2.12, 8.56, 1H), 6.51 (comp, 1H), 1.59 (s, 9H); $^{13}$C NMR (400 MHz, $CDCl_3$, 25 °C) $\delta$ 152.53, 146.67, 135.32, 125.67, 124.77, 120.78, 113.76, 103.59, 102.36, 83.08, 27.58.

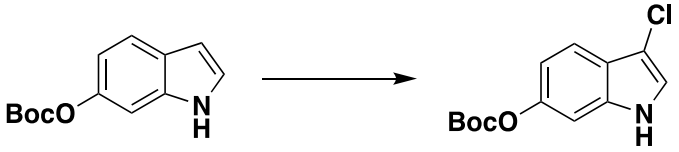


**Chlorinated Indole 4.42.** NCS (2.0 g, 15.4 mmol) was added to a solution of boc indole **4.41** (3.45 g, 14.8 mmol) in DMF (70 mL) and the reactions stirred at room temperature for 2.5 h. The resulting solution was partitioned between $H_2O$ (207 mL) and EtOAc (207 mL). The combined organics were washed with $H_2O$ (69 mL x 2) and saturated aqueous NaCl (138 mL), dried ($Na_sSO_4$), filtered and concentrated. The resulting material was run through a $SiO_2$ plug, eluting with 15% EtOAc/hexanes. The product was recrystallized from EtOAc and hexanes to yield 2.94 g (74.4%) chlorinated indole **4.42** as a white crystal.

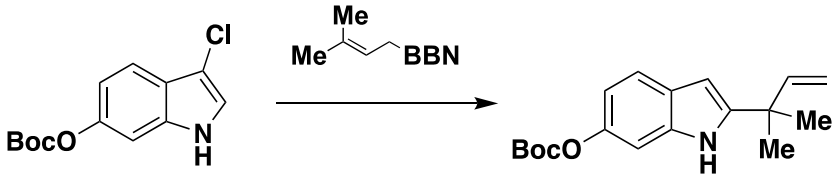


**Prenylated Indole 4.43.** Freshly made allene (3.9 mL, 2.66 g, 39 mmol) was added to a solution of 0.5M 9BBN in THF (64.7 mL, 32.35 mmol) at 0 °C. The reaction was allowed to warm to room temperature and ran at the same temperature for 16 h. Chlorinated indole **4.42** (2.94 g, 11 mmol) was added to the solution and stirred for 15 minutes. $Et_3N$ (4.56 mL, 3.3 g, 32.7 mmol) was added to the solution and the reaction stirred at the same temperature for another 8 h. The resulting mixture was washed sequentially with 1M HCl (77 mL) and saturated aqueous $NaHCO_3$ (77 mL).

The layers were separated and the organic phase was cooled to 0 °C. 2M NaOH (69 mL) and $H_2O_2$ (69 mL) were added to the solution sequentially at a rate in which the temperature remained between 0 °C and 5 °C. The mixture was allowed to warm to room temperature and stirred for another 1.5 h. The resulting crude material was purified by flash chromatography, eluting with 3% - 5% EtOAc/hexanes to yield 2.23 g (67.6& of prenylated indole **4.43** as a yellow solid.

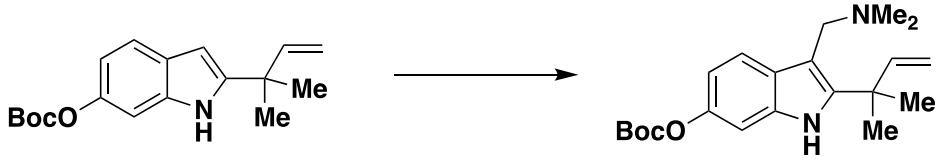


**Gramine 4.44.** 40% $Me_2NH$ (1 mL, 917 mg, 8.14 mmol) and 37% HCHO (0.58 mL, 631 mg, 7.77 mmol) were added to a solution of prenylated indole **4.43** (2.23 g, 7.4 mmol) in AcOH (7 mL) and MeCN (1 mL) at 0 °C. The reaction ran for 5 minutes at the same temperature, and then was allowed to warm to room temperature. The reaction ran at the same temperature for 1.5 h. The resulting solution was partitioned between 1M HCl (40 mL) and $Et_2O$ (80 mL). The organic phase was washed with 1M HCl (40 mL x 2). The aqueous extract was basified with 2M NaOH (140 mL), then was washed with $Et_2O$ (160 mL x 1, 80 mL x 2). The combined organics were washed with saturated aqueous NaCl (80 mL x 2), dried ($MgSO_4$), filtered and choncentrated. The crude material was ran through a $SiO_2$ plug, eluting with 5% MeOH/DCM to yield 1.36 g (51.3%) of gramine **4.44**. $^1$H NMR (400 MHz, $CDCl_3$, 25 °C) $\delta$ 8.79 (bs, 1H), 7.64 (d, *J* = 8.6 Hz, 1 H), 7.09 (d, *J* = 2 Hz, 1 H), 6.88 (dd, *J* = 2.12, 8.6 Hz, 1H), 6.12 (dd, *J* = 10.76, 17.24 Hz, 1H), 5.17 (dd, *J* = 1.08, 7.36 Hz, 1H), 5.13 (s, 1H), 3.56 (s, 2H), 2.20 (s, 6H), 1.57 (s, 9H), 1.54 (s, 6H); $^{13}$C NMR (400 MHz, $CDCl_3$, 25 °C) $\delta$ 152.93, 146.43, 146.21, 142.00, 133.63, 128.57, 119.61, 113.33, 112.17, 108.92, 103.10, 83.25, 54.05, 45.46, 39.50, 27.89, 27.25.

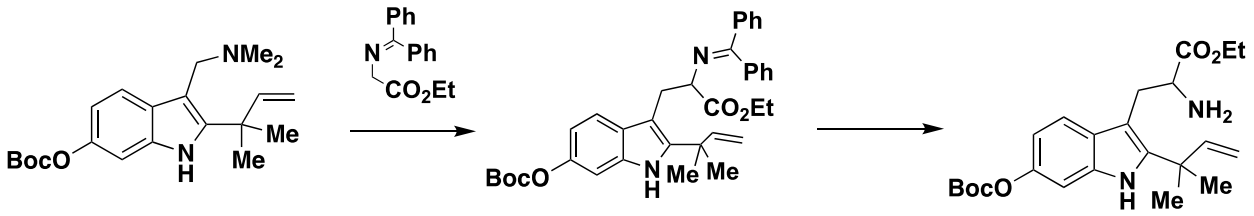


**Tryptophan 4.46.** Freshly distilled $PBu_3$ (0.09 mL, 70 mg, 0.345 mmol) was added to a solution of gramine **4.44** (246 mg, 0.69 mmol) and glycine derivative **4.21** (216.5 g, 0.81 mmol) in MeCN (7 mL). The reaction was heated to reflux and ran for 18 h. The resulting solution was allowed to cool to room temperature, was added 1M HCl (4.6 mL), and stirred for another 30 minutes. The reaction was then basified with 2M NaOH (2.7 mL) and extracted with $Et_2O$ (18.3 mL), washed with saturated aqueous NaCl (9 mL x 2), dried $MgSO_4$), filtered and concentrated. The crude material was purified by flash chromatography, eluting with 100 % DCM (20 mL) to wash away the side product then 3% MeOH/DCM (50 mL) to yield 182.6 mg (63.6%) tryptophan **4.46**.

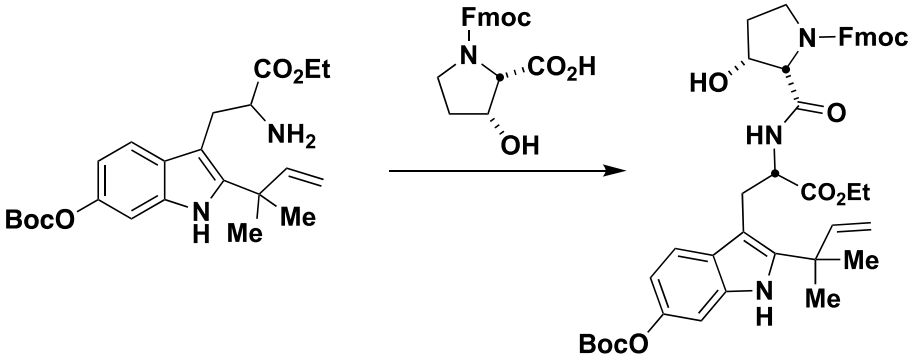


**Dipeptide 4.47.** HATU (227.5 mg, 0.60 mmol) and *i*-$Pr_2NEt$ (0.175 mL, 129.6 mg, 1.00 mmol) were added to a solution of *N*-Fmoc-β-hydroxy-L-proline **4.24** (206 mg, 0.58 mmol) and tryptophan **4.46** (182.6 mg, 0.44 mmol) in $CH_3CN$ (3.6 mL) at room temperature and stirred for 18 h. The reaction was concentrated under reduced pressure, and the residue was taken up in DCM (15 mL). The solution was washed with 1 M HCl (15 mL). The layers were separated, and the aqueous phase was washed with DCM (4 mL x 2). The organic phase was washed with saturated aqueous NaCl (5 mL), then dried ($MgSO_4$), filtered and concentrated under reduced pressure. The residue

was purified by flash chromatography eluting with 60% EtOAc/hexane to yield 268.1 mg (81%) dipeptide **4.47** as an off-white foamy solid. All spectral data matched that of previously reported.

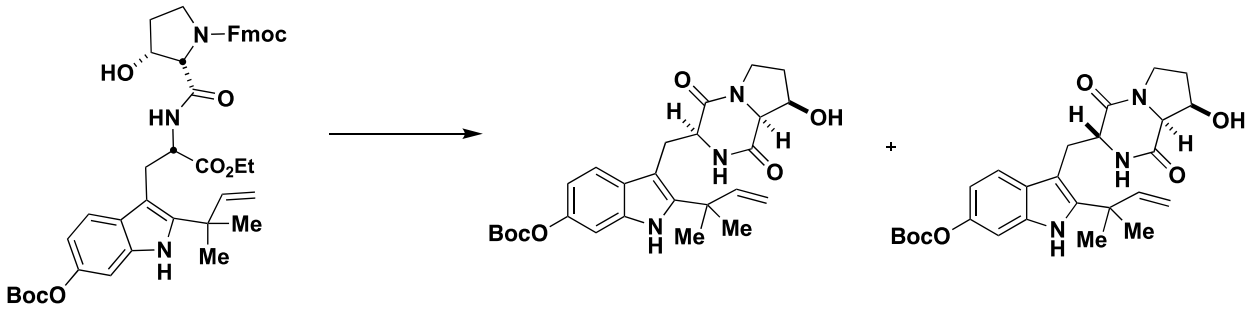

**Diketopiperazine 4.48.** $Et_3N$ (0.50 mL, 361 mg, 3.57 mmol), then hydroxypyridine (7.47 mg, 0.08 mmol) were added to a solution of dipeptide **4.47** (268.1 g, 0.36 mmol) in $CH_3CN$ (7 mL). The reaction was heated to reflux and stirred for 18 h. The resulting solution was allowed to cool to room temperature and was partitioned between DCM (17 mL) and 1M HCl (8.5 mL). The layers were separated, and the aqueous phase was washed with DCM (5 mL x 2). The combined organic layers were washed thoroughly with saturated aqueous NaCl (17 mL), then dried ($MgSO_4$), filtered and concentrated under reduced pressure. The residue was purified by flash chromatography eluting with 3% - 4% MeOH/DCM to yield a diastereomeric mixture of diketopiperazine **4.48** as an off-white foamy solid. $^1$H NMR (400 MHz, $CDCl_3$, 25 °C) $\delta$ 8.15 (bs, 1H), 7.43 (d, *J* = 8.52 Hz, 1H), 7.16 (d, *J* = 2.04 Hz, 1H), 6.93 (dd, *J* = 2.08, 8.6 Hz, 1H), 6.10 (dd, *J* = 17.36, 10.6 Hz, 1H), 5.79 (bs, 1H), 5.19 (d, *J* = 4.16 Hz, 1H), 5.15 (d, *J* = 11.24 Hz, 1H), 4.68 (t, *J* = 3.64, 1H), 4.39 (d, *J* = 9.36 Hz, 1H), 4.11 (bs, 1H), 3.88 (m, 1H), 3.72 (m, 2 H), 3.17 (dd, *J* = 15.34, 11.74 Hz, 1H), 2.17, (m, 1H), 2.03 (m, 1H), 1.56 (s, 9H), 1.52 (s, 6H); $^{13}$C NMR (400 MHz, $CDCl_3$, 25 °C) $\delta$ 167.51, 165.66, 152.56, 147.02, 145.40, 142.45, 134.13, 126.95, 118.27, 114.23, 113.03, 104.57, 103.85, 83.42, 70.85, 64.52, 54.78, 44.05, 39.07, 38.63, 30.21, 27.93, 27.83, 27.74, 26.22.

## II. NMR Data

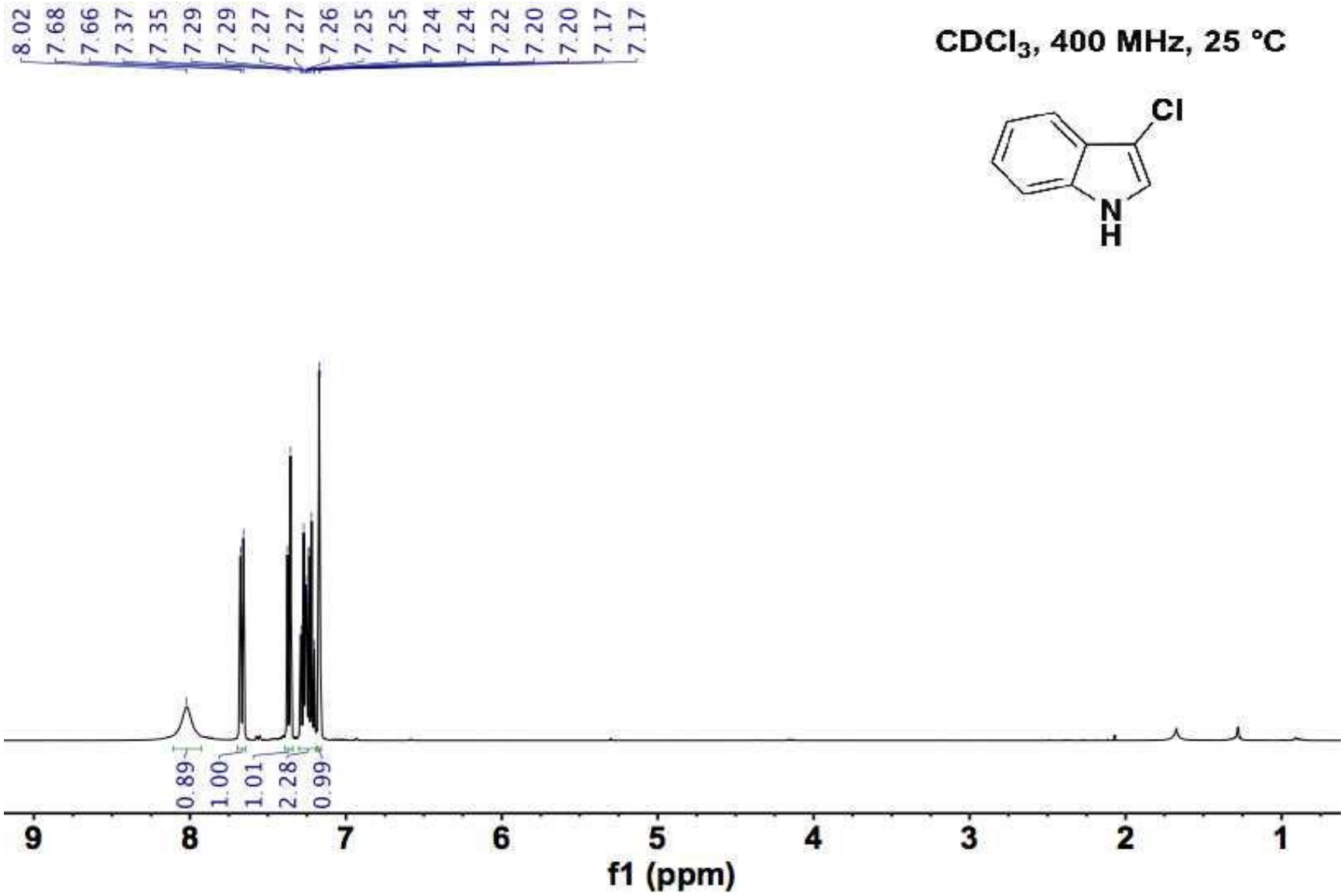


*Figure A2.3.1*. $^{1}$H NMR Spectrum of Compound **3.1**.

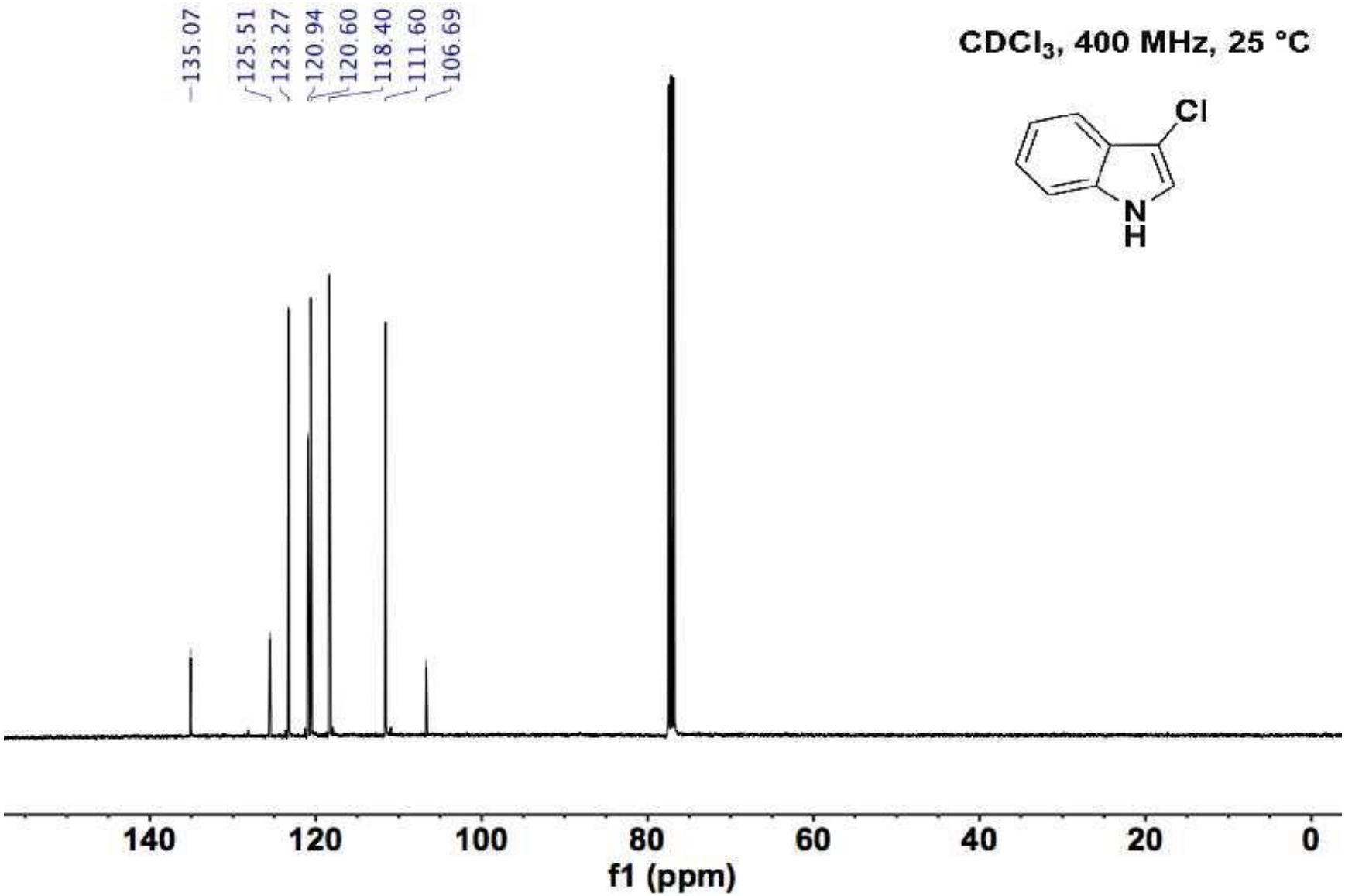


*Figure A2.3.2*. $^{13}$C NMR Spectrum of Compound **3.1**.

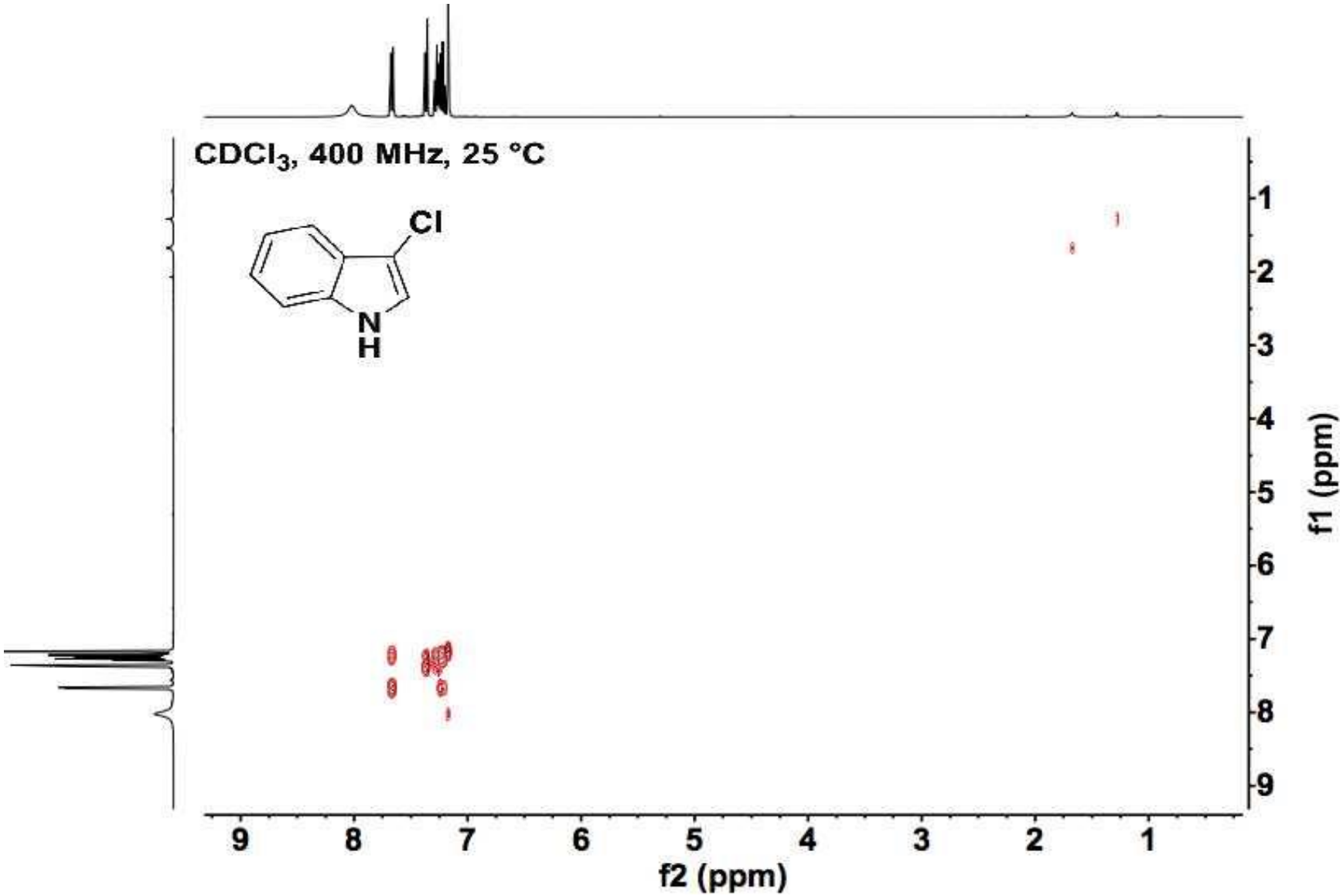


*Figure A2.3.3*. COSY NMR Spectrum of Compound **3.1**.

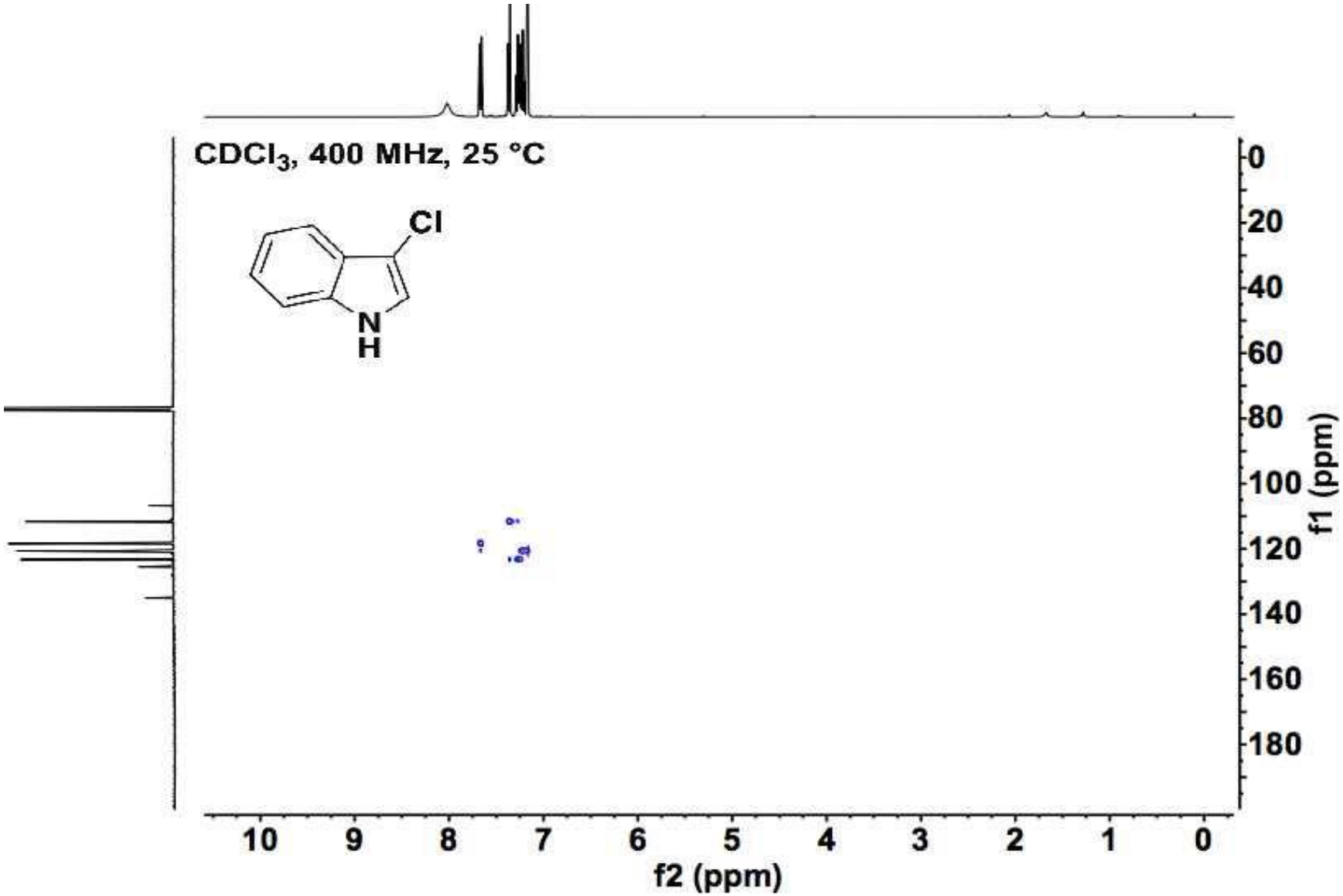


*Figure A2.3.4*. HSQC NMR Spectrum of Compound **3.1**.

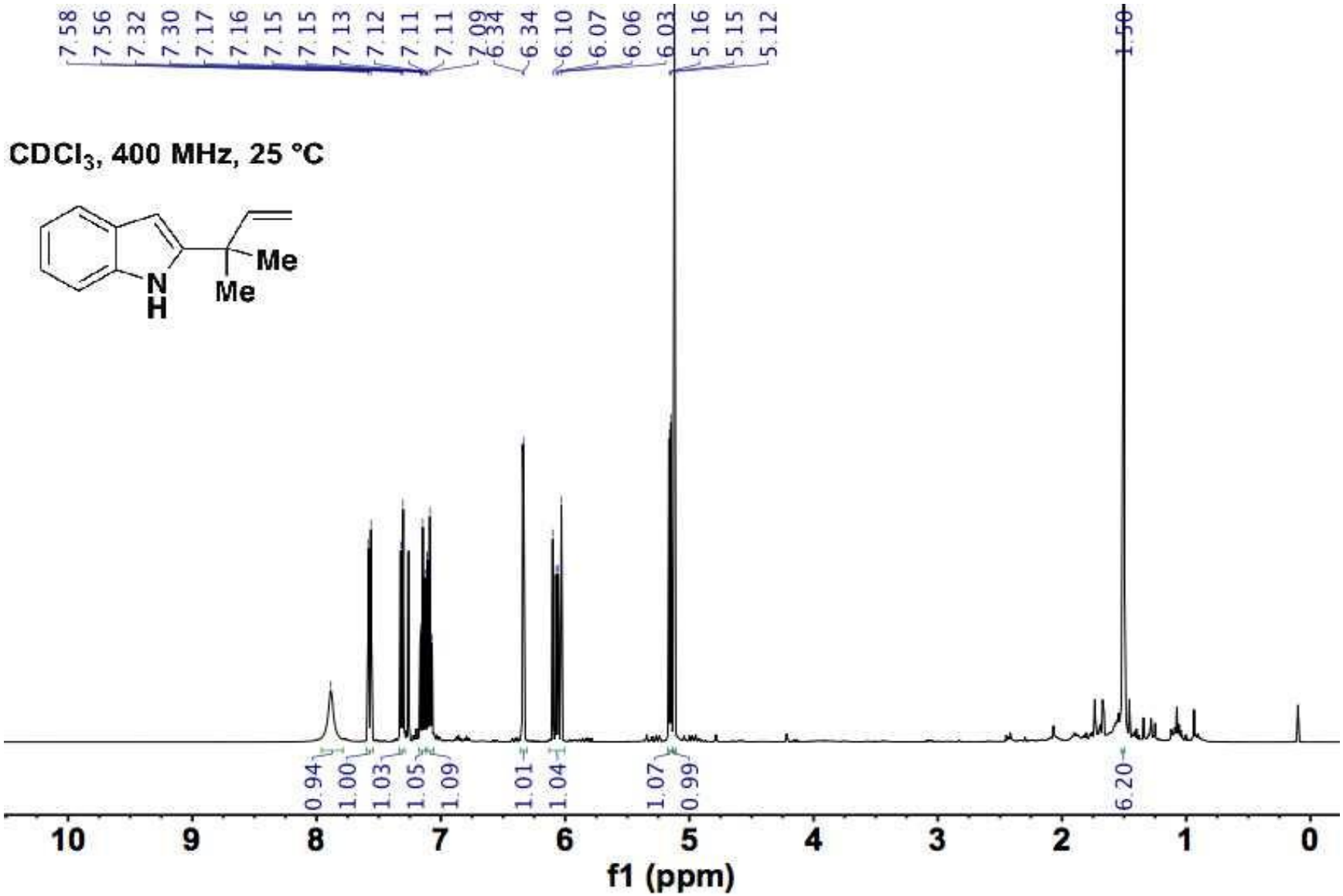


*Figure A2.3.5a*. $^{1}$H NMR Spectrum of Compound **3.3**.

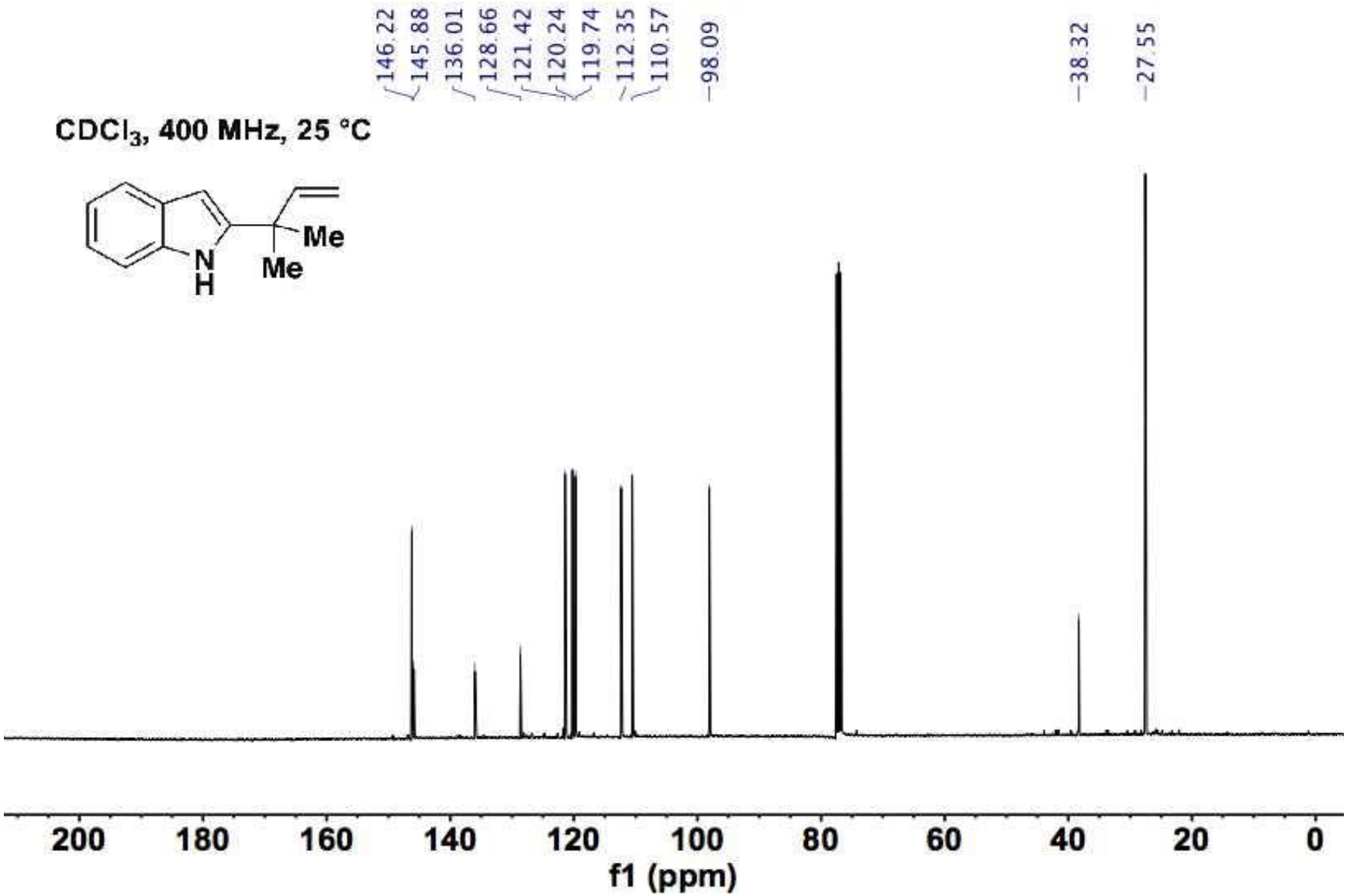


*Figure A2.3.5b*. $^{13}C$ NMR Spectrum of Compound **3.3**.

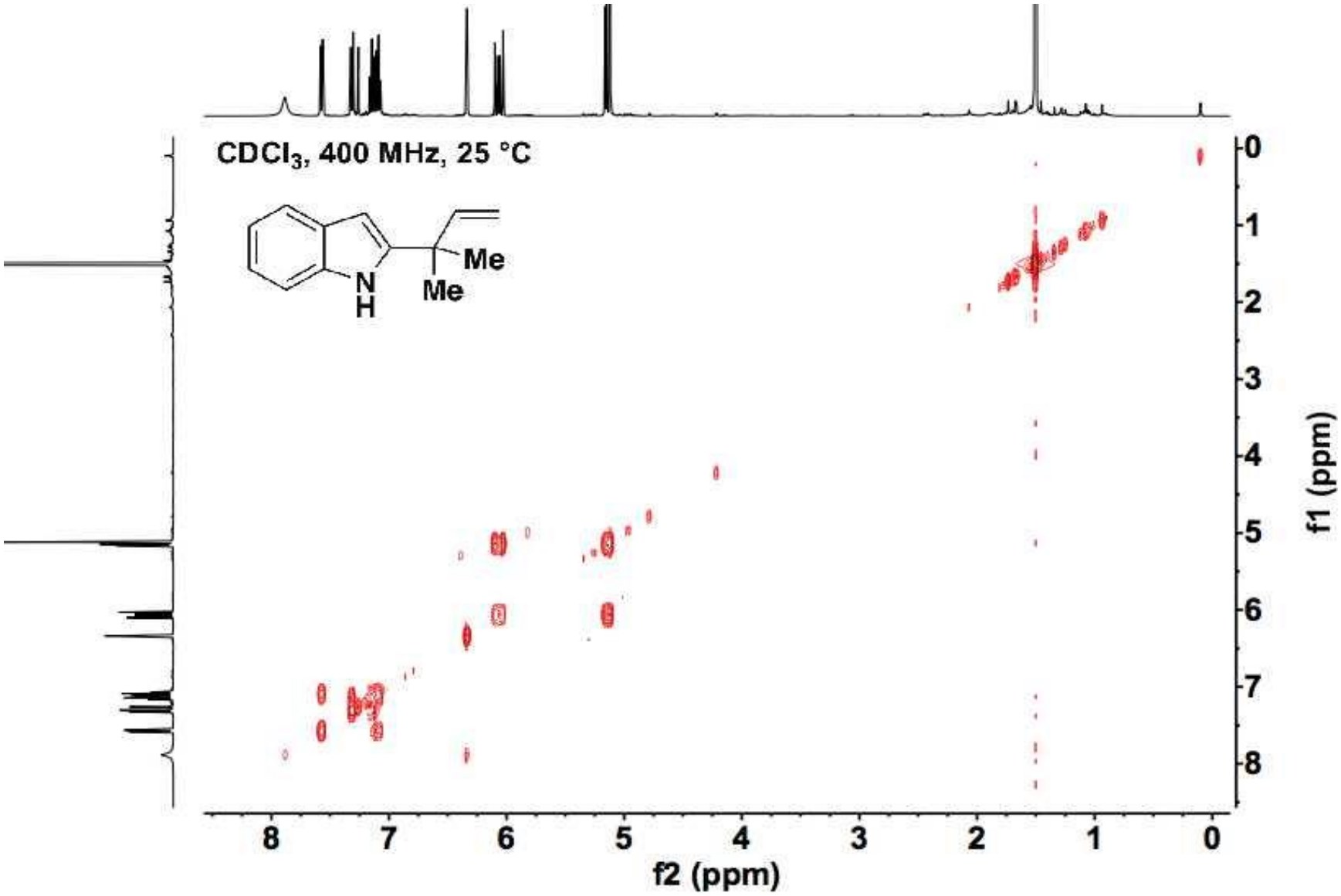


*Figure A2.3.5c*. COSY NMR Spectrum of Compound **3.3**.

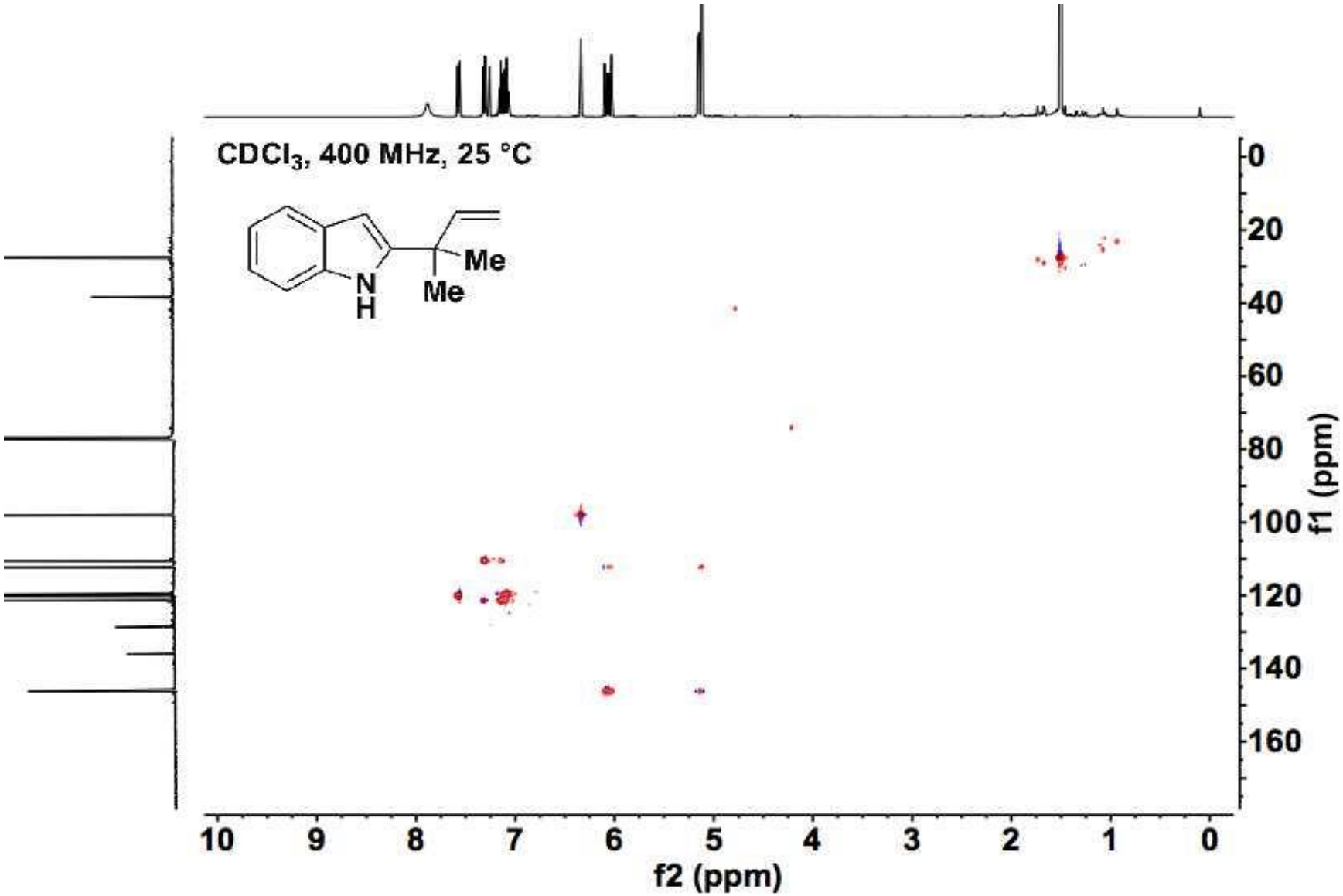


*Figure A2.3.5d*. HSQC Spectrum of Compound **3.3**.

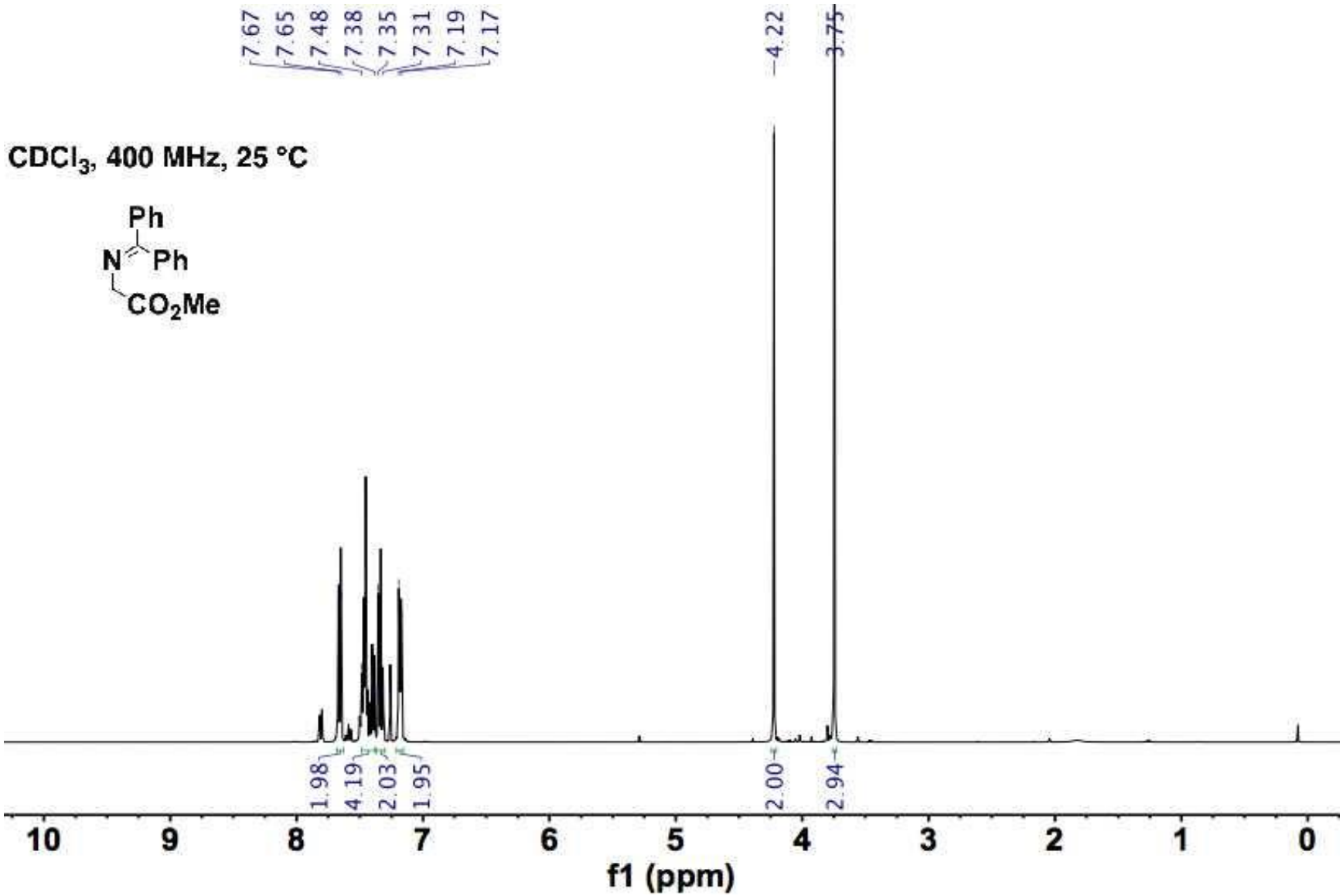


*Figure A2.3.6*. $^{1}$H NMR Spectrum of Compound **3.5**.

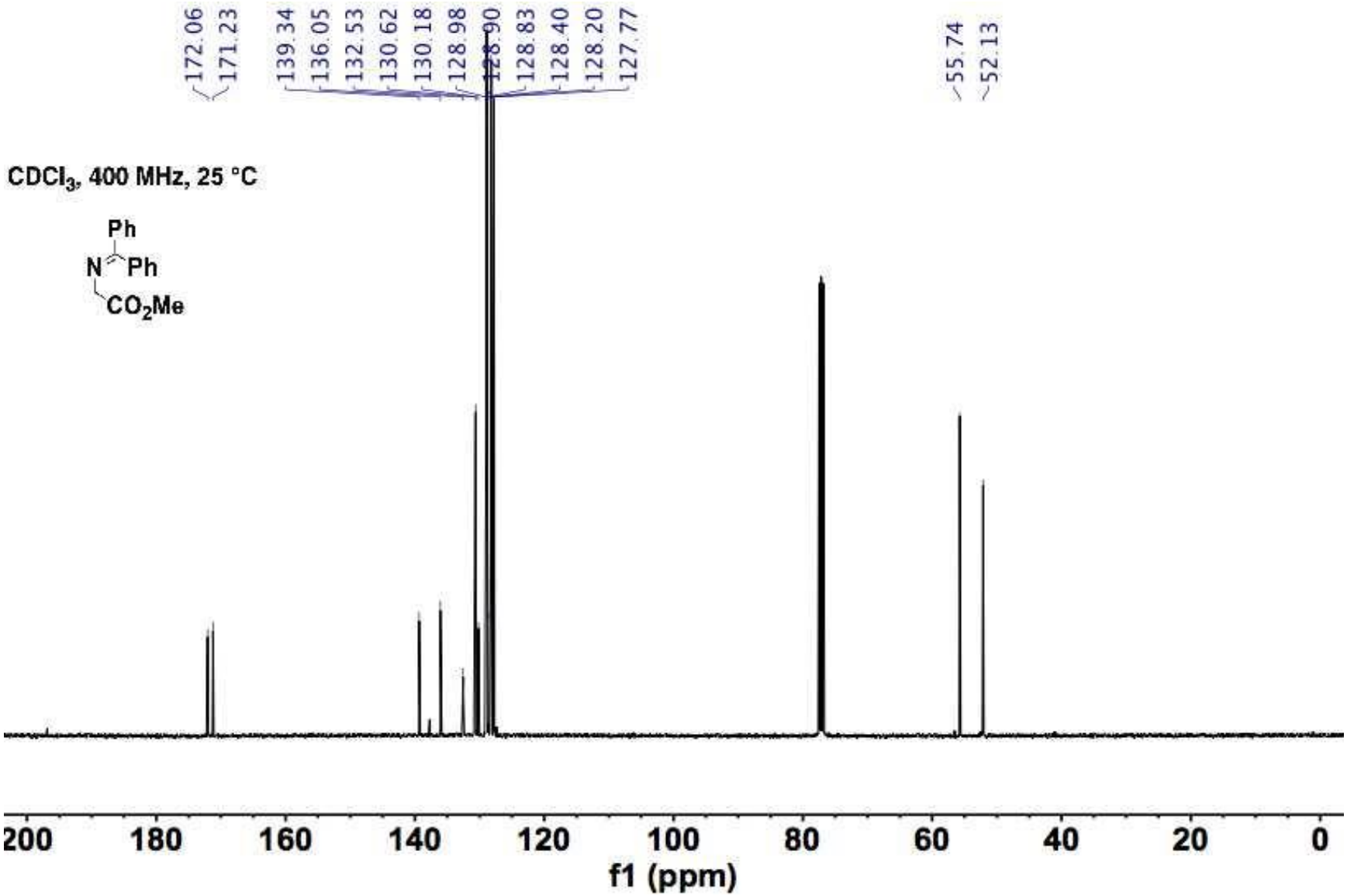


*Figure A2.3.7*. $^{13}C$ NMR Spectrum of Compound **3.5**.

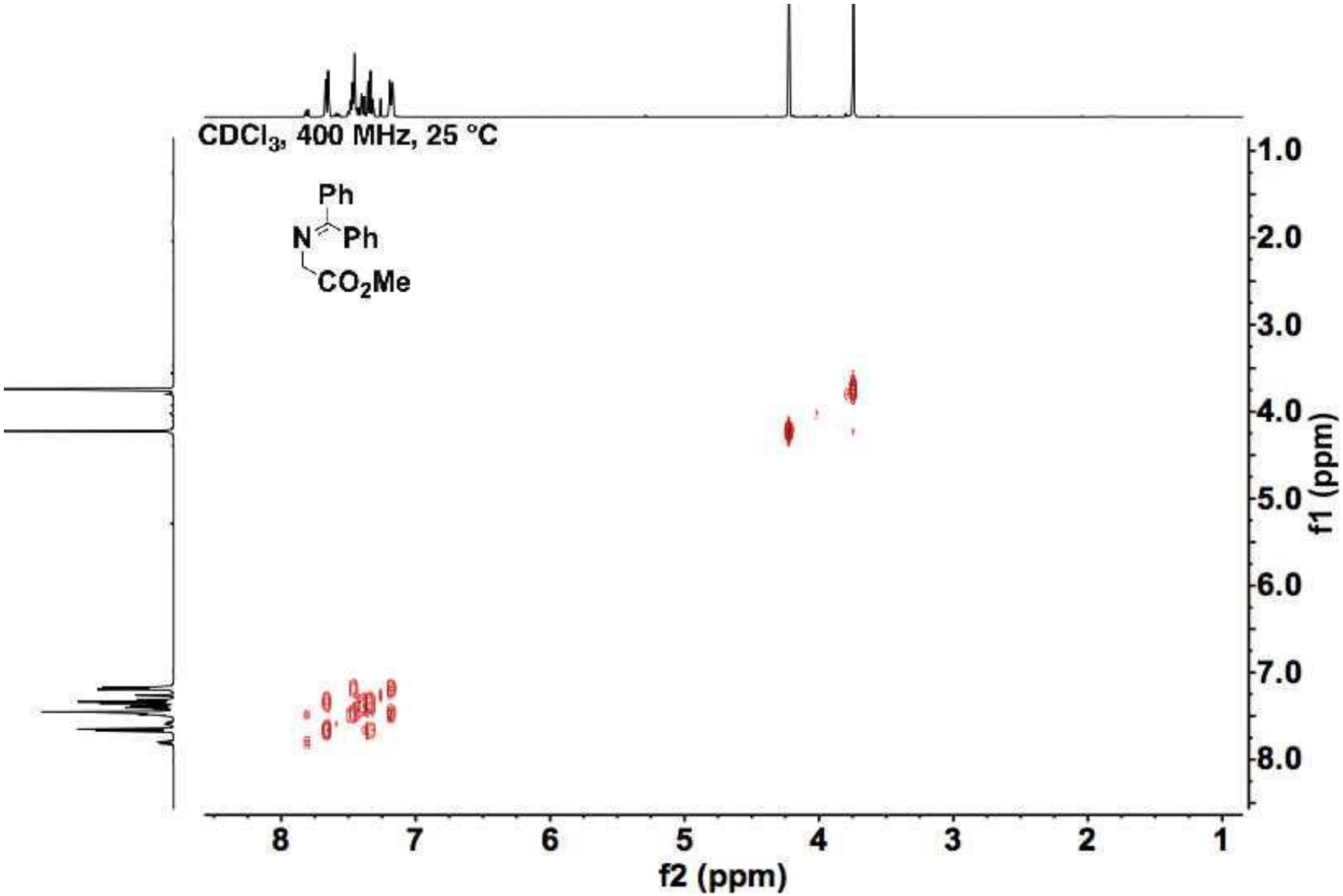


*Figure A2.3.8*. COSY NMR Spectrum of Compound **3.5**.

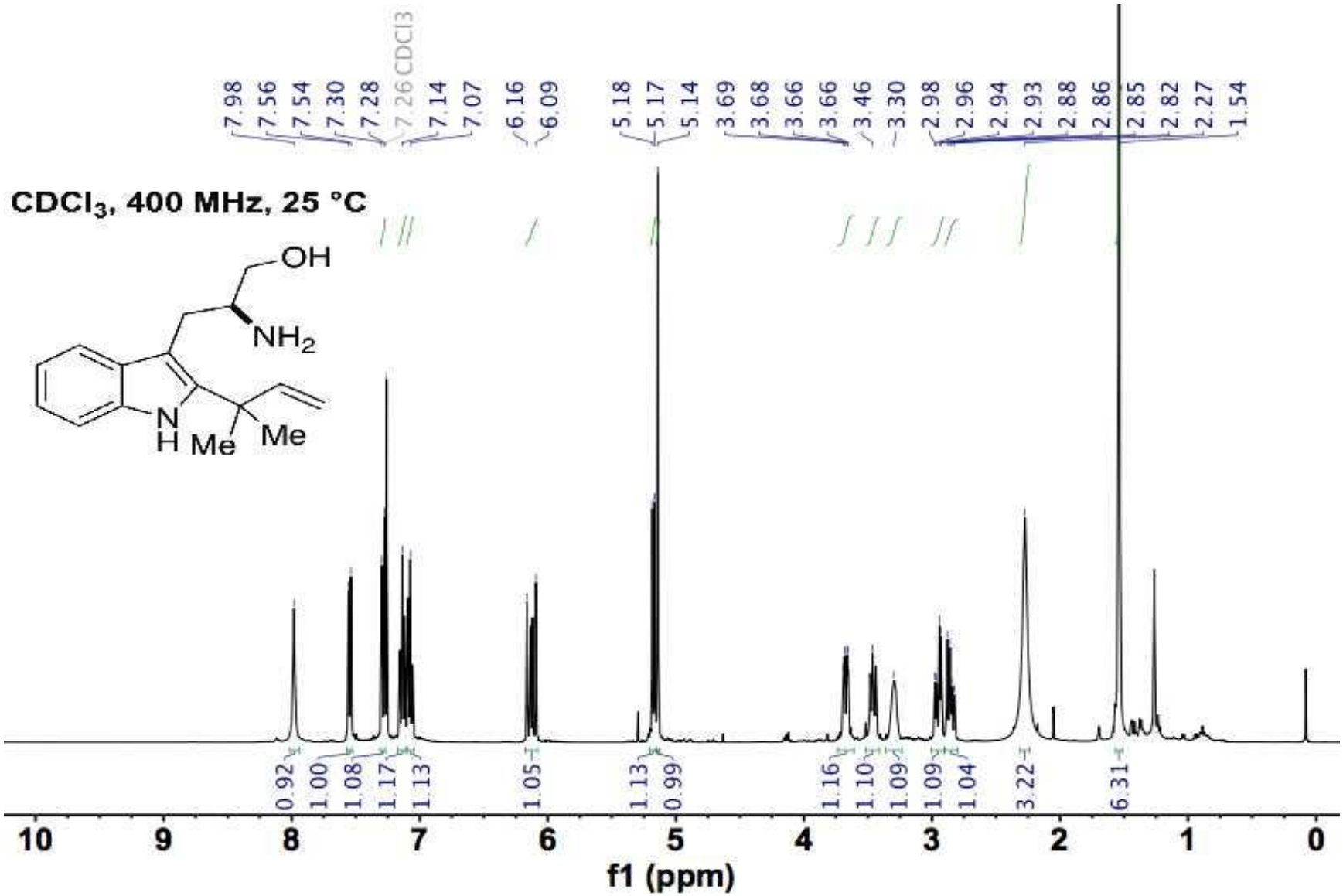


*Figure A2.3.9*. $^{1}$H NMR Spectrum of Compound **3.8**.

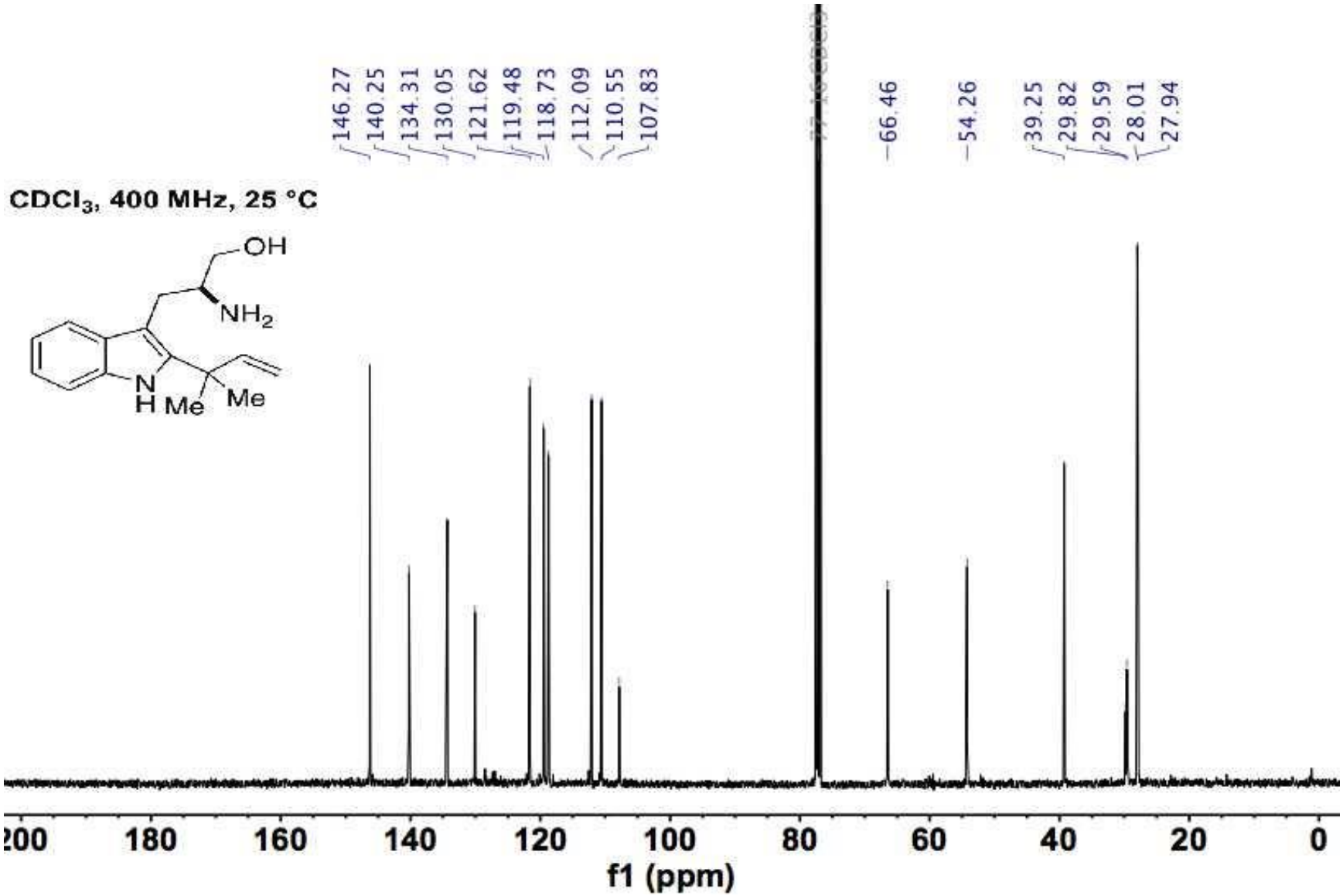


*Figure A2.3.10*. $^{13}$C NMR Spectrum of Compound **3.8**.

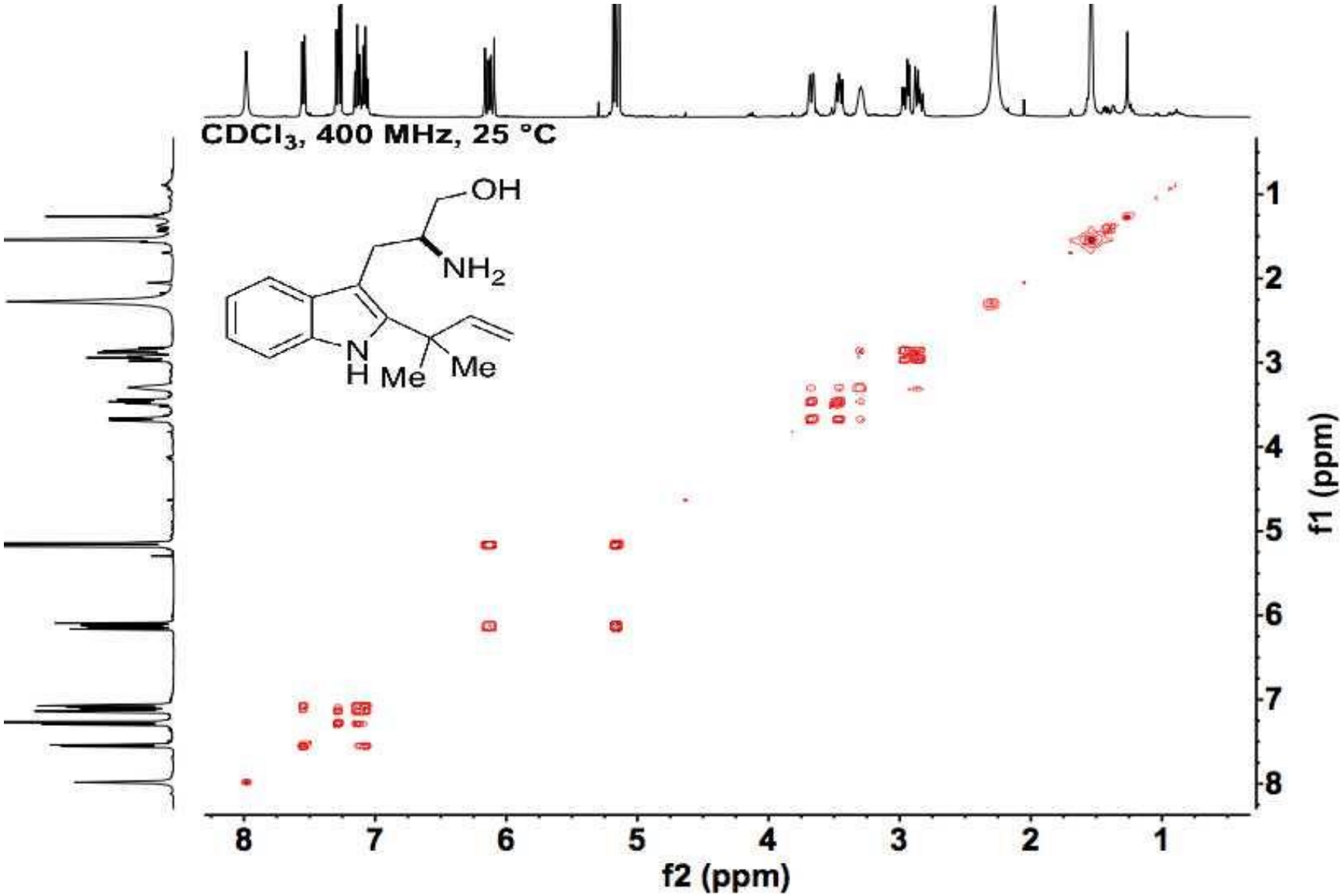


*Figure A2.3.11*. COSY NMR Spectrum of Compound **3.8**.

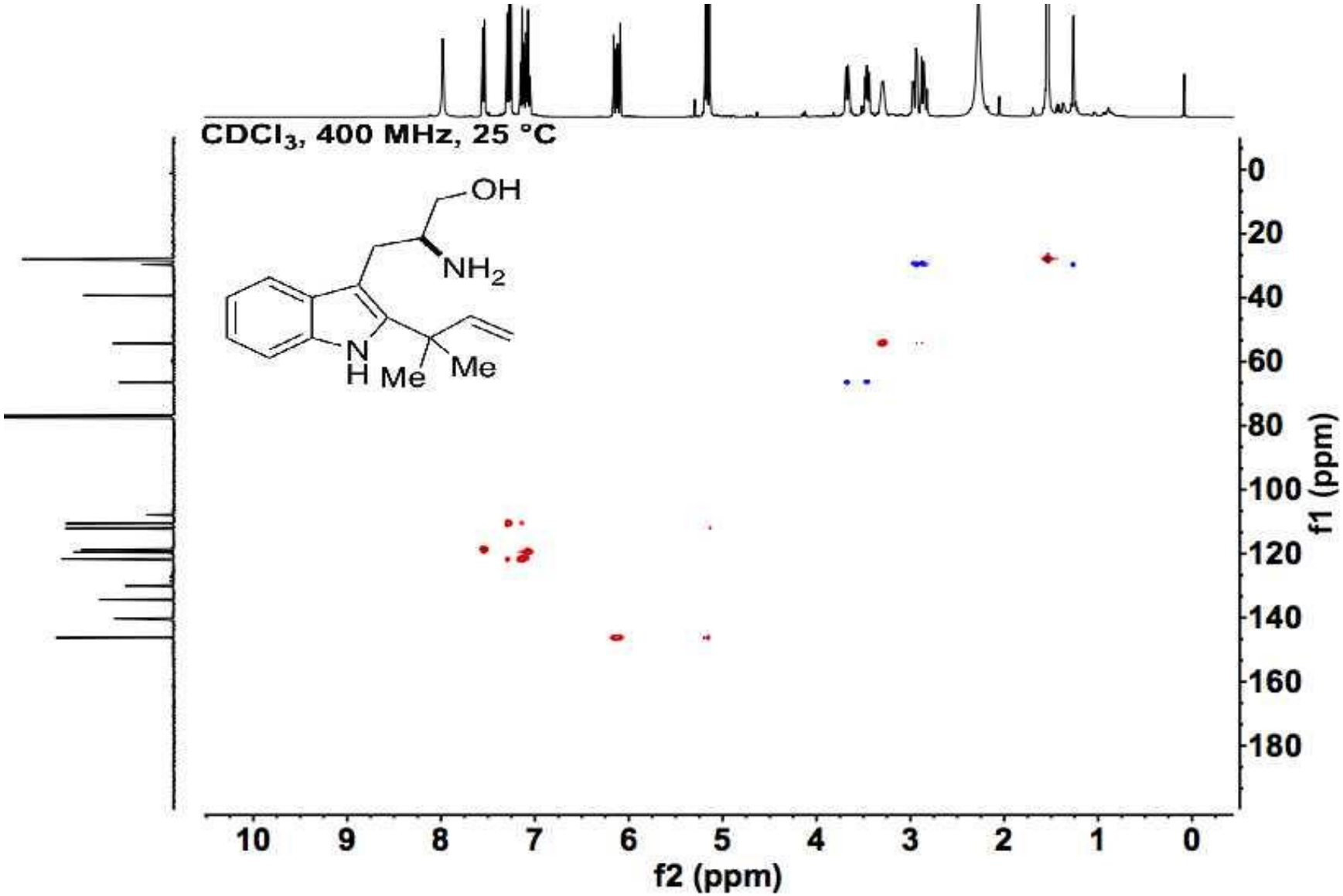


*Figure A2.3.12*. HSQC Spectrum of Compound **3.8**.

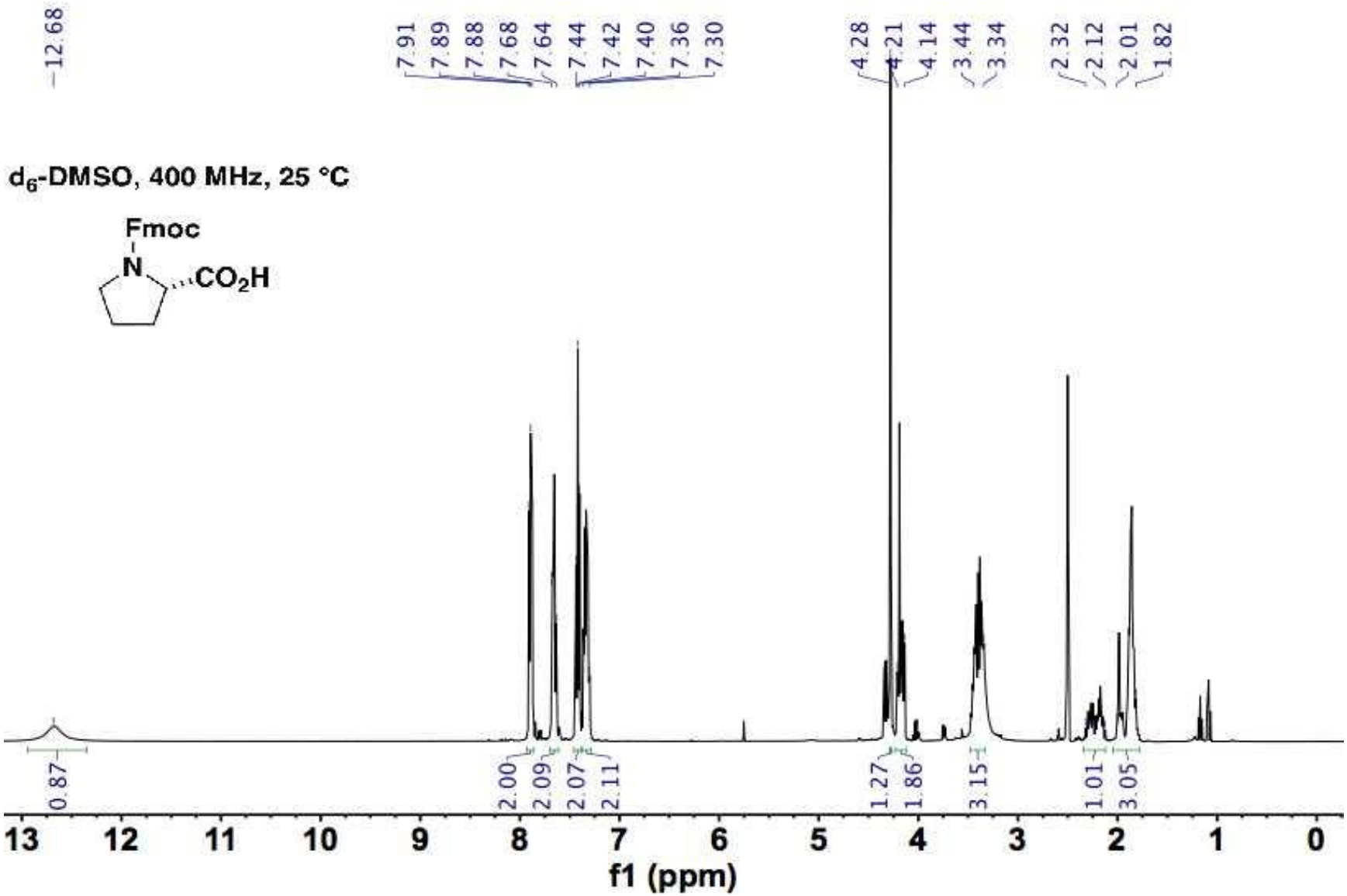


*Figure A2.3.13*. $^{1}$H NMR Spectrum of Compound **3.9**.

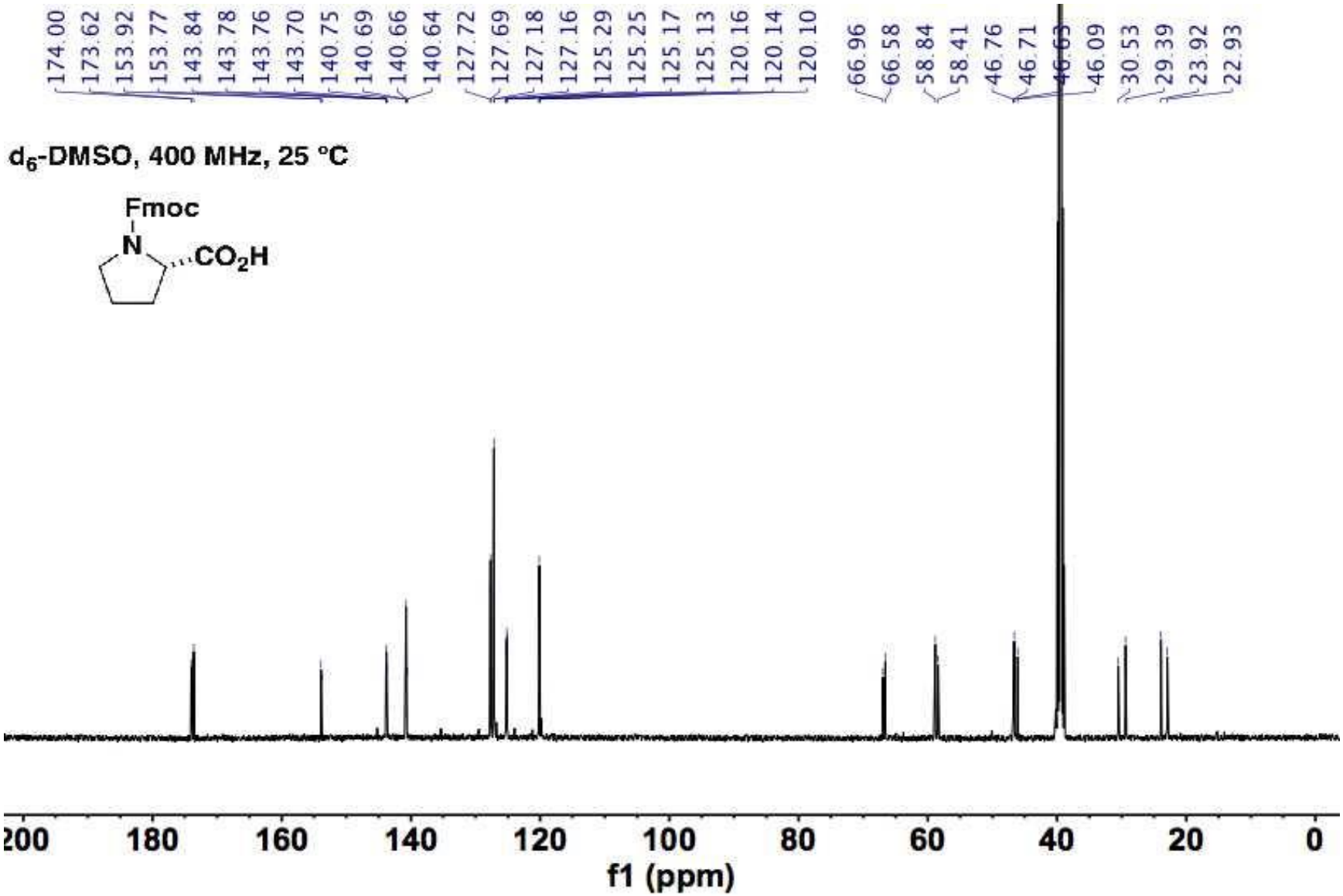


*Figure A2.3.14*. $^{13}$C NMR Spectrum of Compound **3.9**.

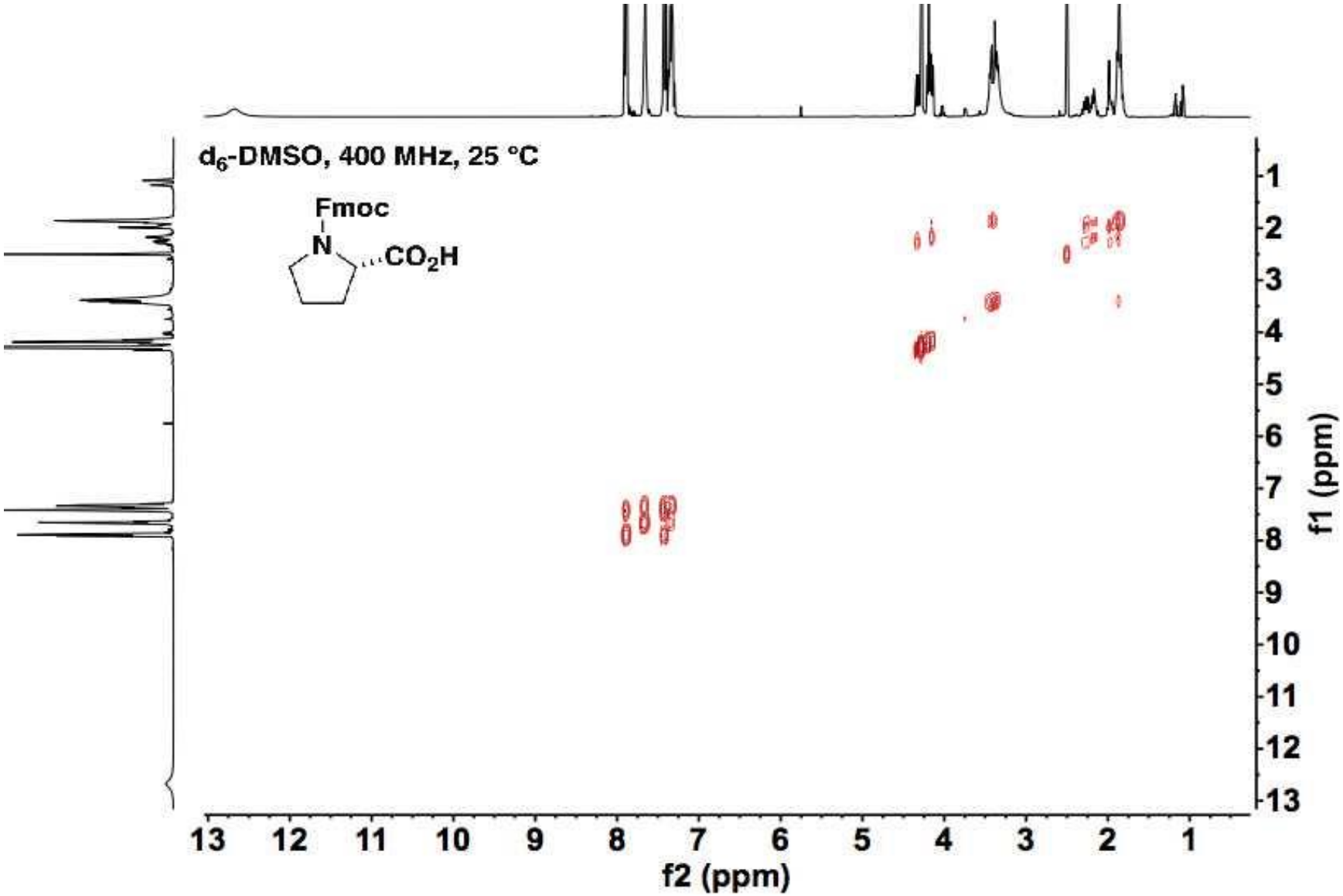


*Figure A2.3.15*. COSY NMR Spectrum of Compound **3.9**.

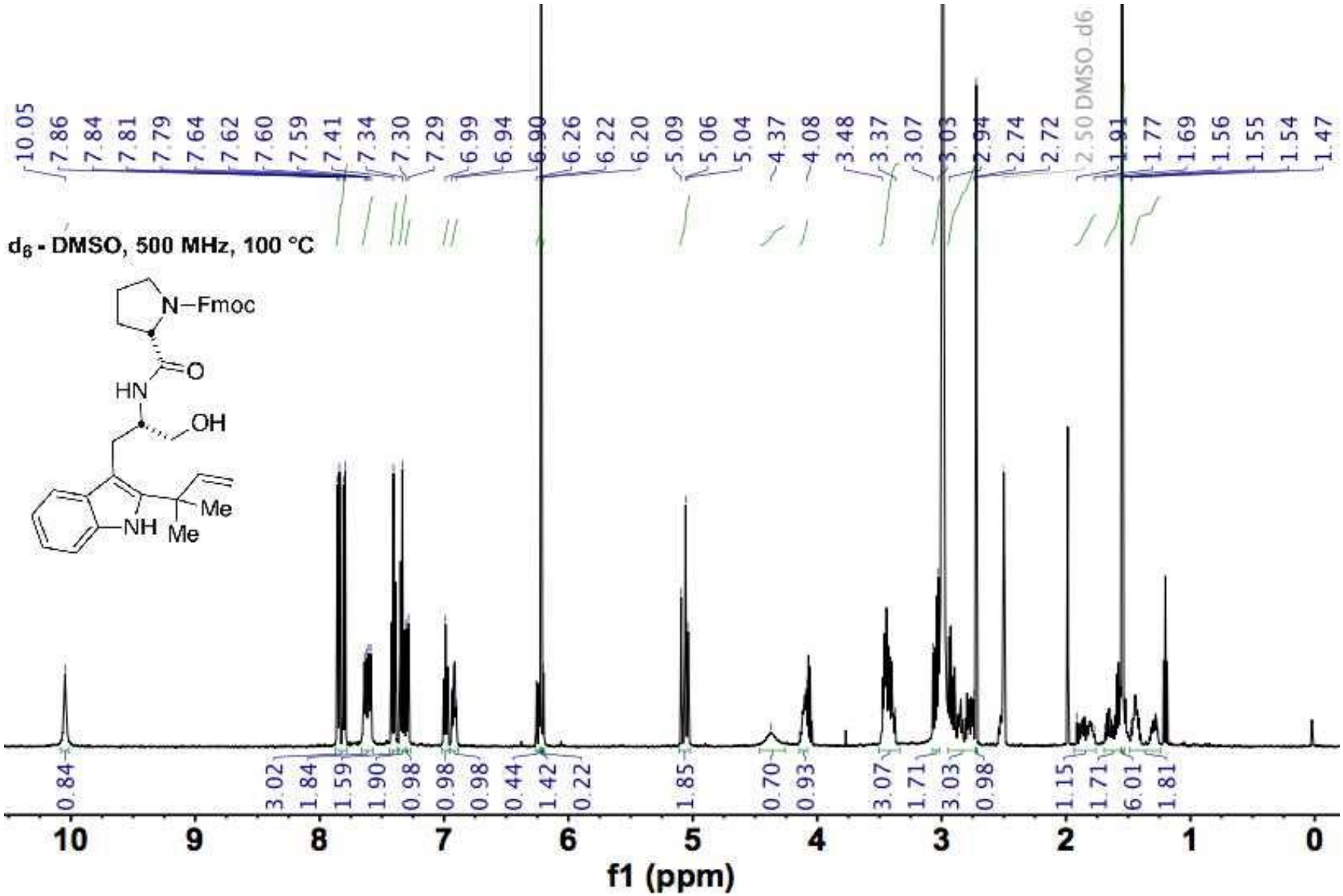


*Figure A2.3.16*. $^{1}$H NMR Spectrum of Compound **3.10**.

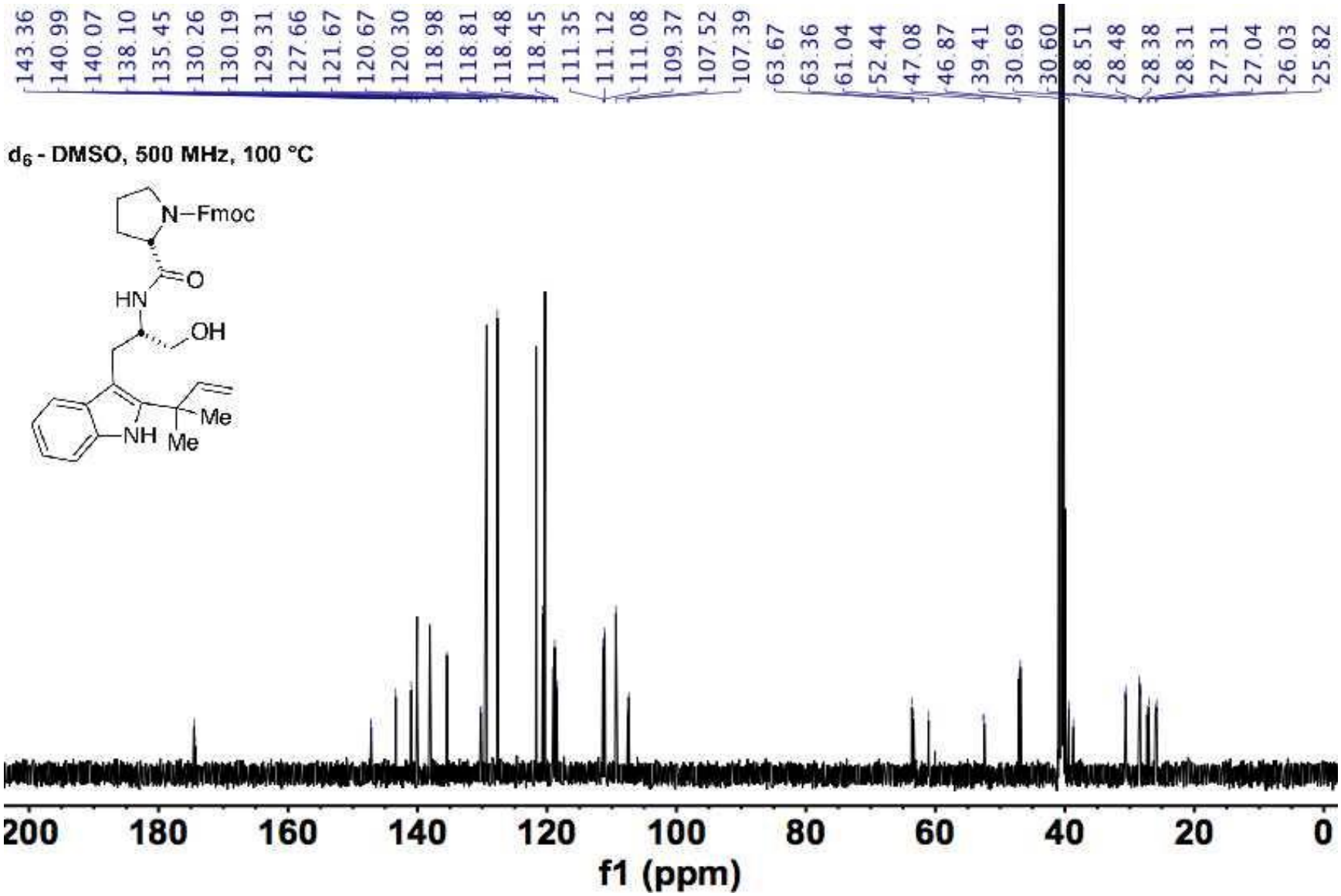


*Figure A2.3.17*. $^{13}$C NMR Spectrum of Compound **3.10**.

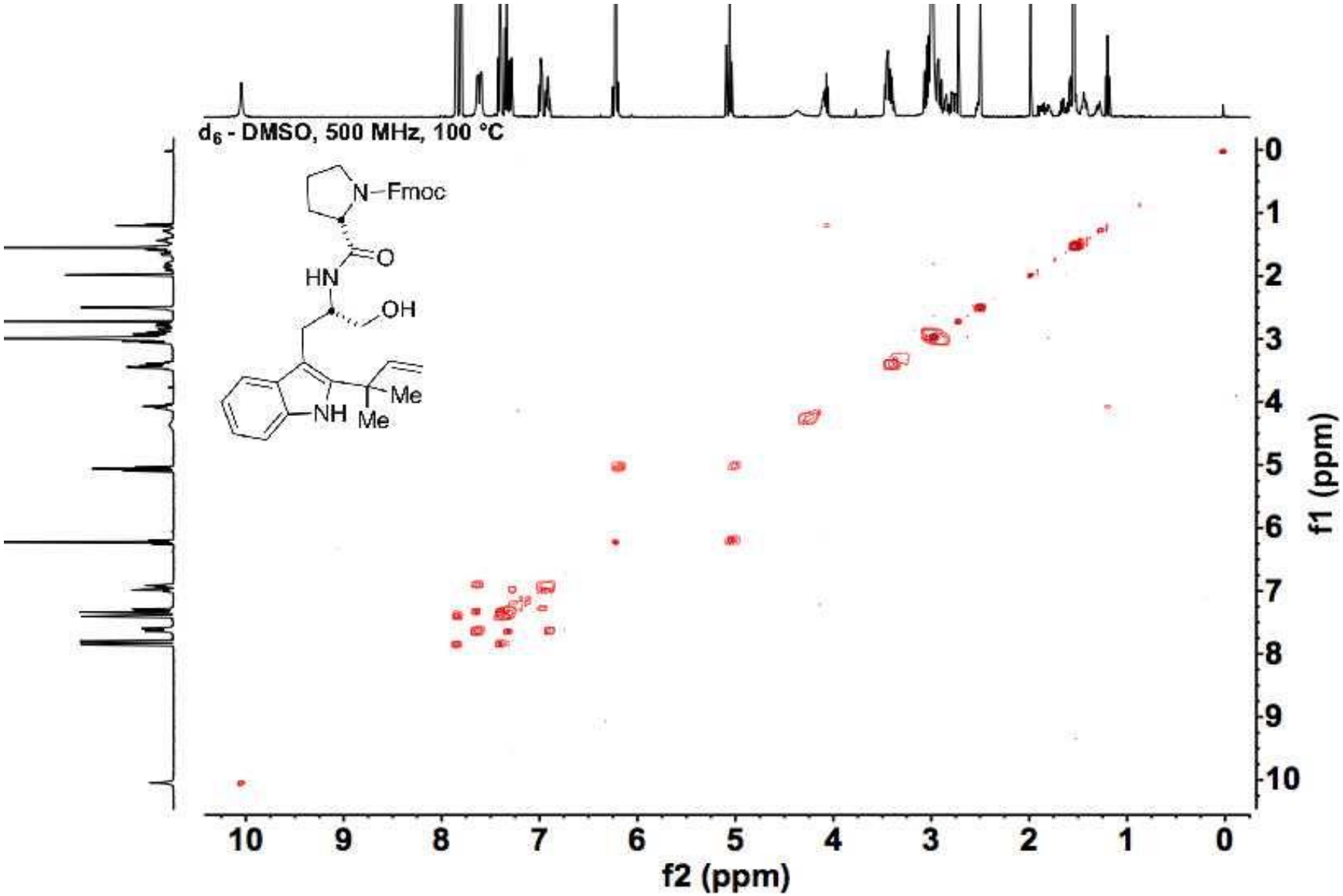


*Figure A2.3.18*. COSY NMR Spectrum of Compound **3.10**.

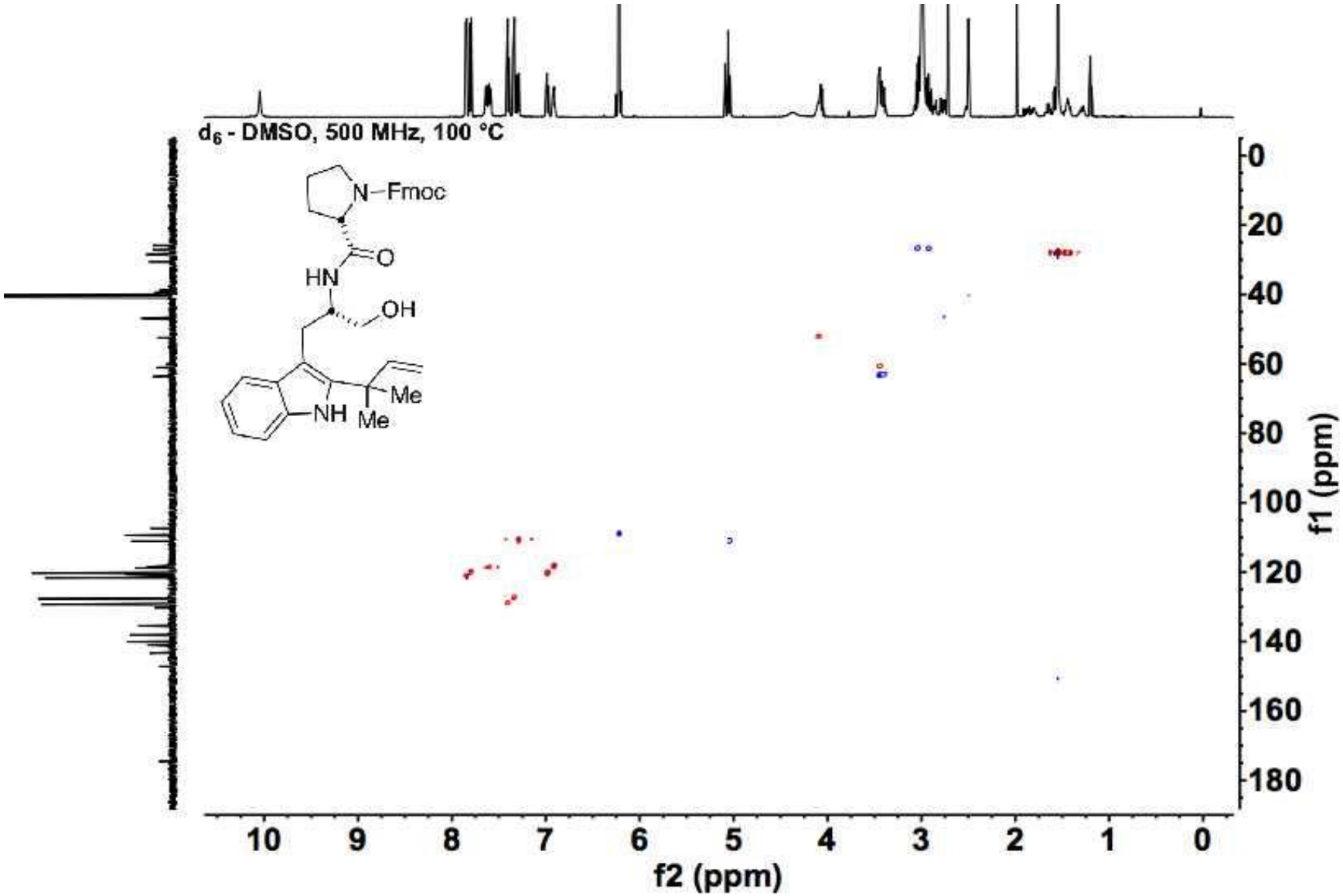


*Figure A2.3.19*. HSQC Spectrum of Compound **3.10**.

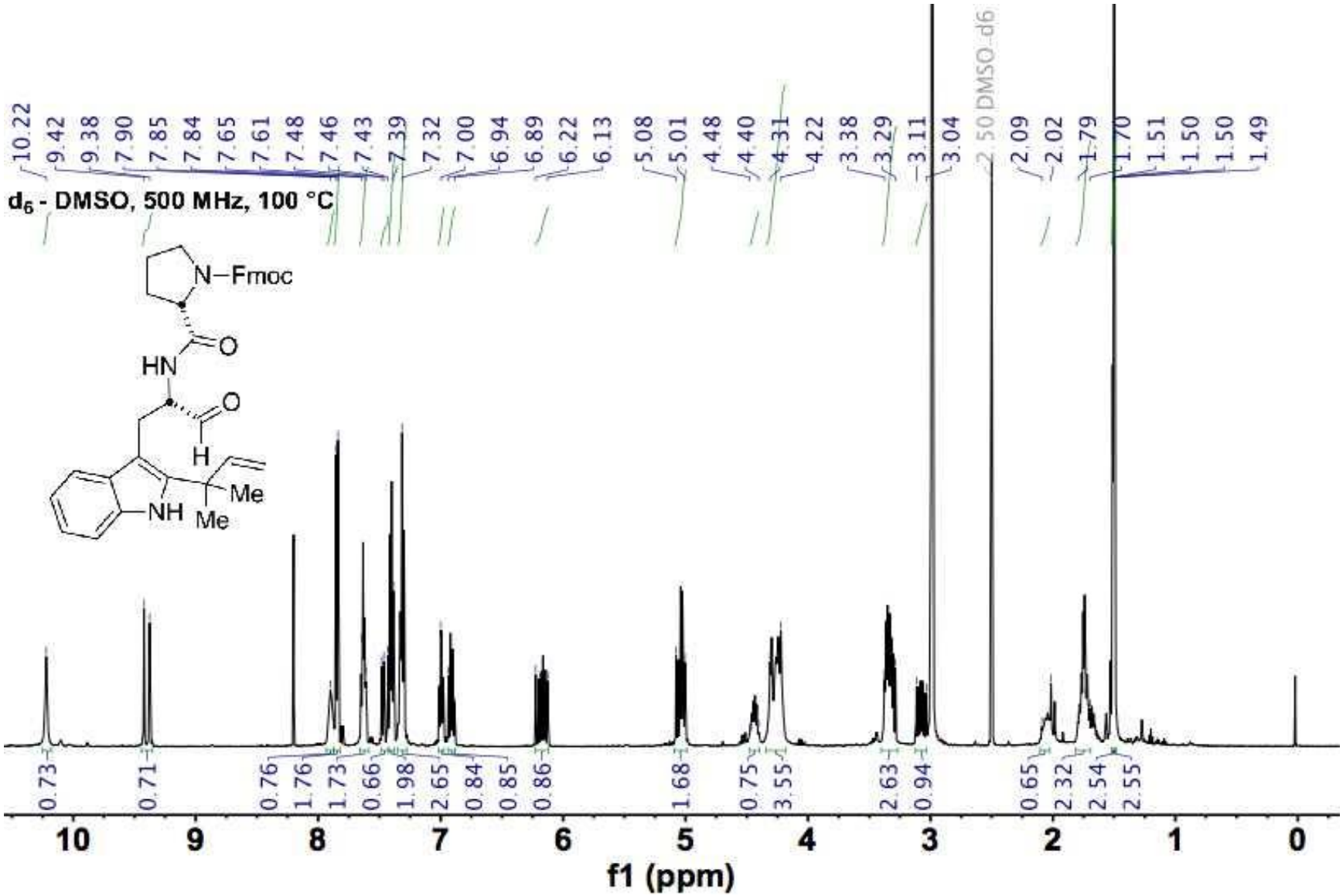


*Figure A2.3.20*. $^{1}$H NMR Spectrum of Compound **3.11**.

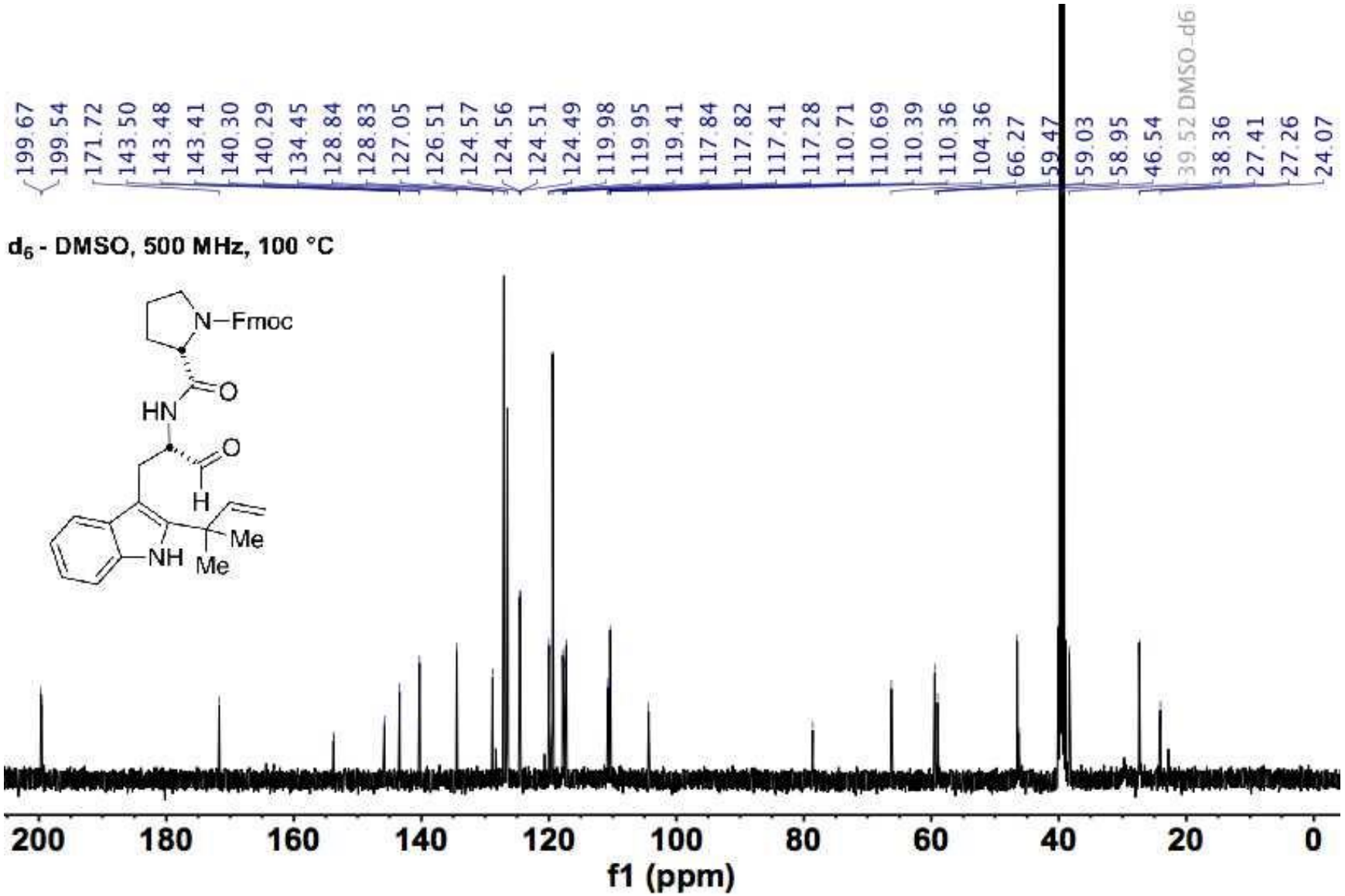


*Figure A2.3.21*. $^{13}$C NMR Spectrum of Compound **3.11**.

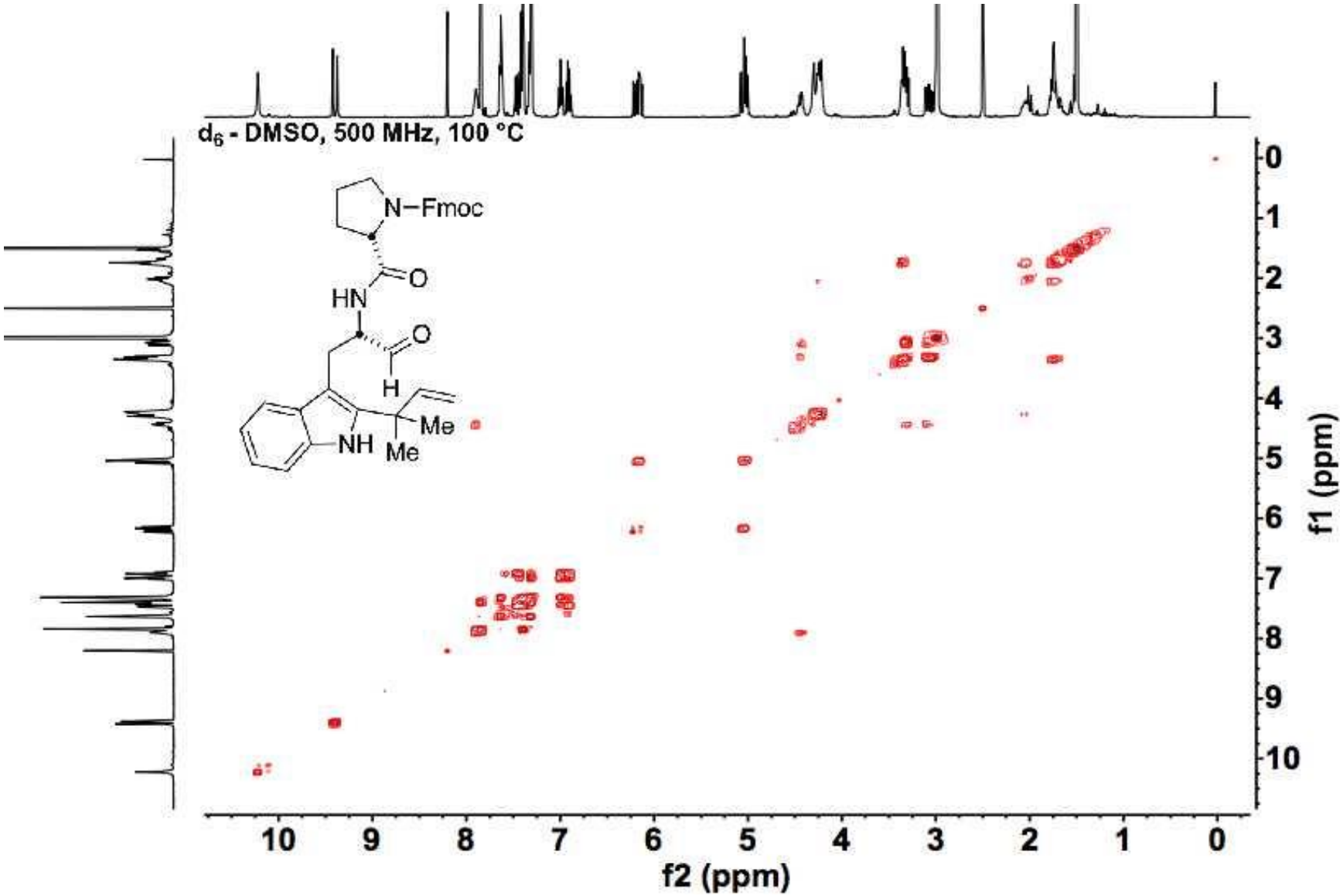


*Figure A2.3.22*. COSY NMR Spectrum of Compound **3.11**.

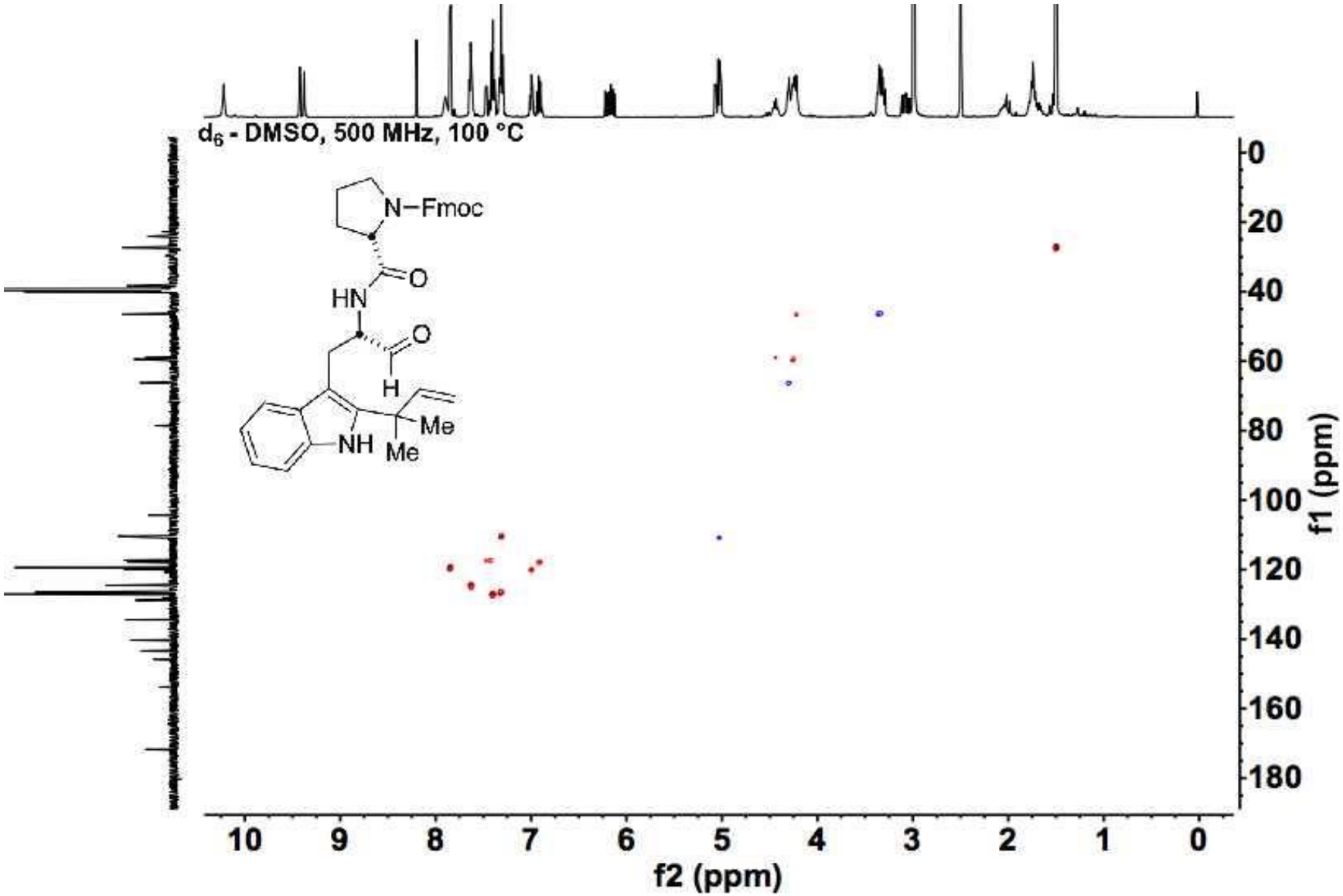


*Figure A2.3.23*. HSQC Spectrum of Compound **3.11**.

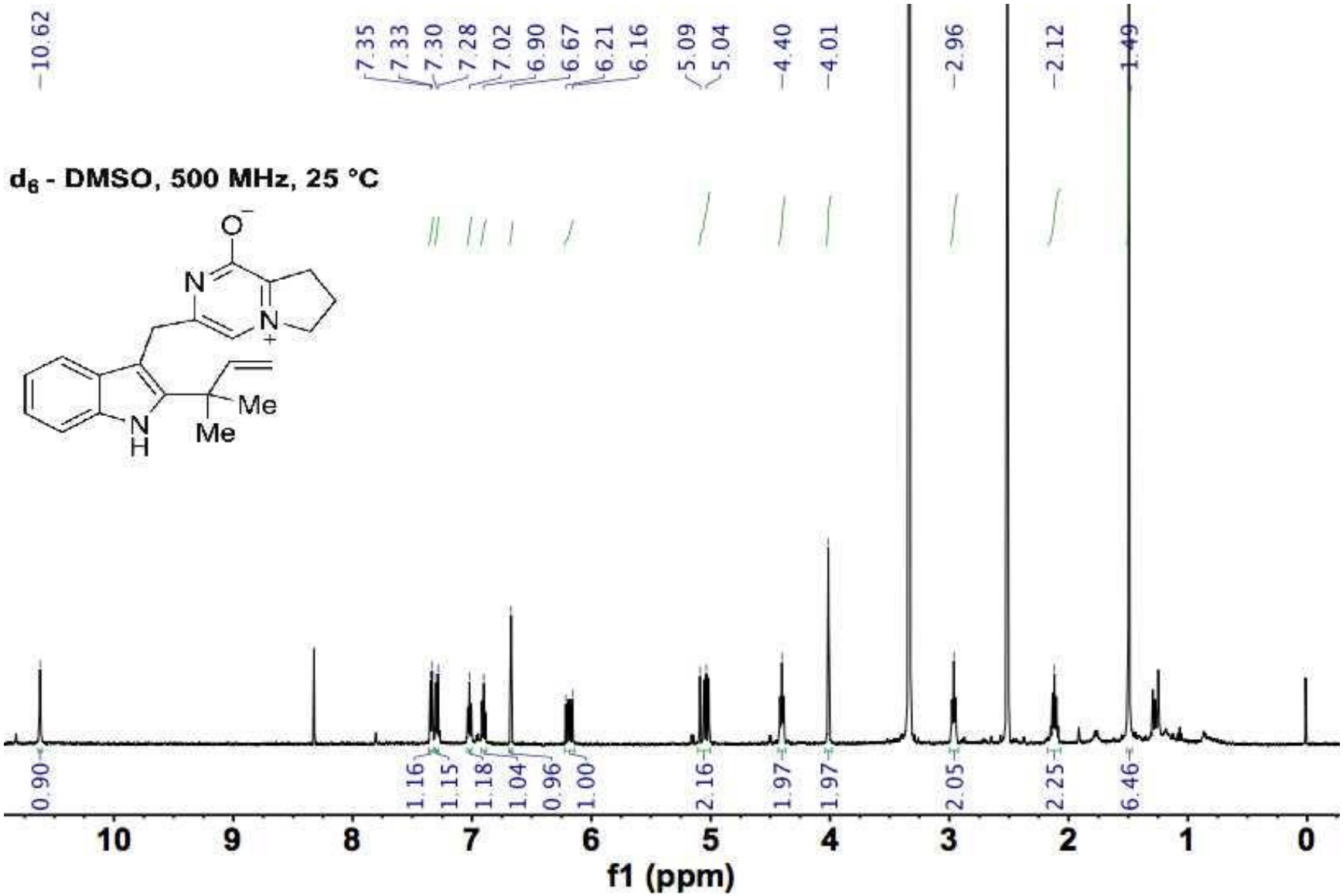


*Figure A2.3.24*. $^{1}$H NMR Spectrum of **ZwtP**.

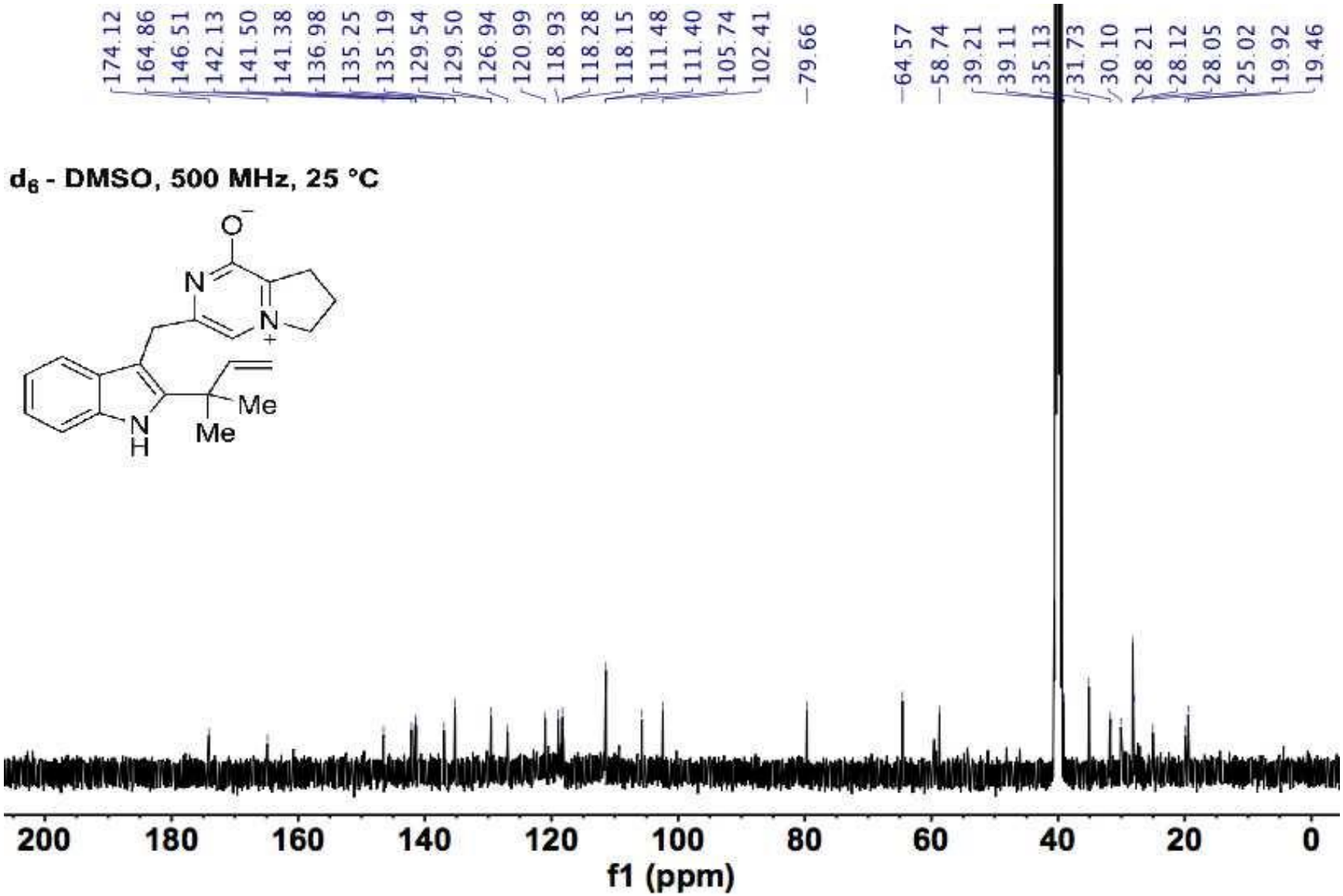


*Figure A2.3.25*. $^{13}$C NMR Spectrum of **ZwtP**.

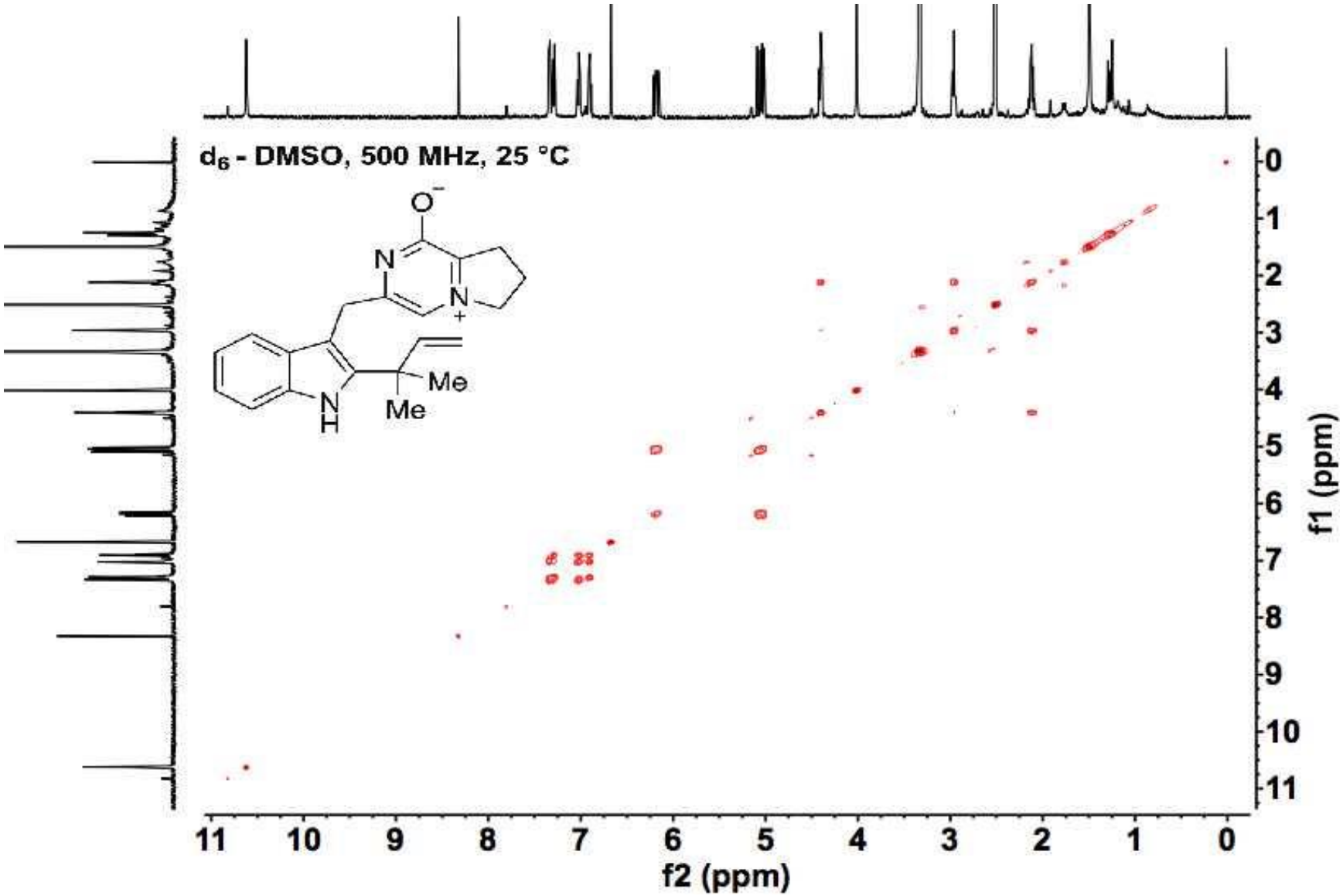


*Figure A2.3.26*. COSY NMR Spectrum of **ZwtP**.

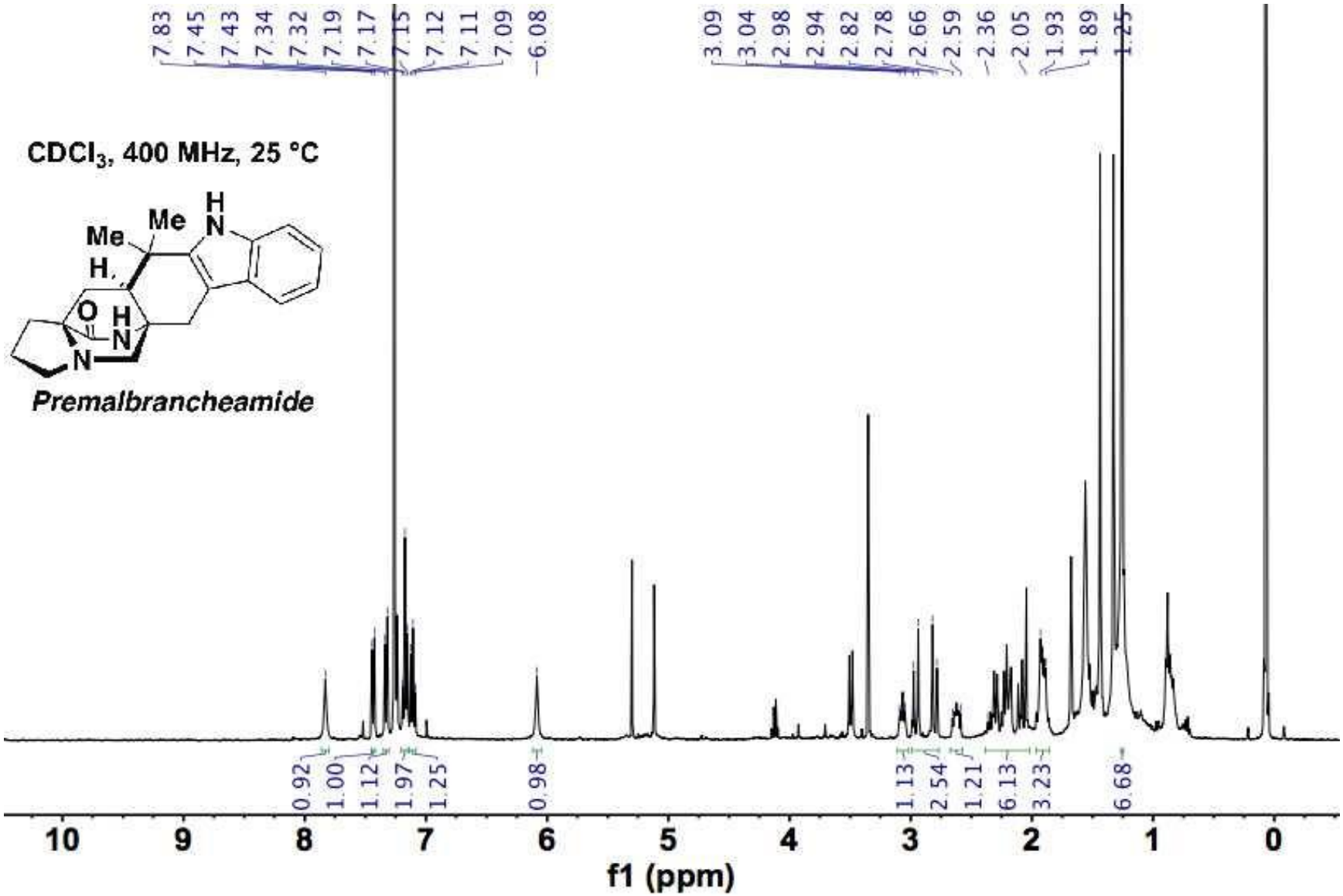


Figure *A2.3.27*. $^{1}$H NMR Spectrum of **Premalbrancheamide**.

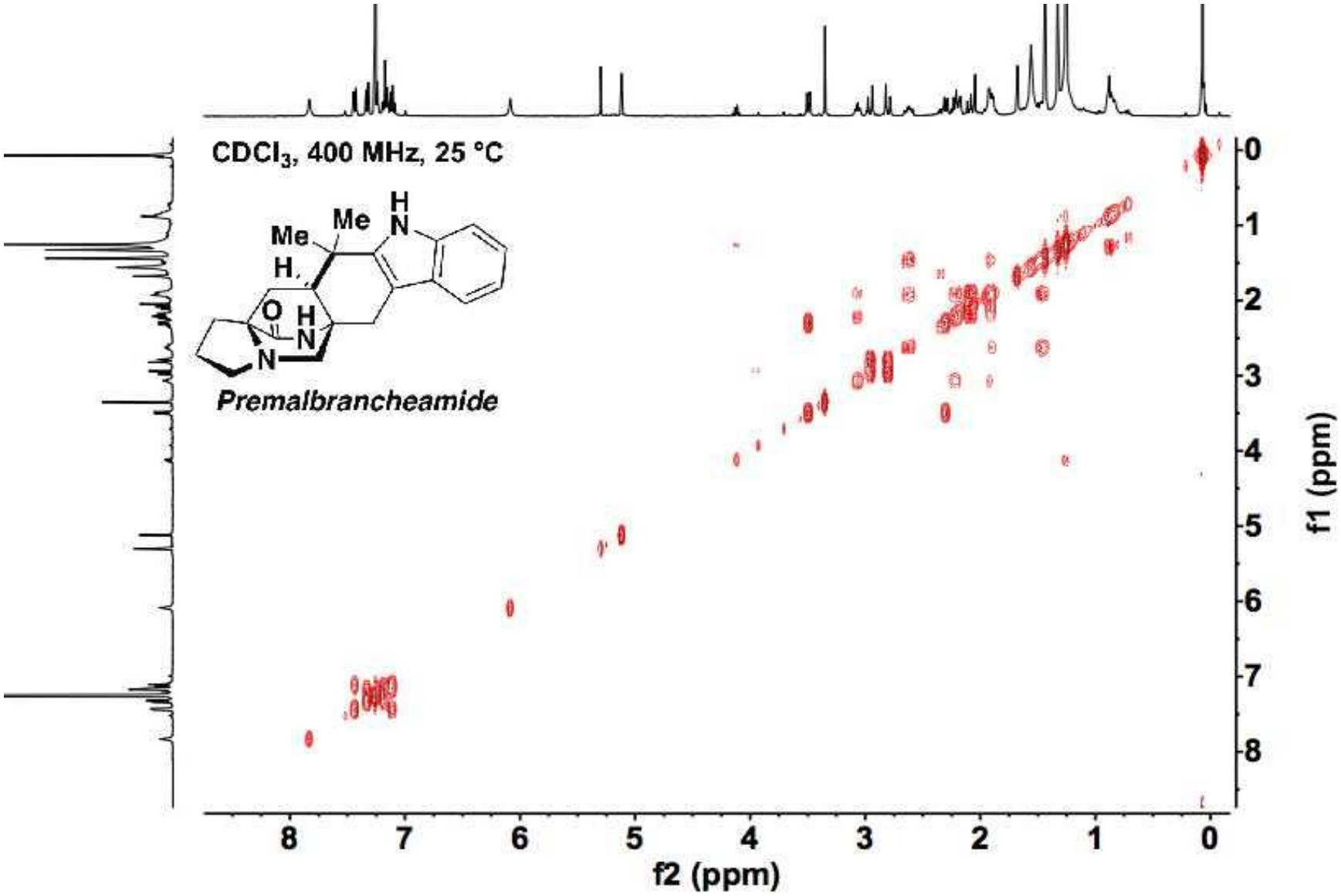


Figure *A2.3.28*. COSY NMR Spectrum of **Premalbrancheamide**.

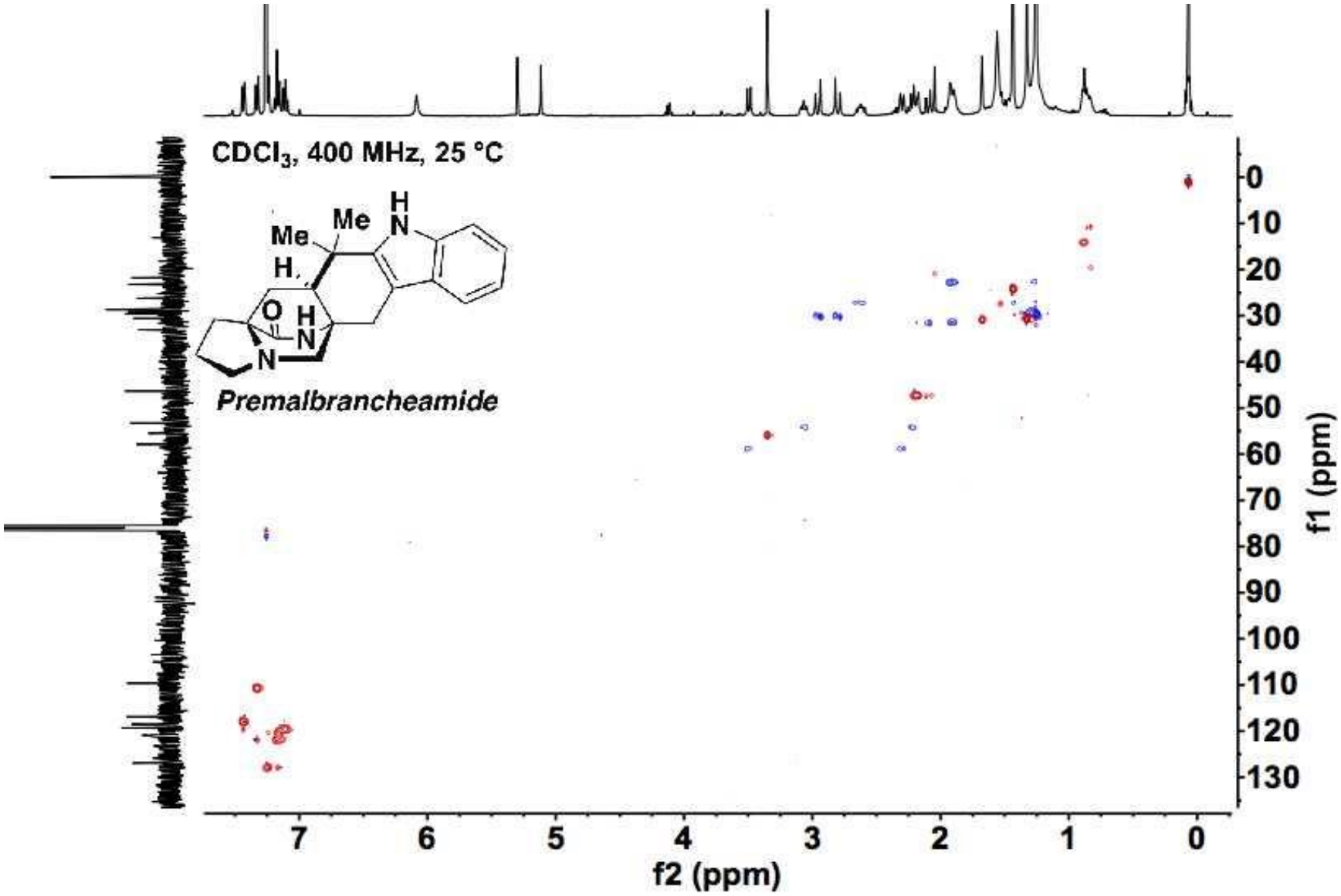


Figure *A2.3.29*. HSQC NMR Spectrum of **Premalbrancheamide**.

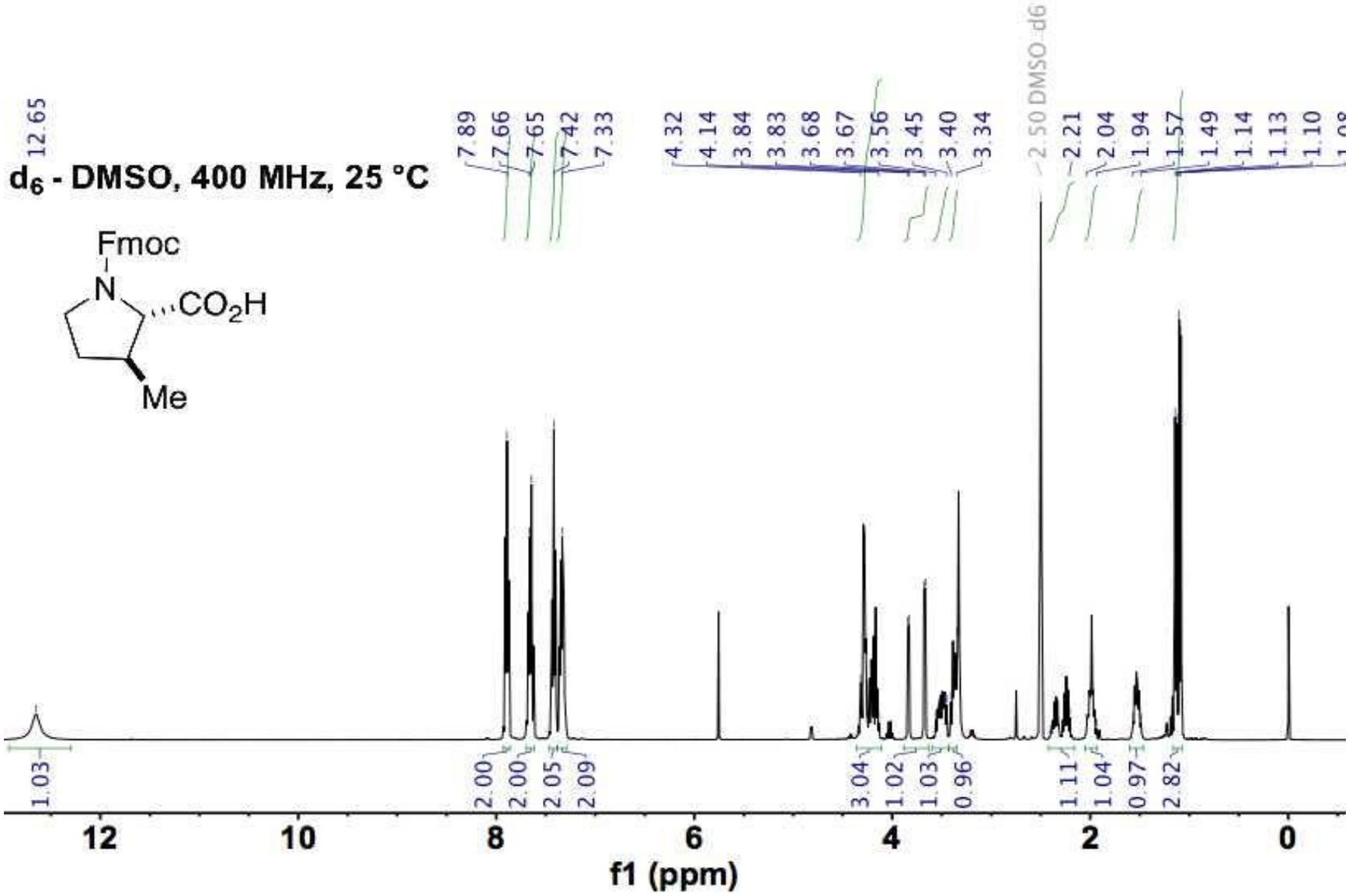


*Figure A2.3.30*. $^{1}$H NMR Spectrum of Compound **3.35**.

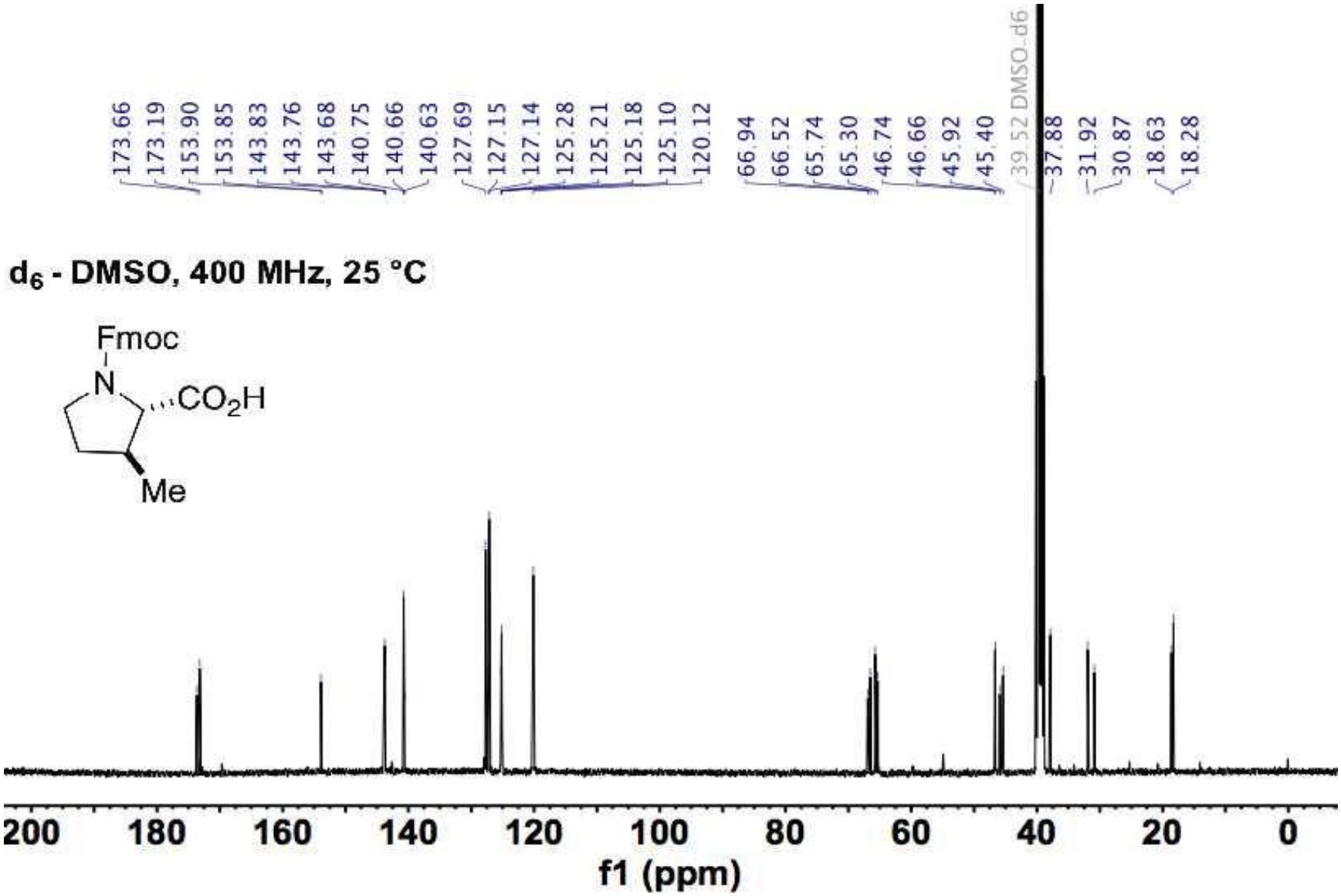


*Figure A2.3.31*. $^{13}C$ NMR Spectrum of Compound **3.35**.

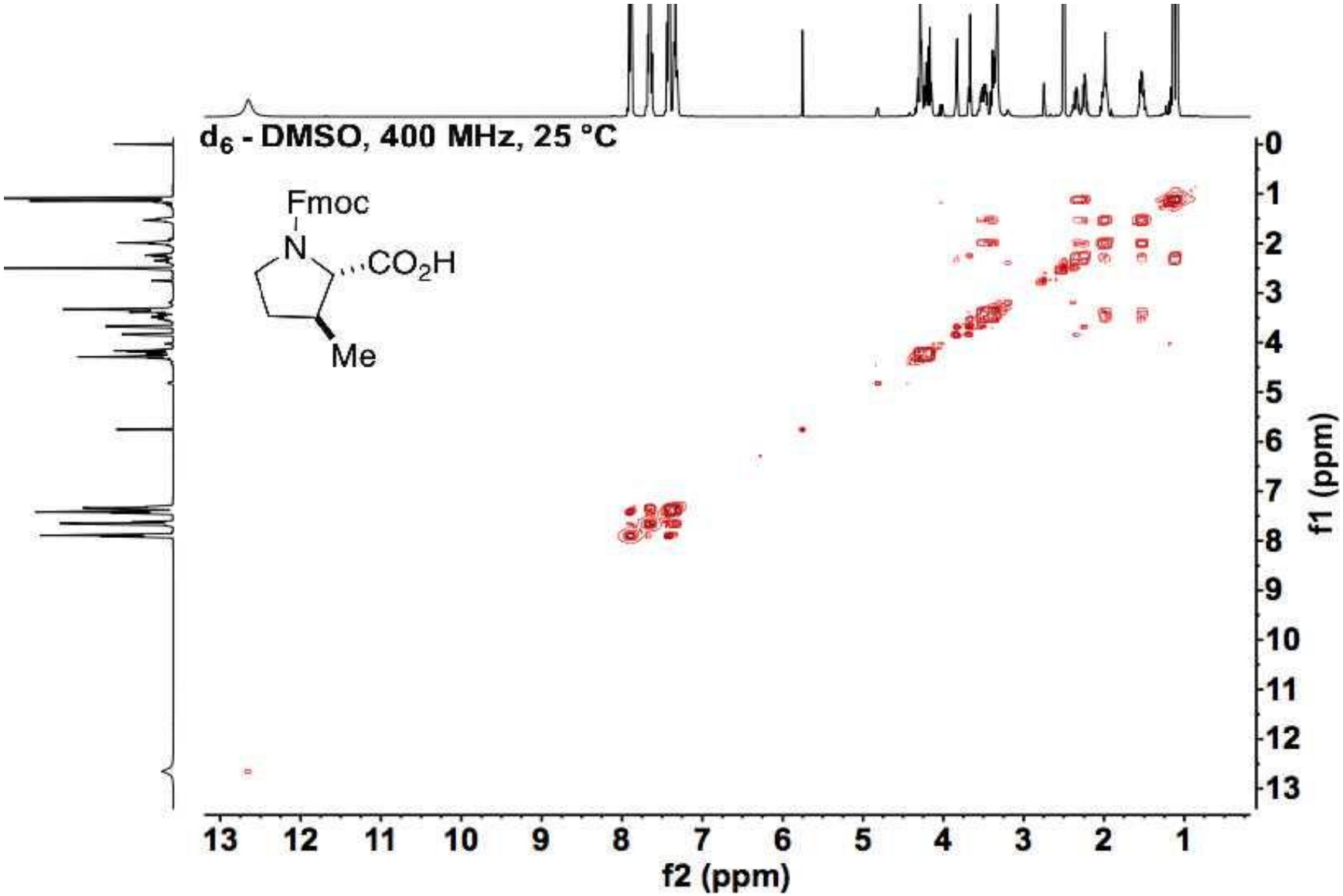


*Figure A2.3.32*. COSY NMR Spectrum of Compound **3.35**.

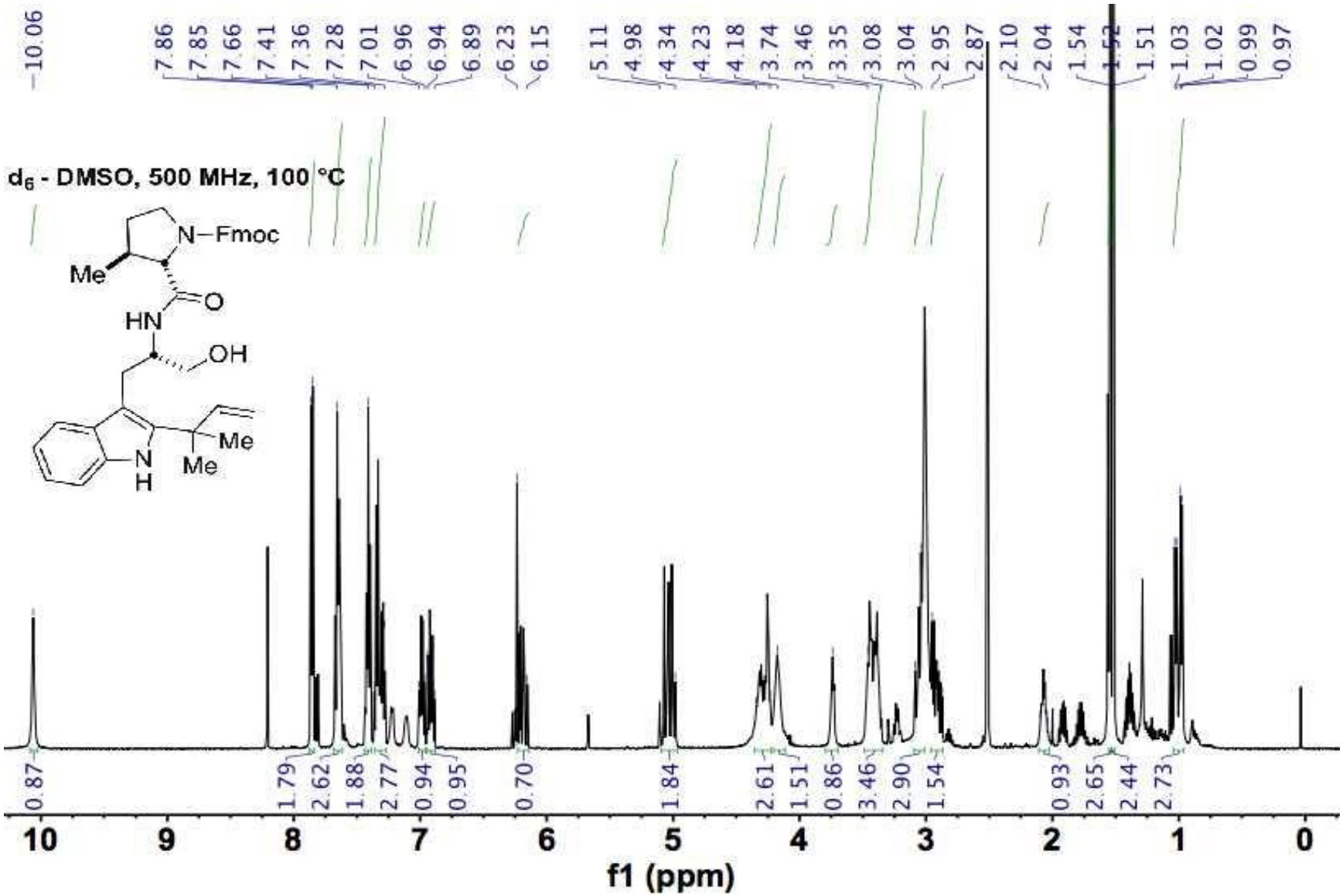


*Figure A2.3.33*. $^{1}$H NMR Spectrum of Compound **3.36**.

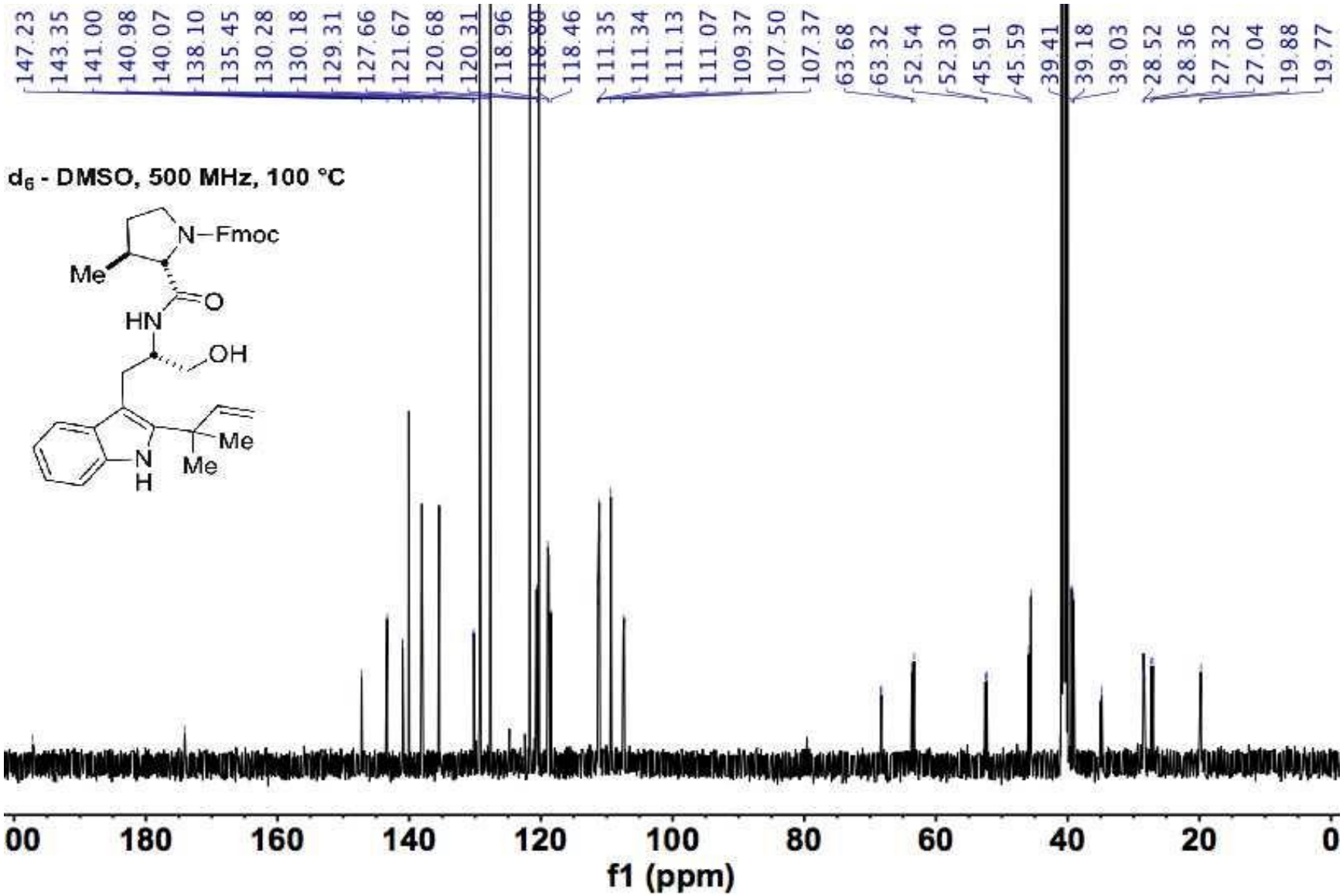


*Figure A2.3.34*. $^{13}$C NMR Spectrum of Compound **3.36**.

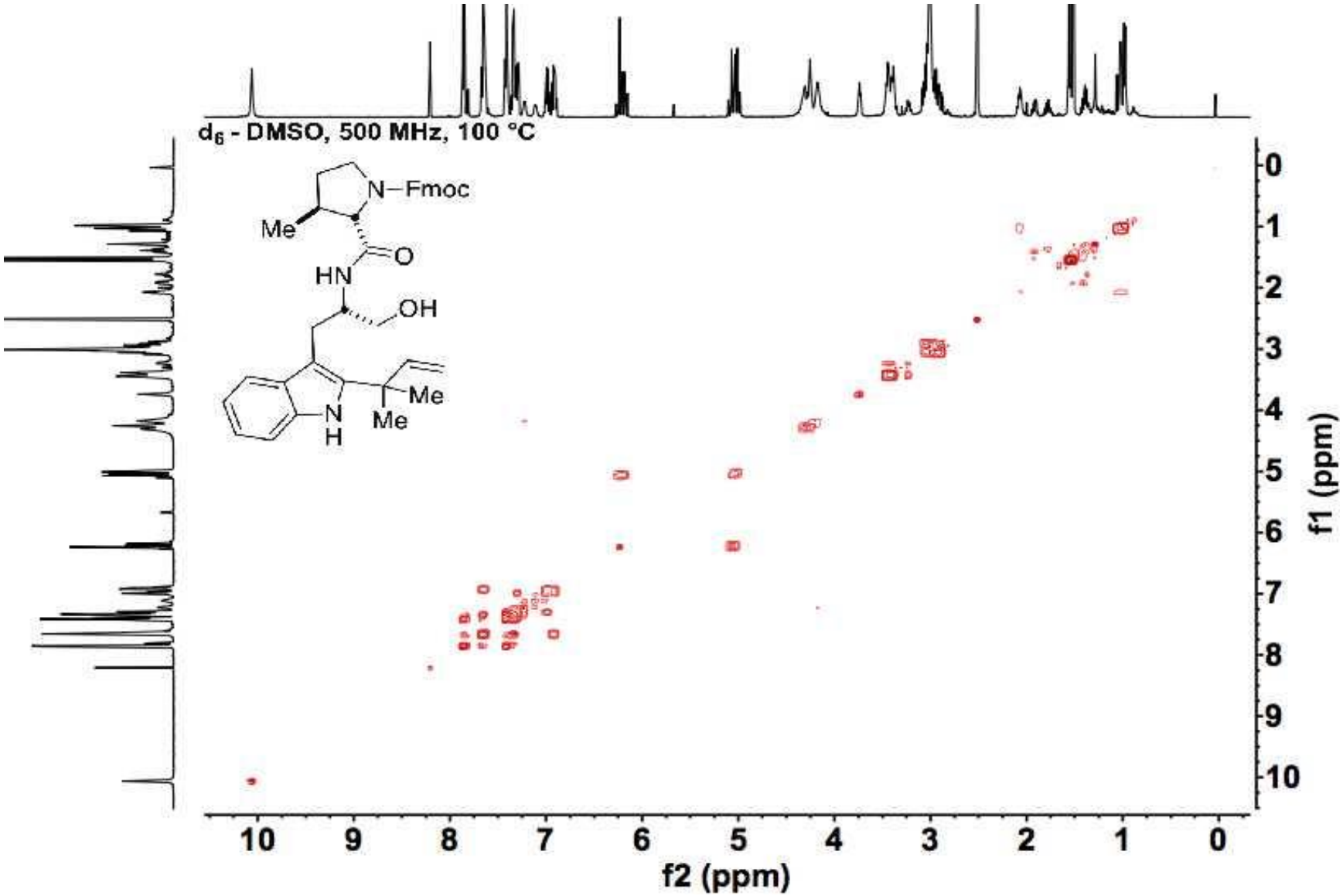


*Figure A2.3.35*. COSY NMR Spectrum of Compound **3.36**.

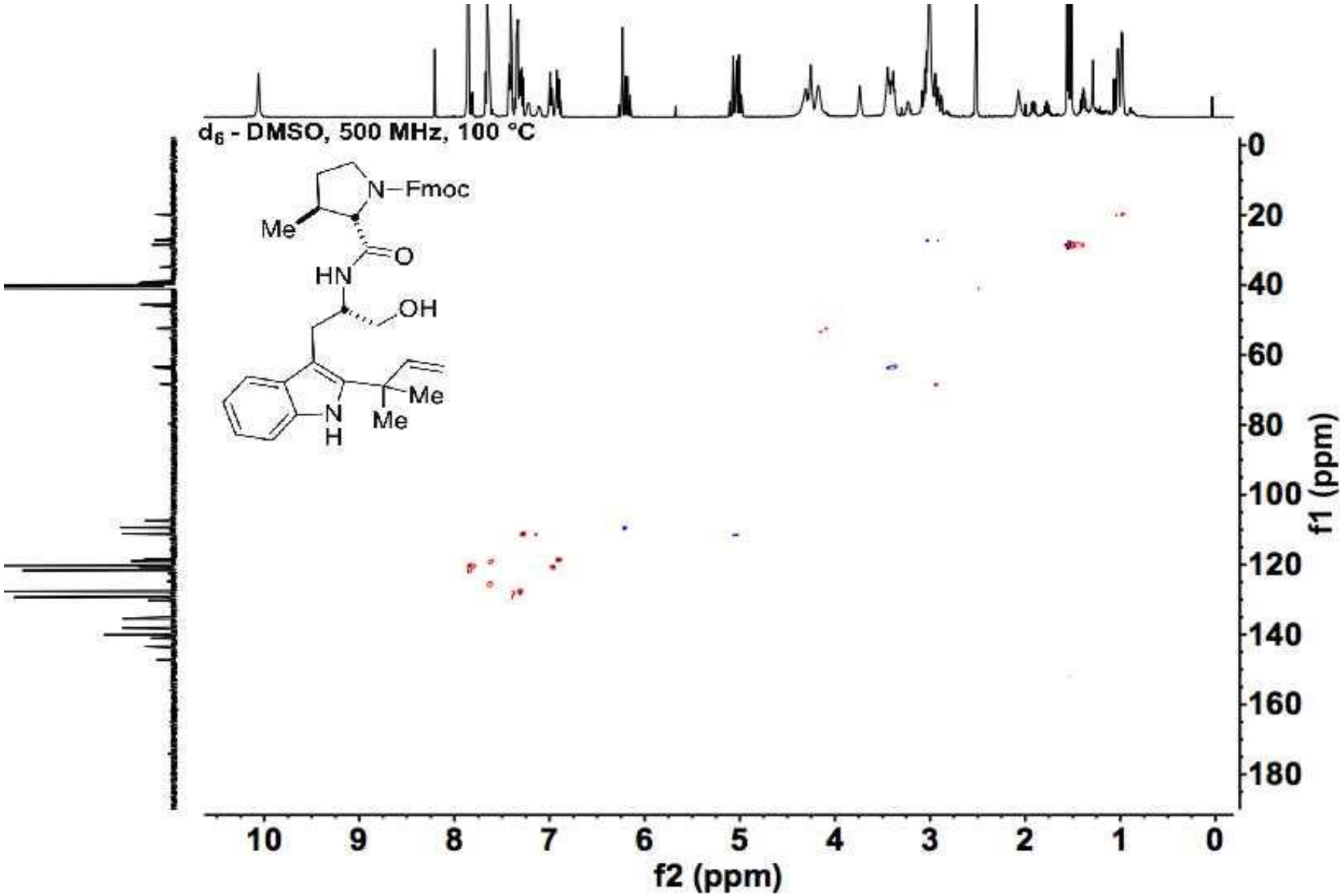


*Figure A2.3.36*. HSQC Spectrum of Compound **3.36**.

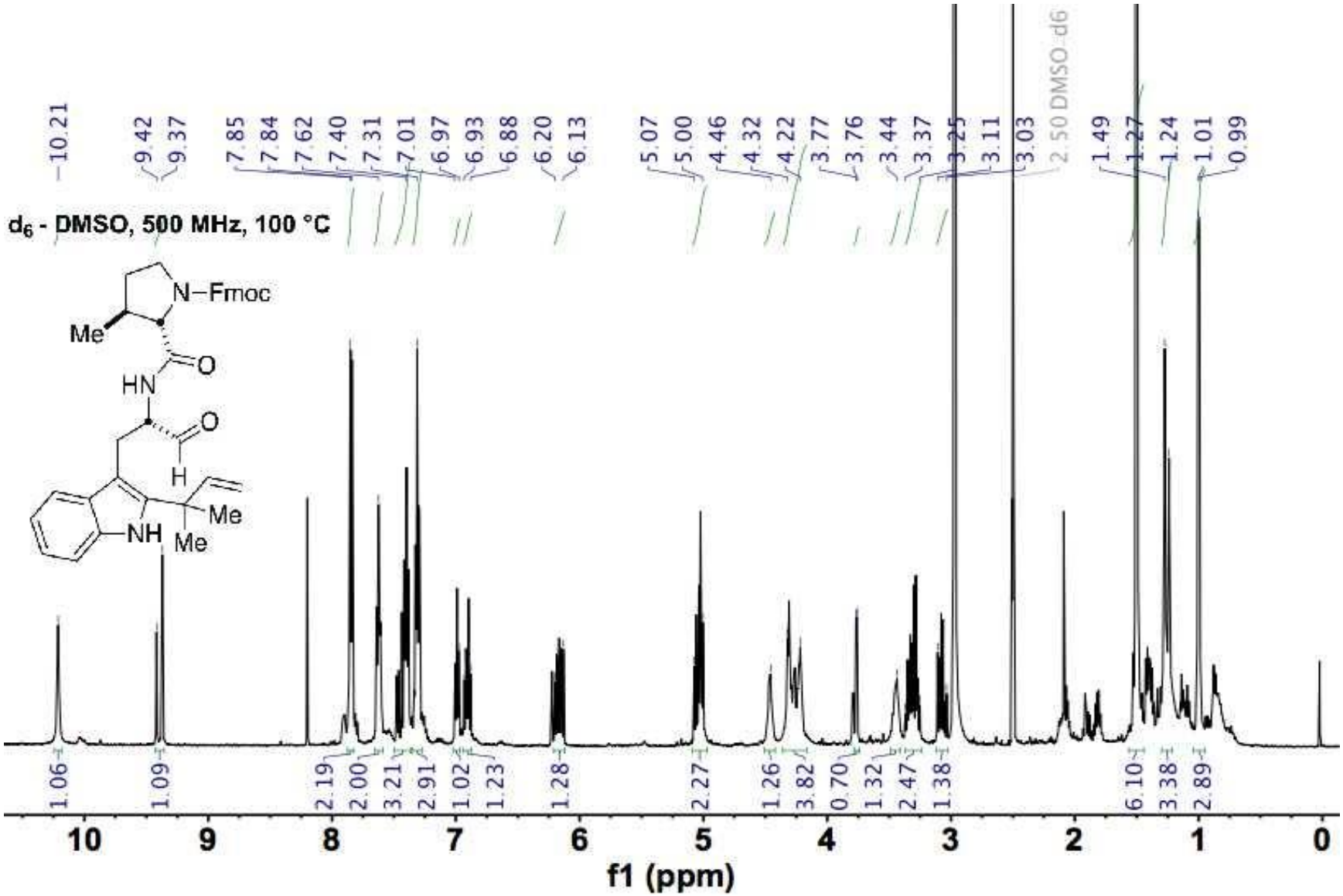


*Figure A2.3.37*. $^{1}$H NMR Spectrum of Compound **3.37**.

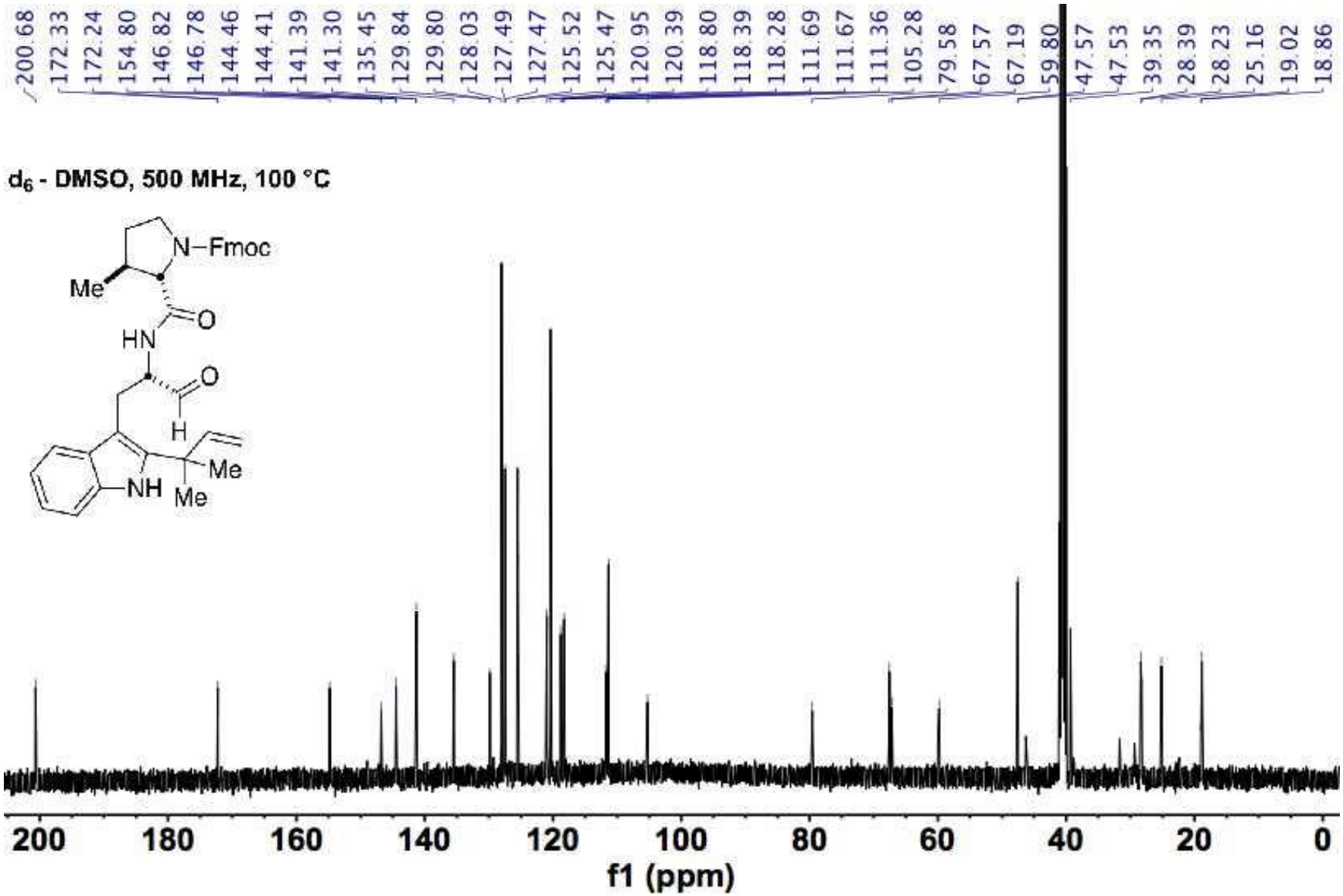


*Figure A2.3.38*. $^{13}$C NMR Spectrum of Compound **3.37**.

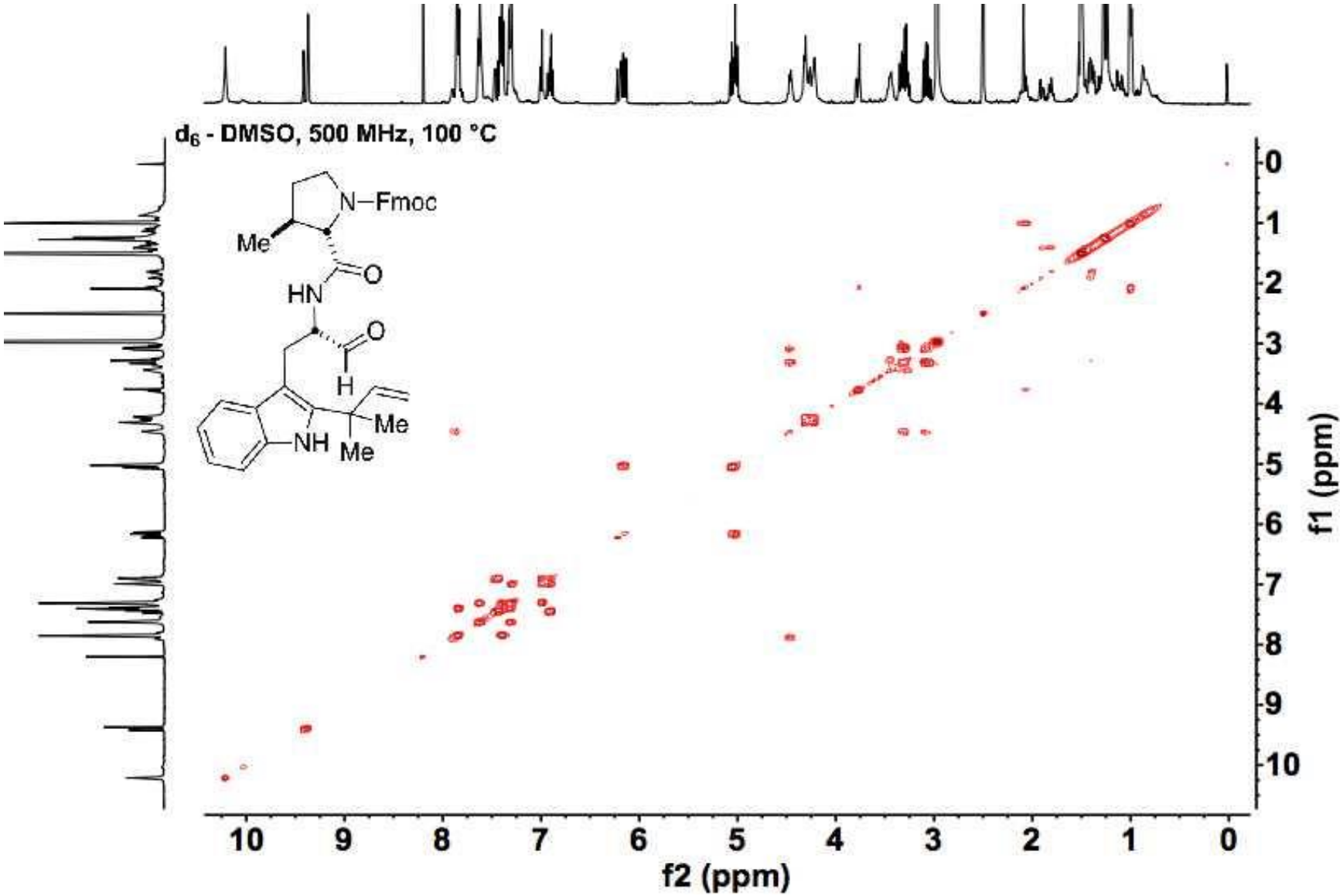


*Figure A2.3.39*. COSY NMR Spectrum of Compound **3.37**.

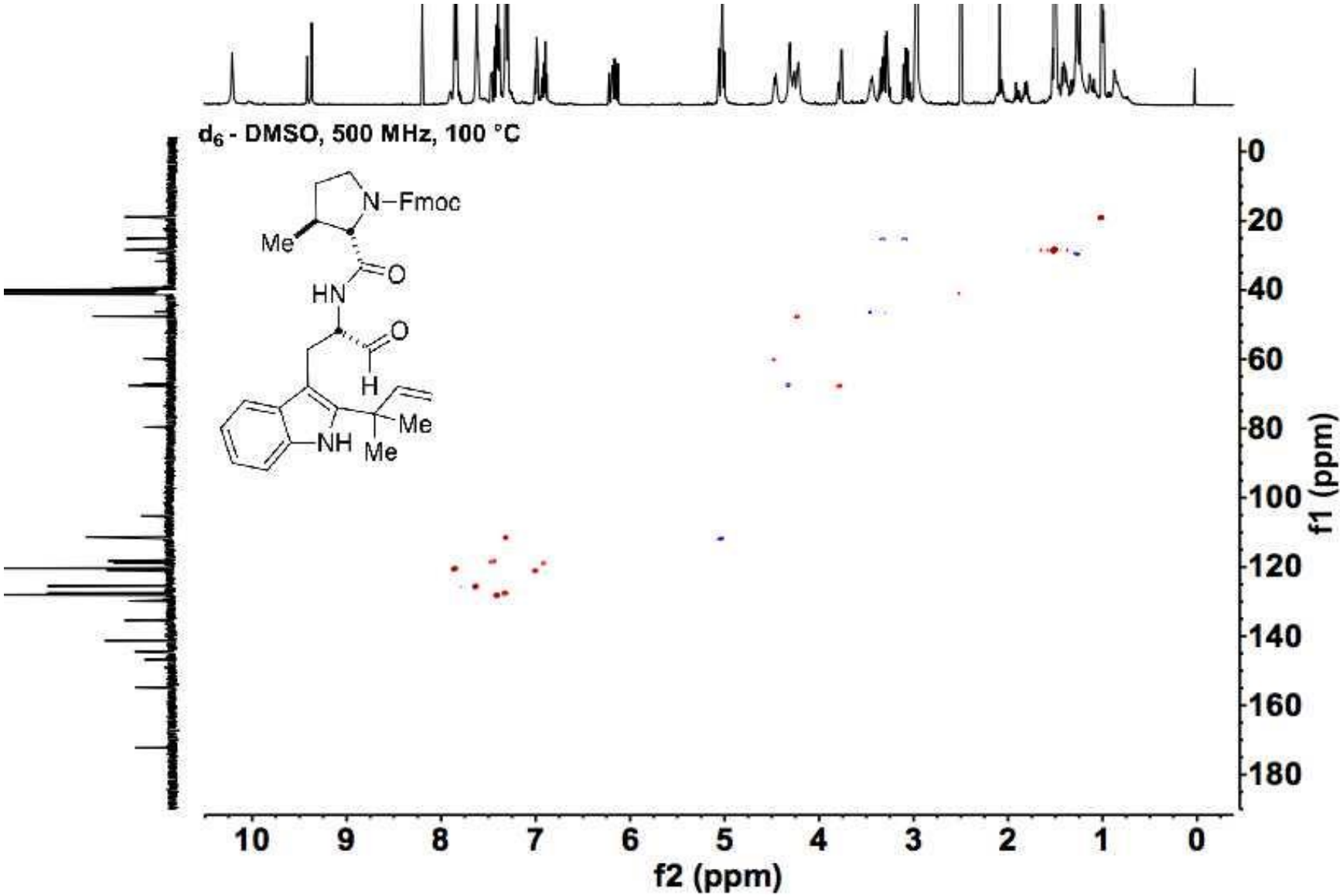


*Figure A2.3.40*. HSQC Spectrum of Compound **3.37**.

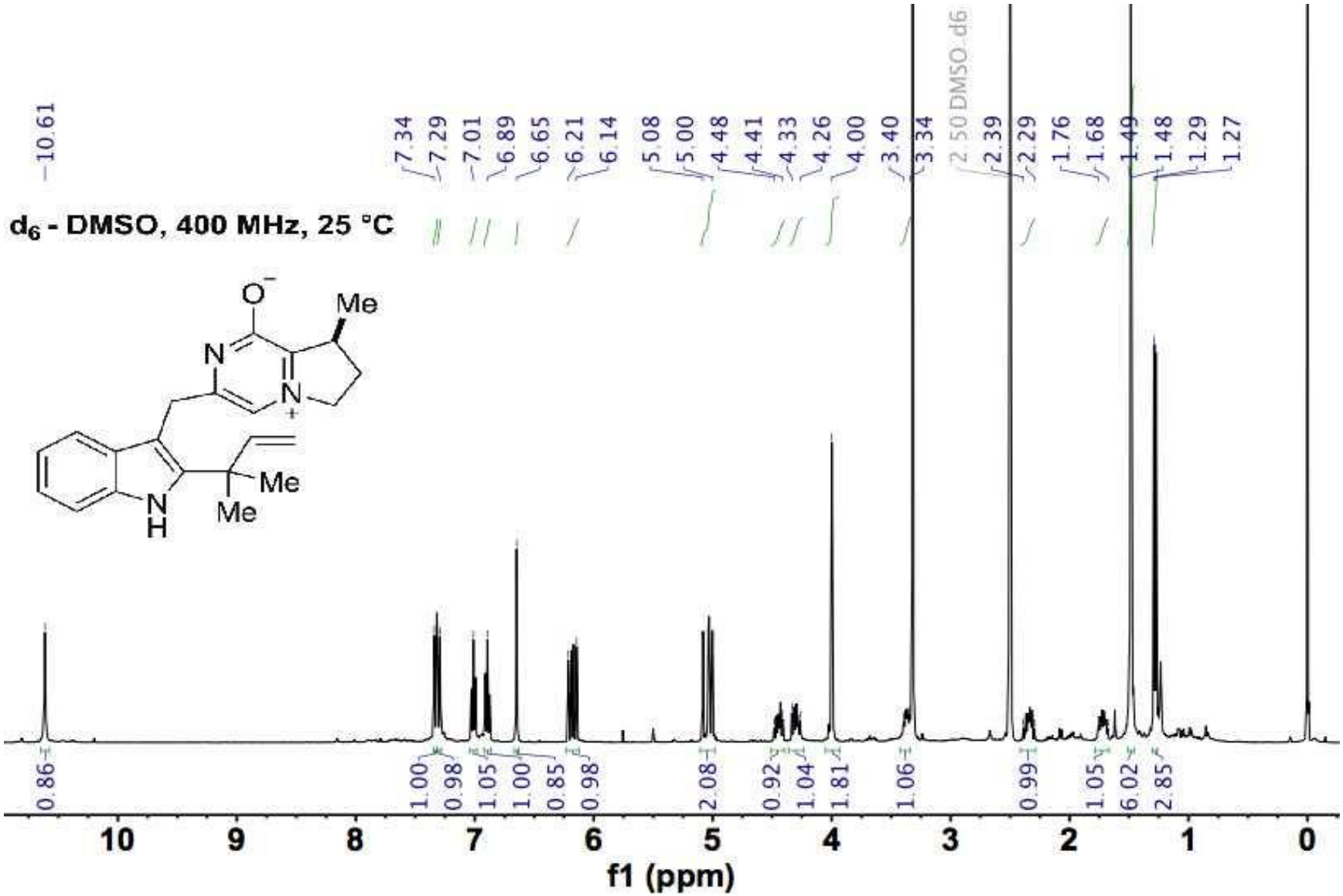


*Figure A2.3.41*. $^{1}$H NMR Spectrum of Compound **MeZwtP**.

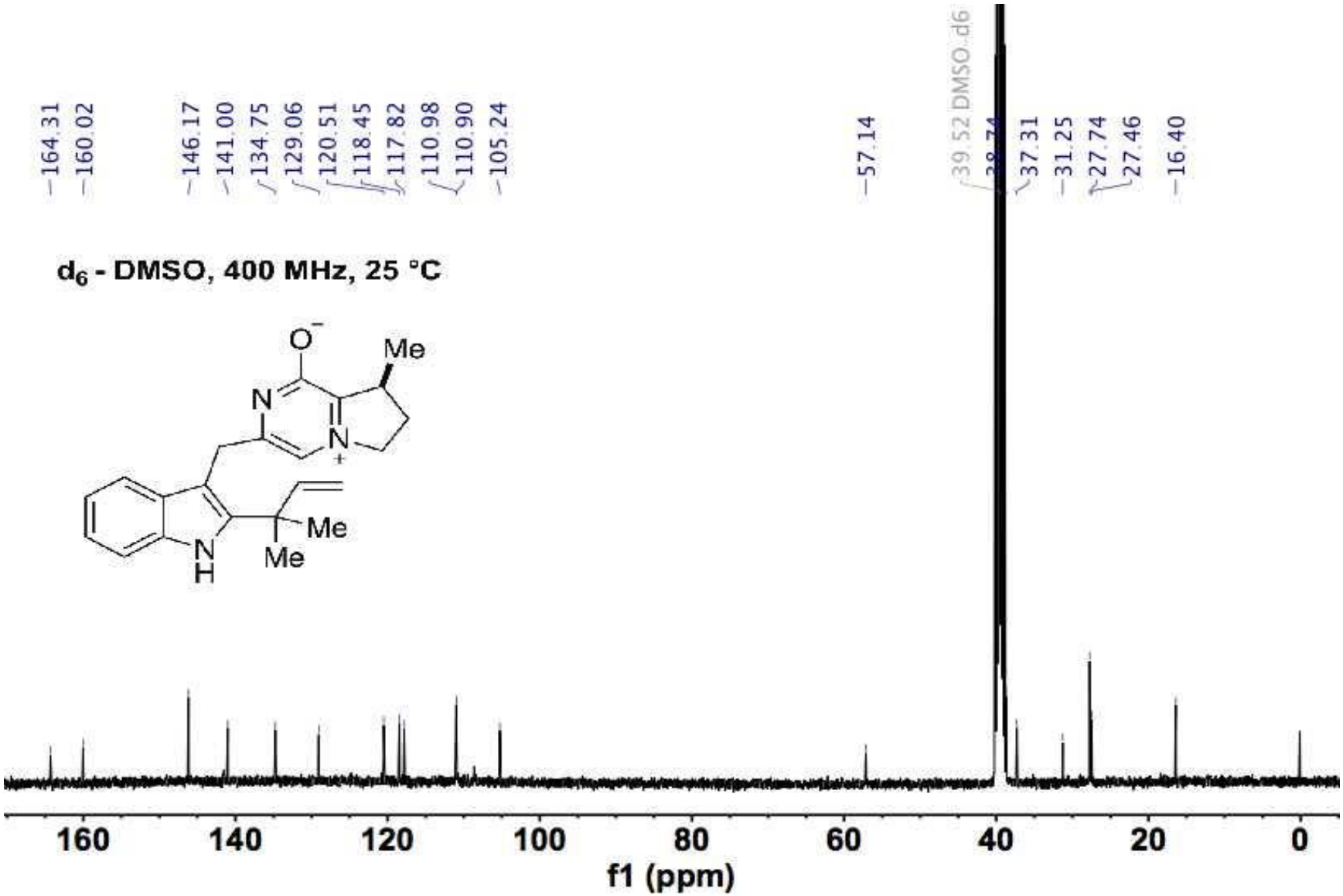


*Figure A2.3.42*. $^{13}$C NMR Spectrum of Compound **MeZwtP**.

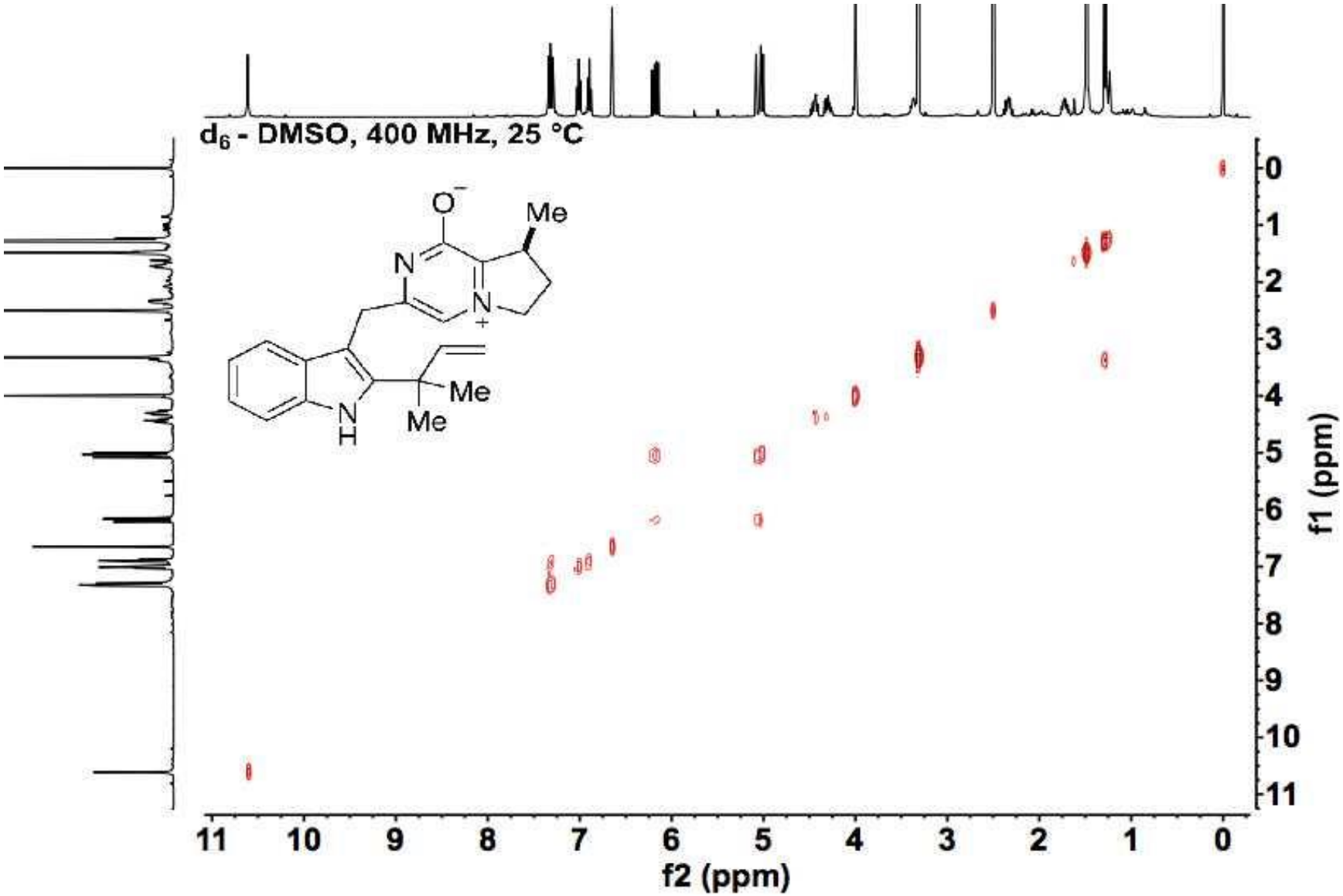


*Figure A2.3.43*. COSY NMR Spectrum of Compound **MeZwtP**.

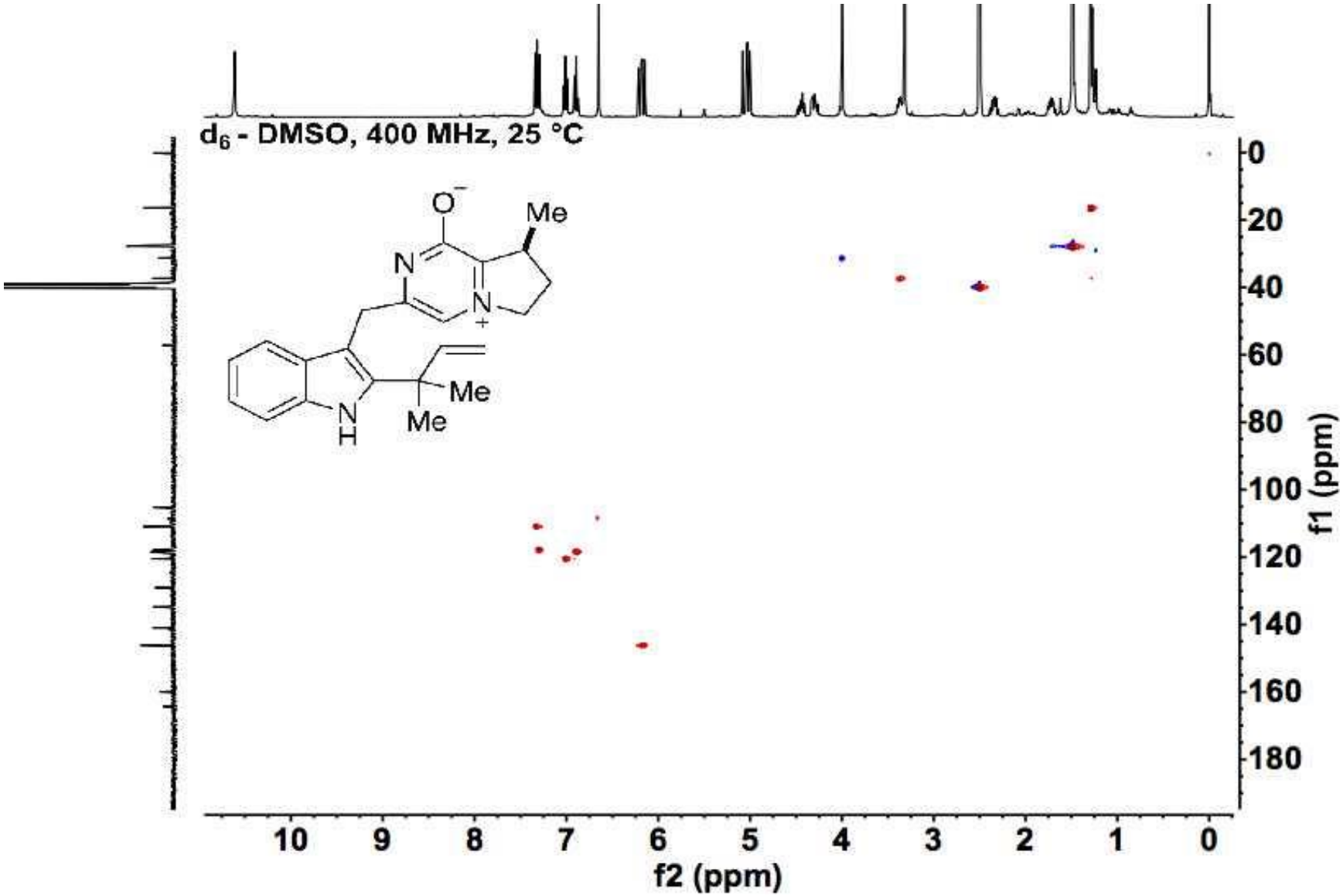


*Figure A2.3.44*. HSQC Spectrum of Compound **MeZwtP**.

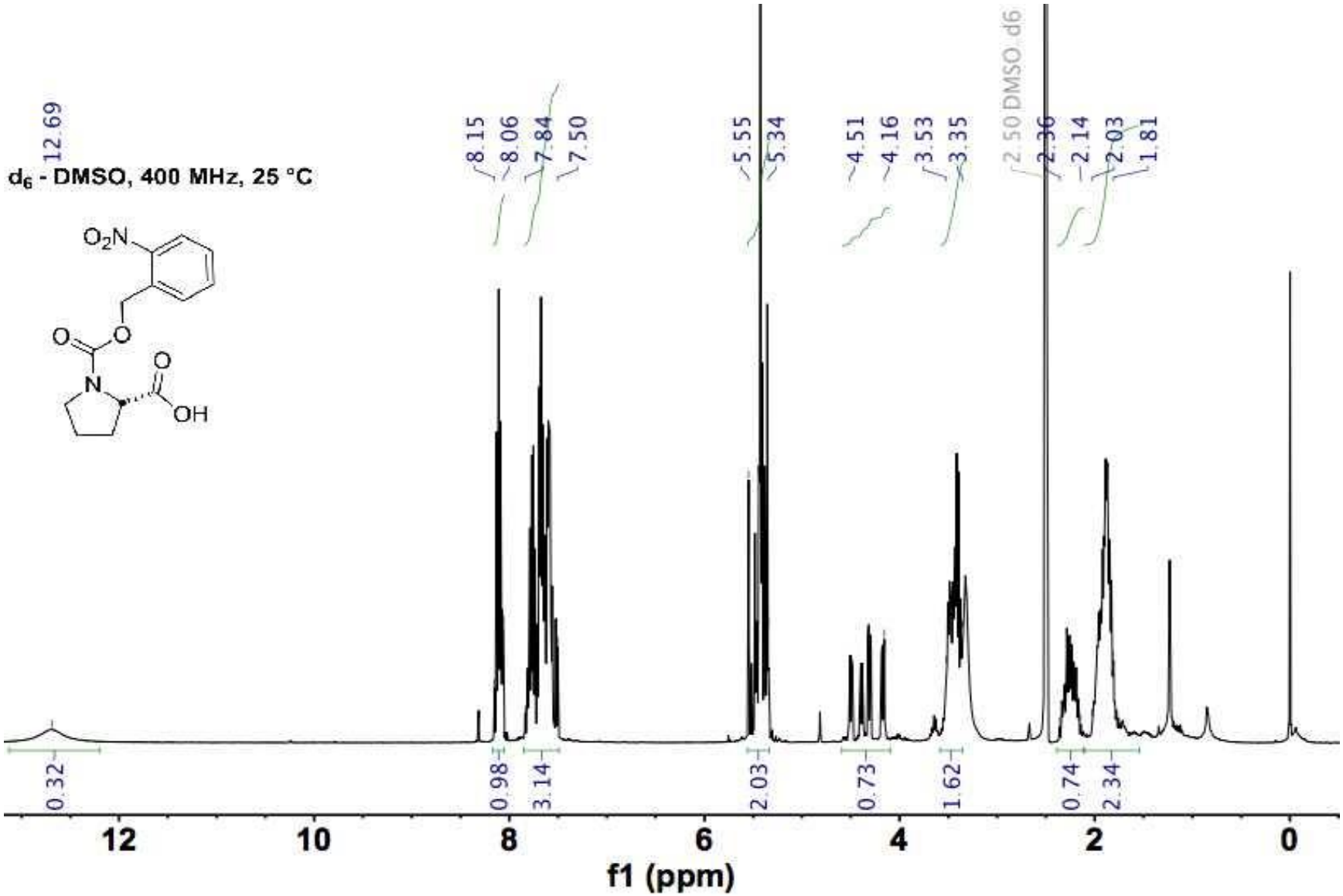


*Figure A2.3.45*. $^{1}$H NMR Spectrum of Compound **3.23**.

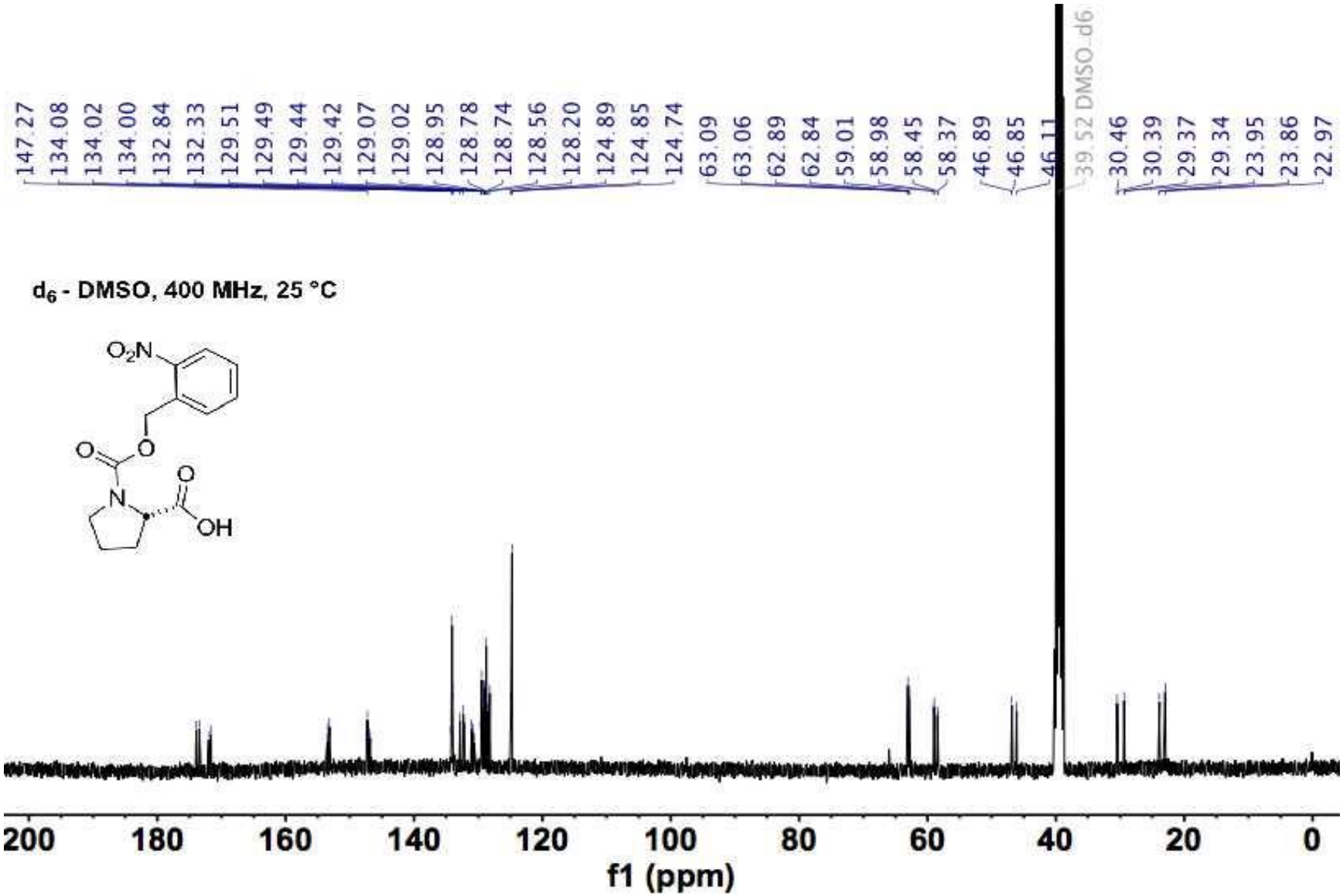


*Figure A2.3.46*. $^{13}$C NMR Spectrum of Compound **3.23**.

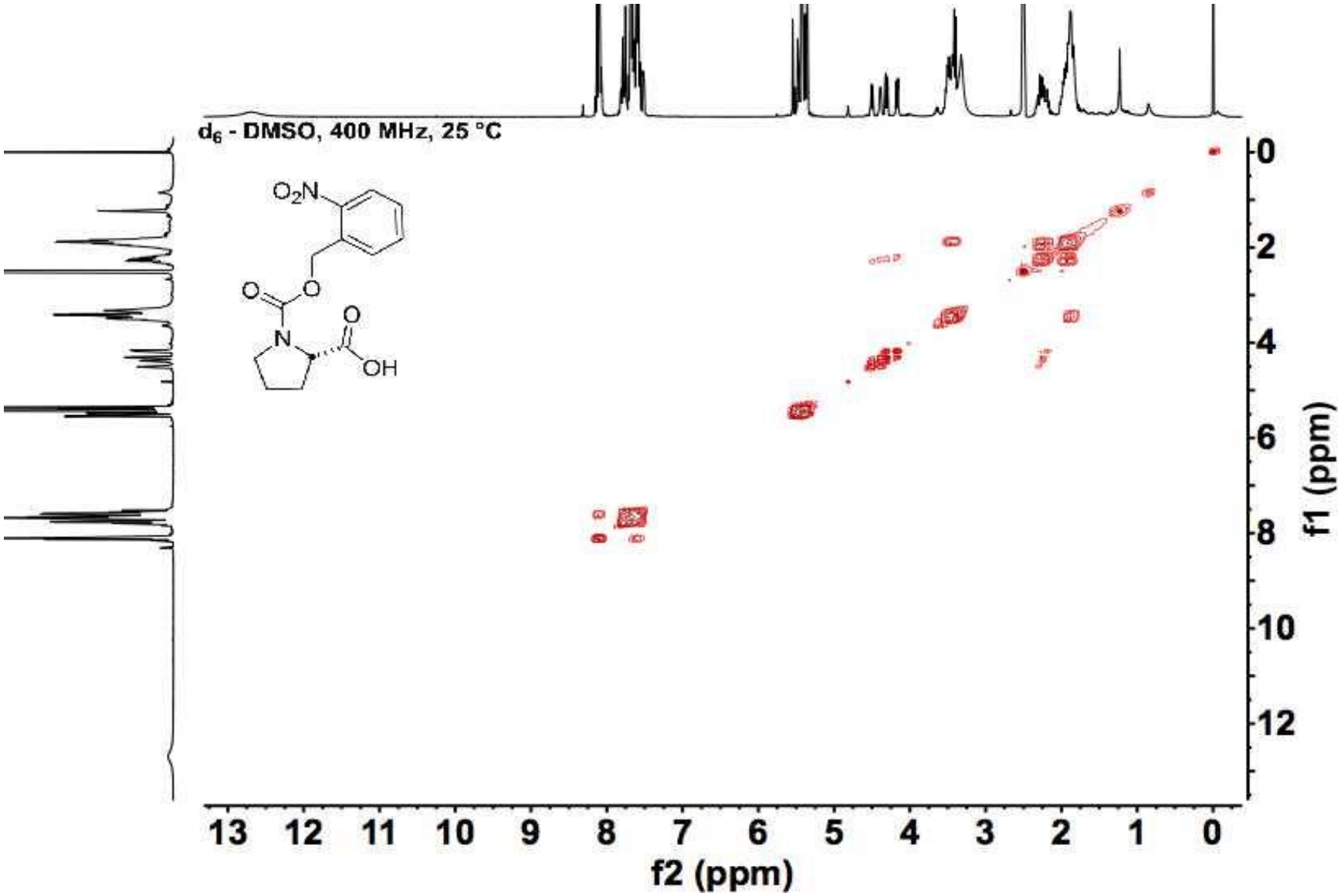


*Figure A2.3.47*. COSY NMR Spectrum of Compound **3.23**.

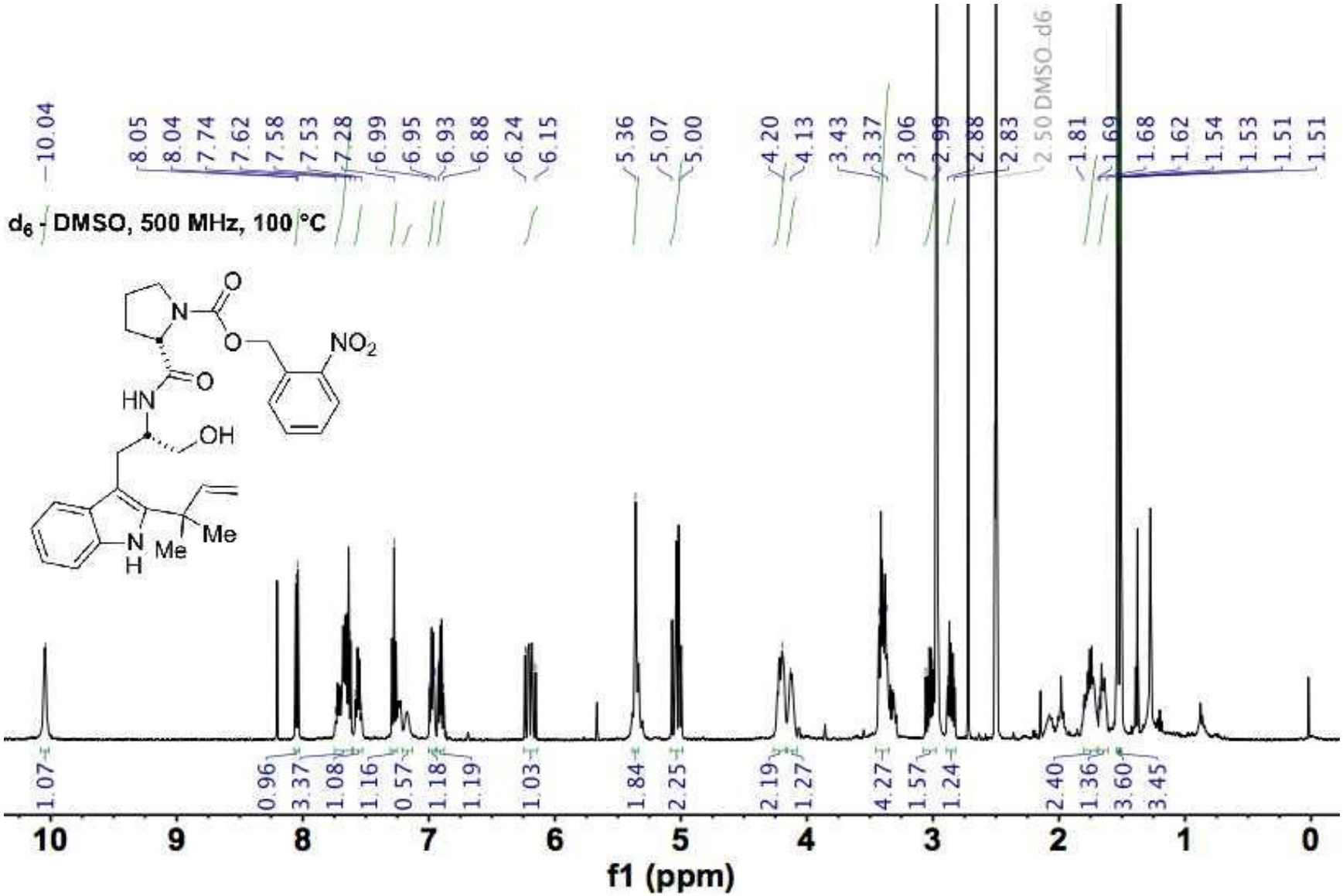


*Figure A2.3.48*. $^{1}$H NMR Spectrum of Compound **3.26**.

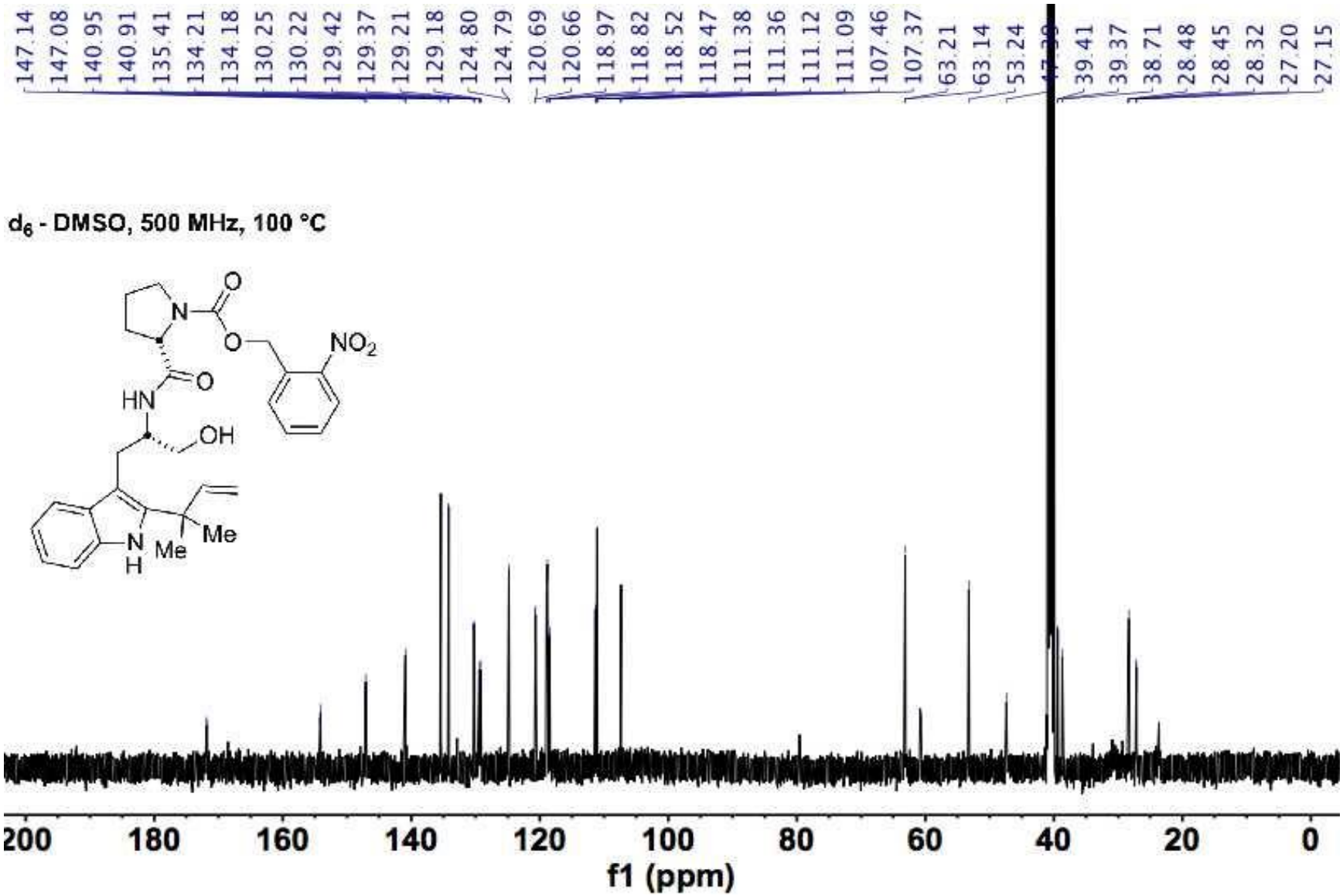


*Figure A2.3.49*. $^{13}$C NMR Spectrum of Compound **3.26**.

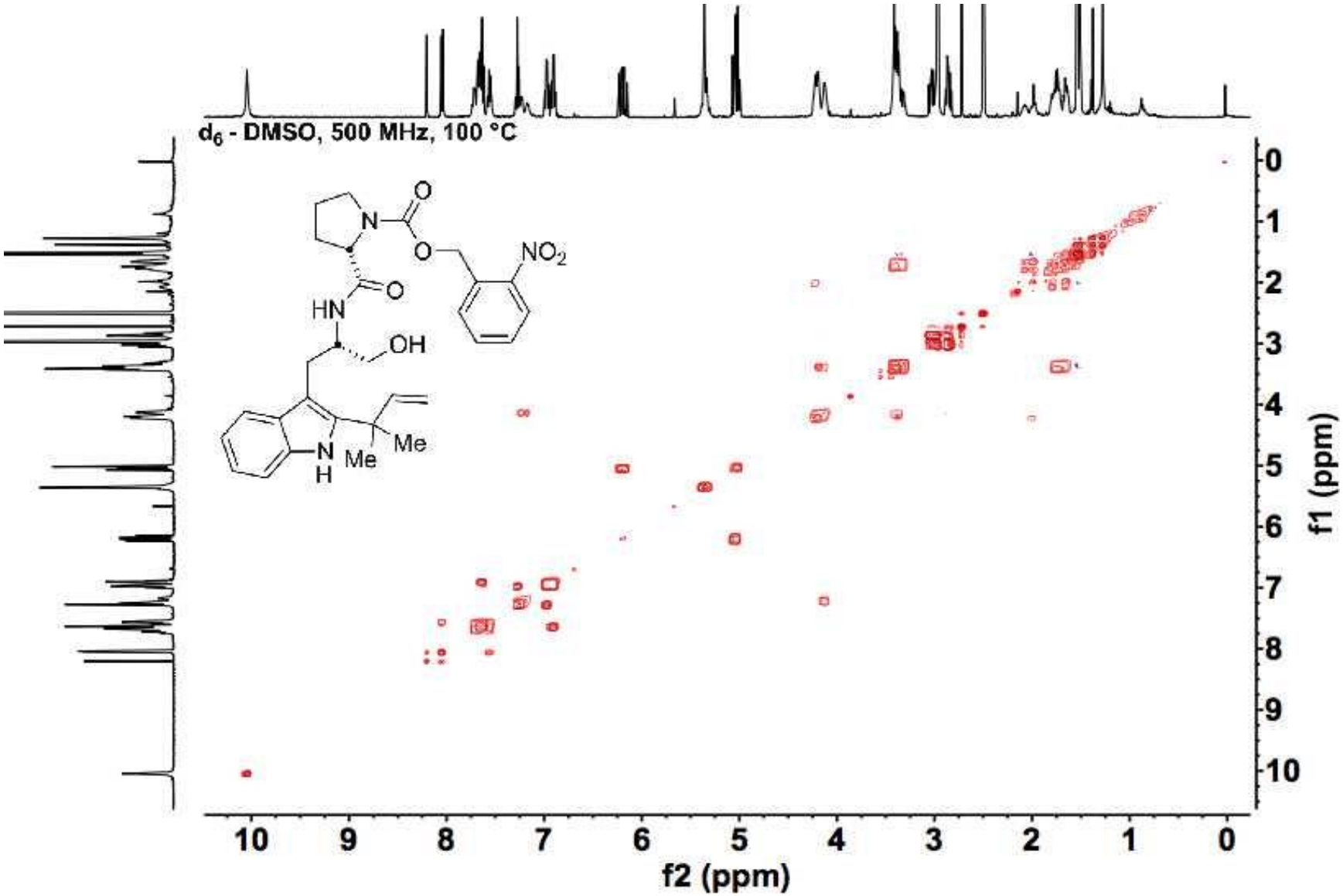


*Figure A2.3.50*. COSY NMR Spectrum of Compound **3.26**.

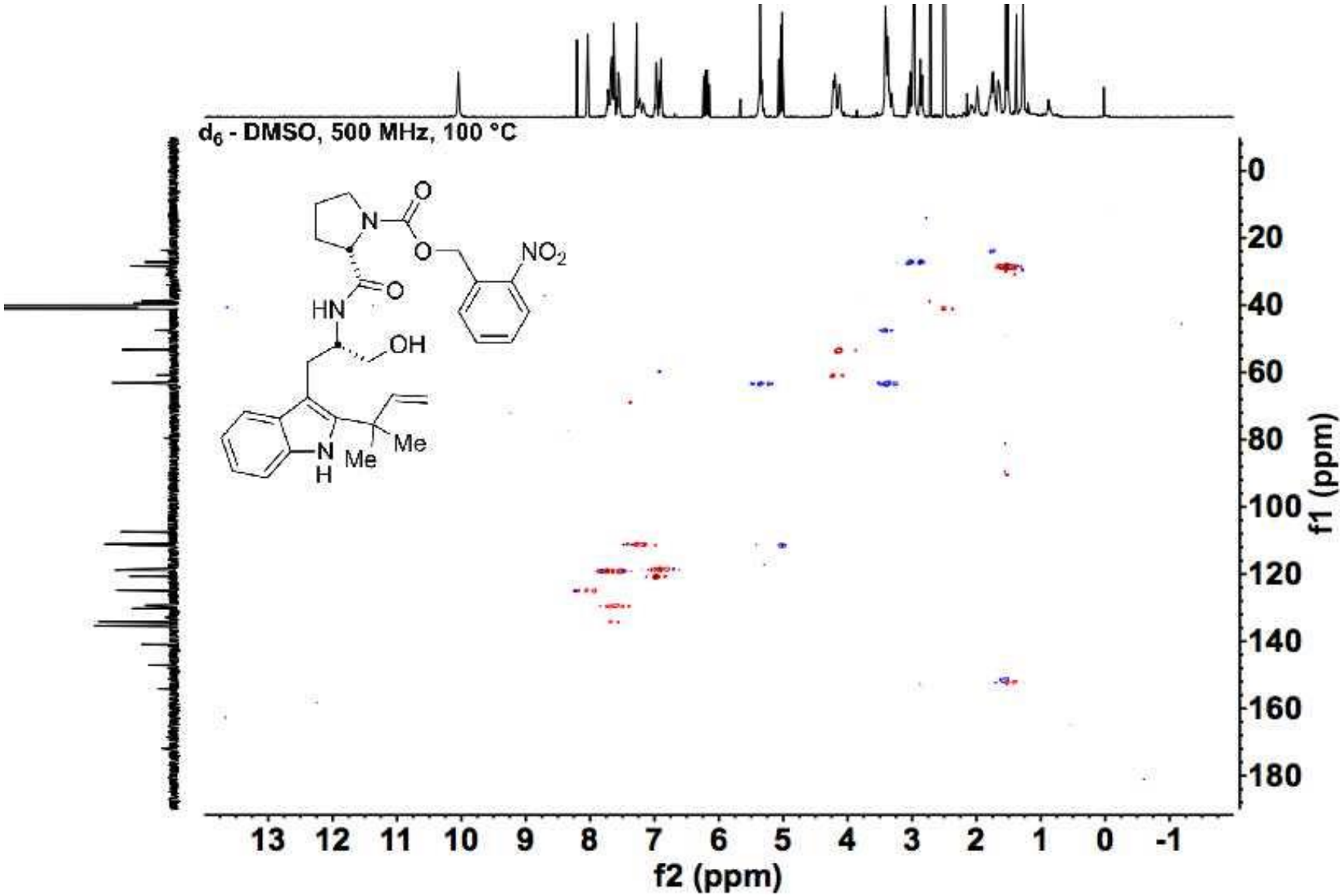


*Figure A2.3.51*. HSQC Spectrum of Compound **3.26**.

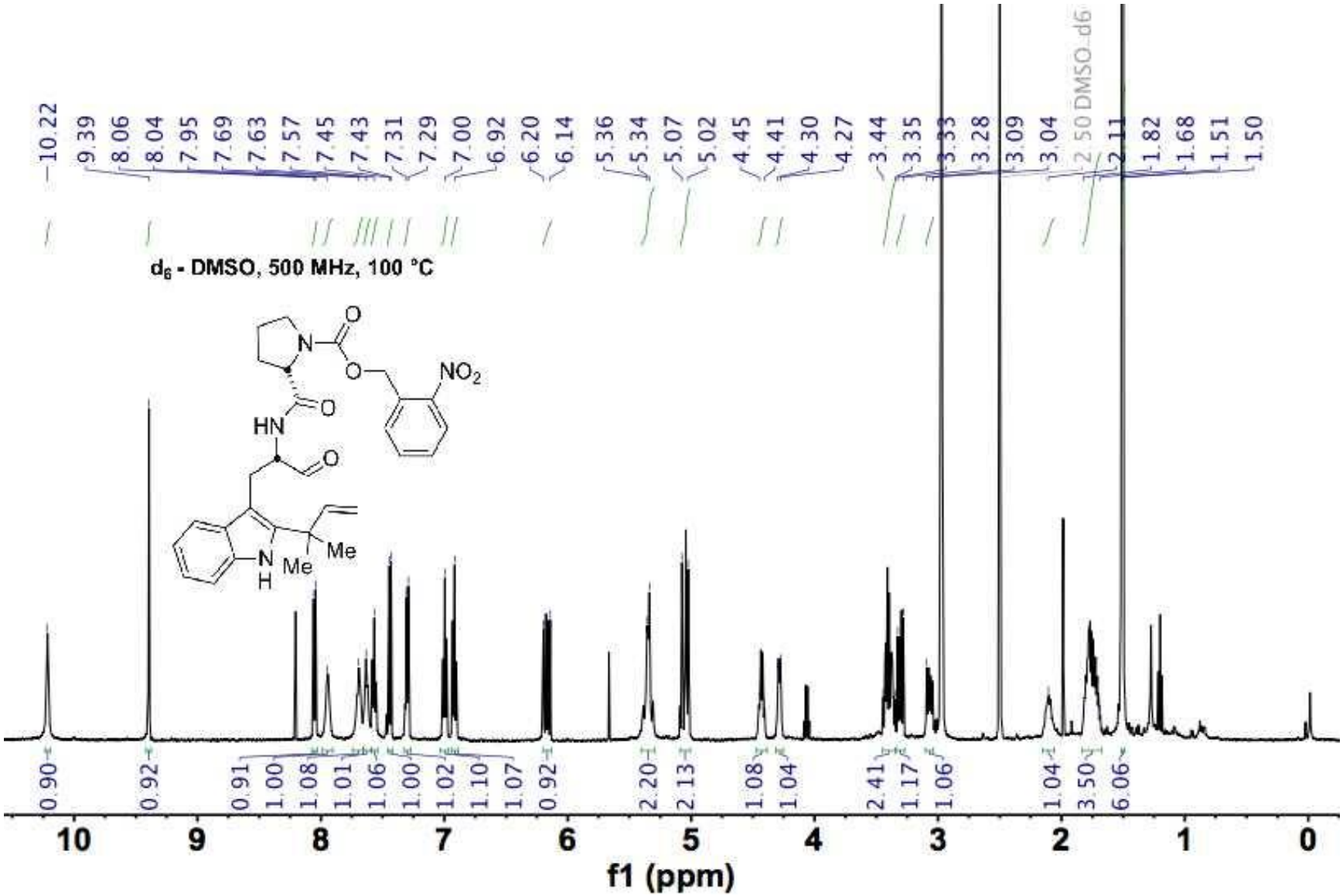


*Figure A2.3.52*. $^{1}$H NMR Spectrum of Compound **3.27**.

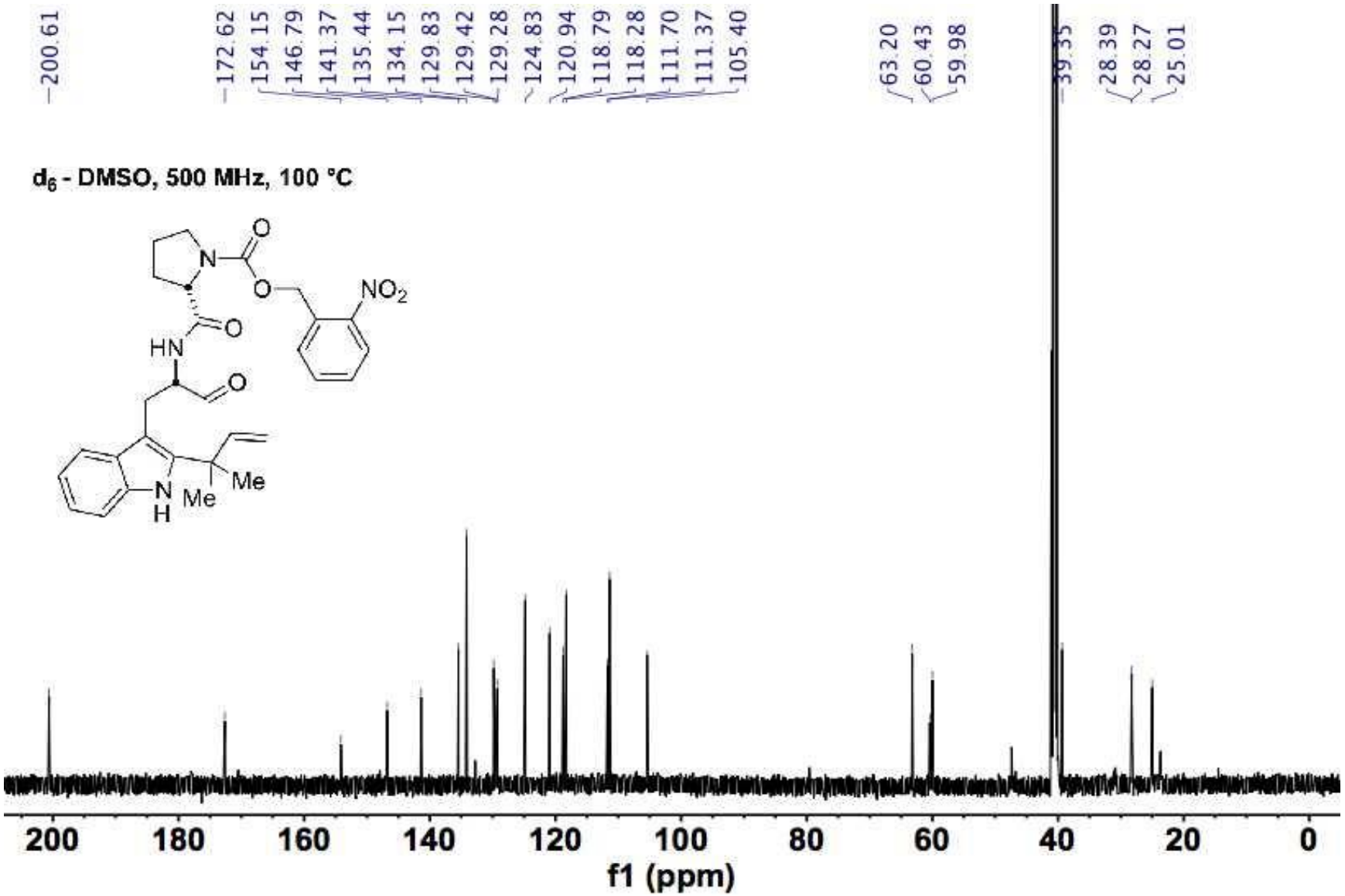


*Figure A2.3.53*. $^{13}$C NMR Spectrum of Compound **3.27**.

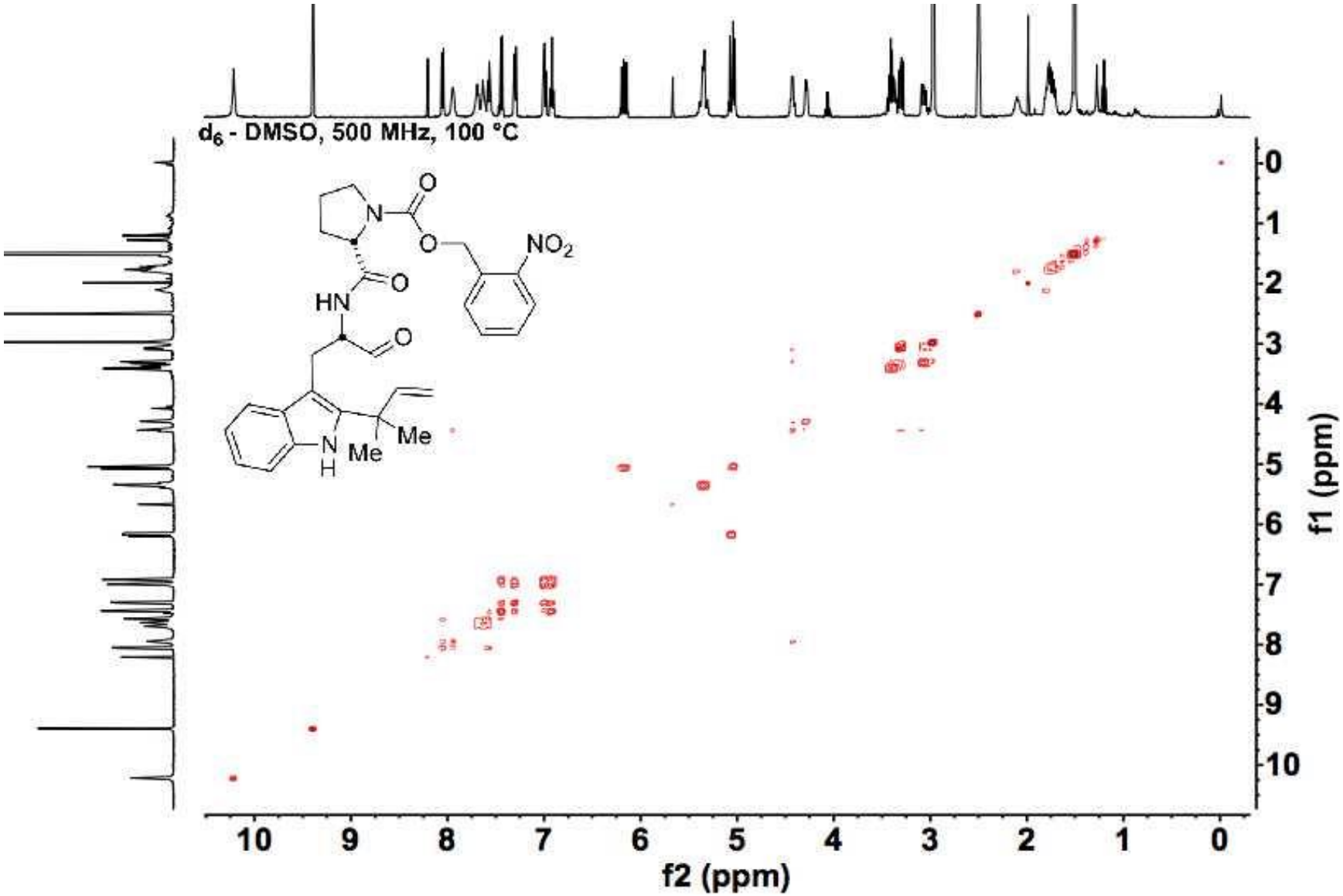


*Figure A2.3.54*. COSY NMR Spectrum of Compound **3.27**.

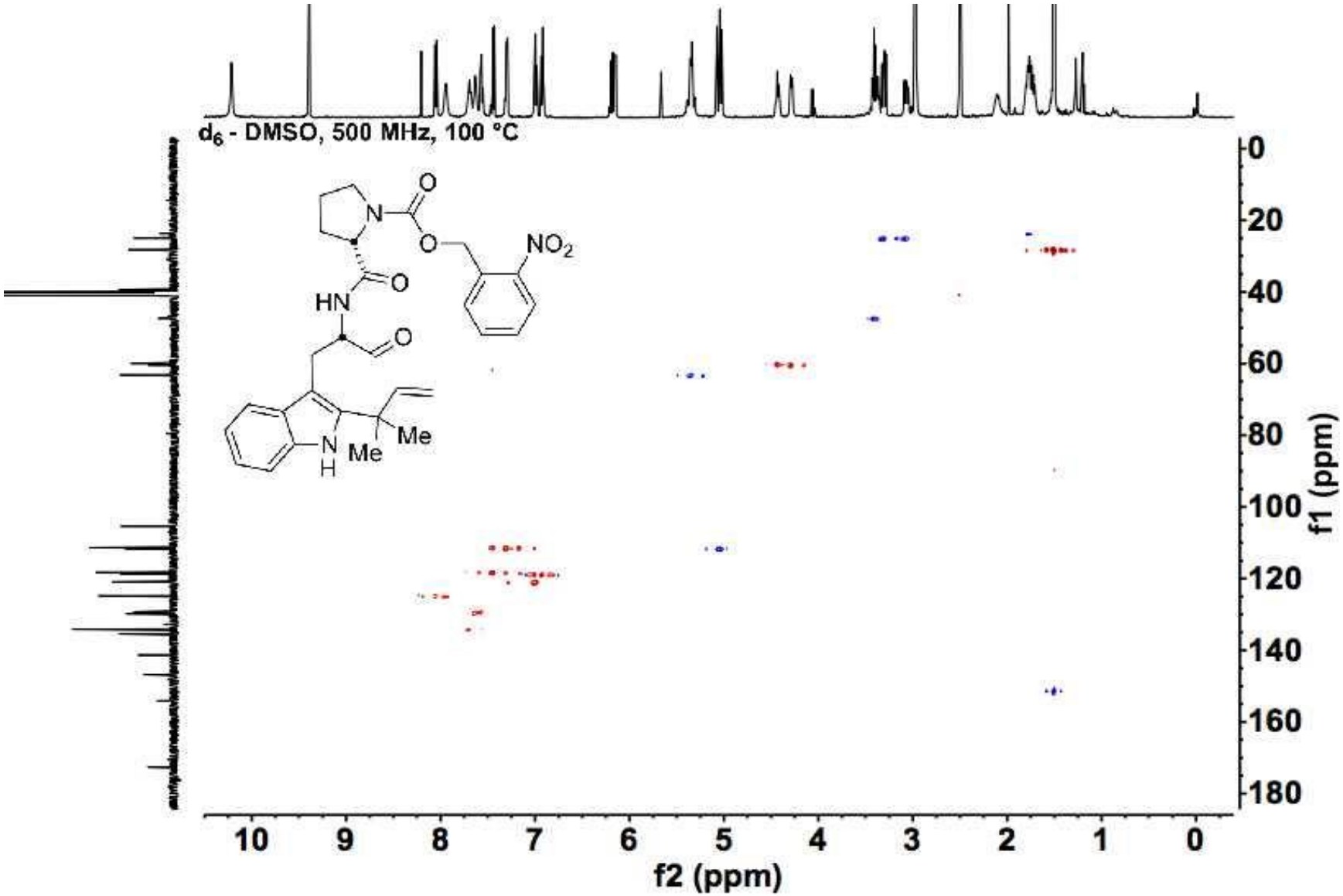


*Figure A2.3.55*. HSQC Spectrum of Compound **3.27**.

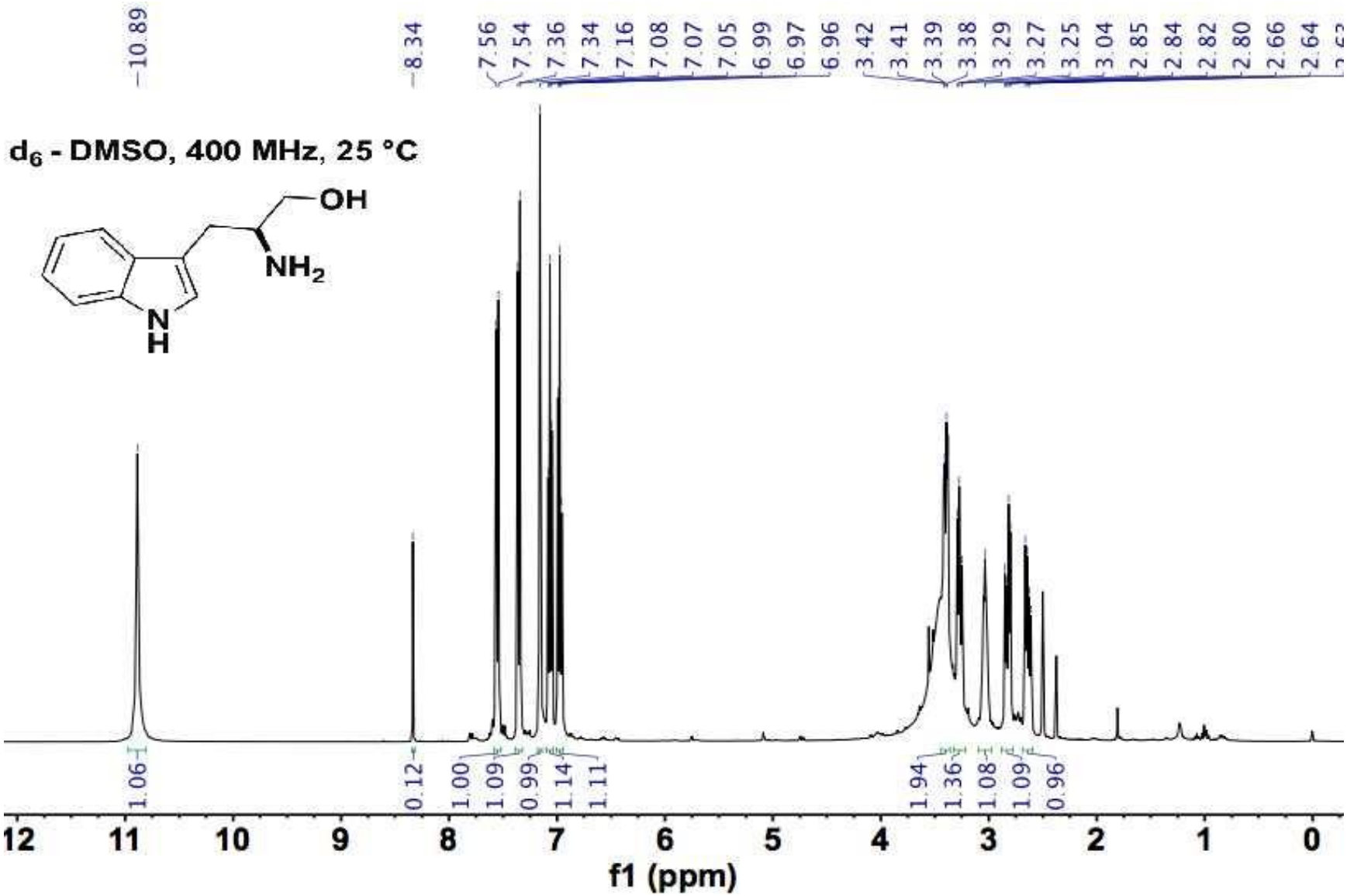


*Figure A2.3.56*. $^{1}$H NMR Spectrum of Compound **3.19.**

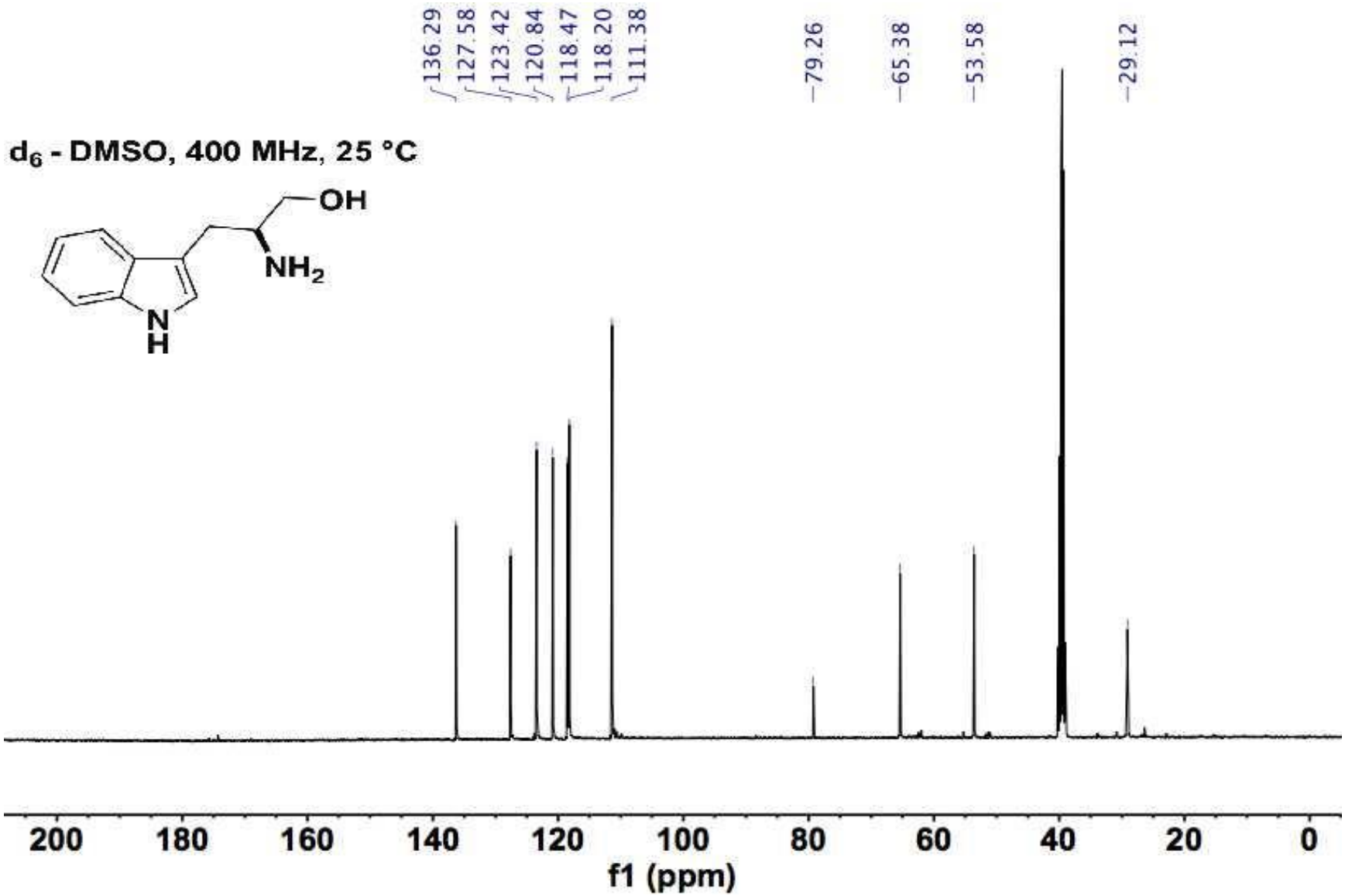


*Figure A2.3.57*. $^{13}$C NMR Spectrum of Compound **3.19**.

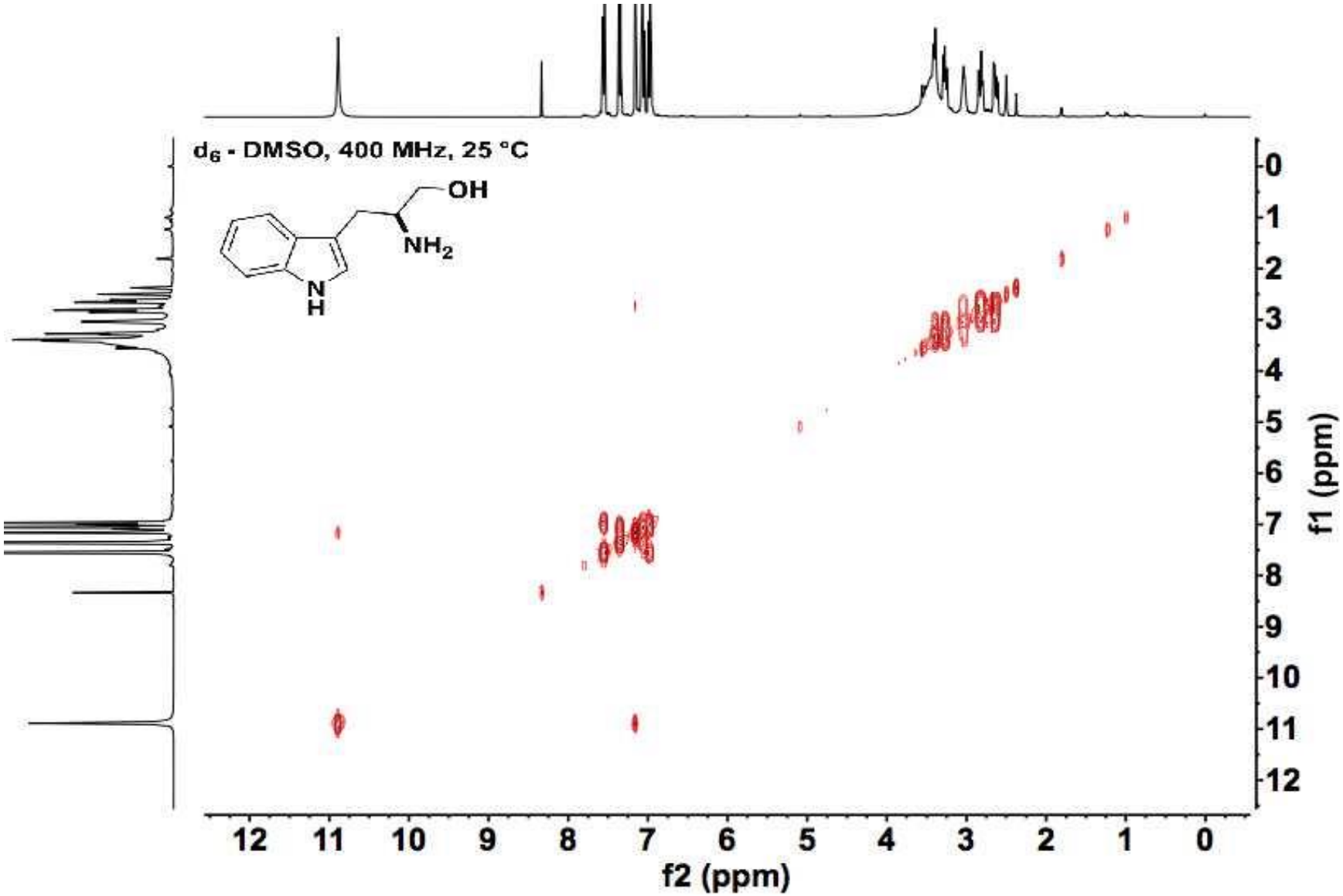


*Figure A2.3.58*. COSY Spectrum of Compound **3.19**.

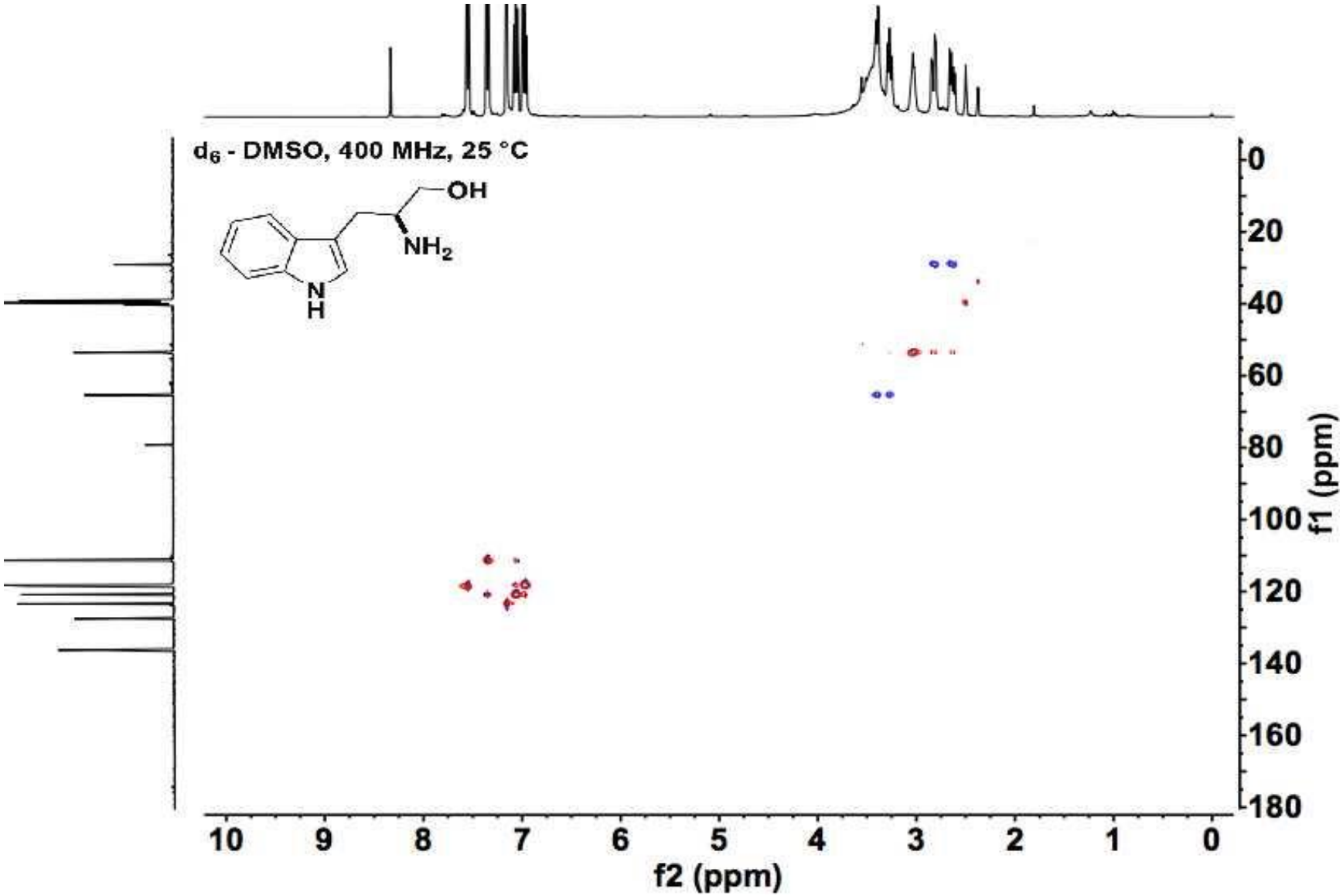


*Figure A2.3.59*. HSQC Spectrum of Compound **3.19**.

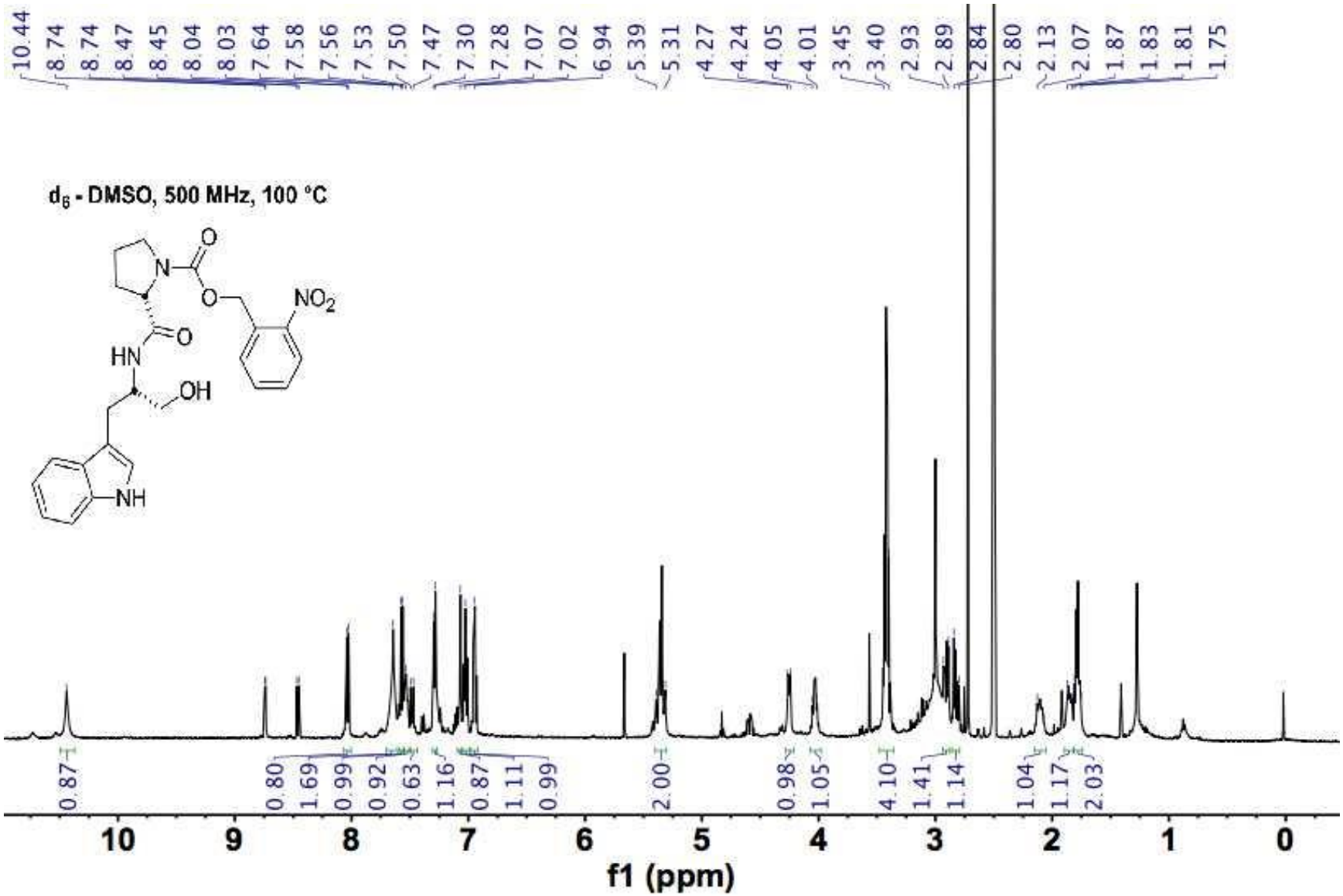


*Figure A2.3.60*. $^{1}$H NMR Spectrum of Compound **3.24**.

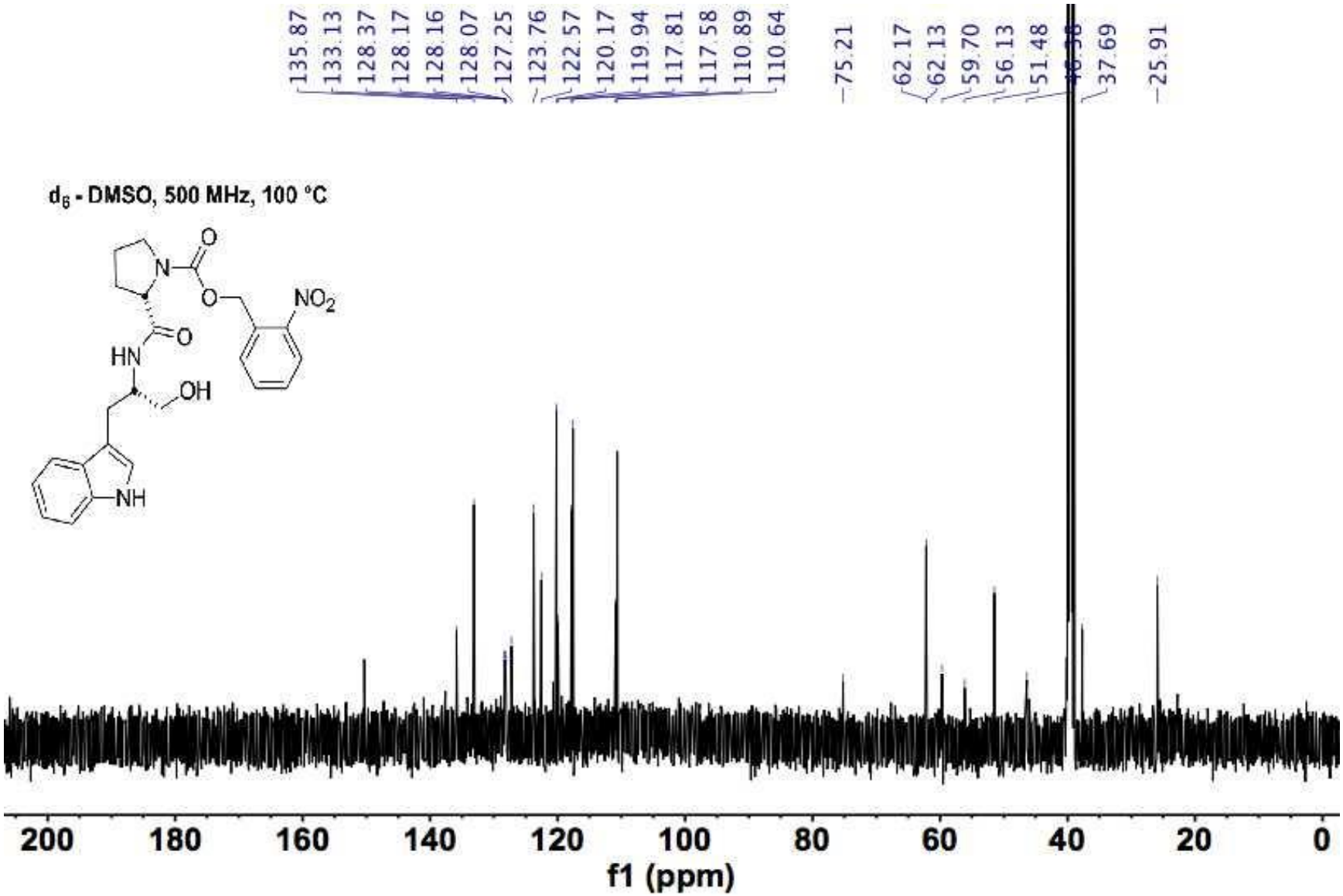


*Figure A2.3.61*. $^{13}$C NMR Spectrum of Compound **3.24**.

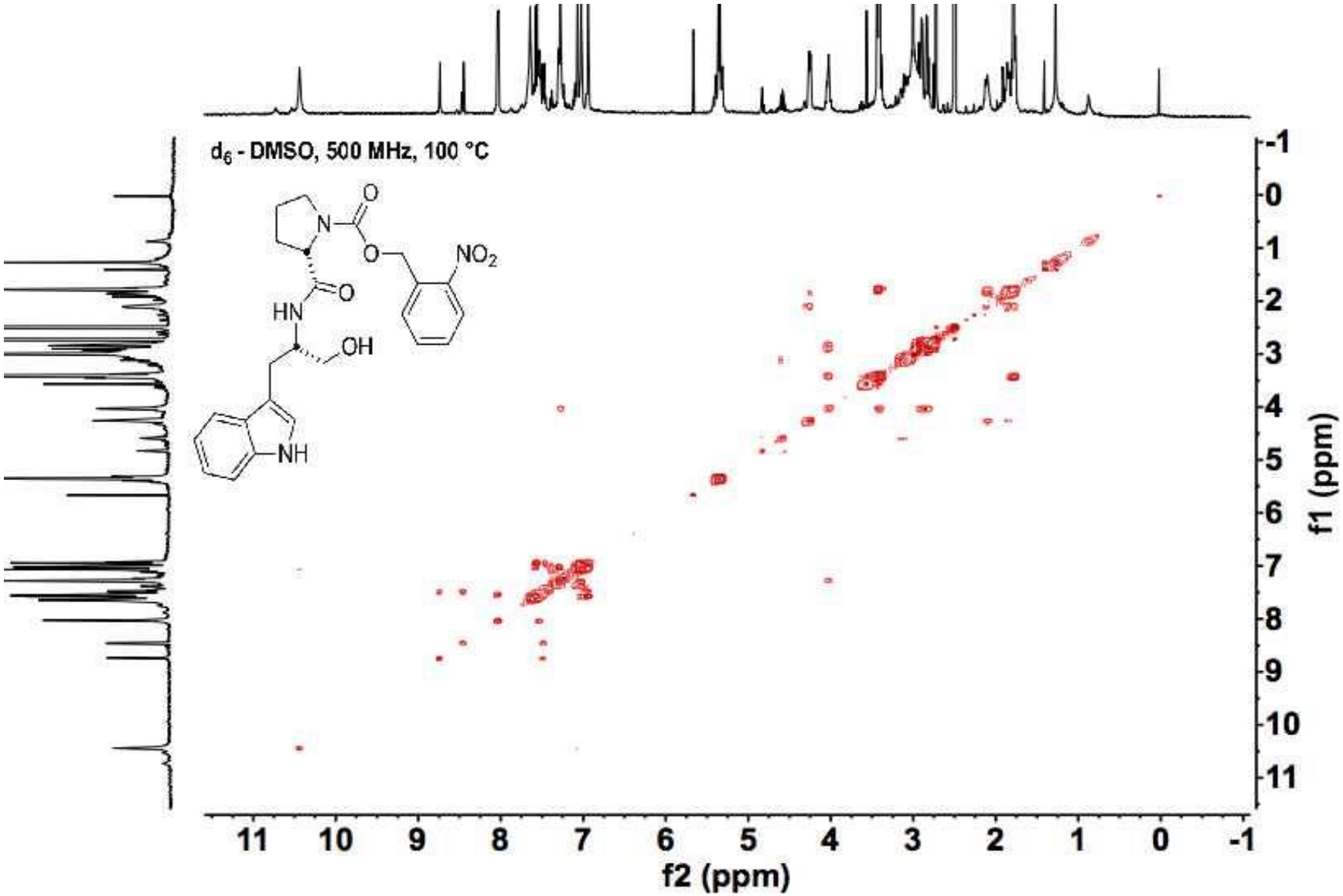


*Figure A2.3.62*. COSY NMR Spectrum of Compound **3.24**.

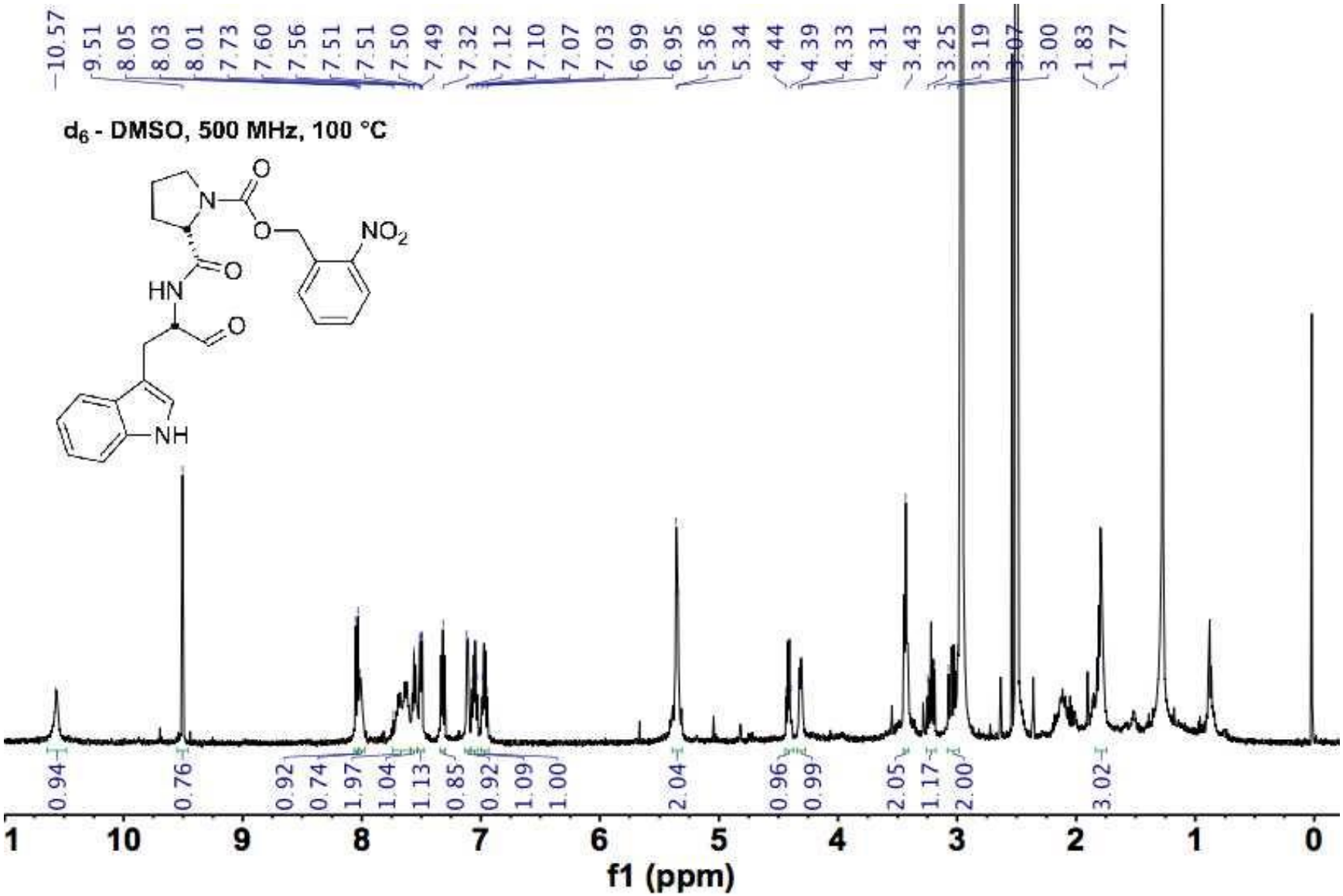


*Figure A2.3.63*. $^{1}$H NMR Spectrum of Compound **3.25**.

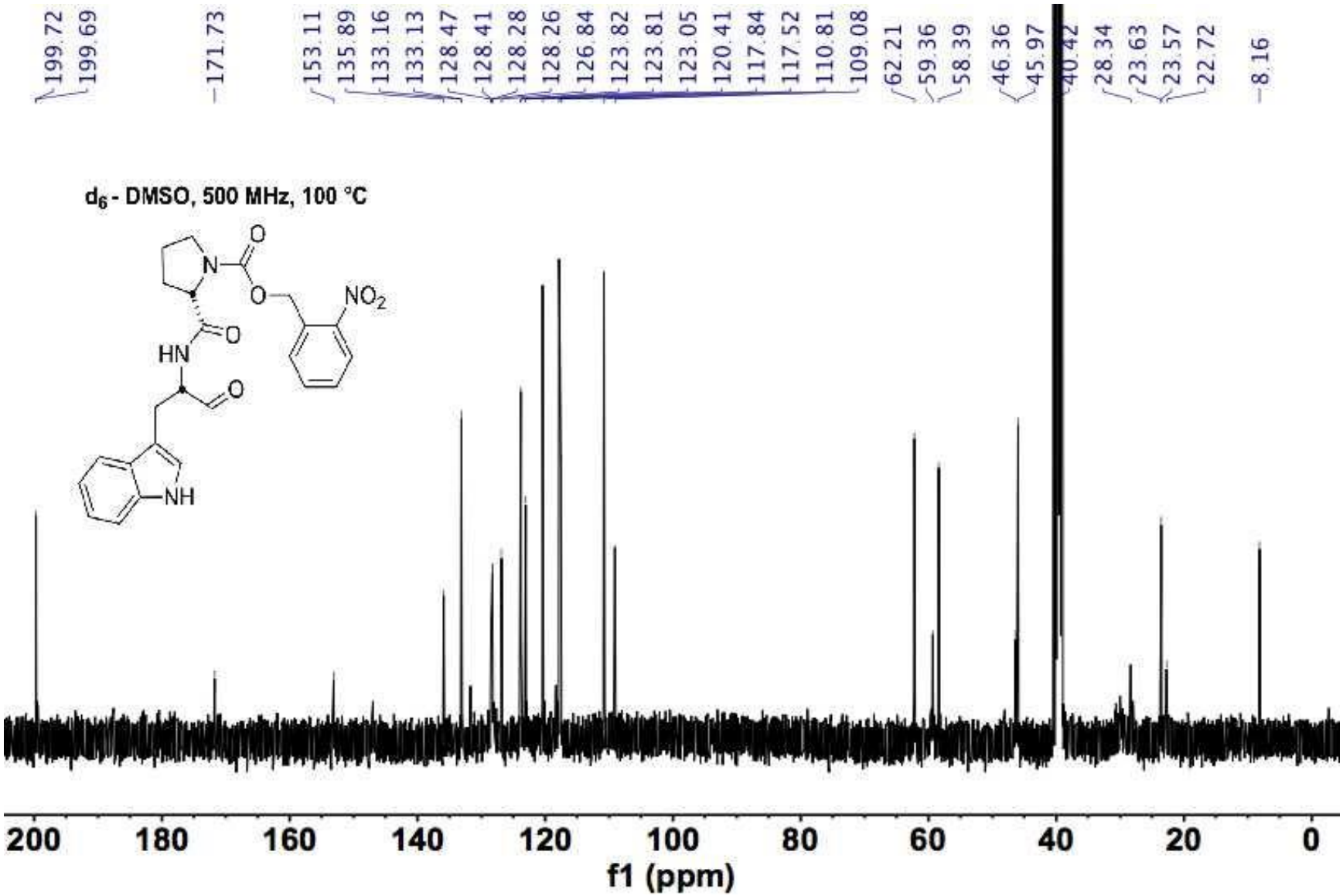


*Figure A2.3.64*. $^{13}$C NMR Spectrum of Compound **3.25**.

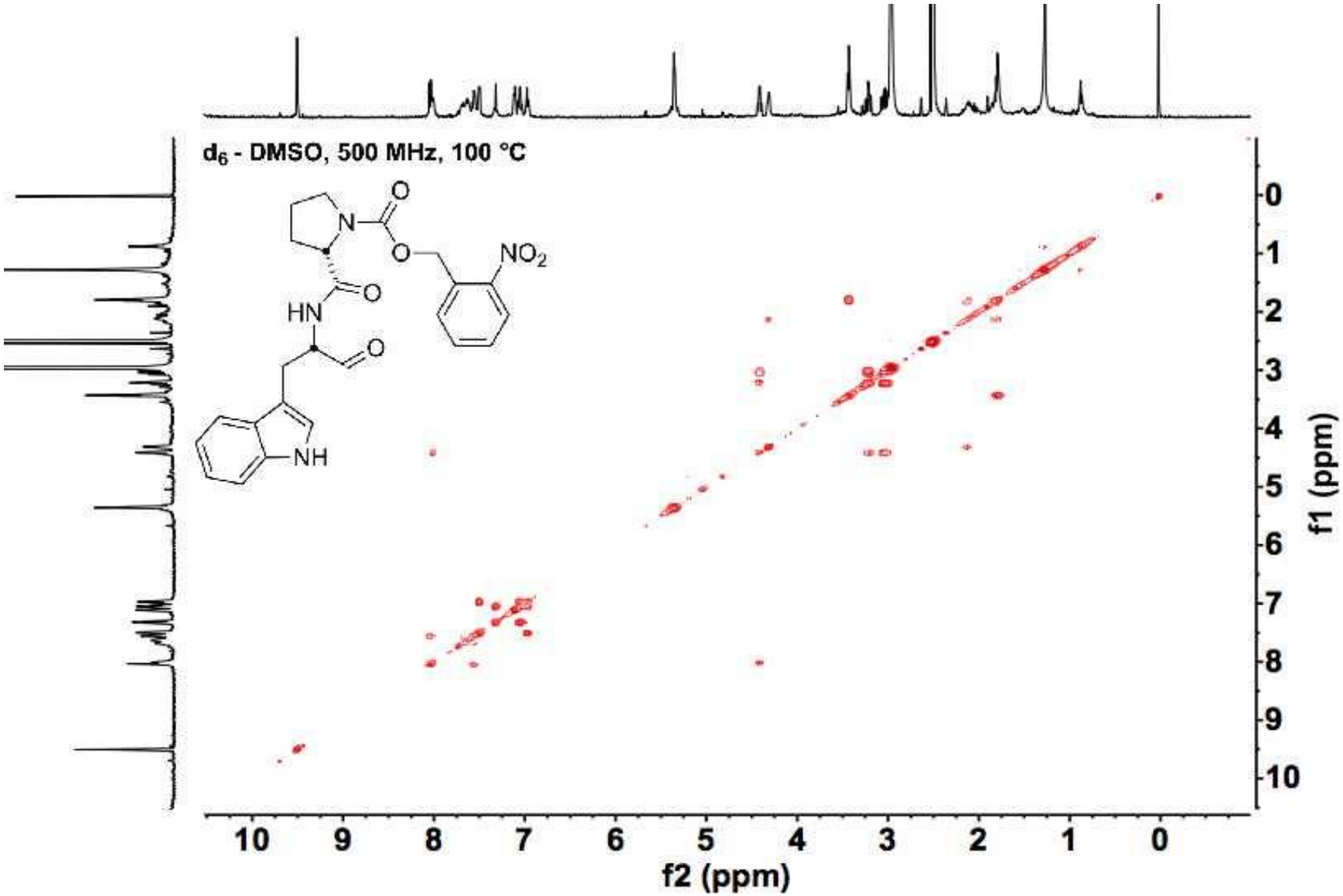


*Figure A2.3.65*. COSY NMR Spectrum of Compound **3.25**.

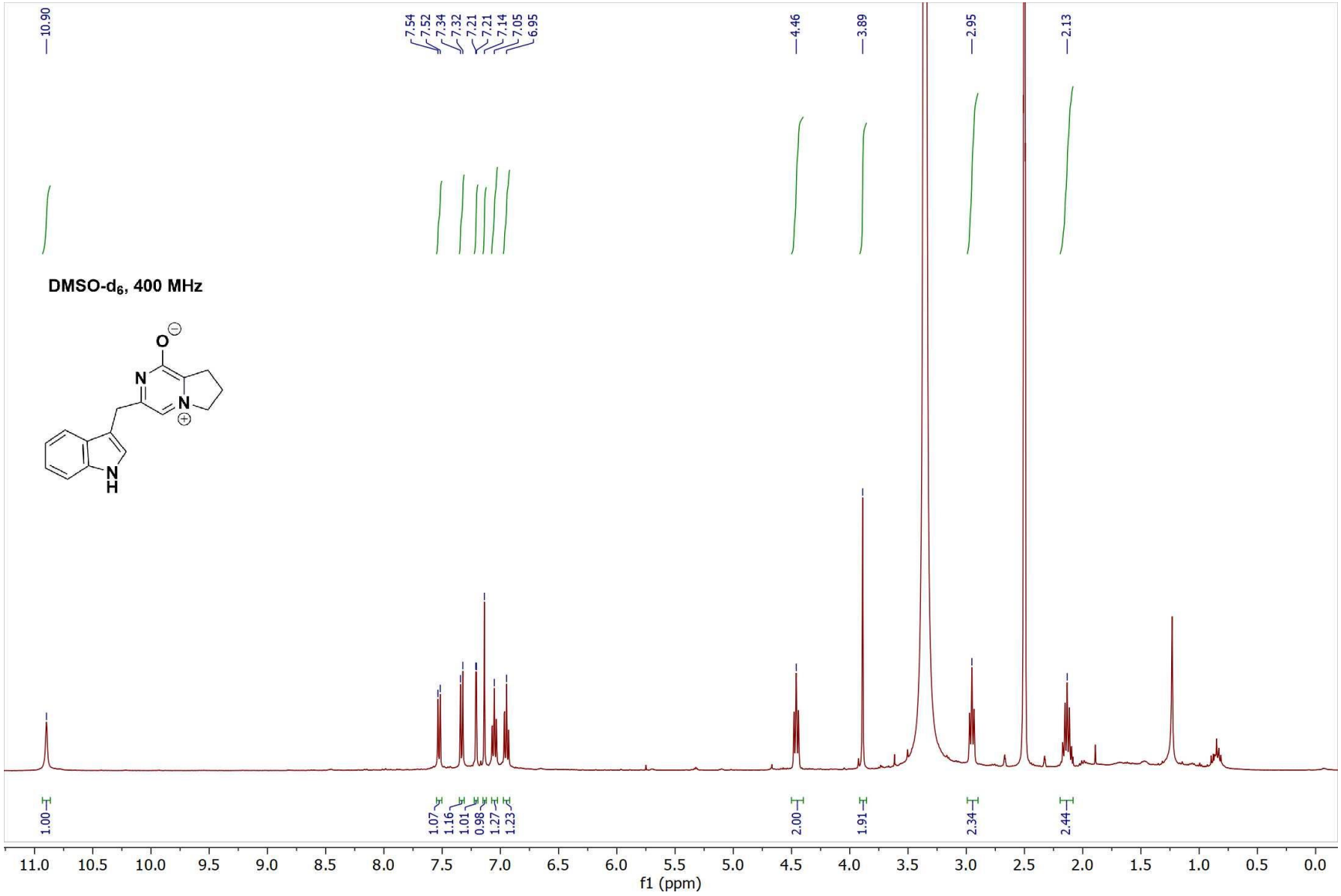


*Figure A2.3.66*. $^{1}$H NMR Spectrum of Compound **3.17**.

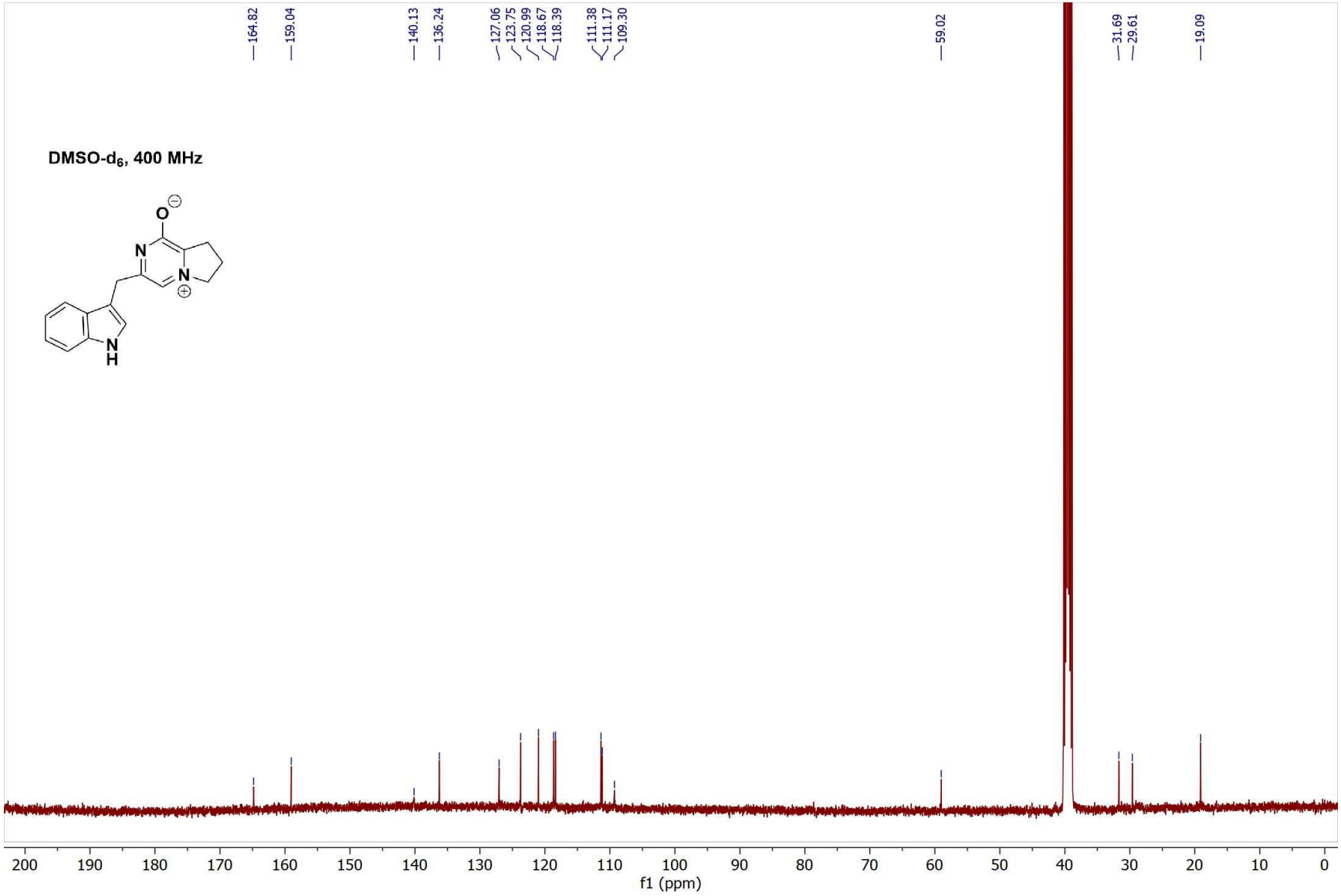


*Figure A2.3.67*. $^{13}$C NMR Spectrum of Compound **3.17**.

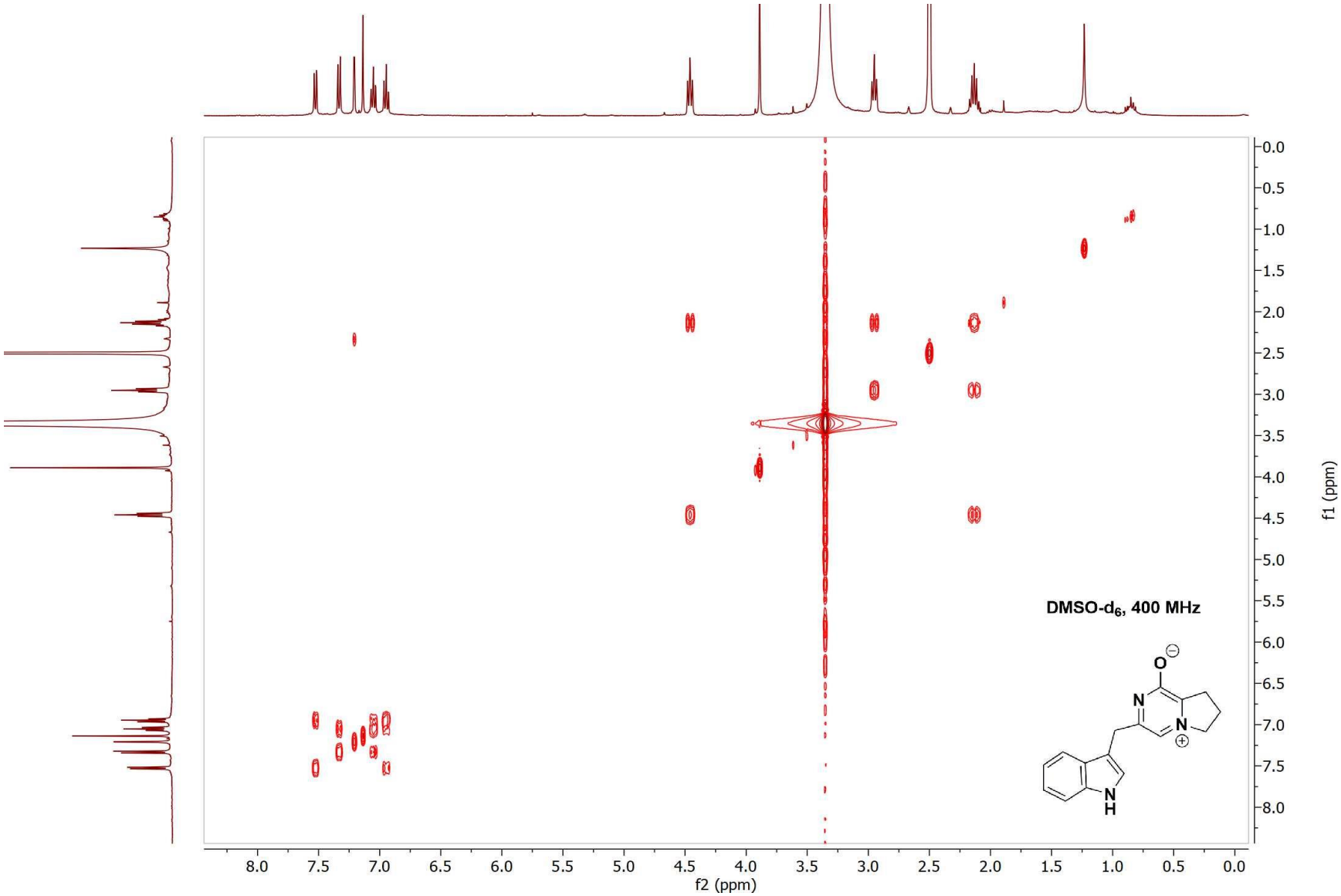


*Figure A2.3.68*. COSY NMR Spectrum of Compound **3.17**.

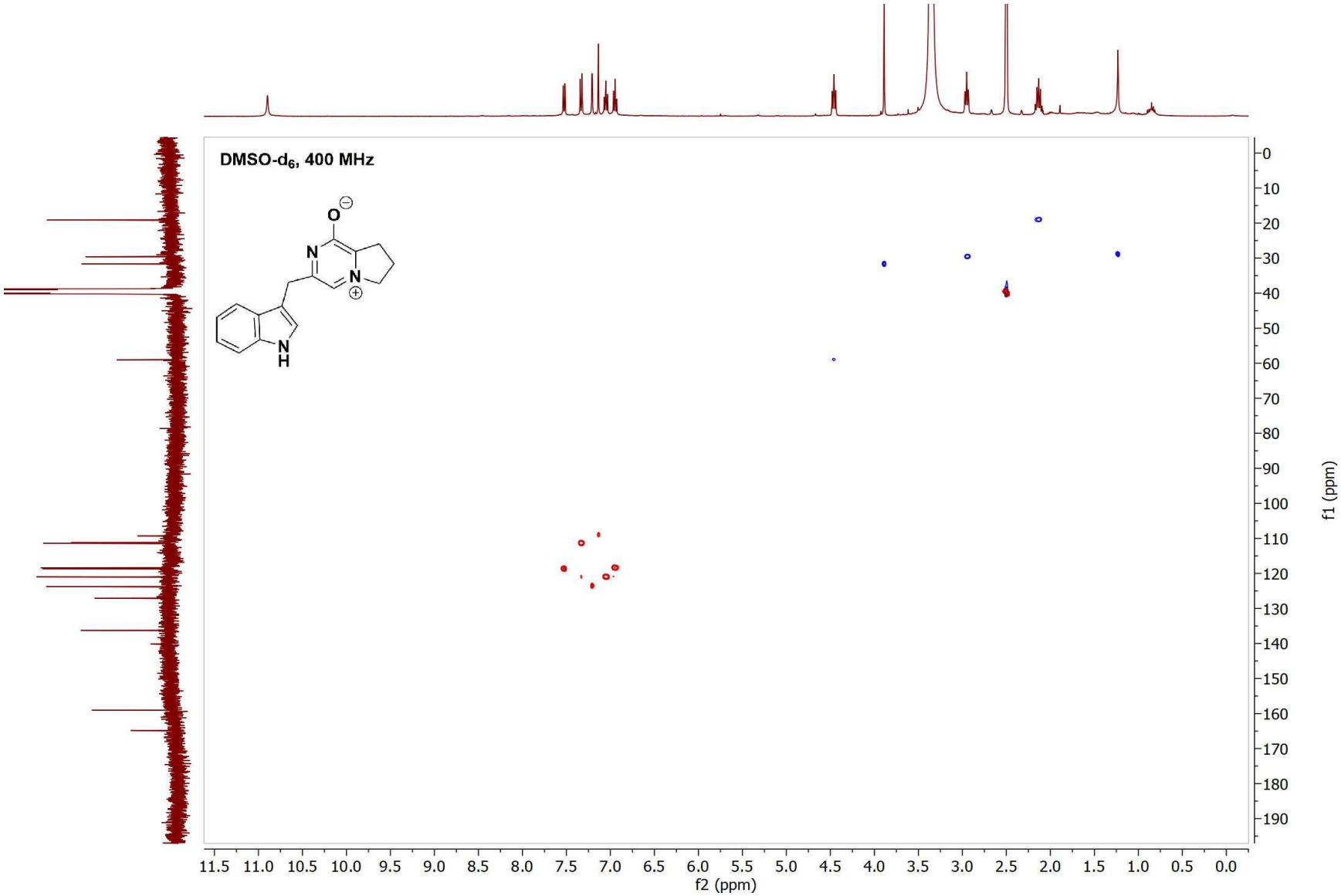


*Figure A2.3.69*. HSQC NMR Spectrum of Compound **3.17**.

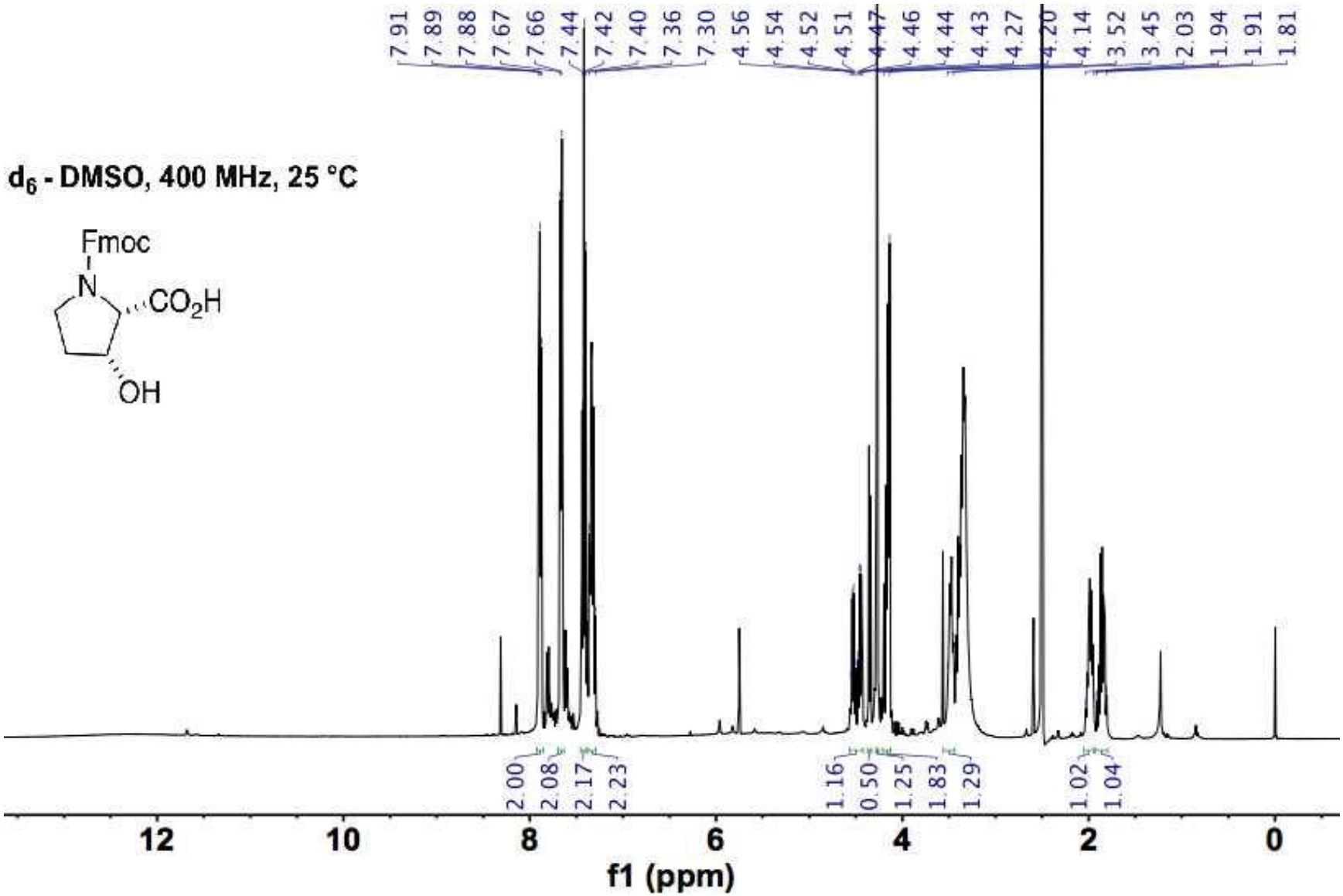


*Figure A2.4.1*. $^{1}$H NMR Spectrum of Compound **4.24**.

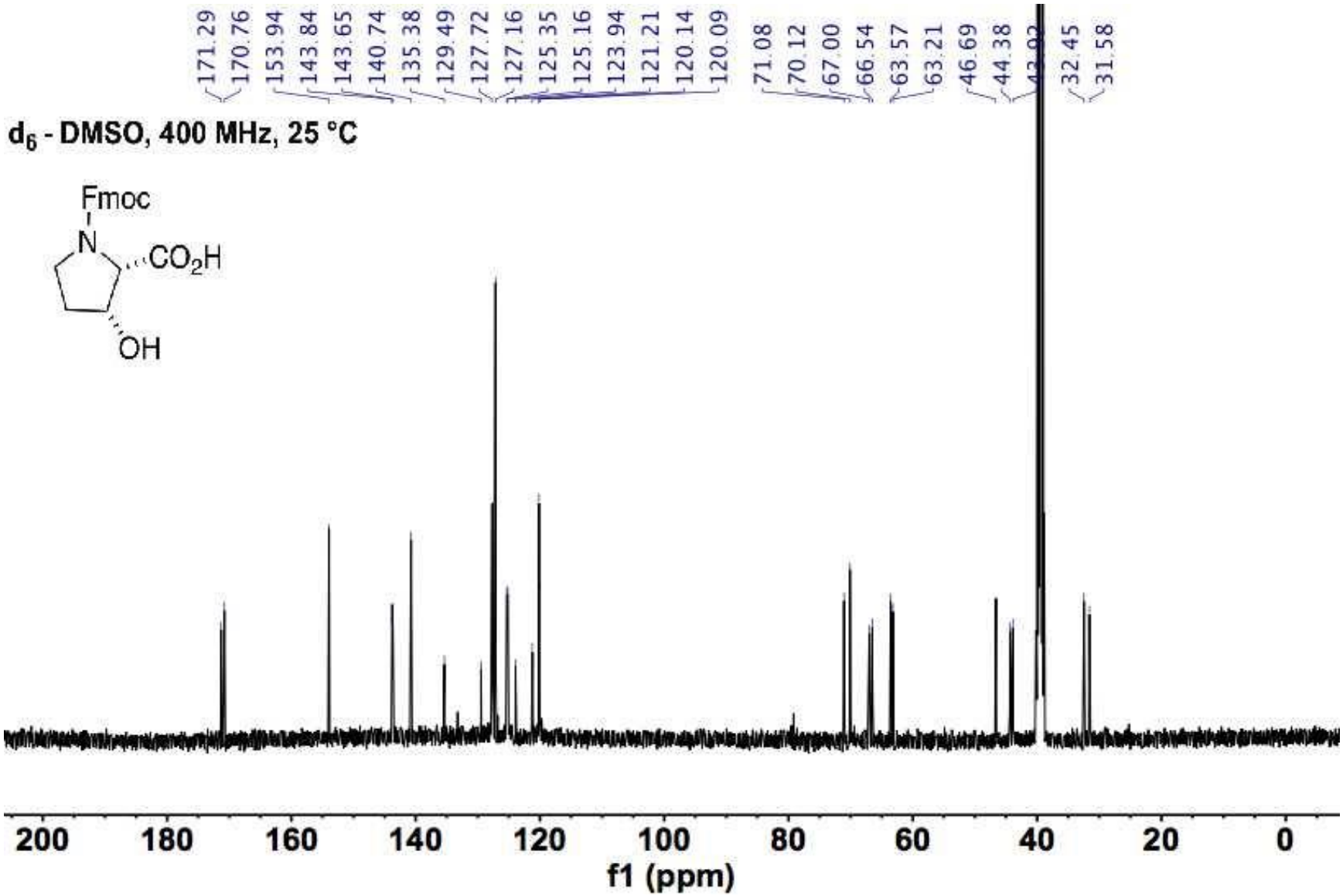


*Figure A2.4.2*. $^{13}$C NMR Spectrum of Compound **4.24**.

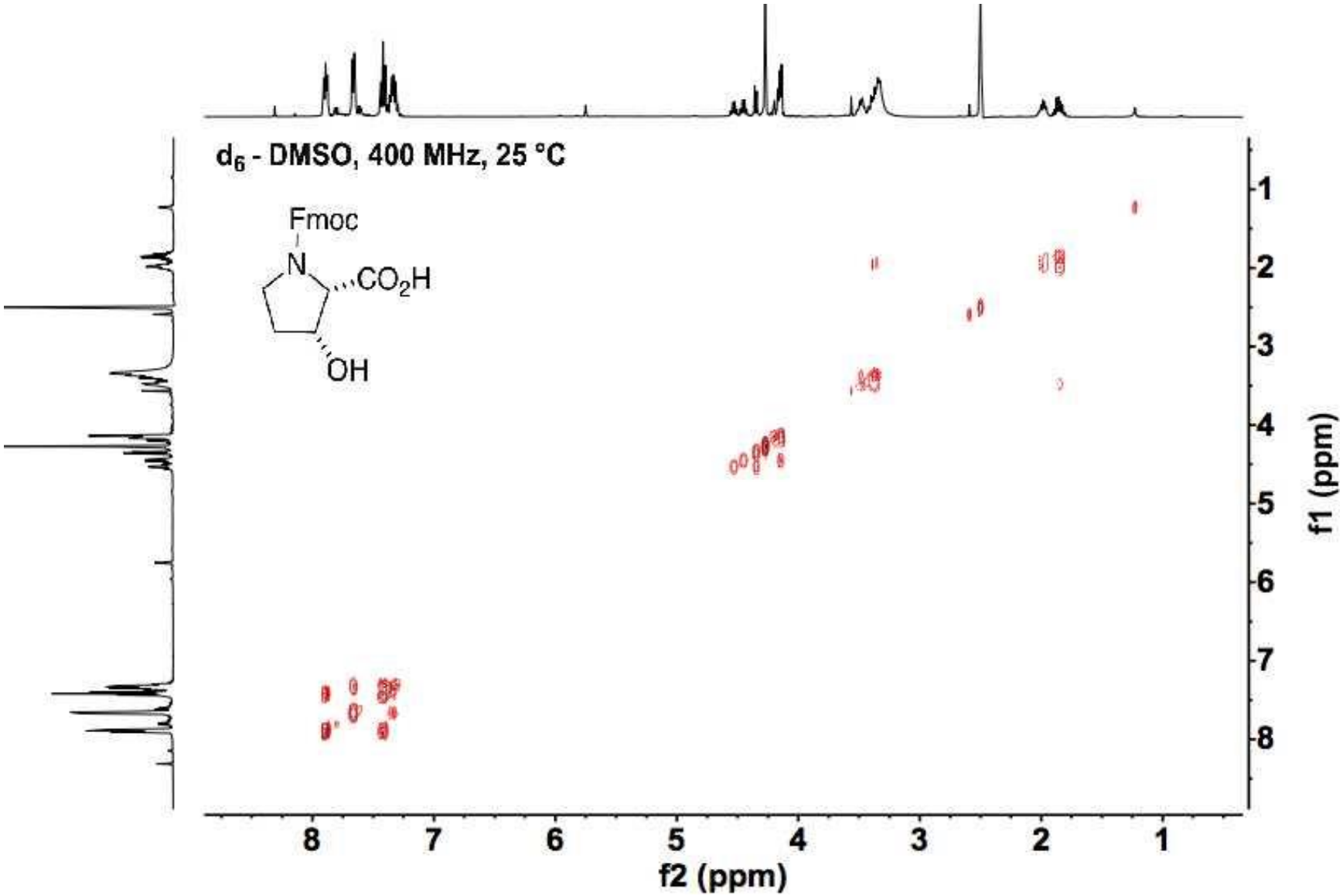


*Figure A2.4.3*. COSY NMR Spectrum of Compound **4.24**.

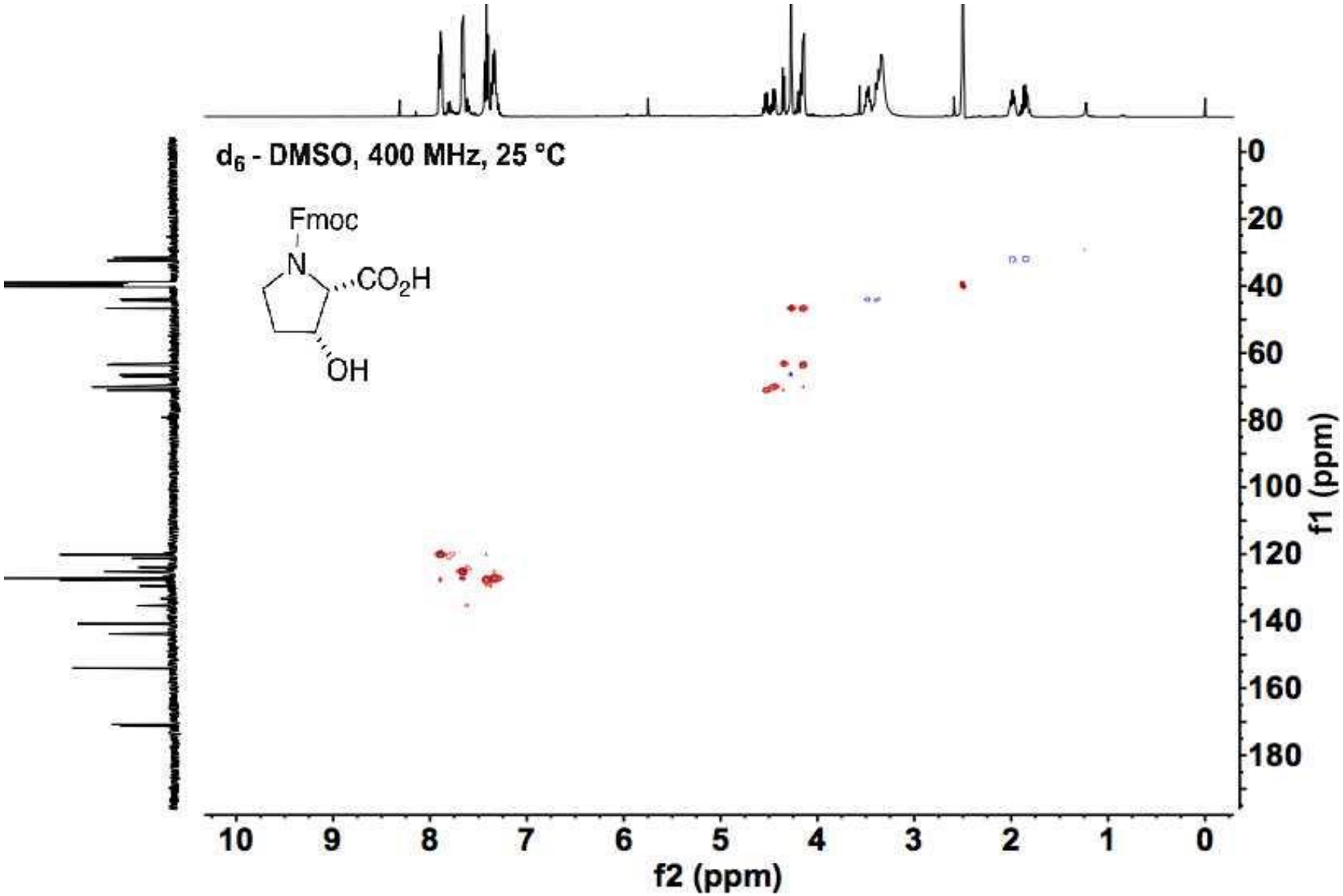


*Figure A2.4.4*. HSQC NMR Spectrum of Compound **4.24**.

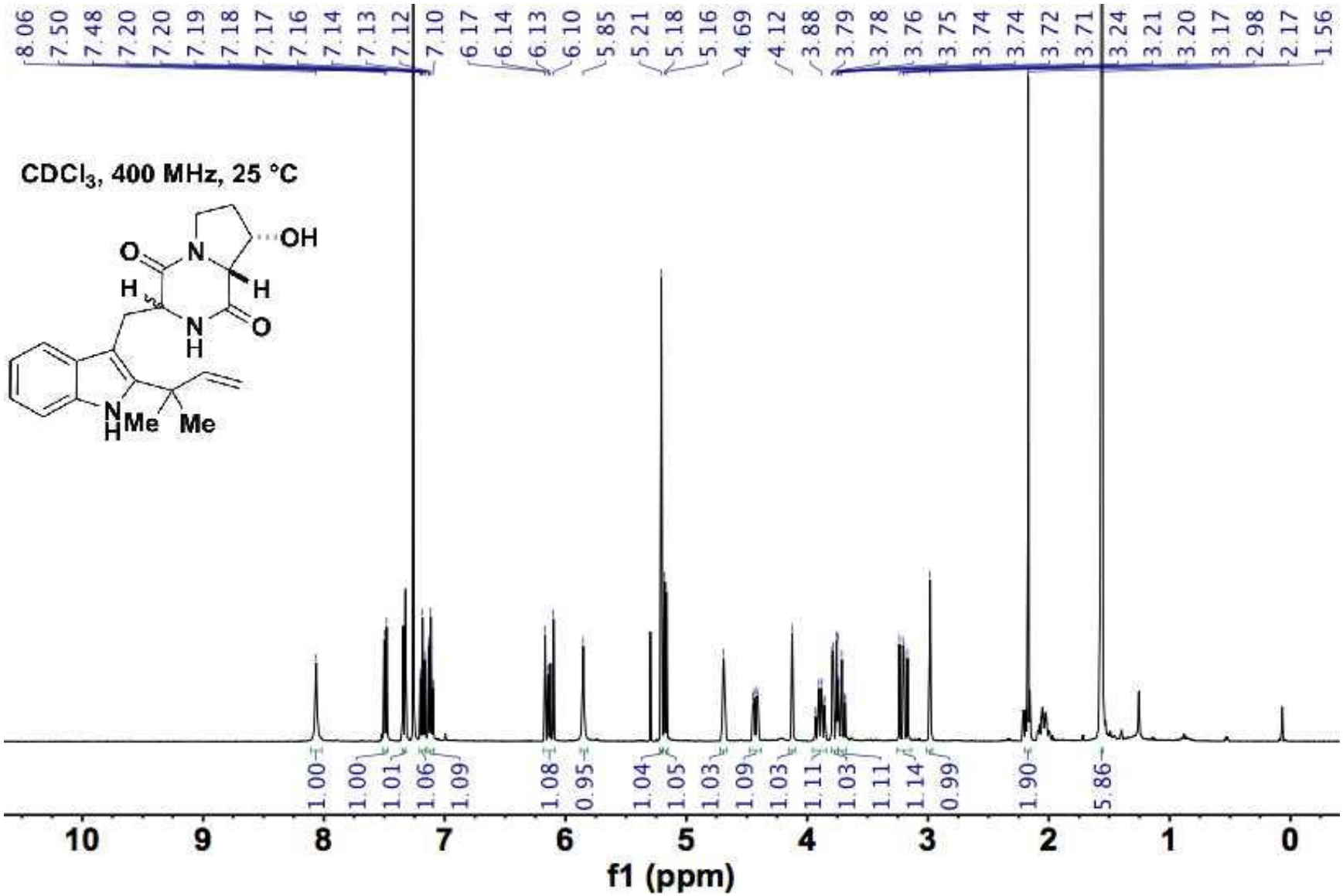


*Figure A2.4.5*. $^{1}$H NMR Spectrum of Compound **4.26** (diastereomer 1).

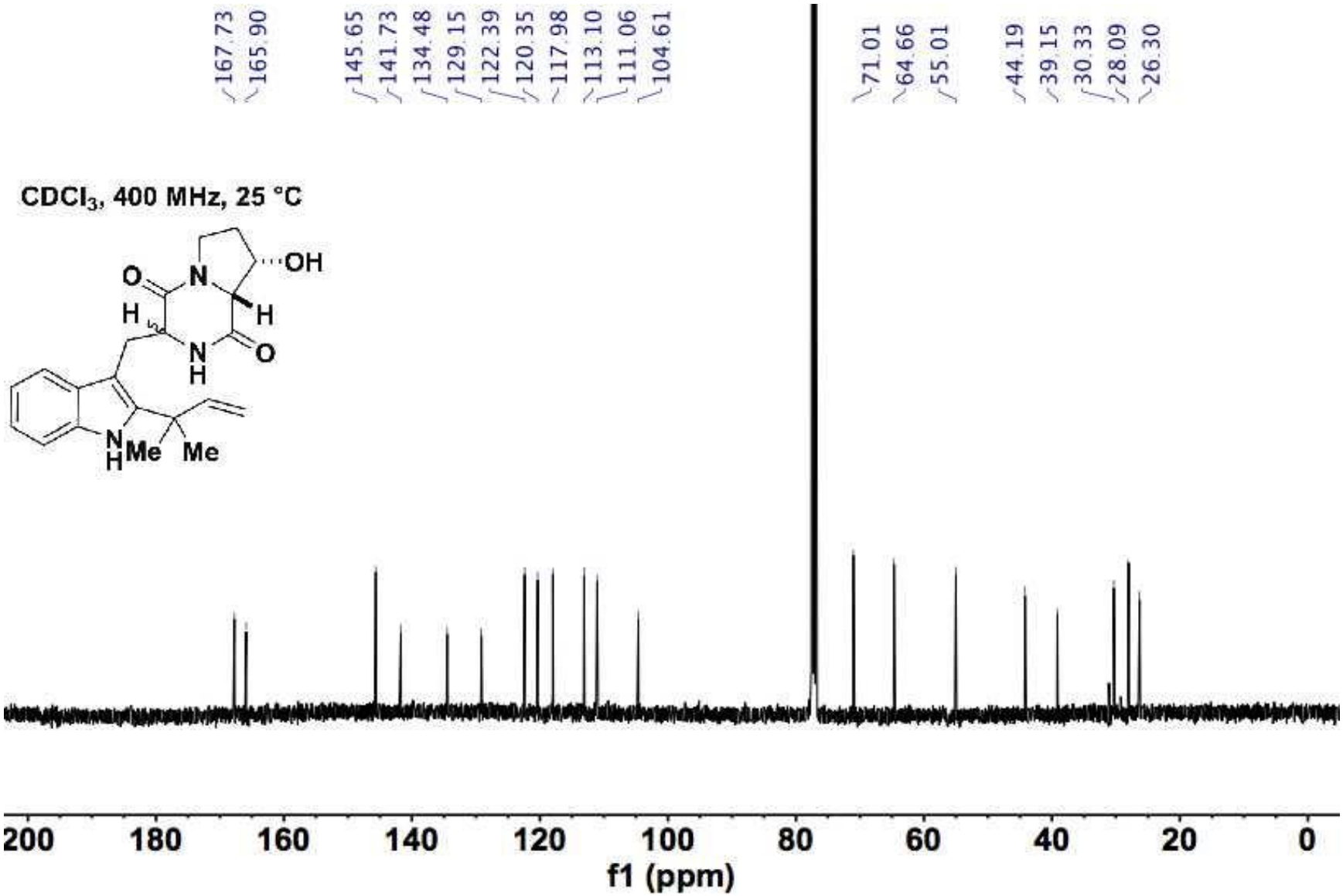


*Figure A2.4.6*. $^{13}$C NMR Spectrum of Compound **4.26** (diastereomer 1).

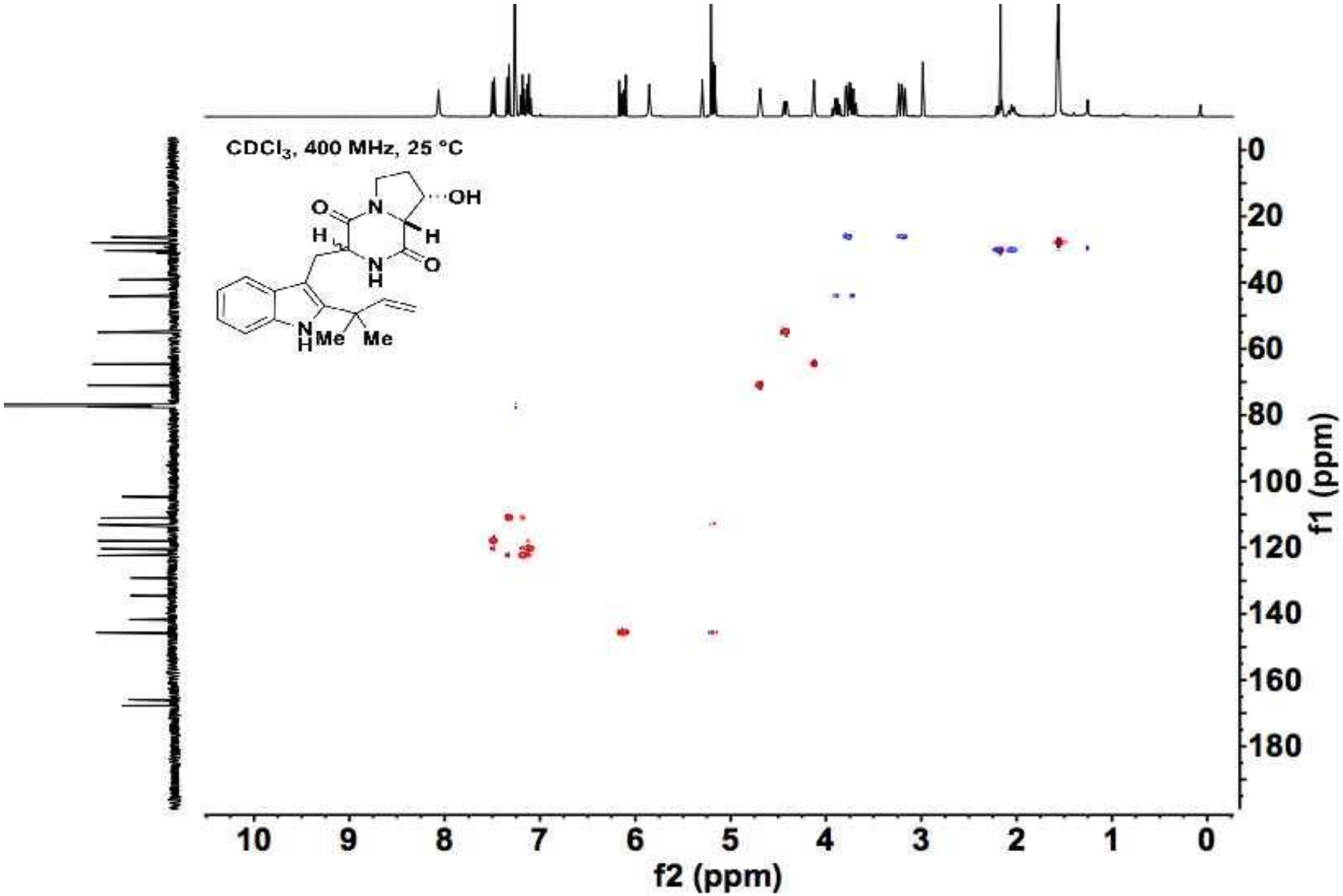


*Figure A2.4.7*. HSQC NMR Spectrum of Compound **4.26** (diastereomer 1).

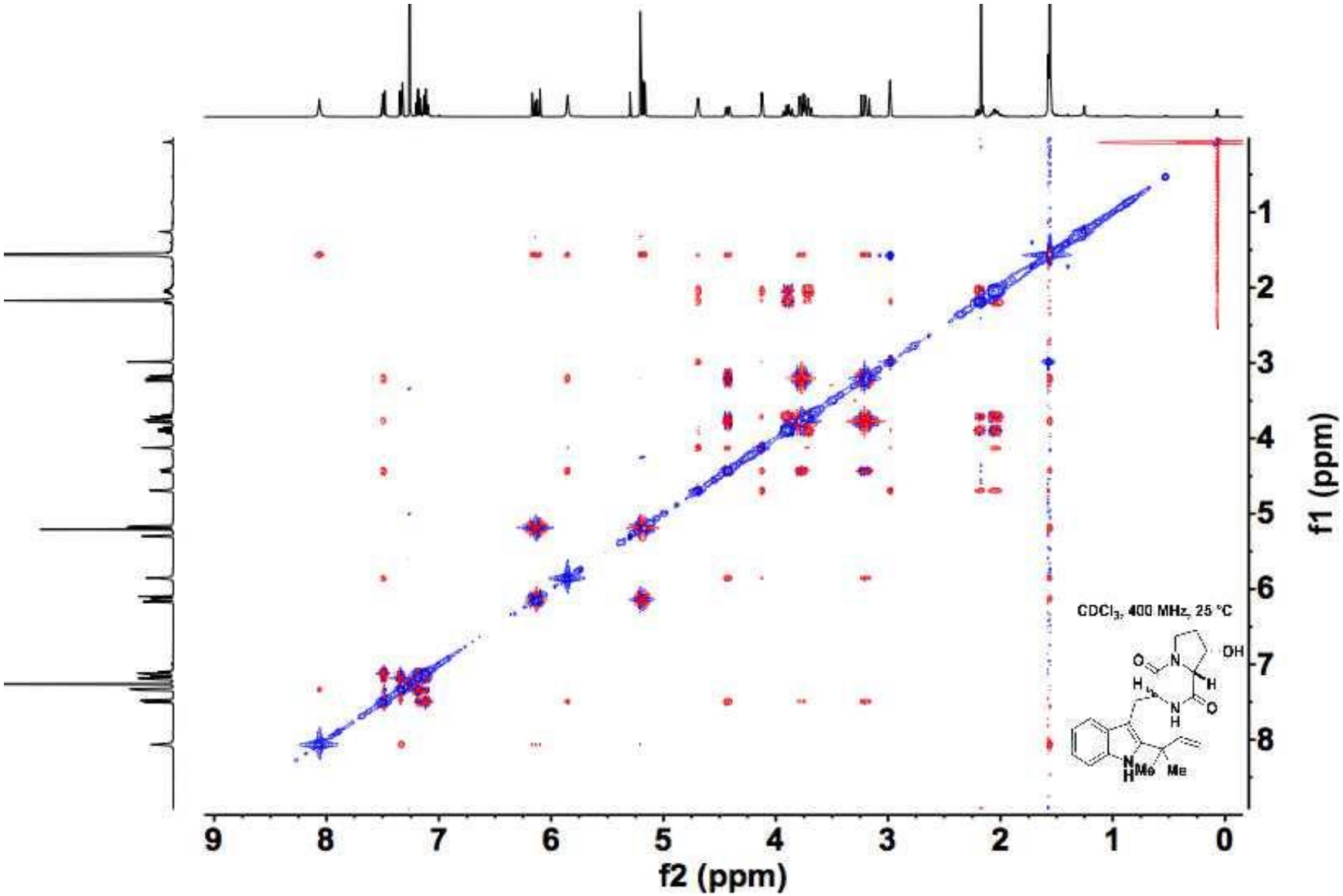


*Figure A2.4.8*. NOESY NMR Spectrum of Compound **4.26** (diastereomer 1).

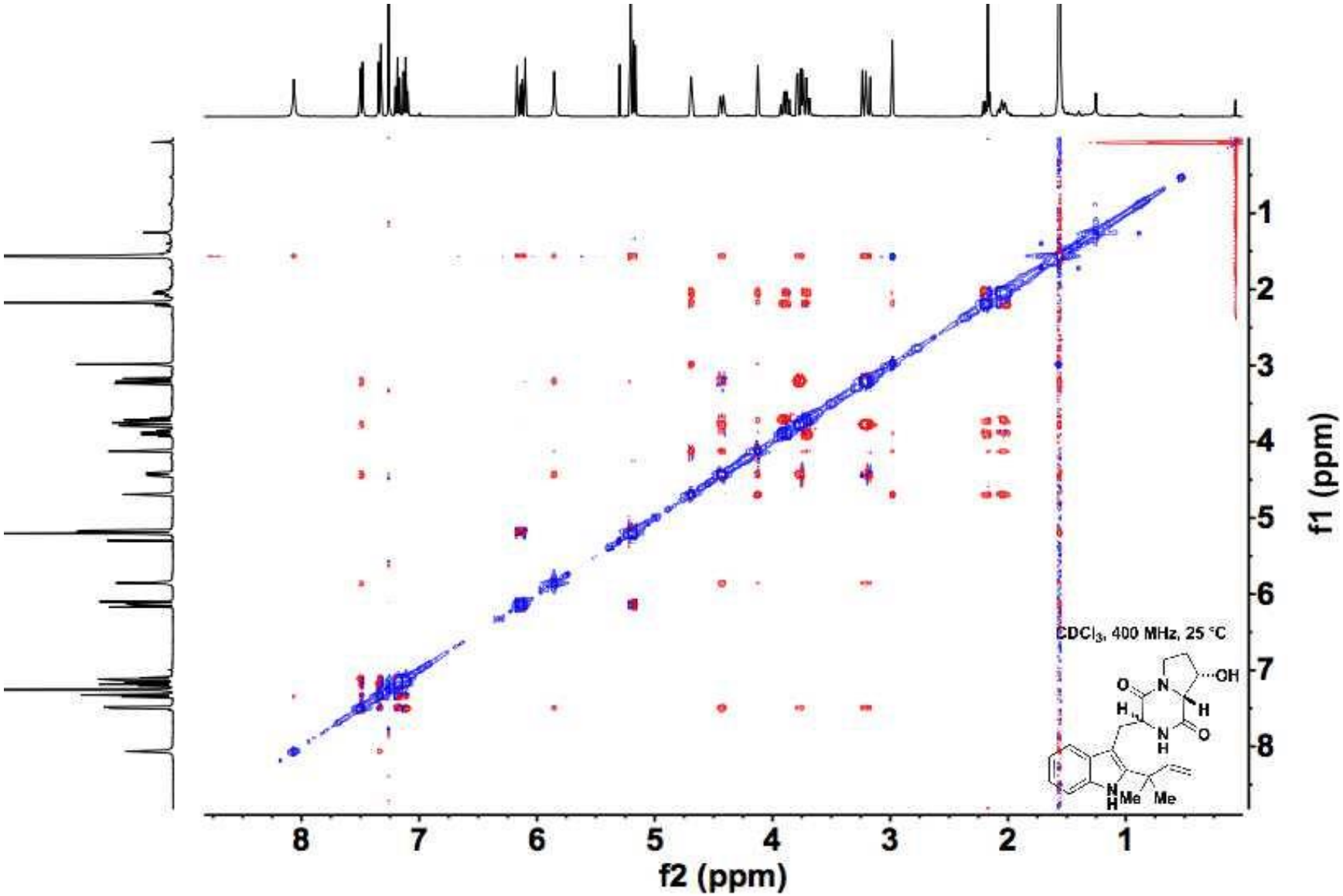


*Figure A2.4.9*. ROESY NMR Spectrum of Compound **4.26** (diastereomer 1).

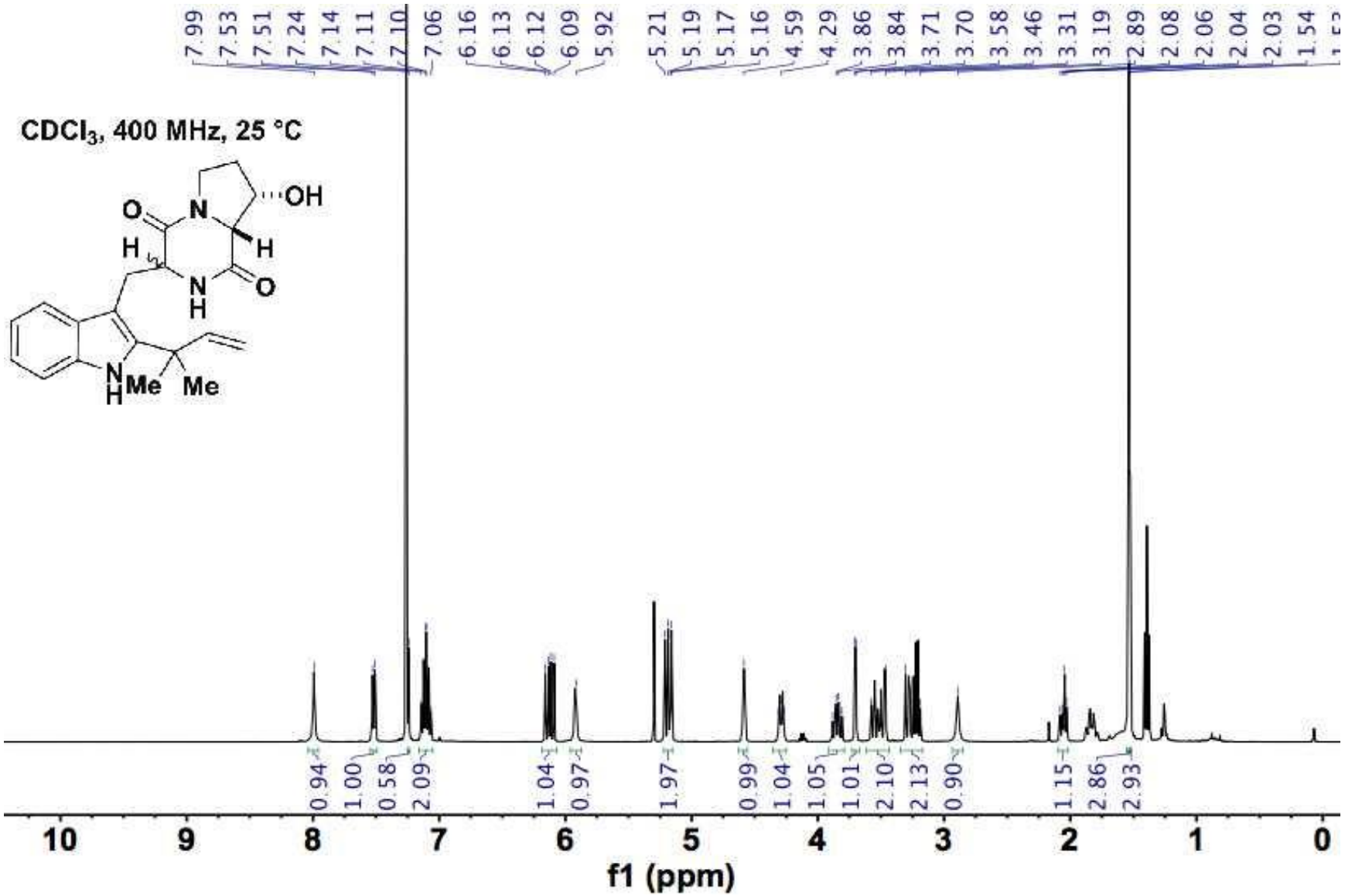


*Figure A2.4.10*. $^{1}$H NMR Spectrum of Compound **4.26** (diastereomer 2).

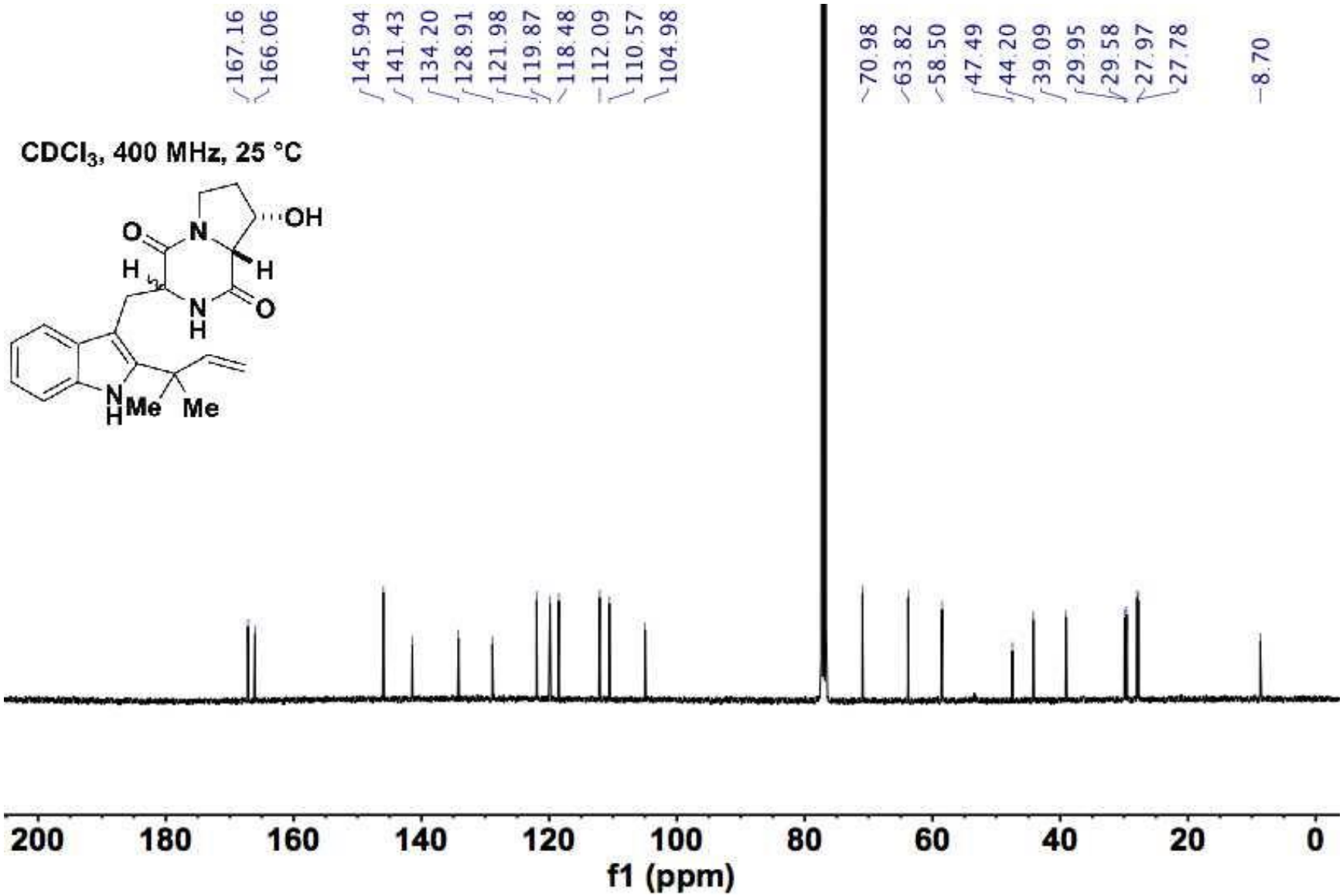


*Figure A2.4.11*. $^{13}C$ NMR Spectrum of Compound **4.26** (diastereomer 2).

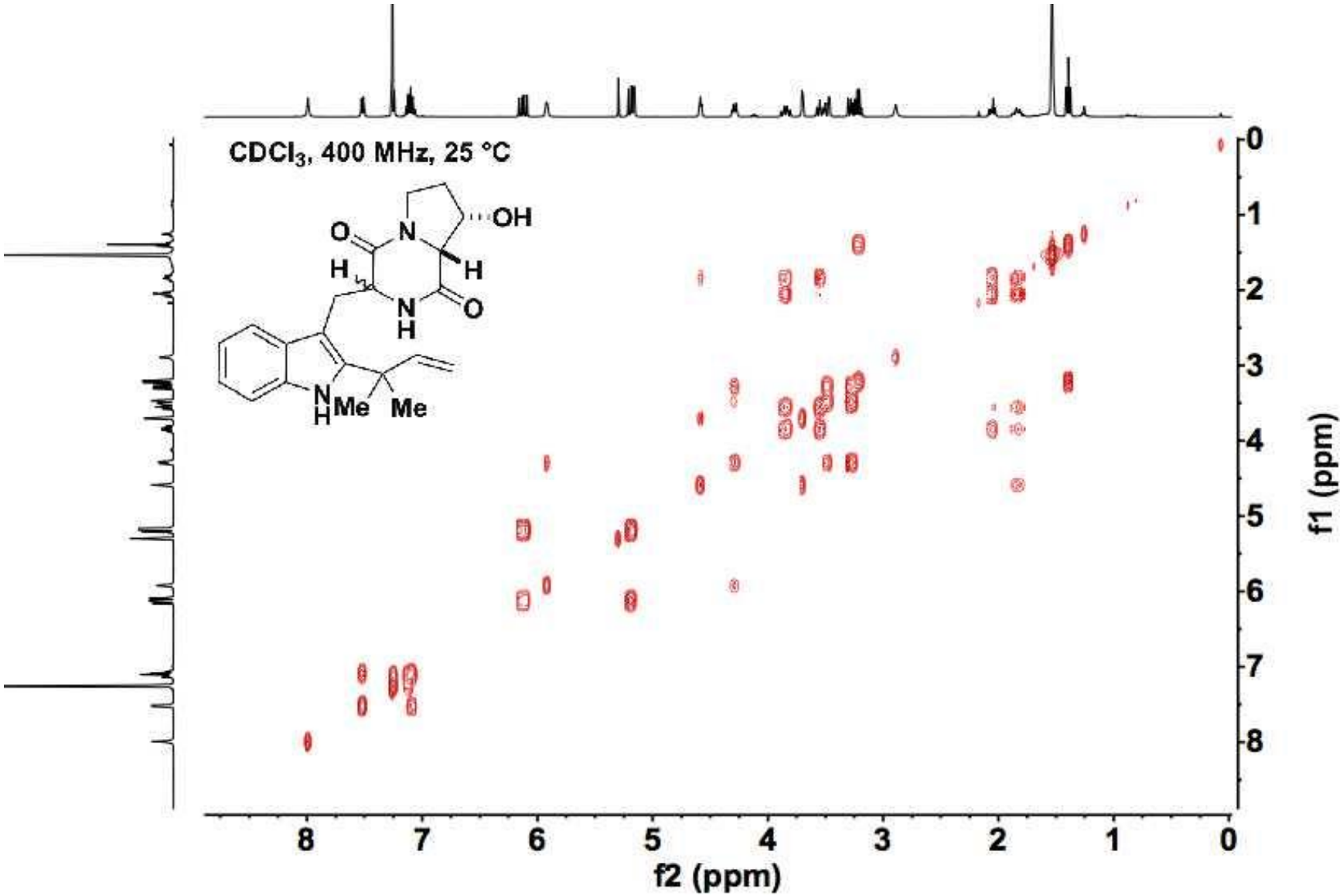


*Figure A2.4.12*. COSY NMR Spectrum of Compound **4.26** (diastereomer 2).

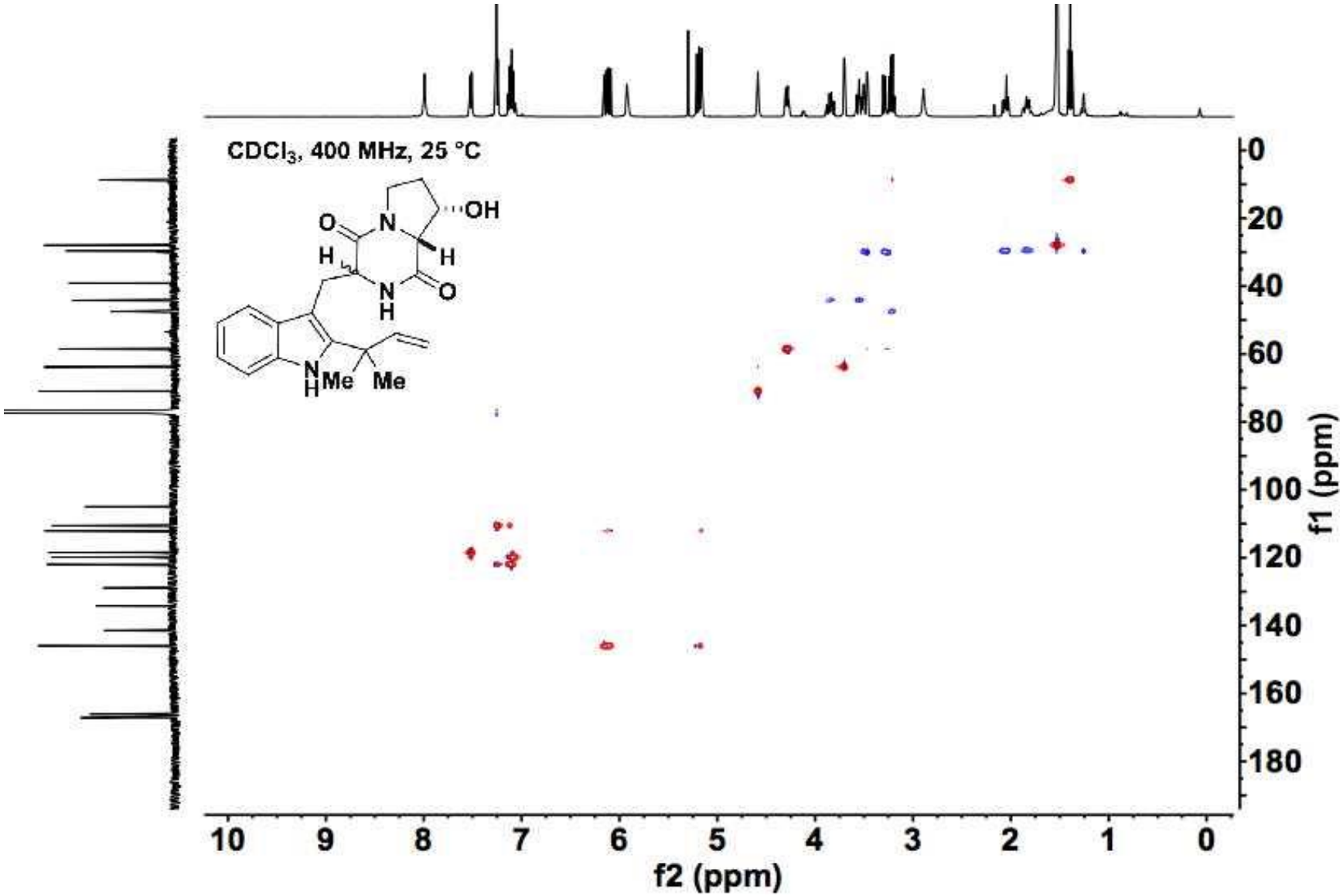


*Figure A2.4.13*. HSQC NMR Spectrum of Compound **4.26** (diastereomer 2).

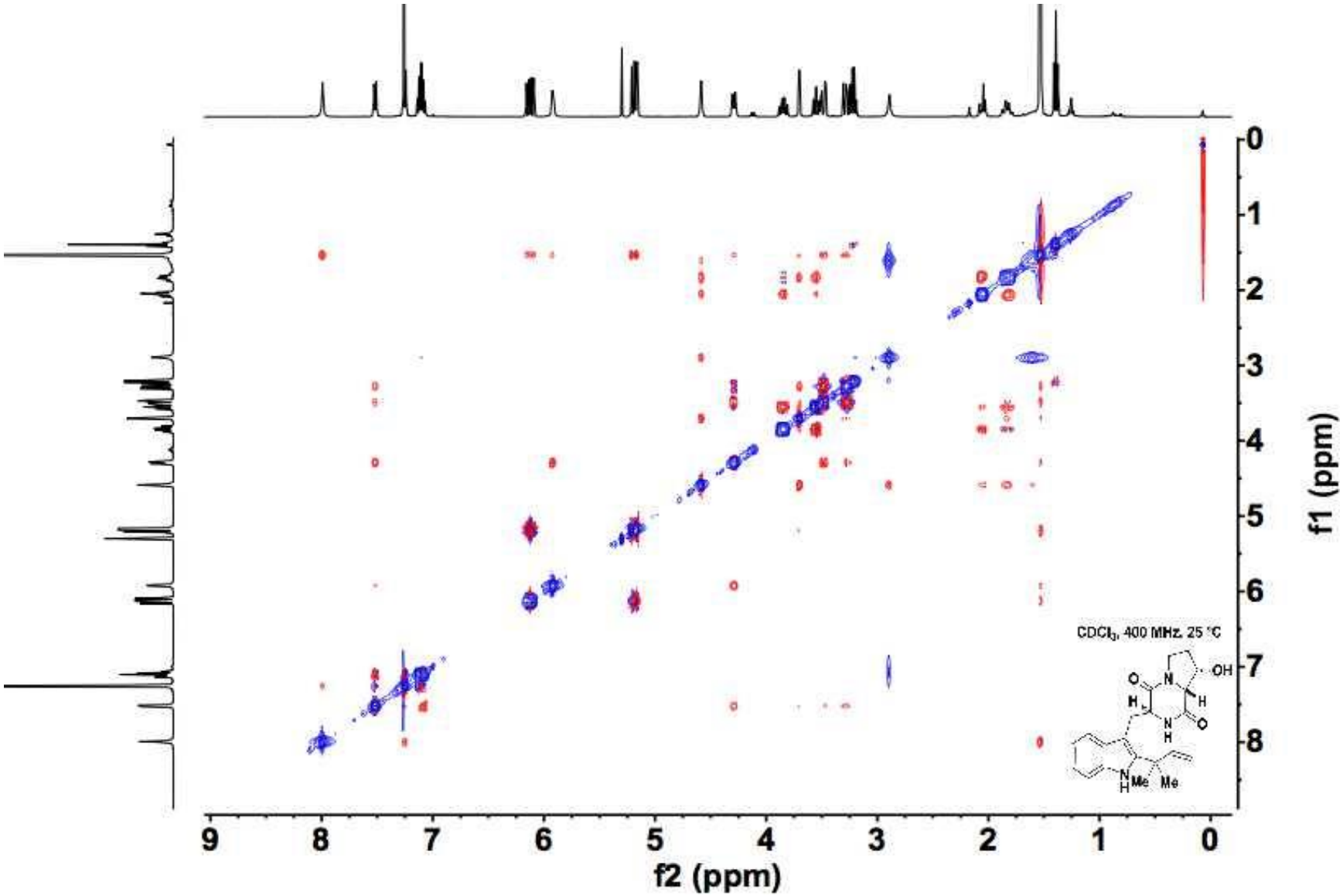


*Figure A2.4.14*. NOESY NMR Spectrum of Compound **4.26** (diastereomer 2).

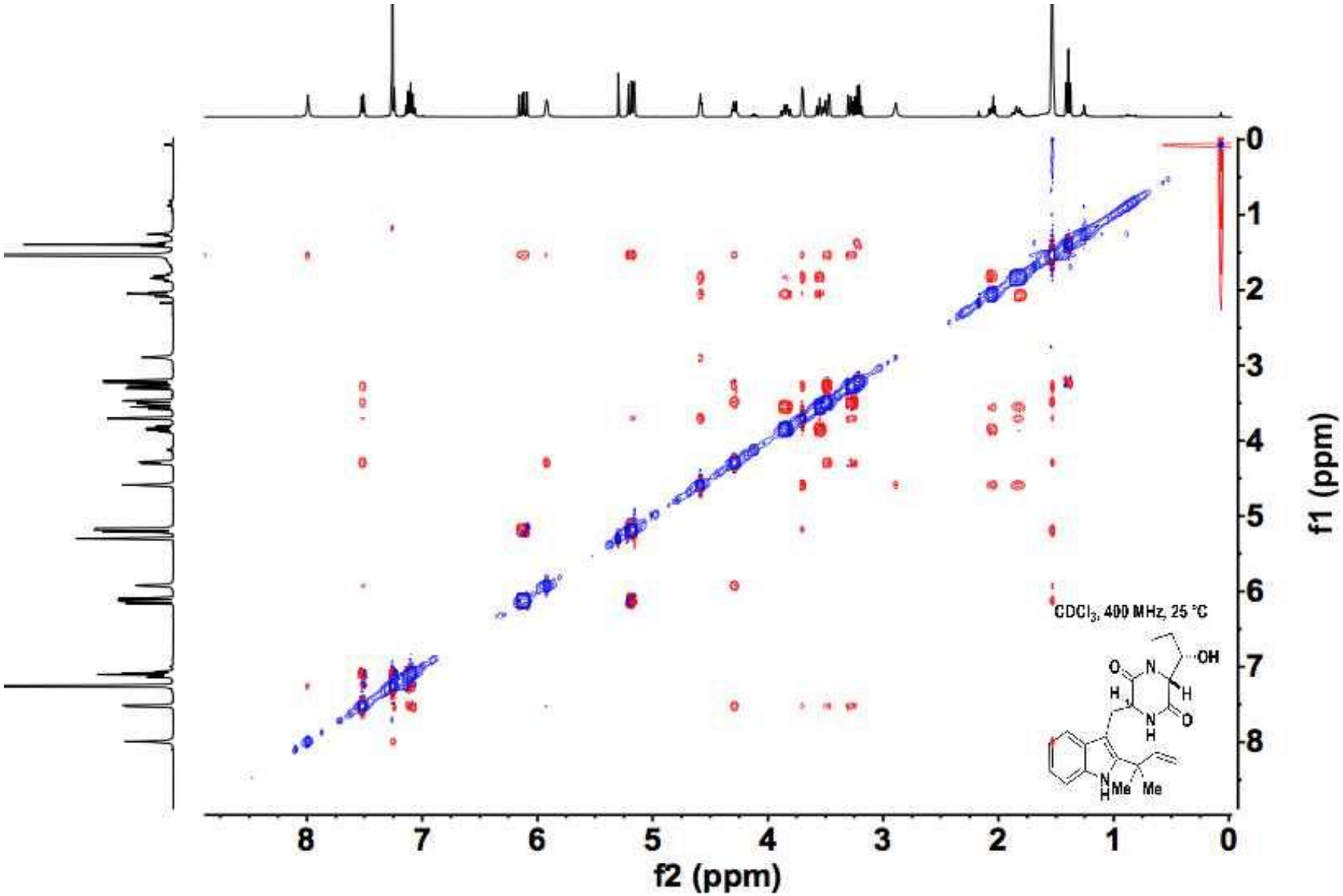


*Figure A2.4.15*. ROESY NMR Spectrum of Compound **4.26** (diastereomer 2).

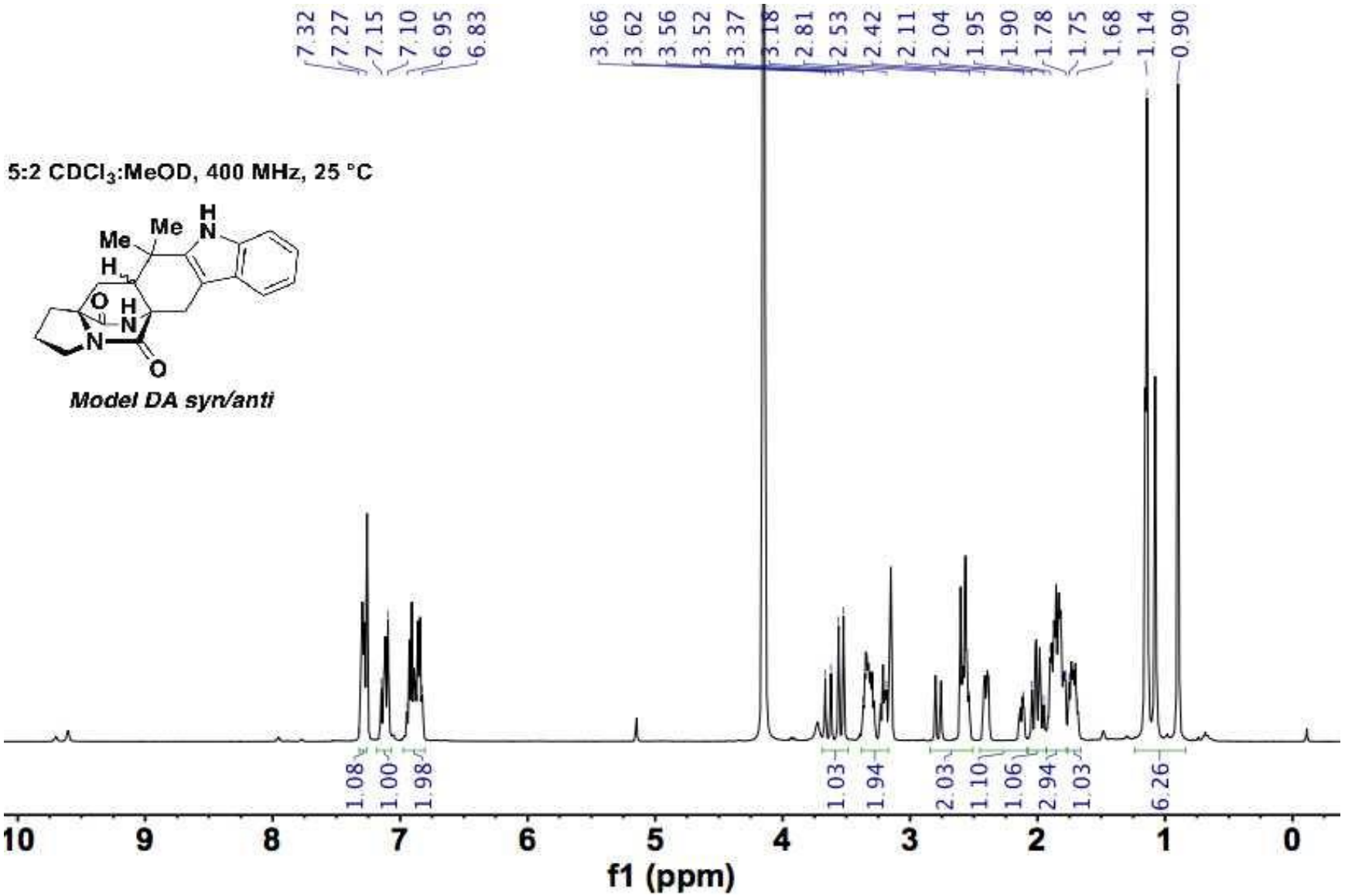


*Figure A2.4.16*. $^{1}$H NMR Spectrum of **Model DA 4.30**.

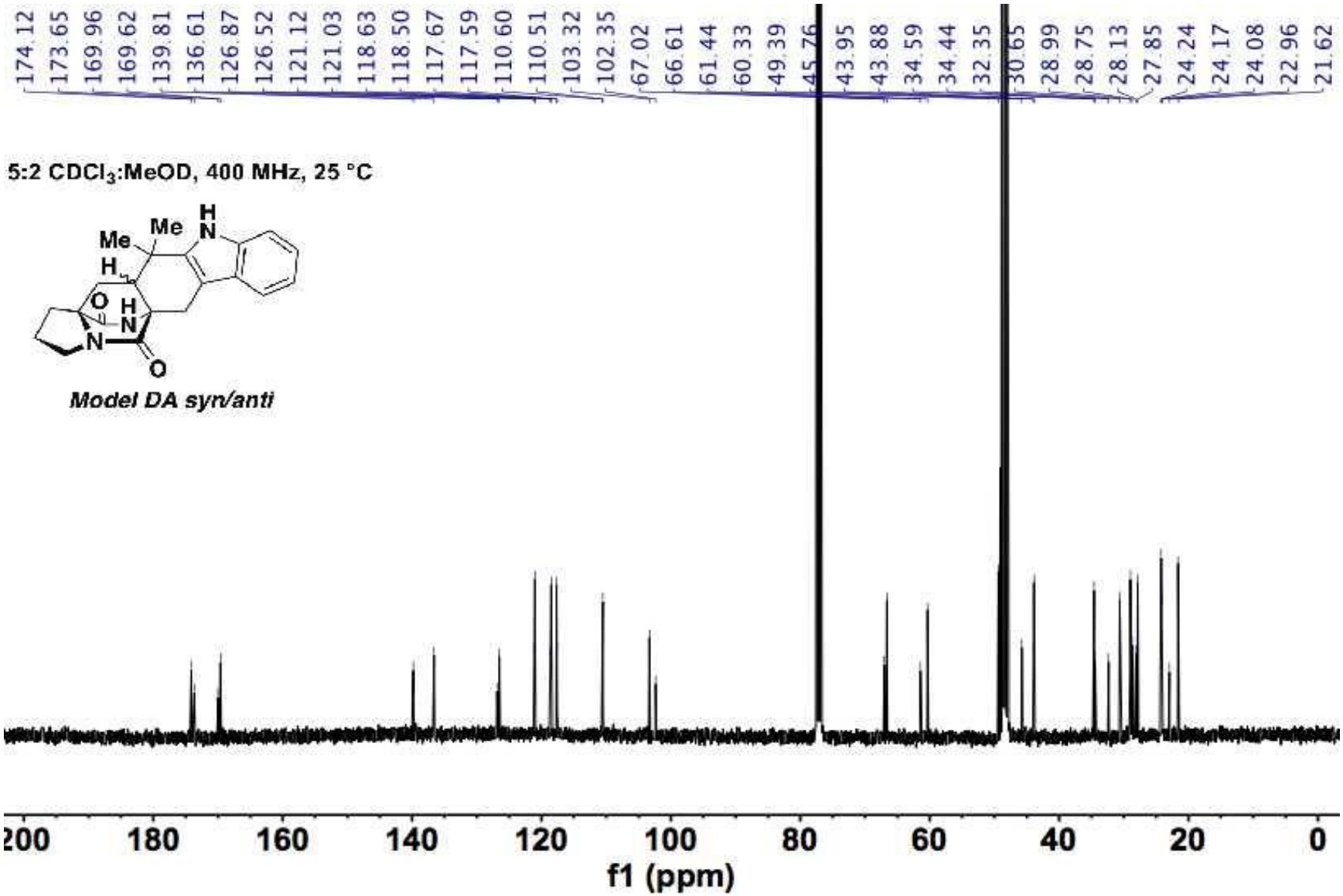


*Figure A2.4.17*. $^{13}$C NMR Spectrum of **Model DA 4.30**.

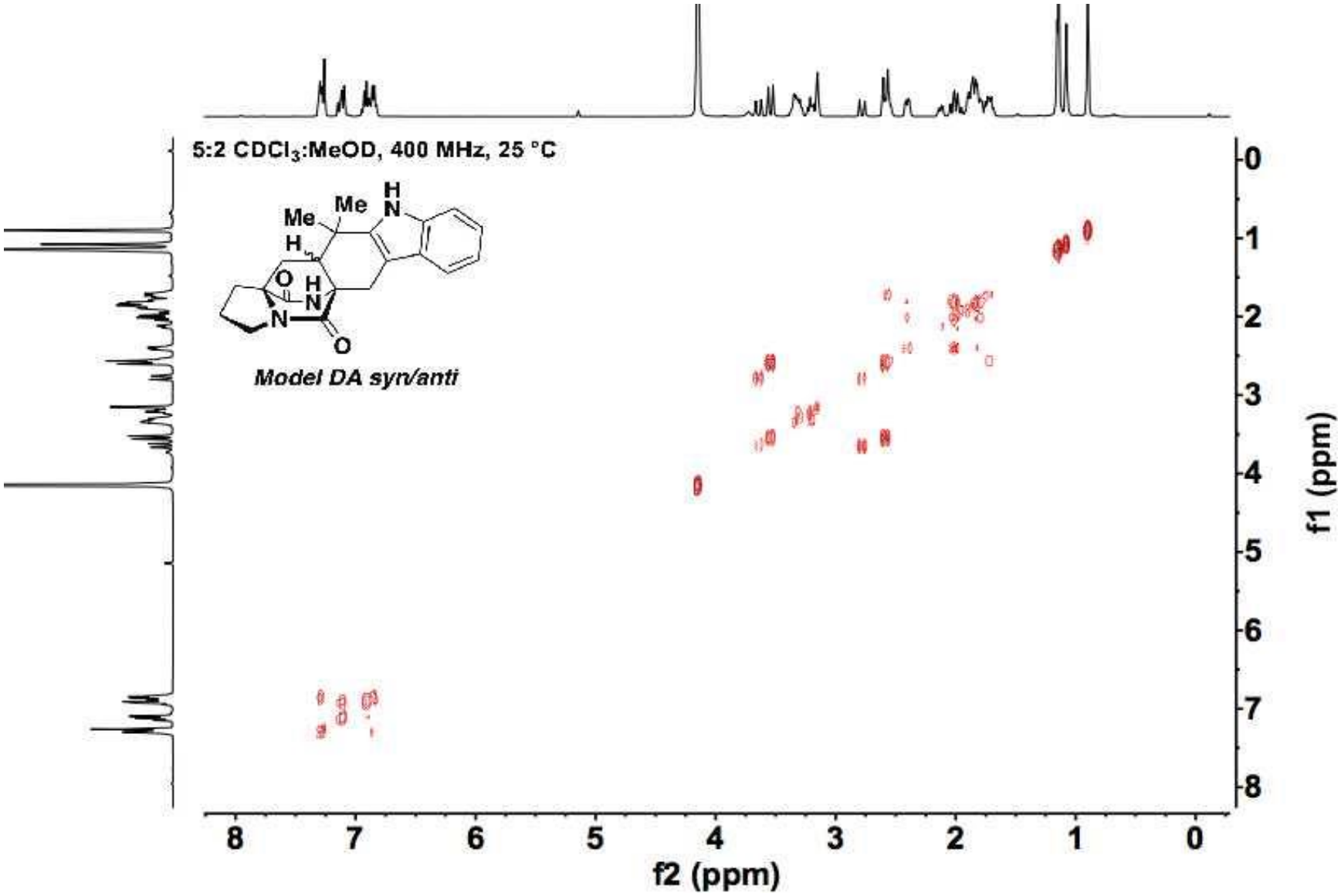


*Figure A2.4.18*. COSY NMR Spectrum of **Model DA 4.30**.

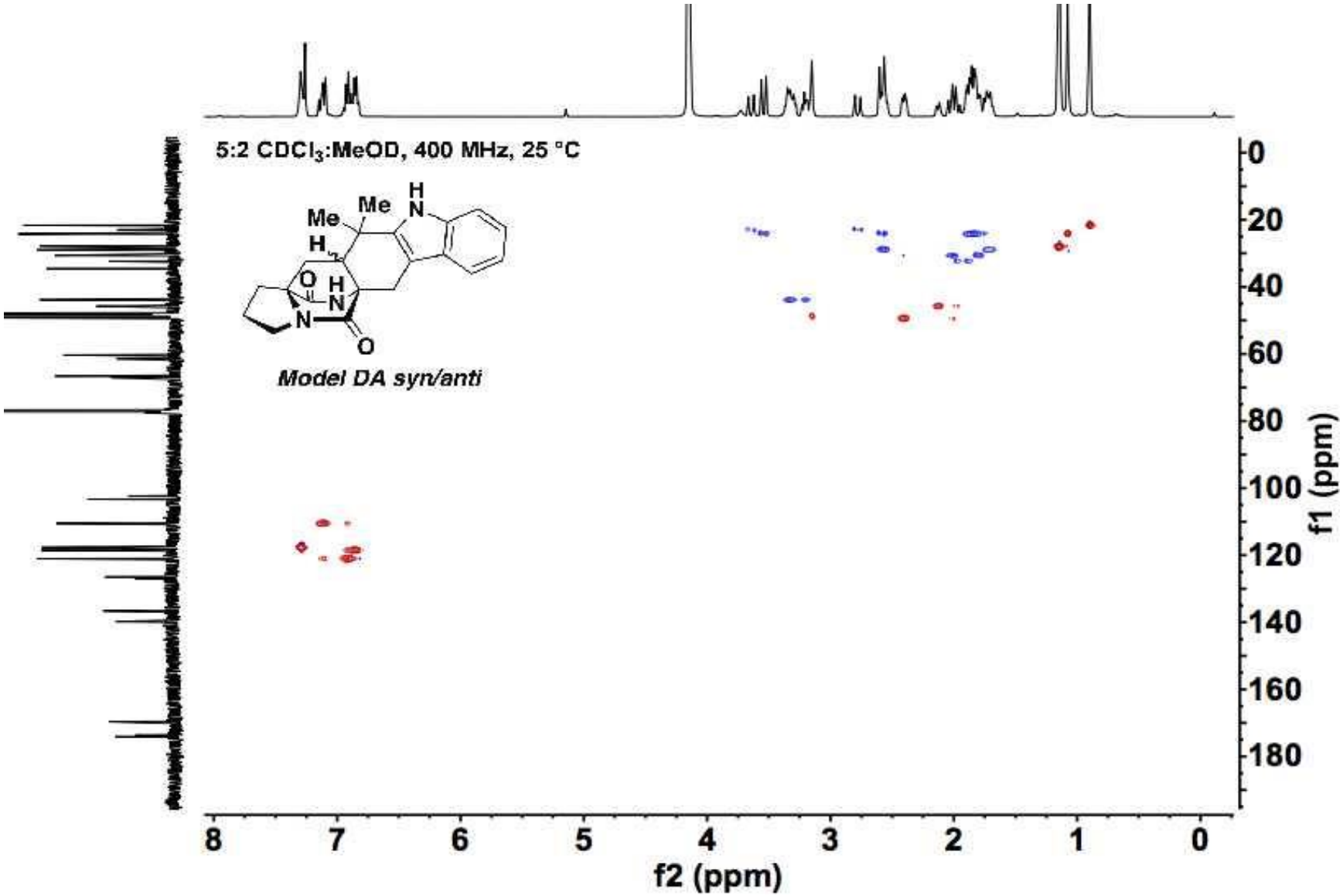


*Figure A2.4.19*. HSQC NMR Spectrum of **Model DA 4.30**.

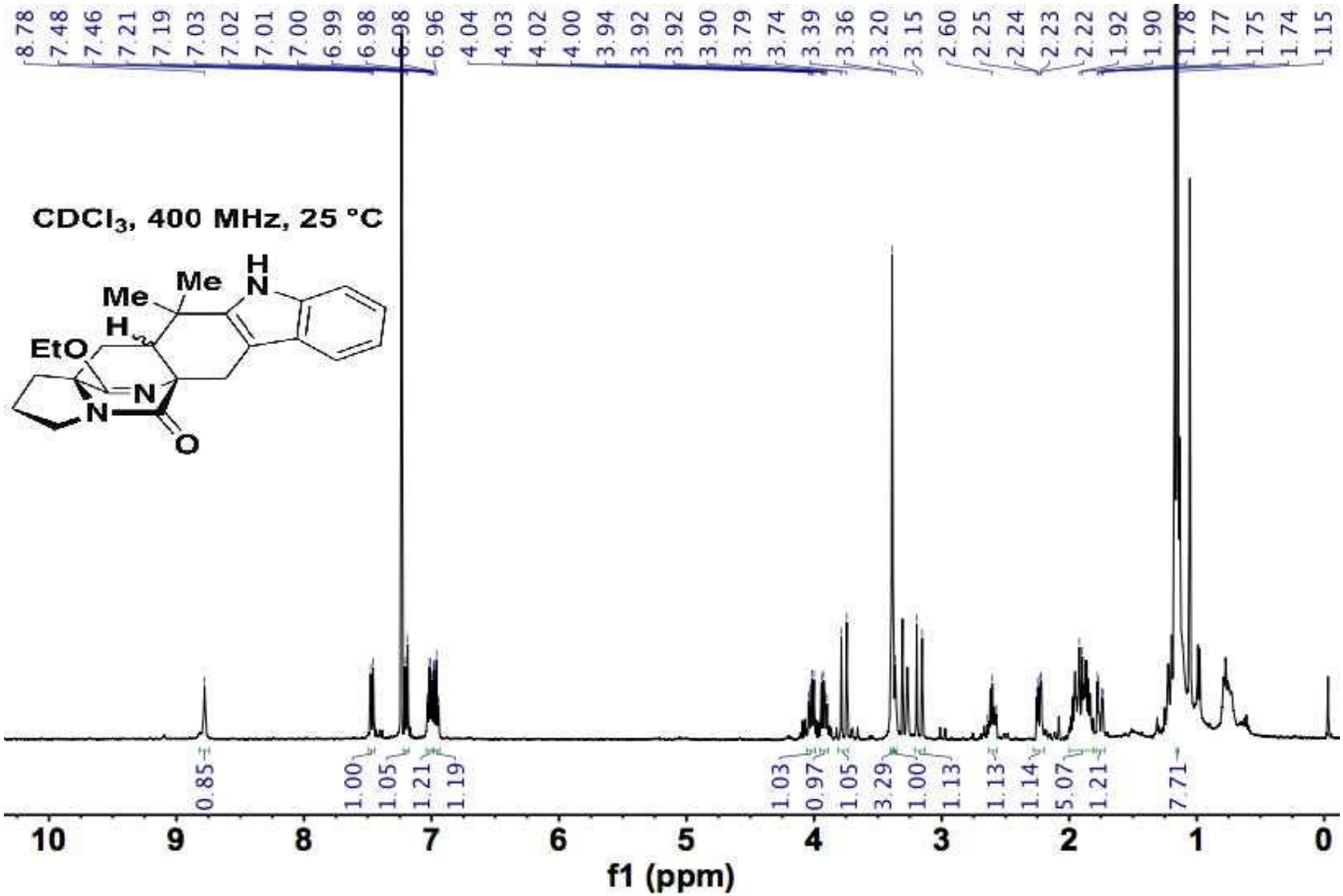


*Figure A2.4.20*. $^{1}$H NMR Spectrum of Compound **4.53**.

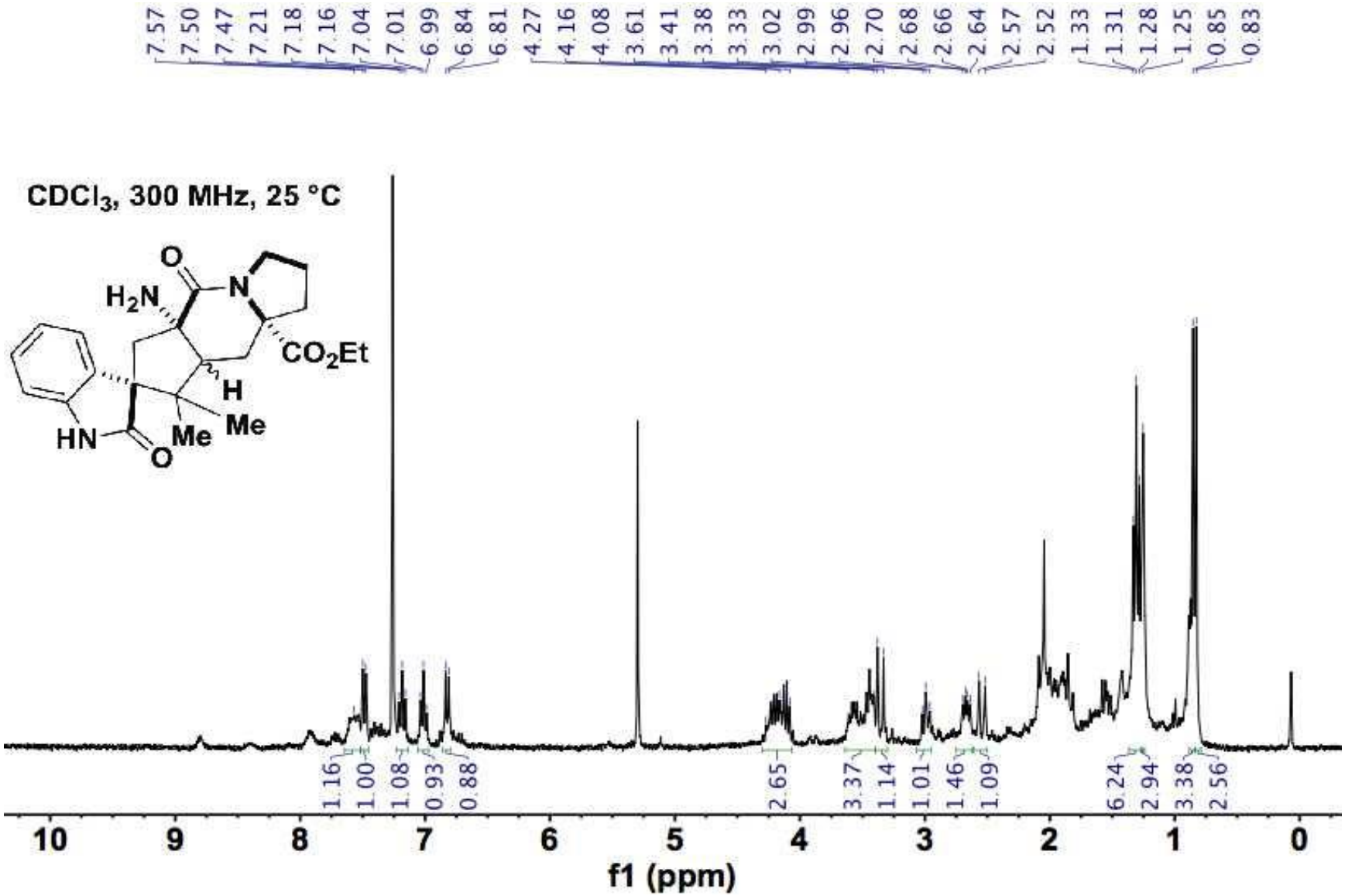


*Figure A2.4.21*. $^{1}$H NMR Spectrum of Compound **4.54**.

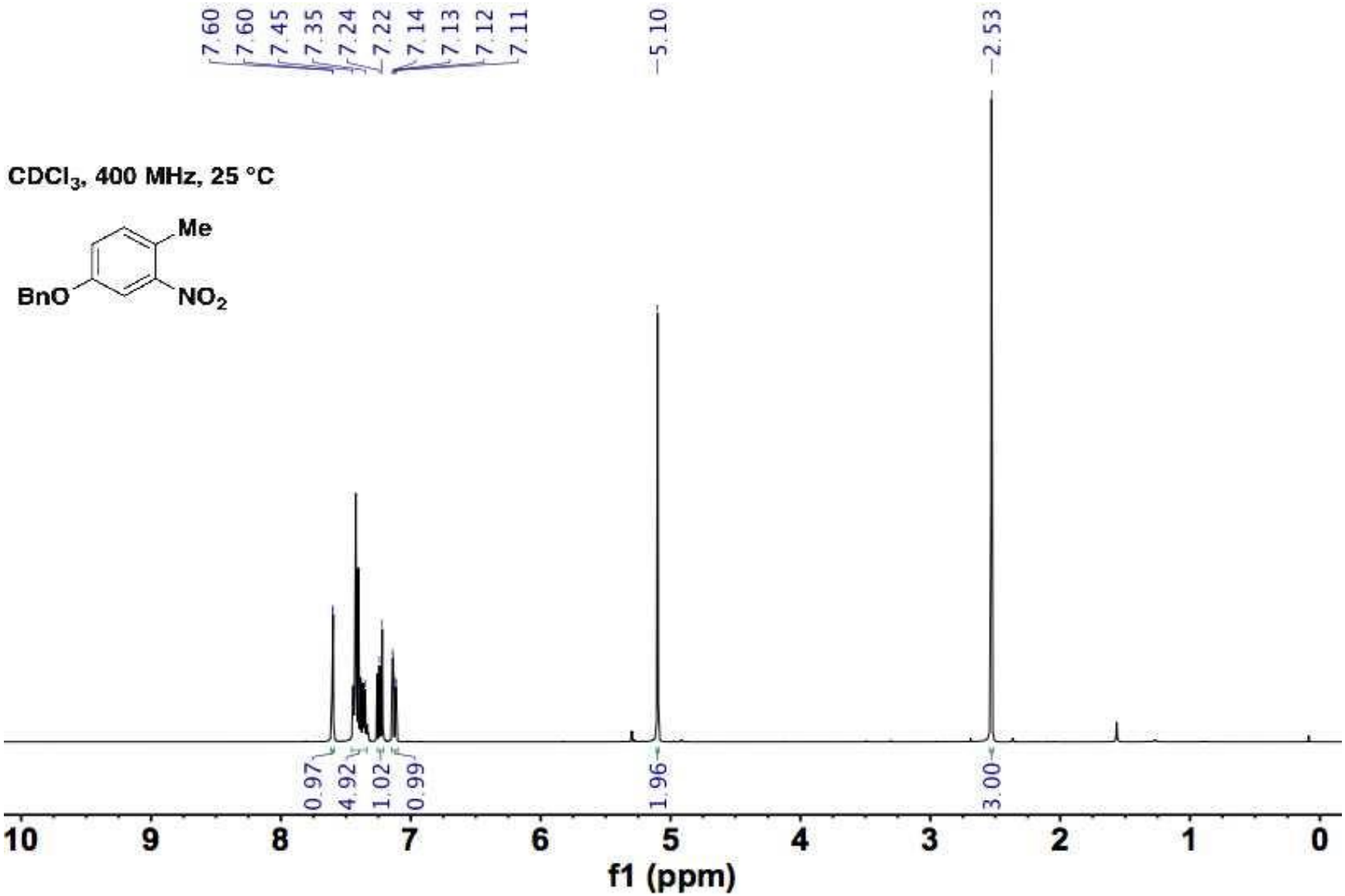


*Figure A2.4.22*. $^{1}$H NMR Spectrum of Compound **4.38**.

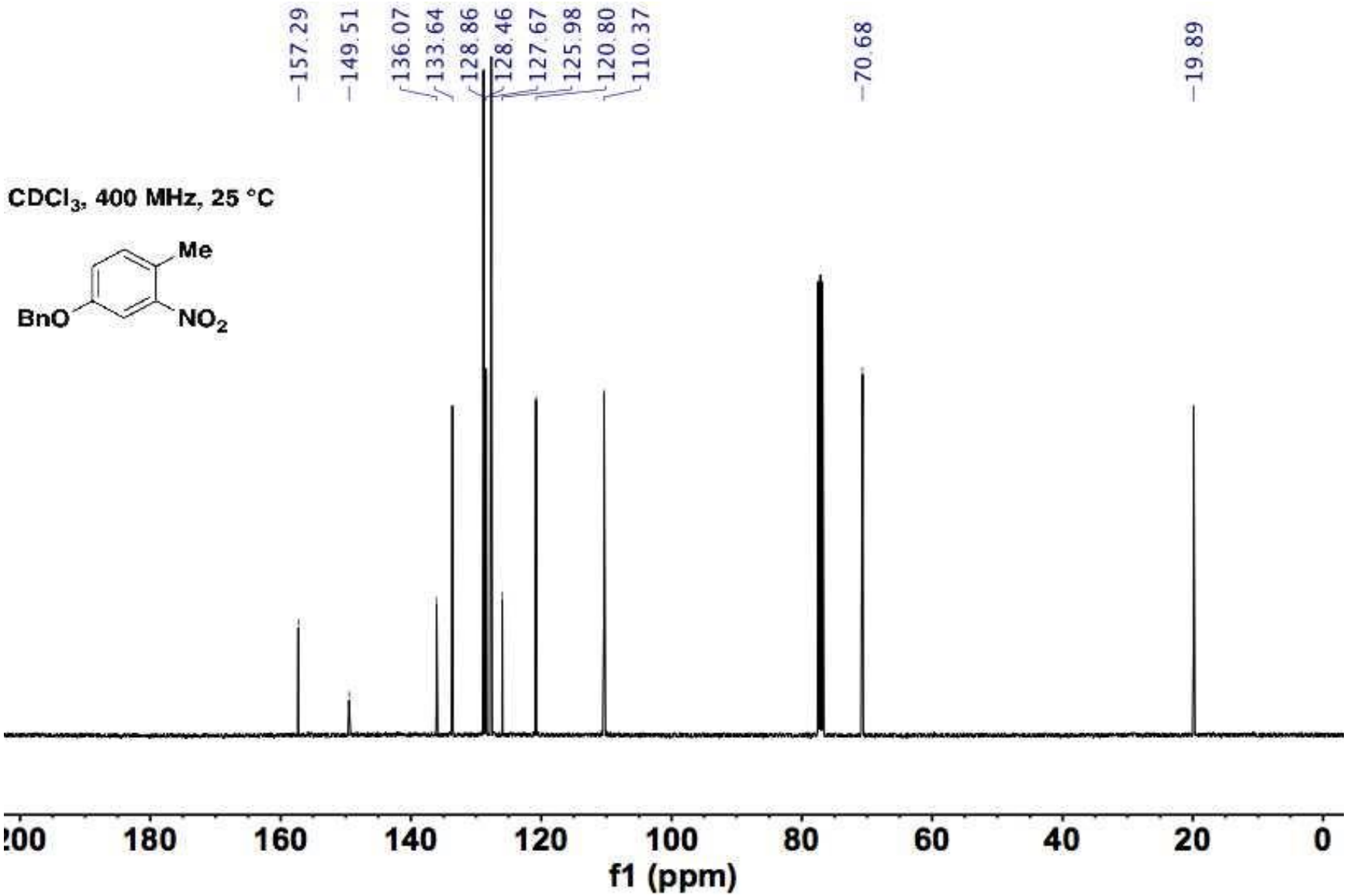


*Figure A2.4.23*. $^{13}C$ NMR Spectrum of Compound **4.38**.

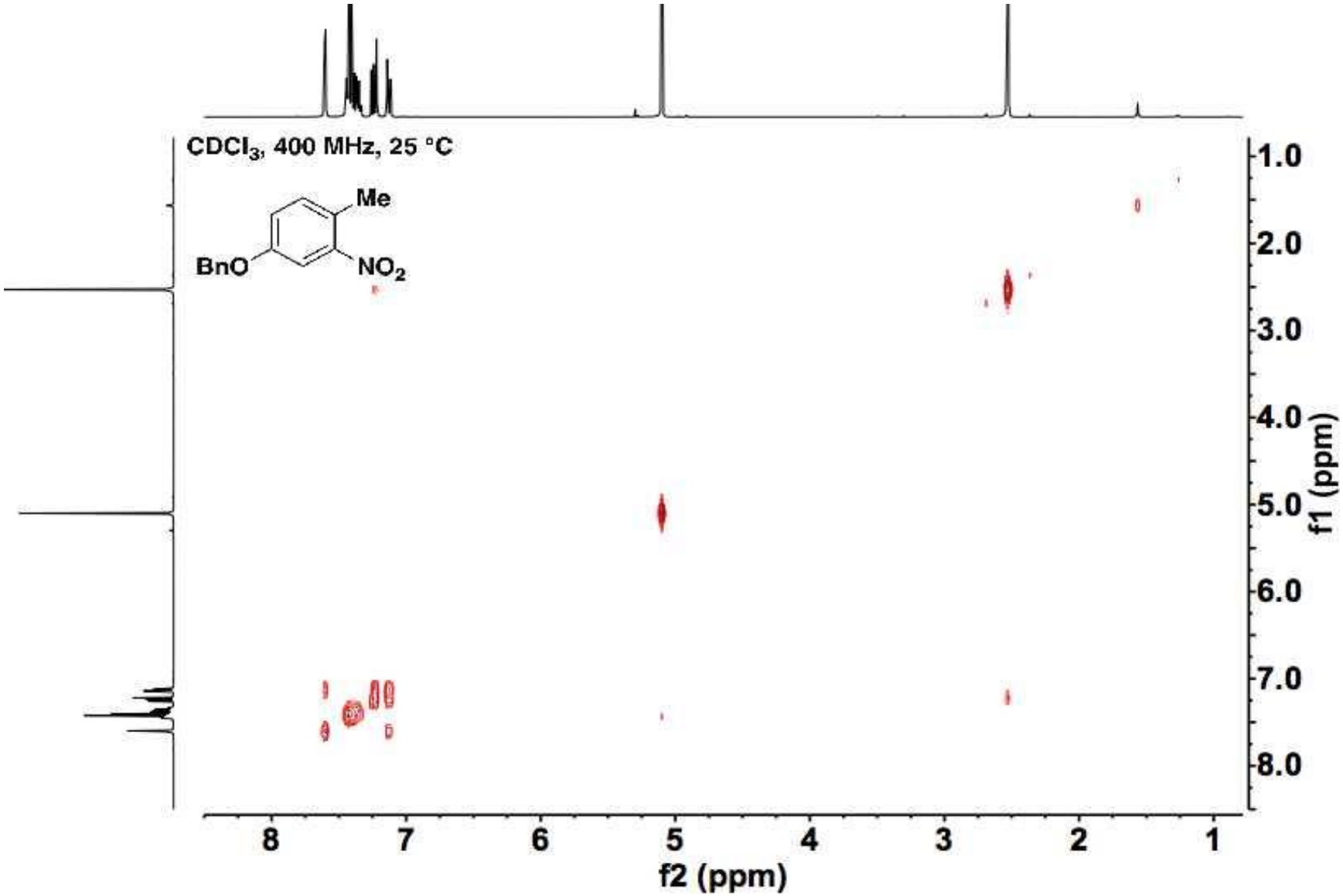


*Figure A2.4.24*. COSY NMR Spectrum of Compound **4.38**.

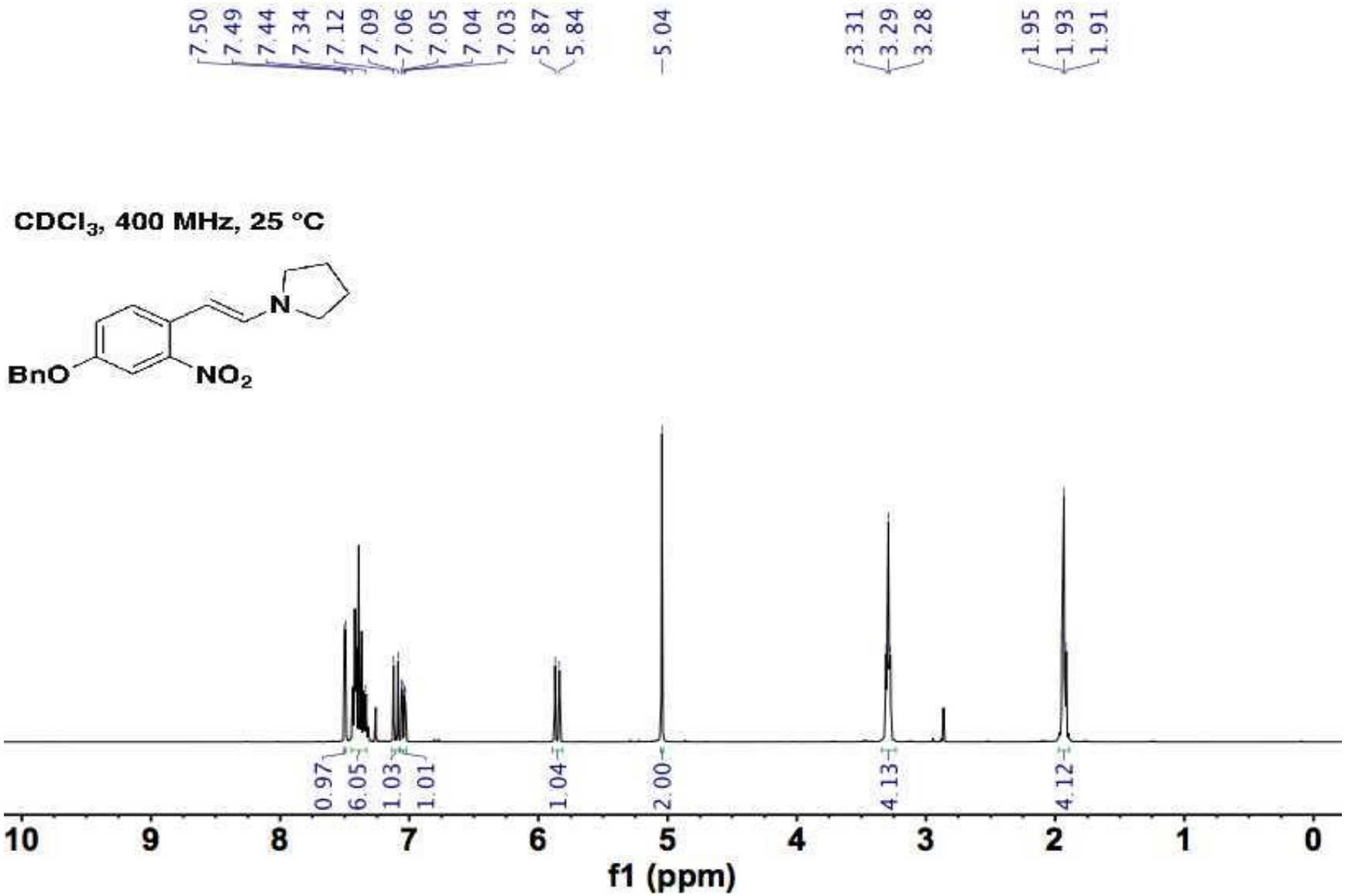


*Figure A2.4.25*. $^{1}$H NMR Spectrum of Compound **4.39**.

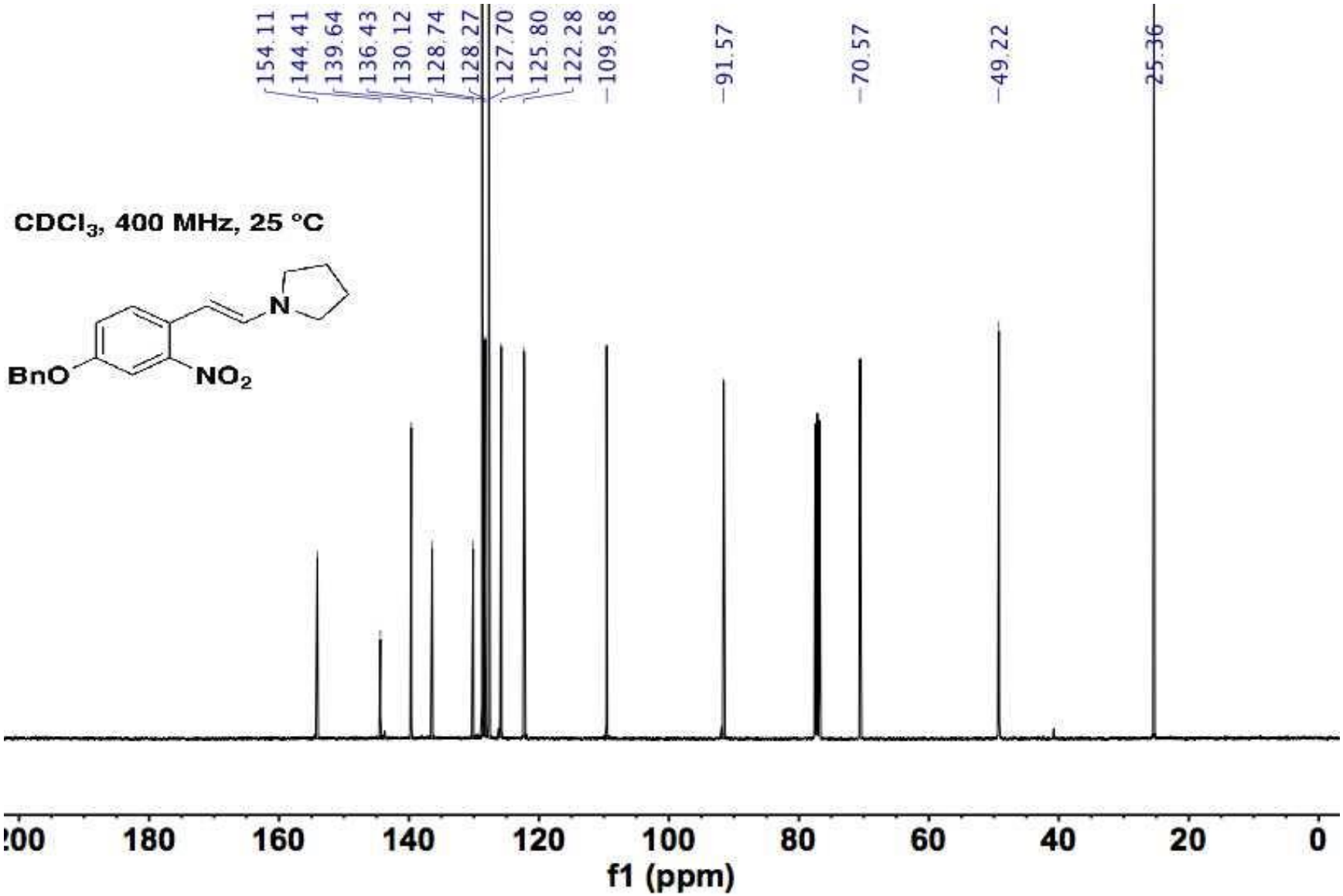


*Figure A2.4.26*. $^{13}$C NMR Spectrum of Compound **4.39**.

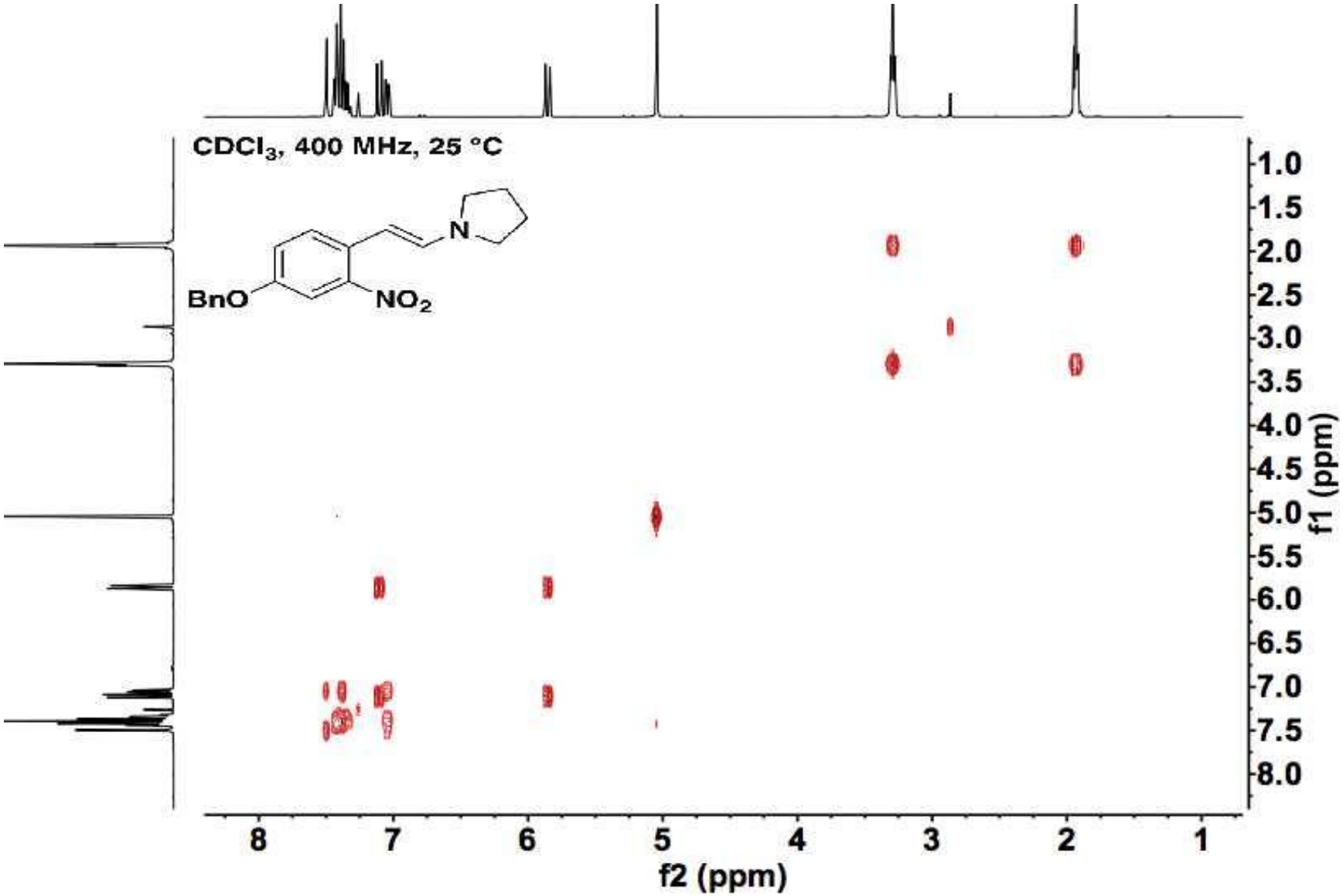


*Figure A2.4.27*. COSY NMR Spectrum of Compound **4.39**.

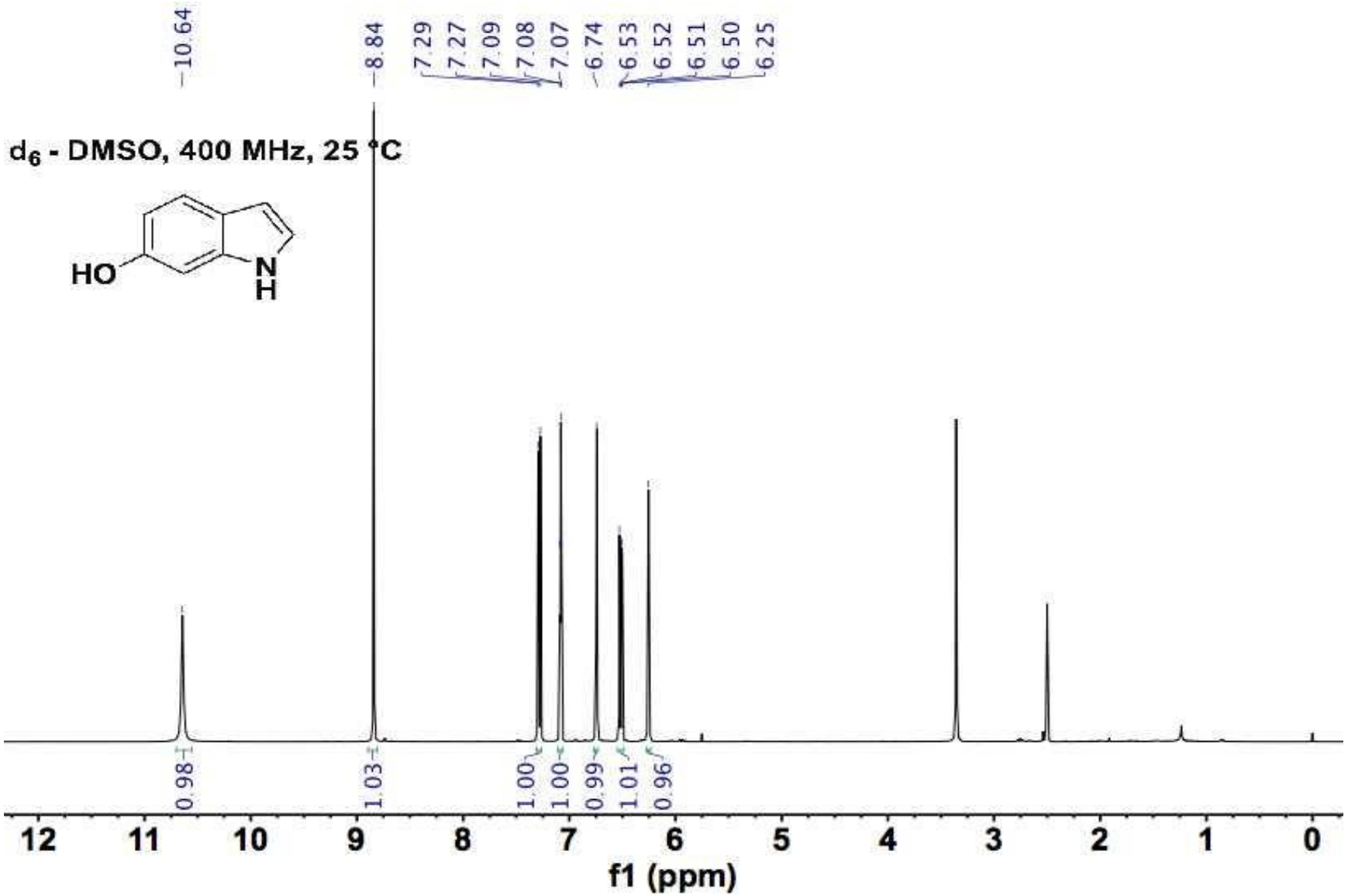


*Figure A2.4.28*. $^{1}$H NMR Spectrum of Compound **4.40**.

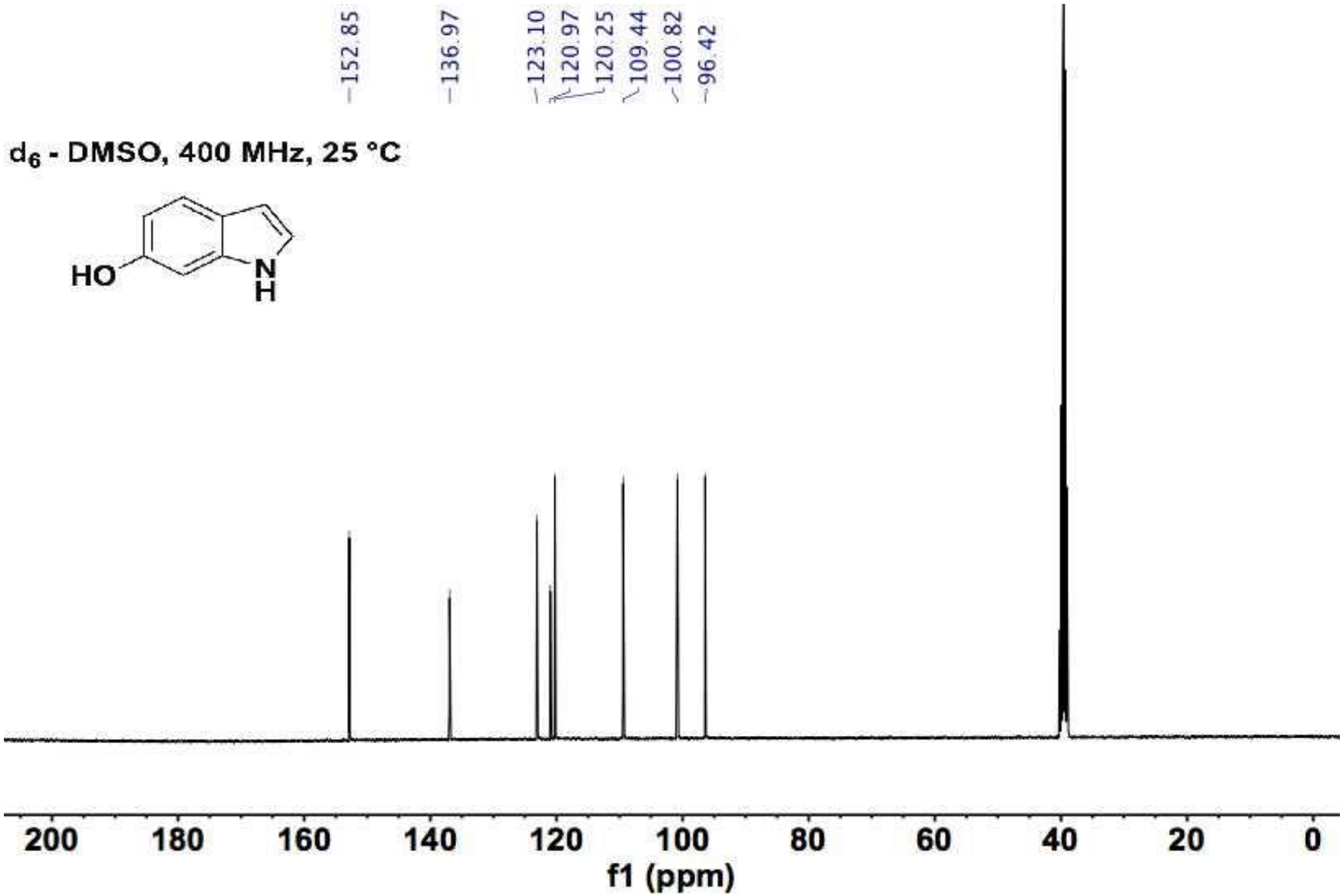


*Figure A2.4.29*. $^{13}$C NMR Spectrum of Compound **4.40**.

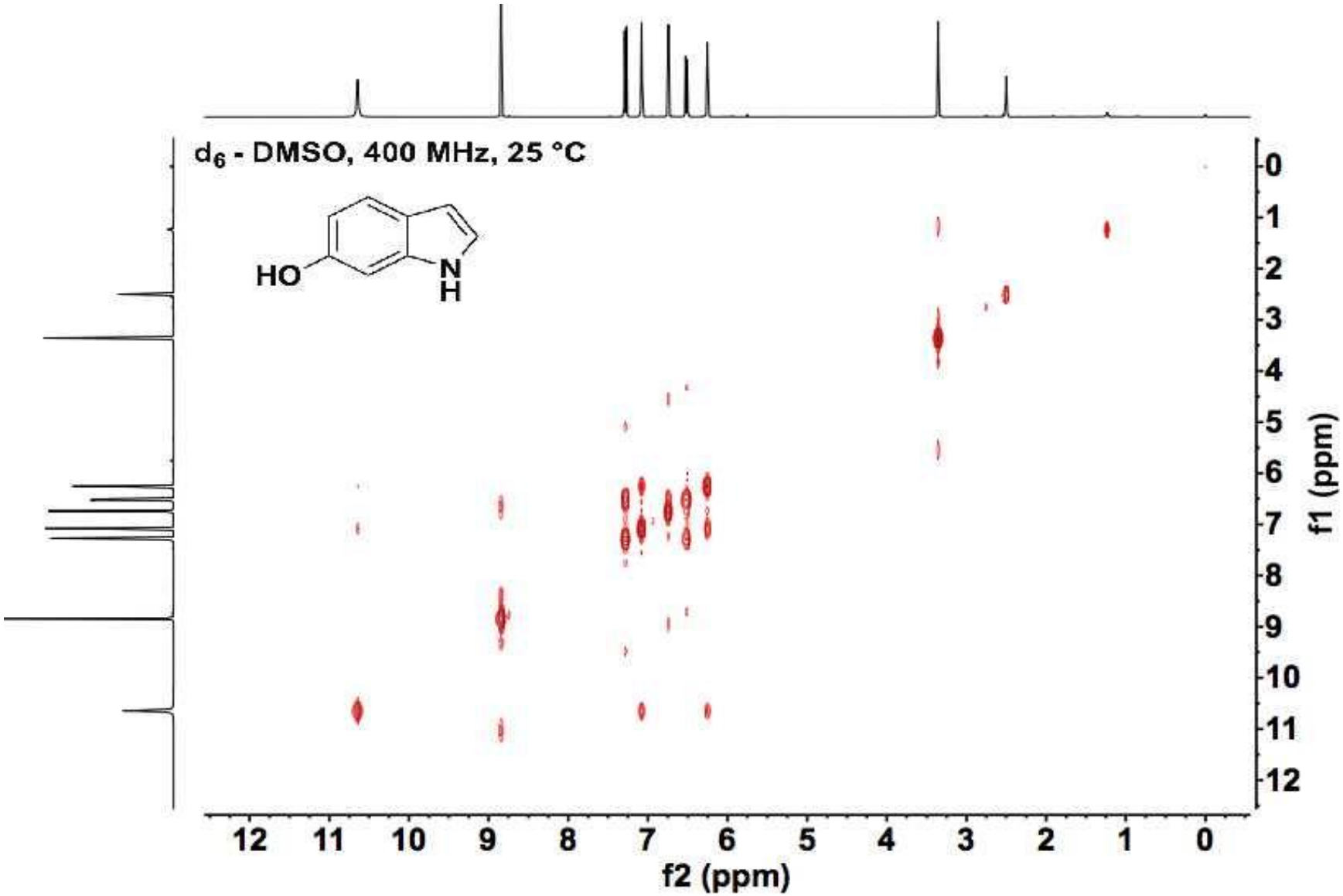


*Figure A2.4.30*. COSY NMR Spectrum of Compound **4.40**.

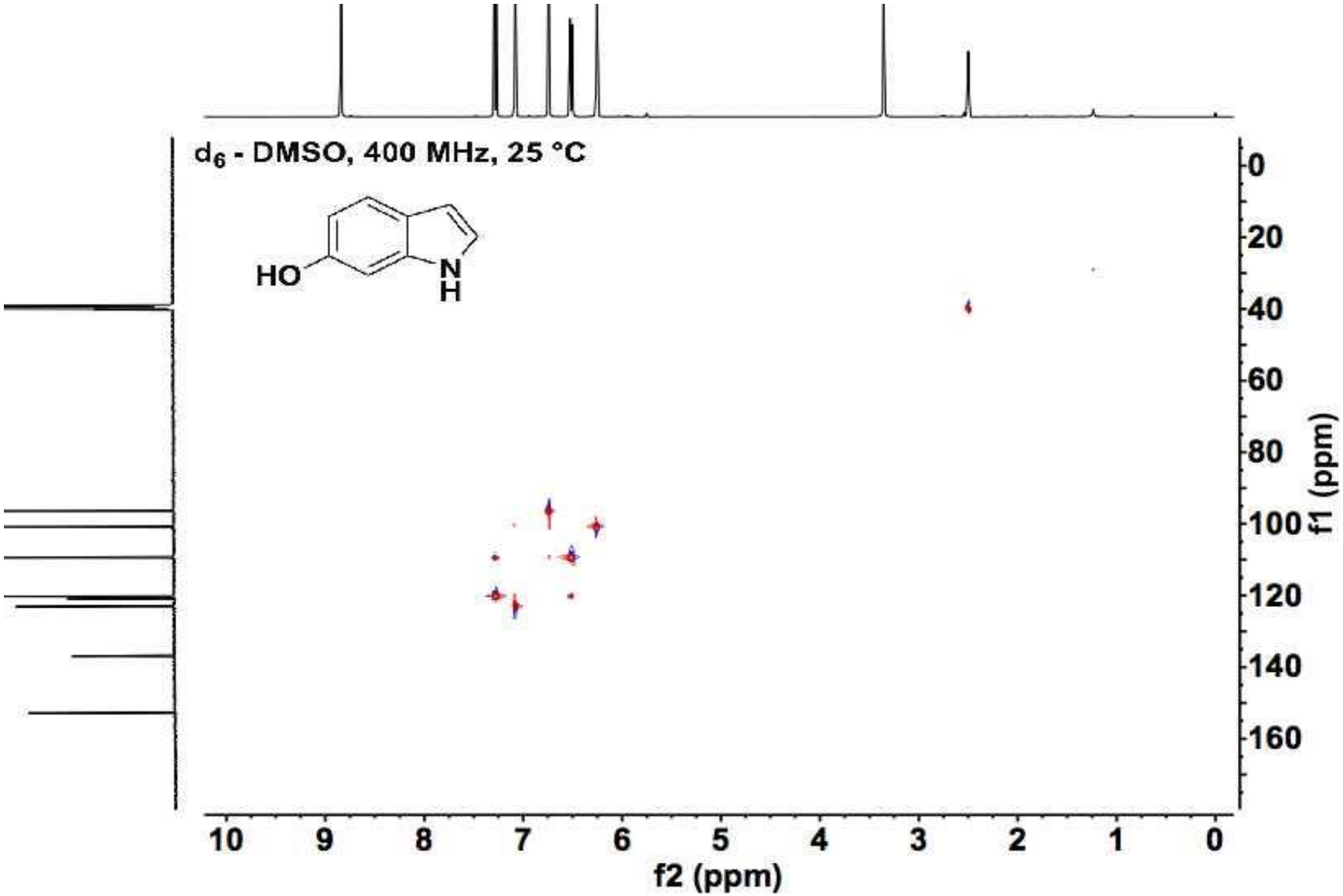


*Figure A2.4.31*. HSQC NMR Spectrum of Compound **4.40**.

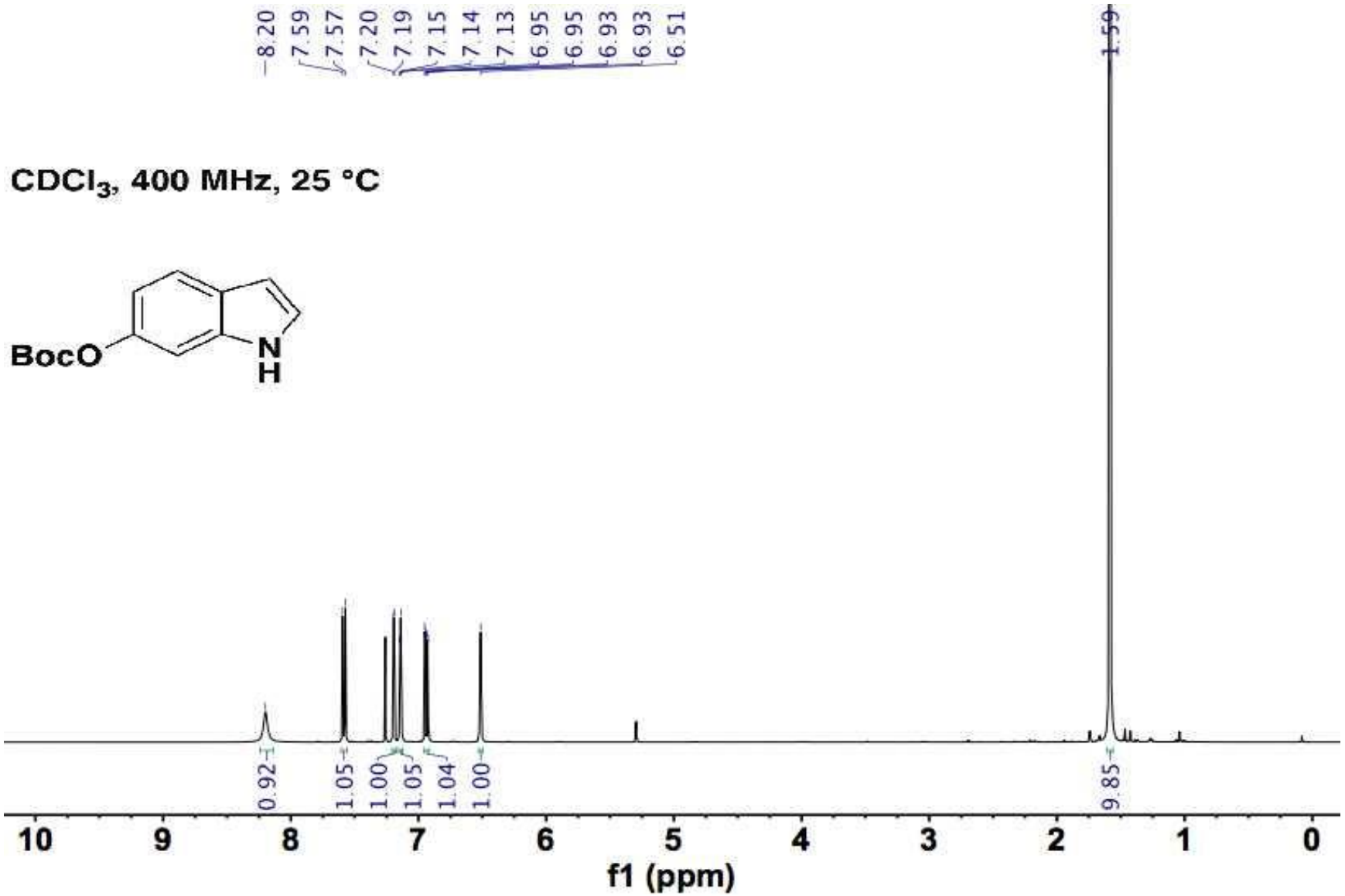


*Figure A2.4.32*. $^{1}$H NMR Spectrum of Compound **4.41**.

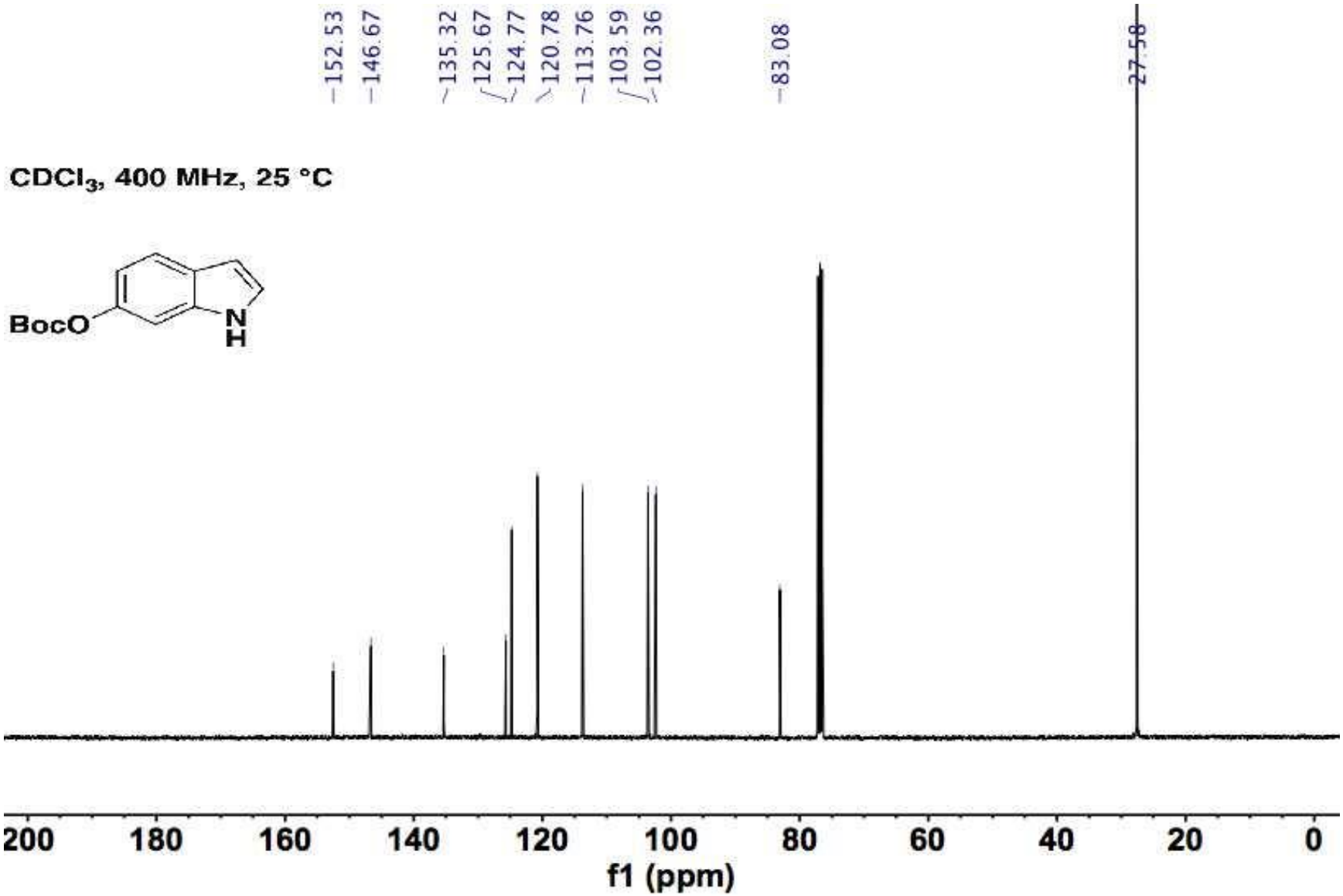


*Figure A2.4.33*. $^{13}C$ NMR Spectrum of Compound **4.41**.

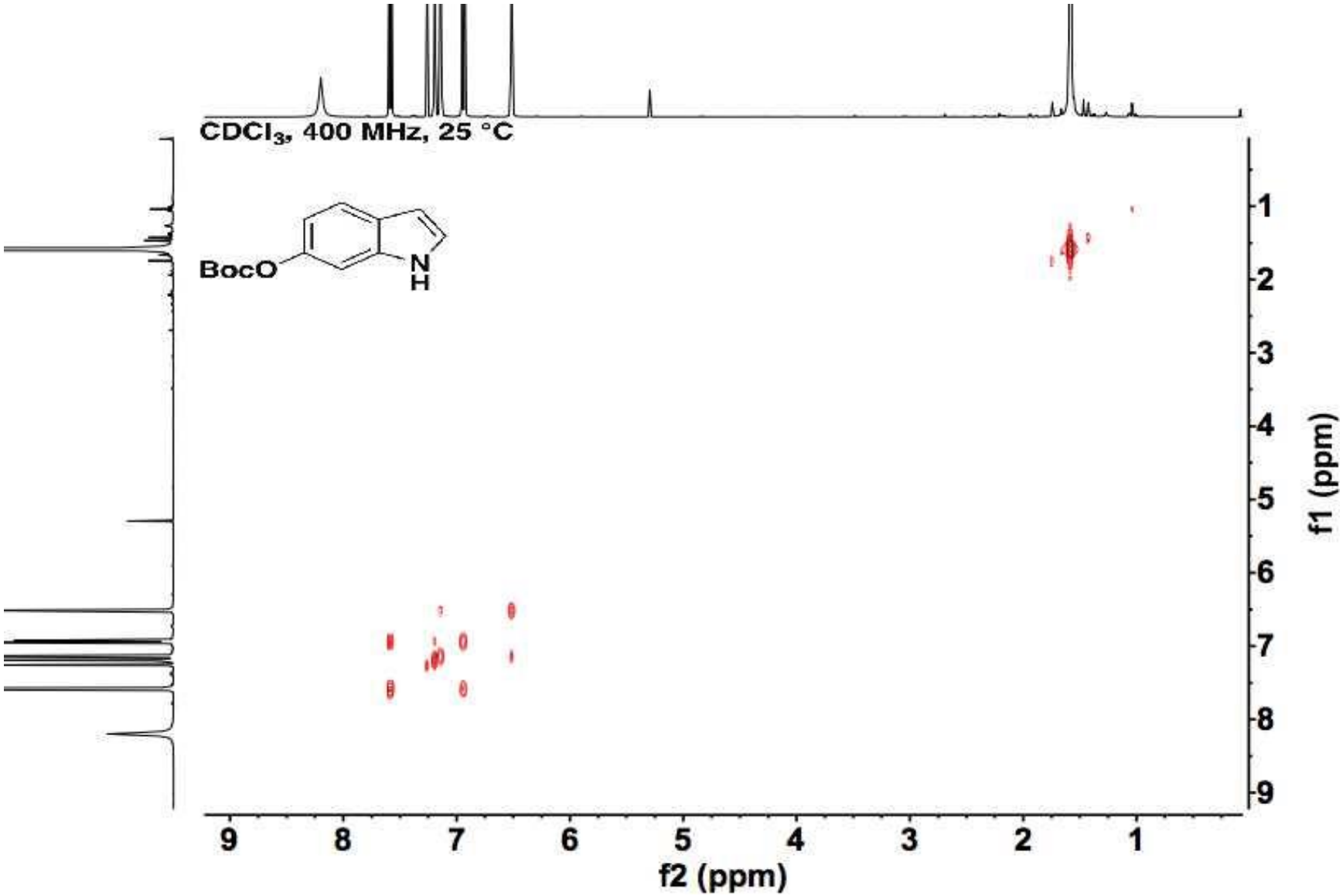


*Figure A2.4.34*. COSY NMR Spectrum of Compound **4.41**.

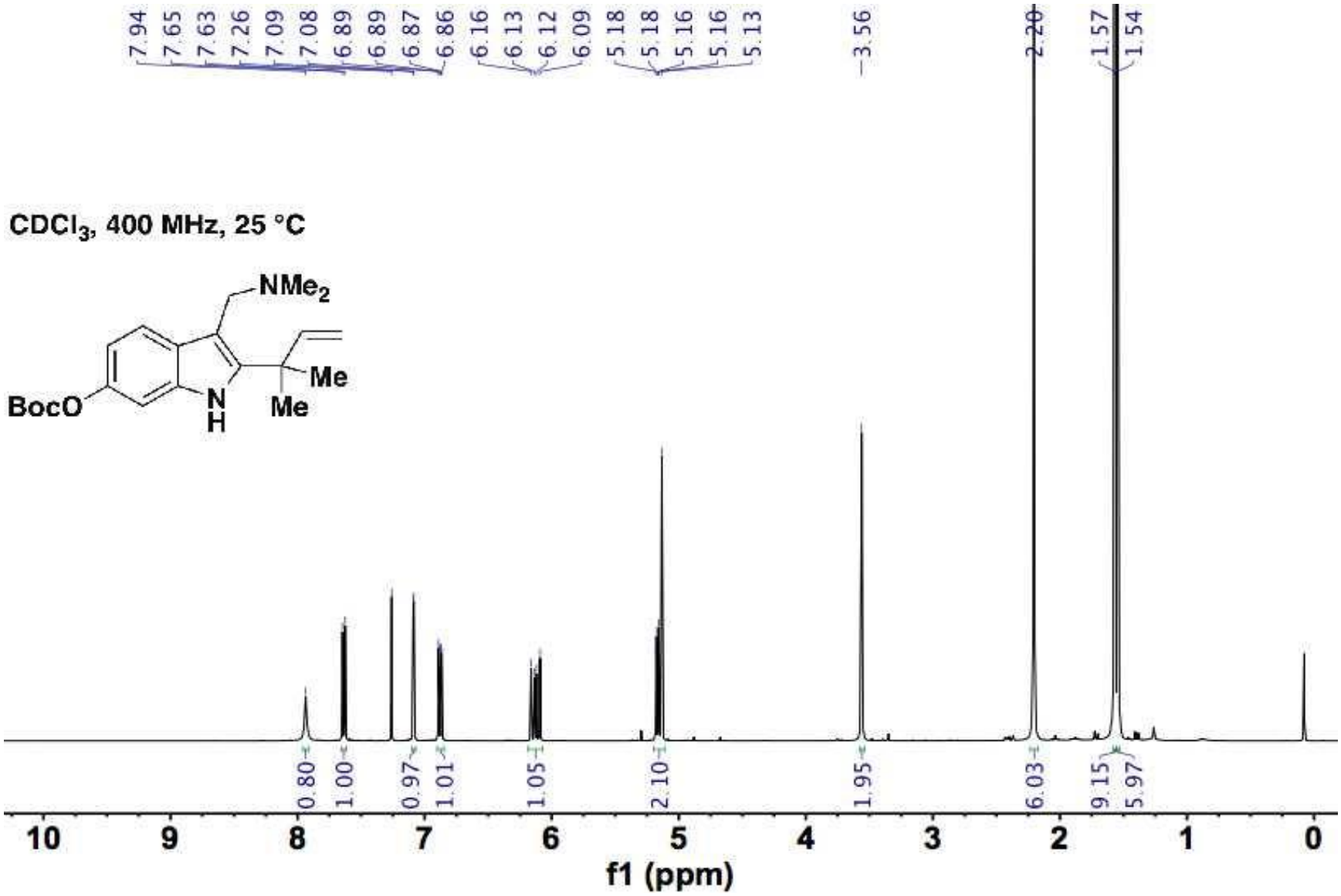


*Figure A2.4.35*. $^{1}$H NMR Spectrum of Compound **4.44**.

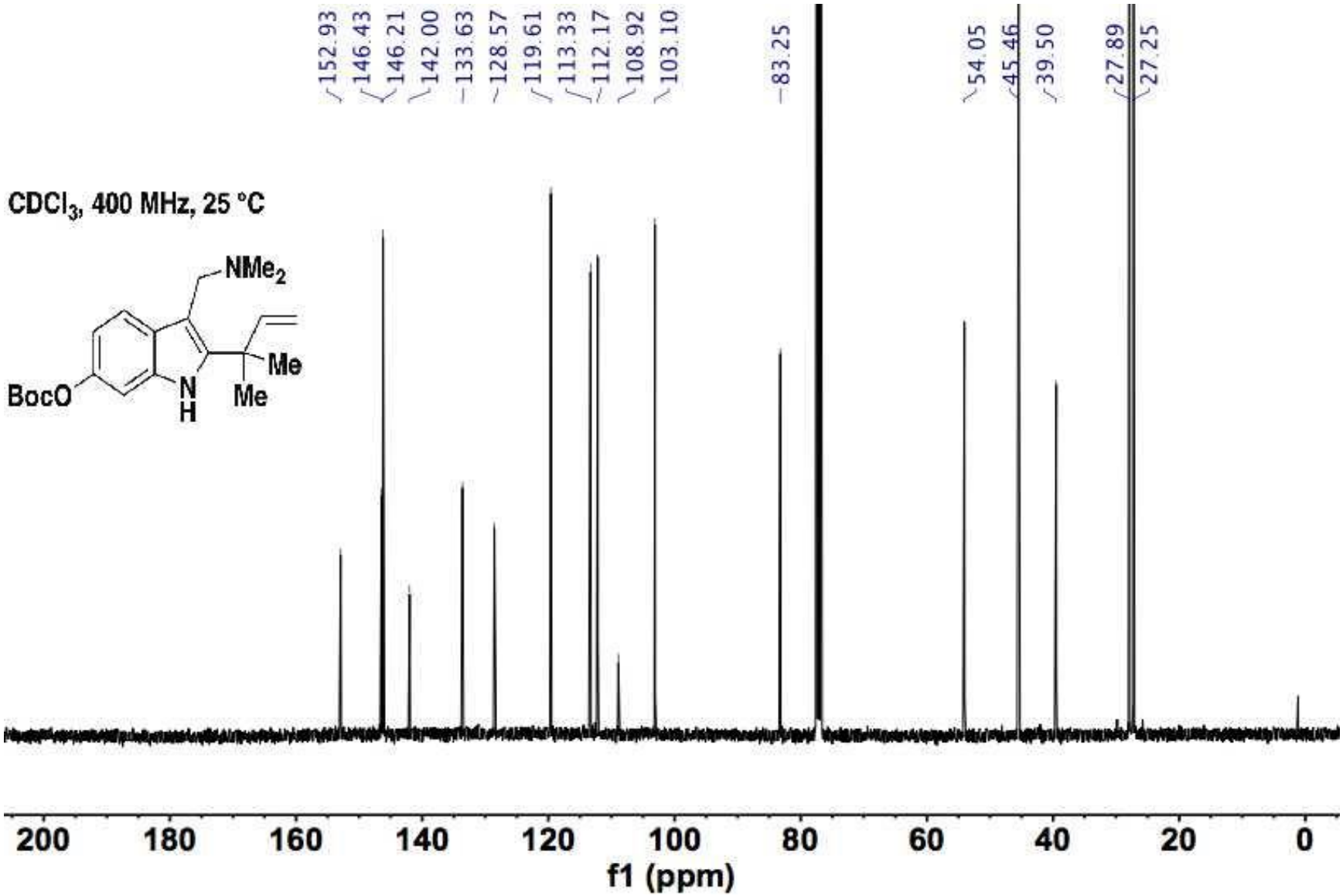


*Figure A.4.36*. $^{13}$C NMR Spectrum of Compound **4.44**.

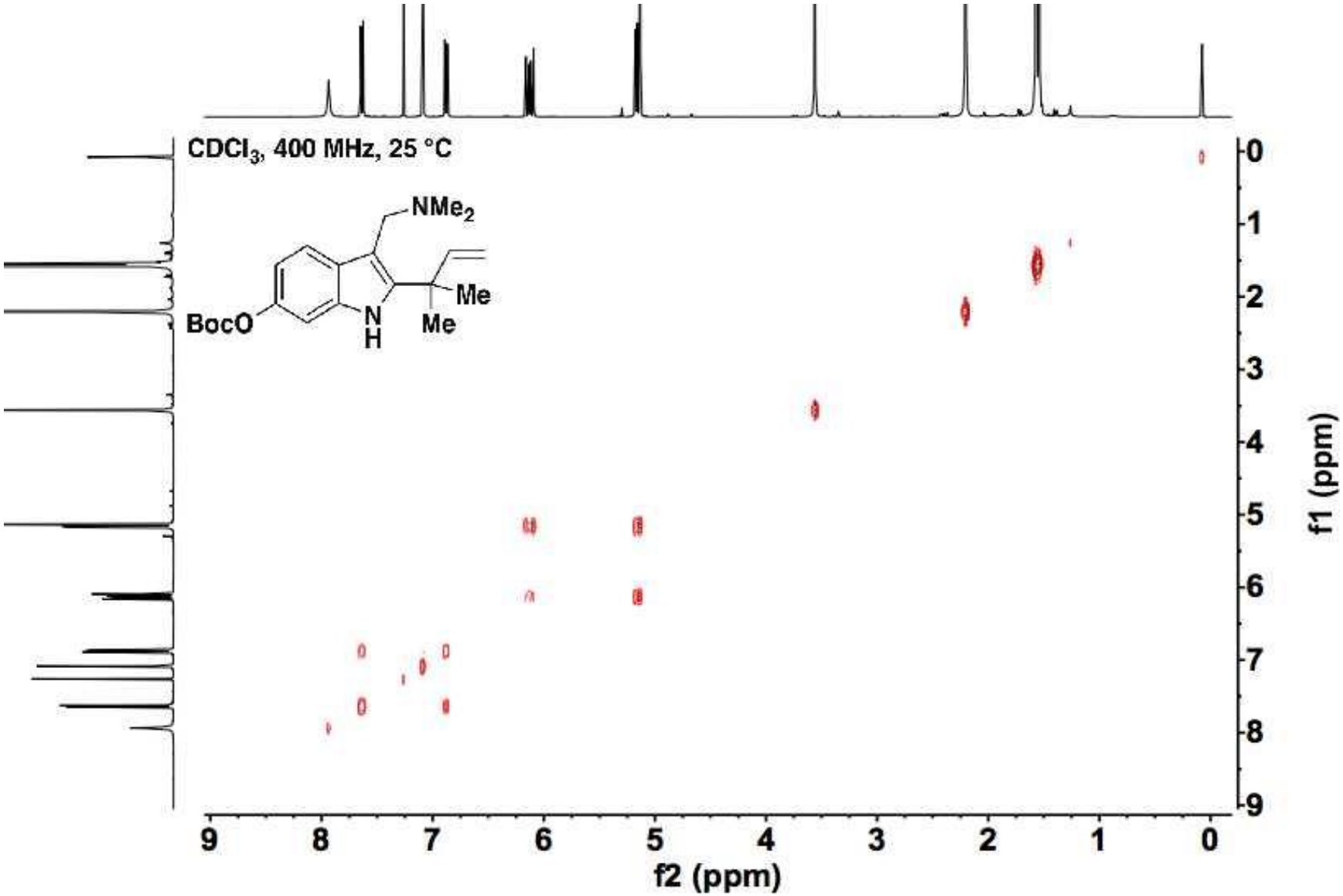


*Figure A2.4.37*. COSY NMR Spectrum of Compound **4.44**.

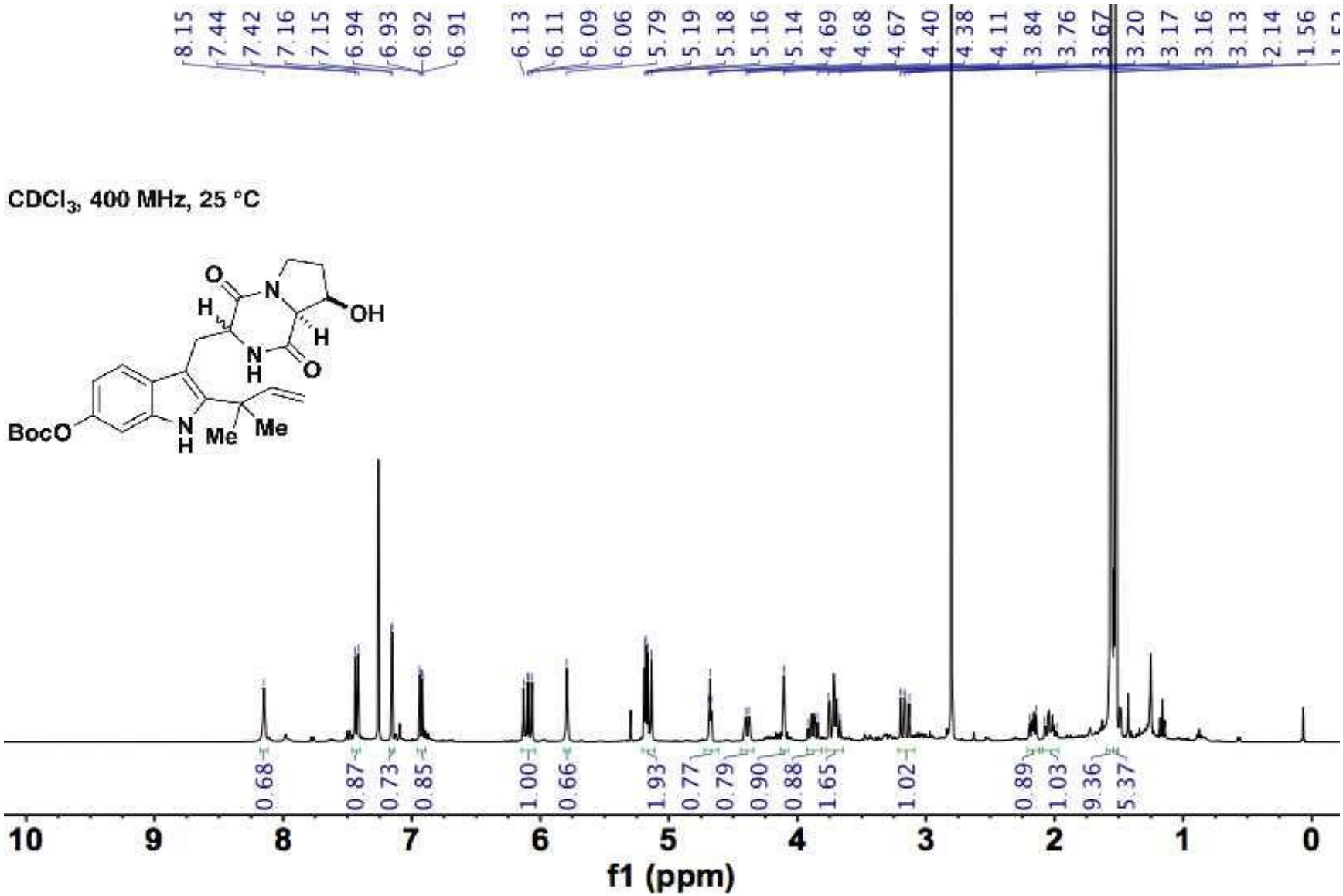


*Figure A2.4.38*. $^{1}$H NMR Spectrum of Compound **4.48**.

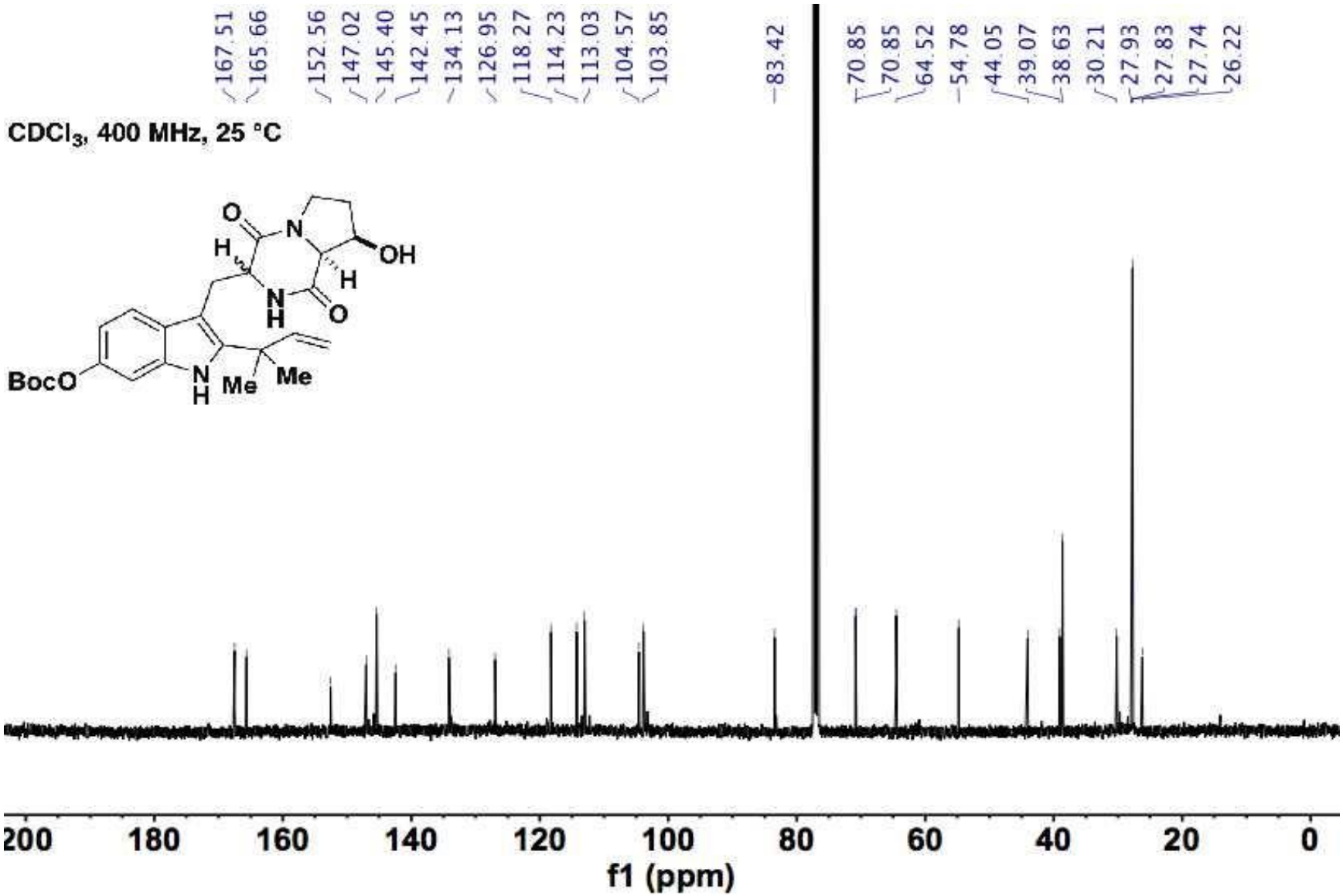


*Figure A2.4.39*. $^{13}$C NMR Spectrum of Compound **4.48**.

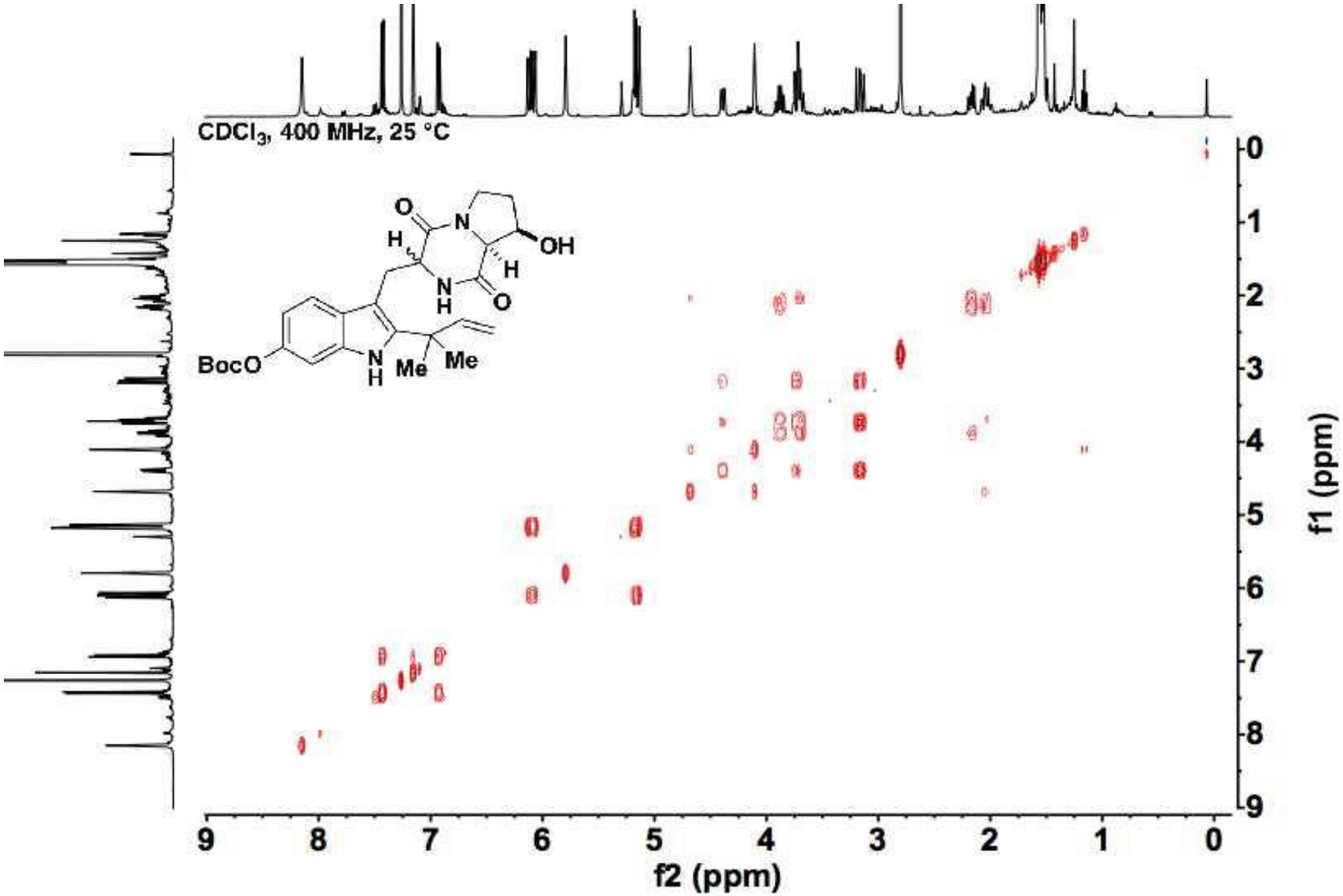


*Figure A2.4.40*. COSY NMR Spectrum of Compound **4.48**.

# Appendix III: The Development of Nonsteroidal Anti-Inflammatory Drug Candidates from the Crop *Portulaca* oleracea

***Specific Aims.*** Nonsteroidal anti-inflammatory drugs (NSAIDs) are known as the most common pain relief medications around the globe. They are also affordable and easily accessible. While Ibuprofen, Aspirin, and Naproxen (Figure 1) are used regularly to relieve pain caused by inflammation, they produce side effects through the inhibition of cyclo-oxygenase (COX-1) alongside the inhibition of the inducible COX-2 enzyme.[159] COX-1 is responsible for the production of the mucous lining in the stomach, however long term and/or high dosage of these anti-inflammatories can result in ulcers and bleeding of the stomach. Patients with gastrointestinal problems cannot take these medications due to their increased risk of damage caused by ulcers. COX-2 selective inhibitors, such as Celecoxib, can be used (a common drug to treat arthritis patients), but they also have serious side effects including heart attack, stroke, bleeding and perforation of the stomach or intestines.[160] These side effects force Celecoxib to be used in moderation.

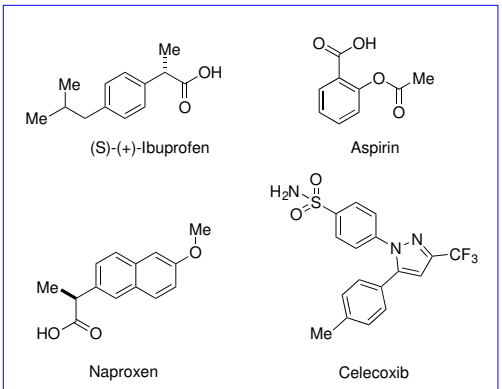

Figure 1. Common Nonsteroidal Anti-inflammatory Drugs

Inflammation is more commonly being recognized as a contributor to many known chronic diseases including but not limited to cancer, diabetes, heart disease, autoimmune disease, and asthma[161] For example, some cancers thrive as an immune response to low-grade inflammation: Cancer causes an inflammatory response resulting in an increased blood flow to the tumor, which in turn promotes proliferation of the cancerous cells. Modern medicine is focused on treating the symptoms of these diseases with pharmaceutical drugs, which commonly have undesirable, and sometimes fatal, side effects. As these diseases continue to be prevalent around the globe, this approach seems to be inefficient.

This proposal aims to develop a library of structural analogs to be studied based on Oleracone B for treatment of inflammation. Oleracone B, an azulene, is one of the five novel compounds (Figure 2) recently isolated from *Portulaca oleracea* L., a crop commonly used as an herb in the Mediterranean and tropical regions of Asia.[162-164] Oleracimine, the most abundant isolate in recent studies, has been reported to exhibit anti-inflammatory activity without any toxic side effects towards white blood cells.[162] Alongside the discovery, the pharmacokinetics of Oleracone displays a high bioavailability in its anti-inflammatory

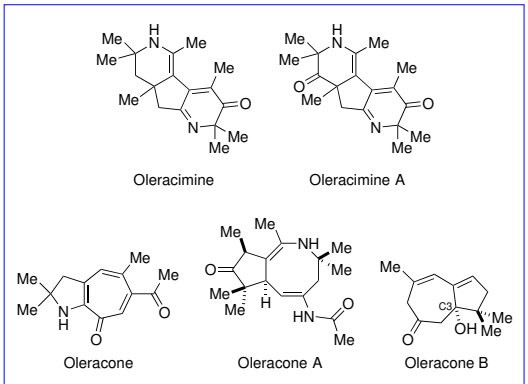

Figure 2. Isolated Novel Alkaloids and Azulene from P. *oleracea* L.

properties.[164] The crop as a whole also contributes the essential ω-3 and ω-6 fatty acids, dietary minerals, antioxidants, as well as antibacterial, analgesic, and neuroprotective properties, among many other benefits towards health.[162] This raises the question: Is the anti-inflammatory response a synergistic effect of the whole vegetable,[162] or can these novel compounds be applied in pharmaceuticals? Having access to the isolates on a large and efficient scale will allow us to begin answering this question.

Advances in this area have focused on manipulation of known selective COX-2 inhibitors to reduce side effects.[165] It has consequently become imperative to better understand the biological pathway to reduce inflammation. Success of this project will allow for the development of a new class of NSAIDs from the isolated natural alkaloids and azulene in *P. oleracea* L.

***Aim 1. Total Synthesis of Natural Alkaloids and Structural Conjugates.*** We will prepare an efficient synthesis towards the novel azulene, Oleracone B, isolated from *P. oleracea* L.[162] Facile transformations will be incorporated to conjugate biological derivatives at the hydroxyl position, C3 (Figure 3). These derivatives will be carefully designed based on prior studies of known NSAIDs and their conjugates as well as new insights. Conjugate development will provide an opportunity to synthesize NSAIDs with an anti-inflammatory response and decreased side effects.

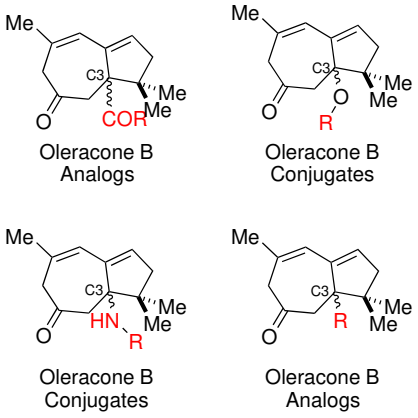

Figure 3. Potential Biological Derivatives of Oleracone B

***Aim 2. Structural Activity Relationship study.*** The natural products isolated maintain very different structural properties than that of the known NSAIDs. This suggests these compounds play a different role in repressing inflammation than the known pathways of NSAIDs. The goal in Aim 2 is to develop a library of analogs (Figure 3) to study the structural activity of Oleracone B.

***Aim 3. Biological Testing***

a) The cytotoxicity of the compounds will be tested against RAW 264.7 cells. The MTT assays will give us insight into understanding the toxicity levels of the new compounds against white blood cells. This data will also be compared to the reported cytotoxicity data of Oleracimine.
b) ELISA assays for both prostaglandin and thromboxane production will follow the development of Oleracone B analogs. This will provide insight into understanding inhibition of substances produced by both isoforms.
c) Western Blot Analysis will be performed to characterize mRNA regulation. This will give us insight into further understanding the mechanism of action of the drug candidates.

# Appendix IV: Natural Diels-Alderases: Elusive and Irresistable

This is the manuscript that corresponds to chapter two and is published in the *Journal of Organic Chemistry*.[82]

JOC The Journal of Organic Chemistry

Perspective

pubs.acs.org/joc

# Natural Diels–Alderases: Elusive and Irresistable

Kimberly Klas,[†] Sachiko Tsukamoto,[‡] David H. Sherman,[§] and Robert M. Williams*[,†,∥]

[†]Department of Chemistry, Colorado State University, Fort Collins, Colorado 80524, United States

[‡]Graduate School of Pharmaceutical Sciences, Kumamoto University, 5-1 Oe-honmachi, Kumamoto 862-0973, Japan

[§]Life Sciences Institute and Departments of Medicinal Chemistry, Microbiology & Immunology, and Chemistry, University of Michigan, Ann Arbor, Michigan 48109, United States

[∥]University of Colorado Cancer Center, Aurora, Colorado 80045, United States

**ABSTRACT:** Eight examples of biosynthetic pathways wherein a natural enzyme has been identified and claimed to function as a catalyst for the [4 + 2] cycloaddition reaction, namely, Diels–Alderases, are briefly reviewed. These are discussed in the context of the mechanistic challenges associated with the technical difficulty of proving that the net formal [4 + 2] cycloaddition under study indeed proceeds through a synchronous mechanism and that the putative biosynthetic enzyme deploys the pericyclic transition state required for a Diels–Alder cycloaddition reaction.

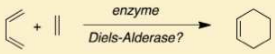


## 1. INTRODUCTION

Among the family of concerted pericyclic reactions governed and understood by the theoretical underpinnings of the conservation of orbital symmetry rules advanced by Woodward and Hoffmann, the [4 + 2] cycloaddition reaction, namely the Diels–Alder reaction, is among the most useful and widely studied reactions in synthetic organic chemistry. A vast array of publications concerning the synthetic utility, mechanism, catalysis, and theoretical bases of the Diels–Alder reaction are evident in the literature. An area of particular controversy concerns the fundamental question regarding the existence of biosynthetic enzymes that have *evolved* to catalyze this tremendously important synthetic construction. Our laboratory previously published a review of biosynthetic Diels–Alder constructions in 2003 covering primarily secondary metabolites that had been suggested by researchers to arise by potential biosynthetic Diels–Alder reactions, both enzyme-catalyzed and nonenzyme-catalyzed.[1] Oikawa has since contributed in highlighting developments in this area by publishing a review in 2005.[2] Kelly provided a more detailed overview of potential Diels–Alderases in 2008, and Liu et al. have provided insight as to the challenges workers face in securing mechanistically, a Diels–Alderase in Nature.[3] Herein, we survey and provide a contextual perspective of recent publications claiming to have identified biosynthetic genes coding for the expression of biosynthetic enzymes that catalyze the Diels–Alder reaction in the formation of primary or secondary metabolites.

Frontier molecular orbital (FMO) theory and molecular dynamics studies have been used to describe and understand the Diels–Alder reaction.[4−6] The highest occupied molecular orbital (HOMO) of the diene has perfect molecular orbital (MO) overlap with the lowest occupied molecular orbital (LUMO) of the dienophile, allowing for electron flow to form two new bonds. The neutral [4 + 2] cycloaddition of 1,3-butadiene with ethylene experiences restricted $HOMO_{diene}$–$LUMO_{dienophile}$ interaction.[4] This limitation requires catalytic and/or electronic support in order for a favorable reaction to occur.[5] Most commonly, an increase in the nucleophilicity of the diene or the electrophilicity of the dienophile is found to be sufficient. Increasing the electron density of the diene raises its HOMO and LUMO to a higher energy, while decreasing the electron density of the dienophile has the opposite effect.[4] This strengthens the $HOMO_{diene}$–$LUMO_{dienophile}$ interaction creating a favorable forward reaction.[6] To further increase reactivity, the use of Lewis acids is common.[4,6] The interaction between the Lewis acid and the electron-withdrawing group of the dienophile further stabilizes its HOMO and LUMO by polarization of the $\alpha,\beta$ double bond, in turn making the dienophile more electrophilic.[7] This is well represented in early work by Kojima and Inukai in the reaction of methyl acrylate with isoprene in the presence of aluminum trichloride ($AlCl_3$).[7] The HOMO and LUMO of the dienophile are lowered, and the electron densities of the orbitals are redistributed by the coordination of $AlCl_3$.[6] Experimental evidence represents an increase in reaction rate of the catalytic reaction, by $10^5$, compared to that of the uncatalyzed reaction expressing higher yields, lower reaction temperatures, and shorter reaction times.[7]

Manipulating the electronics of the addends also plays a significant role in increasing regioselectivity. This is exemplified in the aforementioned work by Kojima and Inukai.[7] The $AlCl_3$-catalyzed reaction of isoprene with acrylate results in a 97:3 regioselective ratio of para/meta products due to the electronic reorganization of Lewis acidic bound acrylate and the electron-donating effect of the alkyl group on the 2-position of diene.[7] The regioselectivity of this reaction was increased from an 80:20 para/meta ratio for the uncatalyzed reaction of isoprene with methyl acrylate.[6−8]

The electron-withdrawing group (EWG) on the dienophile, relative to the diene substitutents, aids in the stereochemistry

**Special Issue:** 50 Years and Counting: The Woodward-Hoffmann Rules in the 21st Century

**Received:** August 20, 2015
**Published:** October 23, 2015





DOI: 10.1021/acs.joc.5b01951
J. Org. Chem. 2015, 80, 11672−11685

established by the Diels–Alder reaction. While the stereochemical relationships on the addends are preserved, secondary interactions between the EWG and the diene determine the relative stereochemistry in a stereoselective transformation. Early work by Houk and Strozier demonstrates this along with the continued effect of a Lewis acid.[5,9] In the [4 + 2] cycloaddition of cyclopentadiene with methyl acrylate, the stereoselective reaction occurs in a 82:18 endo:exo ratio.[6] Studies from the 1970s suggested the explanation for the stereoselective reaction was due to secondary orbital overlap interactions. This subject is discussed later in the manuscript. Enhanced stereoselectivity can be achieved for the lewis-acid catalyzed reaction due to the distribution of electron density within the molecular orbitals of the dienophile. This is exemplified in the work provided by Houk in the reaction of cyclopentadiene and methyl acrylate. The addition of $AlCl_3$ increased the stereoselectivity to a 99:1 ratio of endo:exo.[6]

## 2. DIELS–ALDER REACTION MECHANISM

The mechanistic argument on whether the Diels–Alder reaction proceeds via a concerted or stepwise mechanism dates back to studies carried out by Woodward et al. suggesting a synchronous concerted transition state.[10] Early theoretical calculations of kinetic isotope effects and reaction rates were found not to be conclusive,[11] and the mechanism of the [4 + 2] cycloaddition reaction has been extensively studied experimentally and theoretically by numerous researchers. Figure 1 represents the four transition-state (TS) structures through which the net redox-neutral [4 + 2] cycloaddition may be envisioned to proceed.

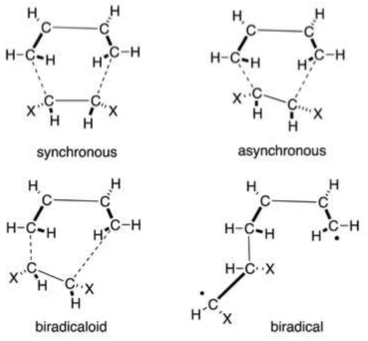


**Figure 1.** Possible transition structures in the Diels–Alder reaction.

On the basis of previous calculations conducted with lower levels of theory by Dewar et al.,[11,12] the Diels–Alder reaction has been rationalized to occur through a biradical intermediate suggesting that multibond reactions cannot proceed via a synchronous transition state.[13] This theory was subsequently contradicted as Houk et al. showed that geometries are more sensitive to electron correlation than to the basis set as it exceeds 3-21G.[14] Further investigations by Houk et al. based on Becke3LYP/6-31G* calculations suggested the concerted transition state is lower in energy than the biradical transition state in the retro-Diels–Alder reaction of norbornene,[15] while highly substituted dienes were found to favor a stepwise mechanism.[16]

**2.1. [4 + 2] Cycloaddition Reaction with Symmetrical Addends.** The simplest or "parent" Diels–Alder reaction involves 1,3-butadiene with ethylene to form cyclohexene (Figure 2). Early high-level ab initio and RH calculations by Burke et al. and Townshend et al. predicted a symmetrical transition state, with perfect synchronicity of formation of the two new C–C bonds.[17] Using the highest level of theory (STO-3G and 4–31G basis sets at CAS1 and CAS2 level) at the time, ab initio calculations by Bernardi et al. suggested a synchronous transition state for the parent Diels–Alder reaction.[18] While the basis sets for the MC-SCF study was limited, Becke3LP and CASSCF calculations at the higher 6-31G* level of theory and CASSCF calculations at the STO-3G level of theory predict a synchronous transition structure for the reaction of ethylene with butadiene (Figure 2).[14,18] The calculated transition structure for the reaction of ethylene with butadiene was favored over a stepwise mechanism by 5 kcal/mol in calculations by Houk et al.[14] Secondary kinetic isotope effects interrogated by Gajewski et al., suggested the reaction of nearly symmetrical dienes and dienophiles is nearly synchronous.[19] These "nearly synchronous" addends refer to alkyl substituents, none of which have significant electronic activating or deactivating effects.

**2.2. D–A Reaction with Unsymmetrical Addends.** The first ab initio calculations and semiempirical studies on a reaction of 1,3-butadiene with an unsymmetrical dienophile were performed by Houk et al. on the reaction of acrolein and 1,3-butadiene.[20] Ab initio quantum mechanical calculations at the 3-21G basis set suggested an asynchronous TS (Figure 3).[20]

These calculations suggested that substituents, particularly ones that form an asymmetric diene, create asynchronicity within the transition state. RHF calculations predicted one substituent to give a 0.3 Å difference in the bond lengths of the nascent $\sigma$ bonds within the transition state.[20] Orbital calculations are given for the *endo* transition structure as they were found most favorable. While the theoretical underpinnings for *endo* preferences are not clear, secondary orbital overlap interactions (now largely assumed moot based on theoretical work) as well as dipolar, electrostatic, and van der Waals forces have been attributed to govern *endo* selectivity.[20]

Further investigations by Bernardi et al. with MC-SCF studies at the minimal STO-3G level predict that reaction of vinylcyclobutane and 1,3-butadiene undergoes a two-step asynchronous (diradicaloid nature) mechanism. This suggested that steric effects can significantly increase the amount of asynchronicity.[21] Based on symmetry, McIver has also concluded that it is highly unlikely that a symmetric transition structure would be relevant.[22]

**2.3. D–A Reactions with Activating Symmetrical Addends.** While recent studies reveal that Diels–Alder reactions with unsymmetrical addends undergo cycloaddition through asynchronous transition states, it was accepted that reactions with symmetrical addends would undergo cycloaddition through synchronous or nearly synchronous transition states.[11,23] Singleton was interested in knowing if this would apply to doubly activated dienophiles[23] due to the observation of attenuated activation by a second activating group.[11,24] Reaction of 1,3-butadiene with bis(boryl)acetylene is predicted by density functional theory to undergo cycloaddition through a highly unsymmetrical transition state.[23] Becke3LYP calculations with a 6-31G* basis set predicted the symmetrical structure, forced $C_s$ symmetry, to be 6.5 kcal/mol higher in energy than the unsymmetrical transition structure.[23] Due to


DOI: 10.1021/acs.joc.5b01951
J. Org. Chem. 2015, 80, 11672–11685

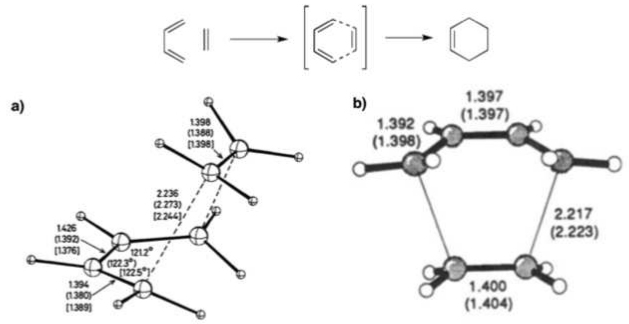


**Figure 2.** Parent Diels–Alder reaction (bond lengths in angstroms). (a) CASSCF/STO-3G calculated transition structures from Bernardi et al. Reprinted with permission from ref 18. Copyright 1985 Royal Society of Chemistry. CAS2 and CAS1 are in parentheses and lower-level 4-31G basis set calculations are in brackets. (b) CASSCF/STO-3G calculated transition structures by Houk et al. Reprinted with permission from ref 14. Copyright 1993 American Chemical Society.

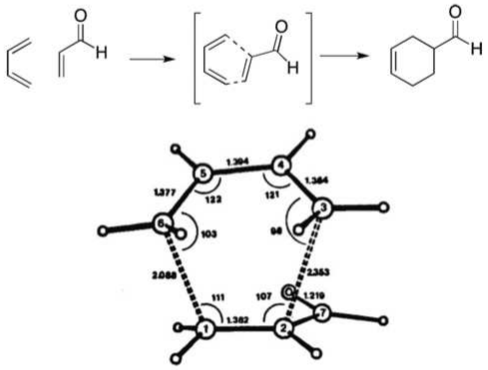

**Figure 3.** Orbital calculations for the asymmetric endo transition structure in the reaction of acrolein with butadiene. Reprinted with permission from ref 20. Copyright 1989 American Chemical Society.

the size of the boron groups and the favorable HOMO–LUMO overlap of the first boryl group with the $\pi$-system of 1,3-butadiene, further investigation with other activating groups was found necessary, and the results were somewhat surprising.[23] Becke3LYP/6-31G* theoretical calculations predicted unsymmetrical and nearly symmetrical transition states for the reaction of acetylenedicarboxylate with isoprene (Figure 4)[23] and an unsymmetrical transition state with cyclopentadiene.[25]

Experimental kinetic isotope effects support asynchronous character as well as theoretical kinetic isotope effects for the reaction of acetylene dicarboxylate with isoprene.[23,26] The asynchronous character of the symmetrical reaction can be explained by the difference in activation by the two activating groups. Stronger activation by the first group over that of the second group accounts for the asynchronous nature of the transition state.

Becke3LYP/6-31G* calculations for the reaction with the highly reactive parent triazolinedione (TAD) represents a highly unsymmetrical transition state being favored by 1.1 kcal/mol by Singleton et al. (Figure 5)[23] and 1.0 kcal/mol by Houk et al.[16] over the second-order saddle point.

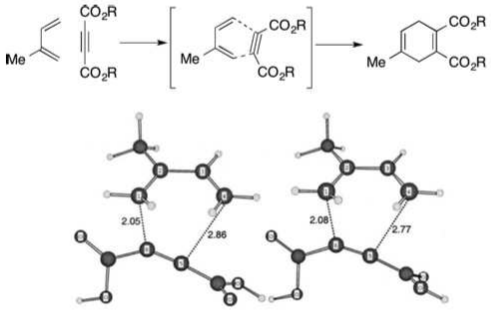


**Figure 4.** Becke3LYP/6-31G* calculations for the asynchronous endo and exo transition structures for the reaction of acetylene dicarboxylic acid with isoprene by Singleton et al. Reprinted from *Tetrahedron*, ref 23, Copyright 2001, with permission from Elsevier.

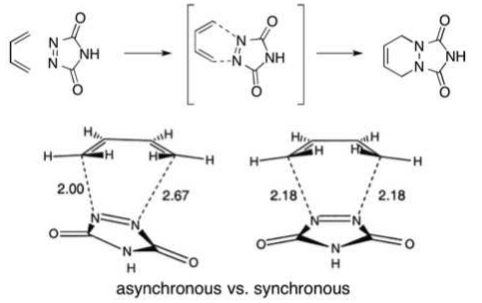


**Figure 5.** Becke3LYP/6-31G* calculated asynchronous and forced Cs symmetry saddle point synchronous transition structures for the reaction of TAD with 1,3-butadiene by Singleton et al. Reprinted from *Tetrahedron*, ref 23, Copyright 2001, with permission from Elsevier. Asynchronous TS is 1.1 kcal/mol lower in energy than synchronous TS.

While Houk et al. found an alternative stepwise diradicaloid mechanism for the reaction of TAD with *tert*-butylbutadiene 3 kcal/mol lower in energy[16] than the concerted transition state,



DOI: 10.1021/acs.joc.5b01951
J. Org. Chem. 2015, 80, 11672–11685

Singleton et al. suggests the reaction can undergo a stepwise or concerted asynchronous transition structure.[23] Calculated kinetic isotope effects of phenyltriazolinedione (PTAD) suggest very little asynchronicity due to the closeness in experimental proton KIE. Theoretical calculations suggest a different interpretation. Beck3LYP/6-31G* calculations suggested a highly asynchronous transition state (TS) (Figure 6), while

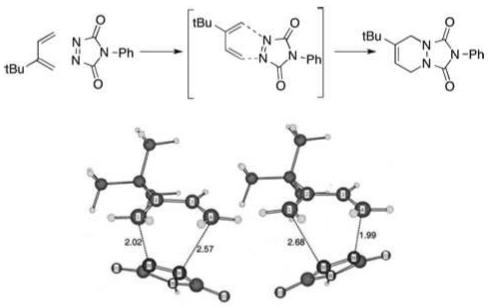


**Figure 6.** Becke3LYP/6-31G* calculated asynchronous *endo*- and *exo*-transition structures for the reaction of PTAD with *tert*-butylbutadiene. Reprinted from *Tetrahedron*, ref 23, Copyright 2001, with permission from Elsevier.

predicted KIEs follow suit. The concern remains if a symmetrical transition structure can account for the observed kinetic isotope effects. Fortunately, calculated isotope effects of the synchronous transition structure are symmetrical and do not agree with the experimental values. Therefore, due to agreement of theoretical isotope effects with the highly unsymmetrical Becke3LYP/6-31G* calculation transition state, reaction of PTAD with butadiene supports highly asynchronous mechanisms and asymmetrical transition states.[23]

It can be concluded that while there has been a lot of attention toward establishing a specific reaction mechanism for the Diels–Alder reaction, many questions still remain. Theoretical evidence suggests that symmetrical substrates undergo cycloaddition via a concerted transition state. Determination of the synchronicity versus asynchronicity of the transition state appears to be highly substituent dependent. The presence of activating groups, which is most common in the putative primary or secondary metabolite substrates to be discussed below, creates intrinsic asymmetry and attendant asynchronicity within the transition structure. It should also be appreciated that the "concertedness" of a putative Diels–Alder reaction, whether it be generated by synthetic chemistry or by a putative enzyme-catalyzed or enzyme-mediated system, lie on a continuum with symmetrical and concerted on one end to highly asynchronous and nonconcerted on the other.

## 3. DIELS–ALDERASES

The possible involvement of Diels–Alder reactions in biosynthesis has been an area of intense interest, and attempts to identify enzymes that might function as catalysts for the Diels–Alder reaction have been an active area of research since the late 1970s.[27] While numerous examples of non-enzyme-catalyzed biosynthetic Diels–Alder constructions are evident in the literature,[1b] the question of evolutionary selection pressure leading to the creation of enzymes that have specifically evolved to catalyze the [4 + 2] cycloaddition reaction via a true pericyclic transition state have attracted the attention of numerous research groups, particularly in the past 20 years. These will be briefly surveyed below.

**3.1. Solanapyrone Synthase.** Ichihara and co-workers performed feeding studies in *Alternaria solani* that provided evidence of oxidation of prosolanapyrone (**1**) to prosolanapyrone (**2**) (Figure 7), followed by a subsequent [4 + 2] cycloaddition in the biosynthesis of solanapyrones A (**4**) and B (**3**).[28] Ichihara et al. isolated a partially purified protein that was named solanapyrone synthase and were the first to claim the identification of a natural Diels–Alderase.[27]

The enzymatic and nonenzymatic reaction of prosolanapyrone **2** was monitored by HPLC analysis utilizing ultraviolet (UV) and circular dicrhoism (CD) detectors. The reaction did occur without presence of crude enzyme, but produced a 3:97 ratio of *exo*/*endo* adducts; whereas in the presence of the partially purified enzyme, the reaction proceeded, from **1** and **2**, in about a 6:1 *exo*-selective ratio. A control experiment with denatured enzyme was carried out to establish the reactivity of the enzyme. While the reaction does occur nonenzymatically, the enzyme-catalyzed reaction proceeded 4.1 times faster with

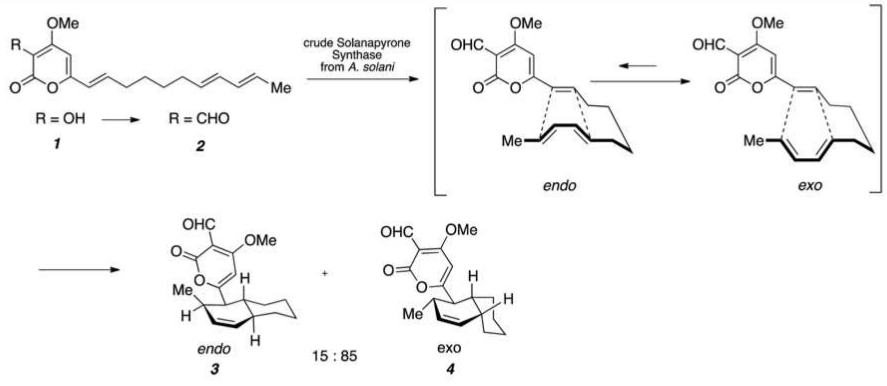


**Figure 7.** Biosynthesis of solanapyrone A (**4**) and B (**3**) with solanapyrone synthase as putative cyclase.



DOI: 10.1021/acs.joc.5b01951
J. Org. Chem. 2015, 80, 11672–11685

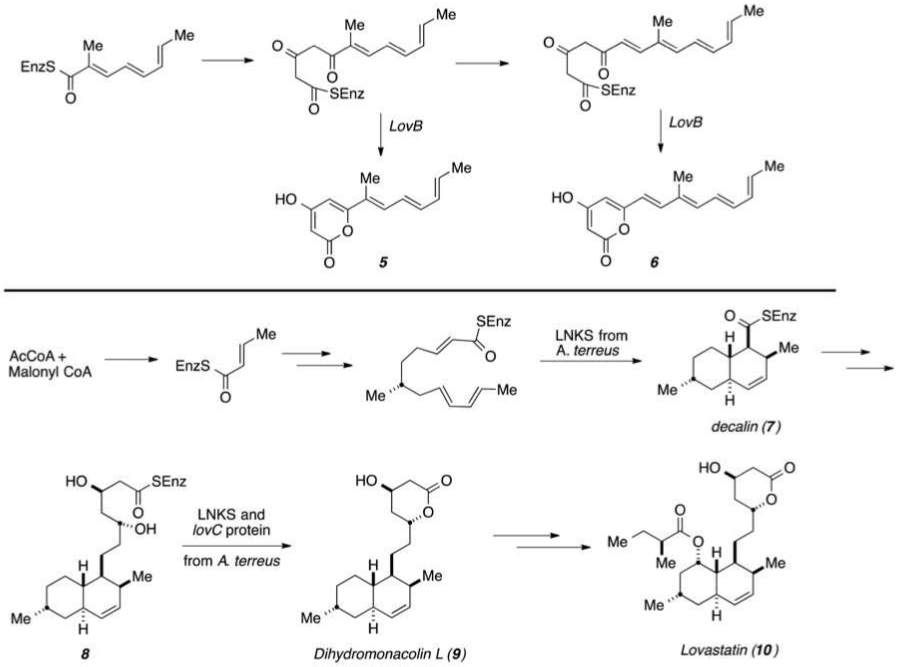


**Figure 8.** Biosynthesis of lovastatin (**10**) with LNKS as cyclase.

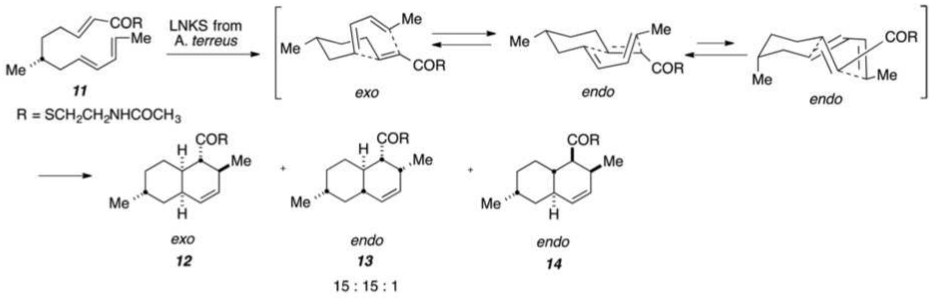


**Figure 9.** Model reaction with LNKS as cyclase in the enzymatic reaction of **11**.

an increase in enzyme concentration.[27] The question remained whether the two-step reaction was carried out by one or two enzymes. Further investigations by Oikawa et al. suggest that solanapyrone synthase is an oxidase that catalyzes the oxidation of **1** to aldehyde **2**, followed by Diels–Alder cyclization in a two-step manner.[29] In this instance, conformational restriction of the in situ generated aldehyde **2** seems a plausible mechanistic explanation for the differences in *endo*/*exo*-selectivity between the protein-free and protein-mediated reactions.

More recently, Oikawa and co-workers have succeeded in cloning and functionally expressing Solanapyrone synthase in the heterologous host *Aspergillus oryzae*. Using purified enzyme, they were able to confirm that this single enzyme effects the net two-electron oxidation of prosolanapyrone (**1**) to the *achiral* substrate aldehyde **2** and mediates the formal [4 + 2] cycloaddition forming optically pure solanapyrone.[30] These workers concluded that *"Expression and purification of SPS confirmed that this single protein catalyzes both the oxidation and the [4+2] cycloaddition, probably acting as a Diels–Alderase."*

The solanapyrone system therefore also introduces the concept that the "Diels–Alderase" function of solanapyrone synthase may be an accidental or spontaneous manifestation of producing the reactive aldehyde substrate (**2**) in the conformationally restricted and chiral environment of the active site of this oxidase. In other words, solanapyrone synthase is functionally constituted as an oxidase, and the "Diels–Alderase" activity is a subsequent fortuitous characteristic of the primary


DOI: 10.1021/acs.joc.5b01951
J. Org. Chem. 2015, 80, 11672–11685

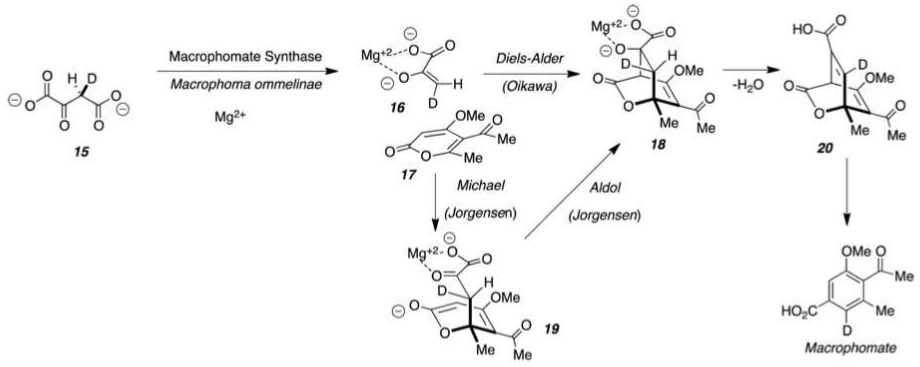


**Figure 10.** Proposed biosynthesis of macrophomate where macrophomate synthase functions as cyclase.

biochemical purpose of the enzyme's major function to oxidize a primary alcohol to an aldehyde. It is significant that the in situ generated aldehyde substrate **2** is *achiral* and the enzymatic product is optically pure. This outcome clearly demonstrates that the enzyme preorganizes the transition-state conformation to proceed in an enantioselective and diastereoselective manner. The high stereoselectivity of the enzyme-mediated process does not, de novo, provide experimental support for a Diels–Alder transition-state and mechanism but seems highly likely based on the corresponding protein-free reaction. The implications of this conceptual framework will be discussed in more detail below.

**3.2. Lovastatin Nonaketide Synthase.** Vederas, Hutchinson, and co-workers have studied the fascinating formation of the decalin system (**7**) in the biosynthesis of the HMG CoA-reductase inhibitor lovastatin (**10**).[31] The lovastatin nonaketide synthase (LNKS) was shown to participate in the synthesis of polyketides,[32] particularly pyrones **5** and **6**,[33] and the formation of dihydromonacolin L (**9**; see Figure 8) with the *lovC* protein in the biosynthesis of lovastatin.[31]

To investigate the involvement of this enzyme in the formation of decalin **7**, incubation of purified, recombinant enzyme was submitted to reaction with **11**.[31] Investigation with NMR studies revealed formation of **12** and **13** from **11** nonenzymatically and formation of **12**, **13**, and **14** enzymatically in the presence of LNKS in a 15:15:1 ratio, respectively (Figure 9).[31] The stereochemistry of *endo*-product **13** corresponds to the natural stereochemistry in the biosynthesis of lovastatin. The authors concluded that the *endo* transition state is a manifestation of van der Waals interactions occurring in the hydrophobic active site of the enzyme.[31]

This seminal work was the first to describe the cloning, functional expression, and isolation of a pure enzyme involved in a putative secondary metabolite Diels–Alder reaction. However, as in virtually all of the systems studied prior to and subsequent to the LNKS work, rigorous biophysical evidence corroborating a concerted, pericyclic transition-state mechanism for the construction of the decalin ring system in lovastatin biosynthesis has not been secured. Indeed, alternative stepwise and/or highly asynchronous mechanisms might indeed be operative and await further, deeper experimental interrogation.

**3.3. Macrophomate Synthase.** The biosynthesis of macrophomate has been the subject of particular controversy and was first proposed by Oikawa et al. to proceed via an enzyme-catalyzed intermolecular Diels–Alder reaction. The putative Diels–Alderase, macrophomate synthase (MPS), was demonstrated by Oikawa et al. to catalyze a multistep reaction from 2-pyrone (**17**) and oxaloacetate **15** to ultimately generate macrophomate. These workers postulated that the key transformation proceeded via the intermolecular Diels–Alder reaction of enol pyruvate **16** and pyrone **17** to yield the unstable bicyclo[2.2.2] Diels–Alder adduct **18**.[34] Dehydration of **18** to **20** and decarboxylation with concomitant aromatization through the proposed enzyme-catalyzed Diels–Alder reaction mechanism is illustrated in Figure 10.[34]

The authors speculated that, upon coordination with $Mg^{2+}$, decarboxylation of **15** occurs to form enolpyruvate **16**. Intermolecular Diels–Alder cycloaddition was proposed to furnish the bicyclo[2.2.2] species **18** which, followed by dehydration and decarboxylation provides macrophomate. In order to determine the stereochemical outcome of the $Mg^{2+}$-dependent enzymatic cycloaddition proposed, deuterium-labeled oxaloacetate and NMR spectroscopy revealed retention of the deuterium in the final macrophomate product.[34] This revealed the high stereospecificity of the transformation that was ascribed as evidence for a concerted process. While the experimental evidence based on NMR studies is only circumstantial, the authors concluded that the enzymatic reaction proceeded via the Diels–Alder route due to the high stereospecificity observed.[34] It should be noted that these studies only revealed that the net process was highly stereospecific and does not conclusively corroborate a concerted or pericyclic mechanism catalyzed by MPS.

Protein X-ray crystallography studies by Oikawa and co-workers provided further insight into the active site of MPS.[35] A binding model was built by Oikawa et al. based on the transition structure of the presumed Diels–Alder cyclization and structural insights from the crystal structure (Figure 11). The carbonyl oxygen of 2-pyrone can hydrogen bond to Arg101 and the acyl oxygen can hydrogen bond to Tyr169 which undergoes $\pi$-stacking with the Phe149 residue, placing Tyr169 in the correct orientation.[35] Experimental evidence with two mutant MPS proteins represents the importance of hydrogen-bonding in the active site, providing further support for the binding site represented in Figure 11.[35]

Jorgensen and co-workers investigated this reaction from a theoretical perspective and conducted mixed quantum and



DOI: 10.1021/acs.joc.5b01951
J. Org. Chem. 2015, 80, 11672−11685

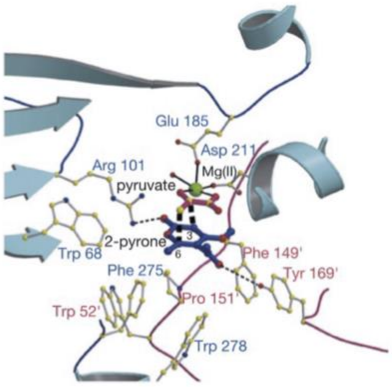


**Figure 11.** Model active site of MPS with binding of **15** and **17** utilizing crystal structure information and proposed transition structure. Reprinted by permission from Macmillan Publishers Ltd: *Nature* ref 35, copyright 2003.

molecular mechanics (QM/MM) combined with Monte Carlo simulations and free-energy perturbation (FEP) calculations and found a lower energy stepwise reaction pathway involving intermolecular Michael addition through intermediate **19**, followed by intramolecular aldol condensation to provide the same bicyclo[2.2.2]intermediate **18** proposed by the Oikawa group.[36] The Jorgensen investigations revealed that the Diels-Alder TS model is 17.7 and 12.1 kcal/mol less stable than the Michael and aldol TSs in the stepwise route, respectively. Jorgensen states in their paper: *"Therefore, this work indicates that the Michael–aldol mechanism is the route used by MPS to catalyze the second step of the overall transformation, and that the enzyme is not a natural Diels–Alderase, as claimed by Ose and co-workers (Nature 2003, 422, 185–189; Acta Crystallogr. 2004, D60, 1187–1197)."*

Significantly, Hilvert and co-workers subsequently demonstrated that MPS was a very competent aldolase, corroborating the second arm of the Jorgensen Michael–aldol mechanism.[37] Hilvert et al. demonstrated that MPS is highly homologous to a known aldolase DDG (2-dehydro-3-deoxygalactarate) and concluded that this lends plausibility to the two-step Michael-aldol alternative originally proposed by Jorgensen.[37] This work, taken in context with the penetrating theoretical insights of Jorgensen, reveals that extreme care must be taken when presuming that a putative Diels–Alder transformation (wherein the substrates appear to be structurally viable Diels–Alder substrates), form a product that ostensibly appears to be the result of a concerted [4 + 2] cycloaddition. It is clear that products can arise by distinct, stepwise, nonconcerted steps that are mechanistically orthogonal to a bona fide Diels–Alder construction.

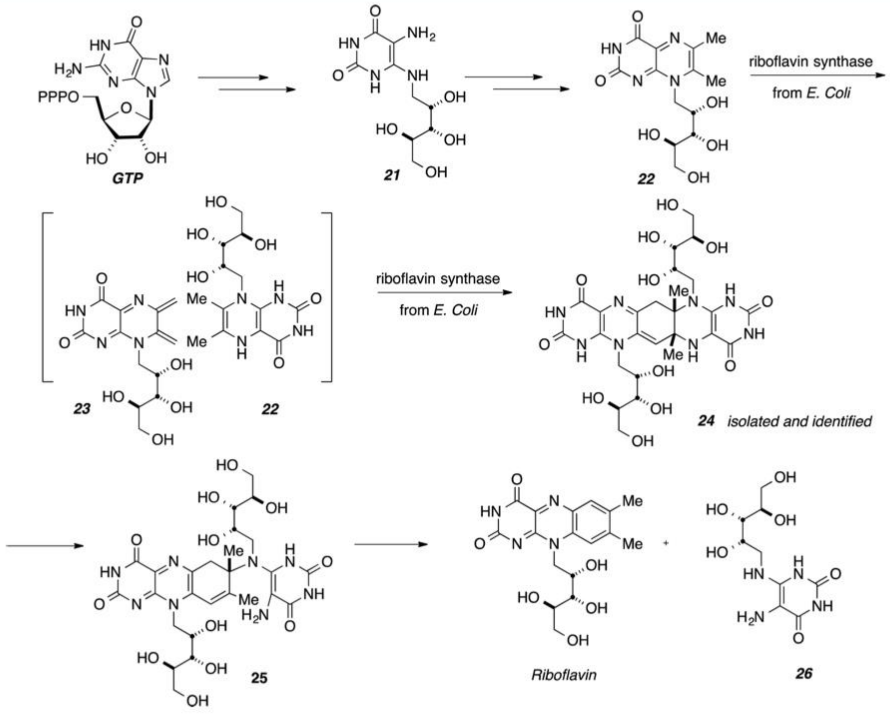


**Figure 12.** Proposed biosynthesis of riboflavin via a key [4 + 2] cycloaddition to provide the isolated and structurally characterized intermediate **24**.



DOI: 10.1021/acs.joc.5b01951
J. Org. Chem. 2015, 80, 11672–11685

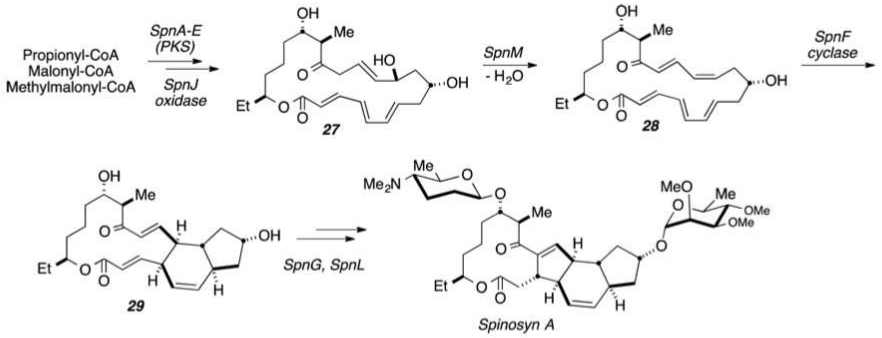


**Figure 13.** Biosynthesis of spinosyn A (**24**) where SpnF has been proposed as the putative cyclase.

**3.4. Riboflavin Synthase.** Riboflavin synthase of *Escherichia coli* is an enzyme that has been extensively studied and appears to be responsible for multiple functions in the biosynthesis of the essential enzymatic cofactor riboflavin.[38] This enzyme catalyzes the fascinating transfer of a four-carbon unit derived from one of the two equivalents of the common substrate, 6,7-dimethyl-8-ribityllumazine (**22**), culminating in the formation of Riboflavin and 5-amino-6-ribitylamino-2,4-(1*H*,3*H*)-pyrimidinedione (**26**). The mechanism proposed by Bacher et al. is illustrated in Figure 12 and features the key intermolecular Diels–Alder condensation between **22** and the oxidized diene species **23** derived from **22** to form **24** – a substance that these workers have isolated and structurally characterized.

Bacher proposes that the enzyme specifically functions as a Diels–Alderase, but there has been no experimental data published supporting this provocative mechanistic hypothesis. The authors discuss that the electronics of the proposed Diels–Alder substrates favor an inverse-electron-demand [4 + 2] reaction wherein the HOMO of the dienophile (**22**) overlaps with the LUMO of the diene (**23**). No corresponding protein-free reaction was reported that would have provided additional mechanistic insights.

Computational work reported later by Houk et al. provided theoretical evidence for other possible mechanistic routes.[39] Density functional theory calculations were used to evaluate the following mechanistic pathways: nucleophilic catalysis, hydride transfer followed by subsequent Diels–Alder, hydrogen atom transfer, and a nucleophilic addition mechanism.[39] While the Diels–Alder transformation cannot yet be ruled out, the alternative pathways are more likely to proceed with nucleophilic addition being of the lowest energy. However, it should be noted that due to high energy intermediates such as **22**, and the likelihood of a stepwise mechanism, the synthesis of riboflavin probably does not proceed via a Diels–Alderase although it formally constitutes a "[4 + 2]" construction.[39]

Access to the purified enzyme provides ample opportunity to study the detailed mechanism of the very interesting heterodimerization of **22** where kinetic isotope effects and double isotope fractionation would be particularly revealing. It is also appreciated that tedious, expensive, and time-consuming experiments are required to conduct such a rigorous mechanistic inquiry, a challenge encountered by all workers in this field.

**3.5. Spinosyn A Biosynthesis.** The fascinating biosynthesis of spinosyn A was recently investigated by Liu et al., and these workers identified the polyketide synthase expressed from the SpnF gene of *Saccharopolyspora spinosa*, suggesting SpnF serves as a natural Diels–Alderase that catalyzes a [4 + 2] cycloaddition in the formation of the cyclohexene ring core of spinosyn A.[40] The authors suggested that this represents the first example of an enzyme whose sole purpose is to catalyze a Diels–Alder reaction, and the basis for such a claim in the context of the lovastatin biosynthesis discussed above resides on the fact that LovB is a multifunctional PKS. The biosynthetic gene cluster of *S. spinosyn* for Spinosyn A also includes SpnJ, SpnL, and SpnM, which were also initially proposed to code for an enzyme that converts product **27** to **29** (Figure 13).[40]

To elucidate if the SpnF cyclase was a true Diels–Alderase, conversion of **27** to cyclized product **29** was observed after a 2 h incubation period with the SpnM gene product and monitored by HPLC.[40] Analysis by NMR, mass spectrometry, and further investigation by HPLC of the reaction time-course led to the discovery of intermediate **28**, identified by spectral analysis.[40] The presence of the monocyclic macrolactone intermediate represents a possible 2-step process that includes a dehydration step followed by the cycloaddition as shown in Figure 13.[40] To determine if the enzyme expressed by the SpnM gene catalyzes both the dehydration and cycloaddition steps, dependence of the rate of each step on the concentration of the SpnM-coded enzyme was determined by HPLC (consumption vs time).[40] Rate enhancement of the dehydration step was observed with an increase in SpnM gene product concentration and the cyclization step was unaffected.[40] While data from Michaelis–Menten kinetics and first order kinetics suggest the cyclization can take place nonenzymatically, the remaining genes from the gene cluster were in turn interrogated. Incubation of SpnF with **28** produced the desired bicyclic species **29** in 20 min, which was compared to the 2 h nonenzymatic reaction time.[40] In order to measure the effect of the SpnF enzyme on the rate of cyclization, HPLC was used with a fixed concentration of SpnM with time as a function of SpnF. Michaelis–Menten kinetics established that SpnF encoded a potential Diels–Alderase in the catalytic conversion of **28** to **29** with an apparent $k_{cat}$ of 14 ± 1.6 $min^{-1}$ for an approximated rate enhancement of 500-fold.[40]



DOI: 10.1021/acs.joc.5b01951
J. Org. Chem. 2015, 80, 11672–11685

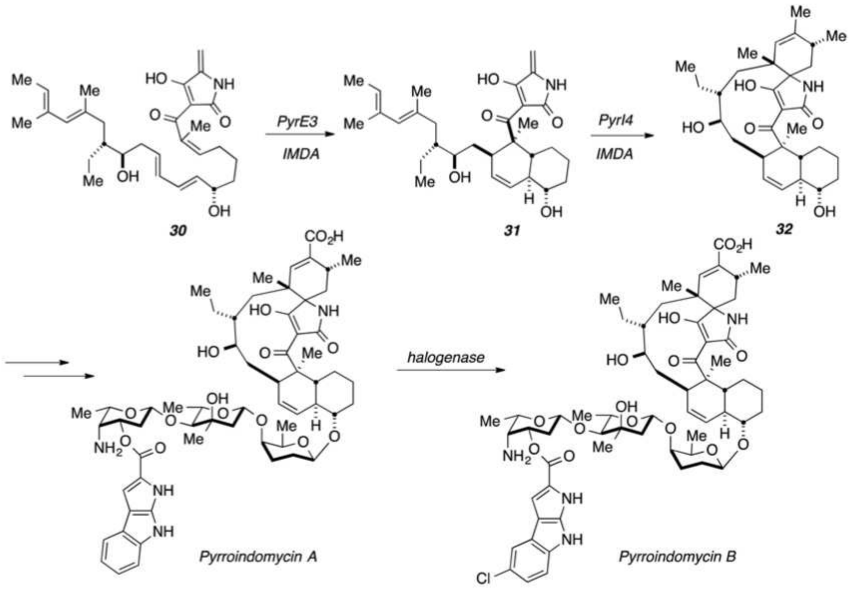


**Figure 14.** Proposed biosynthesis of pyrroindomycins with PyrE3 and PyrI4 as cyclases.

Recent X-ray crystal structure elucidation of the enzyme by Keatinge-Clay et al. was obtained to probe further the putative mechanism of the SpnF-coded PKS-catalyzed cyclization.[41] While the enzyme of interest resembles S-adenosylmethionine (SAM)-dependent methyltransferases (SAM MTs), the activity of SAM MTs could give insight into the activity of the stand-alone enzyme. The activity of SAM MTs in these particular cyclization reactions is currently unknown.[41] The authors conclude, however, that *"The mechanisms by which SpnF and SpnL catalyse their respective cyclization reactions are a point of interest. The SpnF-catalysed endo mode syn-addition of an alkenyl to a dienyl functionality seems consistent with a Diels–Alder reaction; however, confirmation of this hypothesis will require demonstrating that the reaction progresses through a single pericyclic transition state such as [6]. Therefore, a stepwise [4+2] cycloaddition mechanism, for example, one involving a dipolar intermediate such as [7], cannot at present be ruled out."* This comment again gets to the heart of the purely academic argument pervasive in this field regarding the high-resolution details of the synchronicity of the C–C bond-forming step and the exact nature of the transition state.

**3.6. Biosynthesis of Pyrroindomycins.** Biosynthetic studies of the naturally occurring pyrroindomycins, the first naturally occurring spirotetramates, isolated by Ding et al., suggests that the pentacyclic core is constructed via two distinct, sequential [4 + 2] cycloadditions.[42] Bioinformatic analysis of the previously established biosynthetic gene cluster provided two candidates, pyrE3 and pyrI4.[42c] Known functions of enzymes homologous to PyrE3 and PyrI4 suggested that PyrI4 to be responsible for the formation of spiro-indole **32**, via dialkydecalin (**31**) construction by PyrE3 (Figure 14).[42c]

Deactivation of PyrE3 resulted in the isolation of intermediate **30**, while inactive enzymes PyrE3 and PyrI4 failed to generate pyrroindomycins A and B.[42c] Structure elucidation of **30** was confirmed by NMR and mass spectrometry analysis and is consistent with the previously proposed biosynthesis.[42c] Further investigation required addition of both purified enzymes PyrE3 and PyrI4 to intermediate **30** with no additional cofactors.[42c] The enzymes collectively converted **30** into **32** validated by structural characterization.

Based on initial gene disruption and metabolite accumulation studies, the individual function of PyrE3 and PyrI4 was investigated. Incubation of **30** with PyrE3 resulted in essentially complete conversion into **31**, but no reaction occurred in the presence of PyrI4 alone. ESI-MS analysis and site-directed mutagenesis studies were successful in identifying and subsequently determining the dependence of flavin adenine dinucleotide (FAD) for PyrE3 activity. It was assumed that FAD influences the geometry of the active site during the PyrE3-mediated cycloaddition, which was further supported by electronic circular dichroism (ECD) spectra analysis of related proteins in the presence and absence of the FAD cofactor. Intermediate **31** did not convert into **32** upon incubation in aqueous media without the presence of PyrI4.[42c] While this suggests a nonspontaneous, and specifically enzyme-mediated [4 + 2] reaction, initial studies revealed a dependence of PyrI4 activity on the dialkyldecalin system represented as intermediate **31**. Steady-state kinetics indicated a moderate efficiency for the enzymatic conversion of **30** into **31** and **31** into **32**.

**3.7. Thiazolyl Peptide Biosynthesis.** Recent investigations of the remarkably complex thiazolyl peptide biosynthesis by Bowers and co-workers, suggests that a single enzyme, TclM catalyzes the final macrocyclization step that was previously suggested to proceed via a [4 + 2] cycloaddition between dehydroalanine residues (Dha).[43] These investigators synthesized thiocillin **33** to interrogate the enzymatic reaction with


DOI: 10.1021/acs.joc.5b01951
J. Org. Chem. 2015, 80, 11672–11685

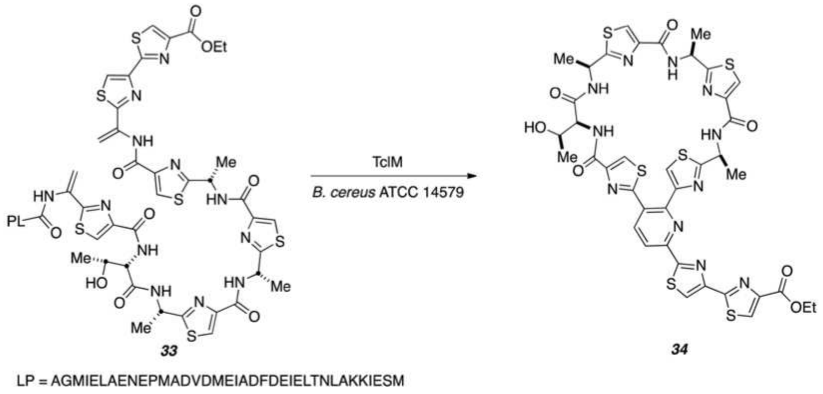


**Figure 15.** Biosynthesis of thiocillin **34** via TclM as cyclase.

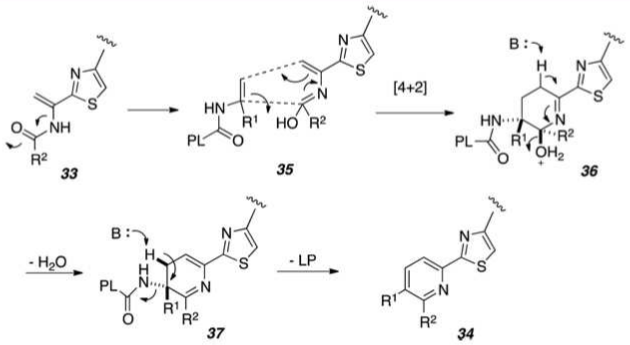


**Figure 16.** Proposed mechanism for the transformation of **33** to **34** in the presence of TclM.

TclM in hopes of forming cycloaddition product **34** (Figure 15).[43]

Substrate **33** was incubated with purified *TclM* gene for 20 h and monitored by high-resolution quadrupole time-of-flight (QTOF) LC/MS and UV–vis. Over time, a new absorption peak was observed as well as full consumption of the intermediate indicative of substrate **33**. The new peak was potentially **34** as the wavelength observed is consistent with that of thiazolyl peptides with the same trisubstituted pyridine core. Further investigation by NMR spectroscopy shows evidence of aromatic protons from the pyridine ring and observation by LC/MS shows an $m/z$ that matches the desired product as well as appropriate fragmentation patterns.[43]

While it is evident that TclM catalyzes the formation of the trisubstituted core present in product **34**, the nature of the mechanism in its formation remains unclear. Figure 16 represents the proposed [4 + 2] cycloaddition mechanism for the net transformation of **33** to **34**.[43] The authors were careful to designate this assembly as a "formal [4 + 2] cycloaddition" and did not overstate the case for TclM necessarily representing a true Diels–Alderase. TclM also apparently conducts the aromatization to the final pyridine ring as putative intermediates corresponding to the intermediate species **36** and **37** were not detectable. Here again, access to the recombinant enzyme provides an ideal opportunity to study the mechanism of this fascinating macrocyclic assembly at high resolution that might involve the intermediacy of a biosynthetic Diels–Alder construction.

**3.8. Stephacidin–Notoamide and Paraherquamide Biosynthesis.** Our laboratories have been studying the biosynthesis of a large family of fungal alkaloids including the dioxopiperazine-containing stephacidins, notoamides, and brevianamides and the related monooxopiperazine alkaloids including the paraherquamides, marcfortines, malbrancheamides, and asperparalines for some time.[44] All of these alkaloids contain a bicyclo[2.2.2]diazaoctane core that is the result of the net oxidative cyclization of a reverse-isoprene moiety to the two $\alpha$-carbons of the amino acid units, typically derived from tryptophan and proline or a proline analogue. Biomimetic laboratory intramolecular Diels–Alder reactions, which occur at ambient temperature and below in aqueous media, provide indirect support for the putative biosynthetic assembly processes.

What is further remarkable about stephacidin–notoamide biosynthesis is the observation that two distinct pairs of terrestrial and marine-derived orthologous *Aspergillus* sp. produce opposite enantiomers of stephacidin A and notoamide B (100% er). We have postulated that the key enantiodivergent step is also the formal [4 + 2] cycloaddition reaction that all


DOI: 10.1021/acs.joc.5b01951
J. Org. Chem. 2015, 80, 11672–11685

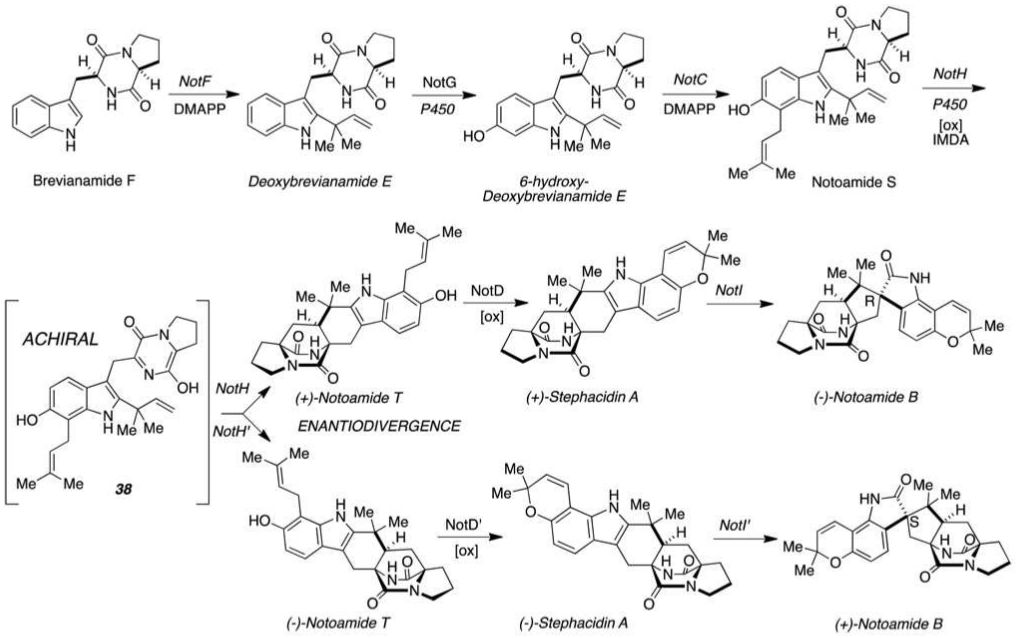


**Figure 17.** Proposed enantiodivergent biogenesis of the stephacidins and notoamides through a formal [4 + 2] cycloaddition.

experimental evidence indicates arises through a common *achiral* azadiene (**38**) as shown in Figure 17.

Whole genome sequencing and bioinformatics analyses of the identified gene clusters has revealed that the conversion of notoamide S into notoamide T appears to be conducted by a cytochrome P450 NotH.[44d] [4] That the putative intermediate IMDA substrate **38** is *achiral* and that the final natural products are optically pure strongly implicates preorganization of the isoprene moiety relative to the azadiene in the active site of the enzyme. It is also noteworthy that the identical Diels–Alder reaction has been successfully conducted through a biomimetic total synthesis producing racemic notoamide T in a 2.4:1 *syn*/*anti*-diasteromeric ratio.

We have recently determined that the biosynthesis of the monooxopiperazine alkaloids (such as paraherquamide and malbrancheamide) and the dioxopiperazine alkaloids (such as stephacidin and notoamide B) arise by distinct pathways but appear to converge on the formation of an azadiene intermediate (**38**) that suffers a net formal [4 + 2] cycloaddition to form the bicyclo[2.2.2]diazaoctane ring system, albeit in two distinct oxidation states (Figure 18, Z = O or $H_2$). Based on our current understanding of the pathway and biosynthetic enzyme function, we hypothesize that the primary function of the enzymes responsible for fashioning the bicyclo[2.2.2]diazaoctane ring systems are oxidation (for the diooxopiperazines) and possibly prenyl transfer or reduction for the monooxopiperazines and are not specifically cyclases. Attempts to functionally express NotH in a heterologous host have not been successful to date and constitute a major focus of our current efforts. In both families of alkaloids, a reactive intermediate is formed in the chiral and conformationally restricted environment of the enzyme active site, which presumably preorganizes the conformation of the azadiene relative to the isoprene moiety resulting in highly enantioselective and diastereoselective cycloadditions. Here as in other systems discussed in this article, the cycloaddition reaction appears to be a fortuitous "auxiliary reaction" leading to new molecular complexity. There is ample evidence that chemical diversification in secondary metabolism is driven by these fascinating "experiments" in enzyme evolution.[45]

**3.9. Versipelostatin.** The synthesis of polyketides is attractive due to the wide variety of pharmaceutical drugs developed from this class of compounds. Their structural variety includes a spirotetronate core, which is proposed to arise from an IMDA.[46] Figure 19 shows the biosynthetic transformation of versipelostatin. To test this proposition, inactivation of the *VstJ* gene resulted in loss of versipelostatin formation and accumulation of an acyclic intermediate (**42**), as shown by liquid chromatography–mass spectrometry (LC/MS) analysis.[46] Further analysis with incubation of purified enzyme with the isolated intermediate, substrate **42**, and Michaelis–Menten kinetics reveal the nonspontaneous catalytic character of VstJ in the biosynthesis of the spirotetronate **44**.[46] Activation of the dienophile and stabilization of the *cis*-diene must be provided by organization and hydrogen bonding within the active site, respectively.

## 4. CONCLUSION

There are at least nine biosynthetic systems to date that have been identified to contain natural enzymes claimed to function as the key cyclase in biosynthetic transformations that appear to constitute biosynthetic formal [4 + 2] cycloadditions or Diels–



DOI: 10.1021/acs.joc.5b01951
J. Org. Chem. 2015, 80, 11672–11685

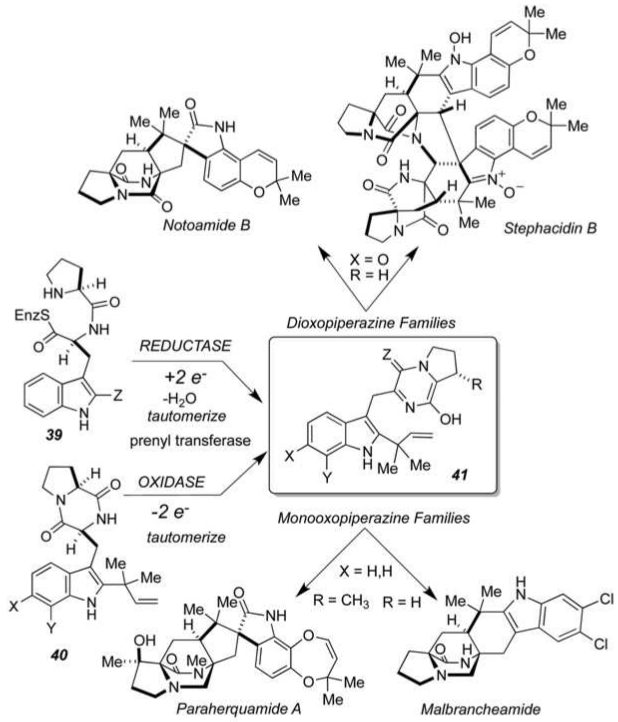


**Figure 18.** Unified biosynthesis of the monooxopiperazine and dioxopiperazine families of alkaloids containing a bicyclo[2.2.2]diazaoctane ring system.

Alder-type constructions. Despite the increasing sophistication of mechanistic tools—both theoretical and experimental—to study the concerted nature of putative enzyme-mediated and/or specifically enzyme-catalyzed biosynthetic Diels–Alder constructions, much remains to be investigated, and rigorous and corroborating biophysical evidence remains elusive.

The fundamental mechanistic conundrum for Diels–Alderases is the issue of turnover. Virtually all known enzymatic reactions lower the activation energy to effect rate acceleration by stabilizing the structure, charge, and geometry of the developing transition state, which does not typically resemble the product structure. For the Diels–Alder reaction, however, the transition state and the product are highly homologous structurally, which would manifest as product inhibition begging the question of how turnover is achieved. This very problem of turnover was evident in the work of Schultz and Hilvert, who designed and generated catalytic antibodies for the Diels–Alder reaction using transition-state mimics as haptens.[47]

In the case of systems where the putative Diels–Alderase is an enzyme that evolved to perform a distinct biochemical transformation, such as oxidation, generating the reactive substrate in the chiral environment of the active site, turnover is presumably not affected by product inhibition. In such systems, such as the solanapyrone and stephacidin biosyntheses discussed above, conformational restriction of the reactive substrate as it is generated in the active site is predisposed to undergo the subsequent "side reaction" of cycloaddition. The entropic benefit of conformational restriction certainly must contribute to increase the rate of the cycloaddition step relative to the laboratory reaction and would also plausibly impact stereoselectivity relative to the laboratory reaction. In fact, the relative changes in stereoselectivity between the cycloaddition reaction in the presence and absence of enzyme has been used, perhaps incorrectly, as "experimental evidence" to support the pericyclic mechanism of these enzyme-mediated transformations. Extreme care should be exercised in this regard when comparing the laboratory reaction (where feasible) to the protein-mediated transformation. Differences in stereoselectivity only reveal that the protein-mediated reaction has a distinct stereoselectivity and does not penetrate the subtle mechanistic details of the protein-mediated reaction.

These authors remain circumspect as to whether a true Diels–Alderase exists that evolved to specifically catalyze the Diels–Alder reaction through the concerted, synchronous pericyclic transition state required. Yet this becomes essentially a philosophical argument as the experimental rigor required to prove that a pericyclic transition state is operative to the exclusion of alternative stepwise, nonsynchronous, or highly asynchronous mechanisms will inevitably loom. In particular, nonenzymatic, synthetic chemical Diels–Alder reactions where the spectrum of substrates, which can undergo cycloaddition through a strictly concerted, synchronous mechanism controlled by orbital symmetry considerations, typically require symmetrical substrates rarely found in natural products studied


DOI: 10.1021/acs.joc.5b01951
J. Org. Chem. 2015, 80, 11672–11685

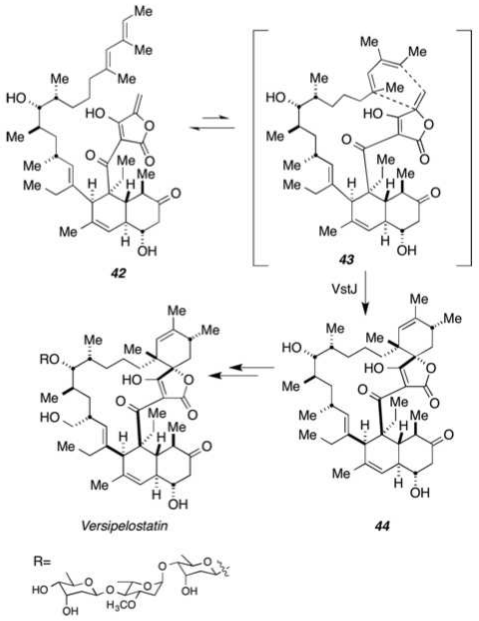


**Figure 19.** Biosynthesis of versipelostatin with VstJ as cyclase.

to date in this context. The polyketide synthases identified in the pyrroindomycin and spinosyn biosyntheses appear to constitute enzymes identified to catalyze a formal [4 + 2] cycloaddition reaction as their sole function.[46] Chemists have been irresistibly drawn to the biosynthetic Diels–Alder construction for the allure of penetrating how Nature has been able to exploit so many chemical reactions familiar in synthetic chemistry to assemble molecular complexity and molecular diversity in primary metabolites and especially secondary metabolites. That Nature might have "accidentally" stumbled upon the Diels–Alder reaction or, more precisely based on the current body of experimental evidence, formal [4 + 2] cycloaddition reactions in the course of secondary metabolic enzyme tailoring is certainly evident, and numerous examples of nonenzyme-catalyzed biosynthetic Diels–Alder constructions are known.[2] The biological activity of such natural substances, if providing an adaptive benefit to the producing organism, furnishes the evolutionary driving force to preserve, propagate, and modify such enzymes. This field remains an area worthy of additional experimentation, theoretical analysis, and pedagogical vetting. As one of the most significant reactions in synthetic organic chemistry, it is very exciting to contemplate the extent to which Nature has interrogated formal [4 + 2] cycloaddition constructions. What remains as an open, and largely unresolved issue, is the extent to which formal [4 + 2] constructions mediated and/or catalyzed enzymatically proceed through concerted, or mostly synchronous, bond constructions as required for a true pericyclic transformation. The same problems here in the formal [4 + 2] cycloadditions evident in Nature permeated an extensive series of papers on chorismate mutase, formally an enzyme-catalyzed Claisen rearrangement.[48]

## AUTHOR INFORMATION

**Corresponding Author**

*E-mail: robert.williams@colostate.edu.

**Notes**

The authors declare no competing financial interest.

**Biography**

Robert M. Williams was born in New York in 1953 and attended Syracuse University where he received a B.A. degree in Chemistry in 1975. He obtained a Ph.D. degree in 1979 at MIT (W. H. Rastetter) and was a postdoctoral fellow at Harvard (1979–1980; R. B. Woodward/Yoshito Kishi). He joined Colorado State University in 1980 and was named a University Distinguished Professor in 2002. His interdisciplinary research program (over 300 publications) at the chemistry–biology interface is focused on the total synthesis of biomedically significant natural products, biosynthesis of secondary metabolites, studies on antitumor drug–DNA interactions, HDAC inhibitors, amino acids, and peptides.

## ACKNOWLEDGMENTS

Our research work in this field has been supported by the National Institutes of Health (Grant No. RO1 CA070375). We also acknowledge Professor Craig Townsend, Professor John C. Vederas, and Professor Christopher Walsh for stimulating discussions and insight.

## DEDICATION

This paper is dedicated to the memory of Professor Robert Burns Woodward and his myriad accomplishments and contributions to science.

## REFERENCES

(1) (a) Laschat, S. *Angew. Chem., Int. Ed. Engl.* **1996**, *35*, 289–291. (b) Stocking, E. M.; Williams, R. M. *Angew. Chem., Int. Ed.* **2003**, *42*, 3078–3115.
(2) Oikawa, H. *Bull. Chem. Soc. Jpn.* **2005**, *78*, 537–554.
(3) (a) Kelly, W. L. *Org. Biomol. Chem.* **2008**, *6*, 4483–4493. (b) Kim, H. J.; Ruszczycky, M. W.; Liu, H. W. *Curr. Opin. Chem. Biol.* **2012**, *16*, 124–131.
(4) Sauer, J.; Sustmann, R. *Angew. Chem., Int. Ed. Engl.* **1980**, *19*, 779–807.
(5) (a) Houk, K. N. *J. Am. Chem. Soc.* **1973**, *95*, 4092–4094. (b) Houk, K. N.; Strozier, R. *J. Am. Chem. Soc.* **1973**, *95*, 4094–4096.
(6) Houk, K. N. *Proc. Natl. Acad. Sci. U. S. A.* **2012**, *109*, 12860–12865.
(7) Inukai, T.; Kojima, T. J. *J. Org. Chem.* **1966**, *31*, 1121–1123.
(8) Houk, K. N. *Acc. Chem. Res.* **1975**, *8*, 361–369.
(9) Hoffmann, R.; Woodward, R. B. *J. Am. Chem. Soc.* **1965**, *87*, 4388–4389.



DOI: 10.1021/acs.joc.5b01951
*J. Org. Chem.* 2015, 80, 11672–11685

(10) Woodward, R. B.; Katz, T. *Tetrahedron* **1959**, *5*, 70.
(11) Dewar, M. J. S.; Olivella, S.; Rzepa, H. S. *J. Am. Chem. Soc.* **1978**, *100*, 5650−5660.
(12) (a) Dewar, M. J. S.; Griffin, A. C.; Kirschner, S. *J. Am. Chem. Soc.* **1974**, *96*, 6225−6226. (b) Dewar, M. J. S.; Olivella, S.; Stewart, J. J. P. *J. Am. Chem. Soc.* **1986**, *108*, 5771−5779.
(13) Dewar, M. J. S. *J. Am. Chem. Soc.* **1984**, *106*, 209−219.
(14) Li, Y.; Houk, K. N. *J. Am. Chem. Soc.* **1993**, *115*, 7478−7485.
(15) Beno, B. R.; Wilsey, S.; Houk, K. N. *J. Am. Chem. Soc.* **1999**, *121*, 4816−4826.
(16) Chen, J. S.; Houk, K. N.; Foote, C. S. *J. Am. Chem. Soc.* **1998**, *120*, 12303−12309.
(17) (a) Townshend, R. E.; Ramunni, G.; Segal, G.; Hehre, W. J.; Salem, L. *J. Am. Chem. Soc.* **1976**, *98*, 2190−2198. (b) Burke, L. A.; Leroy, G.; Sana, M. *Theor. Chim. Acta* **1975**, *40*, 313.
(18) Bernardi, F.; Botoni, A.; Robb, M. A.; Field, M. J.; Hillier, I. H.; Guest, M. F. *J. Chem. Soc., Chem. Commun.* **1985**, 1051−1052.
(19) Gajewski, J. J.; Peterson, K. B.; Kagel, J. R.; Huang, Y. C. J. *J. Am. Chem. Soc.* **1989**, *111*, 9078−9081.
(20) Loncharich, R. J.; Brown, F. K.; Houk, K. N. *J. Org. Chem.* **1989**, *54*, 1129−1135.
(21) Bernardi, F.; Bottoni, A.; Field, M. J.; Guest, M. F.; Hillier, I. H.; Robb, M. A.; Venturini, A. *J. Am. Chem. Soc.* **1988**, *110*, 3050−3055.
(22) (a) McIver, J. W. *J. Am. Chem. Soc.* **1975**, *97*, 3632. (b) McIver, J. W. *Acc. Chem. Res.* **1974**, *7*, 72.
(23) Singleton, D. A. *Tetrahedron* **2001**, *57*, 5149−5160.
(24) Hancock, R. A.; Wood, B. F. *J. Chem. Soc., Chem. Commun.* **1988**, 351−353.
(25) Froese, R. D. J.; Coxon, J. M.; West, S. C.; Morokuma, K. *J. Org. Chem.* **1997**, *62*, 6991−6996.
(26) Singleton, D. A.; Thomas, A. A. *J. Am. Chem. Soc.* **1995**, *117*, 9357−9358.
(27) Oikawa, H.; Katayama, K.; Suzuki, Y.; Ichihara, A. *J. Chem. Soc., Chem. Commun.* **1995**, 1321−1322.
(28) Oikawa, H.; Suzuki, Y.; Naya, A.; Katayama, K.; Ichihara, A. *J. Am. Chem. Soc.* **1994**, *116*, 3605−3606.
(29) (a) Katayama, K.; Kobayashi, T.; Oikawa, H.; Honma, M.; Ichihara, A. *Biochim. Biophys. Acta, Protein Struct. Mol. Enzymol.* **1998**, *1384*, 387−395. (b) Oikawa, H.; Kobayashi, T.; Katayama, K.; Suzuki, Y.; Ichihara, A. *J. Org. Chem.* **1998**, *63*, 8748−8756.
(30) Kasahara, K.; Miyamoto, T.; Fujimoto, T.; Oguri, H.; Tokiwano, T.; Oikawa, H.; Ebizuka, Y.; Fujii, I. *ChemBioChem* **2010**, *11*, 1245−1252.
(31) Auclair, K.; Sutherland, A.; Kennedy, J.; Witter, D. J.; van de Heever, J. P.; Hutchinson, C. R.; Vederas, J. C. *J. Am. Chem. Soc.* **2000**, *122*, 11519−11520.
(32) Ma, S. M.; Li, J. W.-H.; Choi, J. W.; Zhou, H.; Lee, K. K. M.; Moorthie, V. A.; Xie, X.; Kealey, J. T.; Da Silva, N. A.; Vederas, J. C.; Tang, Y. *Science* **2009**, *326*, 589−593.
(33) Kennedy, J.; Auclair, K.; Kendrew, S. G.; Park, C.; Vederas, J. C.; Hutchinson, C. R. *Science* **1999**, *284*, 1368−1372.
(34) Watanabe, K.; Mie, T.; Ichihara, A.; Oikawa, H.; Honma, M. *J. Biol. Chem.* **2000**, *275*, 38393−38401.
(35) Ose, T.; Watanabe, K.; Mie, T.; Honma, M.; Watanabe, H.; Yao, M.; Oikawa, H.; Tanaka, I. *Nature* **2003**, *422*, 185−189.
(36) Guimaraes, C. R. W.; Udier-Blagovic, M.; Jorgensen, W. L. *J. Am. Chem. Soc.* **2005**, *127*, 3577−3588.
(37) Serafimov, J. M.; Gillingham, D.; Kuster, S.; Hilvert, D. *J. Am. Chem. Soc.* **2008**, *130*, 7798−7799.
(38) (a) Eberhardt, S.; Zingler, N.; Kemter, K.; Richter, G.; Cushman, M.; Bacher, A. *Eur. J. Biochem.* **2001**, *268*, 4315−4323. (b) Kim, R.-R.; Illarionov, B.; Joshi, M.; Cushman, M.; Lee, C. Y.; Eisenreich, W.; Fischer, M.; Bacher, A. *J. Am. Chem. Soc.* **2010**, *132*, 2983−2990.
(39) Breugst, M.; Eschenmoser, A.; Houk, K. N. *J. Am. Chem. Soc.* **2013**, *135*, 6658−6668.
(40) Kim, H. J.; Ruszczycky, M. W.; Choi, S.-H.; Liu, Y.-N.; Liu, H.-W. *Nature* **2011**, *473*, 109−112.
(41) Fage, C. D.; Isiorho, E. A.; Liu, Y.; Wagner, D. T.; Liu, H.-W.; Keatinge-Clay, A. T. *Nat. Chem. Biol.* **2015**, *11*, 256−260.
(42) (a) Ding, W.; Williams, D. R.; Northcote, P.; Siegel, M. M.; Tsao, R.; Ashcroft, J.; Morton, G. O.; Alluri, M.; Abbanat, D.; Maiese, W. M.; Ellestad, G. A. *J. Antibiot.* **1994**, *47*, 1250−1257. (b) Singh, M. P.; Petersen, P. J.; Jacobus, N. V.; Mroczenski-Wildey, M. J.; Maiese, W. M.; Greenstein, M.; Steinberg, D. A. *J. Antibiot.* **1994**, *47*, 1258−1265. (c) Tian, Z.; Sun, P.; Yan, Y.; Wu, Z.; Zheng, Q.; Zhou, S.; Zhang, H.; Yu, F.; Jia, X.; Chen, D.; Mandi, A.; Kurtan, T.; Liu, W. *Nat. Chem. Biol.* **2015**, *11*, 259−268.
(43) Wever, W. J.; Bogart, J. W.; Baccile, J. A.; Chan, A. N.; Schroeder, F. C.; Bowers, A. A. *J. Am. Chem. Soc.* **2015**, *137*, 3494−3497.
(44) (a) Li, S.; Srinivasan, K.; Tran, H.; Yu, F.; Finefield, J. M.; Sunderhaus, J. D.; McAfoos, T. J.; Tsukamoto, S.; Williams, R. M.; Sherman, D. H. *MedChemComm* **2012**, *3*, 987−996. (b) Finefield, J. M.; Frisvad, J.; Williams, R. M. *J. Nat. Prod.* **2012**, *75*, 812−833. (c) Sunderhaus, J. D.; Williams, R. M. *Isr. J. Chem.* **2011**, *51*, 442−452. (d) Ding, Y.; de Wet, J. R.; Cavalcoli, J.; Li, S.; Greshock, T. J.; Miller, K. A.; Finefield, J. M.; Sunderhaus, J. D.; McAfoos, T.; Tsukamoto, S.; Williams, R. M.; Sherman, D. H. *J. Am. Chem. Soc.* **2010**, *132*, 12733−12740. (e) Townsend, C. A. *ChemBioChem* **2011**, *12*, 2267−2269.
(45) Gu, L.; Wang, B.; Kulkarni, A.; Geders, T. W.; Grindberg, R. V.; Gerwick, L.; Hakansson, K.; Wipf, P.; Smith, J. L.; Gerwick, W. H.; Sherman, D. H. *Nature* **2009**, *459*, 731−735.
(46) Hashimoto, T.; Hashimoto, J.; Teruya, K.; Hirano, T.; Shin-ya, K.; Ikeda, H.; Liu, H.; Nishiyama, M.; Kuzuyama, T. *J. Am. Chem. Soc.* **2015**, *137*, 572−575.
(47) (a) Romesberg, F. E.; Spiller, B.; Schultz, P. G.; Stevens, R. C. *Science* **1998**, *279*, 1929−1933. (b) Xu, J.; Deng, Q.; Chen, J.; Houk, K. N.; Bartek, J.; Hilvert, D.; Wilson, I. A. *Science* **1999**, *286*, 2345−2348. (c) Piatesi, A.; Hilvert, D. *ChemBioChem* **2004**, *5*, 460−466. (d) Braisted, A. C.; Schultz, P. G. *J. Am. Chem. Soc.* **1990**, *112*, 7430−7431. (e) Hilvert, D.; Hill, K. W.; Nared, K. D.; Auditor, M. T. M. *J. Am. Chem. Soc.* **1989**, *111*, 9261−9262. (f) Piatesi, A.; Aldag, C.; Hilvert, D. *J. Mol. Biol.* **2008**, *377*, 993−1001. (g) Verdino, P.; Aldag, C.; Hilvert, D.; Wilson, I. A. *Proc. Natl. Acad. Sci. U. S. A.* **2008**, *105*, 11725−11730.
(48) (a) Ganem, B. *Angew. Chem., Int. Ed. Engl.* **1996**, *35*, 936−945. (b) Belasco, J. G.; Albery, W. J.; Knowles, J. R. *J. Am. Chem. Soc.* **1983**, *105*, 2475−2477. (c) Sogo, S. G.; Widlanski, T. S.; Hoare, J. H.; Grimshaw, C. E.; Berchtold, G. A.; Knowles, J. R. *J. Am. Chem. Soc.* **1984**, *106*, 2701−2703. (d) Guimarães, C. R. W.; Repasky, M. P.; Chandrasekhar, J.; Tirado-Rives, J.; Jorgensen, W. L. *J. Am. Chem. Soc.* **2003**, *125*, 6892−6899. (e) Wright, S. K.; DeClue, M. S.; Mandal, A.; Lee, L.; Wiest, O.; Cleland, W. W.; Hilvert, D. *J. Am. Chem. Soc.* **2005**, *127*, 12957−12964 and references cited therein.



DOI: 10.1021/acs.joc.5b01951
*J. Org. Chem.* 2015, 80, 11672−11685

# Appendix V: Structural and Stereochemical Diversity in Prenylated Indole Alkaloids Containing the Bicyclo [2.2.2]diazaoctane Ring System from Marine and Terrestrial Fungi

This is the manuscript that corresponds to chapter one and is published in *Natural Product Reports.*[1]

Natural Product Reports

REVIEW

View Article Online
View Journal | View Issue



Cite this: *Nat. Prod. Rep.*, 2018, **35**, 532

# Structural and stereochemical diversity in prenylated indole alkaloids containing the bicyclo [2.2.2]diazaoctane ring system from marine and terrestrial fungi

Kimberly R. Klas,[a] Hikaru Kato,[b] Jens C. Frisvad,[c] Fengan Yu,[d] Sean A. Newmister,[d] Amy E. Fraley,[d] David H. Sherman,*[d] Sachiko Tsukamoto*[b] and Robert M. Williams*[ae]

Covering: up to February 2017

Various fungi of the genera *Aspergillus*, *Penicillium*, and *Malbranchea* produce prenylated indole alkaloids possessing a bicyclo[2.2.2]diazaoctane ring system. After the discovery of distinct enantiomers of the natural alkaloids stephacidin A and notoamide B, from *A. protuberus* MF297-2 and *A. amoenus* NRRL 35660, another fungi, *A. taichungensis*, was found to produce their diastereomers, 6-*epi*-stephacidin A and versicolamide B, as major metabolites. Distinct enantiomers of stephacidin A and 6-*epi*-stephacidin A may be derived from a common precursor, notoamide S, by enzymes that form a bicyclo[2.2.2] diazaoctane core *via* a putative intramolecular hetero-Diels–Alder cycloaddition. This review provides our current understanding of the structural and stereochemical homologies and disparities of these alkaloids. Through the deployment of biomimetic syntheses, whole-genome sequencing, and biochemical studies, a unified biogenesis of both the dioxopiperazine and the monooxopiperazine families of prenylated indole alkaloids constituted of bicyclo[2.2.2]diazaoctane ring systems is presented.

Received 25th August 2017

DOI: 10.1039/c7np00042a

rsc.li/npr





[a]*Department of Chemistry, Colorado State University, 1301 Center Avenue, Fort Collins, CO 80523, USA. E-mail: robert.williams@colostate.edu*

[b]*Graduate School of Pharmaceutical Sciences, Kumamoto University, 5-1 Oe-honmachi, Kumamoto 862-0973, Japan. E-mail: sachiko@kumamoto-u.ac.jp*

[c]*Section for Eukaryotic Biotechnology, Departments of System Biology, Technical University of Denmark, Building 221, 2800 Kongens Lyngby, Denmark*

[d]*Life Sciences Institute, Departments of Medicinal Chemistry, Chemistry, Microbiology & Immunology, The University of Michigan, 210 Washtenaw Avenue, Ann Arbor, MI 48109-2216, USA. E-mail: davidhs@umich.edu*

[e]*University of Colorado, Cancer Center, Aurora, Colorado 80045, USA*

## 1. Introduction

The isolation of natural products from marine and terrestrial-derived fungal species of the *Aspergillus*, *Penicillium* and related genera has allowed for a widely studied diverse class of secondary metabolites. In particular, various prenylated indole alkaloids have been discovered, including the brevianamides,[1–7] marcfortines,[8,9] paraherquamides,[10–14] penicimutamides,[15]

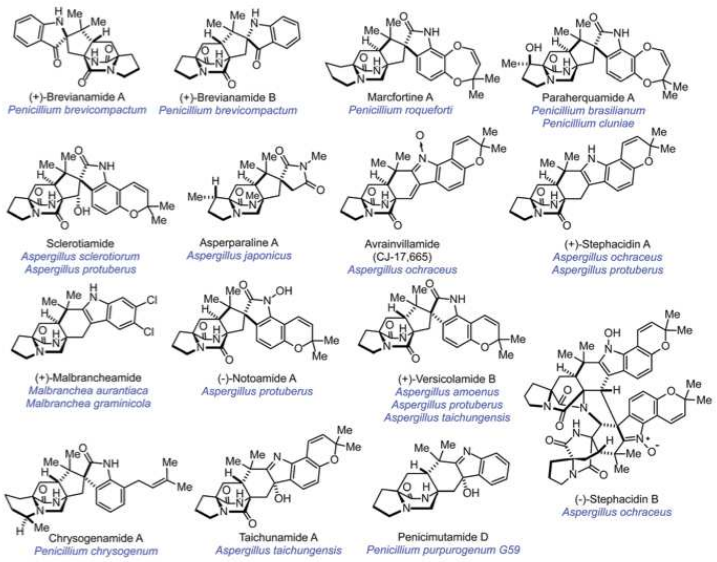


Fig. 1 Structures of representative prenylated indole alkaloids isolated from fungi of the genera *Aspergillus*, *Penicillium*, and *Malbranchea*.

sclerotiamide,[16] asperparalines,[17] avrainvillamide,[18,19] stephacidins,[20] malbrancheamides,[21–23] notoamides,[24–27] versicolamide B,[28] chrysogenamide,[29] and recently the taichunamides (Fig. 1).[30] The presence of a bicyclo[2.2.2]diazaoctane ring system and densely functionalized indole-derived units form the bases for the structural allure of these naturally occurring metabolites. Many of these alkaloids have been found to show a variety of biological activity including insecticidal, cytotoxic, anthelmintic, calmodulin inhibition,[31] osteoclast inhibition, and antibacterial properties.[1–3,5,8–30,32–34] Reviews in this area have included the studies on the discovery of unexpected enantiomeric and diastereomeric relationships (Fig. 2) (see Section 2) as well as developments in the biosynthesis of these compounds (see Section 3), and biomimetic total syntheses (see Section 4).[35–41] Herein, this review will focus on the biogenesis of the notoamides and their congeners, and provide the current understanding of the structural and stereochemical homologies and disparities that are particularly intriguing from a biosynthetic perspective.

Elucidation of the biogenesis of these compounds became of particular interest upon the isolation of antipodal metabolites from different species of the *Aspergillus* genus from both marine and terrestrial sources. Initial studies from the Williams laboratory[42] were based on seminal work first reported by Sammes[43] and Birch,[44] and demonstrated that these natural metabolites arise from L-tryptophan, one or two isoprene units, and L-proline, β-methylproline, or pipecolic acid.

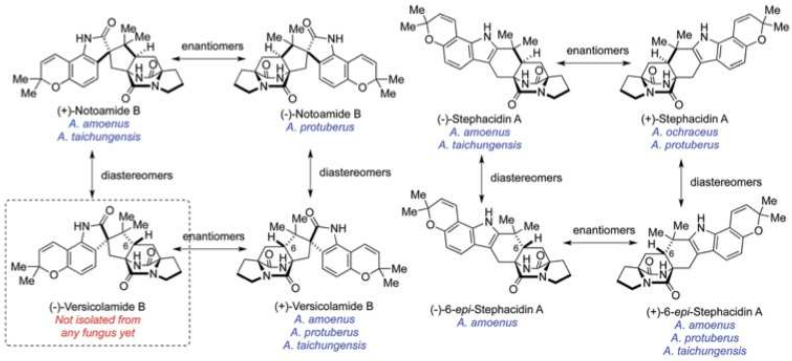


Fig. 2 Structures of several prenylated indole alkaloids isolated from fungi and their stereochemical relationships.

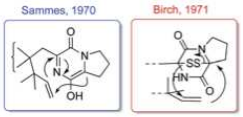


Fig. 3 Early suggestions of Sammes[43] and Birch[45] concerning the biogenesis of the bicyclo[2.2.2]diazaoctane ring system in the brevianamides.

The first proposal concerning the biogenesis of the bicyclo [2.2.2]diazaoctane ring system was that of Sammes in 1970,[43] wherein the intermediacy of an intramolecular hetero Diels–Alder construction through the agency of an azadiene species was proposed (left, Fig. 3). Shortly thereafter, Birch inferred in 1971 (ref. 45) the intermediacy of an epidithiapiperazinedione species, with net extrusion of $S_2$ to form this ring system (right, Fig. 3), although the nature of the C–C bond formations as being heterolytic, radical, or step-wise were not further discussed.

At the time of the Sammes and Birch publications in the early 1970's, the absolute configuration of brevianamide B had not been rigorously assigned, but was thought to be of the same absolute sense as that of brevianamide A and being diastereomeric at the spiro-indoxyl stereogenic center. The Williams laboratory, in 1988,[46] completed the first synthesis of (−)-brevianamide B and re-assigned the absolute configuration of natural (+)-brevianamide B, as depicted in Fig. 1.[47,48] This revealed that brevianamides A and B have a pseudo-enantiomeric relationship (that is, the tricyclic portion constituted with the bicyclo[2.2.2]diazaoctane ring system are enantiomeric, but brevianamides A and B are technically diastereomers) which immediately raised provocative questions regarding the biogenesis of these natural substances in *Penicillium brevicompactum*. Williams suggested a modification to the intramolecular hetero Diels–Alder proposal, originally postulated by Sammes,[43] as shown in Scheme 1.[39,49,50] The differences between the Sammes and Williams biogenetic constructions involves the timing of the indole oxidation relative to the IMDA reaction. The Sammes proposal invokes a spiro-5 IMDA construction whereas the Williams alternative requires a spiro-6 IMDA. The Williams lab interrogated their alternative hypothesis through the synthesis and attempted precursor incorporation of DL-**1**. This potential metabolite was not incorporated into either brevianamide A nor brevianamide B in *Penicillium brevicompactum*,[51,52] leaving the Sammes proposal as the most plausible. However, advances in confirming the assembly details of these fungal indole alkaloids were only made possible with identification of the notoamide gene cluster (see Section 3) as well as through labeled precursor incorporation studies of anticipated intermediates (see Section 2).

A deeper understanding of the enantio- and diastereodivergence of the biosynthetic pathways exhibited by these closely related fungi, has led to the proposal of the functional presence of enzymes putatively mediating a Diels–Alder-type construction, an enzymatic function that is now receiving considerable attention from a number of laboratories investigating natural products biosynthetic pathways.[53] Theoretical[54,55] and experimental[56–61] studies from our laboratories have provided corroborating evidence that an enzyme-mediated IMDA reaction is operative in the biosynthesis of the bicyclo [2.2.2]diazaoctane ring systems.[38,53]

## 2. Fungal metabolites and biosynthetic studies of prenylated bicyclo[2.2.2]diazaoctane indole alkaloids

As to be discussed in detail below, there exists striking stereochemical similarities and differences between various members of this family of alkaloids for which biogenetic constructions need to accommodate. With respect to the construction of the bicyclo[2.2.2]diazaoctane ring system, the progenitor dioxopiperazine **4** (X = O) (or, for the paraherquamides, marcfortines, asperparalines, and malbrancheamides, the progenitor monooxopiperazine, **4**, X = $H_2$) suffers a net two-electron oxidation

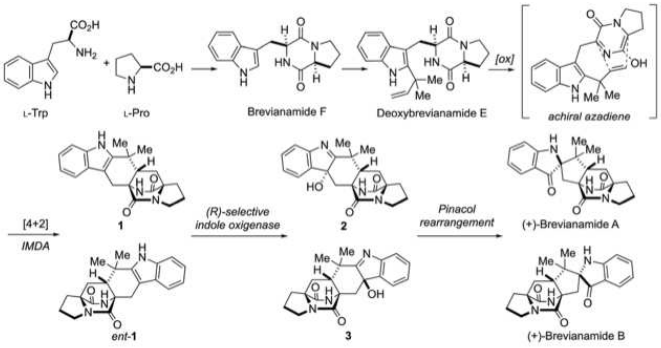


Scheme 1 Alternative brevianamide biogenesis proposed by Williams.[49]

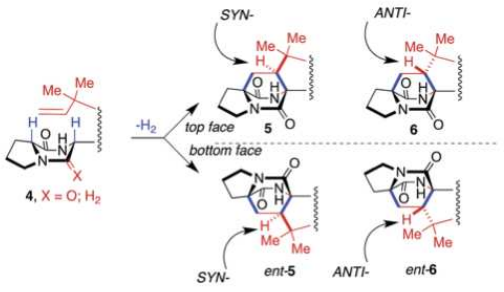


Fig. 4 Stereochemical outcomes of the oxidative isoprene cyclization across the two amino acid α-carbons in the construction of the bicyclo [2.2.2]diazaoctane.[62]

allowing the pendant isoprene-derived vinyl moiety to form the two new C–C bonds of the bicyclo[2.2.2]diazaoctane ring system. Four distinct diastereomeric transition states for this process can be operative resulting in the *syn*- (**5**) or *anti*-(**6**) diastereomeric relationships and a more subtle outcome being the manifestation of top-face or bottom-face cycloaddition as generically summarized in Fig. 4.

These stereochemical outcomes can be specifically identified in the known metabolic fates of notoamide S as illustrated in Scheme 2.[61,63] Various metabolites have been identified, which were biosynthesized through both enantiomers of notoamide T and 6-*epi*-notoamide T.[27,30,61,63–65] It has been suggested that all four of these substances arise *via* the intermediacy of common achiral azadiene species **7** (Scheme 2).

### 2.1 Isolation of prenylated indole alkaloids from the marine-derived fungus *A. protuberus* MF297-2 and the first proposal of the biogenesis of these alkaloids

The marine-derived fungus *A. protuberus* MF297-2 was isolated from the mussel *Mytilus edulis galloprovincialis*, which was collected from the Noto peninsula (Japan) by the Tsukamoto laboratory. The fungal culture showed the activity of cell cycle inhibition in HeLa cells and the bioassay-guided purification afforded a fungal toxin, sterigmatocystin, as a cell cycle inhibitor along with seven prenylated indole alkaloids. Structure elucidation revealed that four of these were new alkaloids, notoamides A–D, and three were known alkaloids, sclerotiamide, stephacidin A, and deoxybrevianamide E.[1,24] The structural relationship of these alkaloids led to the first proposal of the biosynthetic pathway illustrated in Scheme 3.[66,67] Notoamide E was suggested to be a key precursor for this family, although it had not yet been isolated from the culture. The compounds containing a bicyclo [2.2.2]diazaoctane nucleus, namely stephacidin A, notoamides A and B, and sclerotiamide, were hypothesized to be produced from notoamide E through an achiral azadiene intermediate **8** by the IMDA reaction.

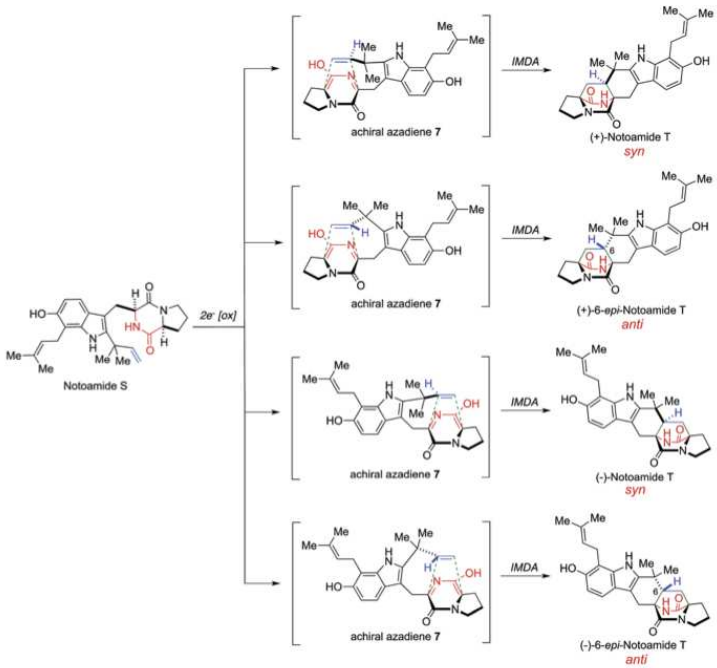


Scheme 2 Putative IMDA reactions in the oxidative enzymatic transformation from notoamide S.[61]

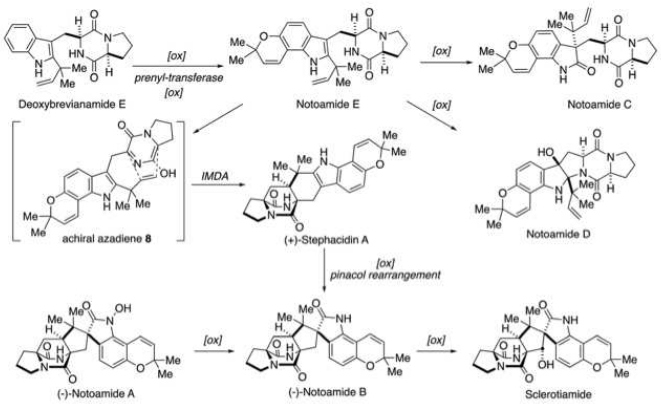


Scheme 3 Structures of prenylated indole alkaloids isolated from *A. protuberus* MF297-2 and initial proposal regarding their possible biogenetic relationships.[24,41,63,66–70]

### 2.2 Precursor incorporation studies of notoamide E and structurally novel metabolites from *A. protuberus* MF297-2

Since notoamide E was identified as a key intermediate in the biosynthesis of prenylated indole alkaloids in *A. protuberus*, Tsukamoto, *et al.* searched for notoamide E in the culture and found that it existed only in the fifth day of culture growth and immediately disappeared the next day.[68,69] These results clearly indicated that notoamide E was produced by the fungus in the early phase of growth and was presumably rapidly converted to other downstream metabolites. Subsequently, precursor incorporation experiments with synthetic, $[^{13}C]_2$–notoamide E were carried out.[68,71] Surprisingly, it was converted only to notoamides C and D as well as four new alkaloids, 3-*epi*-notoamides C and notoamides E2–E4, but not to the alkaloids containing a bicyclo[2.2.2]diazaoctane core, such as stephacidin A, notoamides A and B, nor sclerotiamide (Fig. 5).

Furthermore, in a precursor incorporation experiment, $[^{13}C]_2$–(+)-stephacidin A was, as expected, converted to (−)-notoamide B and (−)-sclerotiamide (Scheme 3).[70] The four new alkaloids (3-*epi*-notoamide C and notoamides E2–E4) were not detected as metabolites from this organism in the normal nutrient-rich medium. Among these, the structure of notoamide E4 is particularly interesting, and two possible biosynthetic pathways from notoamide E can reasonably accommodate the biogenesis of these species (Scheme 4).[68] One of the possible pathways would proceed *via* dioxetane intermediate **9**, followed by fragmentation to the corresponding kynurenine derivative **10**. Then, cyclization of **10** would afford the eight-membered ring derivative, notoamide E4. An alternative pathway is *via* peroxide species **11**, which would be produced by proton-assisted nucleophilic attack of the indole 3-position on molecular oxygen. The results of this precursor incorporation experiment reveals that the addition of excess

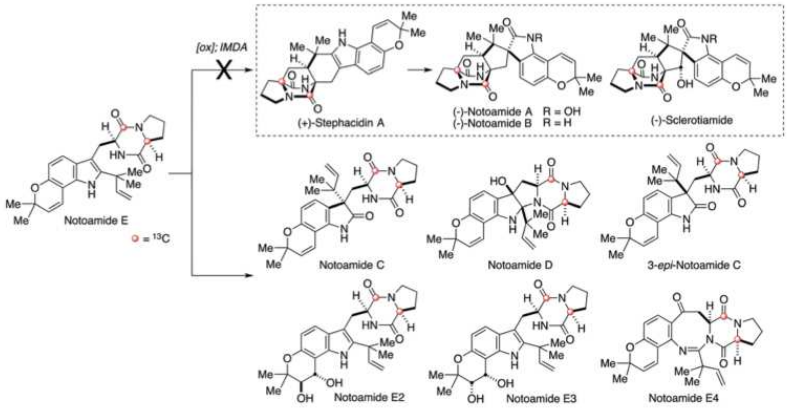


Fig. 5 Precursor incorporation results of $[^{13}C]_2$–notoamide E in *A. protuberus* MF297-2.[68–71]

 

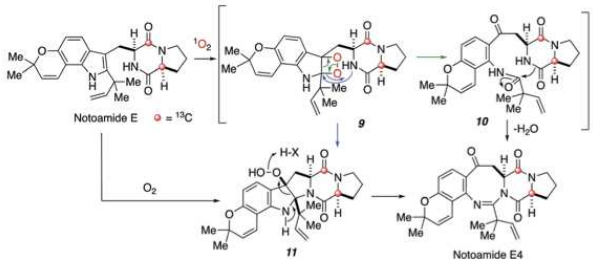


Scheme 4 Possible biosynthetic pathways to notoamide E4 from notoamide E.[68]

[$^{13}$C]$_2$–notoamide E (an endogenous metabolite) above the concentration levels of this metabolite normally produced, appears to alter the secondary metabolite profile of this organism. This provocative result warrants further investigation into how notoamide E, at elevated concentrations, must trigger the expression of dormant tailoring genes present that are not expressed under normal growth conditions.

Tsukamoto, *et al.* succeeded in the isolation of notoamides M[26] and Q,[27] which have hydroxy and methoxyl groups at C-17 positions, respectively (Scheme 5). These metabolites represent the oxidation state of the putative azadiene species that have been strongly implicated in the construction of the bicyclo [2.2.2]diazaoctane ring system. Thus, it is possible that formation of azadiene intermediate (**D**), proceeds through oxidation at C-17 of dioxopiperazine **A** to **B**, followed by loss of water or methanol and tautomerization to **D** (Scheme 5). Alternatively, notoamides M and Q, might be artifacts of hydration/capture of azadiene species (**C**) and experiments to interrogate this possibility are being investigated.

Tsukamoto, *et al.* isolated eighteen new prenylated indole alkaloids, notoamides A–R,[24–27] from the marine fungus *A. protuberus*. Among these, carbon frameworks of notoamides L[26] and O[27] were novel in the family of prenylated indole alkaloids and notoamides N[26] and P[27] contained chlorine and bromine atoms, respectively (Fig. 6). Notoamide L is the first metabolite containing twenty-five carbons in this family, while all other alkaloids possess twenty-six carbons. In the structure of notoamide L, the C-2 carbon derived from tryptophan has been removed.

Notoamide O possesses a novel hemiacetal/hemiaminal ether functionality hitherto unknown among this family. Possibly, notoamides L and O may be derived from (+)-stephacidin A (Scheme 6). In the biogenesis of notoamide L, singlet oxygen reaction at the indole 2,3-position of (+)-stephacidin A would afford a dioxetane intermediate **12** followed by fragmentation to kynurenine **13**. After hydrolysis of the amide bond of **13**, oxidation at C-24 followed by decarboxylative dehydration would afford notoamide L.[26] On the other hand, stephacidin A may be converted to aspergamide B[72] *via* notoamide R. Oxidative cleavage of the tri-substituted alkene in aspergamide B would generate aldehyde hydrate **16**; simple ring closure would afford notoamide O.[27] Notoamide N is one of the rare chlorinated members of the family of prenylated indole alkaloids and this is the third chlorinated derivative following malbrancheamide,[21] malbrancheamide B[22] and spiromalbramide.[23] On the other hand notoamide P is the first brominated member of this family.[27,65] The existence of a halogenase system in these fungi is of interest and the identification of the genes responsible for the halogenations merits further investigation.

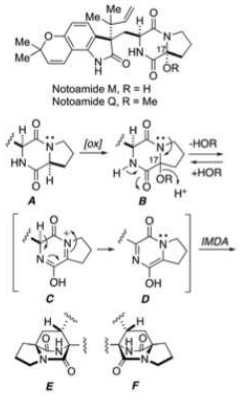


Scheme 5 Structures of notoamides M and Q and possible formation of the bicyclo[2.2.2]diazaoctane ring system, theoretically through notoamides M and Q.[26,27,65]

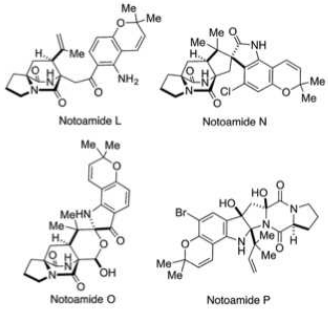


Fig. 6 Structures of notoamides L and N–P.[26,27,65]

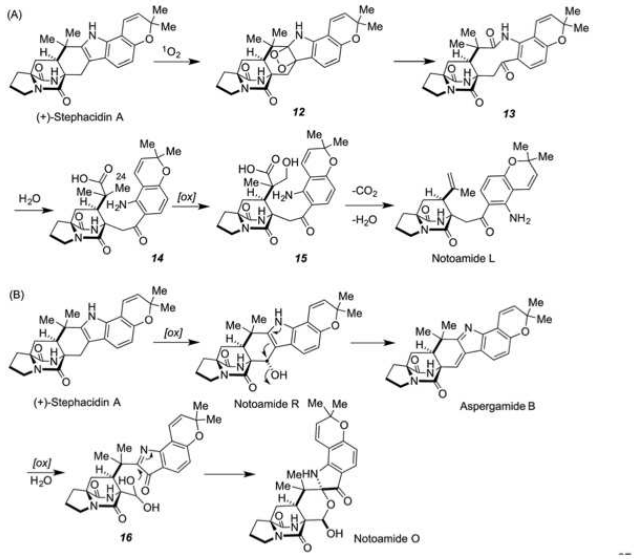


Scheme 6 Possible biosynthetic pathways to notoamides L (A) and O (B).[27]

### 2.3 Isolation of enantiomers of stephacidin A and notoamide B from the terrestrial fungus *Aspergillus amoenus* NRRL 35660

The Gloer laboratory originally isolated (−)-stephacidin A and (+)-notoamide B from the terrestrial fungus *A. amoenus* (formerly *A. versicolor*) NRRL 35660, which was isolated from a basidioma of *Ganoderma australe* collected in a Hawaiian forest, along with a new alkaloid, (+)-versicolamide B (Fig. 2).[28] (+)-Stephacidin A was originally isolated from the terrestrial fungus *A. ochraceus* by Bristol-Myers Squibb[20] and subsequently, (+)-stephacidin A and (−)-notoamide B were isolated from the

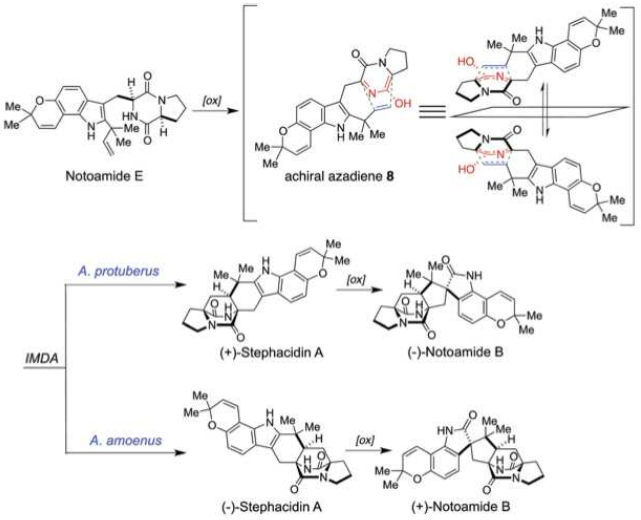


Scheme 7 Initial proposal for the enantiodivergent biogenesis of enantiomeric prenylated indole alkaloids with a bicyclo[2.2.2]diazaoctane core in *A. protuberus* MF297-2 and *A. amoenus* NRRL 35660.[28,70]

 

marine-derived fungus *A. protuberus* MF297-2, by the Tsukamoto laboratory.[24] These facts reveal that these closely related *Aspergillus* fungi biosynthesize the opposite enantiomers of stephacidin A and notoamide B and it has been confirmed that the optical purity of these metabolites are >99%. The initial hypothesis for rationalizing how these opposite enantiomers might arise, is illustrated in Scheme 7 and invokes the oxidation of notoamide E, to the achiral azadiene species **8**, followed by an entirely enantio-selective cycloaddition from this common precursor.[28] Although $[^{13}C]_2$–stephacidin A was converted to $[^{13}C]_2$–notoamide B,[70] as discussed above, the incorporation of $[^{13}C]_2$–notoamide E into stephacidin A and notoamide B, however, was not observed in *A. amoenus*[73] nor *A. protuberus*.[68] These results suggested alternate timing of the pyran and bicyclo[2.2.2]diazaoctane ring constructions as discussed below.

### 2.4 An alternative enantiodivergent biosynthetic pathway for stephacidin A biogenesis

Since $[^{13}C]_2$–notoamide E was not incorporated into stephacidin A in either *A. protuberus* MF297-2 nor *A. amoenus* NRRL 35660, other testable hypotheses needed to be devised. The pathway from deoxybrevianamide E to stephacidin A contains four steps: the putative IMDA, an oxidation at C-6, prenylation, and final oxidation/cyclization to form a pyran ring (Scheme 8). From the results of the precursor incorporation experiments with notoamide E, three compounds, namely deoxybrevianamide E, 6-hydroxy-deoxybrevianamide E, and notoamide S, appeared to be potential precursors for IMDA reactions, although notoamide S had not yet been isolated from any species of the *Aspergillus* fungi.[74] The incorporation experiments of synthetic $[^{13}C]_2$–$[^{15}N]$–deoxybrevianamide E[75] and $[^{13}C]_2$–$[^{15}N]$–6-hydroxy-deoxybrevianamide E[75,76] afforded notoamides C and D but not stephacidin A nor notoamides A and B. Next, the administration of synthetic $[^{13}C]_2$–$[^{15}N]_2$–notoamide S in *A. amoenus* was examined and it was found to be incorporated into (−)-stephacidin A (6.2% incorporation), (+)-notoamide B (6.4% incorporation), and (+)-versicolamide B (6.5% incorporation), together with notoamides C (6.4% incorporation) and D (6.2% incorporation) (Fig. 7).[77] These results clearly indicated that the construction of the bicyclo[2.2.2]diazaoctane ring system occurs prior to the formation of the pyran ring. Although notoamides S and T had not previously been found in the culture extract of *A. amoenus*, Kato, *et al.*, have recently identified notoamide S as a minor metabolite of *A. amoenus*.[61]

### 2.5 The incorporation of notoamide T and 6-*epi*-notoamide T

Since notoamide S was observed to be converted to compounds containing a bicyclo[2.2.2]diazaoctane core *via* notoamide T and 6-*epi*-notoamide T (Scheme 2), the precursor incorporation experiments of these two alkaloids were performed. Unexpectedly, the administration of synthetic $[^{13}C]_2$–(±)-notoamide T in *A. protuberus* afforded racemic mixtures of stephacidin A, notoamide B, notoamide F, notoamide R, and a new compound,

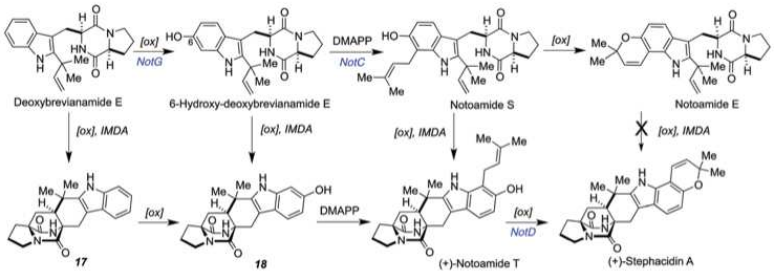


Scheme 8 Possible biosynthetic pathways from deoxybrevianamide E to stephacidin A and potential precursors for IMDA reactions.[74–76]

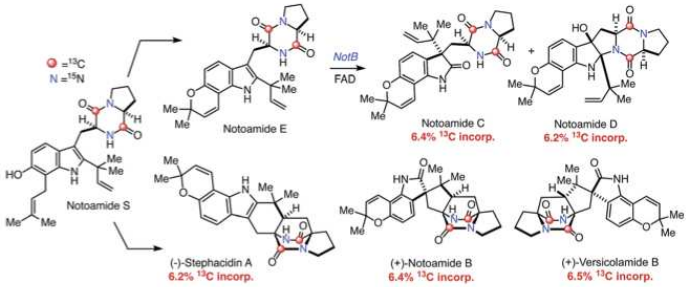


Fig. 7 Results of the incorporation experiment of $[^{13}C]_2$–$[^{15}N]_2$–notoamide S in *A. amoenus* NRRL 35660.[77]

notoamide T2 (Fig. 8A).[63] On the other hand, synthetic [$^{13}$C]$_2$–6-*epi*-(±)-notoamide T was converted to racemic mixtures of versicolamide B and eight new compounds, 6-*epi*-notoamides T3–T8 and 6-*epi*-notoamide I, in a trace element solution (Fig. 8B) and afforded racemic mixtures of 6-*epi*-stephacidin A and four new compounds, 6-*epi*-notoamides T9–T12, on trace element agar plates (Fig. 8C).[64]

Among them, notoamide T2, 6-*epi*-notoamides T3–T12, and 6-*epi*-notoamide I were not produced by the fungus under normal culture conditions to any detectable extent.[63,64] These data suggest that the (presumably) endogenous, natural metabolites [$^{13}$C]$_2$–(±)-notoamide T and [$^{13}$C]$_2$–(±)-6-*epi*-notoamide T activated the expression of dormant tailoring genes that expands the metabolome of the producing organism. While notoamide T and 6-*epi*-notoamide T are presumed to be natural, endogenous metabolites in this organism, the precursor incorporation experiment with the easily accessible synthetic, racemic labeled substances was performed. In order to further interrogate this fascinating observation, sufficient quantities of the respective optically pure enantiomers of each will be required to query whether the metabolite profile alteration is triggered by the presence of the unnatural enantiomer for this producing organism.

Of particular intrigue, 6-*epi*-notoamides T3 and T4 contain unprecedented structures wherein the aromatic benzenoid ring of the tryptophan moiety has suffered oxidative amination, culminating in the formation of the new fused oxazole and 2-oxazolone moieties, respectively. One possible mechanism for the oxidative amination of the tryptophan moiety is suggested in Scheme 9. Oxidation and subsequent pinacol rearrangement of [$^{13}$C]$_2$–(±)-6-*epi*-notoamide T would form the spiro-oxindole, [$^{13}$C]$_2$–(±)-6-*epi*-notoamide T9. Successive oxidation and incorporation of glycine into **20** to form imine **21**, followed by decarboxylation, provides **22** that must cyclize (to **23**) and then be oxidized to the oxazoline moiety of T3. Oxidation of the oxazoline of T3 would produce oxazolidinone in 6-*epi*-notoamide T4.[64] It is reasonable to assume that the initial oxidation of the 2,3-disubstituted indole of 6-*epi*-notoamide T is conducted by NotI that Li, *et al.*, previously predicted this oxidation and spiro-rearrangement.[62] The downstream transformations from 6-*epi*-notoamide T9, requires a minimum of six enzyme-catalyzed reactions: (1) aromatic hydroxylase of T9 to **19**; (2) a catechol oxidase to **20**; (3) glycine aminotransferase to **21**; (4) decarboxylase/cyclase to **23**; (5) oxazolidine oxidase to T3; and (6) oxazolidinone oxidase to T4. The complex array of transformations required to construct T3 and T4 from 6-*epi*-notoamide T mandates that multiple dormant tailoring genes extant

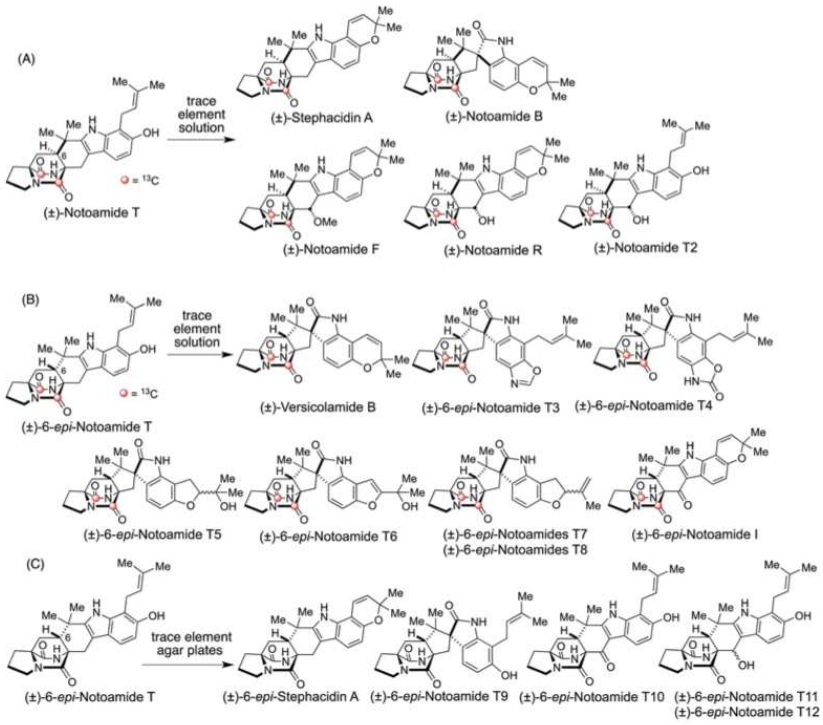


Fig. 8 Results of the incorporation experiments of [$^{13}$C]$_2$–(±)-notoamide T in a trace element solution (A), [$^{13}$C]$_2$–(±)-6-*epi*-notoamide T in a trace element solution (B), and (±)-6-*epi*-notoamide T on trace element agar plates (C) in *A. protuberus* MF297-2.[63,64]

 

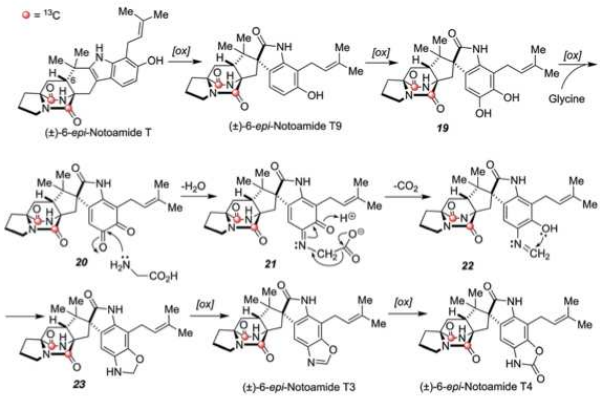


Scheme 9 Possible biosynthetic pathways to 6-*epi*-notoamide T3 and 6-*epi*-notoamide T4 from 6-*epi*-notoamide T.[62,64]

in this organism were activated by the presence of one (or both) enantiomers of 6-*epi*-notoamide T. Significant effort will need to be devoted to elucidating the nature of these remarkable transformations that have significant implications for the plasticity of secondary metabolomes in Nature.

### 2.6 Isolation of an enantiomeric mixture of 6-*epi*-stephacidin A from *A. amoenus* NRRL 35660

The metabolic profiles of *A. protuberus* MF297-2 and *A. amoenus* NRRL 35660 produced the opposite enantiomers of stephacidin A and notoamide B along with the same enantiomer of (+)-versicolamide B. (−)-Versicolamide B has yet to be detected as a natural metabolite in any of the fungi that have been examined to date and poses an enigma (Fig. 2). (+)-6-*epi*-Stephacidin A is the likely precursor of (+)-versicolamide B and was obtained from the culture of *A. protuberus* (Scheme 10).[64] However, 6-*epi*-stephacidin A, which was isolated from *A. amoenus*, was found to be an enantiomeric mixture enriched with the (−)-isomer (1 : 2.4).[61] This result clearly suggested that, in *A. amoenus*, notoamide S was converted to both (+)- and (−)-6-*epi*-stephacidin A and subsequently, only the (+)-isomer was converted into (+)-versicolamide B (Scheme 10). This result mandates that *A. amoenus* contains a highly enantio-specific indole oxidase that exclusively transforms the (+)-enantiomer of 6-*epi*-stephacidin A to (+)-versicolamide B, but apparently does not bind or oxidize the (−)-enantiomer of 6-*epi*-stephacidin A. While the formation of an enantiomerically-enriched metabolite has not yet been observed in any of the other fungal species examined, this begs the question of why this occurs in *A. amoenus*. The lack of optical purity of 6-*epi*-stephacidin A obtained in *A. amoenus* also requires an explanation and it is to such questions, that our labs have recently started investigations.

### 2.7 Isolation of taichunamides A–G from *Aspergillus taichungensis* IBT 19404: biogenetic considerations

The majority of the prenylated indole alkaloids thus far identified containing the bicyclo[2.2.2]diazaoctane ring system, possess the *syn*-configuration (the *syn*- and *anti*-relationship is based on the relative configuration of H21 with respect to the bridging secondary amide; see Fig. 4 and 9). Distinct enantiomers of notoamide B and stephacidin A are the main metabolites present in *A. protuberus* and *A. amoenus*, and

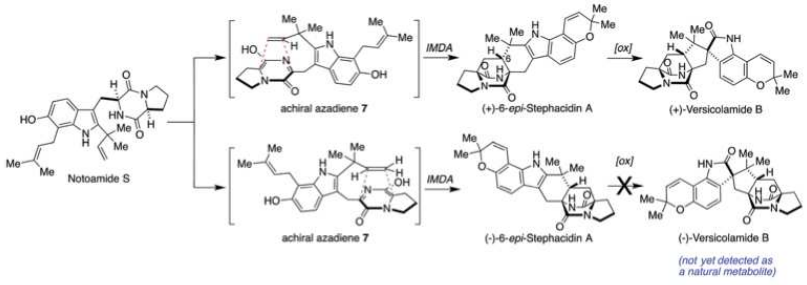


Scheme 10 Possible biosynthetic pathways of an enantiomeric mixture of 6-*epi*-stephacidin A and (+)-versicoclamide B in *A. amoenus* NRRL 35660.[61,64]

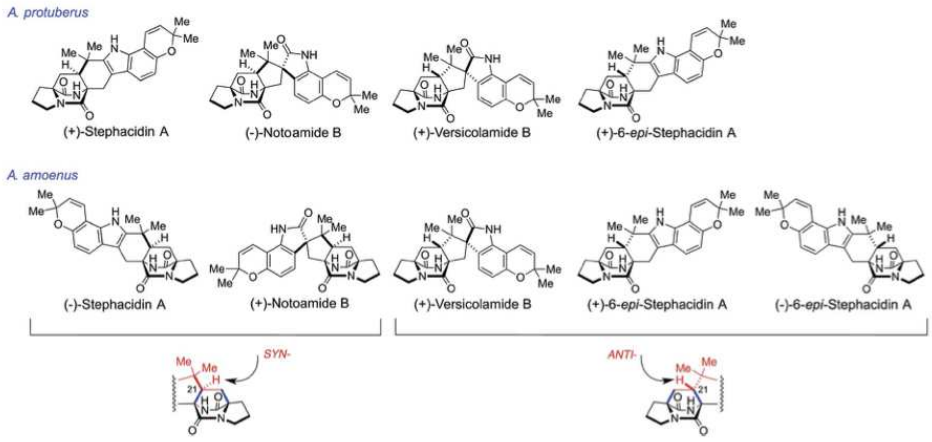


Fig. 9 Prenylated indole alkaloids illustrating the *syn*- and *anti*-diastereomeric relative configurations isolated from *A. protuberus* MF297-2 and *A. amoenus* NRL 35660.[26,28,30,61]

(+)-versicolamide B, a minor metabolite, was the first alkaloid identified within this family with the corresponding *anti* configuration. In 2013, Cai *et al.* isolated (+)-versicolamide B and (+)-6-*epi*-stephacidin A as major metabolites from *A. taichungensis* ZHN-7-07.[78] Kagiyama, *et al.*, have also investigated the isolation of alkaloids from *A. taichungensis* IBT 19404 collected from the soil in Taiwan and succeeded in isolating seven indole alkaloids with unprecedented structures and have named these substances taichunamides A–G (Fig. 10); all of these natural alkaloids possess the *anti*-bicyclo[2.2.2]diazaoctane core.[30] Although the structure of taichunamide A was initially assigned to contain a very rare azetidine unit, recently it was revised as a 3-hydroxyindolenine.[79] Taichunamide B was found to be constituted with a very rare 4-pyridone unit. In DMSO-$d_6$ taichunamide B appears to be an equilibrium mixture of two tautomeric entities: a 4-pyridone and 4-pyridol, in a ratio of 3 : 1. This tautomeric equilibrium is highly solvent-dependent where it was observed a single keto or enol form was observed in $CD_3OD$ or acetone-$d_6$, respectively. Taichunamides C and D contain endoperoxide and methylsulfonyl units, respectively.

These new alkaloids, especially taichunamide B, constitute hitherto unknown structural arrays derived from tailoring of the tryptophan moiety and therefore must deploy a series of fascinating biochemical bond constructions. Biogenetic implications for taichunamides B and E as well as (+)-versicolamide B are represented in Scheme 11.[30] β-Face oxidation (*anti*- to the bridged amide) of 6-*epi*-stephacidin A allows for the formation of a non-isolatable epoxide intermediate **24** which subsequently undergoes a pinacol rearrangement within the active site to form the spirooxindole in (+)-versicolamide B. Oxidation at the α-face (*syn* to the bridged amide) followed by pinacol rearrangement would allow for formation of taichunamide E. Compared with β-face oxidation, α-face oxidation is more sterically demanding with N19, as reflected by the metabolite ratios of (+)-versicolamide B (15.9 mg)/(+)-versicolamide C[30,80] (a N1-OH derivative of versicolamide B)[81] (240 mg) *versus* taichunamide E (0.43 mg). Although, in the biomimetic synthesis that deployed the IMDA reaction, taichunamide E was identified along with (+)-versicolamide B in a ratio of 1 : 1.4; this is the first report of its isolation from the fungal culture.[30] Also, formation of peroxide **26** by oxidation of (+)-6-*epi*-stephacidin A would

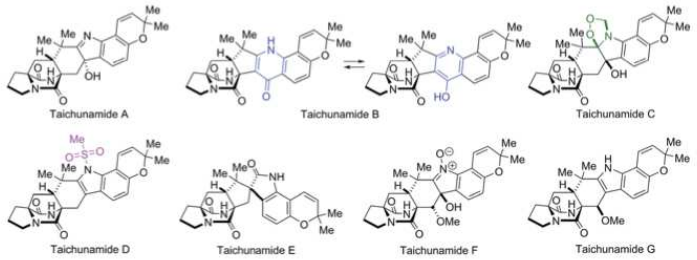


Fig. 10 Structures of the taichunamides isolated from *A. taichungensis* IBT19404.[30]

 

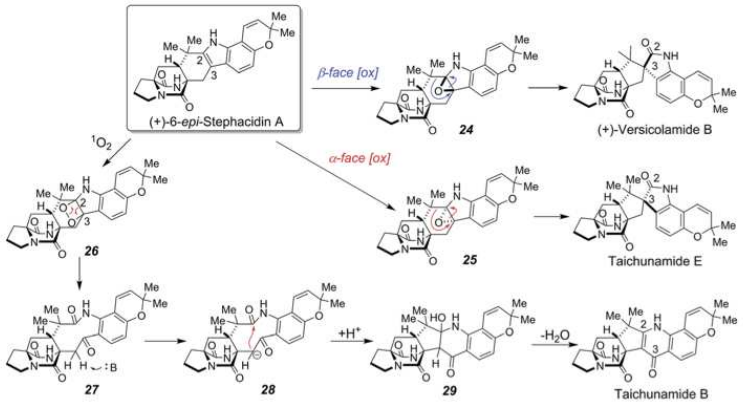


Scheme 11 Possible biogenesis of taichunamides B and E and versicolamide B from 6-*epi*-stephacidin A.[30]

ultimately lead to the ring system found in taichunamide B, theoretically through compound **27**.

A wide structural array of prenylated indole alkaloids have been isolated from the genera of *Aspergillus* and *Penicillium* to date, yet their respective carbon frameworks are very unique. The isolation of these compounds from *A. taichungensis* has greatly expanded the library of these secondary metabolites. Future biochemical studies and genome mining will aid in the identification of genes or gene clusters responsible for the evolution of these unprecedented metabolites.

### 2.8 Biogenetic implications of prenylated indole alkaloids in the *Aspergillus* genus

To date, numerous fungal species in the *Aspergillus* genus, including *A. ochraceus*, *A. protuberus* MF297-2, *A. amoenus* NRRL 35660, and *A. taichungensis* IBT 19404, described in this article that produce prenylated indole alkaloids, bearing the dioxopiperazine-based bicyclo[2.2.2]diazaoctane core most likely biosynthesized by the oxidative cycloaddition reaction of the common precursor, notoamide S (Scheme 12), have been identified. Each organism displays its own unique

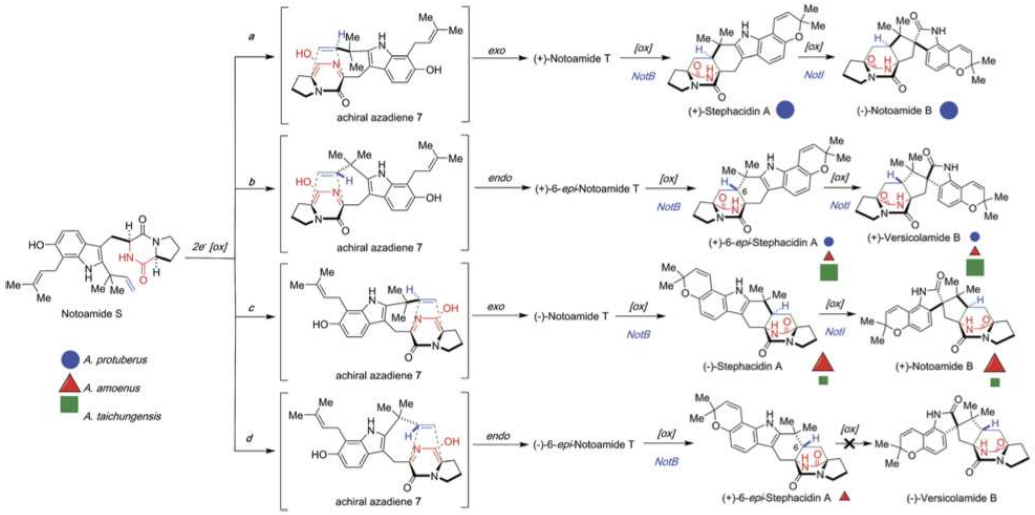


Scheme 12 Proposed facial specificities of IMDA reactions for metabolites in *A. protuberus* MF297-2 (blue circles), *A. amoenus* NRRL 35660 (red triangles), and *A. taichungensis* IBT 19404 (green squares). Major and minor metabolites in each fungus are represented with large and small symbols, respectively.[30]

stereochemical signature wherein the absolute and relative stereochemistry within these molecular frameworks have been constructed are evident. In *A. protuberus*, the orientation of the dienophile to the diene in pathways a (main) and b (minor), respectively, leads to the construction of the corresponding *exo*- and *endo*-products namely, (+)-stephacidin A/(−)-notoamide B and (+)-6-*epi*-stephacidin A/(+)-versicolamide B, respectively. On the other hand, in *A. taichungensis*, the construction of the bicyclo[2.2.2]diazaoctane ring system favors the formation of the C-6-*epi*-diastereomeric *via* pathway b (main) and c (minor).[30] Efforts to clarify the genetic and biochemical bases and relationships between the respective biosynthetic gene clusters are currently under intense investigation in our laboratories.

## 3. Genomic insights

In order to obtain a deeper understanding of the biogeneses of these structurally fascinating natural alkaloids, and in particular, to obtain a higher level elucidation of the enantioselectivity and diastereoselectivity evident in the biogenesis of the stephacidins and notoamides, the genomes of ten fungi known to produce these alkaloids have been sequenced and the identification of relevant biosynthetic gene clusters (Fig. 11) has been realized. The mining of *ftmA*, a NRPS gene from the fumitremorgin *Aspergillus* species, *A. fumigatus*, and production of brevianamide F by heterologous gene expression in 2006 by Turner *et al.*,[82] allowed Ding, *et al.*, to identify the notoamide gene cluster in *A. protuberus*.[83] Due to the crucial role brevianamide F plays in the early biogenesis of an enormous range of prenylated indole alkaloids within the *Aspergillus* genus, it was originally assumed that *ftmA*, or a comparable homolog, would also participate in biosynthetic transformations of *A. protuberus*. Using Roche 454FLX technology and *ftmA* to probe for homologous genes, *notE* was identified as the NRPS module analogous to *ftmA*, sharing a 47% nucleotide identity, in the *A. protuberus* species.[83] Fig. 12 represents the (+)- and (−)-notoamide-producing gene clusters identified by genome sequencing and bioinformatics.[83]

Bioinformatics analysis[83] and deep annotation, has revealed a number of important facts and relationships between *A. protuberus* and *A. amoenus* that produce the opposite enantiomers of stephacidin A and notoamide B. First, it is clear from the structure and directionality of the open-reading frames of genes within the gene clusters, that the gene clusters and thus the organisms are orthologous (ancestrally related through a speciation event that occurred at some time during their evolutionary history). The high level of nucleotide identity overall between the gene clusters is almost 71% and within individual genes, the homology with respect to amino acid identity or similarity, is as high as 95% (for example NotC). Functions have been assigned to a number of genes within these orthologous gene clusters and are identified in Fig. 12, Scheme 13, and Table 1 which

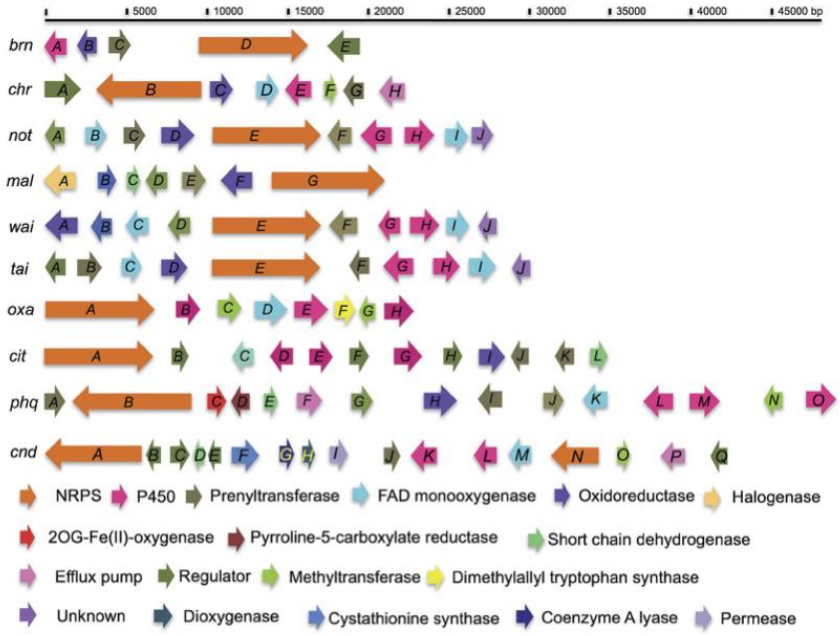


Fig. 11 Mining and annotation of biosynthetic gene clusters of fungal indole alkaloids. Brevianamide (*Aspergillus versicolor* MF030, brn); chrysogenamide (*Penicillium. alligativum*, chr); notoamide A (*A. protuberus* MF297-2, not); malbrancheamide (*Malbranchea aurantiaca* RRC1813, mal); waikialoid A (*Aspergillus* sp., wai); 3-*epi*-notoamide C (*A. taichungensis* IBT 19404, tai); oxaline (*P. oxalicum* F30, oxa); citrinalin (*P. citrinum* F53, cit); parahequamide A (*P. fellutanum* ATCC20841, phq); citrinadins (*P. citrinum* IBT 29821, cnd).[62,84]

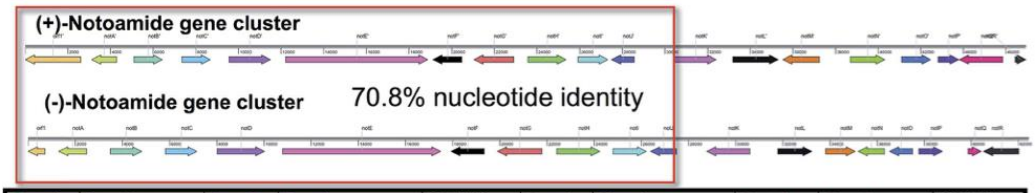


| Protein | Function | Protein | Function | AA id/Sim | Protein | Function | Protein | Function | AA id/Sim |
|---|---|---|---|---|---|---|---|---|---|
| Orf1 | Polysaccharide synthase | Orf1′ | Polysaccharide synthase | Not determined | NotJ | Unknown | NotJ′ | Unknown | 80%/84% |
| NotA | Negative regulator | NotA′ | Negative regulator | 70%/77% | NotK | Efflux pump | NotK′ | Nucleoside transporter | 14%/28% |
| NotB | FAD binding domain protein | NotB′ | FAD binding domain protein | 88%/94% | NotL | Transcriptional activator | NotL′ | Transcription factor | 15%/22% |
| NotC | Prenyl-transferase | NotC′ | Prenyl-transferase | 87%/95% | NotM | Unknown | NotM′ | Unknown | - |
| NotD | Oxidoreductase | NotD′ | Oxidoreductase | 80%/86% | NotM | Dehydrogenase | NotM′ | Unknown | - |
| NotE | NRPS | NotE′ | NRPS | 79%86% | NotO | Short-chain dehydrogenase | NotO′ | Unknown | - |
| NotF | Prenyl-transferase | NotF′ | Prenyl-transferase | 79%/85% | NotP | Unknown | NotP′ | Unknown | - |
| NotG | P450 | NotG′ | P450 | 87%/92% | NotQ | Unknown | NotQ′ | Transcription factor | 12%/21% (NotL) |
| NotH | P450 | NotH′ | P450 | 84%/92% | NotR | Transcriptional co-activator | NotR′ | Unknown | - |
| NotI | FAD binding domain protein | NotI′ | FAD binding domain protein | 85%/90% | | | | | -: No homology |

Fig. 12 Comparison of the biosynthetic gene clusters of the (+)-notoamide (*Aspergillus amoenus*) and (−)-notoamide (*Aspergillus protuberus*) producing fungi.[83]

reflects our current understanding and hypotheses regarding the biogenesis of the enantiomeric pairs.[63,83]

Li, *et al.*, have successfully been able to clone and functionally express the following enzymes: NotF, NotG, NotC, NotD, NotD′, NotI and NotI′.[62,83] Table 1 provides a summary of the relevant data on each individual gene and the heterologous host in which the protein was functionally expressed.

Li, *et al.*, have tentatively assigned roles to other genes in the notoamide gene clusters as follows. NotG appears to be

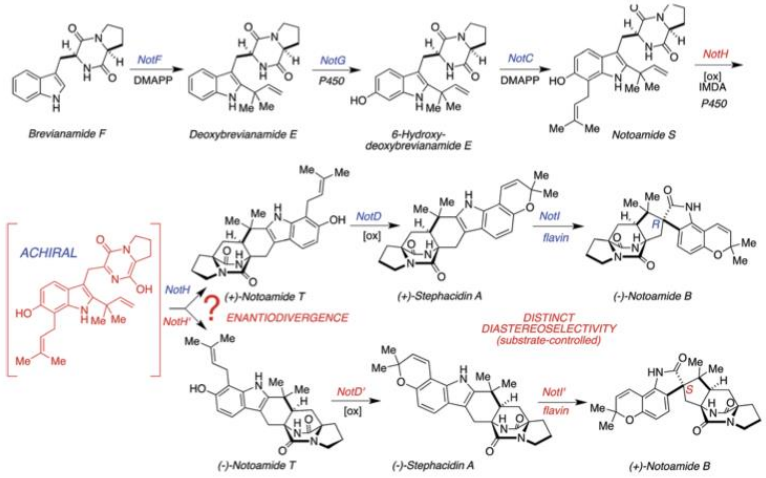


Scheme 13 Current understanding of (+)- and (−)-notoamide biogenesis in *Aspergillus* sp.[63]

Table 1 Select notoamide biosynthetic enzymes

| Enzyme | bp/aa | Heterologous host | Function | Substrate |
|---|---|---|---|---|
| NotB | 1563/456 | *E. coli* | FAD binding domain protein | Notoamide E |
| NotB′ | 1344/455 | — | FAD binding domain protein | Notoamide E |
| NotC | 1350/427 | *E. coli* | Prenyl transferase | 6-Hydroxydeoxybrevianamide E |
| NotD | 2025/621 | *A. oryzae* | Oxidoreductase | (+)-Notoamide T |
| NotD′ | 2025/612 | — | Oxidoreductase | (−)-Notoamide T |
| NotE | 6723/2241 | — | NRPS module | Pro + Trp |
| NotF | 1431/453 | *E. coli* | Reverse prenyl transferase | Brevianamide F |
| NotG | 1901/544 | — | Cytochrome P450 | Deoxybrevianamide E |
| NotH | 1836/502 | — | Cytochrome P450 | Notoamide S |
| NotH′ | 1836/499 | — | Cytochrome P450 | Notoamide S |
| NotI | 1423/434 | *E. coli* | FAD binding domain protein | (+)-Stephacidin A |
| NotI′ | 1423/433 | *E. coli* | FAD binding domain protein | (−)-Stephacidin A |

a cytochrome P450 oxidase responsible for the transformation of deoxybrevianamide E into 6-hydroxydeoxybrevianamide E, which was deduced through a process of elimination by comparative analysis with several fungal gene clusters.[62,83] The other cytochrome P450, NotH is the current most plausible candidate for the oxidative transformation of notoamide S into notoamide T and 6-*epi*-notoamide T.[83] Much to our chagrin, NotH and NotH′, which is currently the focus of where the key enantiodivergence occurs, is a membrane-associated cytochrome P450 that has proven recalcitrant to functional expression in a heterologous host and constitutes the focus of our current efforts.

Biochemical characterization, along with isotopically labeled precursor incorporation studies (*vide supra*), has determined the roles of NotF and NotC as aromatic prenyltransferases.[83] Michaelis–Menten kinetics and isotopically labeled precursor incorporation studies have successfully demonstrated the substrate selectivity of the NotF and NotC enzymes. The reverse-prenylation of brevianamide F into deoxybrevianamide E, the first committed step of the post-NRPS tailoring cascade, is catalyzed by NotF. The subsequent normal prenylation of 6-hydroxydeoxybrevianamide E into notoamide S is catalyzed specifically by NotC.[83]

NotB and NotI are flavin-dependent monooxygenases (FMO). Biochemical characterization of NotB has determined its role as an FAD-dependent oxidase for converting notoamide E into notoamides C and D (Scheme 14).[77] Curiously, 3-*epi*-notoamide C is not observed as a product when notoamide E is exposed to recombinant NotB. 3-*epi*-Notoamide C has been previously isolated from a precursor incorporation experiment with notoamide E as an added substrate, but has not been directly isolated from fermentation extracts of *Aspergillus protuberus*.[68]

NotI and NotI′ which are also flavin-dependent oxygenases, are predicted to catalyze the oxidative spiro-transformation of stephacidin A into notoamide B.[83] The details of how NotI and NotI′ discriminate between the respective enantiomers of stephacidin A and the conversion into the corresponding enantiomers of notoamide B is of great interest, but has not yet been reported.

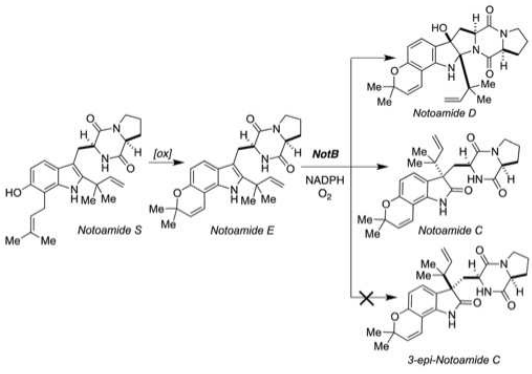


Scheme 14 Role of NotB in the conversion of notoamide E into notoamides C and D.[77]

## 4. Biomimetic total syntheses

With the objective of interrogating the validity of the proposed biosynthetic intramolecular hetero Diels–Alder construction of the characteristic bicyclo[2.2.2]diazaoctane ring nucleus, Williams, *et al.*, have investigated the laboratory version of the IMDA construction which successfully enabled biomimetic syntheses of numerous members of these natural alkaloids. These investigations provided additional insights as to the intrinsic facial bias of this cycloaddition with respect to the *syn*-/*anti*-diastereoselectivity.[56–60] Theoretical calculations on these azadiene IMDA reactions published by our collaborator Domingo *et al.*,[54,55] provide an important backdrop to the laboratory and putative biosynthetic constructions. The strategies for generating the key azadiene species evolved to ever more efficient protocols over the years and are shown here chronologically. Our first successful biomimetic synthesis was that of D,L-brevianamide B, as shown in Scheme 15, where DDQ oxidation of lactam ether **31** was employed to provide the unsaturated proline derivative **32**.[85] Base-mediated tautomerization generated the desired azadiene species, that proved stable enough to

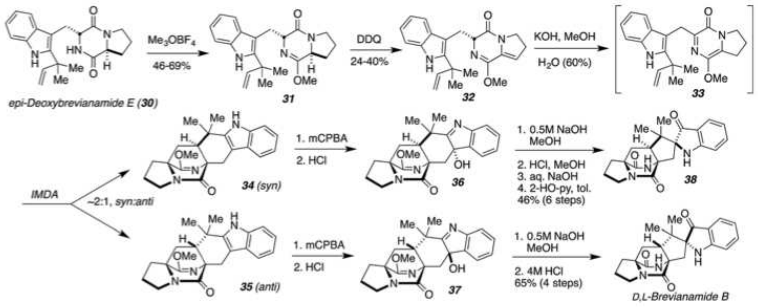


Scheme 15 First-generation biomimetic total synthesis of D,L-brevianamide B.[85]

observe by $^1$H NMR, but spontaneously suffered IMDA cycloaddition to provide an approximately 2 : 1 *syn* : *anti* mixture of cycloadducts **34** and **35**, respectively. Peracid oxidation to the corresponding diastereochemically pure 3-hydroxyindolenines (**36** and **37**) followed by base-mediated pinacol-type spiro-rearrangement and final acidic removal of the lactim ether furnished D,L-brevianamide B from **37** and the corresponding *syn*-diastereomer **38**.[85]

A second-generation synthesis, detailed in Scheme 16, generated the azadiene directly from an α-ketoamide proline amide species (*i.e.*, **42**).[86] The IMDA reaction, carried out under strongly Lewis acidic conditions, interestingly provided the desired *anti*-cycloadduct **44**, exclusively. Fisher indole synthesis to **46** and final peracid oxidation to the indoxyl provided D,L-brevianamide B.[86]

The most efficient biomimetic synthesis of brevianamide B that has been developed and reported to date, relied on using β-hydroxyproline as a surrogate representing the oxidation state of the azadiene, as shown in Scheme 17.[60,85] Reverse-prenylated tryptophan species **47** was coupled with β-hydroxyproline ethyl ester to give dipeptide **48** that was deprotected and cyclized to **49**. Mitsunobu dehydration of **49** in dichloromethane at 40 °C led directly to the production of meta-stable azadiene species **50** that spontaneously underwent IMDA cycloaddition to give a 2.1 : 1, *syn* : *anti* diastereomeric mixture that were readily separated by chromatography. The minor *anti*-cycloadduct **46** was subjected to peracid oxidation as above and rearranged under basic conditions furnishing D,L-brevianamide B. It is important to note that the intrinsic facial bias of the IMDA cycloadditions in all cases, was about 2 : 1 favoring the *syn*-diastereomer and in good agreement with theoretical predictions published by our collaborator Prof. Domingo (see below).

The intrinsic facial bias of these IMDA reactions, have been interrogated by Domingo, *et al.*, quantum chemically at the B3LYP/6-31G* level.[54] He has examined both the dioxopiperazine-based azadienes (**51b**; **54b**) relevant to the stephacidin and notoamide families, as well as the corresponding monooxopiperazine-based azadienes (**51a**; **54a**) relevant to the paraherquamide, malbrancheamide and related family members.

As depicted in Scheme 18, two main substrate platforms were evaluated: the spiro-5 mode, wherein the indole has been

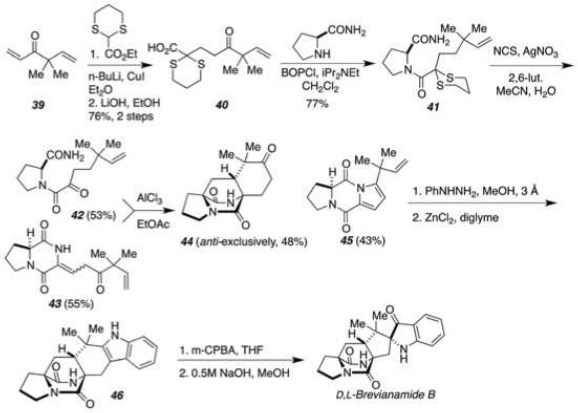


Scheme 16 Second generation biomimetic total synthesis of D,L-brevianamide B.[86]

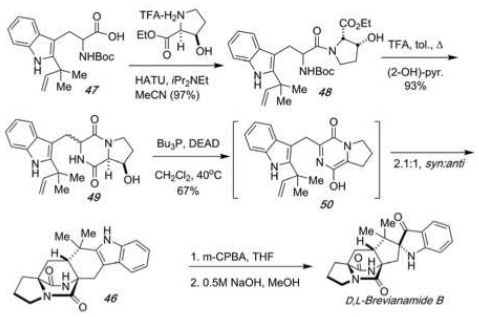


Scheme 17 Third-generation biomimetic total synthesis of D,L-brevianamide B.[60,85]

oxidized to the corresponding oxindole species and the spiro-6 mode, wherein the indole has yet to suffer oxidative tailoring.[54] Strikingly, it was found that the spiro-5 mode greatly favors the *anti*-diastereomer (**52**) over the corresponding *syn*-diastereomer (**53**) by 4–7 kcal $mol^{-1}$. In contradistinction, the corresponding spiro-6 mode from **54**, revealed a modest preference for the *syn*-diastereomers **56** by about 1 kcal $mol^{-1}$.[54] These theoretical predictions have tracked quite well with experiment as can be seen from the modest *syn* : *anti* diastereoselectivities for the laboratory spiro-6 systems described above and below, where the *syn* : *anti* ratio is typically around 2.5 : 1. On the other hand, the experimentally observed spiro-5 cycloadditions have to date, yielded exclusively the *anti*-diastereomers, which will be detailed below.

The biomimetic syntheses developed above for brevianamide B, set the stage for deploying this technology to prepare more complex members of this family. The Williams lab has been able to successfully devise a biomimetic total synthesis of stephacidin A and its C-6-epimer, and more recently demonstrated C6-*epi*-stephacidin A to be a natural metabolite and, as noted above, these stephacidin A congeners are the direct biosynthetic precursors to notoamide B and versicolamide B, respectively. Subsequent to the biomimetic stephacidin A synthesis, these workers have been able to readily adopt this approach for successful biomimetic total syntheses of premalbrancheamide,[87] malbrancheamide,[88] spiromalbramide,[89] marcfortine C,[90] notoamide T and its C-6-epimer,[63] also now known to be a natural metabolite as described above.

As shown in Scheme 19, the reverse-prenylated tryptophan derivative **66** was prepared on multi-gram scale from commercially available 6-hydroxyindole.[63,83,91] Key steps included a Danishefsky 9-BBN reverse-prenylation of 3-chloroindole species **59** (ref. 92 and 100) and Claisen-based rearrangement of the propargyl ether **62** to the requisite pyran **63**. Somei–Kametani[93–96] gramine-based construction of the amino acid and protecting group adjustment furnished the key tryptophan derivative **66** that has been deployed in numerous total syntheses of the stephacidins and notoamides.

As described in Scheme 20, β-hydroxyproline ethyl ester **67** was coupled with tryptophan species **66** employing peptide coupling reagent BOPCl. This provided the incipient dipeptide, which was then subjected to removal of the *N*-Fmoc residue allowing spontaneous cyclization to dioxopiperazine **68**. Mitsunobu dehydration directly led to the tautomerized azadiene species **8**,[97] that was stable enough to be isolated by PTLC and observable by $^1$H NMR, but spontaneously underwent IMDA cycloaddition to give stephacidin A and C6-*epi*-stephacidin A as a 2.4 : 1, *syn* : *anti* mixture in 64% combined yield.[67]

Oxidation of synthetic stephacidin A with the Davis saccharin-derived oxaziridine (**69**)[98] directly provided the spirooxindole product, notoamide B.[67] Asymmetric syntheses of stephacidins A, B, and notoamide B were reported in 2007, utilizing a facially-controlled intramolecular $S_N2'$ reaction.[99] Notably, (−)-stephacidin A was achieved in 17 steps with a 6% overall yield. (+)-Stephacidin B is accessed from (−)-stephacidin

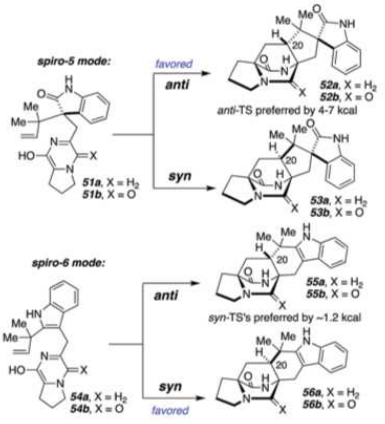


Scheme 18 Theoretical calculations predicting transition state energies and predicted product diastereoselectivities at the B3LYP/6-31G* level.[54]

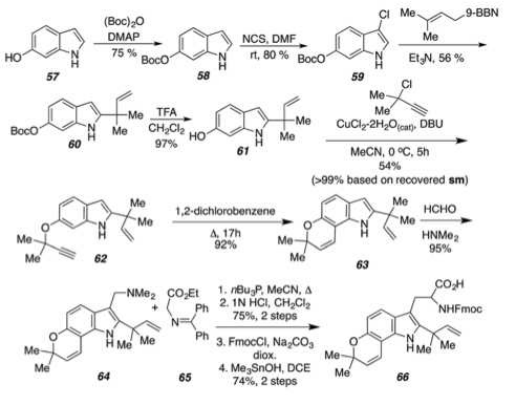


Scheme 19 Synthesis of the reverse-prenylated tryptophan moiety.[63,83,91–95]

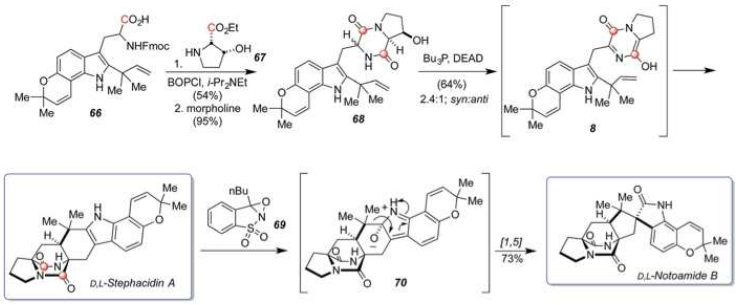


Scheme 20 Biomimetic total synthesis of stephacidin A and notoamide B.[67,97]

A totaling a synthesis of 19 steps with a 1% overall yield. Additionally, (+)-notoamide B can be synthesized from the (−)-enantiomer of stephacidin A *via* the single oxidative pinacol step in 65% yield.[99]

Grubbs, *et al.*, have also been able to conscript the oxaziridine oxidation to a short, biomimetic synthesis of notoamide C, C3-*epi*-notoamide C and notoamide D as shown in Scheme 21.[66] Using the same reverse-prenylated tryptophan species **66**, coupling with (*S*)-proline and cyclization provided a diastereomeric mixture of dioxopiperazines **72** and **73** that were separated and oxidized with the Davis oxaziridine to provide notoamide C (28%), C3-*epi*-notoamide C (48%) and a small amount of notoamide D (together with the corresponding 2,3-epimer in 10% combined yield).[66]

Similarly, notoamide J was prepared as detailed in Scheme 22 deploying the same Davis oxaziridine oxidation of indole **76** to provide notoamide J as a 2 : 1 diastereomeric mixture.[92,100]

As detailed in Scheme 23, biomimetic total syntheses of the malbrancheamides have been successfully realized, deploying the same approach. In contrast to the stephacidin substrate, the Mitsunobu dehydration stops at the stage of dehydroproline derivative **81** that has to be treated with aqueous KOH in methanol at room temperature or below to effect tautomerization to the requisite azadiene that then suffers IMDA cycloaddition to give the cycloadducts **83** and **84** in a ~1 : 2 *anti* : *syn* diastereomeric ratio in good overall yields.[88] Reduction of the tertiary amide in the presence of the secondary amide was readily achieved using di-isobutyl aluminum hydride.[88]

This same approach was also successfully deployed to effect a concise, biomimetic total synthesis of marcfortine C as illustrated in Scheme 24.[90] Readily available β-hydroxypipecolic acid was coupled to reverse-prenylated tryptophan derivative **66** and carried through the analogous sequence deployed for the stephacidin A synthesis. The final spiro-oxindole oxidation required "protecting" the tertiary amine as the corresponding tosylate salt, which permitted smooth and diastereoselective oxidation and spiro-rearrangement to D,L-marcfortine C. This synthesis required a total of fifteen steps from commercially available 6-hydroxyindole with an overall yield of 3.7%.[90]

The asymmetric biomimetic total synthesis of versicolamide B has also been achieved and is described in Scheme 25.[101,102] Similar to the previous discussion, pinacol rearrangement of reverse prenylated indole **68** allows for formation of a set of spiro-oxindole diastereomers. Upon separation, they can consequently be converted into both enantiomers of versicolamide B *via* IMDA cycloaddition. The C3-epimer of (+)-versicolamide B, recently isolated by the Tsukamoto laboratories from *A. taichungensis* and now denoted as *ent*-Taichunamide E,[30] has thus also been achieved *via* this synthetic route (Scheme 25).

Synthetic, isotopically labeled samples of notoamide T and 6-*epi*-notoamide T were prepared by the biomimetic IMDA strategy as shown in Scheme 26.[63] The doubly $^{13}C$-labeled samples of notoamide T and 6-*epi*-notoamide T were deployed

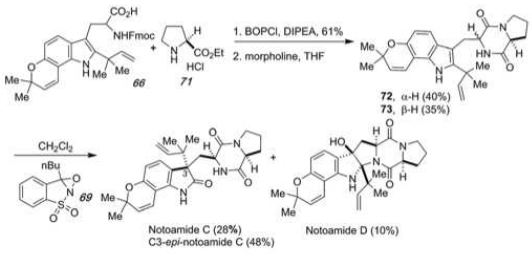


Scheme 21 Biomimetic total syntheses of notoamide C, C3-*epi*-notoamide C and notoamide D.[66]

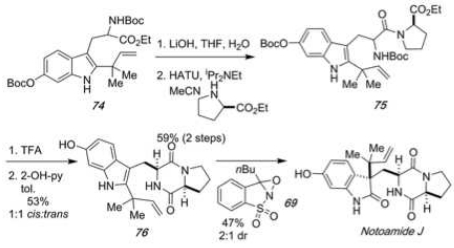


Scheme 22 Biomimetic total syntheses of notoamide J.[92,100]

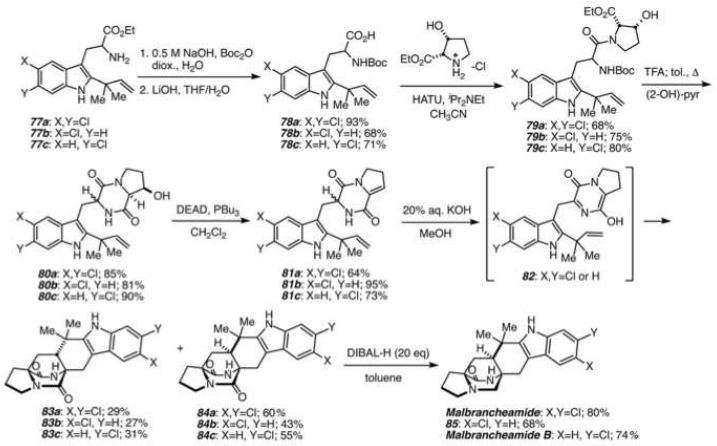


Scheme 23 Biomimetic total synthesis of the malbrancheamides.[88]

in the precursor incorporation experiments described above (Scheme 9, Fig. 8) revealing that 6-*epi*-notoamide T is the biosynthetic precursor to versicolamide B and 6-*epi*-stephacidin A and provided the substrates from which the hitherto unobserved new metabolites were constructed from dormant tailoring genes.[62–64] Efforts are underway to prepare optically pure samples of the individual enantiomers of 6-*epi*-notoamide T to more deeply interrogate the triggering mechanism for the expression of the dormant tailoring genes responsible for the biosynthesis of these new structures which were only produced in the presence of synthetic, racemic 6-*epi*-notoamide T.

For studies relevant to the biosynthesis of the paraherquamides, the IMDA strategy has also been applied to complete the total syntheses of both racemic and optically pure VM55599 and diastereomeric congeners. As shown in Scheme 27, optically pure VM55599, a metabolite co-produced with paraherquamide A, was prepared by the IMDA cycloaddition of *O*-acyl azadiene species **111** generated under conditions reported by Liebscher.[57]

This synthesis enabled the confirmation of the absolute configuration of (−)-VM55599 as the original isolation of this natural, trace metabolite only assigned the relative configuration. As Stocking, *et al.* had demonstrated by labeled precursor incorporation experiments that the biogenetic source of β-methylproline in paraherquamide A was (*S*)-isoleucine,[103] they had tentatively assigned the absolute stereostructure shown (Scheme 27).[104–106] Culturing *Penicillium fellutanum* in a large

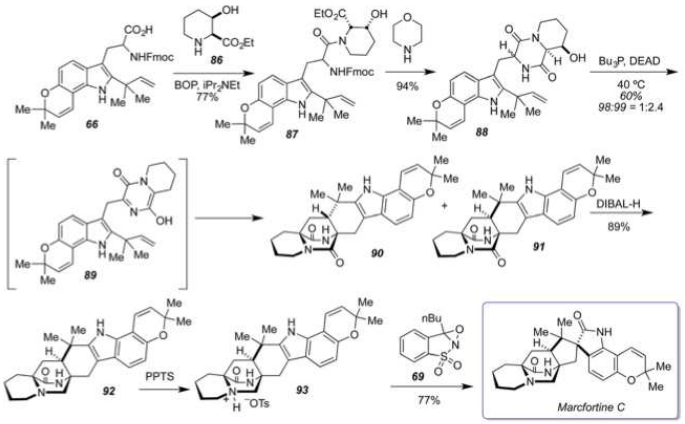


Scheme 24 Biomimetic total synthesis of D,L-marcfortine C.[90]

 

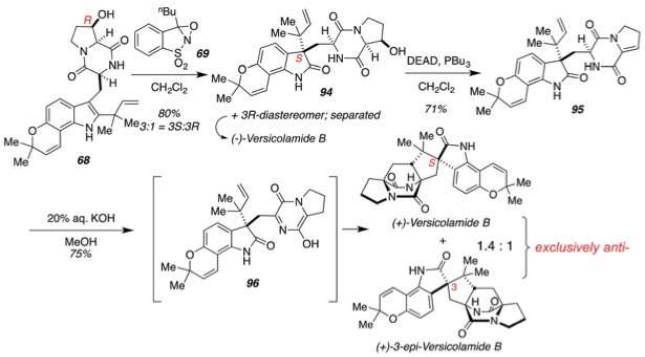


Scheme 25 Biomimetic total synthesis of (+)-versicolamide B and (−)-versicolamide B.[101,102]

format enabled the isolation of about 0.5 mg of natural (−)-VM55599.[107] The synthetic material obtained, which was also derived from (*S*)-isoleucine *via* the Hoffman–Loeffler–Freytag protocol, exactly matched the natural species.[57] Of additional significance, diastereomer **112** was not detected as a reaction product from this laboratory IMDA cycloaddition, revealing that the intrinsic facial bias of this particular IMDA construction favors the VM55599 stereochemistry and not the paraherquamide[108–111] stereochemistry. This provides corroborating, indirect evidence that the enzyme responsible for the key cycloaddition that constructs the bicyclo[2.2.2]diazaoctane core in paraherquamide biosynthesis, must organize the conformation of the putative azadiene (presumably the unacylated congener of **111**) to favor the paraherquamide stereochemistry in both a highly diastereoselective and enantioselective fashion.

Stocking, *et al.*, have also developed a racemic, biomimetic synthesis of VM55599 and the same group of diastereomeric congeners corresponding to **112–114** as illustrated in Scheme 28.[58,112] In this instance, all four diastereomers were produced in the IMDA cycloaddition *via* **121**, which permitted the preparation of an authentic specimen of pre-paraherquamide by diisobutyl aluminum hydride reduction of **122**. As both amino acid subunits **47** and **116** were prepared from glycine, this synthesis was adopted to prepare double $^{13}$C-labeled versions of **122–125**, VM55599 and pre-paraherquamide that were used in precursor incorporation experiments.[112]

## 5. The dioxopiperazine/ monooxopiperazine quandary

It was initially assumed that the bicyclo[2.2.2]diazaoctane ring systems that are common to the monooxopiperazine natural alkaloids, that includes the paraherquamides, marcfortines, asperparalines,[113,114] and malbrancheamides, proceeded *via* biogenetic paths analogous to that of the dioxopiperazine families described in detail above, wherein a late-stage

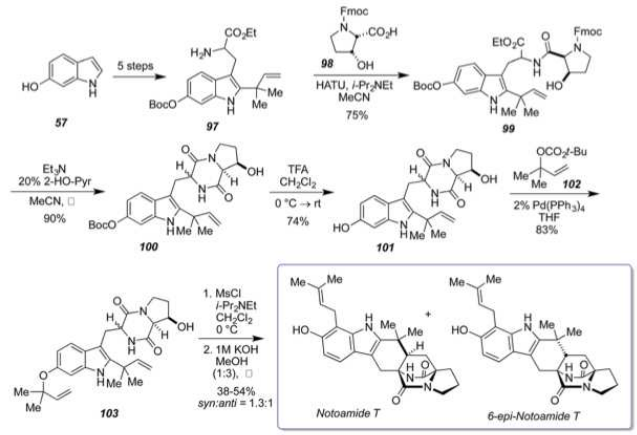


Scheme 26 Biomimetic total synthesis of D,L-notoamide T and D,L-6-*epi*-notoamide T.[63]

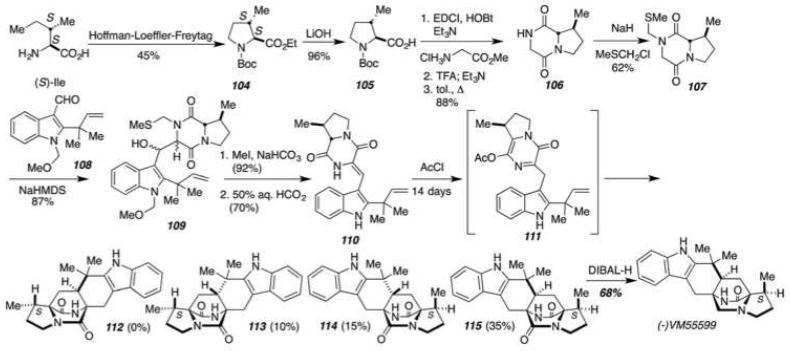

Scheme 27 Biomimetic total synthesis of (−)-VM55599.[57]

reduction of the tryptophan-derived carbonyl group was presumed to occur after the IMDA construction. This assumption has proven to be incorrect based on the following observations. As shown in Scheme 29, precursor incorporation studies with racemic, doubly $^{13}$C-labeled **126**, **127**, VM55599 and pre-paraherquamide were conducted in cultures of *Penicillium fellutanum*, and only pre-paraherquamide incorporated into the paraherquamide A isolated from this experiment (0.73% incorporation).[112] In particular, the observed lack of incorporation of **126** was puzzling, which was presumed as the biosynthetic precursor to pre-paraherquamide.

Ding, *et al.*, observed exactly the same phenomena in malbrancheamide biosynthesis as shown in Scheme 30. Again here, the biomimetic synthesis of pre-malbrancheamide to prepare doubly $^{13}$C-labeled isotopomers of **128** and pre-malbrancheamide was adopted.[115] When both substrates were presented to cultures of *Malbranchea aurantiaca*, only pre-malbrancheamide incorporated into malbrancheamide B (5.5% incorporation). The lack of incorporation of either dioxopiperazine species **126** and **128** begged the question as to when and how the tryptophan-derived carbonyl group is reduced by a net four-electrons? The answer to this quandary came in the most elegant way.

When the NRPS modules from the paraherquamide and malbrancheamide biosynthetic gene clusters were sequenced, it was revealed that the tryptophan module contains a terminal reductase domain, as opposed to the condensation domains evident in both amino acid-loading NRPS modules in notoamide biosynthesis. This is illustrated in Scheme 31.[62] Thus, Li, *et al.*, have devised a new biogenetic hypothesis that envisions

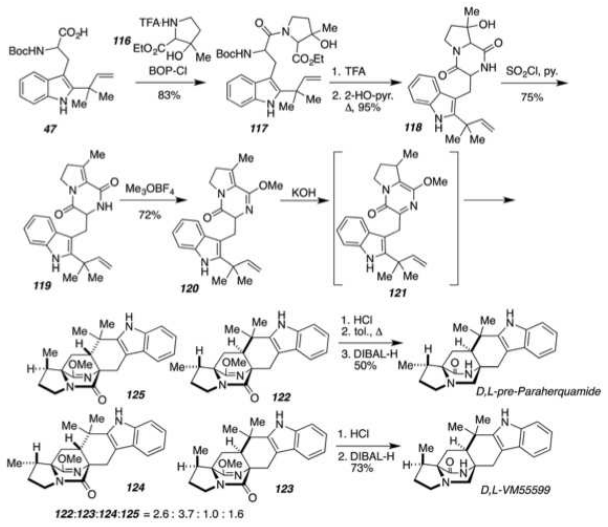

Scheme 28 Biomimetic total synthesis of D,L-VM55599 and D,L-pre-paraherquamide.[58,112]

 

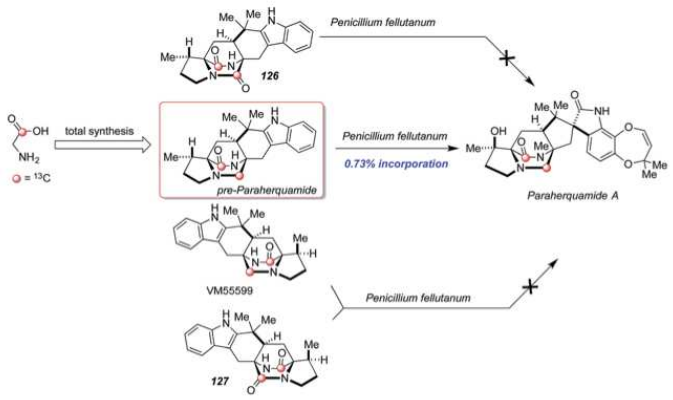


Scheme 29 Results of precursor incorporation studies in *Penicillium fellutanum* with isotopically labeled dioxopiperazine and monooxopiperazine substrates.[112]

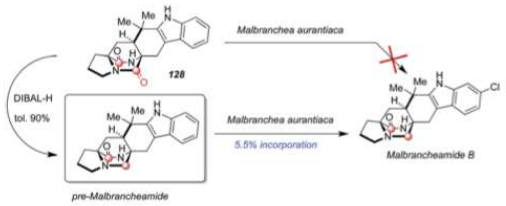


Scheme 30 Results of precursor incorporation studies in *Malbranchea aurantiaca* with isotopically labeled dioxopiperazine and monooxopiperazine substrates.[115]

reductive release of the pro–trp dipeptide from the NRPS module, by either a two-electron or four-electron process (the four-electron reduction is shown) providing species **131** (or, the corresponding aldehyde if the reductive release is a two-electron process) which is then reverse-prenylated and oxidized (for **131**; or just reverse-prenylated for the two-electron process) to give key amino-aldehyde intermediate **132** that should spontaneously cyclize to carbinolamine **133**. Subsequent dehydration to **134** and tautomerization to azadiene species **135** would then allow for IMDA cycloaddition, directly providing pre-paraherquamide (R = Me) and pre-malbrancheamide (R = H), respectively.[62] This proposed biogenetic pathway explains why the dioxopiperazine species **126** and **128** did not incorporate as they are not pathway intermediates!

The gene clusters for the post-NRPS module tailoring enzymes that construct species **132** merits additional scrutiny as the timing of the events leading from the NRPS module to the cycloadducts remains to be resolved.

## 6. Fungal producers of prenylated indole alkaloids

A large number of species of *Penicillium* and *Aspergillus*, both presently with approximately 400 described and accepted species[116–119] are able to produce prenylated indole alkaloids,

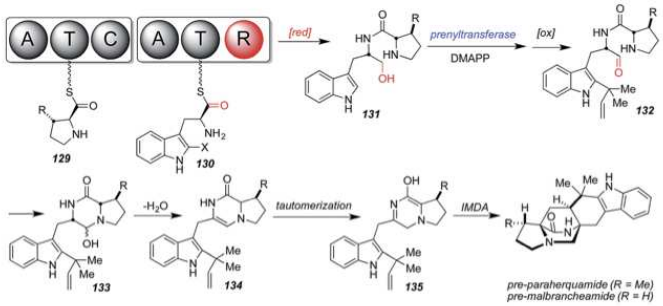


Scheme 31 Molecular architecture of the monooxopiperazine NRPS module and a hypothetical biogenetic pathway to pre-paraherquamide and pre-malbrancheamide.[62]

including penitrems, cyclopiazonic acid, aflavinins, paspalines, fumigaclavines, janthitrems/shearinins, thiersindoles, fumitremorgins, roquefortines, rugulovasines *etc.*[120,121] In *Penicillium*, these secondary metabolites are predominantly produced by species in subgenus *Penicillium*, but several producers are also found in subgenus *Aspergilloides*. While penitrems are restricted to subgenus *Penicillium*, the related shearinins are produced by species in both subgenera. Several species in *Penicillium* produce roquefortine C as the biosynthetic end-product, including *P. expansum*, *P. griseofulvum*, *P. crustosum*, *P. hordei*, *P. robsamsonii*, *P. samsonianum*, *P. roqueforti*, *P. carneum* and *P. paneum*, while other species accumulate meleagrin and oxalines, derived from roquefortine C, for example *P. chrysogenum*, *P. rubens*, *P. oxalicum*, *P. compactum*, *P. concentricum*, *P. coprobium*, *P. glandicola*, *P. crystallinum* and *P. malodoratum*.[117,120,122] Interestingly, neoxaline is also produced by several species in *Aspergillus* section *Nigri*, but only in the uniseriate species.[123,124] None of these secondary metabolites have been found outside the genera *Aspergillus* and *Penicillium*, except that few species in *Talaromyces* can produce rugulovasines.[116,125]

The bicyclo[2.2.2]diazaoctane ring system containing prenylated indole alkaloids are more restricted in their distribution, but again most of them are produced by species of *Penicillium* and *Aspergillus*. The known exception is the malbrancheamides produced by *Malbranchea* species,[22] a species belonging to the *Myxotrichaceae* and unrelated to the *Trichocomaceae*. Since this species already produces the *Penicillium* and *Aspergillus* metabolite penicillic acid,[126] there is a possibility that the fungus was indeed correctly identified as a *Penicillium* or *Aspergillus*. Most of these unique prenylated indole alkaloids are produced by both *Aspergillus* and *Penicillium* species except that the mangrovamides,[127] brevianamides, chrysogenamide, paraherquamides and marcfortines have only been reported from *Penicillium* species, while the asperparalines, sclerotiamides, notoamides, versicolamides, avrainvillamides, stephacidins, and taichunamides have been recorded from *Aspergillus* species. However, chemotaxonomic investigations have shown that the mangrovamides and okaramines have been found in both genera (Frisvad, unpublished data). In *Penicillium,* the brevianamides are produced only by two species in subgenus *Penicillium* section *Fasciculata* (*P. viridicatum*) and subgenus *Penicillium* section *Brevicompacta* (*P. brevicompactum*).[120,122] The marcfortines have until now only been found in *Penicillium paneum* in subgenus *Penicillium* section *Roquefortorum*.[120,122] The paraherquamides have been found in *Penicillium paraherquei*[10] (*Penicillium* section *Lanata-Divaricata*) and *P. canescens* (*Penicillium* section *Canescentia*) (originally determined as *P. charlesii*).[11] Chrysogenamide was reported from *P. chrysogenum*,[29] but the identity of the producing organisms has not been confirmed.

The producers of the related asperparalines (aspergillimides), avrainvillamides, notoamides, sclerotiamides, stephacidins, taichunamides, and versicolamides are produced by species in *Aspergillus* subgenus *Circumdati* sections *Candidi*, *Circumdati*, and *Nigri*, and in subgenus *Nidulantes* section *Versicolores*. Species producing those metabolites in section *Candidi* include *A. subalbidus* and *A. taichungensis*.[128,129] Species in section *Nigri* producing aspergillamides include *A. brunneoviolaceus* (*A. fijiensis*).[124] In section *Circumdati* the species *A. affinis*, *A. auricomus*, *A. bridgeri*, *A. melleus*, *A. ochraceus*, *A. ostianus*, *A. pallidofulvus*, *A. persii*, *A. salwaensis*, *A. sclerotiorum*, *A. sesamicola*, *A. subramanianii*, *A. westerdijkiae* and *A. westlandensis* produce "Aspergamides", which is a mixture of notoamides, avrainvillamides, stephacidins, and sclerotiamide.[116] Finally, *Aspergillus* subgenus *Nidulantes* section *Versicolores* contains producers of "Aspergamides": *A. amoenus* and *A. protuberus*,[35] but "Aspergamides" could not be found in any species in section *Nidulantes*.[130] Further studies will show whether the producing species in these sections of Aspergilli all have stereochemical diversity in their production of these compounds.

## 7. Conclusions

The biogenesis of prenylated indole alkaloid families containing the unique bicyclo[2.2.2]diazaoctane core, obtained from various genera of marine and terrestrial fungi has revealed a number of fascinating aspects of secondary metabolite biosynthesis. First, it is clear that the biosynthetic gene clusters responsible for directing the biosyntheses of these structurally alluring natural compounds are widely distributed in the biosphere. In particular, the orthologous pairs of marine and terrestrial fungi responsible for stephacidin and notoamide biosyntheses, have extensively interrogated the stereochemistry of these molecular frameworks in both a relative and absolute sense. A vast repertoire of tailoring genes is in evidence, and the experiments described in Scheme 9 and Fig. 8 reveal that many dormant tailoring genes likely lie in reserve in the genomes of these complex organisms. It is particularly intriguing to ponder the speciation events that occurred at some time during the evolutionary history of these fungi that resulted in enantiomerically distinct secondary metabolite profiles. Very little is known about the adaptive advantage with which these secondary metabolites embellish the producing fungi as the biological activities of these natural alkaloids have been only superficially examined and demand further elucidation.

It is also now clear that Nature has, perhaps, "accidentally" created the bicyclo[2.2.2]diazaoctane ring system through the generation of reactive, achiral azadiene species (**138**, Scheme 32). The achiral intermediates are conformationally restricted in the chiral environment of the enzyme binding sites that generate these species, and thus orchestrates these reactive azadiene species to undergo highly enantio- and diastereoselective cycloadditions culminating in the formation of the natural substances constituted with the bicyclo[2.2.2]diazaoctane core. Our biomimetic laboratory IMDA reactions, which proceed smoothly at or below room temperature in organic or aqueous solvents, are very facile transformations that in the biochemical setting, only require pre-organization of the pre-transition state conformations.

It is further noteworthy that, in the monooxopiperazine families, the predominant relative stereochemistry is *syn-* (all known paraherquamide alkaloids in this family are *syn-*; see Fig.

 

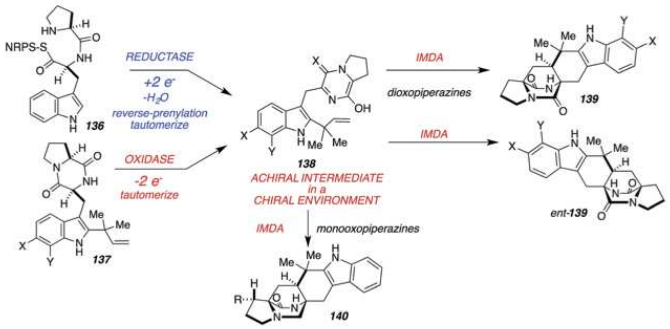


Scheme 32 Unified biogenetic hypothesis for prenylated indole alkaloids containing the bicyclo[2.2.2]diazaoctane nucleus.[53]

1 and 4) and only a single absolute configuration is currently in evidence (with the exception of VM55599, a shunt metabolite of paraherquamide biosynthesis). To date, the only monooxopiperazine-producing fungi that construct the corresponding *anti*-diastereomeric series are *Penicillium purpurogenum* G59 (penicimutamides D and E; *P. purpurogenum* G59 has been mischaracterized and is a *Penicillium citrinum*),[15] *Penicillium chrysogenum* (chrysogenamide A)[29] and *Penicillium citrinum* F53 (the recently described citrinalin C).[146] In stark contradistinction, the dioxopiperazine families display a broader range of relative and absolute stereochemistry, where a myriad of both *syn*- and *anti*-metabolites have been isolated in both enantiomeric forms. Most intriguing from an evolutionary perspective, the enantio-divergence evident in both marine- and terrestrial-producing fungi, provides for a very rich and unique opportunity to study molecular evolution of these organisms.

The application of whole-genome sequencing, bioinformatics analysis, cloning and functional expression of biosynthetic enzymes, synthesis of labeled pathway metabolites, precursor incorporation studies, structure determination of new metabolites and total syntheses of both new/undiscovered and known metabolites has been deployed to gain a deeper understanding of the secondary metabolome of marine and terrestrial fungi that produce these families of alkaloids. It should be noted that many laboratories in the synthetic community have published elegant, yet non-biomimetic total syntheses of numerous natural products in this family of alkaloids.[41,46,47,57,58,66,67,85,86,88,90,95,97,99,102,108,115,131–146] These efforts have been reviewed by Miller and Williams in 2009 (ref. 40) and additional total syntheses have appeared in the literature since 2009.[138–146] Complete knowledge of the structural and stereochemical homologies and disparities among these compounds continues to motivate research into the synthesis, chemistry, biochemistry, genetics and biology of natural fungal metabolites. It is anticipated that exciting new chapters of these fascinating natural alkaloids remain to be written.

## 8. Conflicts of interest

There are no conflicts to declare.

## 9. Acknowledgments

This work was financially supported in part by Grants-in-Aid for Scientific Research (No. 23108518 and 25108719 to S. T. and 24710252 to H.·K.) from the Ministry of Education, Culture, Sports, Science and Technology of Japan and also by grants (S. T.) from the Naito Foundation, the Nagase Science and Technology Foundation, and the Yamada Science Foundation. Financial support from the National Institutes of Health (R01 CA070375 to R. M. W. and D. H.·S.) is gratefully acknowledged. The authors wish to dedicate this manuscript to Professor Yoshito Kishi of Harvard University celebrating his 80th birthday.

## 10. References

1 A. J. Birch and J. J. Wright, *Tetrahedron Lett.*, 1970, **26**, 2329–2344.
2 A. J. Birch and R. A. Russel, *Tetrahedron Lett.*, 1972, **28**, 2999–3008.
3 P. S. Steyn, *Tetrahedron Lett.*, 1973, **29**, 107–120.
4 A. J. Birch and J. J. Wright, *Chem. Commun.*, 1969, 644–645.
5 R. R. M. Paterson and D. L. Hawksworth, *Trans. Br. Mycol. Soc.*, 1985, **85**, 95–100.
6 J. E. Robbers and J. W. Straus, *Lloydia*, 1974, **38**, 355–356.
7 B. J. Wilson, D. T. C. Yang and T. M. Harris, *Appl. Microbiol.*, 1973, **26**, 633–635.
8 J. Polonsky, M.-A. Merrien, T. Prangé, C. Pascard and S. Moreau, *J. Chem. Soc., Chem. Commun.*, 1980, 601–602.
9 T. Prangé, M.-A. Billion, M. Vuilhorgne, C. Pascard and J. Polonsky, *Tetrahedron Lett.*, 1981, **22**, 1977–1980.
10 M. Yamazaki, E. Okuyama, M. Kobayashi and H. Inoue, *Tetrahedron Lett.*, 1981, **22**, 135–136.
11 J. G. Ondeyka, R. T. Goegelman, J. M. Schaeffer, L. Kelemen and L. Zitano, *J. Antibiot.*, 1990, **43**, 1375–1379.
12 J. M. Liesch and C. F. Wichmann, *J. Antibiot.*, 1990, **43**, 1380–1386.
13 S. E. Blanchflower, R. M. Banks, J. R. Everet, B. R. Manger and C. Reading, *J. Antibiot.*, 1991, **44**, 492–497.

14 S. E. Blanchflower, R. M. Banks, J. R. Everet, B. R. Manger and C. Reading, *J. Antibiot.*, 1993, **46**, 1355–1363.
15 C.-J. Wu, C.-W. Li, H. Gao, X.-J. Huang and C.-B. Cui, *RSC Adv.*, 2017, **7**, 24718–24722.
16 C. Authrine and J. B. Gloer, *J. Nat. Prod.*, 1996, **59**, 1093–1095.
17 H. Hayashi, Y. Nishimoto and H. Nozaki, *Tetrahedron Lett.*, 1997, **38**, 5655–5658.
18 W. Fenical, P. R. Jensen and X. C. Cheng, *U.S. Pat.*, 6,066,635, 2000.
19 Y. Sugie, H. Hirai, T. Inagaki, M. Ishiguro, Y.-J. Kim, Y. Kojima, T. Sakakibara, S. Sakemi, A. Sugiura, Y. Suzuki, L. Brennan, J. Duignan, L. H. Huang, J. Sutcliffe and N. Kojima, *J. Antibiot.*, 2001, **54**, 911–916.
20 J. Qian-Cutrone, S. Huang, Y.-Z. Shu, D. Vyas, C. Fairchild, A. Menendez, K. Krampitz, R. Dalterio, S. E. Klohr and Q. Gao, *J. Am. Chem. Soc.*, 2002, **124**, 14556–14557.
21 S. Martínez-Luis, R. Rodriguez, L. Acevedo, M. C. González, A. Lira-Rocha and R. Mata, *Tetrahedron*, 2006, **62**, 1817–1822.
22 M. Figueroa, M. C. González and R. Mata, *Nat. Prod. Res.*, 2008, **22**, 709–714.
23 K. R. Watts, S. T. Loveridge, K. Tenney, J. Media, F. A. Valeriote and P. Crews, *J. Org. Chem.*, 2011, **76**, 6201–6208.
24 H. Kato, T. Yoshida, T. Tokue, Y. Nojiri, H. Hirota, T. Ohta, R. M. Williams and S. Tsukamoto, *Angew. Chem., Int. Ed.*, 2007, **46**, 2254–2256.
25 S. Tsukamoto, H. Kato, M. Samizo, Y. Nojiri, H. Onuki, H. Hirota and T. Ohta, *J. Nat. Prod.*, 2008, **71**, 2064–2067.
26 S. Tsukamoto, T. Kawabata, H. Kato, T. J. Greshock, H. Hirota, T. Ohta and R. M. Williams, *Org. Lett.*, 2009, **11**, 1297–1300.
27 S. Tsukamoto, H. Umaoka, K. Yoshikawa, T. Ikeda and H. Hirota, *J. Nat. Prod.*, 2010, **73**, 1438–1440.
28 T. J. Greshock, A. W. Grubbs, P. Jiao, D. T. Wicklow, J. B. Gloer and R. M. Williams, *Angew. Chem., Int. Ed.*, 2008, **47**, 3573–3577.
29 Z. Lin, J. Wen, T. Zhu, Y. Fang, Q. Gu and W. Zhu, *J. Antibiot.*, 2008, **61**, 81–85.
30 I. Kagiyama, H. Kato, T. Nehira, J. C. Frisvad, D. H. Sherman, R. M. Williams and S. Tsukamoto, *Angew. Chem., Int. Ed.*, 2016, **55**, 1128–1132.
31 K. A. Miller, M. Figueroa, M. W. N. Valente, T. J. Greshock, R. Mata and R. M. Williams, *Bioorg. Med. Chem. Lett.*, 2008, **18**, 6479–6481.
32 R. R. M. Paterson, M. J. S. Simmonds, C. Kemmelmeier and W. M. Blaney, *Mycol. Res.*, 1990, **94**, 538–542.
33 R. R. M. Paterson, M. S. J. Simmonds and W. M. Blaney, *J. Invertebr. Pathol.*, 1987, **50**, 124–133.
34 D. L. Doerfler, C. P. Nulton, C. D. Bartman, F. J. Gottlieb and I. M. Campbell, *Can. J. Microbiol.*, 1978, **24**, 1490–1500.
35 J. M. Finefield, J. C. Frisvad, D. H. Sherman and R. M. Williams, *J. Nat. Prod.*, 2012, **75**, 812–833.
36 J. M. Finefield, D. H. Sherman, M. Kreitman and R. M. Williams, *Angew. Chem., Int. Ed.*, 2012, **51**, 4802–4836.
37 R. M. Williams, *Chem. Pharm. Bull.*, 2002, **50**, 711–740.
38 E. M. Stocking and R. M. Williams, *Angew. Chem., Int. Ed.*, 2003, **42**, 3078–3115.
39 R. M. Williams and R. J. Cox, *Acc. Chem. Res.*, 2003, **36**, 127–139.
40 K. A. Miller and R. M. Williams, *Chem. Soc. Rev.*, 2009, **38**, 3160–3174.
41 J. D. Sunderhaus, D. H. Sherman and R. M. Williams, *Isr. J. Chem.*, 2011, **51**, 442–452.
42 R. M. Williams, E. M. Stocking and J. F. Sanz-Cervera, *Top. Curr. Chem.*, 2000, **209**, 97–173.
43 A. E. A. Porter and P. G. Sammes, *Chem. Commun.*, 1970, 1103.
44 J. Baldas, A. J. Birch and R. A. Russell, *J. Chem. Soc., Perkin Trans. 1*, 1974, **1**, 50.
45 A. J. Birch, *J. Agric. Food Chem.*, 1971, **19**, 1088–1092.
46 R. M. Williams, T. Glinka and E. Kwast, *J. Am. Chem. Soc.*, 1988, **110**, 5927–5929.
47 R. M. Williams, T. Glinka, E. Kwast, H. Coffman and J. K. Stille, *J. Am. Chem. Soc.*, 1990, **112**, 808–821.
48 R. M. Williams and T. Glinka, *Tetrahedron Lett.*, 1986, **27**, 3581–3584.
49 R. M. Williams, E. Kwast, H. Coffman and T. Glinka, *J. Am. Chem. Soc.*, 1989, **111**, 3064–3065.
50 E. M. Stocking, R. M. Williams and J. F. Sanz-Cervera, *J. Am. Chem. Soc.*, 2000, **122**, 9089–9098.
51 J. F. Sanz-Cervera, T. Glinka and R. M. Williams, *J. Am. Chem. Soc.*, 1993, **115**, 347–348.
52 J. F. Sanz-Cervera, T. Glinka and R. M. Williams, *Tetrahedron*, 1993, **49**, 8471–8482.
53 K. Klas, S. Tsukamoto, D. H. Sherman and R. M. Williams, *J. Org. Chem.*, 2015, **80**, 11672–11685.
54 L. R. Domingo, R. J. Zaragozá and R. M. Williams, *J. Org. Chem.*, 2003, **68**, 2895–2902.
55 L. R. Domingo, J. F. Sanz-Cervera, R. M. Williams, M. T. Picher and J. A. Marco, *J. Org. Chem.*, 1997, **62**, 1662–1667.
56 L. A. Adams, C. R. Gray and R. M. Williams, *Tetrahedron Lett.*, 2004, **45**, 4489–4493.
57 J. F. Sanz-Cervera and R. M. Williams, *J. Am. Chem. Soc.*, 2002, **124**, 2556–2559.
58 E. M. Stocking, J. F. Sanz-Cervera and R. M. Williams, *J. Am. Chem. Soc.*, 2000, **122**, 1675–1683.
59 J. F. Sanz-Cervera, R. M. Williams, J. A. Marco, J. M. López-Sánchez, F. González, M. E. Martínez and F. Sancenón, *Tetrahedron*, 2000, **56**, 6345–6358.
60 R. M. Williams, J. F. Sanz-Cervera, F. Sancenón, J. A. Marco and K. M. Halligan, *Bioorg. Med. Chem.*, 1998, **6**, 1233–1241.
61 H. Kato, T. Nakahara, K. Sugimoto, K. Matsuo, I. Kagiyama, J. C. Frisvad, D. H. Sherman, R. M. Williams and S. Tsukamoto, *Org. Lett.*, 2015, **17**, 700–703.
62 S. Li, K. Srinivasan, H. Tran, F. Yu, J. M. Finefield, J. D. Sunderhaus, T. J. McAfoos, S. Tsukamoto, R. M. Williams and D. H. Sherman, *Med. Chem. Commun.*, 2012, **3**, 987–996.
63 J. D. Sunderhaus, T. J. McAfoos, J. M. Finefield, H. Kato, S. Li, S. Tsukamoto, D. H. Sherman and R. M. Williams, *Org. Lett.*, 2013, **15**, 22–25.

64 H. Kato, T. Nakahara, M. Yamaguchi, I. Kagiyama, J. M. Finefield, J. D. Sunderhaus, D. H. Sherman, R. M. Williams and S. Tsukamoto, *Tetrahedron Lett.*, 2015, **56**, 247–251.
65 S. Tsukamoto, H. Umaoka, K. Yoshikawa, T. Ikeda and H. Hirota, *J. Nat. Prod.*, 2013, **76**, 1232–1232.
66 A. W. Grubbs, G. D. Artman III, S. Tsukamoto and R. M. Williams, *Angew. Chem., Int. Ed.*, 2007, **46**, 2257–2261.
67 T. J. Greshock, A. W. Grubbs, S. Tsukamoto and R. M. Williams, *Angew. Chem., Int. Ed.*, 2007, **46**, 2262–2265.
68 S. Tsukamoto, H. Kato, T. J. Greshock, H. Hirota, T. Ohta and R. M. Williams, *J. Am. Chem. Soc.*, 2009, **131**, 3834–3835.
69 S. Tsukamoto, H. Kato, T. J. Greshock, H. Hirota, T. Ohta and R. M. Williams, *J. Am. Chem. Soc.*, 2013, **135**, 10878–10878.
70 J. M. Finefield, H. Kato, T. J. Greshock, D. H. Sherman, S. Tsukamoto and R. M. Williams, *Org. Lett.*, 2011, **13**, 3802–3805.
71 R. J. Cox and R. M. Williams, *Tetrahedron Lett.*, 2002, **43**, 2149–2152.
72 J. Fuchser, Ph. D. Dissertation, University of Gottingen, 1995.
73 J. M. Finefield, T. J. Greshock, D. H. Sherman, S. Tsukamoto and R. M. Williams, *Tetrahedron Lett.*, 2011, **52**, 1987–1989.
74 T. J. McAfoos, S. Li, S. Tsukamoto, D. H. Sherman and R. M. Williams, *Heterocycles*, 2010, **82**, 461–472.
75 H. Kato, Y. Nakamura, J. M. Finefield, H. Umaoka, T. Nakahara, R. M. Williams and S. Tsukamoto, *Tetrahedron Lett.*, 2011, **52**, 6923–6926.
76 J. M. Finefield, D. H. Sherman, S. Tsukamoto and R. M. Williams, *J. Org. Chem.*, 2011, **76**, 5954–5958.
77 S. Li, J. M. Finefield, J. D. Sunderhaus, T. J. McAfoos, R. M. Williams and D. H. Sherman, *J. Am. Chem. Soc.*, 2012, **134**, 788–791.
78 S. Cai, Y. Luan, X. Kong, T. Zhu, Q. Gu and D. Li, *Org. Lett.*, 2013, **15**, 2168–2171.
79 F. Li, Z. Zhang, G. Zhang, Q. Che, T. Zhu, Q. Gu and D. Li, *Org. Lett.*, 2018, **20**, 1138–1141.
80 S. Cai, Y. Luan, X. Kong, T. Zhu, Q. Gu and D. Li, *Org. Lett.*, 2013, **15**, 2168–2171.
81 See ref. 24 for the isolation and structural elucidation of the corresponding N1–OH diastereomer of versicolamide C, notoamide A.
82 S. Maiya, A. Grundmann, S.-M. Li and G. Turner, *ChemBioChem*, 2006, **7**, 1062–1069.
83 Y. Ding, J. R. deWet, J. Cavalcoli, S. Li, T. J. Greshock, K. A. Miller, J. M. Finefield, J. D. Sunderhaus, T. J. McAfoos, S. Tsukamoto, R. M. Williams and D. H. Sherman, *J. Am. Chem. Soc.*, 2010, **132**, 12733–12740.
84 S. A. Newmister, C. M. Gober, S. Romminger, F. Yu, A. Tripathi, L. L. L. Parra, R. M. Williams, R. G. S. Berlinck, M. M. Joullié and D. H. Sherman, *J. Am. Chem. Soc.*, 2016, **138**, 11176–11184.
85 R. M. Williams, J. F. Sanz-Cervera, F. Sancenón, J. A. Marco and K. Halligan, *J. Am. Chem. Soc.*, 1998, **120**, 1090–1091.
86 L. A. Adams, M. W. N. Valente and R. M. Williams, *Tetrahedron*, 2006, **62**, 5195–5200.
87 J. G. Robins, K. J. Kim, A. J. Chinn, J. S. Woo and J. R. Scheerer, *J. Org. Chem.*, 2016, **81**, 2293–2301.
88 K. A. Miller, T. R. Welch, T. J. Greshock, Y. Ding, D. H. Sherman and R. M. Williams, *J. Org. Chem.*, 2008, **73**, 3116–3119.
89 D. H. Sherman, R. M. Williams, *et al.*, unpublished results.
90 T. J. Greshock, A. W. Grubbs and R. M. Williams, *Tetrahedron*, 2007, **63**, 6124–6130.
91 A. W. Grubbs, G. D. Artman III and R. M. Williams, *Tetrahedron Lett.*, 2005, **46**, 9013–9016.
92 J. M. Finefield and R. M. Williams, *J. Org. Chem.*, 2010, **75**, 2785–2789.
93 R. M. Williams, J. Cao and H. Tsujishima, *Angew. Chem., Int. Ed.*, 2000, **39**, 2540–2544.
94 T. D. Cushing, J. F. Sanz-Cervera and R. M. Williams, *J. Am. Chem. Soc.*, 1996, **118**, 557–579.
95 T. D. Cushing, J. F. Sanz-Cervera and R. M. Williams, *J. Am. Chem. Soc.*, 1993, **115**, 9323–9324.
96 (*a*) M. Somei, Y. Karasawa and C. Kaneko, *Heterocycles*, 1981, **16**, 941–949; (*b*) T. Kametani, N. Kanaya and M. Ihara, *J. Chem. Soc., Perkin Trans. 1*, 1981, **3**, 959.
97 T. J. Greshock and R. M. Williams, *Org. Lett.*, 2007, **9**, 4255–4258.
98 F. A. Davis, J. C. Towson, D. B. Vashi, R. ThimmaReddy, J. P. McCauley, M. E. Harakal and D. J. Gosciniak, *J. Org. Chem.*, 1990, **55**, 1254–1261.
99 G. D. Artman III, A. W. Grubbs and R. M. Williams, *J. Am. Chem. Soc.*, 2007, **129**, 6336–6342.
100 J. M. Finefield and R. M. Williams, *J. Org. Chem.*, 2013, **78**, 8214.
101 K. A. Miller, S. Tsukamoto and R. M. Williams, *Nat. Chem.*, 2009, **1**, 165–165.
102 K. A. Miller, S. Tsukamoto and R. M. Williams, *Nat. Chem.*, 2009, **1**, 63–68.
103 E. M. Stocking, J. F. Sanz-Cervera, C. J. Unkefer and R. M. Williams, *Tetrahedron*, 2001, **57**, 5303–5320.
104 E. M. Stocking, J. F. Sanz-Cervera and R. M. Williams, *Angew. Chem., Int. Ed.*, 2001, **40**, 1296–1298.
105 E. M. Stocking, R. A. Martinez, L. A. Silks, J. F. Sanz-Cervera and R. M. Williams, *J. Am. Chem. Soc.*, 2001, **123**, 3391–3392.
106 E. M. Stocking, J. F. Sanz-Cervera, R. M. Williams and C. J. Unkefer, *J. Am. Chem. Soc.*, 1996, **118**, 7008–7009.
107 Y. Ding, S. Gruschow, T. J. Greshock, J. M. Finefield, D. H. Sherman and R. M. Williams, *J. Nat. Prod.*, 2008, **71**, 1574–1578.
108 R. M. Williams, J. Cao, H. Tsujishima and R. J. Cox, *J. Am. Chem. Soc.*, 2003, **125**, 12172–12178.
109 R. M. Williams and J. Cao, *Tetrahedron Lett.*, 1996, **37**, 5441–5444.
110 R. M. Williams and T. D. Cushing, *Tetrahedron Lett.*, 1990, **31**, 6325–6328.
111 R. M. Williams, T. Glinka and E. Kwast, *Tetrahedron Lett.*, 1989, **30**, 5575–5578.

112 K. Sommer and R. M. Williams, *Tetrahedron*, 2009, **65**, 3246–3260.
113 C. R. Gray, J. F. Sanz-Cervera, L. A. Silks and R. M. Williams, *J. Am. Chem. Soc.*, 2003, **125**, 14692–14693.
114 F. Gonzalez, J. F. Sanz-Cervera and R. M. Williams, *Tetrahedron Lett.*, 1999, **40**, 4519–4522.
115 (*a*) Y. Ding, T. J. Greshock, K. A. Miller, D. H. Sherman and R. M. Williams, *Org. Lett.*, 2008, **10**, 4863–4866; (*b*) A. E. Fraley, M. Garcia-Borras, A. Tripathi, D. Khare, E. V. Mercado-Marin, H. Tran, Q. Dan, G. P Webb, K. R. Watts, P. Crews, R. Sarpong, R. M. Williams, J. L. Smith, K. N. Houk and D. H. Sherman, *J. Am. Chem. Soc.*, 2017, **139**, 12060–12068.
116 C. M. Visagie, J. Varga, J. Houbraken, M. Meijer, S. Kocsubé, N. Yilmaz, R. Fotedar, K. A. Seifert, J. C. Frisvad and R. A. Samson, *Stud. Mycol.*, 2014, **78**, 1–61.
117 C. M. Visagie, J. Houbraken, J. C. Frisvad, S. B. Hong, C. H. W. Klaassen, G. Perrone, K. A. Seifert, J. Varga, T. Yaguchi and R. A. Samson, *Stud. Mycol.*, 2014, **78**, 343–371.
118 R. A. Samson, C. M. Visagie, J. Houbraken, S.-B. Hong, V. Hubka, C. H. W. Klaassen, G. Perrone, K. A. Seifert, A. Susca, J. B. Tanney, J. Varga, S. Kocsubé, G. Szigeti, T. Yaguchi and J. C. Frisvad, *Stud. Mycol.*, 2014, **78**, 141–173.
119 J. C. Frisvad, *Front Microbiol.*, 2015, **5**, 773.
120 J. C. Frisvad, J. Smedsgaard, T. O. Larsen and R. A. Samson, *Stud. Mycol.*, 2004, **49**, 201–241.
121 J. C. Frisvad and T. O. Larsen, *Appl. Microbiol. Biotechnol.*, 2015, **99**, 7859–7877.
122 J. Houbraken, L. Wang, H. B. Lee and J. C. Frisvad, *Persoonia*, 2016, **36**, 299–314.
123 R. A. Samson, P. Noonim, M. Meijer, J. Houbraken, J. C. Frisvad and J. Varga, *Stud. Mycol.*, 2007, **59**, 129–145.
124 J. Varga, J. C. Frisvad, S. Kocsubé, B. Brankovics, B. Tóth, G. Szigeti and R. A. Samson, *Stud. Mycol.*, 2011, **69**, 1–17.
125 R. A. Samson, N. Yilmaz, J. Houbraken, H. Spierenburg, K. A. Seifert, S. W. Peterson, J. Varga and J. C. Frisvad, *Stud. Mycol.*, 2011, **70**, 159–183.
126 S. Martínez-Luis, M. C. González, M. Ulloa and R. Mata, *Phytochemistry*, 2005, **66**, 1012–1016.
127 B. Yang, J. Dong, X. Lin, X. Zhou, Y. Zhang and Y. Liu, *Tetrahedron*, 2014, **70**, 3859–3863.
128 J. Varga, J. C. Frisvad and R. A. Samson, *Stud. Mycol.*, 2007, **59**, 75–88.
129 V. Hubka, P. Lyskova, J. C. Frisvad, S. W. Peterson, M. Skorepova and M. Kolarik, *Med. Mycol.*, 2014, **52**, 565–576.
130 A. J. Chen, J. C. Frisvad, B. D. Sun, J. Varga, S. Kocsubé, J. Dijksterhuis, D. H. Kim, S.-B. Hong, J. Houbraken and R. A. Samson, *Stud. Mycol.*, 2016, **84**, 1–118.
131 P. S. Baran, C. A. Guerrero, N. B. Ambhaikar and B. D. Hafensteiner, *Angew. Chem., Int. Ed.*, 2005, **44**, 606–609.
132 P. S. Baran, C. A. Guerrero, B. D. Hafensteiner and N. B. Ambhaikar, *Angew. Chem., Int. Ed.*, 2005, **44**, 3892–3895.
133 P. S. Baran, B. D. Hafensteiner, N. B. Ambhaikar, C. A. Guerrero and J. D. Gallagher, *J. Am. Chem. Soc.*, 2006, **128**, 8678–8693.
134 B. M. Trost, N. Cramer and H. Bernsmann, *J. Am. Chem. Soc.*, 2007, **129**, 3086–3087.
135 T. J. Greshock, A. W. Grubbs, P. Jiao, D. T. Wicklow, J. B. Gloer and R. M. Williams, *Angew. Chem., Int. Ed.*, 2008, **47**, 3573–3577.
136 M. Pichowicz, N. S. Simpkins, A. J. Blake and C. Wilson, *Tetrahedron*, 2008, **64**, 3713–3735.
137 F. Frebault, N. S. Simpkins and A. Fenwick, *J. Am. Chem. Soc.*, 2009, **131**, 4214–4215.
138 F. C. Frebault and N. S. Simpkins, *Tetrahedron*, 2010, **66**, 6585–6596.
139 T. J. McAfoos, S. Li, S. Tsukamoto, D. H. Sherman and R. M. Williams, *Heterocycles*, 2010, **82**, 461–472.
140 S. W. Laws and J. R. Scheerer, *J. Org. Chem.*, 2013, **78**, 2422–2429.
141 N. S. Simpkins, I. Pavlakos, M. D. Weller and L. Male, *Org. Biomol. Chem.*, 2013, **11**, 4957–4970.
142 J. D. Sunderhaus, T. J. McAfoos, J. M. Finefield, H. Kato, S. Li, S. Tsukamoto, D. H. Sherman and R. M. Williams, *Org. Lett.*, 2013, **15**, 22–25.
143 B. M. Trost, D. A. Bringley, T. Zhang and N. Cramer, *J. Am. Chem. Soc.*, 2013, **135**, 16720–16735.
144 E. V. Mercado-Marin and R. Sarpong, *Chem. Sci.*, 2015, **6**, 5048–5052.
145 B. Zhang, W. Zheng, X. Wang, D. Sun and C. Li, *Angew. Chem., Int. Ed.*, 2016, **55**, 10435–10438.
146 K. Mukai, D. P. de Sant'Ana, Y. Hirooka, E. V. Mercado-Marin, D. E. Stephens, K. G. M. Kou, S. C. Richter, N. Kelley and R. Sarpong, *Nat. Chem.*, 2018, **10**, 38–44.

# Appendix VI: Fungal Indole Alkaloid Biogenesis Through Evolution of a Bifunctional Reductase/Diels-Alderase

This manuscript is published online at ChemRXiv and is under revision in *Nature Chemistry*.[143-144]

**Fungal Indole Alkaloid Biogenesis Through Evolution of a Bifunctional Reductase/Diels-Alderase**

Qingyun Dan,[1,2,#] Sean A. Newmister,[1,#] Kimberly R. Klas,[3] Amy E. Fraley,[1,4] Timothy J. McAfoos,[3] Amber D. Somoza,[3] James D. Sunderhaus,[3] Ying Ye,[1] Vikram V. Shende,[1,5] Fengan Yu,[1] Jacob N. Sanders,[6] W. Clay Brown,[1] Le Zhao,[3] Robert S. Paton,[3] K. N. Houk,[6] Janet L. Smith,[1,2] David H. Sherman,[1,4,*] and Robert M. Williams[3,7,*]

[1]Life Sciences Institute, University of Michigan, Ann Arbor, Michigan 48109, USA; [2]Department of Biological Chemistry, University of Michigan, Ann Arbor, Michigan 48109, USA; [3]Department of Chemistry, Colorado State University, Fort Collins, Colorado 80523, USA; [4]Departments of Medicinal Chemistry, Microbiology & Immunology, and Chemistry, University of Michigan, Ann Arbor, Michigan 48109, USA; [5]Program in Chemical Biology, University of Michigan, Ann Arbor, Michigan 48109, USA; [6]Department of Chemistry and Biochemistry, University of California, Los Angeles, California, 90095, USA; [7]University of Colorado Cancer Center, Aurora, Colorado 80045, USA.

[#]These authors contributed equally to this work.

*Robert M. Williams: robert.williams@colostate.edu; David H. Sherman: davidhs@umich.edu.

**Abstract**

Prenylated indole alkaloids isolated from various fungi possess great structural diversity and pharmaceutical utility. Among them are the calmodulin inhibitory malbrancheamides and paraherquamides, used as anthelmintics in animal health. Herein, we report complete elucidation of the malbrancheamide biosynthetic pathway accomplished through complementary approaches. These include a biomimetic total synthesis to access the natural alkaloid and biosynthetic intermediates in racemic form, and *in vitro* enzymatic reconstitution that provides access to the natural antipode (+)-malbrancheamide. Reductive cleavage of a L-Pro-L-Trp dipeptide from the MalG nonribosomal peptide synthetase (NRPS) followed by reverse prenylation and a cascade of post-NRPS reactions culminates in an intramolecular [4+2] hetero-Diels-Alder (IMDA) cyclization to furnish the bicyclo[2.2.2]diazaoctane scaffold. Enzymatic assembly of optically pure (+)-premalbrancheamide involves an unexpected zwitterionic intermediate where MalC catalyzes enantioselective cycloaddition as a bifunctional NADPH-dependent reductase/Diels-Alderase. Crystal structures of substrate and product complexes together with site-directed mutagenesis and molecular dynamics simulations demonstrated how MalC and PhqE, its homolog from the paraherquamide pathway, catalyze diastereo- and enantioselective cyclization in the construction of this important class of secondary metabolites.

Prenylated indole alkaloids comprised of the bicyclo[2.2.2]diazaoctane core have attracted considerable interest due to their wide spectrum of biological activities and offer compelling targets for chemical synthesis and biosynthetic studies.[1-3] Among them, 2-deoxy-paraherquamide A (derquantel) is a commercial therapeutic agent for treating parasitic nematodes in sheep.[4-6] It is now clear that in various genera of fungi, two distinct families containing a bicyclo[2.2.2]diazaoctane system have evolved: (1) the dioxopiperazines such as the anti-cancer stephacidins, insecticidal brevianamides and cytotoxic notoamides, and (2) the monooxopiperazines, including the anthelmintic paraherquamides, asperparalines and calmodulin-inhibitory malbrancheamides (Fig. 1a, **1-5**). In addition, the citrinadins represent another related series of alkaloids that are thought to be derived by deconstruction of monooxopiperazine progenitors containing the [2.2.2] ring system[7,8] (Fig. S1).

The bicyclo[2.2.2]diazaoctane core of these metabolites was first proposed in 1970 to arise from an intramolecular [4+2] Diels-Alder (IMDA) reaction.[9] A long-held hypothesis assumed that both the dioxopiperazine and monooxopiperazine families shared a common biogenesis, with the tryptophan carbonyl of the latter family involved in a net four-electron reduction subsequent to a putative Diels-Alder construction.[3,10] Based on initial genetic studies,[11] and experimental corroboration described in this report, we have discovered that Nature employs divergent biogenetic pathways and biochemical mechanisms to generate the bicyclo[2.2.2]diazaoctane nucleus in these two distinct families of alkaloids[11-15] (Fig. S1). Analysis of the malbrancheamide and paraherquamide biosynthetic gene clusters suggested that the bicyclo[2.2.2]diazaoctane ring system is directly produced in the monooxopiperazine oxidation state[11] (Fig. 1b). We reasoned that it proceeds by the cascade depicted in Figure 1b, **6-12**, following reductive cleavage of the tryptophan thiol ester by the nonribosomal peptide synthetase (NRPS) reductase domain.[11,15] The reduced Pro-Trp dipeptide intermediate is reverse prenylated, and we hypothesized that an intramolecular [4+2] Diels-Alder reaction follows, producing the bicyclo[2.2.2]diazaoctane ring system. However, annotation of the Mal and Phq gene clusters[11] failed to reveal a candidate enzyme for the IMDA reaction. The putative cycloaddition is stereospecific based on the *syn*- or *anti*- configuration of C12a (labeling in premalbrancheamide (**1**), Fig. 1a) and the relative position of the diene and the dienophile. Antipodal bicyclo[2.2.2]diazaoctanes have been isolated from different fungal strains producing the dioxopiperazine indole alkaloid family, while only (+)-malbrancheamide ((+)-**2**) has been isolated from *Malbranchea aurantiaca,*[16] indicating strict diastereo- and enantioselectivity of the biosynthetic IMDA. Thus, the identification and characterization of this presumed catalytic step is fundamental for understanding the formation of these structurally diverse molecules.

Reports of Diels-Alderases remain rare, with few examples over the past decade.[17-23] Among them, four crystal structures have been reported including, 1) the *S*-adenosyl-L-methionine (SAM)-dependent methyltransferase SpnF,[17,24] 2) the β-barrel protein PyrI4[25] and its homolog AbyU,[26] and 3) the flavin-dependent enzyme PyrE3.[27] Tang et al. recently reported functional studies on LepI,[21,28] a SAM-dependent enzyme involved in catalyzing a hetero-Diels-Alder reaction to form the Leporin family of natural products. A common theme in these Diels-

Alderases is their apparent evolution from divergent ancestors, with evident active site reconfiguration. Accordingly, in all reported cases these enzymes have lost ancestral function and the sole remaining activity facilitates a spontaneous [4+2] pericyclic reaction with regio- and stereoselectivity. Cofactors, if present, do not serve their canonical catalytic role for the Diels-Alder cycloaddition, but rather play a structural role in maintaining the active site in a catalytically productive conformation. Similarly, distinct catalytic residues that abolished the enzymatic function were not identified in any previously characterized Diels-Alderase, suggesting that catalysis is achieved primarily through substrate positioning in the protein scaffold. The malbrancheamide and paraherquamide gene clusters lack homologous genes that encode known Diels-Alderases, which indicated the existence of a novel class of biocatalysts. In this article, we reveal the molecular basis for stereocontrolled construction of the monooxopiperazine bicyclic core in the malbrancheamide and paraherquamide biosynthetic pathways. These genetically homologous systems proceed through a bifunctional reductase and Diels-Alderase that evolved from an ancestral short-chain dehydrogenase (SDR) and is also encoded in several other fungal natural product biosynthetic gene clusters.

## Biomimetic Synthesis of Premalbrancheamide, Malbrancheamide and Spiromalbramide

Early considerations regarding biogenesis of the bicyclo[2.2.2]diazaoctane core envisioned a biosynthetic Diels-Alder reaction. In order to chemically validate the sequence of events in malbrancheamide biosynthesis, we prepared the C2 reverse prenylated proposed biosynthetic intermediate, dipeptide aldehyde (**17**),[11] and found that this substance undergoes the cascade of ring closure, dehydration, tautomerization and intramolecular cycloaddition, upon deprotection to give premalbrancheamide (**1**) (Fig. 2). This strategy was applied to two additional natural products, malbrancheamide (**2**) and spiromalbramide (**4**) (Fig. S2), underscoring the utility of the biomimetic paradigm. The key, Fmoc-protected dipeptide aldehyde **17** was prepared through the peptide coupling of N-Fmoc proline (**14**) with the C2 reverse prenylated tryptophan methyl ester **13** through the agency of HATU in acetonitrile in 85% yield. Reduction of the methyl ester with sodium borohydride (82% to **15**) followed by a Parikh-Doering oxidation, furnished the N-Fmoc aldehyde **17** in 72% yield. Removal of the N-Fmoc residue with diethylamine under anaerobic conditions provided the di-enamine **9**, which could be isolated and characterized. Treatment of this substance with TFA in THF at temperatures between 0 °C and 50 °C, resulted in formation of (±)-**1**. The observed modest yield is possibly due to unfavorable tautomerization of **9** to **12**. Under aerobic conditions, **9** spontaneously and rapidly oxidized to aromatic zwitterion **11** (Fig. 1b), which we initially reasoned to be a non-physiological by-product. We later determined that **11** could be chemically reduced by NAD(P)H to **12**, resulting in the spontaneous formation of racemic premalbrancheamide (80 - 90% conversion). This discovery suggested two possible biosynthetic routes – aerobic vs. anaerobic – and the possibility that **11** is an authentic pathway intermediate depending on the intracellular conditions during fungal biosynthesis. Significantly, both routes lead to a single *syn*-diastereomer upon cyclization as the corresponding *anti*-isomer was not detected in even trace amounts from the cycloaddition reactions. This finding agrees

with density functional theory calculations that the azadiene **12** has a calculated relative transition state energy difference of about 2.6 kcal/mol favoring the *syn*-cycloadduct.[29] The *anti*-pathway experiences unfavorable steric interactions between the pyrrolidine ring and the prenyl group (Fig. S3). Our biomimetic synthesis of *syn*-malbrancheamides gave rise to the (+)- and (–)-enantiomers, raising the intriguing question regarding how optically pure (+)-premalbrancheamide is formed by *Malbranchea aurantiaca*. This further indicated the likely presence of an enzyme-directed cyclization *in vivo*, and motivated us to explore the biosynthetic origins of premalbrancheamide by *in vitro* pathway reconstitution.

### *In Vitro* Reconstitution of the Malbrancheamide Biosynthetic Pathway

We aimed to reconstitute the biosynthesis of malbrancheamide as a representative monooxopiperazine alkaloid in a multi-component *in vitro* reaction (Fig. S4). We hypothesized the first step of malbrancheamide biosynthesis involves coupling of L-proline and L-tryptophan by MalG, a dimodular NRPS containing six domains ($A_1$-$T_1$-C-$A_2$-$T_2$-R, Fig. 1b), to produce L-Pro-L-Trp aldehyde **6** through reductive off-loading. Since the full-length NRPS protein could not be produced in soluble form, we identified domain boundaries in MalG, developed expression constructs for the excised $A_1$-$T_1$, C, $T_2$ and R domains (Fig. S5), and loaded the putative amino acid substrates onto the MalG $T_1$ and $T_2$ domains (Fig. S6a, b). Phosphopantetheinylated MalG $A_1$-$T_1$ was loaded with L-proline in the presence of ATP and $Mg^{2+}$, consistent with our functional annotation. With no access to soluble MalG $A_2$, L-tryptophan was loaded onto MalG $T_2$ using Sfp,[30] a nonspecific 4'-phosphopantetheinyl transferase, and L-Trp-coenzyme A (CoA). L-Pro $A_1$-$T_1$ and L-Trp $T_2$ were incubated with the MalG C domain and R domain with the presumed NADPH cofactor. Product formation was determined by LC/MS and comparison with authentic standards. Instead of the proposed dipeptidyl aldehyde-derived product **8**, we identified aromatic zwitterion **10** as the main product (Fig. 1b and 3a). We hypothesized that **10** was produced from spontaneous oxidation of **8**. This was confirmed by chemical synthesis of **8**, which spontaneously and irreversibly converted to **10**. This transformation was suppressed under anaerobic conditions, leading to the conclusion that the malbrancheamide NRPS product rapidly cyclized and dehydrated to **8** and subsequently spontaneously oxidized to **10** under aerobic (i.e. physiological) conditions.

To further test the hypothesis that the MalG terminal R-domain catalyzes an NADPH-dependent two-electron reductive release to produce an aldehyde, we synthesized a dipeptidyl-CoA analog **23**, in which the prolyl-N-atom was replaced with an O-atom to prevent nucleophilic addition of the prolyl-N-atom to the CoA thioester, and loaded **23** onto MalG $T_2$ via Sfp (Fig. S6c). Product standards of aldehyde **24** and alcohol **25** were synthesized chemically. Compound **25** was nonreactive in methanol, while **24** epimerized and reacted to produce the hemiacetal **26** (Fig. S7). Assays with **23**-loaded $T_2$ and MalG R yielded product **26**, confirming that MalG generates an aldehyde product. NADPH was the preferred cofactor in this reaction (Fig. S7d, e). MalG R is an SDR reductase with catalytic Tyr and Lys amino acids, as demonstrated in the 2.6-Å crystal

structure of an NADPH complex of PhqB R, the MalG R homolog of paraherquamide biosynthesis (Figs. S8-10). The essential role of Tyr was confirmed with MalG R/Y2132F, which was incapable of reductive release (Fig. S10d).

We propose that the NRPS product **8** would undergo a reverse prenylation as the next biosynthetic step, thereby installing the dienophile for the IMDA reaction. Two genes, *malE* and *malB* (from the *mal* gene cluster) encode putative prenyltransferases. We incubated MalB or MalE with substrate-loaded MalG domains, NADPH and dimethylallyl pyrophosphate (DMAPP), the prenyl donor. MalE readily catalyzed a C2 reverse prenyl transfer reaction to produce zwitterion **11** (Fig. 3b), whereas MalB displayed modest activity, suggesting that *malB* may be a redundant gene in the pathway (Fig. 3c and S14). Because we could not distinguish in this assay whether **8** or **10** was the MalE substrate, synthetic **8** was produced under anaerobic conditions by UV irradiation of an *O*-nitrobenzyl (ONB) photo-protected dipeptide aldehyde **30** and subjected to the prenyltransferase assay (Fig. S11a). This substrate was rapidly prenylated by MalE in contrast to synthetic **10**, which showed low levels of conversion with the enzyme, indicating that **8** is the native substrate for MalE (Fig. S12). This raised the question regarding how MalE accesses substrate **8** prior to its rapid oxidation to **10**. Thus, we considered the possibility that C2 reverse prenylation occurs with the substrate tethered to the NRPS $T_2$ domain. To address this question, we tested whether MalE or MalB could prenylate L-Trp, L-Trp-loaded MalG $T_2$, or **23**-loaded MalG $T_2$ (Fig. S13). In all cases, no product was detected, confirming that the prenyl transfer reaction occurred on free substrate following the NRPS-catalyzed reaction.

We noticed low levels of premalbrancheamide in the reconstitution assays with MalG and MalE or MalB. Chiral LC/MS analysis revealed a 1:1 racemic mixture of (±)-**1** (Fig. 3f), in agreement with the biomimetic synthesis described above (Fig. 2). Further investigation using synthetic **11** revealed that racemic premalbrancheamide arose through non-enzymatic reduction of **11** by NADPH to azadiene **12**, which undergoes spontaneous cycloaddition in the reaction buffer, thereby explaining the background accumulation of the Diels-Alder products (±)-**1** from *in vitro* assays. From these studies we ascertained that MalG and MalE are the minimal components required for premalbrancheamide biosynthesis, albeit lacking stereocontrol in the IMDA reaction.

Premalbrancheamide isolated from *Malbranchea aurantiaca* is optically pure (+)-**1**, which strongly implicates enzymatic control in the IMDA reaction. Known Diels-Alderases have diverse origins, but the annotated *mal* and *phq* gene clusters did not contain an evident candidate biosynthetic enzyme. Nonetheless, we tested whether MalC, annotated as a short-chain dehydrogenase/reductase (SDR), could function as the presumed Diels-Alderase. When MalC was incubated with substrate-loaded MalG and MalE (NADPH and DMAPP included), neither aromatic zwitterion intermediate, **10** or **11**, was detected; instead the sole product was (+)-**1**, confirming that MalC functions as an intramolecular [4+2] Diels-Alderase (Fig. 3d). To our surprise, when MalC was added to the reaction mixture after significant amounts of **11** had accumulated, the oxidized intermediate was converted to (+)-**1**, indicating that MalC possessed the ability to reduce the zwitterion **11** to the reactive azadiene **12** prior to conducting the

diastereo- and enantio-controlled cycloaddition reaction. This unexpected reactivity of MalC was confirmed using synthetic **11** and NADPH (Fig. S15). To our knowledge, this is a unique example where reduction regenerates the biosynthetic substrate from an oxidized (aromatic) intermediate to provide a productive mode for cycloaddition. The fact that **11** is a MalC substrate indicates that it is an authentic pathway intermediate, and motivated us to address whether an aerobic or anaerobic biosynthetic route is operative *in vivo*. This question was interrogated in two ways; first by performing MalC assays under anaerobic conditions with synthetic **9**, which was generated by photo-deprotection of ONB prenyl dipeptidyl aldehyde **33** (Fig. S11b). Conversion to (+)-**1** was observed only in the presence of MalC and $NADP^+$ (Fig. 3g). However, the efficiency of this reaction was attenuated compared to the MalC-catalyzed conversion of **11** to (+)-**1** under aerobic conditions, indicating that the dienamine tautomer **9** is not optimally recognized by MalC. It is unknown whether MalC can play a role in tautomerization of **9**; notably, background conversion of **9** to racemic premalbrancheamide was not detected under these conditions. Second, gene disruption of the *malC* homolog *phqE* was conducted in the paraherquamide-producing strain *Penicillium simplicissimum* using a CRISPR-Cas9 system.[31] Extracts from the *phqE* mutant strain grown on CYA medium showed the presence of the expected (methyl-Pro-Trp prenyl) zwitterion intermediate **38** (Fig. S16) by LC/MS analysis and co-injection with a synthetic standard, confirming the accumulation of this oxidized metabolite *in vivo* (Fig. S17). Taken together, these data indicate that **11** is the native substrate for MalC en route to (+)-premalbrancheamide.

For the MalC-catalyzed reduction of **11**, NADH or NADPH are effective as the cofactor. However, NADPH is required for strict stereocontrol of the IMDA reaction, as MalC produced a 63:37 mixture of (+)-**1** and (–)-**1** when using NADH (Fig. 3h). This is consistent with the anaerobic experiment in which $NADP^+$ was required to generate (+)-**1**, and further indicates that NADPH plays an important role in the IMDA stereocontrol. The Michaelis-Menten kinetic constants for NADPH and NADH in reactions with MalC and **11** revealed a 10-fold greater catalytic efficiency ($k_{cat}/K_M$) with NADPH compared to NADH (Fig. S15d, e). A 6-fold greater $K_M$ with NADH also suggests that proper cofactor binding is a required component to achieve stereocontrol. Enzymatic rate enhancement of (+)-**1** formation is evident under both assay conditions: aerobically through substrate **11** (post-reduction), or anaerobically through substrate **9** (post-tautomerization) (Fig. 3g). The dramatic shift in enantiomeric excess for the enzymatic reaction (from 0% to 96%) is indicative of enzymatic catalysis for the IMDA reaction.

To complete the biosynthetic pathway, flavin-dependent halogenase MalA was employed to add chlorine atoms on C8 and C9 of premalbrancheamide (+)-**1** to provide malbrancheamide (+)-**2**.[32] We incubated MalA with its pathway partners (L-Pro and L-Trp MalG, MalE and MalC, NADPH, DMAPP, NaCl and $FADH_2$) and identified (+)-**2** as the final product (Fig. 3e). We also found that MalA is stereospecific: when incubated with racemic mixture of **1**, MalA chlorinated only the natural (+) enantiomer (Fig. S18).

**Probing the catalytic mechanism of the bifunctional Diels-Alderase**

To gain further insight into the function of the SDR-derived Diels-Alderase, the crystal structure of ligand-free MalC was solved at 1.6-Å resolution, revealing a classical SDR fold with a nucleotide-binding subdomain that contains an invariant "$TGX_3GXG$" motif (P-loop), and a C-terminal substrate binding region that is less conserved and largely hydrophobic.[33,34] The closest structural homologs are a group of SDRs including RasADH (2.3 Å Cα R.M.S.D., 27% overall sequence identity),[35] which uses NAD(P) to catalyze reversible oxidation of secondary alcohols to aldehydes. Unexpectedly, MalC lacks the characteristic Tyr and Lys catalytic amino acids, and also the essential Asn and Ser residues of typical SDRs,[33,34] suggesting that the active site is reconfigured to fit its unique catalytic roles.

Neither cofactor nor substrate was captured in complex with MalC due to crystal lattice constraints. Thus, we turned to the homologous paraherquamide biosynthetic pathway. PhqE is a MalC homolog (54% identity) and catalyzed formation of (+)-premalbrancheamide using the zwitterionic prenylated Trp-Pro substrate **11** *in vitro* (Fig. S19). The 2.4-Å crystal structure of PhqE in complex with cofactor ($NADP^+$/$NAD^+$) and premalbrancheamide (Fig. S20) is highly similar to the MalC structure (1.0 Å Cα R.M.S.D.; Fig. 4b).

Consistent with our kinetic data, PhqE crystals grown with $NADP^+$ showed strong electron density for the cofactor (Fig. S21a) bound in a manner conserved with bacterial SDR homologs (Fig. S21c), while $NAD^+$ showed weak electron density (Fig. S21b). Lys50 accounts for preferential binding of $NADP^+$ through a salt bridge with the cofactor 2'-phosphate. Premalbrancheamide binds in a groove on the surface and is surrounded by hydrophobic residues. The bicyclo[2.2.2]diazaoctane ring system is buried against the nicotinamide and several amino acids including Arg131 (Fig. 4c). The indole lies in a pocket formed by Ala, Leu and Val side chains. The gem-dimethyl contacts Asp166 and Trp169, which are part of a conserved "PDPGW" motif (Fig. S24-25). Given the dual functions (reductase and Diels-Alderase) of MalC/PhqE, the product complex reveals PhqE to be well-adapted in its capacity as a stereo- and enantioselective biocatalyst due to the shape complementarity between the active site pocket and the product (Fig. 4f). Additionally, the short distance (~4.4 Å) between nicotinamide C4 and the deoxy C5 of premalbrancheamide suggests that reduction to the reactive azadiene also occurs in the same location of the active site and indicates that reduction and cycloaddition are highly coordinated.

We sought a non-reactive substrate complex with $NADP^+$ and **11**, and obtained strong electron density for **11** with indication of a flexible orientation in PhqE/D166N (Fig. 4d), whereas the wild-type PhqE yielded ambiguous density for **11**. The indole of **11** binds in the same pocket as premalbrancheamide while the pyrazinone is pushed towards the nicotinamide (Fig. 4e). Deoxy C5 of **11** lies 3.6 Å from the nicotinamide C4 consistent with hydride delivery to this position. In addition to hydride transfer, protonation of the pyrazinone alkoxide is required to form the reactive azadiene **12**. Curiously the corresponding oxygen atom is part of a hydrogen-bonding network involving the $NADP^+$ 2'-hydroxyl and Arg131, suggesting that the cofactor may play a role in proton-transfer during reduction. Superposition of the substrate and product complexes

revealed a high degree of pre-organization of **11** towards the Diels-Alder reaction and also affirmed that the reduction and IMDA reactions are spatially confined.

We used molecular dynamics (MD) simulations to explore the concepts of coordinated hydride delivery, proton transfer and pre-organization in the active site. First, we monitored the distance between the putative hydride acceptor (C5 of **11**) and nicotinamide C4 over a 1.2 μs simulation. The average distance between these carbon atoms was 4.2 Å, consistent with the crystal structures (Fig. S22). We next explored alkoxide protonation. In the crystal structure, the $NADP^+$ ribose 2'-hydroxyl is hydrogen-bonded to the alkoxide oxygen and Arg131. Within the first few ns of the simulation Arg131 displaces the ribose hydroxyl and interacts with the alkoxide for the remainder of the simulation, lending significance to the role of Arg131 in protonation of **11**. To assess facial selectivity in the cycloaddition reaction that forms the (+)- and (–)-premalbrancheamide enantiomers, we monitored the dihedral angle along N15-C5a-C12a-C13 (Fig. S23). Comparison of this dihedral angle in the constrained premalbrancheamide and unconstrained **11** revealed that the untethered diene explores only a single face of the pyrazinone ring corresponding to the natural (+)-enantiomer (Fig. S23). Interestingly, this pre-organization was lost when $NADP^+$ was omitted from the simulation, consistent with our observation that the cofactor is required for enantio-controlled cycloaddition. Together these results further support the conclusion that MalC/PhqE-catalyzed reduction and cycloaddition are coordinated and take place in the same active site pocket where the enzyme-cofactor complex provides stereocontrol by positioning the diene for [4+2] cycloaddition as the reactive azadiene is generated by reduction of **11**.

Based on this information, we probed the reaction mechanism by site-directed mutagenesis. MalC was chosen for this analysis to directly compare results with the reconstitution assay. All of the targeted amino acids are conserved in MalC and PhqE. With the *in vitro* reconstitution assay, MalC variants were assayed in the presence of the MalG NRPS and MalE prenyltransferase (Fig. 5a, b). Reductase activity was assessed by the levels of oxidized intermediate **11**: higher levels indicate less reductase activity. The effect on the IMDA reaction was determined by measuring levels of unnatural (–)-**1** as a percent of all premalbrancheamide: ~50% (–)-**1** formation indicates loss of enzymatic IMDA function. We identified five MalC substitutions that abolished reductase activity (D108A, R130A, D165A, D165N, W168L), and found that loss of function is highly correlated with loss of stereocontrol in the IMDA reaction. A single exception is MalC D165A, which produced mainly (+)-**1**, suggesting that Asp165 is required for reduction but not the IMDA reaction. The activity of MalC variants was also measured in assays with **11** (Fig. 5c). In agreement with the reconstitution assay, Asp108, Arg130 and Asp165 were required for reduction. Based on these data, we propose a mechanism for MalC in which Arg130 serves as a proton donor potentially in conjunction with 2'-OH of NADPH ribose (Fig. 5d). NADPH is the hydride donor, and Asp165 may stabilize the positive charge of the zwitterionic substrate **11** and facilitate formation of the reactive azadiene intermediate **12**. Stereocontrol of the IMDA reaction is primarily driven by shape

complementarity, with contacts between substrate and Trp168 and the cofactor playing a critical role in the IMDA process.

The MalC/PhqE Diels-Alderases clearly evolved from an ancestral SDR (Fig. S24). The SDR catalytic Tyr and Lys were replaced by shorter, non-polar residues (Ile and Cys) providing space to accommodate the substrate. The "PDPGW" motif positions the essential Asp165 3.0 Å closer to the substrate compared to the corresponding amino acid in canonical SDRs. The SDR hydrogen bonding network is partially maintained since the catalytic Arg side chain of MalC/PhqE occupies the position of the SDR catalytic Lys, providing a compelling example of protein evolution in molecular detail.

## Conclusions

Our comprehensive approach to studying the Diels-Alder mediated construction of bicyclo[2.2.2]diazaoctane indole alkaloids represents a culmination of conceptual, experimental and computational studies initiated almost a half-century ago by Birch.[36] The divergent biogenesis to create the monooxo- and dioxopiperazine-type molecules employed by diverse fungi was revealed through characterization of the respective biosynthetic gene clusters, which suggested a differential release mechanism from the functionally related bimodular NPRS systems (Fig. S1). This information was leveraged to design a biomimetic total synthesis of premalbrancheamide, providing a direct validation of the prenylated dipeptide azadiene intermediate and IMDA construction of the target natural product in racemic form. The basis for creating the (+)-antipodal form of premalbrancheamide via a presumed stereoselective Diels-Alderase motivated our search for the corresponding enzyme from Mal and Phq pathways, resulting in identification of a novel Diels-Alderase and a mechanistic understanding of enantio-induction. We have demonstrated that during biosynthetic assembly, the key step to produce the polycyclic core is catalyzed by a bifunctional reductase and intramolecular [4+2] Diels-Alderase, MalC/PhqE, providing exquisite diastereo- and enantiocontrol. Derived from SDR ancestors, the active site of MalC/PhqE evolved to accommodate an aromatic zwitterion substrate, and both the reduction and the IMDA steps are NADP(H)-dependent. In contradistinction to all other known putative Diels-Alderases[2] which are either redox-neutral cyclases or oxidases, we have discovered the first reductase-dependent Diels-Alderase. Our work reveals a distinct class of Diels-Alder enzymes and provides insights into the nature of IMDA catalysis as well as providing a bold evolutionary thesis. The availability of key intermediates provided from biomimetic synthesis enabled us to probe the molecular mechanism of this transformation in unprecedented detail. The MalC/PhqE-catalyzed reaction includes the remarkable step of "rescuing" an aromatic zwitterionic substrate **11** to create the bicyclic product **1** and avoid premature pathway termination. This brilliant evolutionary solution to protect the structural and stereochemical integrity of this architecturally unique family of alkaloids is, to the best of our knowledge, unprecedented and underscores the expanding plasticity and adaptability of secondary metabolite genes and enzymes. The Mal/Phq biosynthetic sequence represents a novel

"toolbox" for chemoenzymatic diversification of indole alkaloids with opportunities for facile access to improved calmodulin inhibitors, anthelmintics and other therapeutics to treat human and animal diseases.

**Acknowledgements** This work was supported by the National Institutes of Health (R01 CA070375 to R.M.W. and D.H.S.), R35 GM118101, the Hans W. Vahlteich Professorship (to D.H.S.), and R01 DK042303 and the Margaret J. Hunter Professorship (to J.L.S.). J.N.S. and K.N.H. acknowledge the support of the National Institute of General Medical Sciences of the National Institutes of Health under Award Numbers F32GM122218 (to J.N.S.) and R01GM124480 (to K.N.H.). Computational resources were provided by the UCLA Institute for Digital Research and Education (IDRE) and the Extreme Science and Engineering Discovery Environment (XSEDE), which is supported by the NSF (OCI-1053575). Anton 2 computer time was provided by the Pittsburgh Supercomputing Center (PSC) through Grant R01GM116961 from the National Institutes of Health. The Anton 2 machine at PSC was generously made available by D.E. Shaw Research. GM/CA@APS is supported by the National Institutes of Health, National Institute of General Medical Sciences (AGM-12006) and National Cancer Institute (ACB-12002). The Advanced Photon Source is a U.S. Department of Energy (DOE) Office of Science User Facility operated by Argonne National Laboratory under Contract No. DE-AC02- 06CH11357. We thank Prof. Stephen Ragsdale for his assistance with anaerobic enzyme assays.

**Author Contributions** Q.D., S.A.N., J.L.S., R.M.W. and D.H.S. contributed to the experimental design. Q.D., S.A.N., A.E.F. and W.C.B. performed molecular cloning, protein expression and purification. Q.D., S.A.N. and A.E.F. performed all enzymatic assays and LC/MS analysis. S.A.N. and Q.D. carried out all crystallographic experiments, structural analysis and structure-based site-directed mutagenesis. K.R.K., J.D.S., A.D.S., T.J.M., L.Z., S.A.N. and V.V.S. synthesized and validated all compounds described in this study. Y.Y. and F.Y. carried out the genetic knockout experiment, F.Y. and Q.D. performed genetic annotation. J.N.S. and S.A.N. performed MD simulations. R.S.P. performed DFT calculations. Q.D., S.A.N., K.N.H., J.L.S., R.M.W. and D.H.S. evaluated the data and prepared the manuscript.

**Author Information** The authors declare no competing financial interests. Readers are welcome to comment on the online version of the paper. Correspondence and requests for materials should be addressed to D.H.S. (davidhs@umich.edu) and R.M.W. (robert.williams@colostate.edu).

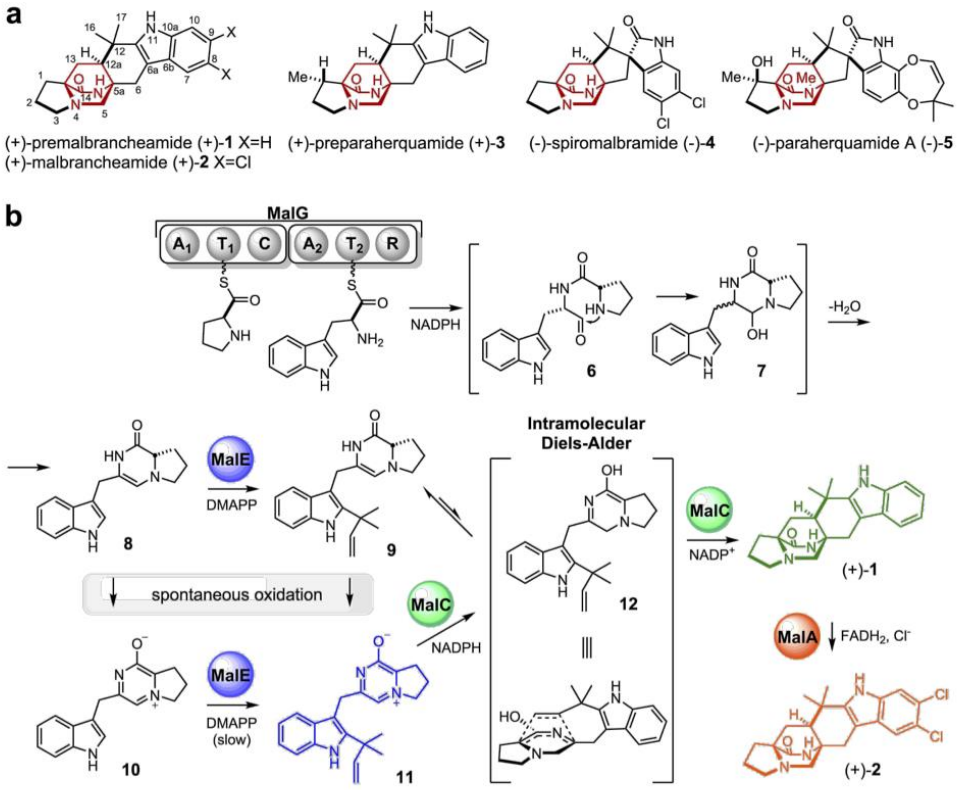


**Figure 1. Fungal bicyclo[2.2.2]diazaoctane indole alkaloids and biosynthesis.**
a. Representative natural products with the biocyclo[2.2.2]diazaoctane group colored in red. b. Scheme of malbrancheamide biosynthesis. The natural substrates are L-proline and L-tryptophan, and the final product is malbrancheamide (**+**)-**2**. The product of each biosynthetic step is colored differently. Proteins are indicated by spheres; MalG domains are adenylation ($A_1$ and $A_2$), thiolation ($T_1$ and $T_2$), condensation (C) and reductase (R).

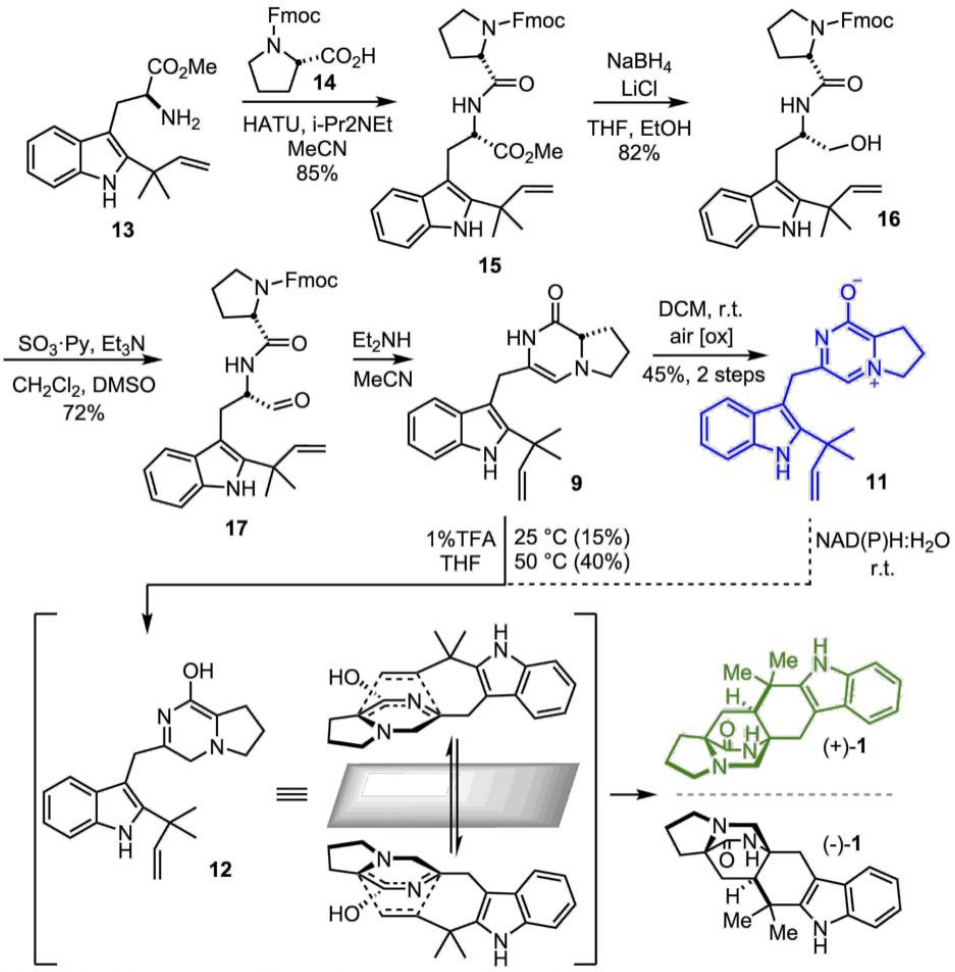


**Figure 2. Biomimetic synthesis of premalbrancheamide.**

The biomimetic synthesis proceeded through a spontaneous intramolecular [4+2] Diels-Alder reaction from a key azadiene intermediate **12** to produce a racemic mixture of *syn*-premalbrancheamides (**1**). Only optically pure (+)-**1** has been isolated from *Malbranchea aurantiaca*. See SI for complete methods.

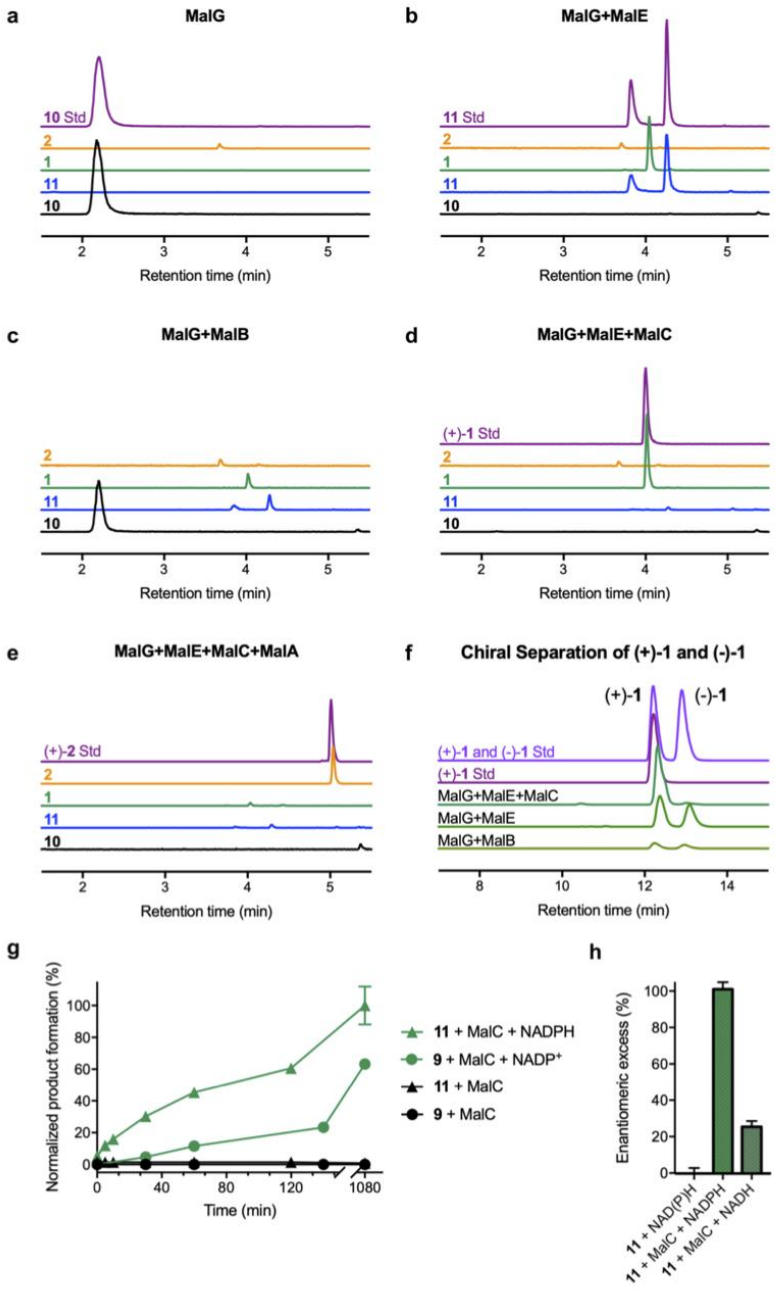
a
MalG
10 Std
2
1
11
10
Retention time (min)
b
MalG+MalE
11 Std
2
1
11
10
Retention time (min)
c
MalG+MalB
2
1
11
10
Retention time (min)
d
MalG+MalE+MalC
(+)-1 Std
2
1
11
10
Retention time (min)
e
MalG+MalE+MalC+MalA
(+)-2 Std
2
1
11
10
Retention time (min)
f
Chiral Separation of (+)-1 and (-)-1
(+)-1
(-)-1
(+)-1 and (-)-1 Std
(+)-1 Std
MalG+MalE+MalC
MalG+MalE
MalG+MalB
Retention time (min)
g
Normalized product formation (%)
Time (min)
11 + MalC + NADPH
9 + MalC + NADP+
11 + MalC
9 + MalC
h
Enantiomeric excess (%)
11 + NAD(P)H
11 + MalC + NADPH
11 + MalC + NADH

**Figure 3. *In vitro* enzymatic reconstitution of malbrancheamide biosynthesis.**
Reactions were monitored by LC/MS. Extracted ion counts (EIC) for key molecules in reaction mixtures are compared to authentic synthetic standards. a. MalG NRPS produced zwitterion **10** by spontaneous oxidation of **8**. b – c. Addition of MalE or MalB prenyltransferase formed three products: a prenylated zwitterion **11**, and (±)-**1**. d. MalC Diels-Alderase addition disabled formation of **11** and (–)-**1** (see panel f). e. Malbrancheamide **2**, the final pathway product, was produced by MalA halogenation of (+)-**1**. f. Chiral separation of (±)-**1** indicates that MalC is an intramolecular [4+2] Diels-Alderase, while MalE or MalB does not provide enantioselectivity for the spontaneous IMDA reaction. g. MalC-catalyzed reactions under aerobic (**11** + MalC) or anaerobic (**9** + MalC) conditions. The aerobic route with **11** as the pathway intermediate was more efficient than the anaerobic route from **9**. h. Effect of cofactor on the enantiomeric excess of the MalC-catalyzed Diels-Alder reaction. MalC provided limited enantioselectivity when NADH was used as cofactor. EIC traces are colored by compound as in Figure 1b, authentic standards are in purple or pink. For panel g and h, all data represent the average of triplicate measurements (error bars, SD; $n = 3$).

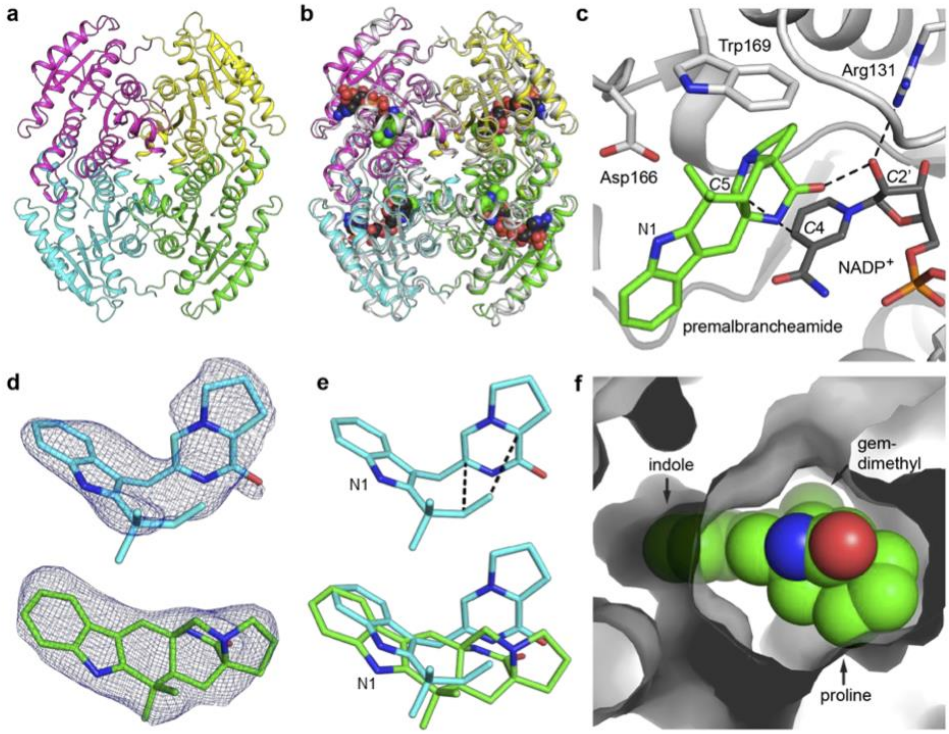


**Figure 4. Structures of MalC and PhqE.**

a. MalC tetramer colored by subunit. b. Superposition of MalC and PhqE product complex (gray); $NADP^+$ (black C) and premalbrancheamide (green C) are shown as spheres. c. PhqE active site showing close arrangement of the product and the $NADP^+$ cofactor. d. Omit electron density ($F_o$-$F_c$; contoured at 2.2 σ) for the substrate **11** (cyan) and the premalbrancheamide (+)-**1** product (green). e. Pre-organization for cycloaddition. Substrate **11** (upper) binds with the prenyl group poised for the IMDA (dashed lines), as seen in the overlay of **11** and premalbrancheamide (+)-**1** (lower). f. Surface representation of the product complex showing high shape complementarity between premalbrancheamide and PhqE.

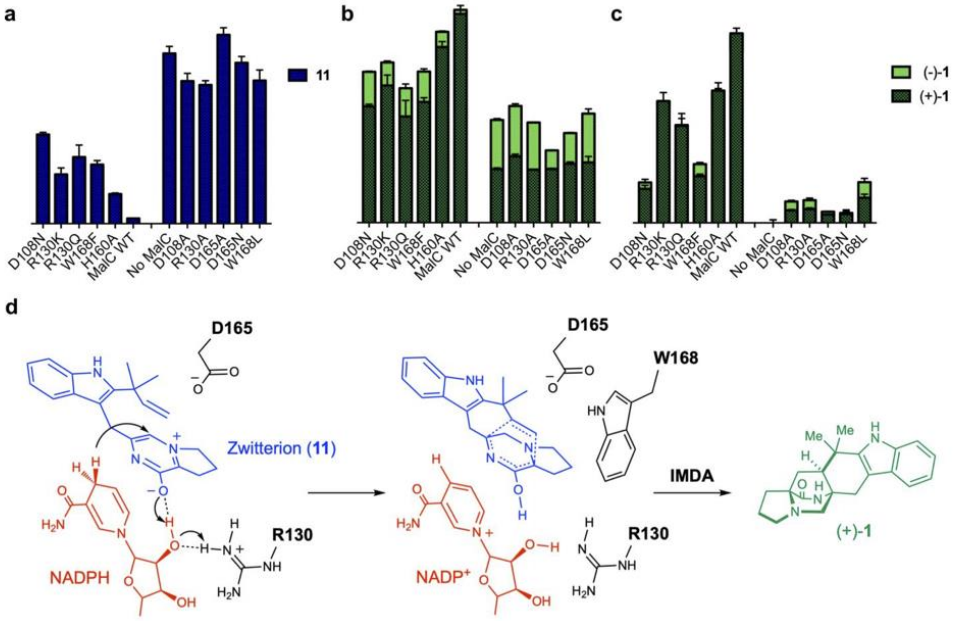


**Figure 5. Catalytic mechanism of the MalC/PhqE-catalyzed Diels-Alder reaction.**
a – b. Product profiles of **11** (blue), (+)-**1** (dark green) and (–)-**1** (light green) in the "MalG+MalE+MalC" reconstitution assay with MalC variants. c. MalC mutagenesis assessed by conversion of synthetic **11** to (+)-**1**. The results agree with those of the reconstitution assay in panel b. Product levels due to non-enzymatic conversion by NADPH were subtracted in all cases. All data represent the average of triplicate measurements (error bars, SD; $n$ = 3). d. Proposed catalytic mechanism for MalC/PhqE, with residue numbers for MalC (PhqE residue number = MalC residue number + 1). Arg130 is the indirect proton donor, possibly mediated via the 2'-OH of NADPH ribose. Asp165 stabilizes the positive charge of **11**, and hydride transfer from NADPH completes the first reduction step, forming an unstable azadiene intermediate. The subsequent IMDA reaction is accelerated primarily via entropy trapping, with diastereo- and enantioselectivity achieved via close packing of the $NADP^+$ nicotinamide, the azadiene and MalC Trp168, which together restrain the conformations of both the diene ring and the dienophile to ensure a single cycloaddition mode.

**REFERENCES**


1 Finefield, J. M., Frisvad, J. C., Sherman, D. H. & Williams, R. M. Fungal origins of the bicyclo[2.2.2]diazaoctane ring system of prenylated indole alkaloids. *J Nat Prod* **75**, 812-833 (2012).

2 Klas, K., Tsukamoto, S., Sherman, D. H. & Williams, R. M. Natural Diels-Alderases: Elusive and Irresistable. *J Org Chem* **80**, 11672-11685 (2015).

3 Klas, K. R. *et al*. Structural and stereochemical diversity in prenylated indole alkaloids containing the bicyclo[2.2.2]diazaoctane ring system from marine and terrestrial fungi. *Nat Prod Rep* **35**, 532-558 (2018).

4 Robertson, A. P. *et al*. Paraherquamide and 2-deoxy-paraherquamide distinguish cholinergic receptor subtypes in ascaris muscle. *J Pharmacol Exp Ther* **303**, 853-860 (2002).

5 Little, P. R. *et al*. Efficacy of a combined oral formulation of derquantel-abamectin against the adult and larval stages of nematodes in sheep, including anthelmintic-resistant strains. *Vet Parasitol* **181**, 180-193 (2011).

6 Buxton, S. K. *et al*. Investigation of Acetylcholine Receptor Diversity in a Nematode Parasite Leads to Characterization of Tribendimidine-and Derquantel-Sensitive nAChRs. *Plos Pathog* **10**, e1003870 (2014).

7 Mugishima, T. *et al*. Absolute stereochemistry of citrinadins a and B from marine-derived fungus. *J Org Chem* **70**, 9430-9435 (2005).

8 Mercado-Marin, E. V. *et al*. Total synthesis and isolation of citrinalin and cyclopiamine congeners. *Nature* **509**, 318-324 (2014).

9 Porter, A. E. A. & Sammes, P. G. A Diels-Alder Reaction of Possible Biosynthetic Importance. *J Chem Soc Chem Comm*, 1103 (1970).

10 Stocking, E. M. & Williams, R. M. Chemistry and biology of biosynthetic Diels-Alder reactions. *Angew Chem Int Ed Engl* **42**, 3078-3115 (2003).

11 Li, S. *et al*. Comparative analysis of the biosynthetic systems for fungal bicyclo[2.2.2]diazaoctane indole alkaloids: the (+)/(-)-notoamide, paraherquamide and malbrancheamide pathways. *Medchemcomm* **3**, 987-996 (2012).

12 Stocking, E. M., Sanz-Cervera, J. F. & Williams, R. M. Studies on the Biosynthesis of Paraherquamide: Synthesis and Incorporation of a Hexacyclic Indole Derivative as an Advanced Metabolite. *Angew Chem Int Ed Engl* **40**, 1296-1298 (2001).

13 Ding, Y. S. *et al*. Detection of VM55599 and preparaherquamide from *Aspergillus japonicus* and *Penicillium fellutanum*: Biosynthetic implications. *J Nat Prod* **71**, 1574-1578 (2008).

14 Ding, Y. S., Greshock, T. J., Miller, K. A., Sherman, D. H. & Williams, R. M. Premalbrancheamide: Synthesis, Isotopic Labeling, Biosynthetic Incorporation, and Detection in Cultures of *Malbranchea aurantiaca*. *Org Lett* **10**, 4863-4866 (2008).

15 Ding, Y. *et al*. Genome-based characterization of two prenylation steps in the assembly of the stephacidin and notoamide anticancer agents in a marine-derived *Aspergillus* sp. *J Am Chem Soc* **132**, 12733-12740 (2010).
16 Martinez-Luis, S. *et al*. Malbrancheamide, a new calmodulin inhibitor from the fungus *Malbranchea aurantiaca*. *Tetrahedron* **62**, 1817-1822 (2006).
17 Kim, H. J., Ruszczycky, M. W., Choi, S. H., Liu, Y. N. & Liu, H. W. Enzyme-catalysed [4+2] cycloaddition is a key step in the biosynthesis of spinosyn A. *Nature* **473**, 109-112 (2011).
18 Hudson, G. A., Zhang, Z. G., Tietz, J. I., Mitchell, D. A. & van der Donk, W. A. *In Vitro* Biosynthesis of the Core Scaffold of the Thiopeptide Thiomuracin. *J Am Chem Soc* **137**, 16012-16015 (2015).
19 Wever, W. J. *et al*. Chemoenzymatic Synthesis of Thiazolyl Peptide Natural Products Featuring an Enzyme-Catalyzed Formal [4+2] Cycloaddition. *J Am Chem Soc* **137**, 3494-3497 (2015).
20 Tian, Z. H. *et al*. An enzymatic [4+2] cyclization cascade creates the pentacyclic core of pyrroindomycins. *Nat Chem Biol* **11**, 259-265 (2015).
21 Ohashi, M. *et al*. SAM-dependent enzyme-catalysed pericyclic reactions in natural product biosynthesis. *Nature* **549**, 502-506 (2017).
22 Li, L. *et al*. Genome Mining and Assembly-Line Biosynthesis of the UCS1025A Pyrrolizidinone Family of Fungal Alkaloids. *J Am Chem Soc* **140**, 2067-2071 (2018).
23 Kato, N. *et al*. Control of the Stereochemical Course of [4+2] Cycloaddition during trans-Decalin Formation by Fsa2-Family Enzymes. *Angew Chem Int Ed Engl* **57**, 9754-9758 (2018).
24 Fage, C. D. *et al*. The structure of SpnF, a standalone enzyme that catalyzes [4 + 2] cycloaddition. *Nat Chem Biol* **11**, 256-258 (2015).
25 Zheng, Q. *et al*. Enzyme-Dependent [4 + 2] Cycloaddition Depends on Lid-like Interaction of the N-Terminal Sequence with the Catalytic Core in PyrI4. *Cell Chem Biol* **23**, 352-360 (2016).
26 Byrne, M. J. *et al*. The Catalytic Mechanism of a Natural Diels-Alderase Revealed in Molecular Detail. *J Am Chem Soc* **138**, 6095-6098 (2016).
27 Zheng, Q. F. *et al*. Structural Insights into a Flavin-Dependent [4+2] Cyclase that Catalyzes trans-Decalin Formation in Pyrroindomycin Biosynthesis. *Cell Chem Biol* **25**, 718-728 (2018).
28 Cai, Y. *et al*. Structural Basis for Stereoselective Dehydration and Hydrogen-Bonding Catalysis by the SAM-Dependent Pericyclase LepI. *bioRxiv*, doi: 10.1101/491761 (2018).
29 Domingo, L. R., Zaragoza, R. J. & Williams, R. M. Studies on the biosynthesis of paraherquamide A and VM99955. A theoretical study of intramolecular Diels-Alder cycloaddition. *J Org Chem* **68**, 2895-2902 (2003).

30 Quadri, L. E. N. *et al*. Characterization of Sfp, a Bacillus subtilis phosphopantetheinyl transferase for peptidyl carrier protein domains in peptide synthetases. *Biochemistry* **37**, 1585-1595 (1998).

31 Nodvig, C. S., Nielsen, J. B., Kogle, M. E. & Mortensen, U. H. A CRISPR-Cas9 System for Genetic Engineering of Filamentous Fungi. *PLoS One* **10**, e0133085 (2015).

32 Fraley, A. E. *et al*. Function and Structure of MalA/MalA', Iterative Halogenases for Late-Stage C-H Functionalization of Indole Alkaloids. *J Am Chem Soc* **139**, 12060-12068 (2017).

33 Filling, C. *et al*. Critical residues for structure and catalysis in short-chain dehydrogenases/reductases. *J Biol Chem* **277**, 25677-25684 (2002).

34 Oppermann, U. *et al*. Short-chain dehydrogenases/reductases (SDR): the 2002 update. *Chem Biol Interact* **143-144**, 247-253 (2003).

35 Man, H. *et al*. Structures of Alcohol Dehydrogenases from Ralstonia and Sphingobium spp. Reveal the Molecular Basis for Their Recognition of 'Bulky-Bulky' Ketones. *Top Catal* **57**, 356-365 (2014).

36 Birch, A. J. & Wright, J. J. Studies in relation to biosynthesis. XLII. The structural elucidation and some aspects of the biosynthesis of the brevianamides-A and -E. *Tetrahedron* **26**, 2329-2344 (1970).

# List of Abbreviations

| | |
|---|---|
| $Ac_2O$ | Acetic anhydride |
| AcOH | Acetic acid |
| 9BBN | 9-Borabicyclo[3.3.1]nonane |
| Bn | Benzyl |
| Boc | *tert*-Butoxycarbonyl |
| $Boc_2O$ | Di-*tert*-butyl dicarbonate |
| BuLi | Butyllithium |
| DBU | 1,8-diazabicyclo[5.4.0]undec-7-ene |
| DCM | Dichloromethane |
| DDQ | 2,3-dichloro-5,6-dicyano-1,4-benzoquinone |
| DEAD | Diethyl azocarboxylate |
| DIBAL | Diisobutylaluminum hydride |
| DIPEA | Diisopropylethylamine |
| DKP | Diketopiperazine |
| DMAP | 4-(Dimethylamino)pyridine |
| DMAPP | Dimethylallyl pyrophosphate |
| DMDO | Dimethyl dioxirane |
| DMF | Dimethylformamide |
| DMF-DMA | Dimethylformamide dimethyl acetal |
| DMSO | Dimethylsulfoxide |

| | |
|---|---|
| DO | Davis' Oxaziridine |
| Et | Ethyl |
| EtOAc | Ethyl acetate |
| $Et_2O$ | Diethyl ether |
| EtOH | Ethanol |
| Fmoc | Fluorenylmethyloxycarbonyl |
| FmocOsu | Fluorenylmethoxycarbonyloxy succinimide |
| HATU | *O*-(7-Azabenzotriazol-1-yl)-*N,N,N',N'*-tetramethyluronium hexafluorophosphate |
| IMDA | Intramolecular Diels-Alder |
| imid. | Imidazole |
| KHMDS | Potassium (bis)trimethylsilyl amide |
| LDA | Lithium diisopropylamine |
| LHMDS (or LiHMDS) | Lithium (bis)trimethylsilyl amide |
| *m*CPBA | *meta*-Chloroperbenzoic acid |
| Me | Methyl |
| MeI | Methyl iodide |
| MeCN | Acetonitirile |
| MeOH | Methanol |
| Ms | Methanesulfonyl (mesylate) |
| MsCl | Methanesulfonyl chloride |
| NADH | Nicotinamide adenine dinucleotide |

| | |
|---|---|
| NADPH | Nicotinamide adenine dinucleotide phosphate |
| NCS | N-chlorosuccinimide |
| NHMDS (or NaHMDS) | Sodium (bis)trimethylsilyl amide |
| NMR | Nuclear magnetic resonance |
| NRPS | Nonribosomal peptide synthetase |
| ONB | *ortho*-nitrobenzyl |
| pMB | *p*-Methoxybenzyl |
| PTLC | Preparative thin layer chromatography |
| *i*-Pr | Isopropyl |
| Py. or Pyr | Pyridine |
| SAM | S-Adenosyl methionine |
| TBAF | Tetrabutylammonium fluoride |
| TBDPS | *tert*-Butyldiphenylsilyl |
| TBS | *tert*-Butyldimethylsilyl |
| TBSCl | *tert*-Butyldimethylsilyl chloride |
| *t*-BuOK | Potassium *tert*-butoxide |
| TFA | Trifluoroacetic acid |
| TFAA | Trifluoroacetic anhydride |
| THF | Tetrahydrofuran |
| TLC | Thin layer chromatography |
| TMS | Trimethylsilyl |
| TMSCl | Trimethylsilyl chloride |